THERMOPHILIC AND HALOPHILIC EXTREMOPHILES IN EURASIAN ENVIRONMENTS

EDITED BY: Hongchen Jiang, Wen-Jun Li, Nils-Kaare Birkeland and Dilfuza Egamberdieva

PUBLISHED IN: Frontiers in Microbiology

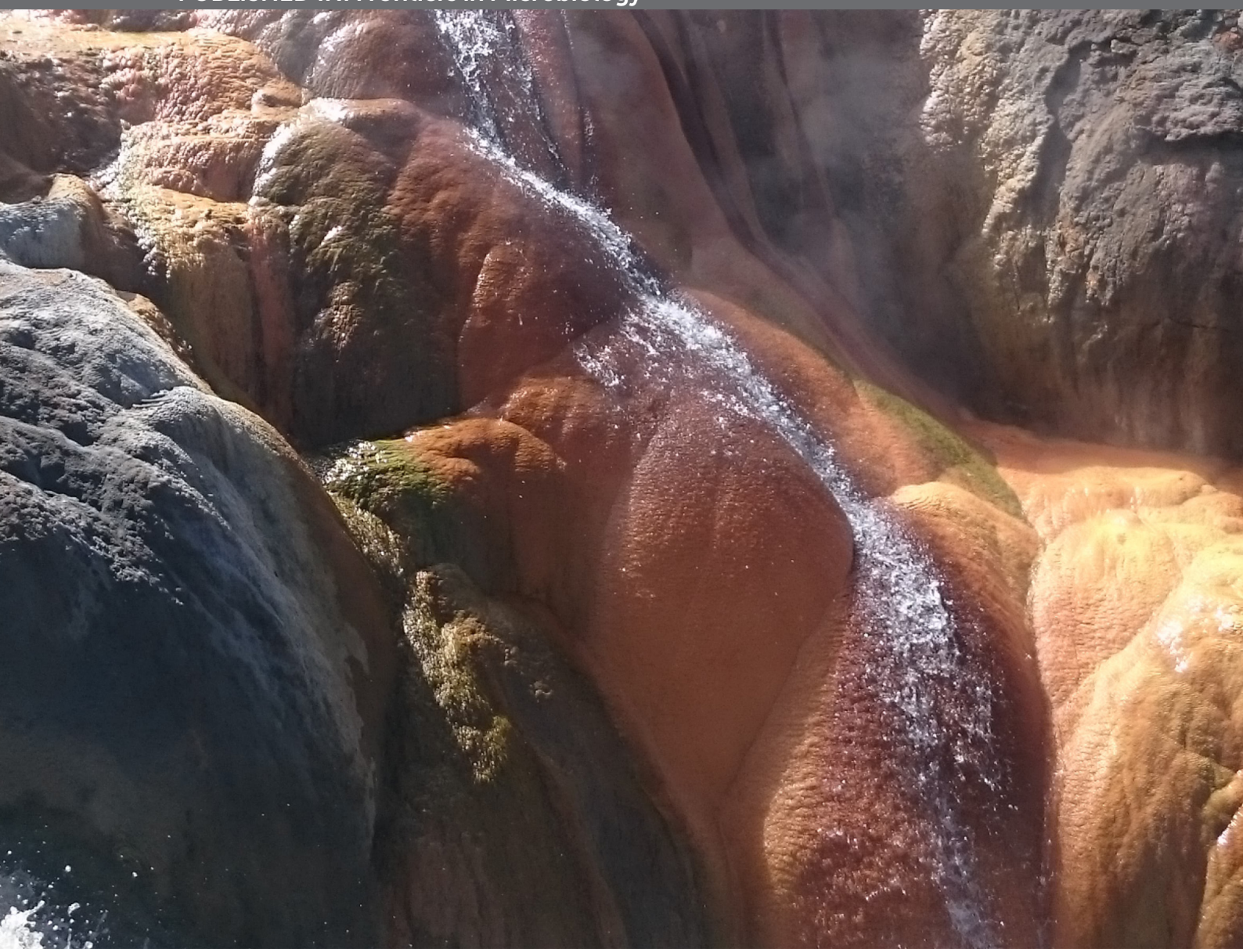

frontiers Research Topics

frontiers

ISSN 1664-8714
ISBN 978-2-88945-835-6
DOI 10.3389/978-2-88945-835-6

About Frontiers

Frontiers is more than just an open-access publisher of scholarly articles: it is a pioneering approach to the world of academia, radically improving the way scholarly research is managed. The grand vision of Frontiers is a world where all people have an equal opportunity to seek, share and generate knowledge. Frontiers provides immediate and permanent online open access to all its publications, but this alone is not enough to realize our grand goals.

Frontiers Journal Series

The Frontiers Journal Series is a multi-tier and interdisciplinary set of open-access, online journals, promising a paradigm shift from the current review, selection and dissemination processes in academic publishing. All Frontiers journals are driven by researchers for researchers; therefore, they constitute a service to the scholarly community. At the same time, the Frontiers Journal Series operates on a revolutionary invention, the tiered publishing system, initially addressing specific communities of scholars, and gradually climbing up to broader public understanding, thus serving the interests of the lay society, too.

Dedication to Quality

Each Frontiers article is a landmark of the highest quality, thanks to genuinely collaborative interactions between authors and review editors, who include some of the world's best academicians. Research must be certified by peers before entering a stream of knowledge that may eventually reach the public - and shape society; therefore, Frontiers only applies the most rigorous and unbiased reviews.
Frontiers revolutionizes research publishing by freely delivering the most outstanding research, evaluated with no bias from both the academic and social point of view. By applying the most advanced information technologies, Frontiers is catapulting scholarly publishing into a new generation.

What are Frontiers Research Topics?

Frontiers Research Topics are very popular trademarks of the Frontiers Journals Series: they are collections of at least ten articles, all centered on a particular subject. With their unique mix of varied contributions from Original Research to Review Articles, Frontiers Research Topics unify the most influential researchers, the latest key findings and historical advances in a hot research area! Find out more on how to host your own Frontiers Research Topic or contribute to one as an author by contacting the Frontiers Editorial Office: researchtopics@frontiersin.org

THERMOPHILIC AND HALOPHILIC EXTREMOPHILES IN EURASIAN ENVIRONMENTS

Topic Editors:
Hongchen Jiang, China University of Geosciences (Wuhan), China
Wen-Jun Li, Sun Yat-Sen University, China
Nils-Kaare Birkeland, University of Bergen, Norway
Dilfuza Egamberdieva, Leibniz Center for Agricultural Landscape Research (ZALF), Germany

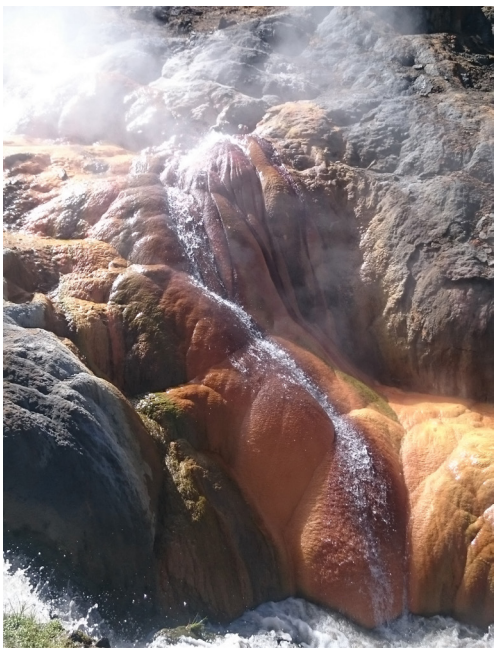

Sinter at the Quzhuomu Hot Spring (E91°48.027′, N28°14.645′) on the Tibetan Plateau, photographed by Dr. Geng Wu (China University of Geosciences-Wuhan).

The eBook is the product of a partnership between the Norwegian Eurasia Program and the China Silk Road Program. At the present, our knowledge on microbiology and biogeochemistry from Eurasian (hyper)saline and thermal ecosystems is limited. Such information is essential to the field and contributes to a comprehensive understanding of microbial metabolic pathways and functions involved in biogeochemical processes in extreme ecosystems. This eBook includes a series of recent progress in microbial diversity, ecological functions, and biogeochemistry in Eurasian (hyper)saline and thermal ecosystems with the use of next generation sequencing, omics technologies and interdisciplinary collaboration. We hope that this eBook would serve as a model for international cooperation and as a source of inspiration for more achievements in Eurasian (hyper)saline and thermal ecosystems in the future. The complete list of authors and co-authors includes 68 highly-qualified specialists from 9 countries.

All chapters in the eBook were edited by authoritative experts. We would like to emphasize the great goodwill, esteem and cooperation extended to each other among the authors, reviewers and editors who contributed to the successful completion of this eBook.

Citation: Jiang, H., Li, W.-J., Birkeland, N.-K., Egamberdieva, D., eds. (2019). Thermophilic and Halophilic Extremophiles in Eurasian Environments. Lausanne: Frontiers Media. doi: 10.3389/978-2-88945-835-6

Table of Contents

06 ***Editorial: Thermophilic and Halophilic Extremophiles in Eurasian Environments***
Hongchen Jiang, Wen-jun Li, Nils-Kåre Birkeland and Dilfuza Egamberdieva

08 ***Morphological and Transcriptomic Analysis Reveals the Osmoadaptive Response of Endophytic Fungus* Aspergillus montevidensis *ZYD4 to High Salt Stress***
Kai-Hui Liu, Xiao-Wei Ding, Manik Prabhu Narsing Rao, Bo Zhang, Yong-Gui Zhang, Fei-Hu Liu, Bing-Bing Liu, Min Xiao and Wen-Jun Li

20 ***Benthic Algal Community Structures and Their Response to Geographic Distance and Environmental Variables in the Qinghai-Tibetan Lakes With Different Salinity***
Jian Yang, Hongchen Jiang, Wen Liu and Beichen Wang

29 ***Macro and Microelements Drive Diversity and Composition of Prokaryotic and Fungal Communities in Hypersaline Sediments and Saline–Alkaline Soils***
Kaihui Liu, Xiaowei Ding, Xiaofei Tang, Jianjun Wang, Wenjun Li, Qingyun Yan and Zhenghua Liu

42 ***Ferric Sulfate and Proline Enhance Heavy-Metal Tolerance of Halophilic/Halotolerant Soil Microorganisms and Their Bioremediation Potential for Spilled-Oil Under Multiple Stresses***
Dina M. Al-Mailem, Mohamed Eliyas and Samir S. Radwan

54 ***Abundant and Rare Microbial Biospheres Respond Differently to Environmental and Spatial Factors in Tibetan Hot Springs***
Yanmin Zhang, Geng Wu, Hongchen Jiang, Jian Yang, Weiyu She, Inayat Khan and Wenjun Li

70 ***Effects of Physiochemical Factors on Prokaryotic Biodiversity in Malaysian Circumneutral Hot Springs***
Chia S. Chan, Kok-Gan Chan, Robson Ee, Kar-Wai Hong, María S. Urbieta, Edgardo R. Donati, Mohd S. Shamsir and Kian M. Goh

84 ***Thioarsenate Formation Coupled With Anaerobic Arsenite Oxidation by a Sulfate-Reducing Bacterium Isolated From a Hot Spring***
Geng Wu, Liuqin Huang, Hongchen Jiang, Yue'e Peng, Wei Guo, Ziyu Chen, Weiyu She, Qinghai Guo and Hailiang Dong

93 ***Genomic Insights Into Energy Metabolism of* Carboxydocella thermautotrophica *Coupling Hydrogenogenic CO Oxidation With the Reduction of Fe(III) Minerals***
Stepan V. Toshchakov, Alexander V. Lebedinsky, Tatyana G. Sokolova, Daria G. Zavarzina, Alexei A. Korzhenkov, Alina V. Teplyuk, Natalia I. Chistyakova, Vyacheslav S. Rusakov, Elizaveta A. Bonch-Osmolovskaya, Ilya V. Kublanov and Sergey N. Gavrilov

113 ***Respiratory Pathways Reconstructed by Multi-Omics Analysis in* Melioribacter roseus*, Residing in a Deep Thermal Aquifer of the West-Siberian Megabasin***
Sergey Gavrilov, Olga Podosokorskaya, Dmitry Alexeev, Alexander Merkel, Maria Khomyakova, Maria Muntyan, Ilya Altukhov, Ivan Butenko, Elizaveta Bonch-Osmolovskaya, Vadim Govorun and Ilya Kublanov

126 ***Sugar Metabolism of the First Thermophilic Planctomycete* Thermogutta terrifontis*: Comparative Genomic and Transcriptomic Approaches***
Alexander G. Elcheninov, Peter Menzel, Soley R. Gudbergsdottir, Alexei I. Slesarev, Vitaly V. Kadnikov, Anders Krogh, Elizaveta A. Bonch-Osmolovskaya, Xu Peng and Ilya V. Kublanov

137 ***Fermentation of Mannitol Extracts From Brown Macro Algae by Thermophilic* Clostridia**
Theo Chades, Sean M. Scully, Eva M. Ingvadottir and Johann Orlygsson

frontiers in Microbiology

EDITORIAL
published: 05 March 2019
doi: 10.3389/fmicb.2019.00379

Editorial: Thermophilic and Halophilic Extremophiles in Eurasian Environments

Hongchen Jiang[1]*, *Wen-jun Li*[2,3], *Nils-Kåre Birkeland*[4] and *Dilfuza Egamberdieva*[5,6]

[1] State Key Laboratory of Biogeology and Environmental Geology, China University of Geosciences, Wuhan, China, [2] State Key Laboratory of Biocontrol and Guangdong Provincial Key Laboratory of Plant Resources, School of Life Sciences, Sun Yat-Sen University, Guangzhou, China, [3] Southern Laboratory of Ocean Science and Engineering, Zhuhai, China, [4] Department of Biological Sciences, University of Bergen, Bergen, Norway, [5] Leibniz Centre for Agricultural Landscape Research, Müncheberg, Germany, [6] Faculty of Biology, National University of Uzbekistan, Tashkent, Uzbekistan

Keywords: saline/hypersaline environments, thermal environments, microbial diversity, adaptation, pathways

Editorial on the Research Topic

Thermophilic and Halophilic Extremophiles in Eurasian Environments

Saline/hypersaline and thermal ecosystems are typical extreme environments. Microbial diversity, ecological function and adaptation in (hyper)saline and thermal ecosystems are attracting more attentions due to the following reasons: (1) (hyper)saline and geothermal ecosystems are analogs to certain extreme environments on early Earth and/or other planets and are thus suitable environments for analog studies on life origin and evolution and extraterrestrial life exploration; (2) microbial community complexity is relatively low in (hyper)saline and thermal ecosystems and thus they are often treated as model ecosystems for environmental microbiologists and biogeochemists to study how microbially mediated element cycling and biogeochemical processes respond to environmental variables (e.g., salinity, temperature); and (3) (hyper)saline and thermal ecosystems are inhabited by abundant and diverse microbial resources that have extensive biotechnological and commercial values.

The Eurasian continent possesses geologically and physiochemically diverse and unique terrestrial saline/hypersaline and thermal environments, which in general have been investigated for microbiology and biogeochemistry to a less extent than those in America. However, research results from Eurasian (hyper)saline and thermal ecosystems are essential to the field. Recently, a series of significant advances have been made on microbial diversity, ecological functions, and biogeochemistry in Eurasian (hyper)saline and thermal ecosystems with the use of next generation sequencing, omics technologies, and interdisciplinary collaboration.

We proposed this Research Topic to highlight the current advances and knowledge related to thermophilic and halophilic extremophiles in Eurasian environments. In this Research Topic "Thermophilic and Halophilic Extremophiles in Eurasian Environments" we accepted 11 original research articles that focus on microbial diversity and ecology, microbe-environment interactions, adaptation and evolution, element cycling, and potential biotechnological and industrial applications of thermophiles and halophiles from Eurasian environments. We are grateful to all authors who have contributed to this Research Topic. We are also grateful to all reviewers and editorial staff who have contributed during the reviewing and article production processes.

In addition, this Research Topic is one of the special issues set up at the fifth and sixth annual meetings of the Chinese Society of Geomicrobiology (CSG), which is an academic exchange platform for Chinese and international geomicrobiological scientists of related disciplines

OPEN ACCESS

Edited by:
Philippe M. Oger, UMR5240 Microbiologie, Adaptation et Pathogenie (MAP), France

Reviewed by:
Doug Bartlett, University of California, San Diego, United States

***Correspondence:**
Hongchen Jiang
jiangh@cug.edu.cn

Specialty section:
This article was submitted to Extreme Microbiology, a section of the journal Frontiers in Microbiology

Received: *19 December 2018*
Accepted: *13 February 2019*
Published: *05 March 2019*

Citation:
Jiang H, Li W, Birkeland N-K and Egamberdieva D (2019) Editorial: Thermophilic and Halophilic Extremophiles in Eurasian Environments. Front. Microbiol. 10:379. doi: 10.3389/fmicb.2019.00379

including mineral petrology, mineral deposits, paleontology, organic geochemistry, molecular paleontology, biogeochemistry, petroleum geology, microbiology, and ecology. This Research Topic is also one of the designated targets of the project "Network for improving research-based higher education in basic and applied microbiology," funded by the Norwegian Eurasia program, using extremophiles as model microorganisms.

Among the accepted articles in this Research Topic, four and seven of them are about halophiles/microbial studies in (hyper)saline ecosystems and thermophiles/microbial studies in thermal ecosystems, respectively. Among the articles related to halophiles/microbial studies in (hyper)saline ecosystems, Liu et al. disclose the osmo-adaptive mechanisms of halophilic endophytic fungi from the molecular perspective. Yang et al. characterized Microbial benthic algal community structures in saline and hypersaline lakes and assessed how they were influenced by spatial and environmental factors on the Qing-Tibetan Plateau. Liu et al. reported that macro- and micro-elements predominate in shaping prokaryotic and fungal diversity and community composition in hypersaline sediments and saline-alkaline soils. Al-Mailem et al. found that addition of ferric sulfate and proline could assist halophilic/halotolerant soil microorganisms to tolerate high concentration of heavy metals, which could be potentially employed in bioremediation of spilled oil.

Among the articles related to thermophiles/microbial studies in thermal ecosystems, Zhang et al. reported on the diversity and composition of microbial communities in Tibetan hot springs and disclosed their different response patterns to environmental and spatial factor from the perspective of abundant and rare biospheres. Chan et al. reported on the prokaryotic biodiversity and its influencing factors in Malaysian hot springs. Wu et al. reported on the role of one thermophilic sulfate-reducing bacterium in the formation of thioarsenates, major As-S-containing compounds ubiquitously distributed in hot spring ecosystems globally. Toshchakov et al. reconstructed the energy metabolism of *Carboxydocella thermautotrophic* that coupled hydrogenogenic CO oxidation with the reduction of Fe(III) minerals from the genomic perspective. Gavrilov et al. presented the multi-omics analysis results on the respiratory pathways of a metabolically versatile thermophilic bacterium isolated from a deep thermal aquifer. Elcheninov et al. reported on the degradation pathways of Xanthan gum by a thermophilic bacterium retrieved from a hot spring in the Far-East of Russia with the use of comparative genomic and transcriptomic techniques. Chades et al. presented the ability of thermophilic anaerobic *Clostridia* to produce bioethanol by fermenting mannitol and mannitol-containing algal extracts.

We are delighted to present this Research Topic in Frontiers in Microbiology. We hope that this Research Topic will be interesting and useful to the readers of the journal and broaden the knowledge of thermophilic and halophilic extremophiles in Eurasian Environments. The findings presented in this Research Topic are promising but still limited. In the future, application of innovative research techniques and intensive and deep international collaborations will undoubtedly unveil more exciting aspects of thermophilic and halophilic extremophiles in Eurasian environments.

AUTHOR CONTRIBUTIONS

HJ organized this topic and wrote the editorial article. WL, N-KB, and DE are co-editors of the topic and discussed the writing.

FUNDING

This work was supported by the National Natural Science Foundation of China (Grant Nos. 91751206 & 41521001), the Special Foundation for Basic Research Program of China Ministry of Science & Technology (MOST) (No. 2015FY110100), the Key Project of International Cooperation of China Ministry of Science and Technology (No. 2013DFA31980), the 111 Program (State Administration of Foreign Experts Affairs & the Ministry of Education of China, grant B18049), the Fundamental Research Funds for the China Central Universities, China University of Geosciences (Wuhan), Xinjiang Uygur Autonomous Region regional coordinated innovation project (Shanghai Cooperation Organization Science and Technology Partnership Program) (Grant No. 2017E01031) and the Eurasia program of the Norwegian Agency for International Cooperation and Quality Enhancement in Higher Education (Diku) (Project No. CPEA-LT-2016/10095).

ACKNOWLEDGMENTS

We are grateful to all editors and reviewers involved in the review process of this Research Topic.

Conflict of Interest Statement: The authors declare that the research was conducted in the absence of any commercial or financial relationships that could be construed as a potential conflict of interest.

frontiers in Microbiology

ORIGINAL RESEARCH
published: 21 September 2017
doi: 10.3389/fmicb.2017.01789

Morphological and Transcriptomic Analysis Reveals the Osmoadaptive Response of Endophytic Fungus *Aspergillus montevidensis* ZYD4 to High Salt Stress

Kai-Hui Liu[1], Xiao-Wei Ding[1], Manik Prabhu Narsing Rao[2], Bo Zhang[1], Yong-Gui Zhang[1], Fei-Hu Liu[3], Bing-Bing Liu[2], Min Xiao[2] and Wen-Jun Li[2, 4]**

[1] School of Biological Science and Engineering, Shaanxi University of Technology, Hanzhong, China, [2] State Key Laboratory of Biocontrol and Guangdong Provincial Key Laboratory of Plant Resources, School of Life Sciences, Sun Yat-Sen University, Guangzhou, China, [3] School of Life Sciences, Yunnan University, Kunming, China, [4] Key Laboratory of Biogeography and Bioresource in Arid Land, Xinjiang Institute of Ecology and Geography, Chinese Academy of Sciences, Ürümqi, China

OPEN ACCESS

Edited by:
Philippe M. Oger, UMR Centre National de la Recherche Scientifique 5240 Institut National des Sciences Appliquées, France

Reviewed by:
Jens Christian Frisvad, Technical University of Denmark, Denmark
Ana Plemenitas, University of Ljubljana, Slovenia

***Correspondence:**
Min Xiao
xiaomin8@mail.sysu.edu.cn
Wen-Jun Li
liwenjun3@mail.sysu.edu.cn

Specialty section:
This article was submitted to Extreme Microbiology, a section of the journal Frontiers in Microbiology

Received: *09 February 2017*
Accepted: *05 September 2017*
Published: *21 September 2017*

Citation:
Liu K-H, Ding X-W, Narsing Rao MP, Zhang B, Zhang Y-G, Liu F-H, Liu B-B, Xiao M and Li W-J (2017) Morphological and Transcriptomic Analysis Reveals the Osmoadaptive Response of Endophytic Fungus Aspergillus montevidensis ZYD4 to High Salt Stress. Front. Microbiol. 8:1789. doi: 10.3389/fmicb.2017.01789

Halophilic fungi have evolved unique osmoadaptive strategies, enabling them to thrive in hypersaline habitats. Here, we conduct morphological and transcriptomic response of endophytic fungus (*Aspergillus montevidensis* ZYD4) in both the presence and absence of salt stress. Under salt stress, the colony morphology of the *A. montevidensis* ZYD4 changed drastically and exhibited decreased colony pigmentation. Extensive conidiophores development was observed under salt stress; conidiophores rarely developed in the absence of salt stress. Under salt stress, yellow cleistothecium formation was inhibited, while glycerol and compatible sugars continued to accumulate. Among differentially expressed unigenes (DEGs), 733 of them were up-regulated while 1,619 unigenes were down-regulated. We discovered that genes involved in the accumulation of glycerol, the storage of compatible sugars, organic acids, pigment production, and asexual sporulation were differentially regulated under salt stress. These results provide further understanding of the molecular basis of osmoadaptive mechanisms of halophilic endophytic fungi.

Keywords: transcriptome, halophilic endophytic fungi, *Aspergillus montevidensis*, high-salt stress, osmoadaptive mechanisms

INTRODUCTION

Extremophilic microorganisms not only survive, but can grow optimally under rough conditions which are considered harsh and inhospitable for other life forms as well (Mesbah and Wiegel, 2012). Hypersaline environment is one of the examples of such extreme environments (Wood, 2015). Generally, high salinity represents high-osmotic stress, which triggers cytoplasm shrinkage and causes lethal damage to salt-sensitive microbes (Koch, 1984; Morris et al., 1986). However, some microbes learn to cope with these high salt concentrations by developing special strategies (Oren, 2002). In hypersaline environments, bacteria are considered to be the only populated microorganisms (Gunde-Cimerman et al., 2009); however, the report by Gunde-Cimermana et al. (2000) show the presence of fungi in saline environments. Since then, many fungal spp. were

reported from different saline environments (Plemenitaš et al., 2008; Gunde-Cimerman et al., 2009).

Fungi use different strategies to overcome salt stress, such as morphological change (Zajc et al., 2013), reinforcement of cell walls, accumulation of osmolytes like glycerol, and change in genetic structures (Duran et al., 2010; Kralj Kuncic et al., 2010; Kis-Papo et al., 2014). Changes to salt stress at the transcriptomic level are still intricate, and the molecular mechanisms are not well-known. With the development of RNA-sequencing, it is easy to detect transcriptomic responses in a given species to varying experimental conditions (Schweder and Hecker, 2004; Dalmolin et al., 2012; Taymaz-Nikerel et al., 2016).

Next-generation sequencing technology (Illumina RNA-seq) enables highly sensitive and accurate quantification of expression, thus providing a myriad of transcript data with high resolution, high quality, and low costs (Riccombeni and Butler, 2012). It has been widely applied in non-model and model species, such as, *Aspergillus nidulans, Hortaea werneckii,* and *Wallemia ichthyophaga,* examining hundreds of stress-tolerance genes (Redkar et al., 1996; Petrovic et al., 2002; Zajc et al., 2013). Although, studies are carried out to understand salt stress-tolerance genes in fungi, there are only a few reports on response of endophytic fungi to high-salt stress. In this study, we made an attempt to isolate an endophytic fungus from a hypersaline region and evaluate its morphological and transcriptomic response under salt stress.

MATERIALS AND METHODS

Isolation and Identification of Endophytic Fungal Strain ZYD4

Medicago sativa L. grew in hypersaline environment (Huama lake region, Northern Shaanxi, China) was chosen as a source plant for the isolation of endophytic fungi. The endophytic strain ZYD4, was isolated using yeast extract-peptone-dextrose (YPD) agar (Difco) from the stems of *Medicago sativa* L. which were surface sterilized by following the protocols of Li et al. (2009) and Salam et al. (2017). For the identification, genomic DNA from strain ZYD4 was extracted by following the protocol of Hinrikson et al. (2005). ITS fragments of strain ZYD4 were amplified using the primers, ITS1 and ITS4 (White et al., 1990).

The analysis of sequences was done at Blast-n site at NCBI server (http://www.ncbi.nlm.nih.gov/BLAST).

The phylogenetic tree was constructed by neighbor-joining (NJ) (Saitou and Nei, 1987) method using MEGA 5.0 software package (Tamura et al., 2011) after multiple alignment of the sequences using CLUSTAL_X program (Thompson et al., 1997). Kimura's two parameter model was used to calculate evolutionary distance matrices (Kimura, 1980). Bootstrap analysis was performed with 1,000 replications (Felsenstein, 1985).

Morphological Response of Endophytic Strain ZYD4 to Salt Stress

The morphological response of endophytic strain ZYD4 to salt stress was evaluated at salt concentrations ranging from 0 to 4.5 M (at an interval of 1.5 M) using YPD agar at 28°C for 6 days.

Evaluation of Salt Stress on the Biosynthesis of Pigment and Accumulation of Glycerol and Compatible Sugars

To evaluate salt stress on the biosynthesis of pigment and accumulation of glycerol and compatible sugars, we grew strain ZYD4 in the presence and absence of 3 M NaCl. The collected mycelium was washed three times with sterilized distilled water and freeze-dried at −30°C.

The mycelium was thoroughly ground in liquid nitrogen. The pigment was extracted with methanol (Liu et al., 2015) and monitored by UV–visible spectrophotometer (Shimadzu UV-1750, Japan) using β-Carotene and flavoglaucin as standard.

Glycerol and compatible sugars were extracted in sterilized distilled water using sonicator (350 W, 1 min) performed on the ice bath followed by centrifugation at 10,000 rpm for 10 min at 4°C. All extracts were filtered through a 0.22-μm filter before the examination. Glycerol and compatible sugars were determined using UV–visible spectrophotometer (Shimadzu UV-1750, Japan) by following the protocols of Kuhn et al. (2015) and Laurentin and Edwards (2003).

RNA Extraction, Library Construction, and Illumina Sequencing

We statically grew endophytic strain ZYD4 on YPD broth at 28°C for 6 days. The fungal mycelium was harvested and induced under salt stress by adding 3 M NaCl at 28°C for 30 min. Total RNA from salt-stress induced and non-induced mycelium was extracted using the Trizol reagent (Invitrogen, Carlsbad, CA, USA), according to manufacturer's instructions. The RNA samples were treated with DNase I for 30 min at 37°C to remove genomic DNA contamination. The quantity and integrity of the total RNAs were verified using an Agilent 2100 bioanalyzer. The cDNA libraries were developed according to manufacturer's instructions (Illumina, Inc., San Diego, CA, USA), and sequenced on the Illumina HiSeq 2000 platform at Beijing Genomics Institute (Shenzhen, China).

De novo Assembly and Analysis

Before the assembly, raw reads were cleaned by removing adaptor sequences, low-quality reads, and reads with unknown nucleotides >5%. All clean reads were *de novo* assembled into contigs using the short-read assembling program Trinity (Grabherr et al., 2011). The contigs were pooled to build into de Brujin graphs by Chrysalis. Contigs from the same transcript and the distances between these contigs were detected by a paired-end sequencing strategy. Unigenes from each samples assembly were further processed with sequence-clustering software to remove sequence splicing and redundancy. The unigenes were divided into clusters (CL prefix) and singletons (unigene prefix) by gene family clustering.

Functional Annotation and Differential Expression Analysis

All unigenes were compared against NCBI non-redundant protein database (NR), the NCBI non-redundant nucleic acid database (NT), the Swiss-Prot database, the Clusters

of Orthologous Groups (COG) database, and the Kyoto Encyclopedia of Genes and Genomes (KEGG) database with an $E < 10^{-5}$. The best aligned results were applied to determine sequence direction of unigenes. The Gene Ontology (GO) was analyzed with Blast2GO software (Conesa et al., 2005). The GO functional classification was performed using WEGO software (Ye et al., 2006). Protein coding region prediction of the unigenes was searched by BLASTx ($E < 0.00001$) against NCBI NR, Swiss-Prot, KEGG, and COG. When unigene was not aligned to any of the above databases, ESTS was used to predict its coding regions and ascertain its sequence direction (Iseli et al., 1999). Differentially expressed unigenes were filtered using a threshold of false discovery rate (FDR ≤ 0.001) and an absolute log2 ratio $\geq$1. These differential expression unigenes were further mapped onto known pathways using the KEGG pathway annotation.

qPCR

qPCR was performed to validate the differential expression of randomly selected genes involved in salt-tolerance on a 7500 Real-Time PCR System (Applied Biosystems, USA) under the following conditions: 95°C for 30 s, followed by 40 cycles of 95°C for 15 s and 60°C for 40 s. The q-PCR mixture (20 μl) comprised of 10 μl of SYBR® Select Master Mix (Applied Biosystems, USA), 10 ng of cDNA, primers (0.4 μM each; Table S1), and RNase-free water. All PCR reactions were run in duplicate for each gene along with the endogenous 18S rRNA reference gene. The $2^{-\Delta\Delta Ct}$ method (Livak and Schmittgen, 2001) was employed to calculate the gene expression levels in salt with and without treated samples.

RESULTS

Identification of Endophytic Fungal Strain ZYD4

The BLAST result showed that, endophytic strain ZYD4 shared 100% similarity with *Aspergillus montevidensis.* The obtained sequences were submitted to GenBank under the accession number MF062488. In NJ tree (**Figure 1**) strain ZYD4 was grouped with *A. montevidensis.* Based on the above, strain ZYD4 was identified as *A. montevidensis.* The strain ZYD4 was deposited in China General Microbiological Culture Collection Center under the deposition number CGMCC 3.15762.

Morphological Response of *A. montevidensis* ZYD4 under Salt Stress

Under salt stress, the morphological characters such as colony shape, color, size, and conidial head formation of *A. montevidensis* ZYD4 changed (**Figures 2b–d**, **Table 1**). Under salt stress, the mycelium was loose while compact in absence of salt stress. The width of hyphae decreased under salt stress (**Table 1**). Under salt stress, *A. montevidensis* ZYD4 colonies were olive green in the center and white at the margin while in the absence of salt stress, colonies were yellow to gray black in center and golden yellow at the margin. The conidial head was extensively developed in the presence of salt stress, while rarely formed in the absence of salt stress. Formation of yellow cleistothecium was dramatically inhibited with an increase of salt stress (**Figures 2e–h**, **Table 1**).

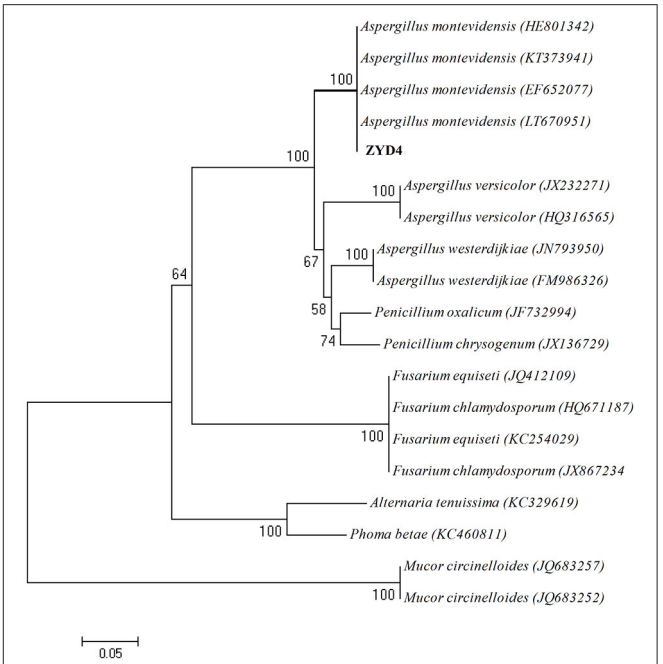

FIGURE 1 | Neighbor-joining tree showing the phylogenetic relationship of the strain ZYD4. Boot strap values (expressed as percentages of 1,000 replications) >50% was given at the node.

Evaluation of Salt Stress on the Biosynthesis of Pigment and Accumulation of Glycerol and Compatible Sugars

Figure 3 shows UV-visible spectra of pigment biosynthesis analysis which suggest that, *A. montevidensis* ZYD4 grown under salt stress did not show any pigment production, while in absence of salt stress pigment production was observed.

The content of glycerol in salt treated mycelium was 2.5-fold high when compared to salt untreated mycelium (**Figure 4A**). Similarly, the contents of total compatible sugars in salt treated mycelium was 2.0-fold high when compared to salt untreated mycelium (**Figure 4B**).

Illumina Sequencing and *De novo* Assembly

To explore osmoadaptive strategies, cDNA libraries of *A. montevidensis* ZYD4 (from salt with and without treated mycelium) were sequenced using the Illumina Hiseq 2000 platform. The raw reads obtained from salt with and without induced mycelium were submitted into GenBank under the accession numbers SRX1794941 and SRX1794940 respectively. After the removal of the adapter sequences, unknown, and low-quality sequences about 104,004,358 clean reads (average length 90 nt) were obtained from raw reads with GC percentage between 50.57 and 51.63%.

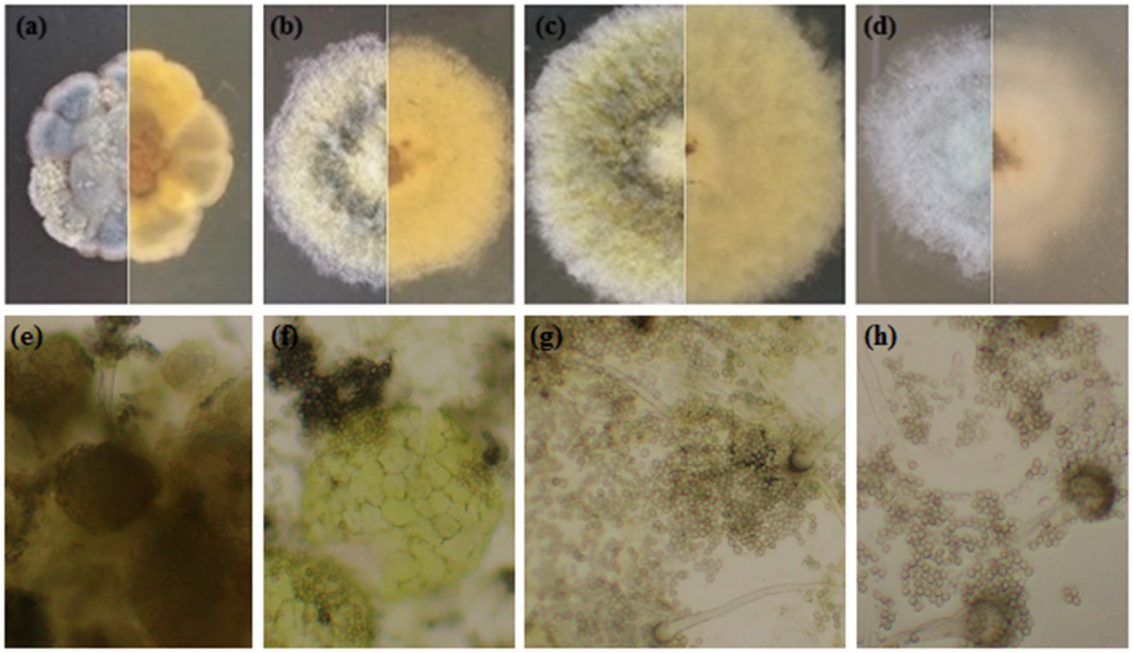

FIGURE 2 | Morphological profile of *A. montevidensis* ZYD4 on solid medium supplemented with varying concentrations of NaCl: **(a,e)** without NaCl; **(b,f)** 1.5 M NaCl; **(c,g)** 3 M NaCl; **(d,h)** 4.5 M NaCl.

These clean reads were *de novo* assembled (**Table 2**) resulting in 34,341, and 28,503 contigs for salt without and with treated samples, with a mean length of 595, and 657 nt and an N50 length of 1,717, and 1,789 nt respectively.

After further clustering and assembly, 27,797 unigenes for salt untreated sample and 24,157 unigenes for salt treated sample, with an average length of 1,199, and 1,253 nt, and N50 length of 2,283, and 2,268 nt respectively were obtained. There were 46,464 unigenes with the length ≥500 nt, and 41,844 unigenes with the length ≥1,000 nt. The length distribution of these contigs and unigenes were shown in **Table 2**.

Functional Annotation

A total of 18,267 unigenes were annotated, among them 17,713, 12,197, 12,018, and 9,029 showed high similarities to the known genes in NR, SwissProt, KEGG, and COG databases. The NR annotation and E-value distribution (**Figure 5A**) of significant hits ($E < 1.0 \times 10^{-45}$) showed that 71.6% of the sequences had strong homologies, 19.2% of the sequences had a high degree of homologies with $E < 1.0 \times 10^{-15}$, and 70.9% of the sequences had high similarity >60%, while 21.9% showed a similarity range between 40 and 60% (**Figure 5B**). Nearly 62.9% of the annotated unigenes assigned to top BLAST hits were closely related to *Aspergillus* species, namely *Aspergillus oryzae* (15.1%), *Aspergillus terreus* (9.4%), *Aspergillus clavatus* (7.7%), *Aspergillus kawachii* (7.1%), *Aspergillus niger* (7%), and *Aspergillus flavus* (4.6%; **Figure 5C**).

GO and COG Classification

FDR ≦ 0.001 and log2 ratio ≧ 1 as the threshold were used to verify the significance of gene expression differences. Based on these criteria, a total of 2,352 unigenes were differentially expressed in presence and absence of salt stress. Among differentially expressed unigenes (DEGs), 733 unigenes were up-regulated while 1,619 unigenes were down-regulated (**Figure 6**). The expression patterns of some DEGs were validated by RT-PCR (**Figure 7**). DEGs were assigned to 44 GO terms consisting of three domains namely biological process, molecular function, and cellular component (**Figure 8**). The representative distributions of the GO terms for biological processes include cellular process, metabolic process, and single-cell process. A majority of molecular function was composed of cells, cell part, and organelle. Cellular component mainly included catalytic activity, and binding. To verify the effectiveness of annotation, COG classification of DEGs was performed resulting in 25 COG groups. Of these, general function prediction cluster (16.7%) was the dominant group, followed by replication, recombination and repair (8.66%), translation, ribosomal structure and biogenesis (7.45%), and RNA processing and modification (0.64%; **Figure 9**).

KEGG Pathway Analysis

To analyze the salt stress functions of DEGs, we mapped DEGs to 100 reference canonical pathways in KEGG database. The significantly enriched DEGs were mainly involved in 20 pathways, such as metabolic pathways (ko01100, 409 unigenes, 32.8%), biosynthesis of secondary metabolites (ko01110, 202 unigenes, 16.2%), ribosome (ko03010, 117 unigenes, 9.38%), starch and sucrose metabolism (ko00500, 79 unigenes, 6.34%), amino sugar and nucleotide sugar metabolism (ko00520, 68 unigenes, 5.45%), oxidative phosphorylation (ko00190,

TABLE 1 | Morphological profile of *A. montevidensis* ZYD4 on solid medium supplemented with varying salt concentration.

Isolate	NaCl in media (M)	Morphology
A. montevidensis ZYD4	0	Compact mycelium; colony was yellow to gray black in the center and golden yellow at the margin; the branched hyphae are septate, and measure about 2.5–6.25 μm in width; conidiophores chain rarely formed from swelling conidial heads; spherical conidia of 3.75 × 3.75 μm size; yellow cleistothecia extensively developed; ascospores measure about 1.67–2.77 × 2.08–3.15 μm.
	1.5	Loose mycelium; colony was yellow to gray black in the center and gray-black at the margin; the branched hyphae are septate, and measure about 2.5–6.25 μm in width; gray pigmented conidial heads developed; spherical/oval conidia of 2.5–4.0 × 3.75–5.0 μm size; yellow cleistothecia extensively produced; ascospores measure about 1.67–2.77 × 2.08–3.15 μm.
	3	Loose mycelium; colony was olive green in the center and white at the margin; the branched hyphae are septate and measure about 2.5–6.25 μm in width; olive green/white pigmented conidial heads extensively developed; spherical/oval conidia of 2.5–4.0 × 3.75–5.0 μm size.
	4.5	Loose and white mycelium; the branched hyphae are septate and measure about 2.0–2.5 μm in width; gray-green pigmented conidial heads extensively developed; spherical/oval conidia of 2.5–4.0 × 3.0–5.0 μm size.

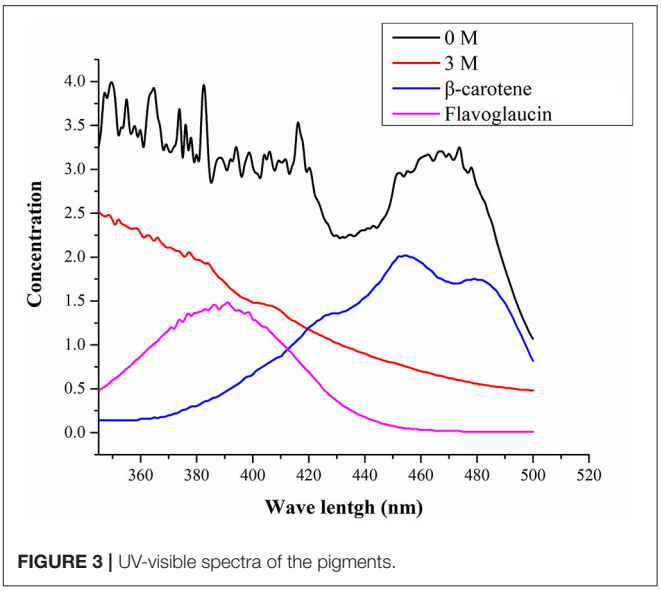

FIGURE 3 | UV-visible spectra of the pigments.

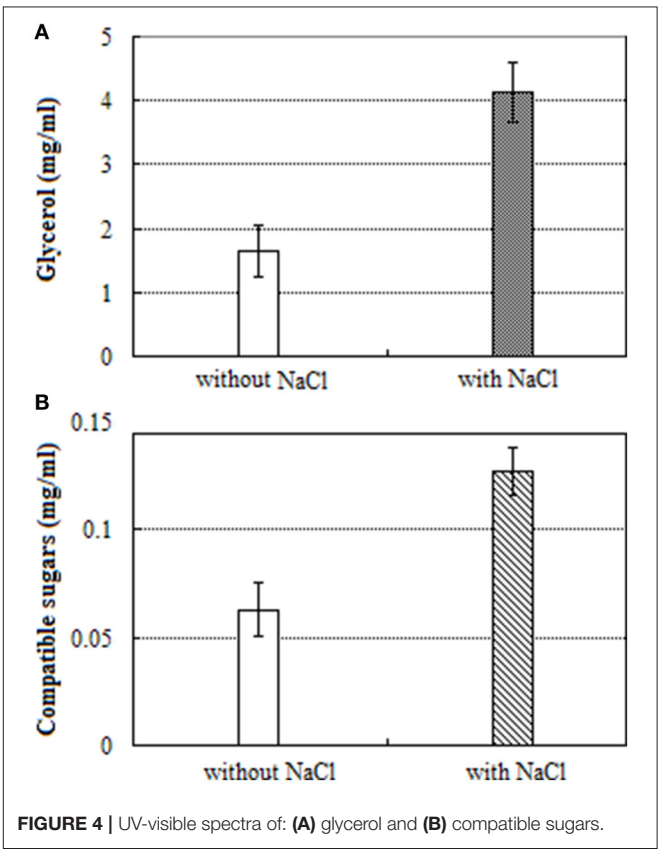

FIGURE 4 | UV-visible spectra of: **(A)** glycerol and **(B)** compatible sugars.

56 unigenes, 4.49%), glycolysis/gluconeogenesis (ko00010, 29 unigenes, 2.33%), glycerophospholipid metabolism (ko00564, 26 unigenes, 2.09%), and cell cycle (ko04111 and ko04113, 38 unigenes, 1.6%). The result of KEGG pathway analysis showed multiple significant enriched pathways which were implicated in response to high salt stress in *A. montevidensis* ZYD4.

Genes Involved in the Development of Asexual Sporulation

After exposure to high-salt stress, *A. montevidensis* ZYD4 extensively developed conidiophores and asexual spores (**Figure 2**). Correspondingly, unigenes homologous to known genes, controlling asexual development of *A. montevidensis* were also up-regulated (**Table 3**).

Genes Involved in the Biosynthesis of Yellow Pigment

The yellow pigment produced by *A. montevidensis* ZYD4 was decreased under salt stress. DEGs related to the biosynthesis of carotenoids in *A. montevidensis* ZYD4 was summarized in **Table 3**. It was observed that, unigenes homologous to geranylgeranyl diphosphate synthase, hydroxymethylglutaryl-CoA (HMG-CoA) synthase, and farnesyl pyrophosphate synthase were down-regulated by 1.1-, 13.1-, and 11.4-fold respectively.

Genes Involved in the Accumulation of Glycerol

Under salt stress, the expression of one unigene encoding glycerol-3-phosphate dehydrogenase (which participates in the

glycerol biosynthetic pathway) was elevated by 1.4-fold (**Table 3**), however, one unigene encoding glycerol dehydrogenase (which converts glycerol into dihydroxyacetone) showed 1.4-fold decrease of expression. Unigenes coding for enzymes responsible for glycerol biosynthesis were up-regulated by 1.1- to 1.4-fold, while unigenes encoding diacylglycerol O-acyltransferase, triacylglycerol lipase, and phospholipase D (these participate in the further transformation of glycerol) were down-regulated by 1.4- to 11.0-fold. These results indicated that glycerol was accumulated in *A. montevidensis* ZYD4 to create a cellular osmotic equilibrium in high-salt conditions.

TABLE 2 | Summary of *A. montevidensis* ZYD4 transcriptome assembly.

	A. montevidensis with NaCl	*A. montevidensis* without NaCl
Number of contings	28,503	34,341
Total length of contings (nt)	18,739,029	20,437,448
Mean length conting (nt)	657	595
N50 contig length (nt)	1789	1717
Total unigenes	24,157	27,797
Total length of unigenes (nt)	30,268,028	33,330,542
Mean length of unigene (nt)	1253	1199
N50 unigene length (nt)	2268	2283
Distinct clusters	8,643	9,765
Distinct singletons	15,514	18,032

Genes Involved in the Biosynthesis of Compatible Sugars

Under salt stress, expression of unigenes homologous to hexokinase, 6-phosphofructo-2-kinase, trehalose-phosphate synthase, and mannose-6-phosphate isomerase increased by 1.0- to 2.2-fold (**Table 3**). Remarkably, 19 DEGs for the further conversion of glucose-6-phosphate into other intermediates via the down-stream pathway of glycolysis and TCA cycle were suppressed up to 10.8- to 13.9-fold. In addition, unigenes responsible for the further transformation of acetyl-CoA (a metabolic intermediate of sugar) into fatty acids, and carotenoids were down-regulated. The above results obtained were consistent with UV-visible spectroscopic analysis (**Figure 4B**).

Genes Involved in the Biosynthesis of Organic Acids

Unigenes of proline oxidase and pyrroline-5-carboxylate dehydrogenase increased the expression by 3.6, and 1.9-fold respectively in salt induced samples (**Table 3**). However, unigenes of glutamate dehydrogenase, and glutamine synthetase (can divide glutamate into glutamine, NH_4^+ and 2-oxo-glutarate) was suppressed more than 11-fold. Moreover, expression level of

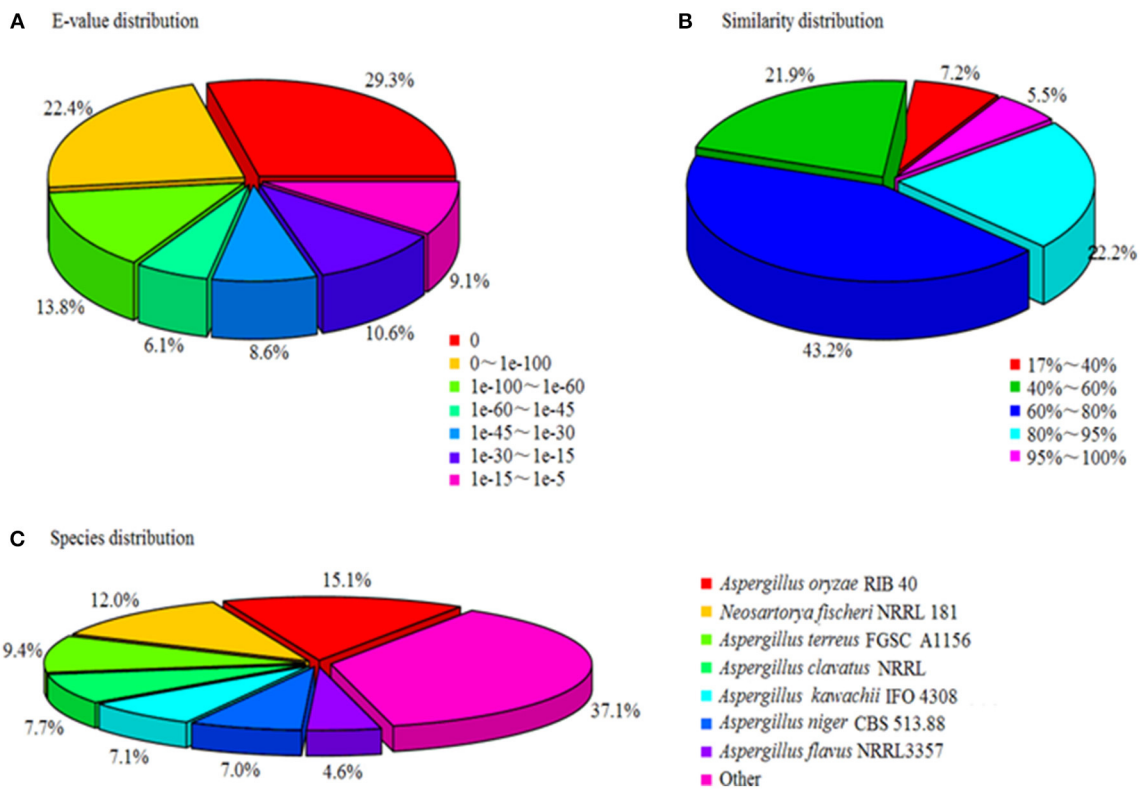

FIGURE 5 | Characteristics of homology search of unigenes against Nr databases. **(A)** *E*-value distribution of BLASTx matches to the unigenes against Nr; **(B)** Similarity in distribution of BLASTx matches to the unigenes against Nr; **(C)** Species distribution of BLASTx matches to the unigenes against Nr.

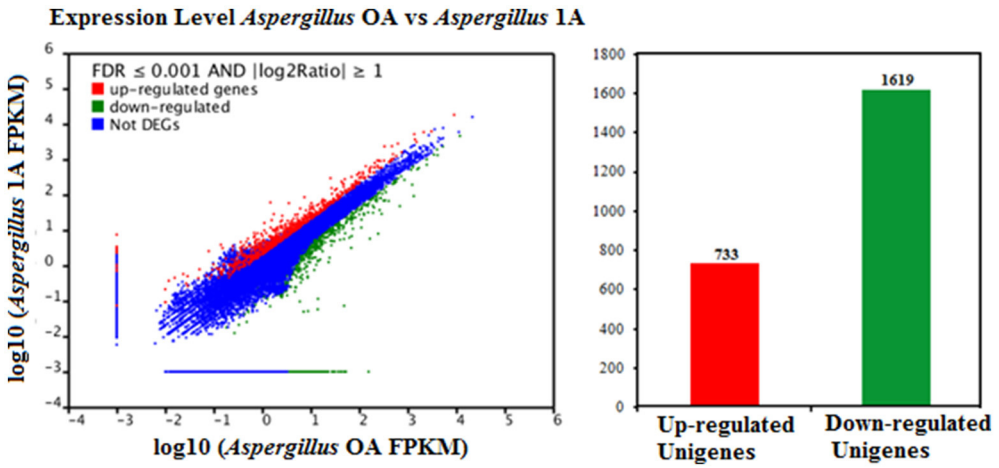

FIGURE 6 | Comparison of gene expression levels in the control and the salt-treated samples. *Aspergillus* OA represents salt untreated sample, and *Aspergillus* 1A represents salt treated samples. Fragments Per Kilobase of transcript per Million fragments mapped abbreviated as FPKM.

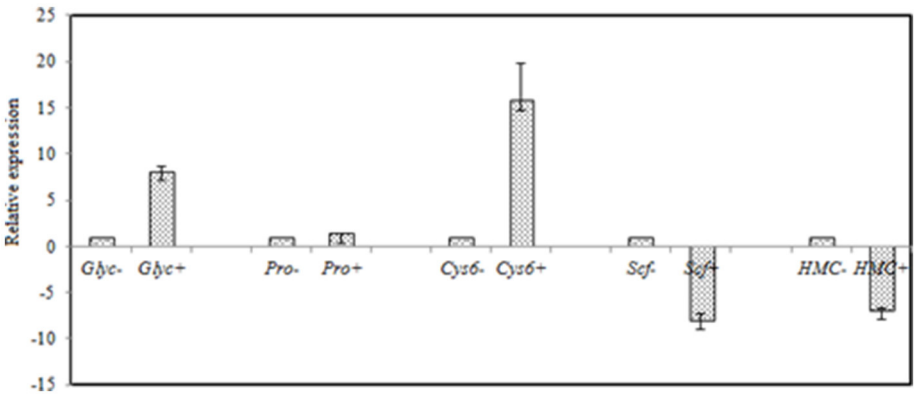

FIGURE 7 | RT-qPCR validation of selected genes with significant differential expression in the control and the salt-treated samples. RT-qPCR data are mean ± *SD* from three biological replicates. "−," and "+" indicates *A. montevidensis* was induced without, and with 3 M NaCl. DEGs putatively encoded glycerol-3-phosphate dehydrogenase (*Glyc*), proline oxidase (*Pro*), Zn(II)2Cys6 transcription factor (*Cys6*), SCF ubiquitin ligase (*Scf*), and hydroxymethylglutaryl-CoA (HMG-CoA) synthase (*HMC*).

one unigene, encoding glutamate decarboxylase, was augmented by 5-fold. A detailed up and down regulated genes involved in biosynthesis of organic acids were mentioned in **Table 3**.

DISCUSSION

Survival and growth of microorganisms in saline environments require numerous morphological ecotypes and adaptations. Salt stress causes changes in colony morphology, colony pigmentation, and cell wall structure (Kralj Kuncic et al., 2010). Hence, in the present study we evaluated the morphological changes caused by salt stress. In the absence of salt stress, mycelium of *A. montevidensis* ZYD4 was compact while loose in the presence of salt stress. Further, the hyphae width was reduced under salt stress. Similar to our results, fungal hyphae growth was effected under salt stress (Matsuda et al., 2006). Under salt stress, *A. montevidensis* ZYD4 conidial heads were extensively developed while without salt stress conidial heads were rarely formed.

It is widely known that carotenoids and flavoglaucin are responsible for yellow, bright red, and orange hues of fungal colonies (Davoli and Weber, 2002; Christaki et al., 2013; Dufosse et al., 2014). *A. montevidensis* ZYD4 subjected to salt stress showed drastic change in colony color. Under salt stress, colonies of *A. montevidensis* ZYD4 were olive green in the center, and white at the margin. Colonies without salt stress, were yellow to gray black in the center, and golden yellow at the margin. Similar to our result, Kralj Kuncic et al. (2010) observed change in the colony color when *Wallemia* sp. subjected to salt stress.

The pigment production showed drastic variation under salt stress. The methanolic extract obtained from *A. montevidensis*

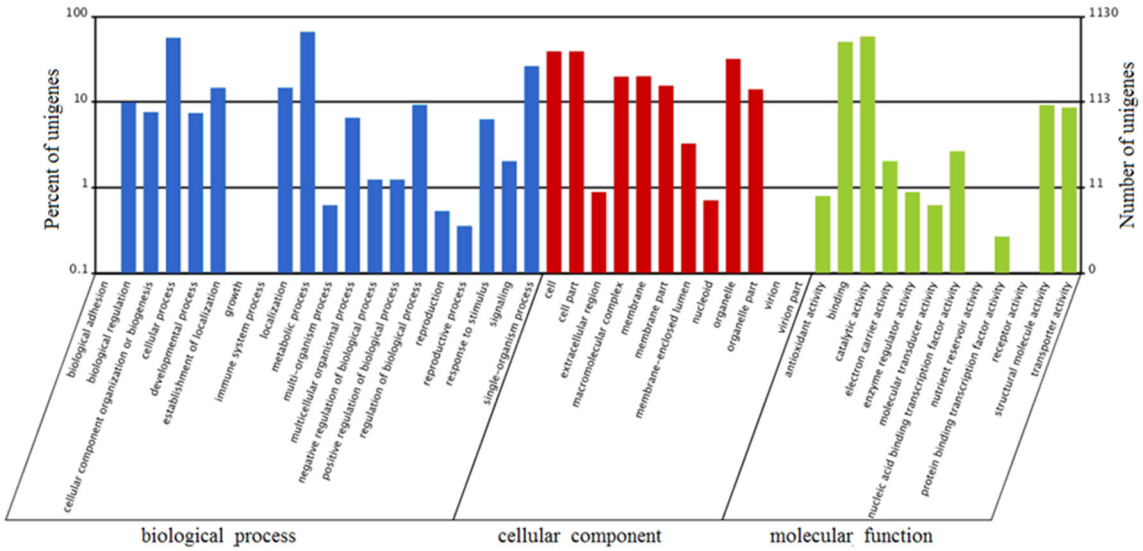

FIGURE 8 | Gene Ontology (GO) terms enrichment of unigenes of *A. montevidensis* ZYD4 at transcriptome level. The results were summarized in three main categories: biological process, cellular component, and molecular function. The right y-axis presents the number of unigenes in the category, while the left y-axis presents the percentage of a specific category of unigenes in that category.

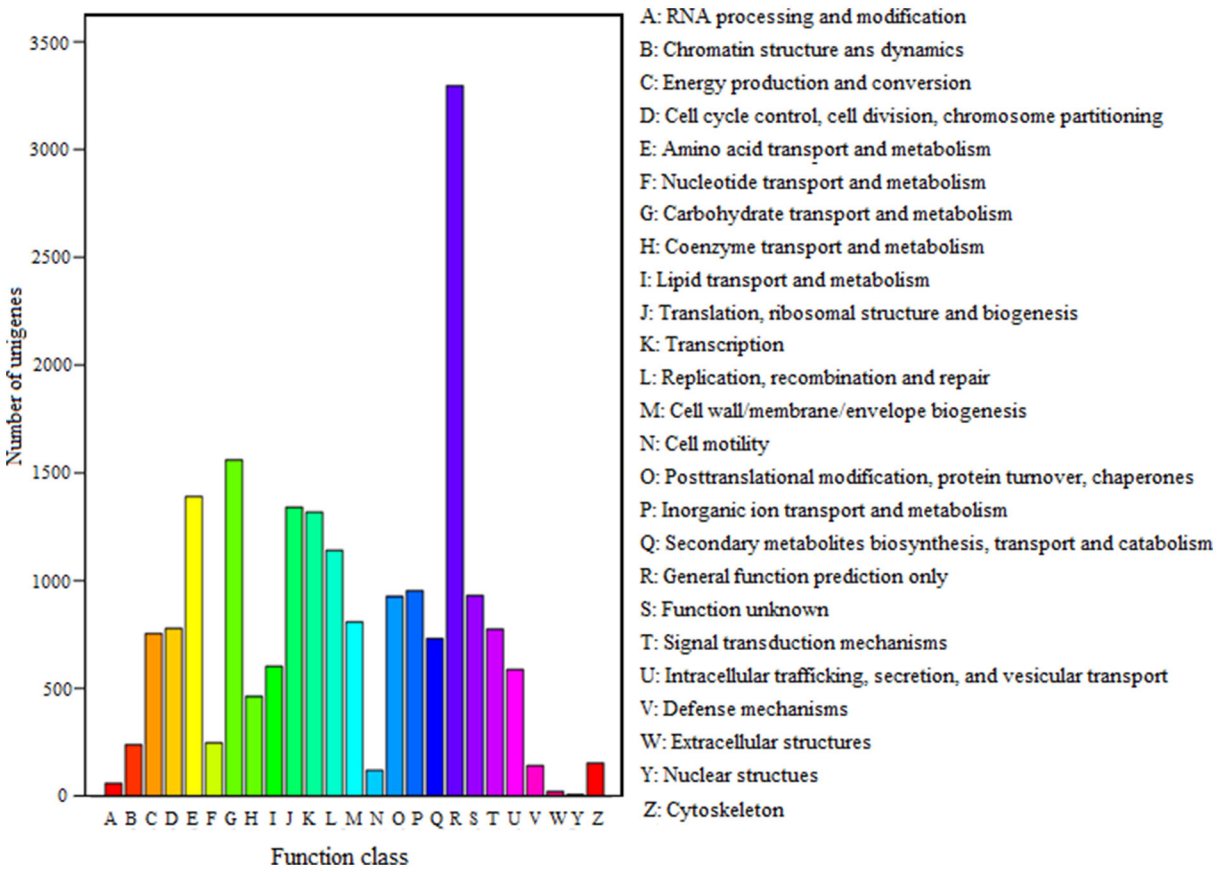

FIGURE 9 | COG classification of unigenes. A total of 7,576 unigenes had a COG classification among the 25 categories. The capital letters on the x-axis indicate the COG categories as listed on the right of the histogram.

TABLE 3 | Summary of some differently expressed genes of *A. montevidensis* in response to high-salt stress.

Unigene ID	Putative function	Log2 fold	Pathway
GLYCEROL			
CL3405	glycerol-3-phosphate dehydrogenase	+1.4	Glycolysis
Unigene 3991	glycerol dehydrogenase	-1.4	Glycolysis
Unigene 788	glycerol dehydrogenase ($NADP^+$)	+1.1	Glycerolipid metabolism
Unigene 2376	aldehyde dehydrogenase (NAD^+)	+1.1	Glycerolipid metabolism
Unigene 9950	diacylglycerol O-acyltransferase	-11.0	Glycerolipid metabolism
CL1785	triacylglycerol lipase	-2.0	Glycerolipid metabolism
Unigene 1646	lysophospholipase	+1.1	Glycero-phospholipid metabolism
Unigene 4940	phospholipase C	+1.3	Glycero-phospholipid metabolism
CL944	glycerol-3-phosphate dehydrogenase (NAD^+)	+1.4	Glycero-phospholipid metabolism
CL3405	glycerol-3-phosphate dehydrogenase	+1.4	Glycero-phospholipid metabolism
Unigene3569	choline kinase	+1.2	Glycero-phospholipid metabolism
Unigene7877	phospholipase D	-1.4	Glycero-phospholipid metabolism
COMPATIBLE SUGARS			
CL184	6-phosphofructo-2-kinase	+2.2	Glycolysis
CL1930	trehalose-phosphate synthase	+1.0	Starch and sucrose metabolism
CL1942	mannose-6-phosphate isomerase	+1.5	Starch and sucrose metabolism
CL1896	hexokinase	+1.4	Glycolysis
Unigene 9250	glucose-6-phosphate isomerase	-11.2	Glycolysis
CL1568	fructose-bisphosphate aldolase	-13.1	Glycolysis
Unigene 8898	triose-phosphate isomerase	-12.5	Glycolysis
CL1944	glyceraldehyde 3-phosphate dehydrogenase	-13.9	Glycolysis
Unigene 8982	Phosphoglycerate kinase	-11.9	Glycolysis
Unigene 8902	enolase	-13.1	Glycolysis
Unigene 8995	pyruvate kinase	-11.8	Glycolysis
Unigene 8882	phosphoenolpyruvate carboxykinase	-11.5	TCA cycle
Unigene 8970	pyruvate dehydrogenase	-12.2	TCA cycle
Unigene 8600	dihydrolipoamide dehydrogenase	-12.2	TCA cycle
Unigene 8566	citrate synthase	-11.5	TCA cycle
Unigene 8945	ATP-citrate synthase	-12.5	TCA cycle
Unigene 9020	aconitate hydratase	-12.1	TCA cycle
Unigene 9386	isocitrate dehydrogenase	-11.4	TCA cycle
Unigene 8508	2-oxoglutarate dehydrogenase E1	-11.9	TCA cycle
Unigene 9002	2-oxoglutarate dehydrogenase E2	-11.8	TCA cycle
Unigene 8600	dihydrolipoamide dehydrogenase	-12.2	TCA cycle
Unigene 10103	succinate dehydrogenase (ubiquinone) iron-sulfur subunit	-10.8	TCA cycle
Unigene8987	malate dehydrogenase	-11.7	TCA cycle
ORGANIC ACIDS			
Unigene 3431	proline oxidase	+3.6	Proline cycle
Unigene 1427	pyrroline-5-carboxylate dehydrogenase	+1.9	Proline cycle
CL601	glutamate decarboxylase	+5.0	Proline cycle
Unigene 8818	glutamate dehydrogenase	-13.8	Proline cycle
Unigene 9009	glutamine synthetase	-11.6	Proline cycle
YELLOW PIGMENT			
Unigene 4069	geranylgeranyl diphosphate synthase	-1.1	HMG-CoA pathway
Unigene 9164	RAB proteins geranylgerany ltransferase component A	-11.5	HMG-CoA pathway
Unigene 9310	farnesyl pyrophosphate synthetase	-11.4	HMG-CoA pathway
Unigene 8875	hydroxymethylglutaryl-CoA (HMG-CoA) synthase	-13.1	HMG-CoA pathway
ASEXUAL SPORULATION			
Unigene 11005	Zn(II)2Cys6 transcription factor	+4.4	Cell cycle

(Continued)

TABLE 3 | Continued

Unigene ID	Putative function	Log2 fold	Pathway
CL66	G1/S-specific cyclin Cln1	+1.5	Cell cycle
CL2000	cell cycle arrest protein BUB2	+1.3	Cell cycle
CL2756	Guanine nucleotide exchange factor LTE1	+1.1	Cell cycle
CL707	DNA replication licensing factor mcm7	+1.0	Cell cycle
Unigene 5683	Spindle assembly checkpoint component MAD1	+1.6	Cell cycle
Unigene 9493	SCF ubiquitin ligase	-11.1	Cell cycle
Unigene 9618	DNA replication licensing factor Mcm5	-3.0	Cell cycle
Unigene 7664	nuclear condensin complex subunit Smc4	-2.9	Cell cycle
CL1202	Spore-wall fungal hydrophobin dewA	+1.6	Cell cycle

ZYD4 grown in absence of 3 M NaCl showed peaks from 400 to 490 nm, indicating the presence of carotenoids (Klassen and Foght, 2008; Liu et al., 2015), while strain ZYD4 grown in presence of 3 M NaCl did not show any significant peak, indicating the absence of carotenoid. Similar to our results, Plemenitaš et al. (2008) found decreased pigment production in *H. werneckii* subjected to high salinity. Further, unigenes homologous to geranylgeranyl diphosphate synthase, hydroxymethylglutaryl-CoA (HMG-CoA) synthase, and farnesyl pyrophosphate synthase were down-regulated under salt stress.

Generally, enhanced expression of these genes increases fungal carotenoid content, which are made from acetyl-CoA through the HMG-CoA pathway (Davoli and Weber, 2002; Alcaino et al., 2014; Nagy et al., 2014). Therefore, down-regulated expression of these unigenes showed decreased synthesis of pigments in *A. montevidensis* ZYD4, and in turn regulated accumulation of intracellular glucose-6-phosphate by slowing down the metabolic flow of acetyl-CoA. The results suggest that the decrease of pigments was an osmoadaptive strategy.

Cleistothecium formation was dramatically inhibited with an increase of salt stress (**Figures 2e–h**, **Table 1**), suggesting that hypersaline condition triggered a transit from sexual to asexual state. The enhanced asexual development in *A. montevidensis* ZYD4 was critical in the life cycle being the primary means for survival under salt stress. Similar effect was observed in the marine-derived *Aspergillus glaucus* under high-salt stress (Liu et al., 2017).

In this study, we also evaluated genes involved in the development of asexual sporulation. The unigene 11005 encoding a $Zn(II)_2Cys_6$ transcription factor was upregulated by 4.4-fold. This factor plays a crucial role for asexual sporulation in different filamentous fungi (Vienken and Fischer, 2006; Chung et al., 2013; Gil-Duran et al., 2015; Son et al., 2016). Seven unigenes with significant identities to *CLN3*, *CIB3/4*, *CIB1/2*, *Bub2*, *Lte1*, *Mcm7*, and *Mad1* required for cell cycle progression through mitosis were up regulated by 1.0- to 2.3-fold, except for unigene 9493, encoding for ubiquitin ligase (E3) complex SCF subunit which was significantly down-regulated by 11.1-fold.

Unlike halophilic Archaea, halotolerant fungi do not accumulate high internal ion concentrations when grown in hypersaline conditions, but rather they counterbalance the osmotic imbalance by the accumulation of polyols (Kogej et al., 2005). Some studies suggest that glycerol accumulation is necessary for living cells to keep osmotic homeostasis and alleviate adverse effects of toxic Na^+ ions (Kogej et al., 2007). In this study, we found that unigenes involved in the accumulation of glycerol were extensively enhanced in expression, however unigenes participated in the transformation of glycerol were down-regulated, suggesting that glycerol was accumulated in cells upon the hypersaline shock. Expression of two unigenes, encoding for glycerol-3-phosphate dehydrogenase, and 6-phosphofructo-2-kinase was augmented by 1.4, and 2.2-fold respectively. These unigenes are essential for glycerol biosynthesis and cell proliferation in hyperosmotic environments (Dihazi et al., 2004; Lenassi et al., 2011). The spectrophotometric analysis demonstrated that the content of glycerol was increased by 2.5 fold (**Figure 4A**) which was consistent with the results of Kogej et al. (2007).

The storage of the compatible sugars and organic acids play a key role for osmotic adjustment of eukaryotic cells (Gagneul et al., 2007; Rosa et al., 2009; Plemenitaš et al., 2014; Sos-Hegedus et al., 2014; Henry et al., 2015). The spectrophotometric analysis demonstrated that the content of compatible sugars was increased by 2.0-fold under salt stress (**Figure 4B**), suggesting that compatible sugars play a significant role in *A. montevidensis* ZYD4 against high salt stress. Further, under salt stress *A. montevidensis* ZYD4 showed 1.0- to 2.2-fold increase in the expression of unigenes homologous to hexokinase, 6-phosphofructo-2-kinase, trehalose-phosphate synthase, and mannose-6-phosphate isomerase which participate in the upper pathways of glycolysis, TCA cycle, starch, and sucrose pathway. Nineteen DEGs for the further conversion of glucose-6-phosphate into other intermediates via the down-stream pathway of glycolysis and TCA cycle were suppressed. Unigenes of proline oxidase and pyrroline-5-carboxylate dehydrogenase that generates glutamate via proline cycle increased the expression by 3.6, and 1.9-fold in the salt-induced samples. Moreover, expression level of one unigene encoding glutamate decarboxylase was augmented by 5-fold which was associated with the conversion of glutamate into γ-aminobutyric acid (GABA) suggesting that GABA was accumulated in the salt-induced fungal cells.

AUTHOR CONTRIBUTIONS

WL, KL, and MX designed research and project outline. KL, XD, and YZ performed growth and morphology observation. KL, XD, MN, and BZ performed transcriptome sample preparation and sequencing. KL, MX, and MN provided the gene functional annotation and differential expression analysis. KL, MN, BL, MX, and WL drafted the manuscript. All authors read and approved the final manuscript.

ACKNOWLEDGMENTS

We are very grateful to the reviewers for their valuable suggestions and comments for greatly improving the manuscript. This work was financed by the National Natural Science Foundation Program of China (No. 31100017), Program of Agricultural Scientific and Technological Innovation of Shaanxi Province (S2018-YF-YBNY-0042), Shaanxi University of Technology (SLGQD16-06, SLGQD16-07), China Postdoctoral Science Foundation Grant (No. 2015M580748) and China Postdoctoral Special Foundation (No. 2016T90811). WL was also supported by Xinjiang Uygur Autonomous Region regional coordinated innovation project (Shanghai cooperation organization science and technology partnership program) (No. 2017E01031) and Project Supported by Guangdong Province Higher Vocational Colleges & Schools Pearl River Scholar Funded Scheme (2014).

SUPPLEMENTARY MATERIAL

The Supplementary Material for this article can be found online at: http://journal.frontiersin.org/article/10.3389/fmicb.2017.01789/full#supplementary-material

REFERENCES

Alcaino, J., Romero, I., Niklitschek, M., Sepulveda, D., Rojas, M. C., Baeza, M., et al. (2014). Functional characterization of the *Xanthophyllomyces dendrorhous* farnesyl pyrophosphate synthase and geranylgeranyl pyrophosphate synthase encoding genes that are involved in the synthesis of isoprenoid precursors. *PLoS ONE* 9:e96626. doi: 10.1371/journal.pone.0096626

Christaki, E., Bonos, E., Giannenas, I., and Florou-Paneri, P. (2013). Functional properties of carotenoids originating from algae. *J. Sci. Food. Agric.* 93, 5–11. doi: 10.1002/jsfa.5902

Chung, H., Choi, J., Park, S. Y., Jeon, J., and Lee, Y. H. (2013). Two conidiation-related Zn(II)2Cys6 transcription factor genes in the rice blast fungus. *Fungal Genet. Biol.* 61, 133–141. doi: 10.1016/j.fgb.2013.10.004

Conesa, A., Gotz, S., Garcia-Gomez, J. M., Terol, J., Talon, M., and Robles, M. (2005). Blast2GO: a universal tool for annotation, visualization and analysis in functional genomics research. *Bioinformatics* 21, 3674–3676. doi: 10.1093/bioinformatics/bti610

Dalmolin, R. J., Gelain, D. P., Klamt, F., Castro, M. A., and Moreira, J. C. (2012). Transcriptomic analysis reveals pH-responsive antioxidant gene networks. *Front. Biosci.* 4, 1556–1567. doi: 10.2741/s352

Davoli, P., and Weber, R. W. S. (2002). Carotenoid pigments from the red mirror yeast, *Sporobolomyces roseus*. *Mycologist* 16, 102–108. doi: 10.1017/S0269915X02001027

Dihazi, H., Kessler, R., and Eschrich, K. (2004). High osmolarity glycerol (HOG) pathway-induced phosphorylation and activation of 6-phosphofructo-2-kinase are essential for glycerol accumulation and yeast cell proliferation under hyperosmotic stress. J. Biol. Chem. 279, 23961–23968. doi: 10.1074/jbc.M312974200

Dufosse, L., Fouillaud, M., Caro, Y., Mapari, S. A., and Sutthiwong, N. (2014). Filamentous fungi are large-scale producers of pigments and colorants for the food industry. *Curr. Opin. Biotechnol.* 26, 56–61. doi: 10.1016/j.copbio.2013.09.007

Duran, R., Cary, J. W., and Calvo, A. M. (2010). Role of the osmotic stress regulatory pathway in morphogenesis and secondary metabolism in filamentous fungi. *Toxins* 2, 367–381. doi: 10.3390/toxins 2040367

Felsenstein, J. (1985). Confidence limits on phylogenies: an approach using the bootstrap. *Evolution* 39, 783–791. doi: 10.1111/j.1558-5646.1985.tb00420.x

Gagneul, D., Ainouche, A., Duhaze, C., Lugan, R., Larher, F. R., and Bouchereau, A. (2007). A reassessment of the function of the so-called compatible solutes in the halophytic plumbaginaceae *Limonium latifolium*. *Plant. Physiol.* 144, 1598–1611. doi: 10.1104/pp.107.099820

Gil-Duran, C., Rojas-Aedo, J. F., Medina, E., Vaca, I., Garcia-Rico, R. O., Villagran, S., et al. (2015). The pcz1 gene, which encodes a Zn(II)2Cys6 protein, is involved in the control of growth, conidiation, and conidial germination in the filamentous fungus *Penicillium roqueforti*. *PLoS ONE* 10:e0120740. doi: 10.1371/journal.pone.0120740

Grabherr, M. G., Haas, B. J., Yassour, M., Levin, J. Z., Thompson, D. A., Amit, I., et al. (2011). Full-length transcriptome assembly from RNA-Seq data without a reference genome. *Nat. Biotechnol.* 29, 644–652. doi: 10.1038/nbt.1883

Gunde-Cimerman, N., Ramos, J., and Plemenitas, A. (2009). Halotolerant and halophilic fungi. *Mycol. Res.* 113(Pt 11), 1231–1241. doi: 10.1016/j.mycres.2009.09.002

Gunde-Cimermana, N., Zalarb, P., De Hoogc, S., and Plemenitasd, A. (2000). Hypersaline waters in salterns-natural ecological niches for halophilic black yeasts. *FEMS. Microbiol. Ecol.* 32, 235–240. doi: 10.1016/S0168-6496(00)00032-5

Henry, C., Bledsoe, S. W., Griffiths, C. A., Kollman, A., Paul, M. J., Sakr, S., et al. (2015). Differential role for trehalose metabolism in salt-stressed maize. *Plant. Physiol.* 169, 1072–1089. doi: 10.1104/pp.15.00729

Hinrikson, H. P., Hurst, S. F., De Aguirre, L., and Morrison, C. J. (2005). Molecular methods for the identification of *Aspergillus* species. *Med. Mycol.* 43(Suppl. 1), S129–S137. doi: 10.1080/13693780500064722

Iseli, C., Jongeneel, C. V., and Bucher, P. (1999). ESTScan: a program for detecting, evaluating, and reconstructing potential coding regions in EST sequences. *Proc. Int. Conf. Intell. Syst. Mol. Biol.* 99, 138–148.

Kimura, M. (1980). A simple method for estimating evolutionary rates of base substitutions through comparative studies of nucleotide sequences. *J. Mol. Evol.* 16, 111–120. doi: 10.1007/BF01731581

Kis-Papo, T., Weig, A. R., Riley, R., Persoh, D., Salamov, A., Sun, H., et al. (2014). Genomic adaptations of the halophilic dead Sea filamentous fungus *Eurotium rubrum*. *Nat Commun.* 5:3745. doi: 10.1038/ncomms4745

Klassen, J. L., and Foght, J. M. (2008). Differences in carotenoid composition among *Hymenobacter* and related strains support a tree-like model of carotenoid evolution. *Appl. Environ. Microbiol.* 74, 2016–2022. doi: 10.1128/AEM.02306-07

Koch, A. L. (1984). Shrinkage of growing *Escherichia coli* cells by osmotic challenge. *J. Bacteriol.* 159, 919–924.

Kogej, T., Ramos, J., Plemenitas, A., and Gunde-Cimerman, N. (2005). The halophilic fungus *Hortaea werneckii* and the halotolerant fungus *Aureobasidium pullulans* maintain low intracellular cation concentrations in hypersaline environments. *Appl. Environ. Microbiol.* 71, 6600–6605. doi: 10.1128/AEM.71.11.6600-6605.2005

Kogej, T., Stein, M., Volkmann, M., Gorbushina, A. A., Galinski, E. A., and Gunde-Cimerman, N. (2007). Osmotic adaptation of the halophilic fungus *Hortaea werneckii*: role of osmolytes and melanization. *Microbiology* 153, 4261–4273. doi: 10.1099/mic.0.2007/010751-0

Kralj Kuncic, M., Kogej, T., Drobne, D., and Gunde-Cimerman, N. (2010). Morphological response of the halophilic fungal genus *Wallemia* to high salinity. *Appl. Environ. Microbiol.* 76, 329–337. doi: 10.1128/AEM.02318-09

Kuhn, J., Müller, H., Salzig, D., and Czermak, P. (2015). A rapid method for an offline glycerol determination during microbial fermentation. *Electron. J. Biotechnol.* 18, 252–255. doi: 10.1016/j.ejbt.2015.01.005

Laurentin, A., and Edwards, C. A. (2003). A microtiter modification of the anthrone-sulfuric acid colorimetric assay for glucose-based carbohydrates. *Anal. Biochem.* 315, 143–145. doi: 10.1016/S0003-2697(02)00704-2

Lenassi, M., Zajc, J., Gostinčar, C., Gorjan, A., Gunde-Cimerman, N., and Plemenitaš, A. (2011). Adaptation of the glycerol-3-phosphate dehydrogenase Gpd1 to high salinities in the extremely halotolerant *Hortaea werneckii* and halophilic *Wallemia ichthyophaga*. *Fungal Biol.* 115, 959–970. doi: 10.1016/j.funbio.2011.04.001

Li, J., Zhao, G. Z., Qin, S., Zhu, W. Y., Xu, L. H., and Li, W. J. (2009). *Streptomyces sedi* sp. nov., isolated from surface-sterilized roots of *Sedum* sp. *Int. J. Syst. Evol. Microbiol.* 59, 1492–1496. doi: 10.1099/ijs.0.007534-0

Liu, L., Zhou, E. M., Jiao, J. Y., Manikprabhu, D., Ming, H., Huang, M. J., et al. (2015). Hymenobacter mucosus sp. nov., isolated from a karst cave soil sample. *Int. J. Syst. Evol. Microbiol.* 65, 4121–4127. doi: 10.1099/ijsem.0.000550

Liu, S., Li, J., Wu, Y., Ren, Y., Liu, Q., Wang, Q., et al. (2017). *De novo* transcriptome sequencing of marine-derived *Aspergillus glaucus* and comparative analysis of metabolic and developmental variations in response to salt stress. *Genes Genomics* 39, 317–329. doi: 10.1007/s13258-016-0497-0

Livak, K. J., and Schmittgen, T. D. (2001). Analysis of relative gene expression data using real-time quantitative PCR and the $2^{-\Delta\Delta CT}$ method. *Methods* 25, 402–408. doi: 10.1006/meth.2001.1262

Matsuda, Y., Sugiyama, F., Nakanishi, K. and Ito, S. I. (2006). Effects of sodium chloride on growth of ectomycorrhizal fungal isolates in culture. *Mycoscience* 47, 212–217. doi: 10.1007/S10267-006-0298-4

Mesbah, N. M., and Wiegel, J. (2012). Life under multiple extreme conditions: diversity and physiology of the halophilic alkalithermophiles. *Appl. Environ. Microbiol.* 78, 4074–4082. doi: 10.1128/AEM.00050-12

Morris, G. J., Winters, L., Coulson, G. E., and Clarke, K. J. (1986). Effect of osmotic stress on the ultrastructure and viability of the yeast *Saccharomyces cerevisiae*. *J. Gen. Microbiol.* 132, 2023–2034. doi: 10.1099/00221287-132-7-2023

Nagy, G., Farkas, A., Csernetics, A., Bencsik, O., Szekeres, A., Nyilasi, I., et al. (2014). Transcription of the three HMG-CoA reductase genes of *Mucor circinelloides*. *BMC Microbiol.* 14:93. doi: 10.1186/1471-2180-14-93

Oren, A. (2002). "Adaptation of halophilic archaea to life at high salt concentrations," in *Salinity: Environment-Plants-Molecules*, eds A. Lauchli and U. Luttge (Springer), 81–96.

Petrovic, U., Gunde-Cimerman, N., and Plemenitas, A. (2002). Cellular responses to environmental salinity in the halophilic black yeast *Hortaea werneckii*. *Mol. Microbiol.* 45, 665–672. doi: 10.1046/j.1365-2958.2002.03021.x

Plemenitaš, A., Lenassi, M., Konte, T., Kejžar, A., Zajc, J., Gostinčar, C., et al. (2014). Adaptation to high salt concentrations in halotolerant/halophilic fungi: a molecular perspective. *Front. Microbiol.* 5:199. doi: 10.3389/fmicb.2014.00199

Plemenitaš, A., Vaupotic, T., Lenassi, M., Kogej, T., and Gunde-Cimerman, N. (2008). Adaptation of extremely halotolerant black yeast *Hortaea werneckii* to increased osmolarity: a molecular perspective at a glance. *Stud. Mycol.* 61, 67–75. doi: 10.3114/sim.2008.61.06

Redkar, R. J., Lemke, P. A., and Singh, N. K. (1996). Altered gene expression in *Aspergillus nidulans* in response to salt stress. *Mycologia* 88, 256–263.

Riccombeni, A., and Butler, G. (2012). Role of genomics and RNA-seq in studies of fungal virulence. *Curr. Fungal Infect. Rep.* 6, 267–274. doi: 10.1007/s12281-012-0104-z

Rosa, M., Prado, C., Podazza, G., Interdonato, R., Gonzalez, J. A., Hilal, M., et al. (2009). Soluble sugars–metabolism, sensing and abiotic stress: a complex network in the life of plants. *Plant Signal. Behav.* 4, 388–393. doi: 10.4161/psb.4.5.8294

Saitou, N., and Nei, M. (1987). The neighbor-joining method: a new method for reconstructing phylogenetic trees. *Mol. Biol. Evol.* 4, 406–425.

Salam, N., Khieu, T. N., Liu, M. J., Vu, T. T., Ky, S. C., Quach, N. T., et al. (2017). Endophytic actinobacteria associated with *Dracaena cochinchinensis* Lour: isolation, diversity, and their cytotoxic activities. *Biomed. Res. Int.* 2017:1308563. doi: 10.1155/2017/1308563

Schweder, T., and Hecker, M. (2004). "Monitoring of stress responses," in *Physiological Stress Responses in Bioprocesses*, ed S.-O. Enfors (Berlin; Heidelberg: Springer), 47–71.

Son, H., Fu, M., Lee, Y., Lim, J. Y., Min, K., Kim, J. C. et al. (2016). A novel transcription factor gene FHS1 is involved in the DNA damage response in *Fusarium graminearum*. *Sci. Rep.* 6:21572. doi: 10.1038/srep 21572

Sos-Hegedus, A., Juhasz, Z., Poor, P., Kondrak, M., Antal, F., Tari, I., et al. (2014). Soil drench treatment with ß-aminobutyric acid increases drought tolerance of potato. *PLoS ONE.* 9:e114297. doi: 10.1371/journal.pone.01 14297

Tamura, K., Peterson, D., Peterson, N., Stecher, G., Nei, M., and Kumar, S. (2011). MEGA5: molecular evolutionary genetics analysis using maximum likelihood, evolutionary distance, and maximum parsimony methods. *Mol. Biol. Evol.* 28, 2731–2739. doi: 10.1093/molbev/msr121

Taymaz-Nikerel, H., Cankorur-Cetinkaya, A., and Kirdar, B. (2016). Genome-wide transcriptional response of *Saccharomyces cerevisiae* to stress-induced perturbations. *Front. Bioeng. Biotechnol.* 4:17. doi: 10.3389/fbioe.2016. 00017

Thompson, J. D., Gibson, T. J., Plewniak, F., Jeanmougin, F., and Higgins, D. G. (1997). The CLUSTAL_X windows interface: flexible strategies for multiple sequence alignment aided by quality analysis tools. *Nucleic Acids Res.* 25, 4876–4882. doi: 10.1093/nar/25.24.4876

Vienken, K., and Fischer, R. (2006). The Zn(II)2Cys6 putative transcription factor NosA controls fruiting body formation in *Aspergillus nidulans*. *Mol. Microbiol.* 61, 544–554. doi: 10.1111/j.1365-2958.2006.05257.x

White, T. J., Bruns, T., Lee, S., and Taylor, J. (1990). "Amplification and direct sequencing of fungal ribosomal RNA genes for phylogenetics," in *PCR Protocols: A Guide to Methods and Applications*, eds M. A. Innis, D. H. Gelfand, J. J. Sninsky, and T. J. White (San Diego, CA: Academic Press), 315–322.

Wood, J. M. (2015). Bacterial responses to osmotic challenges. *J. Gen. Physiol.* 145, 381–388. doi: 10.1085/jgp.201411296

Ye, J., Fang, L., Zheng, H., Zhang, Y., Chen, J., Zhang, Z., et al. (2006). WEGO: a web tool for plotting GO annotations. *Nucleic Acids Res.* 34, W293–W297. doi: 10.1093/nar/gkl031

Zajc, J., Liu, Y., Dai, W., Yang, Z., Hu, J., Gostincar, C., et al. (2013). Genome and transcriptome sequencing of the halophilic fungus *Wallemia ichthyophaga*: haloadaptations present and absent. *BMC Genomics.* 14:617. doi: 10.1186/1471-2164-14-617

Conflict of Interest Statement: The authors declare that the research was conducted in the absence of any commercial or financial relationships that could be construed as a potential conflict of interest.

frontiers in Microbiology

ORIGINAL RESEARCH
published: 27 March 2018
doi: 10.3389/fmicb.2018.00578

Benthic Algal Community Structures and Their Response to Geographic Distance and Environmental Variables in the Qinghai-Tibetan Lakes With Different Salinity

Jian Yang, Hongchen Jiang, Wen Liu and Beichen Wang*

State Key Laboratory of Biogeology and Environmental Geology, China University of Geosciences, Wuhan, China

Uncovering the limiting factors for benthic algal distributions in lakes is of great importance to understanding of their role in global carbon cycling. However, limited is known about the benthic algal community distribution and how they are influenced by geographic distance and environmental variables in alpine lakes. Here, we investigated the benthic algal community compositions in the surface sediments of six lakes on the Qinghai-Tibetan Plateau (QTP), China (salinity ranging from 0.8 to 365.6 g/L; pairwise geographic distance among the studied lakes ranging 8–514 km) employing an integrated approach including Illumina-Miseq sequencing and environmental geochemistry. The results showed that the algal communities of the studied samples were mainly composed of orders of *Bacillariales*, *Ceramiales*, *Naviculales*, *Oscillatoriales*, *Spirulinales*, *Synechococcales*, and *Vaucheriales*. The benthic algal community compositions in these QTP lakes were significantly ($p < 0.05$) correlated with many environmental (e.g., dissolved inorganic and organic carbon, illumination intensity, total nitrogen and phosphorus, turbidity and water temperature) and spatial factors, and salinity did not show significant influence on the benthic algal community structures in the studied lakes. Furthermore, geographic distance showed strong, significant correlation ($r = 0.578$, $p < 0.001$) with the benthic algal community compositions among the studied lakes, suggesting that spatial factors may play important roles in influencing the benthic algal distribution. These results expand our current knowledge on the influencing factors for the distributions of benthic alga in alpine lakes.

Keywords: benthic algal community, salinity, geographic distance, lakes, Qinghai-Tibetan Plateau

OPEN ACCESS

Edited by:
Mark Alexander Lever,
ETH Zürich, Switzerland

Reviewed by:
Olivier Pringault,
Institut de Recherche pour le Développement (IRD), France
Rui Zhang,
Xiamen University, China

****Correspondence:***
Hongchen Jiang
jiangh@cug.edu.cn

Specialty section:
This article was submitted to Extreme Microbiology, a section of the journal Frontiers in Microbiology

Received: *30 June 2017*
Accepted: *13 March 2018*
Published: *27 March 2018*

Citation:
Yang J, Jiang H, Liu W and Wang B (2018) Benthic Algal Community Structures and Their Response to Geographic Distance and Environmental Variables in the Qinghai-Tibetan Lakes With Different Salinity. Front. Microbiol. 9:578. doi: 10.3389/fmicb.2018.00578

INTRODUCTION

The littoral zone of lakes is one of the most productive ecosystems on Earth, and it plays significant roles in the functioning (e.g., carbon cycling) of lacustrine ecosystems (Howard-Williams and Lenton, 1975; Strayer and Likens, 1986; Stoffels et al., 2005). Such inshore habitat hosts diverse algal communities, which are important contributors for primary production in aquatic ecosystems (Nozaki, 2001; Nozaki et al., 2003; Mooij et al., 2005; Nõges et al., 2010). Generally, planktonic algal

community has dominant contribution for primary productions in lakes (Bryant and Frigaard, 2006; Reinfelder, 2011; Althouse et al., 2014). Recent studies reported that littoral benthic algae also make significant or dominant contribution to total primary production within certain lakes (Vadeboncoeur et al., 2001; Ask et al., 2009; Althouse et al., 2014). The primary production is commonly mediated by algal community composition, because different algal species have distinct carbon fixation capability (Reinfelder, 2011). Therefore, studies on the distribution and composition of benthic alga in lakes are of great importance to understanding of carbon cycling in lacustrine ecosystems.

Previous studies reported that planktonic algal distribution was often affected by many environmental factors such as salinity (Huang et al., 2014; Liu X. et al., 2016), pH (Kenneth, 2002), nutrient (Stelzer and Lamberti, 2001; Wyatt et al., 2010), and light (Lange et al., 2011). Furthermore, geographic distance influence on the algal (e.g., diatom) distribution was also reported in some freshwater aquatic ecosystems (e.g., river, wetlands, streams) (Astorga et al., 2012; Wetzel et al., 2012; Goldenberg Vilar et al., 2014), However, studies are limited on benthic algal community composition and distribution in saline lakes. So it is poorly known whether geographic distance and environmental factors can influence the benthic algal community compositions among saline and hypersaline lakes.

The Qinghai-Tibetan Tibetan (QTP) host thousands of lakes (more than 1000 lakes with surface area >1 km^2) with salinity ranging from 0.1 to 426.3 g/L (Zheng, 1997). Many previous studies showed that salinity was the most important factor influencing microbial distribution and function in the QTP lakes (Wu et al., 2006; Jiang et al., 2007, 2012; Xing et al., 2009; Wang et al., 2011; Liu et al., 2013; Huang et al., 2014; Liu Y. et al., 2016; Yang et al., 2016b). However, little is known about the distribution of benthic alga in the QTP lakes and how they respond to the changes of environmental variables (e.g., salinity) and geographic distance among lakes. In this study, the major objectives were to examine the benthic algal community compositions in the QTP lakes and evaluate how they were influenced by geographic distance and environmental factors. In order to fulfill above objectives, a total of 18 littoral sediments were collected from six lakes (triplicates were applied for each of the studied lakes) in the QTP. The pairwise distances of the sampled lakes were 8–514 km. Illumina-Miseq sequencing was employed to investigate the plastid 23S rRNA genes of the benthic algal community compositions in these lake sediments.

MATERIALS AND METHODS

Sample Collection

Sampling cruise was carried out in May 2016. Six Qinghai-Tibetan lakes (Supplementary Figure S1) were selected for this study: Erhai Lake (EHL) is a freshwater lake; Qinghai Lake (QHL) and Tuosu Lake (TSL) are saline lakes; Gahai Lake (GHL), Xiaochaidan Lake (XCDL) and Chaka Lake (CKL) are hypersaline lakes (Yang et al., 2013). The TSL, GHL, and XCDL are located in the Qaidam Basin (QB) hinterland, while the CKL is on the QB fringe and the other lakes (i.e., EHL, QHL) are situated out of the QB (Zheng, 1997) (Supplementary Figure S1). In this study, a total of 18 sampling sites (triplicates from each of the studied lakes) were sampled. At each sampling site, the pH and temperature of lake surface water were measured with a portable SX711 pH meter (SANXIN, Shanghai, China); water turbidity was analyzed using a turbidity meter (HANNA, Romania); In-situ illumination intensity was determined by using a TES1335 light meter (TES, Taiwan, China). Water samples (∼20 mL) for measurements of major ions were collected after filtrating through 0.2-μm Nuclepore filters (Whatman, United Kingdom); water samples (∼20 mL) for measurements of dissolved organic carbon (DOC) were filtered through combusted 0.7-μm Whatman GF/F filters and the resulting filtrate was collected into a dark glass vial pre-acidified with concentrated phosphoric acid (∼40 μL); water samples (∼40 mL each) for measurements of dissolved inorganic carbon (DIC), water samples for total nitrogen (TN) and total phosphorus (TP) were collected into 40 mL dark glass vials without air bubbles, supplemented with saturated mercury chloride (∼40 μL) before covering lid. Additionally, 500 mL water samples were filtered through 0.7-μm glass fiber filters (Whatman, United Kingdom), and the filters were stored in dry ice collected for the measurements of chlorophyll a (Chl-a) concentration. Surface sediments (∼0–1 cm) were collected using a grab-bucket collection sampler in the littoral zones of lakes with water depth of ∼1 meter. The surface sediments were then collected into 50 mL sterilized tubes using sterile spoons for DNA samples. The DNA and Chl-a samples were stored in dry ice in the field and during transportation and then were transferred to a −80°C freezer in the laboratory until further analyses. Other samples (e.g., water samples for major ions, DOC, DIC, TN, and TP) were stored at 4°C during transportation and were analyzed immediately after arrival in laboratory.

Laboratory Geochemical Analyses

Cation and anion concentrations (e.g., K^+, Na^+, Ca^{2+}, Mg^{2+}, SO_4^{2-}, Cl^-) of the lake waters were measured by using ion chromatography (Dionex DX-600, United States). Salinity was calculated by summing up the concentrations of six major ions including K^+, Na^+, Ca^{2+}, Mg^{2+}, SO_4^{2-}, and Cl^-. DOC and TN concentrations were measured on a multi N/C 2100S analyzer (Analytik Jena, Germany). DIC was measured by mean of the potentiometric acid titration method (Bradshaw et al., 1981). TP was analyzed by phosphormolybdic acid colorimetry (Neal et al., 2000). Chl-a was measured using a fluorospectrophotometer (Shimadzu Corp., Japan) following an overnight freeze-thaw extraction in 90% acetone (Liu et al., 2006).

DNA Extraction and Sequencing

Total DNA was extracted from 0.5 g sediment samples using the Fast DNA SPIN Kit for Soil (MP Biomedical, United States). The extracted DNA was amplified with a universal algal 23S rRNA gene primer set p23SrV_f1 and p23SrV_r1, and the detailed PCR conditions were described in a previous study (Sherwood and Presting, 2007). Briefly, a unique 12-bp barcode sequence was added between the sequencing adapter and reverse primer to differentiate among samples. Triplicate PCR reactions

for each sample were conducted and the resulting successful PCR products were purified using a DNA Gel Extraction Kit (Axygen, United States). The PCR amplicons (∼400 bp) from each sample were pooled with equimolar concentrations and then were sequenced by using an Illumina-Miseq platform (paired-ends sequencing of 2 × 250 bp) (Caporaso et al., 2012).

Raw 23S rRNA Gene Sequences Processing and Statistical Analyses

The raw 23S rRNA gene sequences were processed following the pipeline coupling USEARCH (Edgar, 2013) and QIIME (Caporaso et al., 2010) software. The paired reads were joined with FLASH (fast length adjustment of short reads) using default setting (Magoč and Salzberg, 2011). Forward and reverse primers were removed from the joined reads. The remaining reads were then de-multiplexed and quality filtered using QIIME v1.9.0 with *split_libraries_fastq.py* script (Caporaso et al., 2010). Briefly, reads having more than three consecutive low quality (Phred quality score <30) bases were removed, and reads containing ambiguous base were discarded, as well as reads comprising consecutive high quality bases less than 75% of the total read length were culled out. Chimera checking was performed using the UCHIME module with *de novo* method in USEARCH (Edgar et al., 2011). Singleton and read length less than 200 were discarded, and operational taxonomic units (OTUs) were defined at the 97% cutoff (Steven et al., 2012) by using the UCLUST algorithm (Edgar, 2010). OTU representative sequences were then selected and their taxonomy were assigned using *parallel_assign_taxonomy_blast.py* with default set (sequences similarity >90% and blasted exception value $<10^{-3}$) against the SILVA 128 LSU database in the QIIME program. Sequences failing to be assigned into *Cyanobacteria* and eukaryotic algae were removed. In order to validate these assignments of taxonomy, OTU representative sequences were locally BLASTed in NCBI database[1]. The BLASTed results were provided in Supplementary Table S1. The final OTU table was rarefied to equal sequence number (n = 8843) for each sample with 1000 times, and then alpha diversity was calculated at the 97% identity level in QIIME. A variety of alpha diversity indices were calculated including Simpson, Shannon, Equitability and Chao1.

All environmental variables in this study were normalized to values ranged between 1 and 100 as described previously (Yang et al., 2016a). The non-metric dimensional scaling (NMDS) ordination with 500 random starts were performed to depict the difference of algal community compositions among lakes based on the Bray-Curtis dissimilarity using the package "vegan." Cluster analysis was performed according to the Bray-Curtis dissimilarity among samples using PAST software[2]. Simple Mantel tests were performed to assess the Spearman's correlations between algal community compositions and geographic distance/environmental variables by using the "vegan" package. Geographical distances among sampling sites were calculated based on the GPS locations of each sites using Euclidean method in PAST software (Supplementary Table S2). Canonical correspondence analysis (CCA) was also performed to explore the relationships between algal communities and environmental and spatial variables. Before the CCA, a set of spatial variables were generated through the method of principal coordinates of neighbor matrices (PCNM) analysis according to the longitude and latitude coordinates of the sampling sites (Borcard and Legendre, 2002). Subsequently, we used a forward selection procedure to select environmental and spatial variables through the '*ordiR2step*' function in R package "vegan" (Blanchet et al., 2008). Only significant ($p < 0.05$) environmental and spatial variables were shown in the CCA ordination.

In order to discern the difference between benthic and planktonic algal community composition in lakes, planktonic algal 23S rRNA gene sequences were collected from the two published studies (Steven et al., 2012; Liu X. et al., 2016). To avoid any bias resulting from different primers, only 23S rRNA gene sequences derived from the same primer set (p23SrV_f1 and p23SrV_r1) and the same PCR protocol were included in this analysis. Sequences were processed according to the procedures described above. NMDS ordination with 500 random starts were conducted to discern the difference between benthic (this study) and planktonic (previous studies) algal community compositions in lakes according to the Bray-Curtis dissimilarity. In addition, the dominant OTU representative sequences of *Cyanobacteria* (average relative abundance >0.1%) were selected to perform BLAST[3] against available 23S rRNA genes in the GenBank. Meanwhile, their closest references were retrieved for constructing phylogenic tree. All the OTU representative sequences were aligned with their references by using Clustal W implemented in the Bioedit program. Maximum-likelihood tree was constructed from the representative cyanobacterial 23S rRNA sequences and their references by using the MEGA 6.0.

Nucleotide Sequence Accession Numbers

The sequence data generated in this study were deposited at the Sequence Read Archive (SRA) in the National Center for Biotechnology Information (NCBI) under the BioProject PRJNA376846 with accession no. SRP101378.

RESULTS

Environmental Parameters of the Studied Samples

The studied lakes have a large range of environmental parameters (Supplementary Table S3). For example, the salinity was 0.8–365.6 g/L and the pH was 7.4–9.2; DOC was 1.9–26.3 mM and DIC was 6.2–29.8 mM; turbidity was 0.6–17.4 NTU

[1] http://blast.ncbi.nlm.nih.gov

[2] http://folk.uio.no/ohammer/past/

[3] www.ncbi.nlm.nih.gov/blast

(Nephelometric Turbidity Unit) and the concentration of Chl-a was 0.1–21.4 μg/L; TN and TP ranged 97.7–441.1 and 3.8–13.7 μM, respectively.

Benthic Algal Community Composition

A total of 2, 244, 853 qualified sequence reads were obtained after data processing, and 89.1% of total qualified sequence reads (1, 999, 487 sequence reads) were assigned to *Cyanobacteria* and eukaryotic algae. The algal sequences per sample ranged from 8,843 to 764,193 with an average of 101, 082. Alpha diversity indices of the studied samples were summarized in **Table 1**. The number of the observed algal OTUs of the studied samples ranged 9.0–65.2 with Shannon indices and Chao 1 being 0.6–3.9 and 9.0–83.4, respectively (**Table 1**). These alpha-diversity indices were not significantly correlated with any environmental parameters of the studied lakes (data not shown). The relative abundances of *Cyanobacteria* and eukaryotic algae ranged 0.2–99.2 and 0.8–99.8% among the samples, respectively (**Figure 1**). *Cyanobacteria* was dominant (relative abundance >45%) in the samples of EHL, QHL, and CKL, whereas eukaryotic algae largely dominated (relative abundance >60%) in the samples of TSL, GHL and XCDL (**Figure 1**). The algal communities of the studied samples were composed of seven dominant (relative abundance >5% at least in one sample) orders (i.e., *Bacillariales*, *Ceramiales*, *Naviculales*, *Oscillatoriales*, *Spirulinales*, *Synechococcales*, and *Vaucheriales*) (**Figure 2**). Algal

TABLE 1 | Alpha diversity of the studied samples (a, b, and c indicate replicate samples).

Sample	Total sequences	Algal sequences	Observed OTUs	Simpson	Shannon	Equitability	Chao1
EHLSa	90131	80292	65.2	0.8	3.3	0.5	81.5
EHLSb	172207	143090	61.8	0.8	2.9	0.5	78.5
EHLSc	169488	145123	63.4	0.9	3.4	0.6	83.4
QHLSa	379250	375963	52.7	0.4	1.2	0.2	74.1
QHLSb	69241	68707	49.0	0.4	1.3	0.2	63.0
QHLSc	774594	764193	40.1	0.3	1.0	0.2	59.8
TSLSa	16018	14269	31.0	0.7	2.5	0.5	32.4
TSLSb	17156	16902	24.3	0.7	2.3	0.5	25.0
TSLSc	9057	8843	22.0	0.7	2.3	0.5	22.0
GHLSa	22469	16270	33.8	0.7	2.0	0.4	37.1
GHLSb	19691	18299	22.0	0.6	1.7	0.4	25.1
GHLSc	19467	11671	19.7	0.2	0.6	0.1	20.2
XCDLSa	12405	11996	9.9	0.5	1.2	0.4	9.9
XCDLSb	10727	10665	9.0	0.5	1.2	0.4	9.0
XCDLSc	25109	24899	10.8	0.5	1.2	0.3	11.6
CKLSa	149077	86339	23.8	0.4	1.1	0.2	30.2
CKLSb	123130	75456	36.0	0.9	3.9	0.8	41.8
CKLSc	165636	126510	32.6	0.9	3.3	0.7	45.1

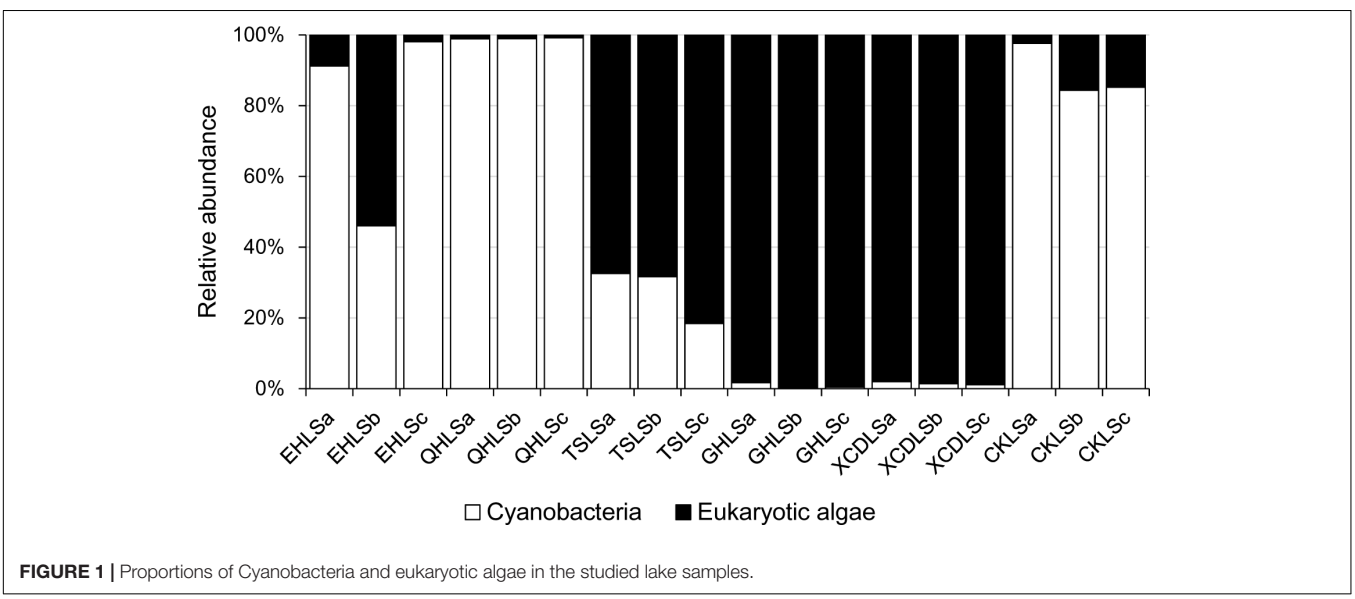

FIGURE 1 | Proportions of Cyanobacteria and eukaryotic algae in the studied lake samples.

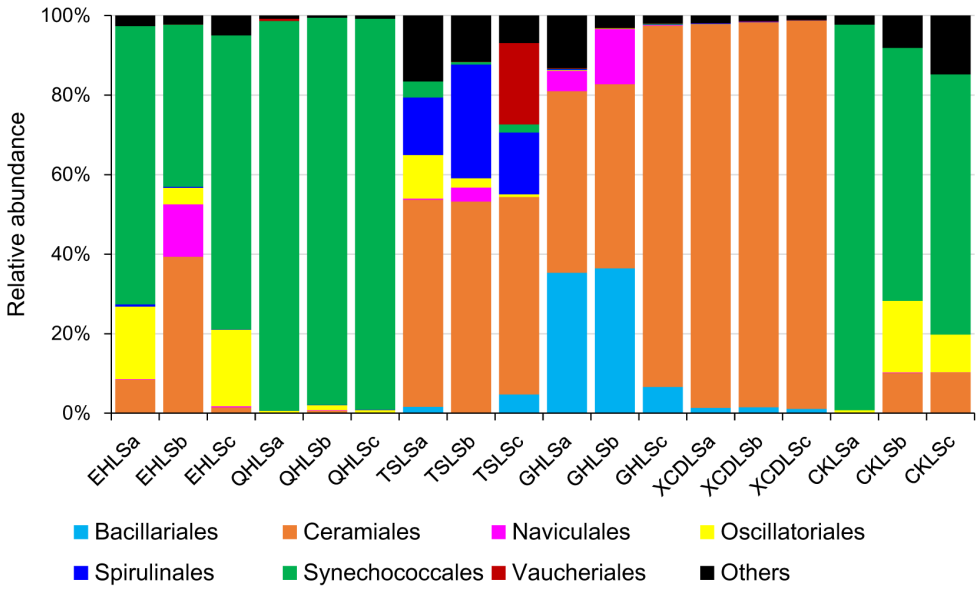

FIGURE 2 | Relative abundance of algal sequences at the order level in the studied lake samples.

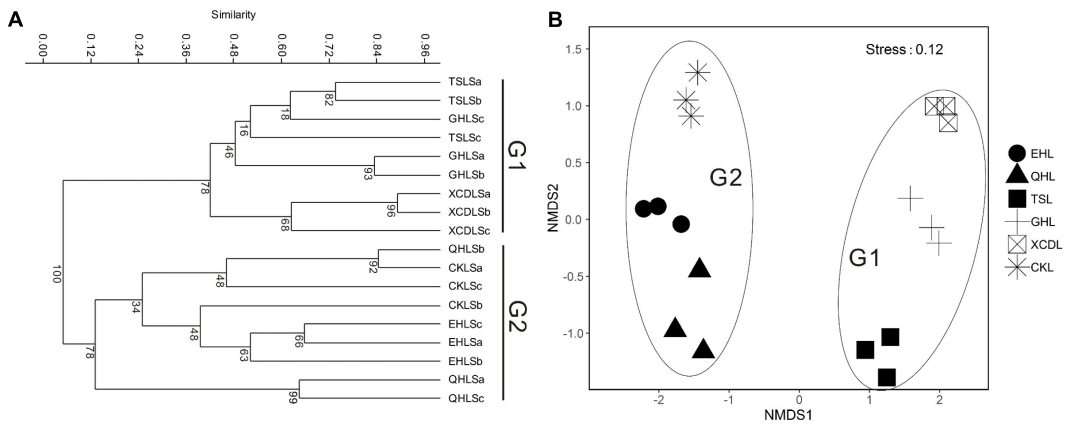

FIGURE 3 | Clustering **(A)** and NMDS ordination **(B)** analysis on the basis of Bray-Curtis dissimilarities among the studied lake samples. G1: the group of samples from lakes in the Qaidam Basin hinterland; G2: the group of samples from the fringe (CKL) and out (EHL and QHL) of the Qaidam Basin.

sequences belonging to *Synechococcales* were dominant in the samples of EHL, QHL, and CKL, whereas *Ceramiales* sequences dominated in the samples of TSL, GHL, and XCDL (**Figure 2**).

Influence of Environmental and Spatial Variables on Algal Distribution

The clear geographic patters of benthic algal community were observed among the studied lakes (**Figure 3**): the benthic algal communities in the lakes (i.e., TSL, GHL, XCDL) within the Qaidam Basin (QB) hinterland were grouped into the G1 cluster, and those from EHL, QHL, and CKL were grouped into the G2 cluster (**Figure 3A**). Similar grouping patterns were also observed in the NMDS and CCA ordination, which showed that the distributions of algal communities in TSL, GHL, and XCDL (G1) were separated from those of EHL, QHL and CKL (G2) along the axis NMDS1 (**Figures 3B**, **4**). The CCA result also indicated that many local environmental (i.e., DOC, DIC, illumination intensity, TN, TP, turbidity, water temperature) and spatial (i.e., PCNM1, PCNM3, and PCNM4) variables significantly ($p < 0.05$) affect the benthic algal distribution in the studied lakes (**Figure 4**). Furthermore, Mantel tests showed that the algal community compositions of the studied samples were significantly ($p < 0.05$) correlated with DIC, DOC, geographic distance, pH, salinity and water temperature (**Table 2**). Geographic distance possessed higher correlation coefficient than other environmental variables (e.g., salinity, pH, etc.). Linear analysis gave a R^2 of 0.341 ($p < 0.001$) between the dissimilarities of benthic algal community among lakes and geographic distances (**Figure 5**).

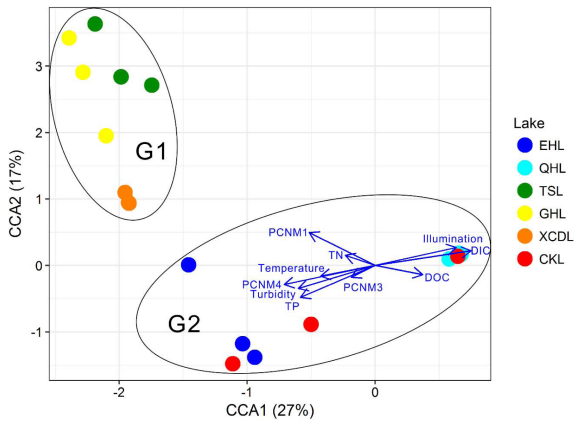

FIGURE 4 | CCA ordination showing the benthic algal community composition in relation to significant environmental and spatial factors ($p < 0.05$).

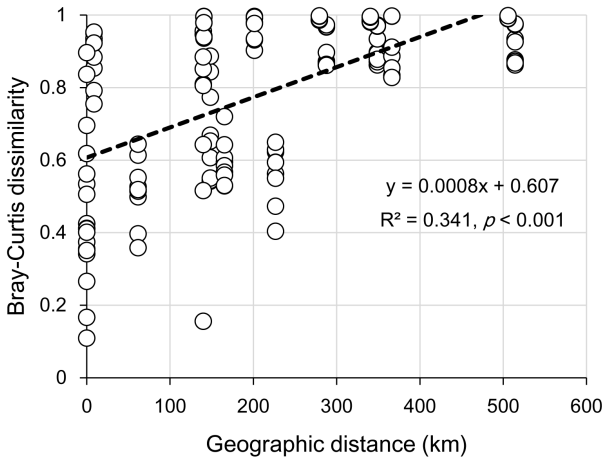

FIGURE 5 | Linear relationship between geographic distance and the Bray-Curtis dissimilarities of the benthic algal communities among the studied lake samples.

TABLE 2 | Mantel test-based correlations between algal community compositions and the measured environmental factors in the studied samples.

Factors	r	p
Chlorophyll-a	0.129	0.094
DIC	**0.350**	**0.004**
DOC	**0.446**	**0.001**
Geographic distance	**0.578**	**<0.001**
Illumination intensity	0.101	0.122
pH	**0.161**	**0.048**
Salinity	**0.214**	**0.033**
TN	0.113	0.095
TP	0.075	0.184
Turbidity	0.153	0.054
Water temperature	**0.178**	**0.043**

r: Spearman correlation coefficient. Bold face indicate a significant correlation with $p < 0.05$.

Comparisons Between Benthic and Planktonic Algal Community Compositions in Lakes

Non-metric dimensional scaling (NMDS) ordinations on the basis of both presence-absence and abundance data showed that benthic (this study) and planktonic (previous studies) algal community compositions were distinctly different (**Figure 6**). Moreover, the algal community composition in American lakes were different from that in Chinese lakes (**Figure 6**). Additionally, phylogenetic analysis indicated that the dominant cyanobacterial OTUs (average relative abundance >0.1%) were mainly affiliated with *Synechococcales* and *Oscillatoriophycideae* (Supplementary Figure S2A) and the relative abundances of those OTUs ranged 0–74.5% (Supplementary Figure S2B) in the studied lakes. Some cyanobacterial OTUs (e.g., OTU98, OTU248, OTU134) occurred in both water and sediment samples, whereas other OTUs only occurred in either water (e.g., OTU80, OTU135) or sediment (e.g., OTU13, OTU14) samples (Supplementary Figure S2B).

DISCUSSION

It is expected that environmental variables significantly affected the distribution of the benthic algal community in the studied lakes, which was evidenced by the significant correlation between benthic algal community composition and water temperature, light intensity, turbidity, and nutrient-related variables (i.e., DIC, DOC, TP, TN) (**Figure 4**). This finding was in agreement with previous studies on planktonic algal distribution (Riebesell et al., 1993, Riebesell, 2004; Chen and Durbin, 1994; Kenneth, 2002; Elliott et al., 2006; Hare et al., 2007), suggesting that environmental factors could affect the distributions of both planktonic and benthic algal communities. These results were reasonable, because temperature, light intensity and nutrient are crucial factors for algal growth (Geider et al., 1998; Cloern, 1999).

It is remarkable to observe a strong correlation between benthic algal community structures and geographic distance in the studied lakes (**Table 2**), and that the dissimilarities of benthic algal communities increased with increasing geographic distance among the studied lakes (**Figure 5**). This finding is inconsistent with one recent study, which indicated that geographic distance did not significantly affected planktonic algal community structures among lakes (Huang et al., 2014). Such inconsistency may be ascribed to the different studied objects between Huang et al. (2014) and this study (planktonic vs. benthic algal communities). Previous studies have indicated that distinct microbial communities were inhabited in waters (planktonic) and sediments (benthic) (DeLong et al., 1993; Francis et al., 2005; Jiang et al., 2006; Mesbah et al., 2007; Yang et al., 2013), and thus planktonic and benthic microbes may be influenced by different factors among lakes (Yang et al., 2016a). Therefore, it is not surprising to observe the different response of planktonic and benthic algal communities to geographic distance between this and previous studies (Huang et al., 2014). Strong geographic distance effect on benthic algal distribution could be

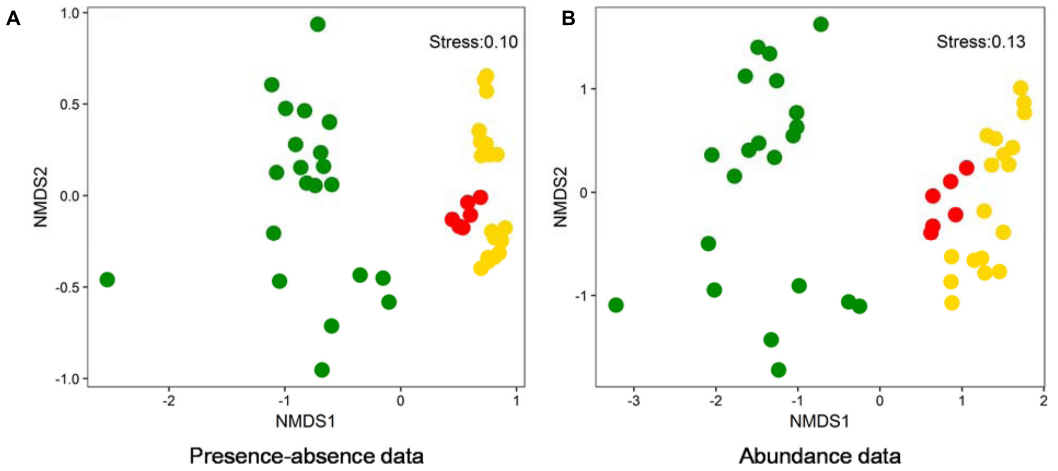

FIGURE 6 | NMDS ordination analysis based on presence-absence **(A)** and abundance data **(B)** showing the algal community compositions of different lake samples collected from this study and two previous studies (Steven et al., 2012; Liu X. et al., 2016). Green solid circles: water samples from LaBonte and Rock Lake, United States (Steven et al., 2012); Red solid circles: water samples from Qinghai-Tibetan lakes, China (Liu X. et al., 2016); Gold solid circles: samples from this study.

ascribed to the facts that (1) benthic alga were relatively difficult to travel a long distance because they were attached on the benthic sediments and their dispersal might be readily limited by geographic distance; and (2) some environmental variables that might be related to spatial distribution of algal communities were not measured in present study.

It is surprising that salinity did not exhibit significant influence on the benthic algal community structures among the studied lakes (**Figure 4**). Many previous studies have reported that salinity was the strongest limiting factor for microbial distribution in lakes of a large range of salinity (Xing et al., 2009; Liu et al., 2013; Logares et al., 2013; Huang et al., 2014; Liu Y. et al., 2016; Yang et al., 2016b). The studied lakes in present study had a very large salinity range of 0.8–365.6 g/L, and thus salinity was supposed to have strong influence on the benthic algal distribution. Such inconsistency may be ascribed to the following reasons: (1) the impact of water temperature, light and nutrient-related variables (e.g., DIC, DOC, illumination intensity, TN, TP, turbidity) exceeded salinity on the distribution of benthic algal communities, which also was supported by the CCA ordination (**Figure 4**); and (2) micro-niches in the sediments make some attached algal species capable of tolerating a broad salinity range (freshwater to hypersaline), resulting in their insensitivity to salinity change (Oren, 2011, 2015). However, the underlying reasons still await further investigation.

Benthic algal communities in the studied lakes showed different composition from their planktonic counterparts (**Figure 6**), suggesting that the source of some benthic algal taxa could be indigenous. Lake water and sediment are different habitats (having different environmental conditions), and thus they are prone to host distinct microbial communities (DeLong et al., 1993; Jiang et al., 2006; Mesbah et al., 2007; Yang et al., 2013). However, it cannot still be excluded that some benthic algal taxa were derived from upper water column, because we indeed observed the occurrence of some cyanobacterial OTUs in both lake waters and surface sediments (Supplementary Figure S2). Such common algal taxa may be generalists that can utilize a wide spectrum of substrates and thus easily adapt to another new habitat (Hambright et al., 2015). In addition, the distinct algal diversity difference between Chinese and American lakes (**Figure 6**) suggested that geographic isolation may play an important role in influencing algal distribution in lakes. Such geographic isolation effect on microbial distribution has already been reported in many previous studies (Papke et al., 2003; Whitaker et al., 2003; Valverde et al., 2012). However, further investigation is needed to validate the geographic isolation effect on algal distribution observed in this study.

In summary, water temperature, light and nutrient-related variables were more important than salinity in influencing the community compositions of the benthic algae in the studied lakes, and geographic distance could also play an important role in influencing the distribution of benthic algal community. The source of benthic algal taxa in lakes could be partially indigenous or derived from upper water column. The results of this study gave insights into the influence of environmental and spatial factors on the benthic algal distribution in alpine lakes.

AUTHOR CONTRIBUTIONS

JY and HJ conceived and designed the experiments. JY, WL, and BW performed the experiments. JY analyzed the data. All authors assisted in writing the manuscript, discussed the results, and commented on the manuscript.

FUNDING

This research was supported by grants from the National Natural Science Foundation of China (Grant Nos. 41602346,

41422208, 41672337, and 41521001), and Fundamental Research Funds for the Central Universities, China University of Geosciences (Wuhan).

ACKNOWLEDGMENTS

We are thankful to Enming Zhou from Sun Yat-sen University for helping manuscript revision. We are also grateful to the reviewers whose constructive comments significantly improved the quality of the manuscript.

SUPPLEMENTARY MATERIAL

The Supplementary Material for this article can be found online at: https://www.frontiersin.org/articles/10.3389/fmicb.2018.00578/full#supplementary-material

REFERENCES

Althouse, B., Higgins, S., and Zanden, M. J. V. (2014). Benthic and planktonic primary production along a nutrient gradient in Green Bay, Lake Michigan, USA. *Freshw. Sci.* 33, 487–498. doi: 10.1086/676314

Ask, J., Karlsson, J., Persson, L., Ask, P., Byström, P., and Jansson, M. (2009). Whole-lake estimates of carbon flux through algae and bacteria in benthic and pelagic habitats of clear-water lakes. *Ecology* 90, 1923–1932. doi: 10.1890/07-1855.1

Astorga, A., Oksanen, J., Luoto, M., Soininen, J., Virtanen, R., and Muotka, T. (2012). Distance decay of similarity in freshwater communities: do macro- and microorganisms follow the same rules? *Global Ecol. Biogeogr.* 21, 365–375. doi: 10.1111/j.1466-8238.2011.00681.x

Blanchet, F. G., Legendre, P., and Borcard, D. (2008). Forward selection of explanatory variables. *Ecology* 89, 2623–2632. doi: 10.1890/07-0986.1

Borcard, D., and Legendre, P. (2002). All-scale spatial analysis of ecological data by means of principal coordinates of neighbour matrices. *Ecol. Model.* 153, 51–68.

Bradshaw, A. L., Brewer, P. G., Shafer, D. K., and Williams, R. T. (1981). Measurements of total carbon dioxide and alkalinity by potentiometric titration in the GEOSECS program. *Earth Planet. Sci. Lett.* 55, 99–115. doi: 10.1016/0012-821X(81)90090-X

Bryant, D. A., and Frigaard, N.-U. (2006). Prokaryotic photosynthesis and phototrophy illuminated. *Trends Microbiol.* 14, 488–496. doi: 10.1016/j.tim.2006.09.001

Caporaso, J. G., Kuczynski, J., Stombaugh, J., Bittinger, K., Bushman, F. D., Costello, E. K., et al. (2010). QIIME allows analysis of high-throughput community sequencing data. *Nat. Methods* 7, 335–336. doi: 10.1038/nmeth.f.303

Caporaso, J. G., Lauber, C. L., Walters, W. A., Berg-Lyons, D., Huntley, J., Fierer, N., et al. (2012). Ultra-high-throughput microbial community analysis on the Illumina HiSeq and MiSeq platforms. *ISME J.* 6, 1621–1624. doi: 10.1038/ismej.2012.8

Chen, C. Y., and Durbin, E. G. (1994). Effects of pH on the growth and carbon uptake of marine phytoplankton. *Mar. Ecol. Prog. Ser.* 109, 83–94.

Cloern, J. E. (1999). The relative importance of light and nutrient limitation of phytoplankton growth: a simple index of coastal ecosystem sensitivity to nutrient enrichment. *Aquat. Ecol.* 33, 3–15. doi: 10.1023/A:1009952125558

DeLong, E. F., Franks, D. G., and Alldredge, A. L. (1993). Phylogenetic diversity of aggregate-attached vs. free-living marine bacterial assemblages. *Limnol. Oceanogr.* 38, 924–934. doi: 10.4319/lo.1993.38.5.0924

Edgar, R. C. (2010). Search and clustering orders of magnitude faster than BLAST. *Bioinformatics* 26, 2460–2461. doi: 10.1093/bioinformatics/btq461

Edgar, R. C. (2013). UPARSE: highly accurate OTU sequences from microbial amplicon reads. *Nat. Methods* 10, 996–998. doi: 10.1038/nmeth.2604

Edgar, R. C., Haas, B. J., Clemente, J. C., Quince, C., and Knight, R. (2011). UCHIME improves sensitivity and speed of chimera detection. *Bioinformatics* 27, 2194–2200. doi: 10.1093/bioinformatics/btr381

Elliott, J. A., Jones, I. D., and Thackeray, S. J. (2006). Testing the sensitivity of phytoplankton communities to changes in water temperature and nutrient load, in a temperate lake. *Hydrobiologia* 559, 401–411. doi: 10.1007/s10750-005-1233-y

Francis, C. A., Roberts, K. J., Beman, J. M., Santoro, A. E., and Oakley, B. B. (2005). Ubiquity and diversity of ammonia-oxidizing archaea in water columns and sediments of the ocean. *Proc. Natl. Acad. Sci. U.S.A.* 102, 14683–14688. doi: 10.1073/pnas.0506625102

Geider, R. J., Maclntyre, H. L., and Kana, T. M. (1998). A dynamic regulatory model of phytoplanktonic acclimation to light, nutrients, and temperature. *Limnol. Oceanogr.* 43, 679–694. doi: 10.4319/lo.1998.43.4.0679

Goldenberg Vilar, A., van Dam, H., van Loon, E. E., Vonk, J. A., van Der Geest, H. G., and Admiraal, W. (2014). Eutrophication decreases distance decay of similarity in diatom communities. *Freshwat. Biol.* 59, 1522–1531. doi: 10.1111/fwb.12363

Hambright, K. D., Beyer, J. E., Easton, J. D., Zamor, R. M., Easton, A. C., and Hallidayschult, T. C. (2015). The niche of an invasive marine microbe in a subtropical freshwater impoundment. *ISME J.* 9, 256–264. doi: 10.1038/ismej.2014.103

Hare, C. E., Leblanc, K., DiTullio, G. R., Kudela, R. M., Zhang, Y., Lee, P. A., et al. (2007). Consequences of increased temperature and CO2 for phytoplankton community structure in the Bering Sea. *Mar. Ecol. Prog. Ser* 352, 9–16. doi: 10.3354/meps07182

Howard-Williams, C., and Lenton, G. M. (1975). The role of the littoral zone in the functioning of a shallow tropical lake ecosystem. *Freshwat. Biol.* 5, 445–459. doi: 10.1111/j.1365-2427.1975.tb00147.x

Huang, S., Liu, Y., Hu, A., Liu, X., Chen, F., Yao, T., et al. (2014). Genetic diversity of picocyanobacteria in Tibetan lakes: assessing the endemic and universal distributions. *Appl. Environ. Microbiol.* 80, 7640–7650. doi: 10.1128/AEM.02611-14

Jiang, H., Dong, C. Z., Huang, Q., Wang, G., Fang, B., Zhang, C., et al. (2012). Actinobacterial diversity in microbial mats of five hot springs in central and central-eastern Tibet, China. *Geomicrobiol. J.* 29, 520–527. doi: 10.1080/01490451.2011.590872

Jiang, H., Dong, H., Yu, B., Liu, X., Li, Y., Ji, S., et al. (2007). Microbial response to salinity change in Lake Chaka, a hypersaline lake on Tibetan plateau. *Environ. Microbiol.* 9, 2603–2621. doi: 10.1111/j.1462-2920.2007.01377.x

Jiang, H., Dong, H., Zhang, G., Yu, B., Chapman, L. R., and Fields, M. W. (2006). Microbial diversity in water and sediment of Lake Chaka, an athalassohaline lake in northwestern China. *Appl. Environ. Microbiol.* 72, 3832–3845.

Kenneth, R. H. (2002). Effects of pH on coastal marine phytoplankton. *Mar. Ecol. Prog. Ser.* 238, 281–300. doi: 10.3354/meps238281

Lange, K., Liess, A., Piggott, J. J., Townsend, C. R., and Matthaei, C. D. (2011). Light, nutrients and grazing interact to determine stream diatom community composition and functional group structure. *Freshwat. Biol.* 56, 264–278. doi: 10.1111/j.1365-2427.2010.02492.x

Liu, X., Hou, W., Dong, H., Wang, S., Jiang, H., Wu, G., et al. (2016). Distribution and diversity of cyanobacteria and eukaryotic algae in Qinghai–Tibetan lakes. *Geomicrobiol. J.* 33, 860–869. doi: 10.1080/01490451.2015.1120368

Liu, Y., Priscu, J. C., Xiong, J., Conrad, R., Vick-Majors, T., Chu, H., et al. (2016). Salinity drives archaeal distribution patterns in high altitude lake sediments on the Tibetan Plateau. *FEMS Microbiol. Ecol.* 92:fiw033. doi: 10.1093/femsec/fiw033

Liu, Y., Yao, T., Jiao, N., Kang, S., Zeng, Y., and Huang, S. (2006). Microbial community structure in moraine lakes and glacial meltwaters, Mount Everest. *FEMS Microbiol. Lett.* 265, 98–105. doi: 10.1111/j.1574-6968.2006.00477.x

Liu, Y., Yao, T., Jiao, N., Zhu, L., Hu, A., Liu, X., et al. (2013). Salinity impact on bacterial community composition in five high-altitude lakes from the Tibetan plateau, Western China. *Geomicrobiol. J.* 30, 462–469. doi: 10.1080/01490451.2012.710709

Logares, R., Lindstrom, E. S., Langenheder, S., Logue, J. B., Paterson, H., Laybourn-Parry, J., et al. (2013). Biogeography of bacterial communities exposed to progressive long-term environmental change. *ISME J.* 7, 937–948. doi: 10.1038/ismej.2012.168

Magoč, T., and Salzberg, S. L. (2011). FLASH: fast length adjustment of short reads to improve genome assemblies. *Bioinformatics* 27, 2957–2963. doi: 10.1093/bioinformatics/btr507

Mesbah, N. M., Abou-El-Ela, S. H., and Wiegel, J. (2007). Novel and unexpected prokaryotic diversity in water and sediments of the alkaline, hypersaline lakes of the Wadi An Natrun. *Egypt. Microb. Ecol.* 54, 598–617. doi: 10.1007/s00248-006-9193-y

Mooij, W. M., Hülsmann, S., Domis, L. N. D. S., Nolet, B. A., Bodelier, P. L., Boers, P. C., et al. (2005). The impact of climate change on lakes in the Netherlands: a review. *Aquat. Ecol.* 39, 381–400.

Neal, C., Neal, M., and Wickham, H. (2000). Phosphate measurement in natural waters: two examples of analytical problems associated with silica interference using phosphomolybdic acid methodologies. *Sci. Total Environ.* 251–252, 511–522.

Nõges, T., Luup, H., and Feldmann, T. (2010). Primary production of aquatic macrophytes and their epiphytes in two shallow lakes (Peipsi and Võrtsjärv) in Estonia. *Aquat. Ecol.* 44, 83–92.

Nozaki, K. (2001). Abrupt change in primary productivity in a littoral zone of Lake Biwa with the development of a filamentous green-algal community. *Freshwat. Biol.* 46, 587–602. doi: 10.1046/j.1365-2427.2001.00696.x

Nozaki, K., Darijav, K., Akatsuka, T., Goto, N., and Mitamura, O. (2003). Development of filamentous green algae in the benthic algal community in a littoral sand-beach zone of Lake Biwa. *Limnology* 4, 161–165.

Oren, A. (2011). Thermodynamic limits to microbial life at high salt concentrations. *Environ. Microbiol.* 13, 1908–1923. doi: 10.1111/j.1462-2920.2010.02365.x

Oren, A. (2015). Cyanobacteria in hypersaline environments: biodiversity and physiological properties. *Biodivers. Conserv.* 24, 781–798. doi: 10.1007/s10531-015-0882-z

Papke, R. T., Ramsing, N. B., Bateson, M. M., and Ward, D. M. (2003). Geographical isolation in hot spring cyanobacteria. *Environ. Microbiol.* 5, 650–659. doi: 10.1046/j.1462-2920.2003.00460.x

Reinfelder, J. R. (2011). Carbon concentrating mechanisms in eukaryotic marine phytoplankton. *Ann. Rev. Mar. Sci.* 3, 291–315. doi: 10.1146/annurev-marine-120709-142720

Riebesell, U. (2004). Effects of CO2 enrichment on marine phytoplankton. *J. Oceanogr.* 60, 719–729. doi: 10.1007/s10872-004-5764-z

Riebesell, U., Wolf-Gladrow, D. A., and Smetacek, V. (1993). Carbon dioxide limitation of marine phytoplankton growth rates. *Nature* 361, 249–251. doi: 10.1038/361249a0

Sherwood, A. R., and Presting, G. G. (2007). Universal primers amplify a 23S rDNA plastid marker in eukaryotic algae and cyanobacteria. *J. Phycol.* 43, 605–608. doi: 10.1111/j.1529-8817.2007.00341.x

Stelzer, R. S., and Lamberti, G. A. (2001). Effects of N: P ratio and total nutrient concentration on stream periphyton community structure, biomass, and elemental composition. *Limnol. Oceanogr.* 46, 356–367. doi: 10.4319/lo.2001.46.2.0356

Steven, B., McCann, S., and Ward, N. L. (2012). Pyrosequencing of plastid 23S rRNA genes reveals diverse and dynamic cyanobacterial and algal populations in two eutrophic lakes. *FEMS Microbiol. Ecol.* 82, 607–615. doi: 10.1111/j.1574-6941.2012.01429.x

Stoffels, R. J., Clarke, K. R., and Closs, G. P. (2005). Spatial scale and benthic community organisation in the littoral zones of large oligotrophic lakes: potential for cross-scale interactions. *Freshwat. Biol.* 50, 1131–1145. doi: 10.1111/j.1365-2427.2005.01384.x

Strayer, D., and Likens, G. E. (1986). An energy budget for the zoobenthos of Mirror Lake, New Hampshire. *Ecology* 67, 303–313. doi: 10.2307/1938574

Vadeboncoeur, Y., Lodge, D. M., and Carpenter, S. R. (2001). Whole-lake fertilization effects on distribution of primary production between benthic and pelagic habitats. *Ecology* 82, 1065–1077.

Valverde, A., Tuffin, M., and Cowan, D. (2012). Biogeography of bacterial communities in hot springs: a focus on the actinobacteria. *Extremophiles* 16, 669–679. doi: 10.1007/s00792-012-0465-9

Wang, J., Yang, D., Zhang, Y., Shen, J., Van Der Gast, C., Hahn, M. W., et al. (2011). Do patterns of bacterial diversity along salinity gradients differ from those observed for macroorganisms? *PLoS One* 6:e27597. doi: 10.1371/journal.pone.0027597

Wetzel, C. E., Bicudo, D. D. C., Ector, L., Lobo, E. A., Soininen, J., Landeiro, V. L., et al. (2012). Distance decay of similarity in neotropical diatom communities. *PLoS One* 7:e45071. doi: 10.1371/journal.pone.0045071

Whitaker, R. J., Grogan, D. W., and Taylor, J. W. (2003). Geographic barriers isolate endemic populations of hyperthermophilic archaea. *Science* 301, 976–978. doi: 10.1126/science.1086909

Wu, Q. L., Zwart, G., Schauer, M., Kamst-van Agterveld, M. P., and Hahn, M. W. (2006). Bacterioplankton community composition along a salinity gradient of sixteen high-mountain lakes located on the Tibetan Plateau, China. *Appl. Environ. Microbiol.* 72, 5478–5485.

Wyatt, K. H., Stevenson, R. J., and Turetsky, M. R. (2010). The importance of nutrient co-limitation in regulating algal community composition, productivity and algal-derived DOC in an oligotrophic marsh in interior Alaska. *Freshwat. Biol.* 55, 1845–1860. doi: 10.1111/j.1365-2427.2010.02419.x

Xing, P., Hahn, M. W., and Wu, Q. L. (2009). Low taxon richness of bacterioplankton in high-altitude lakes of the eastern Tibetan Plateau, with a predominance of Bacteroidetes and *Synechococcus* spp. *Appl. Environ. Microbiol.* 75, 7017–7025. doi: 10.1128/AEM.01544-09

Yang, J., Jiang, H., Dong, H., Wang, H., Wu, G., Hou, W., et al. (2013). amoA-encoding archaea and thaumarchaeol in the lakes on the northeastern Qinghai-Tibetan Plateau, China. *Front. Microbiol.* 4:329. doi: 10.3389/fmicb.2013.00329

Yang, J., Jiang, H., Wu, G., Liu, W., and Zhang, G. (2016a). Distinct factors shape aquatic and sedimentary microbial community structures in the lakes of western China. *Front. Microbiol.* 7:1782. doi: 10.3389/fmicb.2016.01782

Yang, J., Ma, L., Jiang, H., Wu, G., and Dong, H. (2016b). Salinity shapes microbial diversity and community structure in surface sediments of the Qinghai-Tibetan Lakes. *Sci. Rep.* 6:25078. doi: 10.1038/srep25078

Zheng, M. (1997). *An Introduction to Saline Lakes on the Qinghai-Tibet Plateau*, 1st Edn. Dordrecht: Kluwer Academic Publisher, 1–17.

Conflict of Interest Statement: The authors declare that the research was conducted in the absence of any commercial or financial relationships that could be construed as a potential conflict of interest.

frontiers in Microbiology

ORIGINAL RESEARCH
published: 27 February 2018
doi: 10.3389/fmicb.2018.00352

Macro and Microelements Drive Diversity and Composition of Prokaryotic and Fungal Communities in Hypersaline Sediments and Saline–Alkaline Soils

Kaihui Liu[1], Xiaowei Ding[1]*, Xiaofei Tang[1], Jianjun Wang[2], Wenjun Li[3], Qingyun Yan[4] and Zhenghua Liu[5]*

[1] School of Biological Science and Engineering, Shaanxi University of Technology, Hanzhong, China, [2] State Key Laboratory of Lake Science and Environment, Nanjing Institute of Geography and Limnology, Chinese Academy of Sciences, Nanjing, China, [3] State Key Laboratory of Biocontrol and Guangdong Provincial Key Laboratory of Plant Resources, School of Life Sciences, Sun Yat-sen University, Guangzhou, China, [4] Environmental Microbiome Research Center and School of Environmental Science and Engineering, Sun Yat-sen University, Guangzhou, China, [5] School of Minerals Processing and Bioengineering, Central South University, Changsha, China

Understanding the effects of environmental factors on microbial communities is critical for microbial ecology, but it remains challenging. In this study, we examined the diversity (alpha diversity) and community compositions (beta diversity) of prokaryotes and fungi in hypersaline sediments and salinized soils from northern China. Environmental variables were highly correlated, but they differed significantly between the sediments and saline soils. The compositions of prokaryotic and fungal communities in the hypersaline sediments were different from those in adjacent saline–alkaline soils, indicating a habitat-specific microbial distribution pattern. The macroelements (S, P, K, Mg, and Fe) and Ca were, respectively, correlated closely with the alpha diversity of prokaryotes and fungi, while the macronutrients (e.g., Na, S, P, and Ca) were correlated with the prokaryotic and fungal beta-diversity ($P \leq 0.05$). And, the nine microelements (e.g., Al, Ba, Co, Hg, and Mn) and micronutrients (Ba, Cd, and Sr) individually shaped the alpha diversity of prokaryotes and fungi, while the six microelements (e.g., As, Ba, Cr, and Ge) and only the trace elements (Cr and Cu), respectively, influenced the beta diversity of prokaryotes and fungi ($P < 0.05$). Variation-partitioning analysis (VPA) showed that environmental variables jointly explained 55.49% and 32.27% of the total variation for the prokaryotic and fungal communities, respectively. Together, our findings demonstrate that the diversity and community composition of the prokaryotes and fungi were driven by different macro and microelements in saline habitats, and that geochemical elements could more widely regulate the diversity and community composition of prokaryotes than these of fungi.

Keywords: prokaryotic and fungal community, soils and saline sediments, macroelement, microelement, high-throughput sequencing, variance partitioning analysis

OPEN ACCESS

Edited by:
Nils-Kaare Birkeland, University of Bergen, Norway

Reviewed by:
James A. Coker, University of Maryland University College, United States
Jian Yang, China University of Geosciences, China
Juan M. Gonzalez, Consejo Superior de Investigaciones Científicas (CSIC), Spain

****Correspondence:***
Kaihui Liu
Kaihhui168@hotmail.com
Xiaowei Ding
dxw518@163.com

Specialty section:
This article was submitted to Extreme Microbiology, a section of the journal Frontiers in Microbiology

Received: *03 December 2017*
Accepted: *14 February 2018*
Published: *27 February 2018*

Citation:
Liu K, Ding X, Tang X, Wang J, Li W, Yan Q and Liu Z (2018) Macro and Microelements Drive Diversity and Composition of Prokaryotic and Fungal Communities in Hypersaline Sediments and Saline–Alkaline Soils. Front. Microbiol. 9:352. doi: 10.3389/fmicb.2018.00352

INTRODUCTION

Microbial communities are ubiquitous and can even thrive in extreme environments such as hypersaline lakes, marine habitats and saline–alkaline soils (Jiang et al., 2007; Andrei et al., 2015; Yakimov et al., 2015; Xie et al., 2017). They are key components of these extreme ecosystems, and thus play central roles in their geochemical cycles and ecological stability (Nunoura et al., 2013; Liang et al., 2014; Sorokin et al., 2015). Microbial communities in extreme environments have formed unique community structures (Oren, 2013). Moreover, the species diversity and distribution patterns of microbial assemblages vary, together with dynamic ecological variables such as pH, geochemical elements, moisture and terrestrial locations (Xiong et al., 2012; Liu K. et al., 2014; Bryanskaya et al., 2016; Fernandez et al., 2016; Zhong et al., 2016). Revealing the linkage between the diversity and structures of microbial communities and environmental driving forces will provide significant insight into the mechanisms that microbial communities use to adapt to extreme habitats, community succession and ecological functioning.

Accumulating evidence suggests that geochemical elements could be major factors influencing microbial assemblages (Oren, 2013). For example, macroelements such as K^+, Ca^{2+}, and Mg^{2+}significantly contributed to the species richness and compositions of prokaryotic communities in soils and hypersaline sediments (Podell et al., 2014; Bryanskaya et al., 2016; Xia et al., 2016; Zhong et al., 2016) and Ca and P significantly affect fungal community compositions in forest soils (Sun et al., 2016). Although some microelements are regarded as toxic to most forms of life, they regulated microbial communities in extreme conditions. For instance, they are significantly correlated with bacterial community composition in hot springs (Jiang et al., 2016) and certain elements (Co, Ni, and Mn) explained variations of prokaryotic and fungal assemblages in polymetallic mining areas (Reith et al., 2015). These previous studies have enriched our knowledge of microbial biogeography, but the respective reports are mainly focused on various macroelements. In fact, microbial communities are jointly driven by various factors. What's more, these two types of elements drive different physiological processes of microbial life (Stolz et al., 2006; Wintsche et al., 2016). Therefore, it is important to investigate the effects of these multiple variables on the diversity and composition of microbial communities. However, the relevant knowledge is still unavailable especially as regards saline habitats.

Salt lakes and saline–alkaline lands are widely distributed across the earth, where they are characterized by high osmotic pressure and high ionic concentrations (Oren, 2002; Hallsworth et al., 2007). Microbial communities in saline habitats are adapted to high ionic conditions, and salt ions play an important role in driving the diversity and composition of microbial communities. In this study, we collected 36 samples (including hypersaline sediments and saline soils) from salt lakes and saline–alkaline regions of northwest China. The diversity and composition of prokaryotic and fungal communities in these saline samples were determined based on the sequencing data of 16S rRNA genes and fungal ITS regions on an Illumina HiSeq. Specifically, this study has two major objectives: (1) evaluate the influence of macro- and microelements on the diversity of prokaryotic and fungal communities; (2) assess the relative importance of macro- and microelements in driving the distribution of prokaryotic and fungal communities.

MATERIALS AND METHODS

Site Description and Sample Collection

A total of 27 hypersaline sediment samples were collected from three salt lakes (Gouchi, Yuncheng, and Luyang lakes), and nine salinized soil samples were collected from areas adjacent to these lakes (**Figure 1**). Gouchi and Luyang lakes represent typical chloride-type lakes and are located in Dingbian County and Weinan City of Shaanxi Province in Northern China. Lake Yuncheng, known as one of the world's three largest sodium-sulfate-type inland saline lakes, is located in Yuncheng City, in Shaanxi Province. Sediment samples from Gouchi, Yuncheng and Luyang lakes were numbered with the prefixes G, Y and W, respectively, and saline soil samples surrounding these three salt lakes were assigned the prefixes GT, YT and WT, respectively. Each sample was obtained by mixing five 10-g subsamples from 1 m × 1 m quadrants, which were taken from a depth of approximately 10–15 cm from a sediment or soil surface. Each set of five subsamples was combined as one sample, giving three biological replicates per plot. All samples were collected in sterile 50-ml plastic screw-top tubes, transported to the laboratory on ice, and stored at −80°C until the extraction of DNA.

Measurements of Environmental Factors

Macroelements and trace elements in the soil and sediment samples were measured using an inductively coupled plasma mass spectrometer (ICP-MS; Perkin-Elmer Sciex Elan+ 5000). Briefly, sediment and soil samples were dried in a hot-air oven at 40°C until a stable weight was achieved, and sieved through a 0.25-μm filter. Each test sample (200 mg) was fully digested in a microwave digestion system with the addition of a mixture of HNO_3 and HF (Arslan and Tyson, 2008), and the resulting solutions were transferred to 25-ml volumetric flasks and diluted to the fixed volume with 3% HNO_3. The digestion procedure was performed in triplicate for each test sample. The calibration curve was prepared using a working standard solution with concentrations ranging from 0.01 to 10 μg ml^{-1} for all macroelements (Na, Mg, K, Ca, S, P, and Fe) and microelements (Al, As, B, Ba, Cd, Co, Cr, Cu, Ga, Ge, Hg, Li, Mn, Ni, Pt, Sr, Ti, Zn, and Rb). The concentrations of macroelements and trace elements in the soil and saline sediments were determined by ICP-MS (Sandroni and Smith, 2002). In addition, moisture was reported based on the water content of the samples. Geographic locations of each site were recorded in situ, and pH values of the samples were measured using pH strips with 1:5 (wt/vol) sediment to water.

DNA Extraction, PCR Amplification, and Illumina-Based Sequencing

DNA was extracted from 0.5-g samples of soil or saline sediments using a FastDNA^{TM} SPIN Kit for soil (MP Biomedicals, LLC)

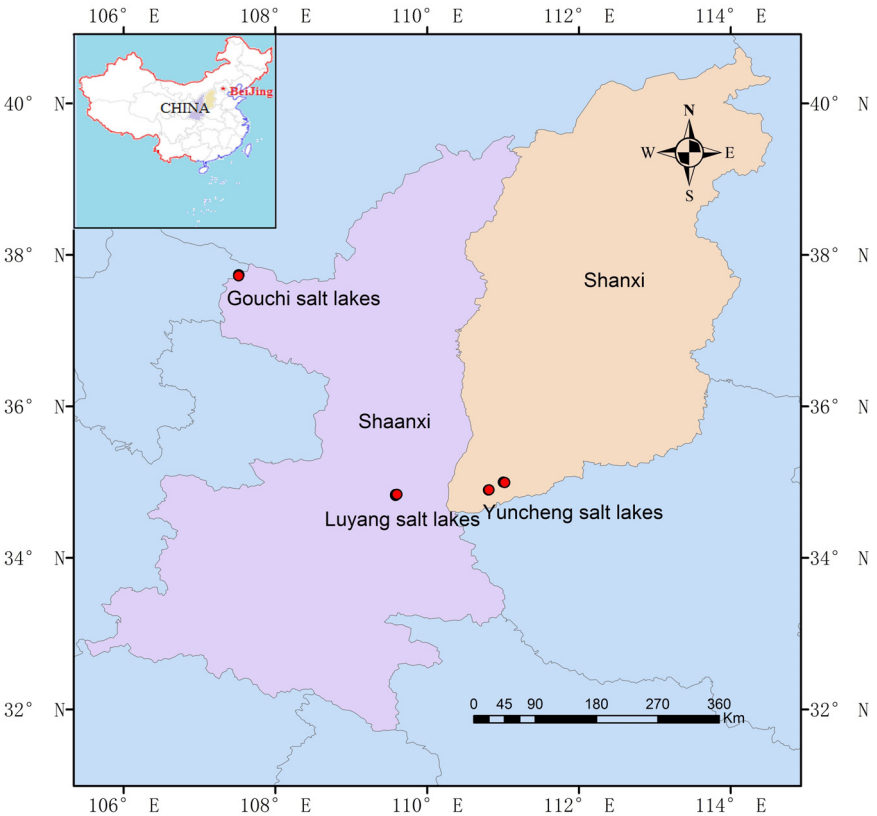

FIGURE 1 | Geographic location of the Gouchi salt lake, Yuncheng salt lake, and Luyang salt lake. Location map of the sampling sites was created using ArcGIS software by Esri.

according to the manufacturer's instructions. Triplicate DNA extracts from the same sample were combined and analyzed using a NanoDrop® TM ND-1000 spectrophotometer (Thermo Scientific, Wilmington, DE, United States). The 16S rRNA genes and the ITS regions of the extracted DNA were amplified using general bacterial primers 515F/806R (Caporaso et al., 2011) and fungal-specific primers ITS1F (Gardes and Bruns, 1993)/ITS4 (White et al., 1990). PCR was performed in triplicate for each sample with the following thermal cycling: an initial denaturation at 94°C for 5 min, followed by 25 cycles of 30 s at 94°C, 30 s at 50°C (ITS) or 55°C (16S rRNA) and 30 s at 72°C. Replicates were further pooled, and the resulting amplicons from each sample were sequenced on the HiSeq2500 system (Illumina Inc., San Diego, CA, United States).

Sequence Processing

The quality filtering, chimera removal and operational taxonomic unit (OTU)-based clustering of the sequences were performed using the Mothur software V 1.35.1 (Quast et al., 2013). Briefly, sequences with a barcode ambiguity at one end and more than one ambiguous nucleotide (N), and those shorter than 200 bp in length after removal of the barcode and primer were discarded. Chimeric sequences were removed using the UCHIME modules in Mothur. The quality-filtered sequences were truncated to a constant length and were then clustered into OTUs with a 3% dissimilarity cutoff using the UPARSE pipeline (Edgar, 2013). The OTUs that contained fewer than two reads were excluded from further analysis. A representative sequence from each OTU was assigned to bacteria, archaea, and fungi using the Ribosomal Database Project (RDP) classifier (Wang et al., 2007). At the phylum-taxonomy level, OTUs in each of the three samples from the same saline pools or soil plots were combined and assigned, for example, (G1, G2, and G3) to G_1, (G4, G5, and G6) to G_2, (G7, G8, and G9) to G_3, (Y11, Y12, and Y13) to Y_1, (Y21, Y22, and Y23) to Y_2, (Y31, Y32, and Y33) to Y_3, (GT1, GT2, and GT3) to GT, (YT1, YT2, and YT3) to YT and (WT1, WT2, and WT3) to WT.

Multivariate Statistical Analysis

All statistical analyses in this study were performed using the vegan package in R software, except where otherwise noted. Prior to data analysis, the number of sequences was normalized by randomly sub-sampling reads of prokaryotes (30,126 sequences) and fungi (30,198 sequences) for each sample to avoid a potential bias caused by different sequencing depths. The alpha and beta diversities were calculated using species-level OTUs in QIIME (Caporaso et al., 2010). Relationships of environmental variables and alpha-diversity indices (species richness and Shannon) with factors were tested based on Pearson's correlation. Principal component analyses (PCoA), based on unweighted

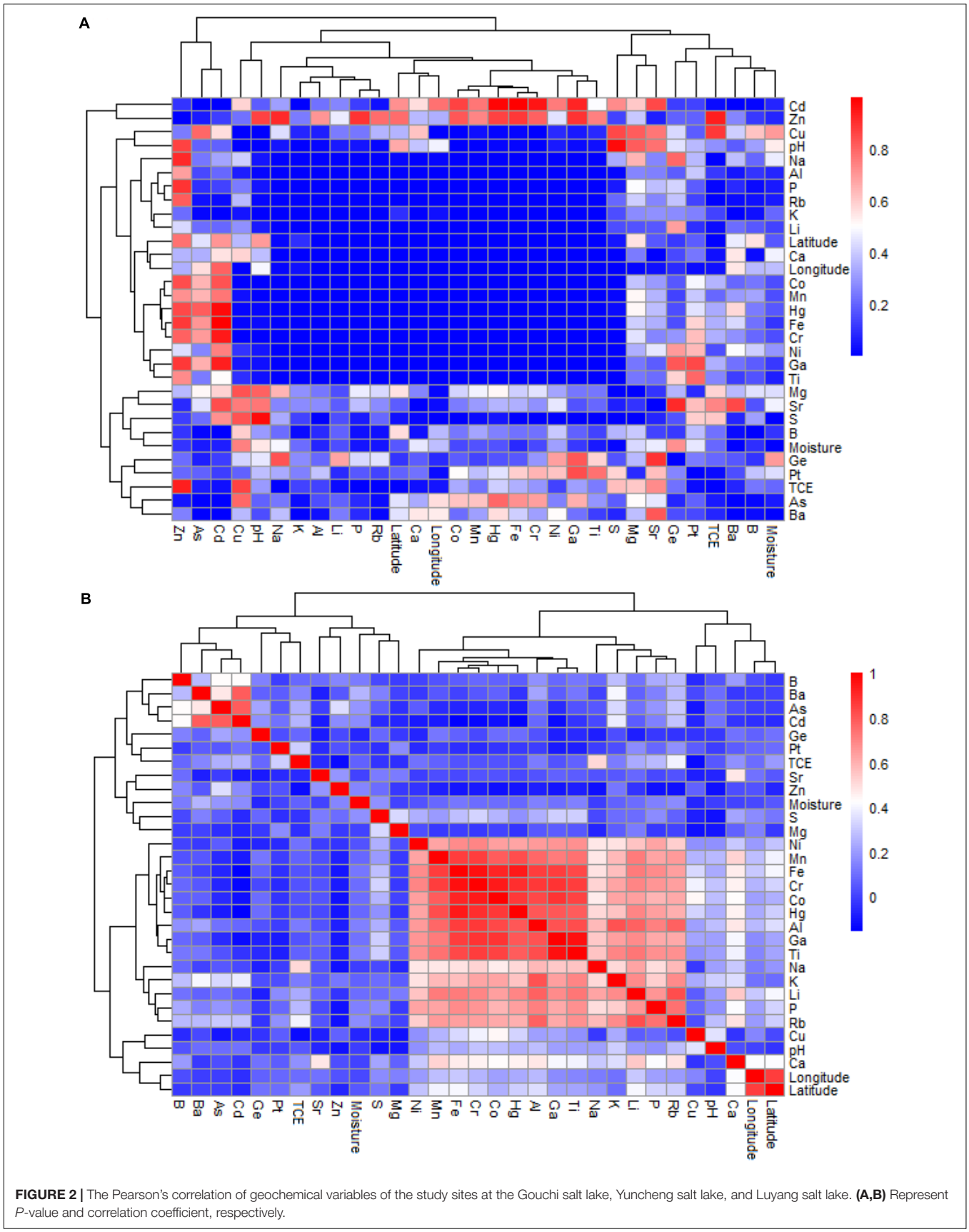

FIGURE 2 | The Pearson's correlation of geochemical variables of the study sites at the Gouchi salt lake, Yuncheng salt lake, and Luyang salt lake. **(A,B)** Represent *P*-value and correlation coefficient, respectively.

UniFrac metrics, were performed to reveal the spatial patterns of the microbial communities within the samples. Canonical correspondence analysis (CCA) was used to identify the significant factors ($P \leq 0.05$) to the community composition of prokaryotes and fungi. The permutational multivariate analysis of variance (PerMANOVA) was performed using the distance matrices (R: adonis) in vegan with 999 permutations, and variation partitioning analyses (VPA) were performed by the vegan package in R 2.14.0 to evaluate the relative contribution of significant factors ($P \leq 0.05$, variance inflation coefficient < 10) to the prokaryotic and fungal community structures. Due to the microbial community shaped by multiple factors, we also analyzed the joint effects of macroelements, microelements and other factors on the community composition.

Accession Numbers

The raw sequencing data generated in this study were deposited into the National Center for Biotechnology Information (NCBI) database under accession numbers SAMN07764381-SAMN07764416 (16S rRNA) and SAMN 07764417-SAMN07764452 (ITS).

RESULTS

Characteristics of Environmental Variables

The macroelemental contents differed significantly among the 36 samples of salt-lake sediments and saline–alkaline soils (Supplementary Table S1). The Na content in all samples was variable. The concentrations of P, Ca, K, and Fe were low in samples G1, G2, and G3 compared to the other 33 samples, as expected. Moreover, the average P concentration in the saline sediments from Gouchi Lake (G4 to G9) was higher than that in the adjacent soils, whereas the average P concentrations in the hypersaline sediments from Yuncheng Lake and Luyang Lake were lower than those in the adjacent soils. In contrast, the average concentrations of S and Mg in the sediments from the

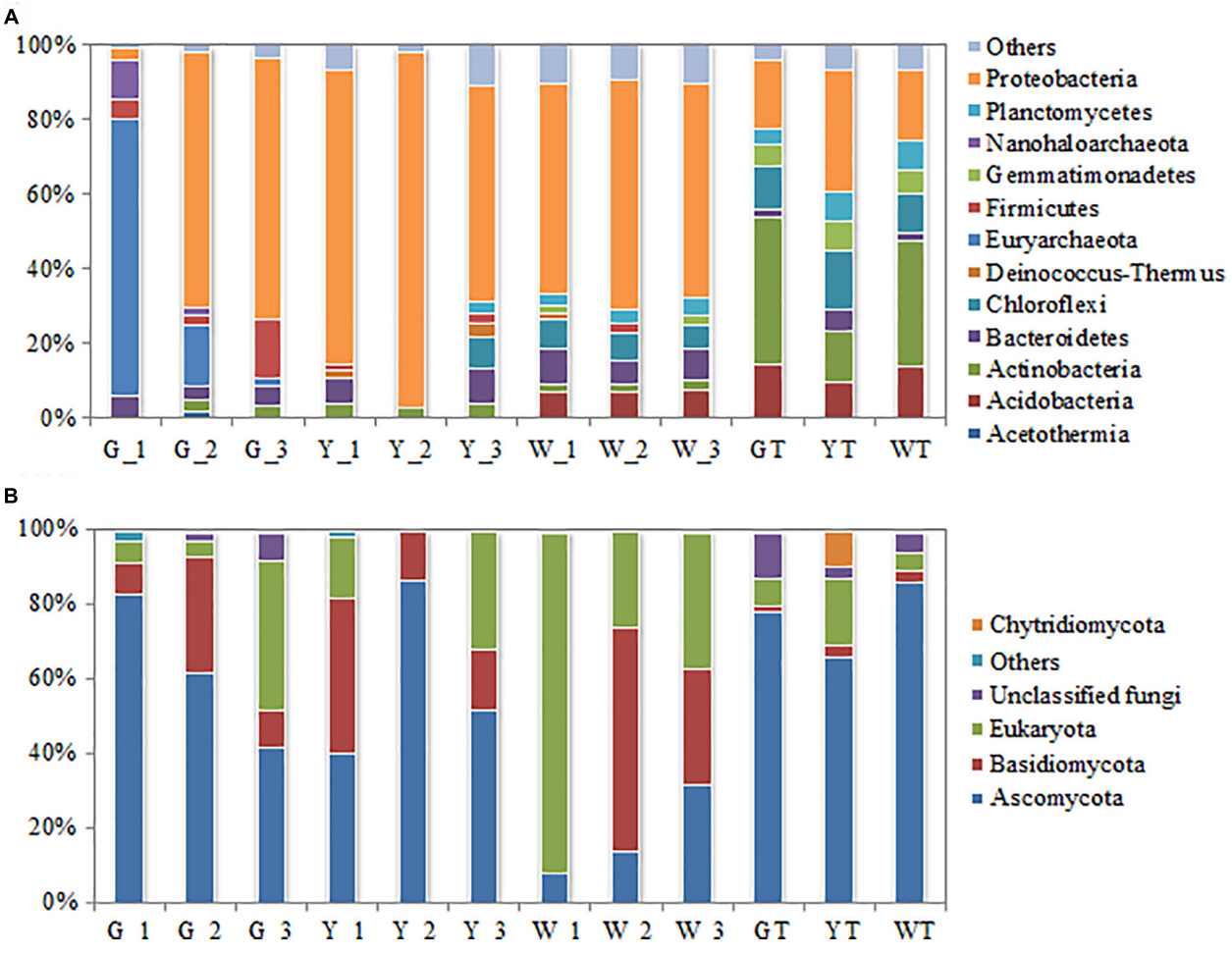

FIGURE 3 | Relative abundance of the dominant phyla in the prokaryotic **(A)** and fungal **(B)** communities from the soil-saline sediment regions. Observed OTUs in three samples from the same saline pool (or soil plot) were combined and further assigned to G_1, G_2, G_3, Y_1, Y_2, Y_3, W_1, W_2, W_3, GT, YT and WT. Only the phyla with >1% mean abundance were shown.

salt lakes were significantly higher than in the neighboring saline soils.

As shown in Supplementary Table S1, the microelemental contents (Al, Co, Cr, Ga, Hg, Mn, Ni, Sr, and Ti) of the 33 samples were higher than those of G1, G2, and G3. The concentrations of Al and Ba fluctuated greatly among all samples. Moreover, the average Al content was found to be greater in the saline soils surrounding Yuncheng and Luyang lakes than in the sediments from those salt lakes. The Sr content varied significantly in saline sediments from each lake but was relatively constant in the soil samples. Mn and Ti concentrations were relatively constant in the all samples, except for samples G1, G2, and G3, in which they were exceptionally low. The contents of Co, Cr, Ga, Hg, and Ni were relatively constant in all samples. In general, moisture content in saline sediments was greater than in their corresponding surrounding soils.

The Pearson's correlations showed significant relationships between many environmental variables of the investigated sites (**Figure 2** and Supplementary Table S2). For example, the presence of S positively correlated with that of Cr ($P = 0.005$, $r = 0.327$) and Ga ($P = 0.004$, $r = 0.310$). The P content was significantly correlated with Na, K, Ca, Fe, Al, Co, Cr, Ga, Hg, Li, Mn, Ni, Rb, Ti, latitude and longitude, with $P = 0.001$ and r ranging from 0.213 to 0.740 for all correlations. The concentrations of Ca were correlated with Fe, Al, Co, Cr, Hg, Li, Mn, Rb, Sr, latitude and longitude ($P = 0.001$), with r values ranging from 0.420 to 0.541. The K content was correlated with Fe, Al, Co, Cr, Ga, Li, Mn, Ni, Rb and Ti, with $P = 0.001$ and r values of 0.491–0.809. The presence of Ba was positively related to Cd ($P = 0.001$ and $r = 0.782$). The Cr content had an even higher correlation to Na, Fe, Al, Co, Ga, Hg, Li, Mn, Ni, Rb, Ti, longitude and latitude ($P = 0.001$ and r values in the range of 0.258–0.959). The Ga content was correlated with Fe, Al, Co, Hg, Li, Mn, Ni, Rb and Ti at ($P = 0.001$ and r values of 0.616–0.959). The Ti content correlated with Na, Fe, Al, Co, Hg, Li, Mn, Ni, and Rb, with $P = 0.001$ and r values of 0.555 to 0.847. Moisture correlated with S ($P = 0.015$, $r = 0.174$) and Ba ($P = 0.005$, $r = 0.256$).

Distribution Patterns of Microbial Communities

Illumina sequencing yielded 1,152,000 prokaryotic reads and 1,156,000 fungal sequences from the 36 samples, after removing low-quality tags and chimeras, resulting in a total of 43,579 OTUs and 3,182 OTUs, respectively (Supplementary Table S3). We found that the Chao1 index and observed OTUs for prokaryotes were significantly higher than these for fungi, and that the diversity of prokaryotes and fungi was higher in saline soils than in hypersaline samples (Supplementary Table S4). We normalized the sequence numbers to 30,124 and 30,198 reads per sample for prokaryotes and fungi, respectively, based on the fewest reads available among the 36 samples. These normalized reads were used in the subsequent analyses.

The phylum-level distribution patterns of prokaryotes differed significantly between the hypersaline sediments and saline–alkaline soils (**Figure 3A**). A total of 74 prokaryotic phyla, including 13 abundant groups, were found across all samples. Proteobacteria were quite abundant in hypersaline sediments, accounting for 57–95% of the total reads per sediment sample (other than G_1, which was dominated by Euryarchaeota), while they exhibited lower richness in the soils. By contrast, Actinobacteria were the most abundant in saline soil samples (14–39%) but represented a relatively small proportion of prokaryotic reads in saline samples (<4%). This phylum was not detected in G_1. Bacteroidetes were more abundant in saline sediments than in soil samples, with the exception of sample Y_2, and Firmicutes were only present in some saline samples. However, Chloroflexi and Acidobacteria were

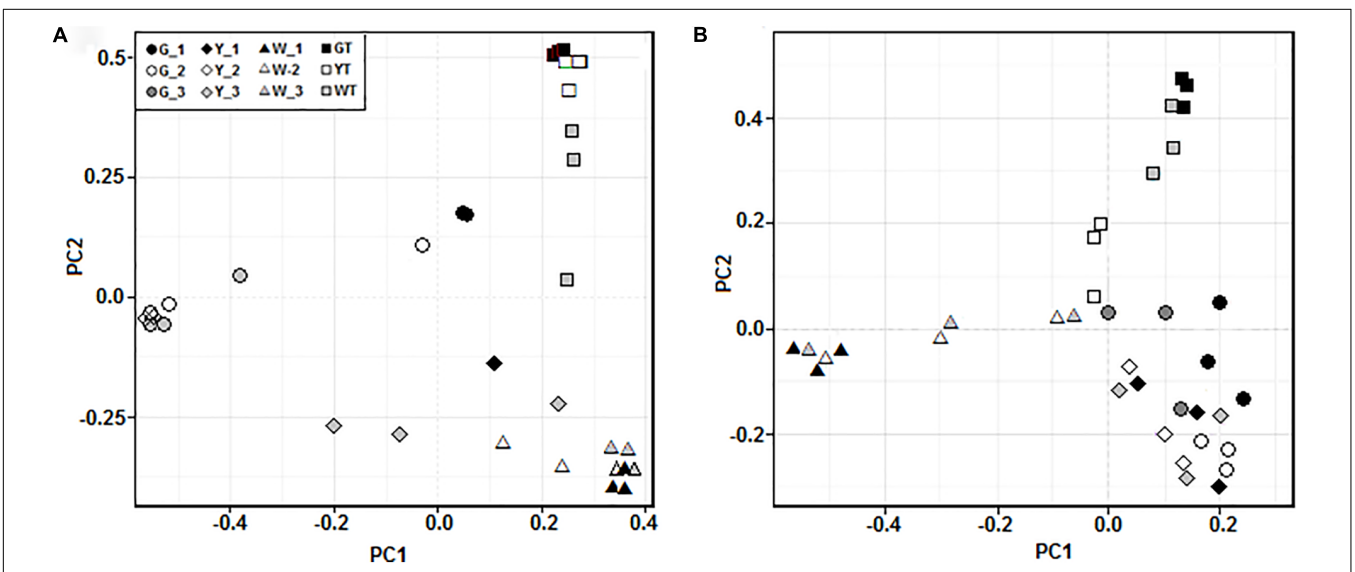

FIGURE 4 | Principal coordinates analysis (PCoA) of the prokaryotic **(A)** and fungal **(B)** communities in all the samples along a salinity gradient. Microbial communities in three samples from the same saline pool (or soil plot) were represented by G_1, G_2, G_3, Y_1, Y_2, Y_3, W_1, W_2, W_3, GT, YT, and WT, respectively.

TABLE 1 | The Pearson correlations of alpha-diversity indices of prokaryotic and fungal communities with environmental factors.

Factor	Prokaryotic community (*P*/R)		Fungal community (*P*/R)	
	Chao1 (Richness)	Shannon	Chao1 (Richness)	Shannon
Na	0.489/−0.006	0.592/−0.033	0.280/0.042	0.067/0.156
S	**0.001/0.526**	**0.001/0.610**	0.320/0.012	0.319/0.029
P	**0.021/0.100**	0.214/0.049	0.067/0.181	0.188/0.080
Ca	0.223/0.026	0.085/0.088	0.690/−0.056	**0.004/0.228**
K	**0.007/0.118**	0.150/0.080	0.340/0.053	0.431/0.006
Mg	**0.002/0.156**	**0.002/0.350**	0.646/−0.075	0.158/0.103
Fe	**0.001/0.238**	**0.047/0.136**	0.494/−0.027	0.404/0.007
Al	**0.001/0.225**	**0.020/0.165**	0.347/0.029	0.356/0.023
As	0.878/−0.049	0.627/−0.042	0.143/0.146	0.776/−0.078
B	0.549/−0.012	0.269/0.033	0.299/0.031	0.784/−0.079
Ba	**0.001/0.287**	**0.012/0.196**	**0.001/0.467**	0.261/0.044
Cd	0.461/0.001	0.553/−0.030	**0.017/0.362**	0.514/−0.019
Co	**0.001/0.245**	**0.012/0.187**	0.414/0.013	0.491/−0.011
Cr	**0.001/0.295**	**0.011/0.201**	0.421/−0.012	0.455/−0.003
Cu	0.317/0.017	0.627/−0.037	0.591/−0.071	0.971/−0.156
Ga	**0.001/0.270**	**0.009/0.206**	0.342/0.008	0.215/0.064
Ge	0.200/0.033	0.072/0.144	0.322/−0.008	0.969/−0.125
Hg	**0.001/0.167**	0.159/0.072	0.417/−0.009	0.326/0.024
Li	0.259/0.022	0.475/−0.002	0.332/0.035	0.148/0.101
Mn	**0.001/0.218**	0.062/0.121	0.337/0.026	0.266/0.047
Ni	**0.004/0.167**	**0.025/0.158**	0.462/−0.021	0.216/0.072
Pt	0.918/−0.056	0.454/−0.025	0.524/−0.044	0.574/−0.047
Sr	0.417/0.004	0.177/0.064	0.712/−0.064	**0.001/0.433**
Ti	**0.001/0.282**	**0.009/0.225**	0.225/0.079	0.195/0.062
Zn	0.813/−0.041	0.931/−0.092	0.979/−0.117	0.837/−0.110
Rb	0.136/0.051	0.398/0.01	0.094/0.178	0.139/0.097
TCE	0.985/−0.076	0.899/−0.084	0.177/0.099	0.091/0.122
pH	0.779/−0.035	0.849/−0.07	0.396/0.015	0.390/0.016
Moisture	**0.004/0.158**	0.057/0.101	**0.005/0.275**	0.281/0.043
Longitude	**0.020/0.129**	**0.006/0.162**	0.930/−0.075	0.287/0.021
Latitude	**0.007/0.160**	**0.047/0.107**	0.836/−0.065	0.205/0.046

Shannon: the Shannon index; Chao1: the Chao1 estimator. Significant $P \leq 0.05$ are shown in bold. TCE represents the concentration of total elements.

richer in the soils than in the several salt-lake sediment samples.

Similarly, the community composition of fungi at the phylum level was distinct between the saline sediments and soils (**Figure 3B**). The relative abundances of Ascomycota varied greatly in the saline sediment samples (8–87%), while they were more consistent in the different soil samples (66–86%). Basidiomycota was more abundant in hypersaline sediments (9–60%) than in salinized soils (<3%), with the exception of sample W_1, which did not contain this group. Eukaryota inhabited all investigated sites but could not be assigned to any known group at the phylum level.

The PCoA analyses showed that prokaryotic (**Figure 4A**) and fungal (**Figure 4B**) communities in all samples were sorted by habitat, which was demonstrated by the community distributions at the phylum-level (**Figures 3A,B**). For example, the prokaryotic communities in hypersaline sediments were better separated along the PC1 axis, while these groups in saline soils were partly arrayed along the PC2 axis. The fungal communities in the sediments and saline soils exhibited the similar separation trend. Moreover, prokaryotic and fungal communities from the same saline pools or plots tended to be assembled together.

Effects of Environmental Factors on Microbial Alpha Diversity

The rarefaction curves for all samples approached the saturation plateau (Supplementary Figure S1), indicating that the sequencing depths for each sample were sufficient to cover the microbial diversity. The species diversity of the prokaryotic community was higher in the soil samples than in the corresponding hypersaline sediments; the fungal community showed similar trends, with the exception of samples G3, Y13, and Y31 (Supplementary Table S4). In addition, species diversity of prokaryotic and fungal microbes was highly variable in the hypersaline sediment samples, with OTUs ranging from 74 to 2,394 and 12 to 366, respectively.

The Pearson's analyses showed that the alpha-diversity of prokaryotic and fungal communities was influenced differently by macroelements (**Table 1**). The macroelements S ($P = 0.001$, $r = 0.562$ and 0.610, respectively), Mg ($P = 0.002$, $r = 0.156$ and 0.350, respectively) and Fe ($P \leq 0.047$, $r = 0.238$ and 0.136, respectively) were significantly correlated with the Chao1 (species richness) and Shannon (diversity and evenness) indices of the prokaryotic community. Meanwhile, P ($P = 0.021$, $r = 0.100$) and K ($P = 0.007$, $r = 0.118$) were positively correlated with the Chao1 index of these groups. In contrast, Ca ($P = 0.004$, $r = 0.228$) correlated with the Shannon index of the fungal community.

As shown in **Table 1**, the microelements had a greater effect on the species diversity of prokaryotic assemblages than on those of fungal communities. The microelements (Al, Ba, Co, Cr, Ga, Ni, and Ti) were significantly correlated with the Chao1 ($P \leq 0.004$, $r = 0.231 \pm 0.064$) and Shannon indices ($P \leq 0.025$, $r = 0.192 \pm 0.033$) of the prokaryotic community. Concentrations of Hg and Mn significantly influenced the Chao1 of prokaryotic taxa ($P = 0.001$, $r = 0.167$ and 0.218, respectively). However, for the fungal community, Ba and Cd were positively related to Chao1 ($P \leq 0.017$, $r = 0.467$ and 0.362, respectively), and Sr was significantly correlated with Shannon index ($P = 0.001$, $r = 0.433$) as well.

Of other environmental variables, moisture was significantly correlated with the Chao1 index of the prokaryotic and fungal communities ($P \leq 0.005$, $r = 0.158$ and 0.275, respectively). And, longitude and latitude were linked to the Chao1 ($P \leq 0.020$, $r = 0.129$ and 0.160, respectively) and Shannon indices ($P \leq 0.047$, $r = 0.162$ and 0.107, respectively) of the prokaryotic assemblages.

Effects of Environmental Factors on Microbial Beta Diversity

The CCA results showed significant correlations ($P \leq 0.05$) between macro and microelements (e.g., Na, S, P, Ca, Ba, Cr, and Ge) and the prokaryotic microbial assemblages (**Figure 5A**), indicating that these geochemical parameters have strong impacts on the composition of the prokaryotic communities. In contrast, the CCA analysis also indicated that the trends of the factors, e.g., S, P, Ca, Cr, Cu, and moisture, correlated with the two axes and that these nutrient components significantly influenced the fungal community structures ($P \leq 0.05$) (**Figure 5B**).

The PerMANOVA results indicated that the compositions of the prokaryotic communities in all samples were strongly driven by macroelements, including Na, S, P and Ca, with *P*-values ranging from 0.001 to 0.023 and r^2-values ranging from 0.036 to 0.192. They were influenced by microelements As, Ba, Cr, Cu, Ge and Zn, with *P*-values varying from 0.001 to 0.048 and r^2-values varying from 0.030 to 0.075. In addition, pH ($P = 0.049$, $r^2 = 0.031$) correlated significantly with the compositions of the prokaryotic communities (**Table 2**). However, the fungal community structures were significantly influenced by the macroelements, including Na ($P = 0.007$, $r^2 = 0.041$), S ($P = 0.001$, $r^2 = 0.074$), P ($P = 0.004$, $r^2 = 0.043$), Ca ($P = 0.016$, $r^2 = 0.036$), and K ($P = 0.003$, $r^2 = 0.043$), and by the microelements Cr ($P = 0.006$, $r^2 = 0.039$) and Cu ($P = 0.008$, $r^2 = 0.039$). Latitude shaped the compositions of fungal communities ($P = 0.038$, $r^2 = 0.033$) (**Table 2**).

Determinants of the Microbial Community Composition

Variance partitioning analyses were used to further quantify the relative effects of environmental factors on prokaryotic and fungal community structures. Macroelements (Na, S, P, and Ca),

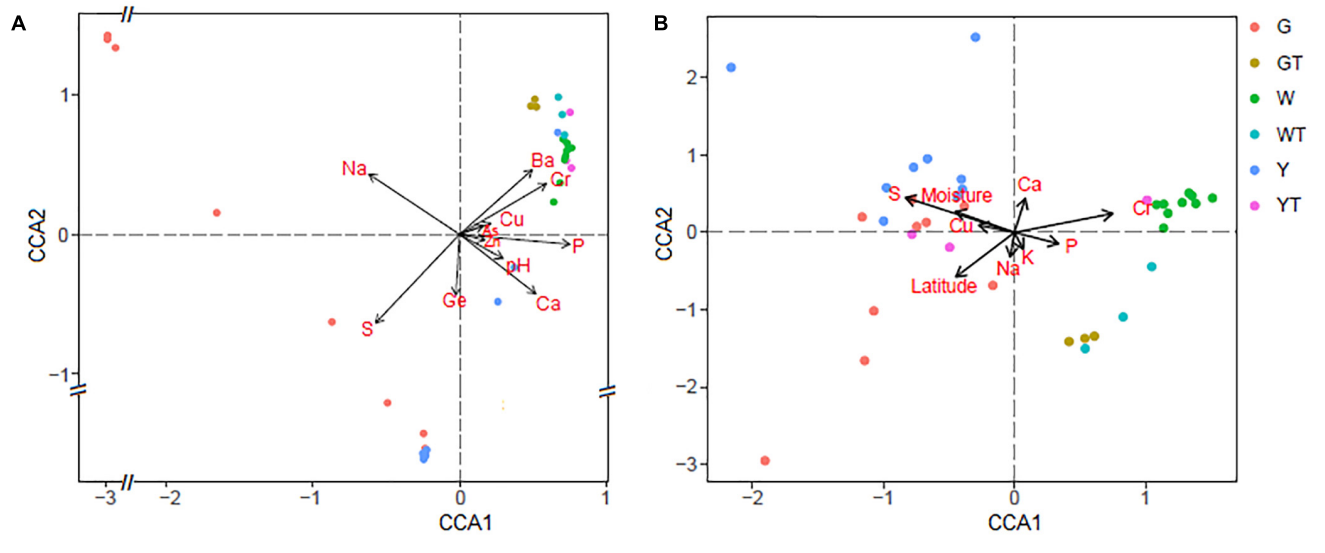

FIGURE 5 | Canonical correspondence analysis (CCA) of the prokaryotic **(A)** and fungal **(B)** communities with the significant variables ($P \leq 0.05$). G, Y, W, GT, YT, and WT represent microbial communities from Gouchi, Yuncheng, Luyang lakes, and the surrounding soils.

TABLE 2 | The PerMANOVA of the community compositions of prokaryotes and fungi with geochemical factors.

Factor	R^2	P
Prokaryotic community		
Na	0.092	**0.001**
S	0.191	**0.001**
P	0.047	**0.006**
Ca	0.036	**0.023**
Mg	0.007	0.846
As	0.040	**0.008**
B	0.019	0.251
Ba	0.031	**0.048**
Cr	0.036	**0.029**
Cu	0.030	**0.048**
Ge	0.034	**0.014**
Ni	0.017	0.277
Zn	0.075	**0.001**
pH	0.031	**0.049**
Moisture	0.031	0.066
Fungal community		
Na	0.041	**0.007**
S	0.074	**0.001**
P	0.043	**0.004**
Ca	0.036	**0.016**
K	0.043	**0.003**
Mg	0.027	0.117
Fe	0.029	0.088
Al	0.021	0.533
As	0.025	0.267
B	0.020	0.592
Ba	0.030	0.081
Cr	0.039	**0.006**
Cu	0.039	**0.008**
Ga	0.022	0.401
Ge	0.025	0.251
Hg	0.024	0.306
Li	0.021	0.534
Mn	0.027	0.171
Ni	0.030	0.073
Sr	0.026	0.194
Ti	0.026	0.169
Zn	0.021	0.531
Rb	0.026	0.170
TCE	0.020	0.593
pH	0.022	0.430
Moisture	0.032	0.051
Longitude	0.030	0.061
Latitude	0.033	**0.038**

Significant $P \leq 0.05$ are indicated in bold. TCE represents the concentration of total elements.

microelements (As, Ba, Cr, Cu, Ge and Zn) and pH contributed 19.34, 21.28, and 3.23% to the prokaryotic community variation, respectively. The combination of the significant geochemical variables (Na, S, P, Ca, As, Ba, Cr, Cu, Ge, Zn, and pH) ($P \leq 0.05$) explained 55.49% of the prokaryotic community variation, leaving 44.51% of the variation unexplained (**Figure 6A**). In contrast, macronutrients (Na, S, P, Ca, and K), trace elements (Cr and Cu), other variables (latitude and moisture) accounted for 17.13%, 6.93% and 6.79% of the prokaryotic community compositions, respectively. The combination of the significant environmental factors (Na, S, P, Ca, K, C, Cu, moisture and latitude) ($P \leq 0.05$) accounted for 32.27% of the observed variation in the fungal community, leaving 67.73% of the variation unexplained (**Figure 6B**).

DISCUSSION

In this study, we found that the average diversity index (Shannon index) of prokaryotes and fungi in the hypersaline sediments of salt lakes was consistently lower than in the adjacent saline–alkaline soils, and examined a noticeable decreasing trend in average species richness (Chao1 index) of the microbial communities in the hypersaline sediments (Supplementary Table S4), suggesting that the extreme saline environments harbor the lowest alpha-diversity of prokaryotes and fungi. It was agreed well with the general principle for ecology that microbial diversity is low in extreme habitats (Benlloch et al., 2002; Pavloudi et al., 2017). Furthermore, we found that the species richness and diversity of prokaryotes and fungi in the sediments drastically changed but remained relatively constant in the soils. This fluctuation of alpha-diversity indices might be caused by geochemical variations in the hypersaline sediments (Supplementary Table S1).

As expected, prokaryotic and fungal communities in hypersaline sediments and saline soils exhibited a habitat-dependent distribution pattern. Proteobacteria dominated hypersaline sediments (except for G_1), whereas many classes, such as Proteobacteria, Actinobacteria, Chloroflexi and Acidobacteria, were relatively evenly distributed in the saline soils (**Figure 3A**). Some groups of Proteobacteria widely occupied hypersaline habitats (Hollister et al., 2010; Quaiser et al., 2011; Kambura et al., 2016). Similarly, Ascomycota dominated the fungal communities in the soil samples, while its abundance varied obviously in the sediments. Basidiomycota were more abundant in the various hypersaline sediments and less in the soils (**Figure 3B**). Notably, prokaryotic and fungal communities were similar to each other when their habitats (hypersaline sediments versus saline soils) were similar, even if geographic distance between sample sites was greater, suggesting that habitat types play an important role in driving the microbial beta diversity.

The findings in this study demonstrate that the macroelements S, P, K, Mg, and Fe were drivers of the alpha-diversity of the prokaryotic communities in the salt-lake sediments and saline soils ($P \leq 0.05$) (**Table 1**). Previous reports have mainly addressed that elements K^+, S^{2-}, and Mg^{2+} determine the species richness of archaeal communities in a hypersaline lake (Podell et al., 2014), and that K^+, Mg^{2+}, and total P affect the OTU richness of soil bacterial groups such as Chloroflexi, Actinobacteria, Proteobacteria, and Bacteroidetes (Kim et al., 2016; Xia et al., 2016). Aside from the macronutrients (S, P, K, and Mg) associated

with the diversity, we also explored the importance of Fe driving the prokaryotic alpha diversity. Here, we only analyzed the correlation of Ca ($P = 0.004$) with the Shannon index of the fungi in saline habitats (**Table 1**). Ca as well was found to regulate global soil fungal diversity (Tedersoo et al., 2014). It might be because Ca^{2+}-mediated signals pathways are indispensable for eukaryotes' life processes including salt-stress tolerance (Shi et al., 2011; Asano et al., 2012; An et al., 2014). In contrast, K^+ is crucial to the survival of halotolerant and halophilic prokaryotes in saline environments because these microbes concentrate K^+ inside cells to maintain their abundance (Edbeib et al., 2016). This could partially explain why the alpha-diversity of prokaryotes and fungi in saline habitats are driven by different macroelements.

Studies have showed that the geochemical conditions of habitats govern microbial community compositions (Wang et al., 2013, 2017; Hazard et al., 2014; Oloo et al., 2016). Here, we observed that macroelements (Na, S, P, and Ca) shaped prokaryotic community compositions across the studied sites ($P \leq 0.05$) (**Table 2**). These macroelements explained 19.34% of the total variation in prokaryotic community structures (**Figure 6A**). The significance of Na, S, and Ca concentrations for bacterial community structures has been suggested by research conducted on the mine tailings and salt lakes of the Tibetan Plateau (Valentín-Vargas et al., 2014; Zhong et al., 2016). We showed that Na, S, P, Ca, and K were significantly correlated with fungal community compositions (**Table 2**) and that these macronutrients explained 17.13% of the total variation (**Figure 6B**). S, P, and Ca were found to regulate fungal community compositions in a variety of soil habitats (Jie et al., 2012; Tedersoo et al., 2014), however, K and Na as drivers of fungal beta diversity were rarely reported in previous studies. Macroelements are responsible for multiple microbial processes, such as the synthesis of biological macromolecules, signal transduction and osmotic balance (Dominguez, 2004; Jung and Bahn, 2009; Madigan et al., 2009; Edbeib et al., 2016); thus, they play a crucial role in driving the community composition of prokaryotes and fungi.

We revealed a series of microelements (Al, Ba, Co, Cr, Ga, Hg, Mn, Ni, and Ti) influencing the alpha-diversity of prokaryotes (**Table 1**). As shown in previous studies, metal elements Al, Cr, Hg, Mn, and Ni shape the species richness of bacteria in soils or in marine sediments (Faoro et al., 2010; Liu Y.R. et al., 2014; Pereira et al., 2014; Quero et al., 2015; Zhang et al., 2015), but correlations between microchemicals (Ba, Co, Ga, and Ti) and prokaryotic alpha diversity had not been previously discerned. Although some microelements (e.g., Co, Cr, Hg, and Mn) are toxic to life, microchemicals with a suitable content serve as electron donors or acceptors and enzymatic activators of bacterial cells (Stolz et al., 2006; Huang et al., 2015; Wintsche et al., 2016). What' more, it is known that diverse prokaryotes tolerate the effects of certain metals, and that microbial assemblages are significantly more resistant to heavy metals than pure cultures (Oregaard and Sørensen, 2007; Mejias Carpio et al., 2018). Therefore, microelements might be not toxic and instead be

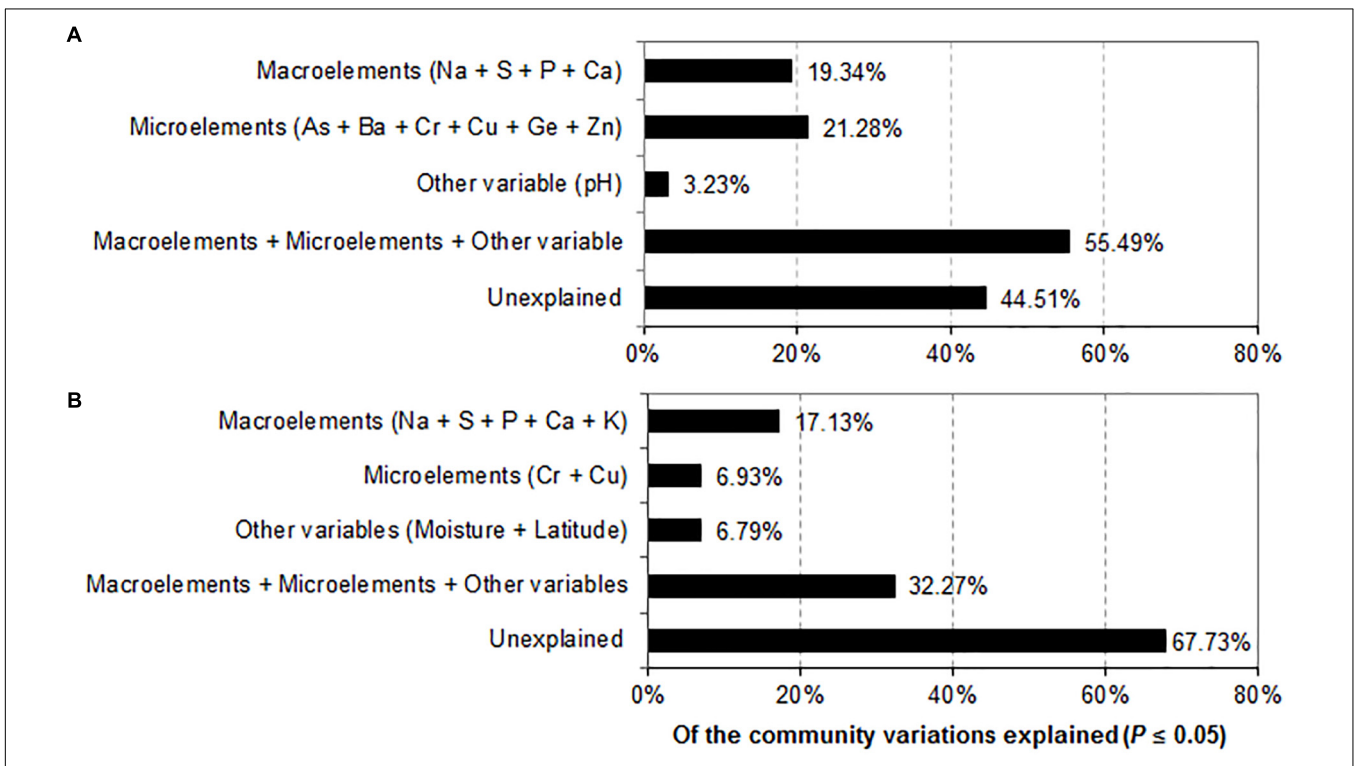

FIGURE 6 | Variance partitioning analysis (VPA) demonstrating the effects of environmental factors on the variation of the prokaryotic **(A)** and fungal **(B)** community compositions.

drivers of alpha-diversity of prokaryotic groups. Moreover, one study has shown that deep-sea hydrothermal sediments, rich in metal elements such as Ba and Sr, harbored the highest level of species diversity and phylogenetic uniqueness for eukaryotes (López-García et al., 2003), suggesting that some microelements could modulate fungal alpha-diversity. Here, our results showed that Ba correlated with the species richness of fungi ($P = 0.001$), while Sr correlated with the Shannon diversity, highlighting the importance of alkali-metal elements for the fungal alpha-diversity.

Similarly, microelements explained the variations in prokaryotic community composition (**Table 2**). For example, the elements As, Ba, Cr, Cu, Ge, and Zn significantly contributed to the differences in prokaryotic community structures in both hypersaline sediments and saline soils. Our findings are supported by research showing that microelements, including As, Cr, Cu, and Zn, affected bacterial community structures in coastal sediments and metal-rich soils (Quero et al., 2015; Reith et al., 2015). The combined microelements (As, Ba, Cr, Cu, Ge, and Zn) and variables (Cr and Cu) individually explained 21.28% and 6.93% of the total variation in community structures of prokaryotes and fungi (**Figure 6**), indicating the relative importance of micronutrients in modulating prokaryotic composition. Together, the alpha and beta-diversities of prokaryotes were more widely influenced by macro and microelements as compared to fungi, suggesting that geochemical element profiles could better predict the diversity and community compositions of prokaryotes.

Furthermore, we observed that variables including moisture, longitude and latitude had relationships with the species richness and community compositions of prokaryotes and fungi, supported by previously published accounts (Talley et al., 2002; Tedersoo et al., 2014; Ding et al., 2015; Shay et al., 2015). However, it should be noted that given terrestrial coordinates determine the specific geochemical characteristics, which could have direct effects on microbial diversity and community composition. Moreover, latitudes, on a broad scale, are related to temperature, which is a well-known controller of the primary productivities and nutrient uptake of cells (Fuhrman et al., 2008). The diversity and community compositions of prokaryotes and fungi were driven by different variables, suggesting that distinct mechanisms are involved in the maintenance and succession of these two communities.

CONCLUSION

We found that the prokaryotic and fungal community compositions in hypersaline sediments and saline–alkaline soils exhibited habitat-dependent patterns. We explored the concept that the diversity and composition of prokaryotic and fungal communities were driven by different macro and microelements. We also found that the diversity and composition of prokaryotes were more widely influenced by geochemical elements than those of fungal communities. Geochemistry selects unique microbial communities and, conversely, microbes drive geochemical cycles. Further studies could focus on the functional microbial communities involved in geochemical recycling in hypersaline environments.

AUTHOR CONTRIBUTIONS

KL and XD collected the samples and designed the research. KL, XD, and XT produced the data. KL, XD, JW, WL, QY, and ZL performed the data analysis. KL and XD wrote the manuscript.

FUNDING

This work was financed by the National Natural Science Foundation of China (No. 31100017), Program of Agricultural Scientific and Technological Innovation of Shaanxi Province (S2018-YF-YBNY-0042), and Shaanxi University of Technology (SLGQD16-06 and SLGQD16-07). The manuscript has been linguistically edited by Natalie Kaplan, Johns Hopkins University.

ACKNOWLEDGMENTS

We are especially grateful to the editor and reviewers for their valuable comments on the manuscript.

SUPPLEMENTARY MATERIAL

The Supplementary Material for this article can be found online at: https://www.frontiersin.org/articles/10.3389/fmicb.2018.00352/full#supplementary-material

REFERENCES

An, B., Chen, Y., Li, B., Qin, G., and Tian, S. (2014). Ca^{2+}-CaM regulating viability of *Candida guilliermondii* under oxidative stress by acting on detergent resistant membrane proteins. *J. Proteomics* 109, 38–49. doi: 10.1016/j.jprot.2014.06.022

Andrei, A. S., Robeson, M. S. II, Baricz, A., Coman, C., Muntean, V., Ionescu, A., et al. (2015). Contrasting taxonomic stratification of microbial communities in two hypersaline meromictic lakes. *ISME J.* 9, 2642–2656. doi: 10.1038/ismej.2015.60

Arslan, Z., and Tyson, J. F. (2008). Determination of trace elements in siliceous samples by ICP-MS after precipitation of silicon as sodium fluorosilicate. *Mikrochim. Acta* 160, 219–225. doi: 10.1007/s00604-007-0809-9

Asano, T., Hayashi, N., Kobayashi, M., Aoki, N., Miyao, A., Mitsuhara, I., et al. (2012). A rice calcium-dependent protein kinase OsCPK12 oppositely modulates salt-stress tolerance and blast disease resistance. *Plant J.* 69, 26–36. doi: 10.1111/j.1365-313X.2011.04766.x

Benlloch, S., López-López, A., Casamayor, E. O., Øvreås, L., Goddard, V., Daae, F. L., et al. (2002). Prokaryotic genetic diversity throughout the salinity gradient of a coastal solar saltern. *Environ. Microbiol.* 4, 349–360. doi: 10.1046/j.1462-2920.2002.00306.x

Bryanskaya, A. V., Malup, T. K., Lazareva, E. V., Taran, O. P., Rozanov, A. S., Efimov, V. M., et al. (2016). The role of environmental factors for the composition of microbial communities of saline lakes in the Novosibirsk region (Russia). *BMC Microbiol.* 16(Suppl. 1):4. doi: 10.1186/s12866-015-0618-y

Caporaso, J. G., Kuczynski, J., Stombaugh, J., Bittinger, K., Bushman, F. D., Costello, E. K., et al. (2010). QIIME allows analysis of high-throughput community sequencing data. *Nat. Methods* 7, 335–336. doi: 10.1038/nmeth.f.303

Caporaso, J. G., Lauber, C. L., Walters, W. A., Berg-Lyons, D., Lozupone, C. A., Turnbaugh, P. J., et al. (2011). Global patterns of 16S rRNA diversity at a depth of millions of sequences per sample. *Proc. Natl. Acad. Sci. U.S.A.* 108, 4516–4522. doi: 10.1073/pnas.1000080107

Ding, X., Peng, X. J., Jin, B. S., Xiao, M., Chen, J. K., Li, B., et al. (2015). Spatial distribution of bacterial communities driven by multiple environmental factors in a beach wetland of the largest freshwater lake in China. *Front. Microbiol.* 6:129. doi: 10.3389/fmicb.2015.00129

Dominguez, D. C. (2004). Calcium signalling in bacteria. *Mol. Microbiol.* 54, 291–297. doi: 10.1111/j.1365-2958.2004.04276.x

Edbeib, M. F., Wahab, R. A., and Huyop, F. (2016). Halophiles: biology, adaptation, and their role in decontamination of hypersaline environments. *World J. Microbiol. Biotechnol.* 32:135. doi: 10.1007/s11274-016-2081-9

Edgar, R. C. (2013). UPARSE: highly accurate OTU sequences from microbial amplicon reads. *Nat. Methods* 10, 996–998. doi: 10.1038/nmeth.2604

Faoro, H., Alves, A. C., Souza, E. M., Rigo, L. U., Cruz, L. M., Al-Janabi, S. M., et al. (2010). Influence of soil characteristics on the diversity of bacteria in the Southern Brazilian Atlantic forest. *Appl. Environ. Microbiol.* 76, 4744–4749. doi: 10.1128/AEM.03025-09

Fernandez, A. B., Rasuk, M. C., Visscher, P. T., Contreras, M., Novoa, F., Poire, D. G., et al. (2016). Microbial diversity in sediment ecosystems (evaporites domes, microbial mats, and crusts) of hypersaline laguna Tebenquiche, Salar de Atacama, Chile. *Front. Microbiol.* 7:1284. doi: 10.3389/fmicb.2016.01284

Fuhrman, J. A., Steele, J. A., Hewson, I., Schwalbach, M. S., Brown, M. V., Green, J. L., et al. (2008). A latitudinal diversity gradient in planktonic marine bacteria. *Proc. Natl. Acad. Sci. U.S.A.* 105, 7774–7778. doi: 10.1073/pnas.0803070105

Gardes, M., and Bruns, T. (1993). ITS primers with enhanced specificity for basidiomycetes–application to the identification of mycorrhizae and rusts. *Mol. Ecol.* 2, 113–118. doi: 10.1111/j.1365-294x.1993.tb00005.x

Hallsworth, J. E., Yakimov, M. M., Golyshin, P. N., Gillion, J. L., D'Auria, G., de Lima Alves, F., et al. (2007). Limits of life in MgCl2-containing environments: chaotropicity defines the window. *Environ. Microbiol.* 9, 801–813. doi: 10.1111/j.1462-2920.2006.01212.x

Hazard, C., Gosling, P., Mitchell, D. T., Doohan, F. M., and Bending, G. D. (2014). Diversity of fungi associated with hair roots of ericaceous plants is affected by land use. *FEMS Microbiol. Ecol.* 87, 586–600. doi: 10.1111/1574-6941.12247

Hollister, E. B., Engledow, A. S., Hammett, A. J., Provin, T. L., Wilkinson, H. H., and Gentry, T. J. (2010). Shifts in microbial community structure along an ecological gradient of hypersaline soils and sediments. *ISME J.* 4, 829–838. doi: 10.1038/ismej.2010.3

Huang, L., Wang, Q., Jiang, L., Zhou, P., Quan, X., and Logan, B. E. (2015). Adaptively evolving bacterial communities for complete and selective reduction of Cr(VI), Cu(II), and Cd(II) in biocathode bioelectrochemical systems. *Environ. Sci. Technol.* 49, 9914–9924. doi: 10.1021/acs.est.5b00191

Jiang, H., Dong, H., Yu, B., Liu, X., Li, Y., Ji, S., et al. (2007). Microbial response to salinity change in Lake Chaka, a hypersaline lake on Tibetan Plateau. *Environ. Microbiol.* 9, 2603–2621. doi: 10.1111/j.1462-2920.2007.01377.x

Jiang, Z., Li, P., Van Nostrand, J. D., Zhang, P., Zhou, J., Wang, Y., et al. (2016). Microbial communities and arsenic biogeochemistry at the outflow of an alkaline sulfide-rich hot spring. *Sci. Rep.* 6:25262. doi: 10.1038/srep25262

Jie, W., Cai, B., Zhang, Y., Li, J., and Ge, J. (2012). The effect of sulfur on the composition of arbuscular mycorrhizal fungal communities during the pod-setting stage of different soybean cultivars. *Curr. Microbiol.* 65, 500–506. doi: 10.1007/s00284-012-0183-7

Jung, K. W., and Bahn, Y. S. (2009). The stress-activated signaling (SAS) pathways of a human fungal pathogen, *Cryptococcus neoformans*. *Mycobiology* 37, 161–170. doi: 10.4489/MYCO.2009.37.3.161

Kambura, A. K., Mwirichia, R. K., Kasili, R. W., Karanja, E. N., Makonde, H. M., and Boga, H. I. (2016). Bacteria and Archaea diversity within the hot springs of Lake Magadi and little Magadi in Kenya. *BMC Microbiol.* 1:136. doi: 10.1186/s12866-016-0748-x

Kim, J. M., Roh, A. S., Choi, S. C., Kim, E. J., Choi, M. T., Ahn, B. K., et al. (2016). Soil pH and electrical conductivity are key edaphic factors shaping bacterial communities of greenhouse soils in Korea. *J. Microbiol.* 54, 838–845. doi: 10.1007/s12275-016-6526-5

Liang, Y., Zhao, H., Zhang, X., Zhou, J., and Li, G. (2014). Contrasting microbial functional genes in two distinct saline-alkali and slightly acidic oil-contaminated sites. *Sci. Total Environ.* 487, 272–278. doi: 10.1016/j.scitotenv.2014.04.032

Liu, K., Ding, X., Wang, H. F., Zhang, X., Hozzein, W. N., Wadaan, M. A., et al. (2014). Eukaryotic microbial communities in hypersaline soils and sediments from the alkaline hypersaline Huama Lake as revealed by 454 pyrosequencing. *Antonie Van Leeuwenhoek* 105, 871–880. doi: 10.1007/s10482-014-0141-4

Liu, Y. R., Wang, J. J., Zheng, Y. M., Zhang, L. M., and He, J. Z. (2014). Patterns of bacterial diversity along a long-term mercury-contaminated gradient in the paddy soils. *Microb. Ecol.* 68, 575–583. doi: 10.1007/s00248-014-0430-5

López-García, P., Philippe, H., Gail, F., and Moreira, D. (2003). Autochthonous eukaryotic diversity in hydrothermal sediment and experimental microcolonizers at the Mid-Atlantic Ridge. *Proc. Natl. Acad. Sci. U.S.A.* 100, 697–702. doi: 10.1073/pnas.0235779100

Madigan, M. T., Martinko, J. M., Dunlap, P. V., and Clark, D. P. (2009). "Nutrition and cultures of microorganisms," in *Brock Biology of Microorganisms*, 12th Edn (San Francisco, CA: Benjamin-Cummings Publishing Company), 108–140.

Mejias Carpio, I. E., Ansari, A., and Rodrigues, D. F. (2018). Relationship of biodiversity with heavy metal tolerance and sorption capacity: a meta-analysis approach. *Environ. Sci. Technol.* 52, 184–194. doi: 10.1021/acs.est.7b04131

Nunoura, T., Nishizawa, M., Kikuchi, T., Tsubouchi, T., Hirai, M., Koide, O., et al. (2013). Molecular biological and isotopic biogeochemical prognoses of the nitrification-driven dynamic microbial nitrogen cycle in hadopelagic sediments. *Environ. Microbiol.* 15, 3087–3107. doi: 10.1111/1462-2920.12152

Oloo, F., Valverde, A., Quiroga, M. V., Vikram, S., Cowan, D., and Mataloni, G. (2016). Habitat heterogeneity and connectivity shape microbial communities in South American peatlands. *Sci. Rep.* 6:25712. doi: 10.1038/srep25712

Oregaard, G., and Sørensen, S. J. (2007). High diversity of bacterial mercuric reductase genes from surface and sub-surface floodplain soil (Oak Ridge. USA). *ISME J.* 1, 453–467. doi: 10.1038/ismej.2007.56

Oren, A. (2002). Molecular ecology of extremely halophilic Archaea and Bacteria. *FEMS Microbiol. Ecol.* 39, 1–7. doi: 10.1111/j.1574-6941.2002.tb00900.x

Oren, A. (2013). "Life at high salt concentrations," in *The Prokaryotes–Prokaryotic Communities And Ecophysiology*, 4th Edn, eds E. Rosenberg, E. F. DeLong, F. Thompson, S. Lory, E. Stackebrandt (Berlin: Springer-Verlag), 421–440.

Pavloudi, C., Kristoffersen, J. B., Oulas, A., De Troch, M., and Arvanitidis, C. (2017). Sediment microbial taxonomic and functional diversity in a natural salinity gradient challenge Remane's "species minimum" concept. *PeerJ* 5:e3687. doi: 10.7717/peerj.3687

Pereira, L. B., Vicentini, R., and Ottoboni, L. M. (2014). Changes in the bacterial community of soil from a neutral mine drainage channel. *PLoS One* 9:e96605. doi: 10.1371/journal.pone.0096605

Podell, S., Emerson, J. B., Jones, C. M., Ugalde, J. A., Welch, S., Heidelberg, K. B., et al. (2014). Seasonal fluctuations in ionic concentrations drive microbial succession in a hypersaline lake community. *ISME J.* 8, 979–990. doi: 10.1038/ismej.2013.221

Quaiser, A., Zivanovic, Y., Moreira, D., and López-García, P. (2011). Comparative metagenomics of bathypelagic plankton and bottom sediment from the Sea of Marmara. *ISME J.* 5, 285–304. doi: 10.1038/ismej.2010.113

Quast, C., Pruesse, E., Yilmaz, P., Gerken, J., Schweer, T., Yarza, P., et al. (2013). The SILVA ribosomal RNA gene database project: improved data processing and web-based tools. *Nucleic Acids Res.* 41, 590–596. doi: 10.1093/nar/gks1219

Quero, G. M., Cassin, D., Botter, M., Perini, L., and Luna, G. M. (2015). Patterns of benthic bacterial diversity in coastal areas contaminated by heavy metals, polycyclic aromatic hydrocarbons (PAHs) and polychlorinated biphenyls (PCBs). *Front. Microbiol.* 6:1053. doi: 10.3389/fmicb.2015.01053

Reith, F., Zammit, C. M., Pohrib, R., Gregg, A. L., and Wakelin, S. A. (2015). Geogenic factors as drivers of microbial community diversity in soils overlying polymetallic deposits. *Appl. Environ. Microbiol.* 81, 7822–7832. doi: 10.1128/AEM.01856-15

Sandroni, V., and Smith, C. M. M. (2002). Microwave digestion of sludge, soil and sediment samples for metal analysis by inductively coupled plasma-atomic emission spectrometry. *Anal. Chim. Acta* 468:335. doi: 10.1016/S0003-2670(02)00655-4

Shay, P. E., Winder, R. S., and Trofymow, J. A. (2015). Nutrient-cycling microbes in coastal Douglas-fir forests: regional-scale correlation between communities, in situ climate, and other factors. *Front. Microbiol.* 6:1097. doi: 10.3389/fmicb.2015.01097

Shi, S., Chen, W., and Sun, W. (2011). Comparative proteomic analysis of the Arabidopsis cbl1 mutant in response to salt stress. *Proteomics* 11, 4712–4725. doi: 10.1002/pmic.201100042

Sorokin, D. Y., Banciu, H. L., and Muyzer, G. (2015). Functional microbiology of soda lakes. *Curr. Opin. Microbiol.* 25, 88–96. doi: 10.1016/j.mib.2015.05.004

Stolz, J. F., Basu, P., Santini, J. M., and Oremland, R. S. (2006). Arsenic and selenium in microbial metabolism. *Annu. Rev. Microbiol.* 60, 107–130. doi: 10.1146/annurev.micro.60.080805.142053

Sun, H., Terhonen, E., Kovalchuk, A., Tuovila, H., Chen, H., Oghenekaro, A. O., et al. (2016). Dominant tree species and soil type affect the fungal community structure in a boreal peatland forest. *Appl. Environ. Microbiol.* 82, 2632–2643. doi: 10.1128/AEM.03858-15

Talley, S. M., Coley, P. D., and Kursar, T. A. (2002). The effects of weather on fungal abundance and richness among 25 communities in the Intermountain West. *BMC Ecol.* 2:7. doi: 10.1186/1472-6785-2-7

Tedersoo, L., Bahram, M., Põlme, S., Kõljalg, U., Yorou, N. S., Wijesundera, R., et al. (2014). Fungal biogeography. Global diversity and geography of soil fungi. *Science* 346:1256688. doi: 10.1126/science.1256688

Valentín-Vargas, A., Root, R. A., Neilson, J. W., Chorover, J., and Maier, R. M. (2014). Environmental factors influencing the structural dynamics of soil microbial communities during assisted phytostabilization of acid-generating mine tailings: a mesocosm experiment. *Sci. Total Environ.* 500–501, 314–324. doi: 10.1016/j.scitotenv.2014.08.107

Wang, J., Shen, J., Wu, Y., Tu, C., Soininen, J., Stegen, J. C., et al. (2013). Phylogenetic beta diversity in bacterial assemblages across ecosystems: deterministic versus stochastic processes. *ISME J.* 7, 1310–1321. doi: 10.1038/ismej.2013.30

Wang, Q., Garrity, G. M., Tiedje, J. M., and Cole, J. R. (2007). Naive Bayesian classifier for rapid assignment of rRNA sequences into the new bacterial taxonomy. *Appl. Environ. Microbiol.* 73, 5261–5267. doi: 10.1128/AEM.00062-07

Wang, X. B., Lü, X. T., Yao, J., Wang, Z. W., Deng, Y., Cheng, W. X., et al. (2017). Habitat-specific patterns and drivers of bacterial β-diversity in China's drylands. *ISME J.* 11, 1345–1358. doi: 10.1038/ismej.2017.11

White, T. J., Bruns, T., Lee, S., and Taylor, J. W. (1990). "Amplification and direct sequencing of fungal ribosomal RNA genes for phylogenetics," in *PCR Protocols, a Guide to Methods and Applications*, eds M. A. Innis, D. H. Gelfand, J. J. Sninsky, and T. J. White (New York, NY: Academic Press), 315–322.

Wintsche, B., Glaser, K., Sträuber, H., Centler, F., Liebetrau, J., Harms, H., et al. (2016). Trace elements induce predominance among methanogenic activity in anaerobic digestion. *Front. Microbiol.* 7:2034. doi: 10.3389/fmicb.2016.02034

Xia, Z., Bai, E., Wang, Q., Gao, D., Zhou, J., Jiang, P., et al. (2016). Biogeographic distribution patterns of bacteria in typical Chinese forest soils. *Front. Microbiol.* 7:1106. doi: 10.3389/fmicb.2016.01106

Xie, K., Deng, Y., Zhang, S., Zhang, W., Liu, J., Xie, Y., et al. (2017). Prokaryotic community distribution along an ecological gradient of salinity in surface and subsurface saline soils. *Sci. Rep.* 7:13332. doi: 10.1038/s41598-017-13608-5

Xiong, J., Liu, Y., Lin, X., Zhang, H., Zeng, J., Hou, J., et al. (2012). Geographic distance and pH drive bacterial distribution in alkaline lake sediments across Tibetan Plateau. *Environ. Microbiol.* 14, 2457–2466. doi: 10.1111/j.1462-2920.2012.02799.x

Yakimov, M. M., La Cono, V., Spada, G. L., Bortoluzzi, G., Messina, E., Smedile, F., et al. (2015). Microbial community of the deep-sea brine Lake Kryos seawater-brine interface is active below the chaotropicity limit of life as revealed by recovery of mRNA. *Environ. Microbiol.* 17, 364–382. doi: 10.1111/1462-2920.12587

Zhang, D. C., Liu, Y. X., and Li, X. Z. (2015). Characterization of bacterial diversity associated with deep sea ferromanganese nodules from the South China Sea. *J. Microbiol.* 53, 598–605. doi: 10.1007/s12275-015-5217-y

Zhong, Z. P., Liu, Y., Miao, L. L., Wang, F., Chu, L. M., Wang, J. L., et al. (2016). Prokaryotic community structure driven by salinity and ionic concentrations in Plateau Lakes of the Tibetan Plateau. *Appl. Environ. Microbiol.* 82, 1846–1858. doi: 10.1128/AEM.03332-15

Conflict of Interest Statement: The authors declare that the research was conducted in the absence of any commercial or financial relationships that could be construed as a potential conflict of interest.

frontiers in Microbiology

ORIGINAL RESEARCH
published: 07 March 2018
doi: 10.3389/fmicb.2018.00394

Ferric Sulfate and Proline Enhance Heavy-Metal Tolerance of Halophilic/Halotolerant Soil Microorganisms and Their Bioremediation Potential for Spilled-Oil Under Multiple Stresses

*Dina M. Al-Mailem, Mohamed Eliyas and Samir S. Radwan**

Microbiology Program, Department of Biological Sciences, Faculty of Science, Kuwait University, Safat, Kuwait

The aim of this study was to explore the heavy-metal resistance and hydrocarbonoclastic potential of microorganisms in a hypersaline soil. For this, hydrocarbonoclastic microorganisms were counted on a mineral medium with oil vapor as a sole carbon source in the presence of increasing concentrations of $ZnSO_4$, $HgCl_2$, $CdSO_4$, $PbNO_3$, $CuSO_4$, and Na_2HAsO_4. The colony-forming units counted decreased in number from about 150 g^{-1} on the heavy-metal-free medium to zero units on media with 40–100 mg l^{-1} of $HgCl_2$, $CdSO_4$, $PbNO_3$, or Na_2HAsO_4. On media with $CuSO_4$ or $ZnSO_4$ on the other hand, numbers increased first reaching maxima on media with 50 mg l^{-1} $CuSO_4$ and 90 mg l^{-1} $ZnSO_4$. Higher concentrations reduced the numbers, which however, still remained considerable. Pure microbial isolates in cultures tolerated 200–1600 mg l^{-1} of $HgCl_2$, $CdSO_4$, $PbNO_3$, $CuSO_4$, and Na_2HAsO_4 in the absence of crude oil. In the presence of oil vapor, the isolates tolerated much lower concentrations of the heavy metals, only 10–80 mg l^{-1}. The addition of 10 $Fe_2(SO_4)_3$ and 200 mg l^{-1} proline (by up to two- to threefold) enhanced the tolerance of several isolates to heavy metals, and consequently their potential for oil biodegradation in their presence. The results are useful in designing bioremediation technologies for oil spilled in hypersaline areas.

Keywords: bioremediation, haloarchaea, halophilic bacteria, heavy metals, hypersaline, environments, oil bioremediation

OPEN ACCESS

Edited by:
Hongchen Jiang,
China University of Geosciences, China

Reviewed by:
M. Oves,
King Abdulaziz University, Saudi Arabia
Karen Trchounian,
Yerevan State University, Armenia

****Correspondence:***
Samir S. Radwan
samir.radwan@ku.edu.kw

Specialty section:
This article was submitted to Extreme Microbiology, a section of the journal Frontiers in Microbiology

Received: *11 January 2018*
Accepted: *21 February 2018*
Published: *07 March 2018*

Citation:
Al-Mailem DM, Eliyas M and Radwan SS (2018) Ferric Sulfate and Proline Enhance Heavy-Metal Tolerance of Halophilic/Halotolerant Soil Microorganisms and Their Bioremediation Potential for Spilled-Oil Under Multiple Stresses. Front. Microbiol. 9:394. doi: 10.3389/fmicb.2018.00394

INTRODUCTION

Oil started to be extensively produced and used as energy and raw-material sources since about 80 years. This was associated with increasing rates of pollution of terrestrial, aquatic, and atmospheric environments with spilled oil, oil vapor, and processed oil products. It has been estimated that alone the marine environment is charged yearly with 10 Mt of hydrocarbon pollutants (Banerjee et al., 2006). As expected, pollution rates are particularly high in oil-producing countries such as the Arabian Gulf states. The Gulf water-body is used by vessels that carry about 50% of the marine-transported oil worldwide (Hunter, 1982). Those states

belong geographically to the semiarid region and are characterized by harsh climates. For example, the temperature in the small state of Kuwait during the long, dry summer frequently exceeds 50°C. Under such harsh conditions, oil bioremediation and self-cleaning via activities of nonextremophilic microorganisms are minimal (Margesin and Schinner, 2001; Oren, 2002). At such high temperatures, coastal seawaters trapped during tidal movement lose water by excessive evaporation, and the respective areas become thus hypersaline with NaCl concentrations reaching 4 M and higher. Like elsewhere (Lefebvre and Moletta, 2006), the hypersaline coastal areas in Kuwait are subjected to contamination with spilled oil. Bioremediation of such polluted areas cannot be achieved by nonextremophilic microorganisms (Pieper and Reineke, 2000; Oren, 2002); only halophilic/halotolerant microorganisms could be effective.

Halophilic/halotolerant microorganisms with hydrocarbon-utilization potential were recorded and isolated from hypersaline areas all over the globe (Oren et al., 1992; Emerson et al., 1994; Margesin and Schinner, 2001; Garcia et al., 2004; Nicholson and Fathepure, 2005; Zhao et al., 2009; Bonfa et al., 2011; Fathepure, 2014). Those hydrocarbonoclastic halophiles include prokaryotes (bacteria and archaea) and eukaryotes (yeasts and molds). Our group in Kuwait contributed to such studies and published extensive information on numbers, identities, and hydrocarbonoclastic potential of hydrocarbonoclastic microorganisms from hypersaline coastal areas in this region (Al-Mailem et al., 2012, 2014a). Emphasis was put on the feasibility of using these indigenous microorganisms in bioremediation and self-cleaning of local oil spills. The Gulf microorganisms naturally are stressed, not only by high salinity, harsh climatic conditions, and oil spills, but also by toxic heavy metals that may be associated with crude oil (Osuji and Onojake, 2004; Basumatary et al., 2012). Within this context, toxicity and resistance of heavy metals have been studied using predominantly nonextremophilic microorganisms (for review, see Nies, 1999). Those metals have a density above 5 g cm^{-3} (atomic weights > 50 amu) (Weast, 1984). They potentially form unspecific complex compounds in the cell which leads to toxicity. Yet, some heavy metals are essential trace elements. Two systems for heavy-metal uptake are known. The fast, unspecific system which is constitutively expressed; it depends solely on concentration gradient force. The second is the slow uptake system, with high substrate specificity in which ATP is consumed. Heavy-metal toxicity arises when the heavy-metal cations bind to SH groups leading to the inhibition of the activity of sensitive (especially respiratory) enzymes. Ions may also bind with O_2 leading to oxidative stress. Three mechanisms for heavy-metal resistance are known. The first involves the active extrusion (efflux) of ions from the cell. The second is the segregation of cations (especially the S-lovers) into complex compounds by thiol-containing molecules. Thirdly, metal ions may be reduced to a less toxic oxidation (sometimes volatile, e.g., Hg^o) state.

Within a research project on the bioremediation of oily hypersaline regions in Kuwait, we reported recently on biostimulation of pure, hydrocarbonoclastic microorganisms from those habitats by the addition of cations including Fe^{3+} (Al-Mailem et al., 2017). The major objective of this current study was to elaborate on the previous work by investigating the sensitivity and tolerance of the same microorganisms to common heavy metals, and to measure the effects of individual heavy metals on crude-oil removal by such microorganisms under salt stress. In other words, the main aim was jointly exploring the heavy-metal tolerance and hydrocarbon-degrading potential of novel halotolerant/halophilic isolates from hypersaline coastal soil in Kuwait. We started this study by counting the numbers of colony-forming units (CFU) of hydrocarbonoclastic, halophilic/halotolerant microorganisms for the hypersaline soil on media containing increasing concentrations of heavy metals. This part was followed by another one in which pure cultures from the hypersaline soil were used. It was also proposed to investigate whether or not, Fe^{3+} and proline (a compatible solute) may affect the microbial tolerance to the toxicity of individual heavy metals. Information gained from this research would help in designing biotechnologies for bioremediation of spilled oil in areas under multiple stresses. Within this context, our group recently found that calcium and dipicolinic acid (constituents of heat-tolerant endospores) biostimulated oil bioremediation under multiple stresses by heat, oil, and heavy metals (Radwan et al., 2017).

MATERIALS AND METHODS

Counting Heavy-Metal-Tolerant Microorganisms in Hypersaline Soil

The aim of this experiment was to study the inhibition pattern of increasing concentrations of heavy metals on the numbers of CFU of halophilic/halotolerant, hydrocarbonoclastic microorganisms counted by the dilution-plating method. A solid (1.5% agar) mineral medium with oil vapor as sole source of carbon and energy (Sorkhoh et al., 1990) was used, it had the following composition (g l^{-1}): 0.85 $NaNO_3$, 0.56 KH_2PO_4, 0.86 Na_2HPO_4, 0.17 K_2SO_4, 0.37 $MgSO_4.7H_2O$, 0.7 $CaCl_2.2H_2O$, 2.5 ml of a trace element mixture consisting of (g l^{-1}): 2.32 $ZnSO_4$, 1.78 $MnSO_4$, 0.56 H_3BO_3, 1.0 $CuSO_4$, 0.39 Na_2 MoO_4, 0.42 $CoCl_2$, 0.66 KI, 1.0 EDTA, 0.4 $FeSO_4$, 0.004 $NiCl_2$, pH 7.0. With oil vapor as a sole carbon and energy source, this medium obviously would support hydrocarbonoclastic microorganisms selectively. The medium salinity was adjusted to 2 M NaCl, and different concentrations of individual heavy-metal salts were added. Medium portions, 25 ml, were dispensed in sterile Petri dishes. After medium solidification at room temperature, inoculum aliquots, 0.25 ml [from down series of dilutions of the hypersaline soil (about 4 M NaCl) in sterile hypersaline water, about 3 M NaCl], were spread on the solid medium surfaces. Filter papers impregnated with 2 ml crude oil as source of oil vapor were fixed in dish lids, and the dishes were sealed. The heavy-metal salts tested were $HgCl_2$, $CdSO_4$, $PbNO_3$, $CuSO_4$, and Na_2HAsO_4 at concentrations from 0 (controls) to 300 mg l^{-1}. Three replicates for each soil dilution and heavy-metal concentration were prepared. The plates were incubated at 30°C for 12 days (d) and the CFUs were counted and the mean numbers per gram soil were calculated.

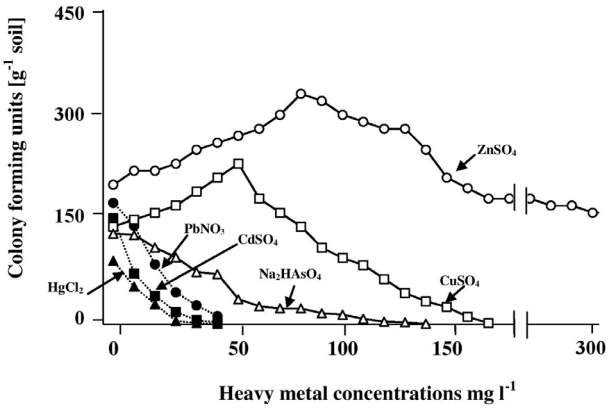

FIGURE 1 | Numbers of CFU of hydrocarbonoclastic microorganisms in hypersaline soil as determined by the dilution-plating method on heavy-metal containing mineral medium with oil vapor as a sole source of carbon and energy. The medium salinity was adjusted to 2 M NaCl (section "Materials and Methods"). The CFU numbers are obviously those of cultivable microorganism only.

Halophilic/Halotolerant, Hydrocarbonoclastic Microorganisms

Pure cultures of the four halophilic, hydrocarbonoclastic bacteria, *Arhodomonas aquaeolei*, *Marinobacter lacisalsi*, *Halomonas axialensis*, and *Kocuria flava*, and the two haloarchaea, *Haloferax elongans* and *Halobacterium salinarum*, that had been used in our earlier investigation (Al-Mailem et al., 2014a,b, 2017) were used in this study. These cultures had been isolated from the hypersaline coastal soil (about 4 M NaCl), about 90 km, south of Kuwait city, 10 km north of the Saudi Arabian borders, using the mineral medium with oil vapor as sole source of carbon and energy. Those isolates had been identified by comparing sequences of their 16S rRNA genes with those of type strains in the GenBank database. For this, total genomic DNA was extracted from the cells using the PrepMan Ultra Kit (Applied Biosystems, United States) and the 16S rRNA genes were amplified using the primer pairs GM5F and 907R (Santegoeds et al., 1998) for bacteria and the pairs of 0018F and 1518R for archaea (Cui et al., 2009). The PCR products were purified, sequenced, and obtained sequences were subjected to basic local alignment search tool analysis. The sequences were deposited in the GenBank database. A phylogenetic tree was constructed by neighbor joining including bootstrap analysis using PAUP* V.4 (Swofford, 1998).

Effects of Crude Oil, $Fe_2(SO_4)_3$, and Proline on Heavy-Metal Tolerance by Pure Halophilic/Halotolerant Isolates

Heavy-metal tolerance is measured either as "maximum tolerated concentrations" (MTCs) or as "minimum inhibitory concentrations" (MIC). The MTC measurement was chosen here because it was more related to the objectives of this study than the MIC measurement.

For this experiment, saline (2 M NaCl) nutrient agar was used, once as such, and once with oil vapor in the dish head spaces. Obviously, the mineral medium with oil vapor as a sole carbon source is not suitable because in the absence of oil vapor, the sole carbon source, no microbial activity would occur at all. Aliquots of the media were provided with individual heavy-metal salts at concentrations of 0–1600 mg l^{-1}. To study the effects of $Fe_2(SO_4)_3$ (10 mg l^{-1}) and proline (200 mg l^{-1}) (those concentrations were based on the results of preliminary experiments and the concentrations used by earlier researchers), they were added, separately. Common inocula (one loopful of biomass in 5 ml of sterile hypersaline water) were prepared, and the medium aliquots were inoculated by streaking one loopful of the inoculum on medium surfaces. Triplicates were prepared throughout. The cultures were incubated at 30°C for 12 d, and examined for the highest heavy-metal concentrations, above which the tested organisms failed to grow MTC.

Effects of $Fe_2(SO_4)_3$, Proline, and Heavy Metals on Crude-Oil Consumption by Halophilic/Halotolerant Isolates

In this experiment, the liquid mineral medium was provided with 2 M NaCl and used. Aliquots, 50 ml, dispensed in screw-caped flasks were provided with 0.3%, w/v, crude oil alone and together with the individual heavy-metal salts: $HgCl_2$ (10 mg l^{-1}), $PbNO_3$ (10 mg l^{-1}), $CuSO_4$ (20 mg l^{-1}), $CdSO_4$ (10 mg l^{-1}), and Na_2HAsO_4 (20 mg l^{-1}). In addition, $Fe_2(SO_4)_3$ (10 mg l^{-1}) and proline (200 mg l^{-1}) were amended, separately. Triplicates were prepared throughout. The media were inoculated with 1 ml portions of common inocula, sealed, and incubated at 30°C on a reciprocal shaker, 110 rpm, for 12 d. The residual oil in each flask was recovered with three 10 ml successive portions of pentane. The combined extract was raised to 35 ml using pure pentane, and 1 μl aliquots were analyzed by gas–liquid chromatography (GLC) using a Chrompack (Chrompack, Middelburg, Netherlands) CP-9000 instrument equipped with a FID, a WCOT-fused silica CP-SIL-5CB capillary column, and a temperature program, which raised the temperature from 45 to 310°C, 10°C min^{-1}. The oil consumption was calculated as percent decreases of the total peak areas in the GLC profiles at the end of incubation based on the total peak areas of the abiotic controls (similarly treated, but using previously autoclaved inocula). Mean readings of the triplicates ± standard deviation values were calculated.

Effects of Heavy Metals on Growth of Halophilic/Halotolerant Isolates at Different Salinities

In this experiment, nutrient broth was used. Medium aliquots in test tubes were provided with NaCl at concentrations from 0.0 to 4.5 M. To study the effects of heavy metals on microbial growth, the medium aliquots were provided in addition with individual heavy-metal salts ranging in concentration from 0.0 to 80 mg l^{-1} of $HgCl_2$ or $PbNO_3$, and from 0.0 to 160 mg l^{-1} of $CdSO_4$, $CuSO_4$, or Na_2HAsO_4. Selection of those concentrations was based on results of preliminary experiments. Triplicates were prepared throughout. The test-tube cultures were inoculated

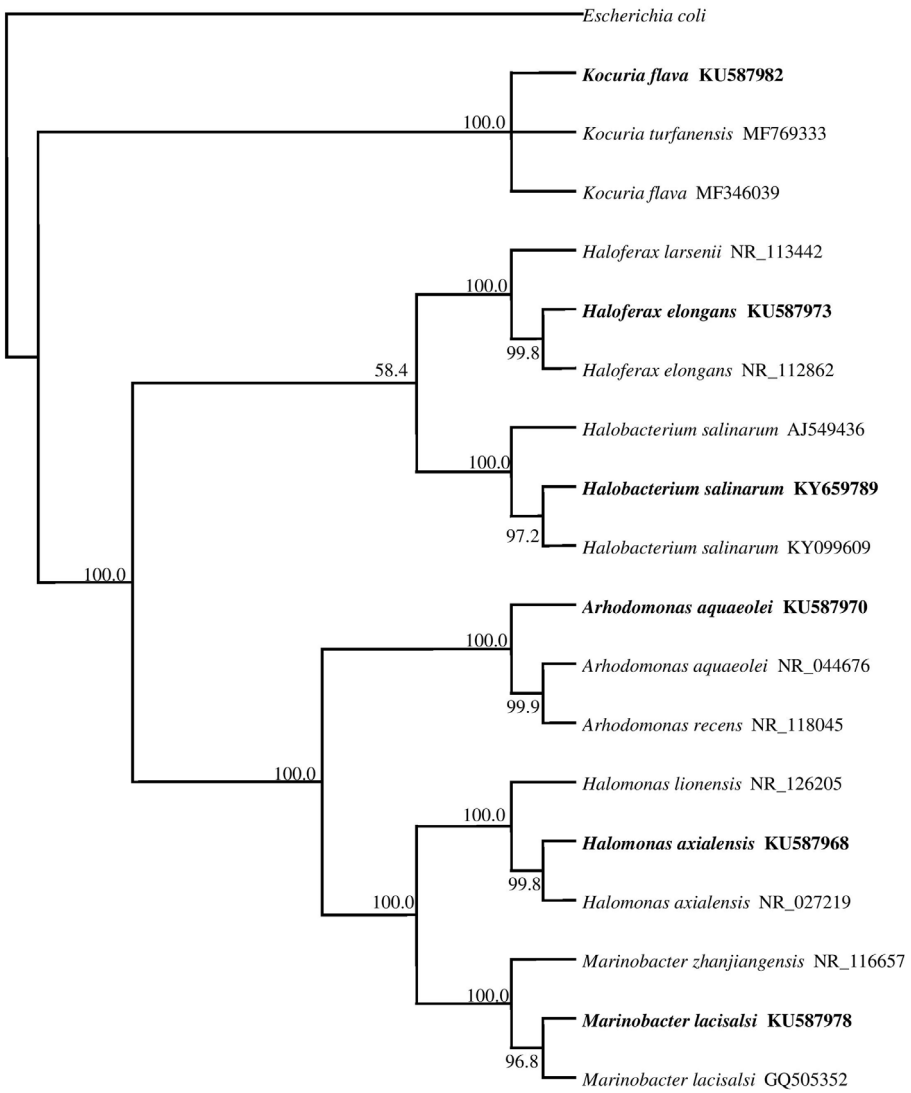

FIGURE 2 | 16S rRNA gene phylogeny of hydrocarbonoclastic bacterial and archaeal isolates used in this study. Values used in each node of the tree are bootstrap values; 2000 bootstrap replicates were performed. The tree includes the accession numbers of the isolates.

with common inocula, and incubated at 30°C for 5 d. Growth was measured as optical density values at the commonly used wavelength of 660_{nm}, using a spectrophotometer (Spectronic 21D, Milton Roy, United States). The use of oil-containing medium was avoided because the water-immiscible oil would have interfered with optical density measurement.

Effects of Salinity on Heavy-Metal Uptake by Halophilic/Halotolerant Isolates

The cells were first allowed to propagate in a heavy-metal-free medium, and were subsequently suspended in solutions of the metals whose uptake was to be measured.

Nutrient broth as a medium and the heavy-metal salts, $HgCl_2$ and $PbNO_3$, were used in this experiment. The oil-containing medium was not used because oil would interfere with heavy-metal uptake. Medium salinities were adjusted to 0, 1, 2, and 3 M NaCl. Heavy-metal-free medium aliquots were inoculated as described above, and incubated at 30°C for 24 h to allow for cell growth without heavy metals. Cells were harvested by centrifugation, 10,000 × *g*, for 10 min at 4°C and washed twice for a few minutes with sterile deionized water. The results of a preliminary experiment had confirmed that cells of *H. salinarum* (known to lyse in pure water) remained intact in deionized water for up to 3 h (duration of OD determination), but after 24 h complete cell lysis occurred. To recall, cell washing with water in this experiment took only minutes. The cells were subsequently suspended in 50 ml portions of deionized water containing 0, 1, 2, or 3 M NaCl, 0.2%, w/v, glucose and either $HgCl_2$ (10 mg l^{-1}) or $PbNO_3$ (10 mg l^{-1}). The suspensions were incubated for 40 min at 30°C. Longer incubation could have led to cell lysis

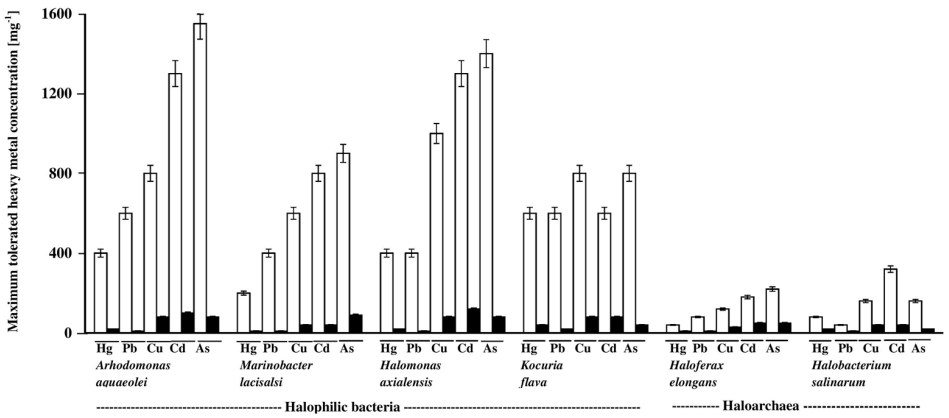

FIGURE 3 | Heavy-metal tolerance by halophilic/halotolerant bacterial and archaeal cultures in the presence (black columns) and absence (white columns) of crude oil. Hg, $HgCl_2$; Pb, $PbNO_3$; Cu, $CuSO_4$; Cd, $CdSO_4$; As, Na_2HAsO_4. Each reading was the mean of three parallel replicates, whose maximum tolerated values were identical, i.e., no deviation. The medium salinity was adjusted to 2 M NaCl (section "Materials and Methods").

after 3 h (at 0 M NaCl) as the preliminary experiments revealed. At time 0 and in 5 min intervals, 5 ml samples were harvested and centrifuged (10,000 $\times$ *g*) for 2 min at 4°C. Cells were digested with conc. HNO_3 and HCl, 2:1 on a hot plate. The digestion solutions were filtered, diluted with 1% HNO_3, and the heavy-metal-salt concentrations therein were determined by the USEPA method 6010B using Inductively Coupled Plasma Optical Emission Spectrometry (ICP-OES; PerkinElmer Optima 7300DV, United States) and Certified Reference Materials (multi-elements) (Oyetibo et al., 2010). As blank, the uninoculated liquid medium containing all the reagents was used. Reportedly, this method produces an average heavy-metal recovery of 100% with only 0.92% relative error (Han et al., 2006). The differences from the start concentrations were considered as the heavy-metal uptake values.

Statistical Analysis

As already mentioned, three parallel replicates for each analysis were prepared throughout, and the mean values $\pm$ standard deviation values were calculated using Microsoft Excel 2003. Statistical Package for Social Sciences, version 12 was used to assess the degree of significance, where the analysis of variance (ANOVA) was used to differentiate between the means of the tested parameters.

RESULTS AND DISCUSSION

Numbers of Cultivable Heavy-Metal-Resistant CFU in Hypersaline Soil

To recall, the culture-dependent analysis captures the cultivable, hydrocarbonoclastic microorganisms only. Heavy metals are grouped into toxic and less toxic ones (Massadeh et al., 2005; Salgaonkar et al., 2013). This study focused on the first group that comprises mercury, cadmium, lead, and arsenic. For comparison, two representatives of the much less toxic heavy metals, copper and zinc, were used.

The results in **Figure 1** show that the CFU numbers of hydrocarbonoclastic microorganisms (capable of growth on the mineral medium with oil vapor as a sole source of carbon and energy) as counted on the heavy-metal-free medium (control) ranged between about 170 ± 7 and 200 ± 11 CFU g^{-1}. Addition of salts of mercury, cadmium, lead, and arsenic led to the lowest numbers of CFU counted. Increasing concentrations of those salts led to immediate decreases of the CFU numbers, until no more colonies appeared at heavy-metal-salt concentrations around 40 mg l^{-1}. Basically, the same result was obtained with Na_2HAsO_4, although the maximum concentration of this heavy-metal salt above which no CFU appeared was >100 mg l^{-1}. The results with $CuSO_4$ and $ZnSO_4$ were quite different. Within the concentration ranges of 0–50 and 80 mg l^{-1} of those salts, respectively, concentration increases were associated with immediate increases in the CFU numbers. Maximum numbers were counted in the presence of 50 mg l^{-1} $CuSO_4$ (a concentration at which Hg^{2+}, Cd^{2+}, and Pb^{+} prevented CFU growth) and about 80 mg l^{-1} $ZnSO_4$. Those enhancing effects are probably related to the roles of Cu^{2+} and Zn^{2+} in certain enzymatic activities (Salgaonkar et al., 2013). Furthermore, Cu^{2+} and Zn^{2+} with their low toxicity may be involved in cytoplasmic osmolarity regulation under high salinity, just like the conventional cations, Na^{+} and K^{+}. Copper was more potent in its inhibitory effect than zinc, the maximum $CuSO_4$ concentration above which no CFU appeared was 140 mg l^{-1}, while as high as 300 mg l^{-1} $ZnSO_4$ did not result in reducing the CFU numbers below those counted in the complete absence of this salt.

Pure Isolates of Hydrocarbonoclastic Microorganisms

The phylogenetic tree in **Figure 2** shows the phylogenetic affiliations among the pure isolates studies and includes their accession numbers in the GenBank database.

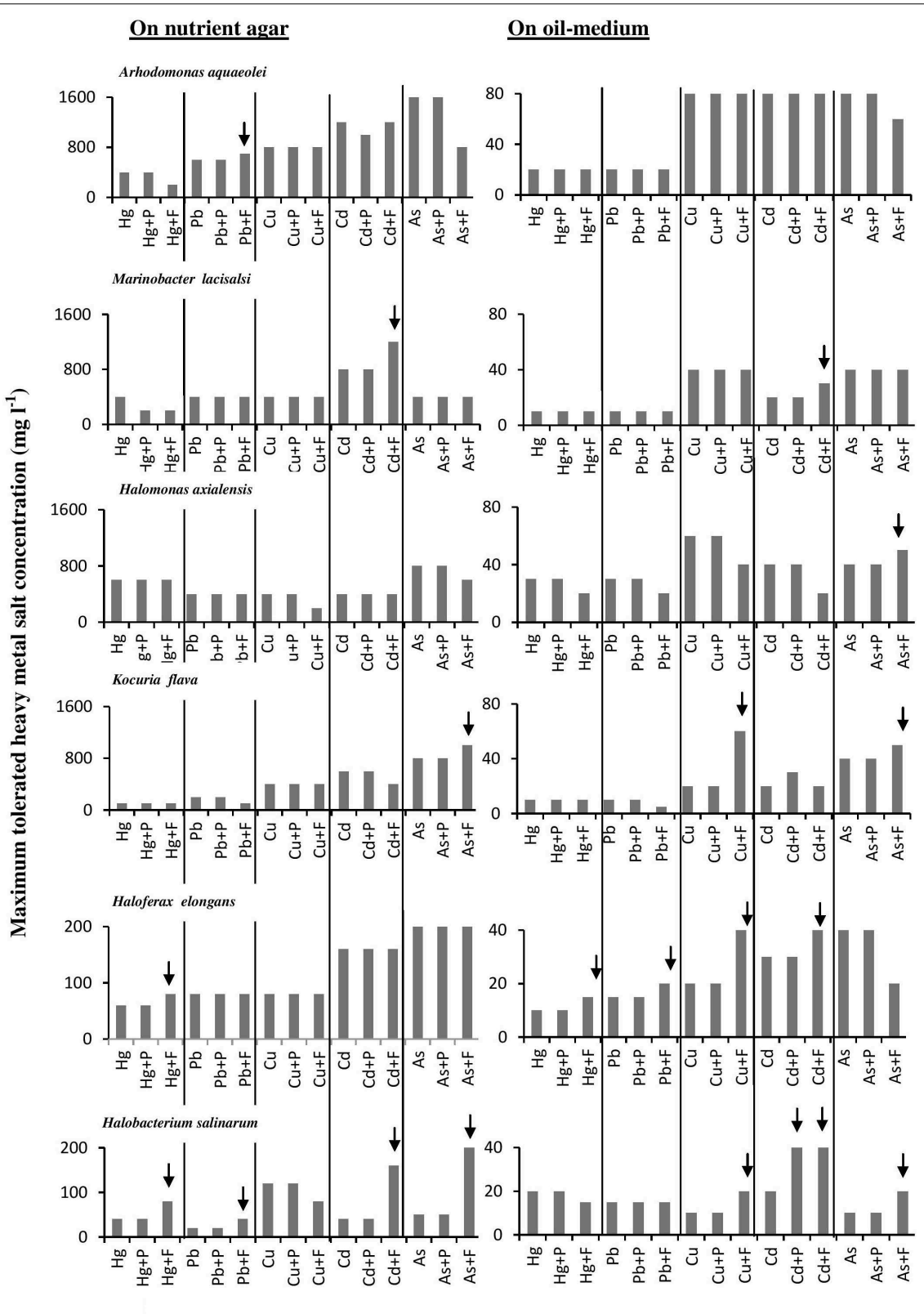

FIGURE 4 | Effects of Fe^{3+} and proline on maximum-heavy-metal concentrations tolerated by halophilic/ halotolerant microorganisms. Arrows highlight positive effects of added Fe^{3+} and proline. Hg, $HgCl_2$; Pb, $PbNO_3$; Cu, $CuSO_4$; Cd, $CdSO_4$; As, Na_2HAsO_4. Each reading was the mean of three parallel replicates, whose maximum tolerated values were identical, i.e., there were no deviations. The medium salinity was adjusted to 2 M NaCl (section "Materials and Methods").

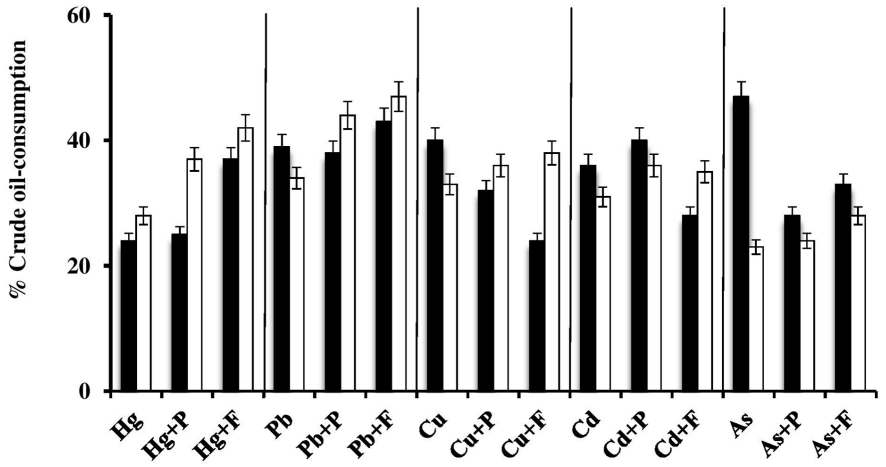

FIGURE 5 | Effects of Fe^{3+} and proline on heavy-metal-mediated inhibition of crude oil consumption by the halophilic/halotolerant bacterium, *Kocuria flava* (black columns) and the haloarchaeon, *Halobacterium salinarum* (white columns). Hg, $HgCl_2$; Pb, $PbNO_3$; Cu, $CuSO_4$; Cd, $CdSO_4$; As, Na_2HAsO_4; P, proline; F, $Fe_2(SO_4)_3$. The medium salinity was adjusted to 2 M NaCl (section "Materials and Methods").

Heavy-Metal Tolerance by Halophilic/Halotolerant Isolates on Oil-Free and Oil-Containing Media

The histograms in **Figure 3** illustrate the dramatic inhibitory effects of crude oil on the heavy-metal tolerance by the four hydrocarbonoclastic bacterial and the two hydrocarbonoclastic haloarchaeal species from the hypersaline soil. Interestingly, the two haloarchaeal species seemed to be more sensitive to the tested heavy metals (showing weaker growth) than the four halophilic bacterial species, particularly on the crude-oil-free nutrient agar. Earlier researchers noted that numerous halophilic bacteria but only a few haloarchaea possess heavy-metal resistance (for review, see Voica et al., 2016). The highest tolerance measured in our study was that of *A. aquaeolei* which tolerated up to 1600 mg l^{-1} Na_2HAsO_4, and the lowest was that of *M. lacisalci* which tolerated up to only 200 mg l^{-1} $HgCl_2$. High tolerance values were also measured for *H. axialensis*, which tolerated up to 1200 mg l^{-1} of $CdSO_4$, $CuSO_4$, and Na_2HAsO_4. *K. flava* tolerated up to 800 mg l^{-1} of $CuSO_4$ and Na_2HAsO_4 and up to 600 mg l^{-1} of $HgCl_2$, $CdSO_4$, and $PbNO_3$. In contrast, the highest tolerance of the haloarchaeon, *H. elongans* was at 200 mg l^{-1} Na_2HAsO_4, and that of *H. salinarum* was at 320 mg l^{-1} $CdSO_4$. The heavy-metal-tolerance values on the oil-containing medium were lower than on the oil-free medium. A simple calculation showed that the highest concentrations of heavy metals tolerated by bacteria in the presence of oil were between only about 3 and 10% (in one case only reaching 13%) of the corresponding values in the absence of oil (on nutrient agar). Corresponding tolerance values for the archaeal species were considerably higher, between 20 and 25% (with 13% in three cases only).

There are no relevant result in the available literature to compare them with the above results. However, the weaker heavy-metal tolerance in the presence of oil than in its absence may be due to additional stress by aromatic hydrocarbons in the oil used (Shukla and Singh, 2012).

Effects of $Fe_2(SO_4)_3$ and Proline on the "Maximum Heavy-Metal Concentrations" Tolerated by Halophilic/Halotolerant Isolates

The histograms in **Figure 4** confirm that bacterial cultures commonly tolerated higher concentrations of heavy metals than archaeal cultures. The data also show that the tested microorganisms tolerated higher heavy-metal concentrations on the oil-free than in the oil-containing media. In many cases (highlighted by arrows in **Figure 4**), the addition of Fe^{3+} and, albeit to a less extent, proline enhanced this tolerance. The highest tolerated heavy-metal concentrations were double to triple as high as the concentrations tolerated in the absence of $Fe_2(SO_4)_3$ and proline. This result was more frequent among the tested haloarchaea than among the halophilic bacteria. In several other cases, $Fe_2(SO_4)_3$ and proline did not affect the heavy-metal tolerance at all. There are no relevant results in the available literature to compare them with those results. However, Fe^{3+} and proline might have contributed to osmoregulation of the cytoplasm leading to less salt stress and thus to enhanced heavy-metal tolerance. Why this did not happen in several other cases as **Figure 4** shows, this could be due to the fact that concerned microorganisms accumulate other compatible solutes for osmoregulation.

Effects of $Fe_2(SO_4)_3$ and Proline on Heavy-Metal-Mediated Inhibition of Crude-Oil Consumption by Halophilic/Halotolerant Isolates

In view of the extensive setup, this experiment was done on one bacterial and one haloarchaeal species only. The histograms

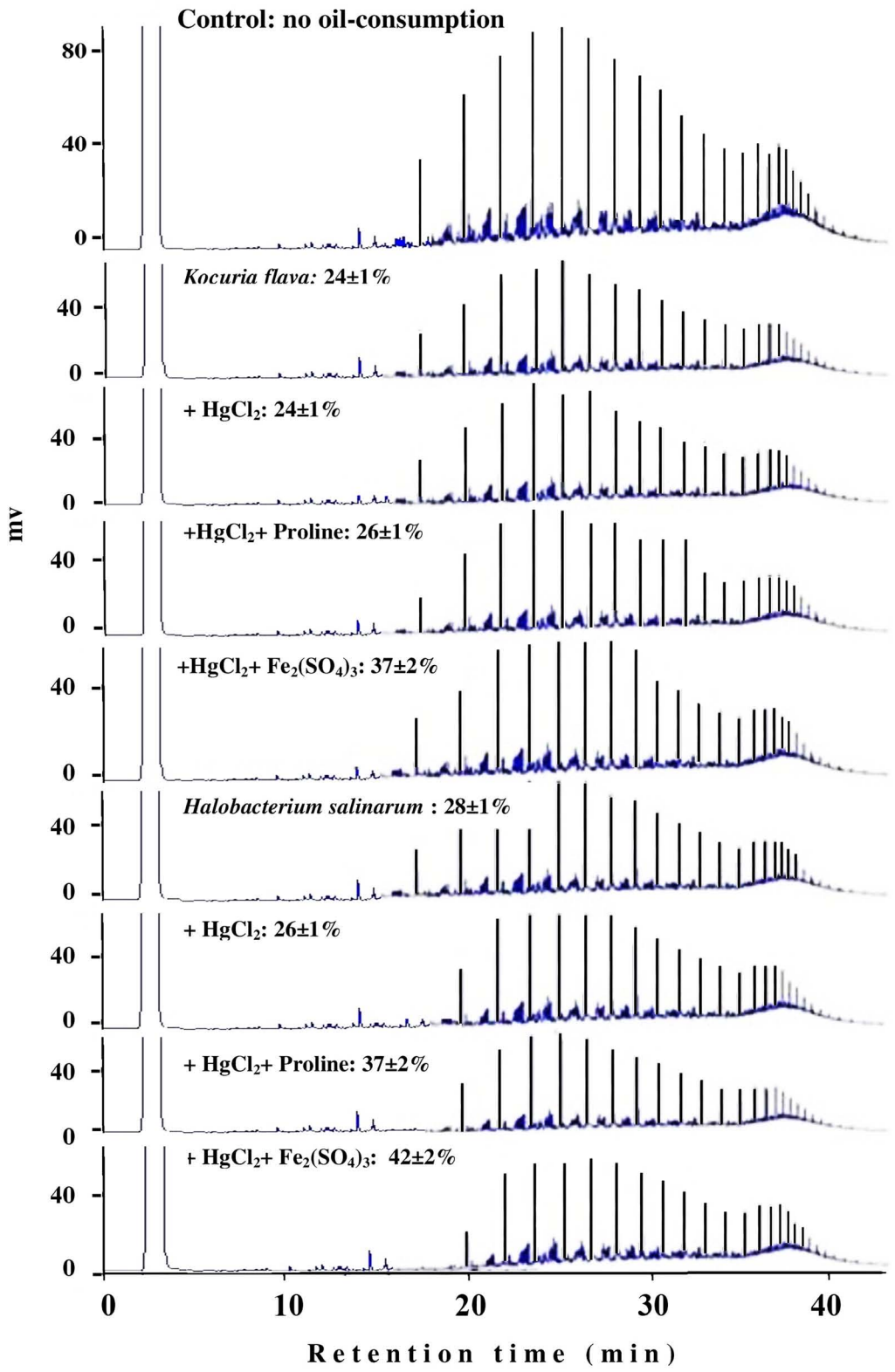

FIGURE 6 | Typical GLC profiles of residual hydrocarbons in microbial cultures treated with $Fe_2(SO_4)_3$ and proline. Percent values on the individual profiles are those of oil-consumption ± standard deviation. Note that small peaks mean more consumption, and that amendment with $Fe_2(SO_4)_3$ and proline significantly enhanced the oil-consumption values by both organisms compared with the values in the presence of the heavy metals alone.

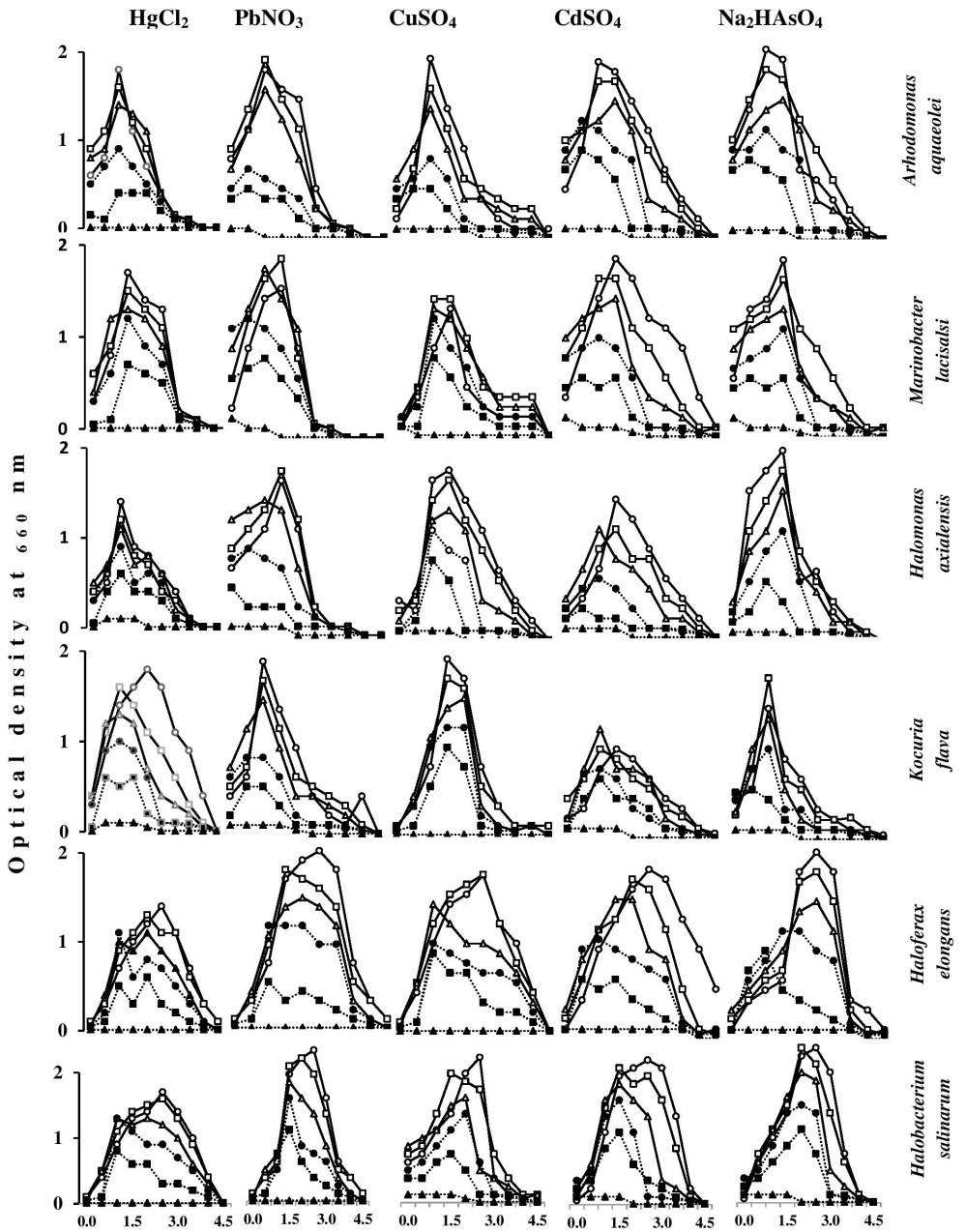

FIGURE 7 | Effects of heavy-metal concentrations on the growth magnitudes of halophilic/halotolerant isolates at different salinities. $HgCl_2$ and $PbNO_3$ concentration (mg l^{-1}): -o-, 0; -□-, 5; -Δ-, 10; -●-, 20; -■-, 40; -▲-, 80. $CuSO_4$, $CdSO_4$, Na_2HAsO_4 concentration (mg l^{-1}): -o-, 0; -□-, 10; -Δ-, 20; -●-, 40; -■-, 80; -▲-, 160.

in **Figure 5** show that, in most of the cases, Fe^{3+} and proline significantly ($P < 0.05$) enhanced the oil consumption by the studied microorganisms in the presence of heavy metals. In many cases, the Fe^{3+}-amendments led to consumption values much higher even than those in the absence of heavy metals. Still in some other cases, these amendments had even negative effects on oil consumption. Again the enhancement of oil consumption could have been due to the osmoregulatory effects of Fe^{3+} and proline, thus reducing the salt stress and supporting the heavy-metal tolerance of the respective oil-utilizing microorganisms. Furthermore, it has been reported that Fe^{3+} may serve as an electron acceptor during anaerobic respiration of bacteria and archaea (Lovley et al., 1991).

The typical GLC profiles in **Figure 6** illustrate this novel result using the most toxic heavy-metal Hg^{2+}. Irrespective of the actual mechanism(s) by which Fe^{3+} and proline may enhance the oil consumption by some microorganism, this result could obviously be of practical value in designing bioremediation biotechnologies for oil-contaminated, hypersaline environments.

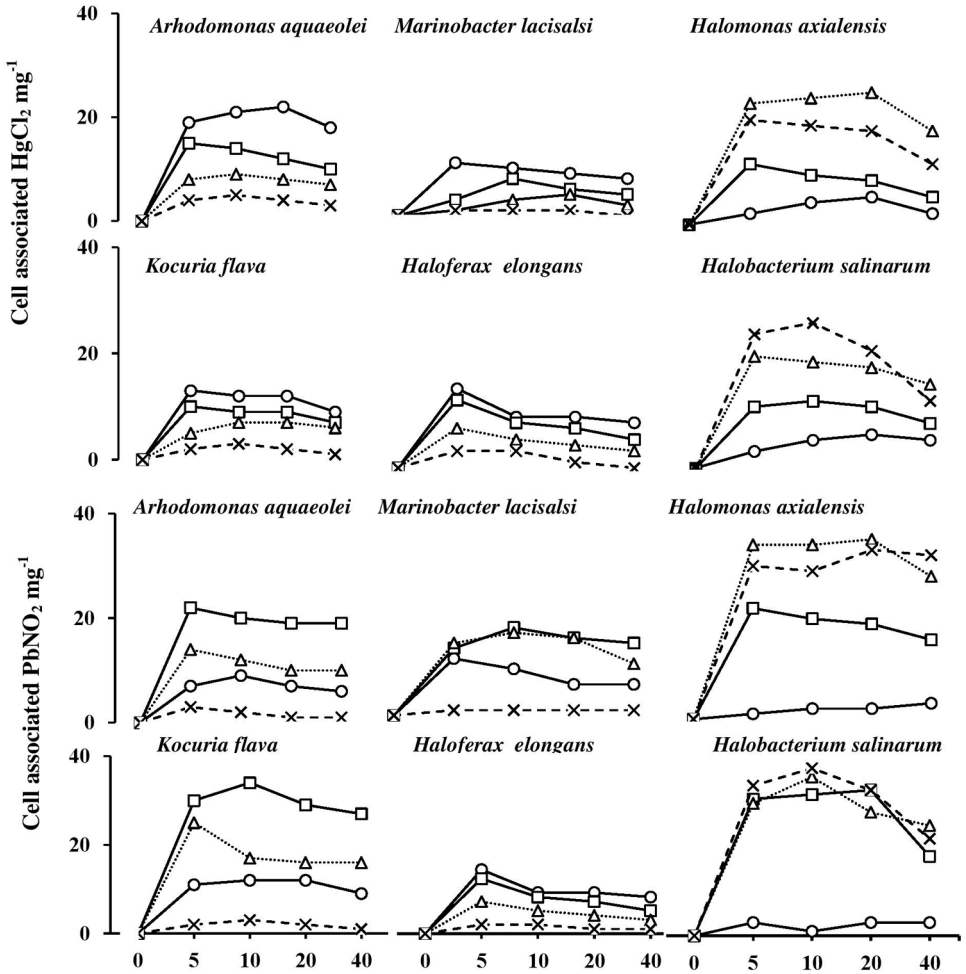

FIGURE 8 | Heavy-metal uptake by halophilic microorganisms at various salinities. NaCl concentrations (M): circles, 0 M; squares, 1 M; triangles, 2 M; cross, 3 M.

Effects of Heavy Metals on the Growth Magnitudes of Halophilic/Halotolerant Microorganisms Under Salt Stress

Figure 7 shows the effects of heavy metals on the growth magnitudes of tested isolates in nutrient broth containing various NaCl concentrations. The heavy metals did not only affect the growth magnitudes but also resulted in changing the optimum NaCl concentrations for growth of some isolates. As should be expected, the growth of the tested species was frequently best in the absence of heavy metals, and decreased with increasing heavy-metal concentrations. Exceptions, which are obvious in this figure, are quite interesting. Thus, with some organisms, $HgCl_2$ and $PbNO_3$ concentrations of 5 and 10 mg l^{-1} at certain salinities resulted in growth values similar to or higher than the values in the absence of those heavy metals. This was also true for $CdSO_4$, $CuSO_4$, and Na_2HAsO_4 at concentrations of 10 and 20 mg l^{-1}. Higher heavy-metal-salt concentrations of up to 40 mg l^{-1} $HgCl_2$ and up to 80 mg l^{-1} of all other heavy-metal salts did not arrest the growth of the tested organisms at most of the salinities. These results may imply that the "toxic" heavy-metal cations at low concentrations may be beneficial, probably by affecting cytoplasmic osmolality under environmental salt stress, like conventional cations do (K^+, Mg^{2+}, Ca^{2+}, and Fe^{3+}) (Al-Mailem et al., 2017). Furthermore, toxic heavy metals at trace concentrations were reported to serve as essential micronutrients in metabolic reactions and enzyme stabilization (Bruins et al., 2000).

Heavy-Metal Uptake by Halophilic/Halotolerant Isolates at Various Salinities

It is important to recall that this experiment extended for only 40 min, and that it took haloarchaeal cells at least 3 h to start lysis in the absence of NaCl (see above). The results proved, however, that this short period was adequate to fulfill the objectives targeted.

Figure 8 shows the uptake rates of $HgCl_2$ and $PbNO_3$ by the six tested isolates. The uptake of both salts was almost completed during the first 5 min of incubation. Their cell-associated concentrations remained nearly constant or exhibited

some decreases with time. The smallest proportions of $HgCl_2$ and $PbNO_3$ were taken up by the bacterium, *H. axialensis* and the haloarchaeon, *H. salinarum* in the absence of NaCl, whereas the highest uptake values by both microorganisms were in the hypersaline range (2 and 3 M NaCl). Conversely, the greatest amounts of $HgCl_2$ were taken up in the absence of NaCl by *A. aqueoleoi*, *M. lacisalsi*, *K. flava*, and *H. elongans*; the latter species also took up the greatest amount of $PbNO_3$ in the absence of NaCl. In the remaining cases, the highest concentrations of the two studied heavy-metal salts were taken up at 1 and 2 M NaCl, but 3 M NaCl inhibited the heavy-metal uptake. The fact that there was a direct relationship between salinity and heavy-metal uptake consolidates the assumption that heavy-metal cations may play some role in affecting cytoplasmic osmolality under salt stress. It may be argued that the heavy metals were just adsorbed on the cell envelops as it happens in many microorganisms as a part of the heavy-metal tolerance strategy (Nies, 1999; Deb et al., 2013). However, the tolerance of Hg^{2+}, one of the two studied metals, is known to follow a completely different strategy which involves the reduction of the toxic Hg^{2+} to the less toxic volatile Hg^{o} form (Nies, 1999; Wiatrowski et al., 2006; De et al., 2008). The patterns of $HgCl_2$ uptake in **Figure 8**, however, are more similar to the active-transport pattern than to the pattern of metal loss by volatilization.

CONCLUSION

The results of this study provide novel information complementary to our recent findings on biostimulation for oil bioremediation in salt-stressed environments. Although hydrocarbonoclastic bacteria and archaea indigenous to hypersaline soil occur permanently under multiple stresses, they still maintain the potential for active growth and biodegradation of spilled oil. In batch cultures, those organisms proved capable of growth and crude-oil removal in the presence of certain concentrations of heavy metals and high NaCl concentrations. For some isolates, those activities were significantly biostimulated by amended substances. Thus, Fe^{3+} and proline enhanced the tolerance of some organisms to toxic heavy metals, thus raising their potential for spilled-oil bioremediation under the prevailing multiple stresses. This study offers experimental evidence for quick uptake of heavy metals by tested microorganisms under salt stress. Although toxic, some metals enhanced salt tolerance and biodegradation of spilled oil in hypersaline environments.

AUTHORS CONTRIBUTIONS

DA-M, ME, and SR drafted the manuscript and performed the microbiological studies and genome sequencing analysis. DA-M and SR participated in the design of the study. All authors read and approved the final manuscript.

FUNDING

This work was supported by Kuwait University, Research Grant RS 01/12.

ACKNOWLEDGMENTS

We acknowledge Kuwait University for funding (Research Grant RS 01/12). Thanks are due also to the RSPU unit, Kuwait University, for providing the Genetic Analyzer (GS 01/02) and to the NUERS unit, Kuwait University, for providing facilities for GLC and metal analysis (SRUL 01/13) and to Mrs. Majida Khanafer for technical help.

REFERENCES

Al-Mailem, D. M., Al-Deieg, M., Eliyas, M., and Radwan, S. S. (2017). Biostimulation of indigenous microorganisms for bioremediation of oily hypersaline microcosms from the Arabian Gulf Kuwaiti coasts. *J. Environ. Manage.* 193, 576–583. doi: 10.1016/j.jenvman.2017.02.054

Al-Mailem, D. M., Eliyas, M., Khanafer, M., and Radwan, S. S. (2014a). Culture-dependent and culture-independent analysis of hydrocarbonoclastic microorganisms indigenous to hypersaline environments in Kuwait. *Microb. Ecol.* 67, 857–865. doi: 10.1007/s00248-014-0386-5

Al-Mailem, D. M., Eliyas, M., and Radwan, S. S. (2012). Enhanced haloarcaheal oil removal in hypersaline environments via organic nitrogen fertilization and illumination. *Extremophiles* 16, 751–758. doi: 10.1007/s00792-012-0471-y

Al-Mailem, D. M., Eliyas, M., and Radwan, S. S. (2014b). Enhanced bioremediation of oil-polluted, hypersaline, coastal areas in Kuwait via vitamin-fertilization. *Environ. Sci. Pollut. Res.* 21, 3386–3394. doi: 10.1007/s11356-013-2293-6

Banerjee, S. S., Joshi, M. V., and Jayaram, R. V. (2006). Treatment of oil spill by sorption technique using fatty acid grafted sawdust. *Chemosphere* 64, 1026–1031. doi: 10.1016/j.chemosphere.2006.01.065

Basumatary, B., Bordoloi, S., Sarma, H. P., and Das, H. C. (2012). A study on the physico-chemical properties and heavy metal content in crude oil contaminated soil of Duliajan, Assam, India. *Int. J. Adv. Biotechnol. Res.* 2, 64–66.

Bonfa, M. R. L., Grossman, M. J., Mellado, E., and Durrant, L. R. (2011). Biodegradation of aromatic hydrocarbons by haloarchaea and their use for the reduction of the chemical oxygen demand of hypersaline petroleum produced water. *Chemosphere* 84, 1671–1676. doi: 10.1016/j.chemosphere.2011.05.005

Bruins, M. R., Kapil, S., and Oehme, F. W. (2000). Microbial resistance to metals in the environment. *Ecotoxicol. Environ. Saf.* 45, 198–207. doi: 10.1006/eesa.1999.1860

Cui, H. L., Zhou, P. J., Oren, A., and Liu, S. J. (2009). Intraspecific polymorphism of 16S rRNA genes in two halophilic archaeal genera, *Haloarcula* and *Halomicrobium*. *Extremophiles* 13, 31–37. doi: 10.1007/s00792-008-0194-2

De, J., Ramaiah, N., and Vardanyan, L. (2008). Detoxification of toxic heavy metals by marine bacteria highly resistant to mercury. *Mar. Biotechnol.* 10, 471–477. doi: 10.1007/s10126-008-9083-z

Deb, S., Ahmed, S. F., and Basu, M. (2013). Metal accumulation in cell wall: a possible mechanism of cadmium resistance by *Pseudomonas stutzeri*. *Bull. Environ. Contam. Toxicol.* 90, 323–328. doi: 10.1007/s00128-012-0933-z

Emerson, D., Chauhanm, S., Oriel, P., and Breznak, J. A. (1994). Haloferax sp. D1227, a halophilic archaeon capable of growth on aromatic compounds. *Arch. Microbiol.* 61, 445–452. doi: 10.1007/BF00307764

Fathepure, B. Z. (2014). Recent studies in microbial degradation of petroleum hydrocarbons in hypersaline environments. *Front. Microbiol.* 5:173. doi: 10.3389/fmicb.2014.00173

Garcia, M. T., Mellado, E., Ostos, J. C., and Ventosa, A. (2004). *Halomonas organivorans* sp. nov., a moderate halophiles able to degrade aromatic compounds. *Int. J. Syst. Evol. Microbiol.* 54, 1723–1728. doi: 10.1099/ijs.0.63114-0

Han, F. X., Patterson, W. D., Xia, Y., Sridhar, B. M. M., and Su, Y. (2006). Rapid determination of mercury in plant and soil samples using inductively coupled plasma atomic emission spectroscopy, a comparative study. *Water Air Soil Pollut.* 170, 161–171. doi: 10.1007/s11270-006-3003-5

Hunter, J. R. (1982). "The physical oceanography of the Arabian Gulf. A review and theoretical interpretation of previous observations," in *The First Arabian Gulf Conference on Environment and Pollution*, eds R. Halwagy, D. Clayton, and M. Behbehani (Kuwait City: Kuwait University), 1–23.

Lefebvre, O., and Moletta, R. (2006). Treatment of organic pollution in industrial saline wastewater: a literature review. *Water Res.* 40, 3671–3682. doi: 10.1016/j.watres.2006.08.027

Lovley, D. R., Phillips, E. J. P., Gorby, Y. A., and Landa, E. R. (1991). Microbial reduction of uranium. *Nature* 350, 413–416. doi: 10.1038/350413a0

Margesin, R., and Schinner, F. (2001). Biodegradation and bioremediation of hydrocarbons in extreme environments. *Appl. Microbiol. Biotechnol.* 56, 650–663. doi: 10.1007/s002530100701

Massadeh, A. M., Al-Momani, F. A., and Haddad, H. I. (2005). Removal of lead and cadmium by halophilic bacteria isolated from the Dead Sea Shore, Jordan. *Biol. Trace Elem. Res.* 108, 259–269. doi: 10.1385/BTER:108:1-3:259

Nicholson, C. A., and Fathepure, B. Z. (2005). Aerobic biodegradation of benzene and toluene under hypersaline conditions at the Great Salt Plains, Oklahoma. *FEMS Microbiol. Lett.* 245, 257–262. doi: 10.1016/j.femsle.2005.03.014

Nies, D. H. (1999). Microbial heavy-metal resistance. *Appl. Microbiol. Biotechnol.* 51, 730–750. doi: 10.1007/s002530051457

Oren, A. (2002). Diversity of halophilic microorganisms: environments, phylogeny, physiology, and applications. *J. Indus. Microbiol. Biotechnol.* 28, 56–63. doi: 10.1038/sj/jim/7000176

Oren, A., Gurevich, P., Azachi, M., and Hents, Y. (1992). Microbial degradation of pollutants at high salt concentrations. *Biodegradation* 3, 387–398. doi: 10.1007/BF00129095

Osuji, L. C., and Onojake, C. M. (2004). Trace heavy metals associated with crude oil: a case study of Ebocha-8 oil-spill-polluted site in Niger Delta, Nigeria. *Chem. Biodivers.* 1, 1708–1715. doi: 10.1002/cbdv.200490129

Oyetibo, G. O., Ilori, M. O., Adebusoyem, S. A., Oluwafemi, S., Obayori, O. S., and Amund, O. O. (2010). Bacteria with dual resistance to elevated concentrations of heavy metals and antibiotics in Nigerian contaminated systems. *Environ. Monit. Assess.* 168, 305–314. doi: 10.1007/s10661-009-1114-3

Pieper, D., and Reineke, W. (2000). Engineering bacteria for bioremediation. *Curr. Opin. Biotechnol.* 11, 262–270. doi:10.1016/S0958-1669(00)00094-X

Radwan, S. S., Al-Mailem, D. M., and Kansour, M. K. (2017). Calcium (II)- and dipicolinic acid mediated-biostimulation of oil-bioremediation under multiple stresses by heat, oil and heavy metals. *Sci. Rep.* 7:9534. doi: 10.1038/s41598-017-10121-7

Salgaonkar, B. B., Mani, K., and Braganca, J. M. (2013). Characterization of polyhydroxyalkanoates accumulated by a moderately halophilic salt pan isolate *Bacillus megaterium* strain H16. *J. Appl. Microbiol.* 114, 1347–1356. doi: 10.1111/jam.12135

Santegoeds, C. M., Ferdelman, T. G., Muyzer, G., and Beer, D. (1998). Structural and functional dynamics of sulfate-reduction populations in bacterial biofilms. *Appl. Environ. Microbiol.* 64, 3731–3739.

Shukla, A., and Singh, C. S. (2012). "Hydrocarbon pollution: Effects on living organisms, remediation of contaminated environments, and effects of heavy metals co-contamination on bioremediation," in *Introduction to Enhanced oil Recovery (EOR) Processes and Bioremediation of Oil Contaminated Sites*, ed. L. Romero-Zerón (Rijeka: In Tech).

Sorkhoh, N. A., Ghannoum, M. A., Ibrahim, A. S., Stretton, R. J., and Radwan, S. S. (1990). Crude oil and hydrocarbon-degrading strains of *Rhodococcus rhodochrous* isolated from soil and marine environments in Kuwait. *Environ. Pollut.* 65, 1–17. doi: 10.1016/0269-7491(90)90162-6

Swofford, D. L. (1998). *PAUP*. Phylogenetic Analysis Using Parasimony (* and Other Methods), Version 4*. Sunderland, MA: Sinauer Associates.

Voica, D. M., Bartha, L., Banciu, H. L., and Oren, A. (2016). Heavy metal resistance in halophilic bacteria and Archaea. *FEMS Microbiol. Lett.* 363:fnw146. doi: 10.1093/femsle/fnw146

Weast, R. C. (1984). *CRC Handbook of Chemistry and Physics*, 64 Edn. Boca Raton, FL: CRC.

Wiatrowski, H. A., Ward, P. M., and Barkey, T. (2006). Novel reduction of mercury (II) by mercury-sensitive dissimilatory metal reducing bacteria. *Environ. Sci. Technol.* 40, 6690–6696. doi: 10.1021/es061046g

Zhao, B., Wang, H., Mao, X., and Li, R. (2009). Biodegradation of phenanthrene by a halophilic bacterial consortium under aerobic conditions. *Curr. Microbiol.* 58, 205–210. doi: 10.1007/s00284-008-9309-3

Conflict of Interest Statement: The authors declare that the research was conducted in the absence of any commercial or financial relationships that could be construed as a potential conflict of interest.

frontiers in Microbiology

ORIGINAL RESEARCH
published: 19 September 2018
doi: 10.3389/fmicb.2018.02096

Abundant and Rare Microbial Biospheres Respond Differently to Environmental and Spatial Factors in Tibetan Hot Springs

Yanmin Zhang[1†], Geng Wu[1†], Hongchen Jiang[1], Jian Yang[1], Weiyu She[1], Inayat Khan[1] and Wenjun Li[2]*

[1] State Key Laboratory of Biogeology and Environmental Geology, China University of Geosciences, Wuhan, China, [2] State Key Laboratory of Biocontrol and Guangdong Provincial Key Laboratory of Plant Resources, School of Life Sciences, Sun Yat-sen University, Guangzhou, China

OPEN ACCESS

Edited by:
Andreas Teske,
The University of North Carolina at Chapel Hill, United States

Reviewed by:
Matthew Schrenk,
Michigan State University, United States
Jeremy Dodsworth,
California State University, San Bernardino, United States

***Correspondence:**
Hongchen Jiang
jiangh@cug.edu.cn

[†] These authors have contributed equally to this work

Specialty section:
This article was submitted to Extreme Microbiology, a section of the journal Frontiers in Microbiology

Received: *24 December 2017*
Accepted: *16 August 2018*
Published: *19 September 2018*

Citation:
Zhang Y, Wu G, Jiang H, Yang J, She W, Khan I and Li W (2018) Abundant and Rare Microbial Biospheres Respond Differently to Environmental and Spatial Factors in Tibetan Hot Springs. Front. Microbiol. 9:2096. doi: 10.3389/fmicb.2018.02096

Little is known about the distribution and ecological functions of abundant, intermediate, and rare biospheres and their correlations with environmental factors in hot springs. Here, we explored the microbial community composition of total, abundant, intermediate, and rare biospheres in 66 Tibetan hot springs (pairwise geographic distance 0–610 km, temperature 32–86°C, pH 3.0–9.5, and salinity 0.13–1.32 g/L) with the use of Illumina MiSeq high-throughput sequencing. The results showed that the abundant sub-communities were mainly composed of *Chloroflexi*, *Proteobacteria*, *Deinococcus-Thermus*, *Aquificae*, *Bacteroidetes,* and *Firmicutes*. In contrast, the rare sub-communities mainly consisted of most newly proposed or candidate phyla of *Dictyoglomi*, *Hydrogenedentes*, *Atribacteria*, *Hadesarchaea*, *Aminicenantes*, *Microgenomates*, *Calescamantes*, *Omnitrophica*, *Altiarchaeales,* and *Chlamydiae*. However, the abundant and rare sub-communities shared some common phyla (e.g., *Crenarchaeota*, *Bathyarchaeota*, and *Chlorobi*), which were composed of different OTUs. The abundant, intermediate, and rare sub-communities were mainly influenced by different environmental variables, which could be ascribed to the fact that they may have different growth and activity and thus respond differently to these variables. Spatial factors showed more contribution to shaping of the intermediate and rare communities than to abundant sub-community, suggesting that the abundant taxa were more easily dispersed than their rare counterparts among hot springs. Microbial ecological function prediction revealed that the abundant and rare sub-communities responded differently to the measured environmental factors, suggesting they may occupy different ecological niches in hot springs. The rare sub-communities may play more important roles in organic matter degradation than their abundant counterparts in hot springs. Collectively, this study provides a better understanding on the microbial community structure and potential ecological functions of the abundant and rare biospheres in hot spring ecosystems. The identified rare taxa provide new opportunities of ecological, taxonomic and genomic discoveries in Tibetan hot springs.

Keywords: Tibetan hot springs, abundant biosphere, rare biosphere, environment factors, spatial factors

INTRODUCTION

Microbes are the dominant life form in hot springs, and their community compositions are commonly linked with ecological functions. Therefore investigation of microbial community composition and their metabolic functions is of great importance to understanding of biogeochemical cycling of carbon, nitrogen and sulfur elements in geothermal environments (Rothschild and Mancinelli, 2001; Fuhrman, 2009). So far a large number of microbial investigations have been performed in hot springs worldwide, such as Yellowstone National Park (Meyer-Dombard et al., 2005) and the Great Basin in the United States (Costa et al., 2009), Kamchatka in Russia (Kublanov et al., 2009), Malaysian (Chan et al., 2015), Yunnan (Hou et al., 2013), and Tibetan Plateau in China (Lau et al., 2009; Song et al., 2010, 2013; Huang et al., 2011; Wang et al., 2013). Among some of these previous studies, temperature was shown more important in shaping microbial community than other environmental parameters (e.g., pH and water chemistry) and spatial factors (biogeography) (Skirnisdottir et al., 2000; Pearson et al., 2008; Hou et al., 2013; Wang et al., 2013; Saxena et al., 2017). However, the microbial diversity did not show a monotonic relationship with temperature, suggesting other environmental variables and/or spatial factors may also jointly shape the microbial community (Yim et al., 2006; Purcell et al., 2007). For example, microbial communities were dominated by different phylogenetic groups in the low- and high-sulfide hot spring mats with same temperature (Skirnisdottir et al., 2000); and hyperthermophilic archaeal communities showed geographical distribution pattern in various hot springs (Whitaker et al., 2003). Thus it can be seen that environmental and spatial variables are two types of important factors shaping microbial community compositions in natural ecosystems (Nemergut et al., 2013). However, few researches have ever investigated the relative contribution of environmental and spatial factors to shaping of microbial communities in hot springs.

Considering the contribution of different microbial species to the diversity and biomass in ecosystems, microbial communities could be classified into abundant and rare (relative abundance >1 and $<0.01\%$, respectively) taxa, with the former contributing major biomass but minor biodiversity and the latter contributing minor biomass but major biodiversity (Galand et al., 2009; Pedrós-Alió, 2012). Abundant taxa were the basis of most of our up-to-date knowledge on microbial diversity and response to environmental and spatial factors in hot springs, while rare taxa were usually treated as analytical annoyance (Jousset et al., 2017). However, recent 16S rRNA gene-based high-throughput sequencing surveys have revealed that rare taxa should also be considered as the indispensable component of full microbial communities due to their over-proportional roles in biogeochemical cycles and they could function as the "seed bank" of the vast gene pool (Sogin et al., 2006; Logares et al., 2015; Jousset et al., 2017). Thus abundant and rare taxa should be included in holistic analysis on microbial diversity.

Recent studies suggested abundant and rare biosphere might show contrasting response patterns to environmental and spatial factors when considering their relative importance in shaping community composition. For example, the abundant sub-community in freshwater lakes showed much stronger response to spatial factors than its rare counterpart (Liu et al., 2015; Yang et al., 2016). In contrast, abundant and rare taxa were shown to present similar biogeography in coastal saline lakes (Galand et al., 2009; Logares et al., 2013). Such inconsistency could be ascribed to different ranges of environmental factors (e.g., salinity) and geographic distance among those investigated ecosystems (Galand et al., 2009; Logares et al., 2013; Liu et al., 2015; Yang et al., 2016). However, few studies have ever differentiated abundant, and rare taxa from total microbial community when assessing microbial diversity and its response to environmental and spatial factors in hot springs.

The Tibetan Plateau (>4500 m above sea level) is located on the Indian-Eurasia collision orogenic belt, belonging to the Mediterranean-Himalayan hydrothermal areas (Wang et al., 2013). The southern Tibetan Plateau hosts one of the most active geothermal areas in the world and possesses a large number of hot springs with various environmental gradients, such as pH (3.0–8.6), temperature (30–97°C), and sulfate concentrations (3.3–850.5 mg/L) (Wang et al., 2013; Guo et al., 2014). So far several studies have been performed to investigate the microbial community in Tibetan hot springs. For example, clone library-based phylogenetic analysis showed that the bacterial communities were predominated by *Firmicutes, Proteobacteria, Cyanobacteria,* and *Chloroflexi* (Lau et al., 2009; Huang et al., 2011) and that archaeal and bacterial diversity did not show statistically significant correlation with temperature in the Tibetan hot springs (Lau et al., 2009; Huang et al., 2011). In contrast, another two 454 pyrosequencing-based studies uncovered a higher number of dominant phylogenetic groups and showed that temperature controlled the microbial structure in Tibetan hot springs (Song et al., 2013; Wang et al., 2013). However, in these previous microbial studies the rare sub-community was not differentiated from total microbial community due to the intrinsic limitations of clone library-based and/or 454 Pyrosequencing techniques (Jiang et al., 2018) and to the limited number of sampled hot springs (Song et al., 2013; Wang et al., 2013). Therefore, a holistic investigation is needed on the taxonomic diversity and potential ecological functions of total community, and abundant and rare sub-communities in Tibetan hot springs.

The aims of this study were to investigate (1) the taxonomic diversity and potential ecological functions of the microbial communities (in total, abundant, and rare biospheres) in the Tibetan hot springs; (2) the influences of environmental variables on the ecological functions of the microbial communities in total, abundant, and rare biospheres; and (3) the relative importance of environmental variables (e.g., temperature) and spatial factors to shaping of microbial communities in total, abundant, and rare biospheres in the Tibetan hot springs.

MATERIALS AND METHODS

Field Measurements and Sample Collection

In summer of 2015 and 2016, field measurements and sample collection were performed in a total of 66 hot springs from five areas located on the southern Tibetan Plateau. These five sampling areas included the Quzemu zone (QZM) in Cuona County located in the valley areas from the Gonzáles Mountain to southern Tanggula Mountain, the Daggyai (DGJ) zone in Angren County, the Qucai (QC) zone in Naqu County, the Gudui (GD) zone in Cuomei County, and the Semi (SM) zone in Luozha County (**Figure 1**). Most hot springs distributed in these five zones were shaped as small (diameter < 1 m) wells (deep or shallow) with or without small outlets (**Supplementary Figures S1A,B,G–L**), while only several hot springs were shaped as lakes (**Supplementary Figure S1F**). Some hot spring waters flows directly out of the rock of the mountain in the QZM zone (**Supplementary Figures S1C,D**). Most hot springs in the DGJ zone were featured as geysers (**Supplementary Figures S1E–G**).

In the field, at each sampled hot spring water temperature, pH and concentrations of dissolved oxygen (DO) and Fe^{2+} were measured with a temperature/pH probe (DR850, HACH Company, CO, United States) and Hach kits. For water chemistry measurement, about 50 mL hot spring water was filtered through polycarbonate membrane filters (pore size 0.22 μm). A half of the resulting filtrate was collected into polyethylene bottles for major anion measurement, and the other half of resulting filtrate was collected for major cation measurement into glass bottles supplemented with concentrated HNO_3 (to a final concentration of 0.1 M). For dissolved organic carbon (DOC) analysis, hot spring water was filtrated through 0.7-mm Whatman GF/F filters followed by acidification with concentrated phosphoric acid (to a final concentration of 0.1 M). The resulted DOC samples were stored on ice in the field and during transportation, and were then stored at 4°C in the laboratory until further analysis. After field measurements, the sediment/water interface (top 1 cm) was collected for DNA extractions and total organic carbon (TOC) measurements from each studied hot spring and then stored on dry ice in the field and during transportation. On arrival in laboratory, the frozen samples were transferred to a −80°C freezer until further analyses.

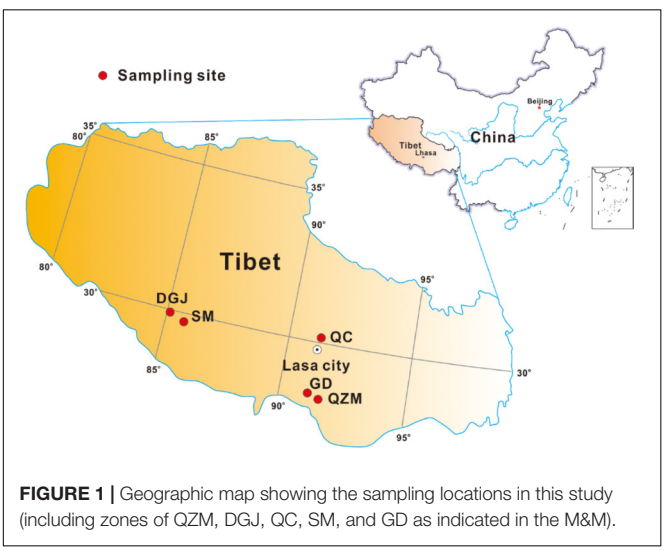

FIGURE 1 | Geographic map showing the sampling locations in this study (including zones of QZM, DGJ, QC, SM, and GD as indicated in the M&M).

Laboratory Geochemical Analyses

Major cation and anion concentrations (e.g., K^+, Na^+, Ca^{2+}, Mg^{2+}, SO_4^{2-}, and Cl^-) of the collected hot spring waters were measured by using ion chromatography (Dionex DX-600, United States). Salinity was obtained by summing the concentrations of the eight abovementioned major ions. Water DOC and sediment TOC concentrations were measured on a multi N/C 2100S analyzer (Analytik Jena, Germany). Before sediment TOC analysis, carbonates in the sediment samples were removed by overnight acidification with 1 N HCl, and then the acidified sediments were washed to neutral pH, dried in an oven and ground into fine powder.

DNA Extraction and Sequencing

DNA was extracted from 0.5 g surface sediment samples using the Fast DNA SPIN Kit for Soil according to the manufacturer's instruction (MP Biomedical, Solon, OH, United States). The extracted DNA was amplified with a universal 16S rRNA gene primer set of barcoded 515F (5′-GTGYCAGCMGCCGCGGTA-3′)/806R (5′-GGACTACVSGGGTATCTAAT-3′), and the detailed PCR conditions were described in a previous study (Tamaki et al., 2011). Briefly, a unique 12 bp barcode sequence was added between the sequencing adapter and the forward primer to differentiate among samples. In order to minimize technical artifacts (Zhou et al., 2011) and ruling out contaminations from the laboratory reagents, triplicate PCRs and experimental blanks (replacement of DNA with the same amount of sterilized deionized water) were conducted for each sample. The successful PCR products were purified using a DNA Gel Extraction Kit (Axygen, Union City, CA, United States). The DNA quality and concentrations were assessed based on the absorbance ratios of 260/280 and 260/230 using a NanoDrop ND-1000 Spectrophotometer (NanoDrop Technology, DE, United States). The bar-coded amplicons (291 bp in length) from each sample were pooled with equimolar concentrations and then were sequenced by using an Illumina MiSeq platform (Caporaso et al., 2012).

Data Processing and Statistical Analyses

In order to increase the validity of the OTU grouping and to make the classification of intermediate and rare taxa more credible in the sampled hot springs, the obtained Illumina sequencing data were filtered according to the strategies described previously (Lynch and Neufeld, 2015). The data analyses were following the UPARSE pipeline (Edgar, 2013). Briefly, the paired reads were joined using FLASH (fast length adjustment of short reads) with default settings (Magoè and Salzberg, 2011). Both forward and reverse primer sequences were removed from the resulting joined reads, which were then demultiplexed and quality filtered using QIIME v1.8.0 with *split_libraries_fastq*.py script (Caporaso et al.,

2012). Reads having the following properties were discarded: (1) containing more than three consecutive low quality (Phred quality score <30) bases, (2) containing ambiguous base, and (3) comprising consecutive high quality bases less than 75% of the total read length. Chimera checking was performed using the UCHIME module with *de novo* method in USEARCH[1] (Edgar et al., 2011). Subsequently, qualified reads were de-replicated and clustered using the USEARCH. All the qualified reads were truncated to identical length with 235 nt. All singletons and reads with length less than 235 nt were discarded, and operational taxonomic units (OTUs) were defined at the 97% cutoff by using the UPARSE-OTU algorithm (Edgar, 2013). The OTU representative sequences were then selected and their taxonomy was assigned using the ribosomal data base project (RDP) classifier algorithm at the 80% threshold (Wang et al., 2007) against the SILVA 123 database in the QIIME program. The OTU table was rarefied to equal sequence number (n = 22938) for each sample with 1000 replicates, and then the alpha diversity (i.e., Simpson, Shannon, Equitability, and Chao1) was calculated at the 97% cutoff by QIIME. The rarefied OTU table was used for downstream analyses unless otherwise specified. Abundant and rare OTUs were arbitrarily defined as the OTUs with relative abundance of >1 and <0.01% within one sample, respectively (Galand et al., 2009), the intermediate OTUs were arbitrarily defined as the OTUs with relative abundance between 0.01–1%. In order to identify potential microbial ecological functions in the studied hot springs, the obtained OTUs were compared against the FAPROTAX 1.1 database to predict potential metabolic functions of the microbial community (Louca et al., 2016). The spearman correlation was assessed between the dominant taxa (or the dominant metabolic phenotypes) and the measured environmental factors with the use of "vegan" and "ggplot" in the R package.

In order to identify sites with similar water geochemistry, the measured environmental variables were subjected to cluster analysis by employing the PAST software with the unweighted pair group method with arithmetic mean (UPGMA) of Euclidean distance (Yang et al., 2013). In order to compare microbial similarity among the samples, UPGMA cluster analysis was conducted for the total, abundant and rare biosphere of the studied 66 hot spring samples based on Bray-Curtis dissimilarities of at the 97% cutoff. Mantel test was performed to assess the correlation between the microbial community (of total, abundant, intermediate, and rare biosphere) and the measured environmental variables/geographic distance by using the PAST software. In order to evaluate the relative importance of environmental and spatial factors in shaping microbial community, aggregated boosted tree (ABT) analysis was performed to quantitatively evaluate the relative influence of individual environmental factors and geographic distance on the distribution of microbial community using R package "gbm" (De'Ath, 2007). Variance inflation factors (VIFs) were computed to check the presence of collinearities among the environmental variables using the function VIF in the "car" package. The environmental variables that had VIF >10 (which indicated evident collinearities with the other measured environmental variables) were removed from subsequent ABT analysis until all VIFs of the variables were <10 (De'Ath, 2007). The parameters for ABT analysis were set as follows: distribution = gaussian, n.trees = 10000, shrinkage = 0.001, bag.fraction = 0.5, train.fraction = 0.5, cv.folds = 10, interaction.depth = 3.

In order to identify the difference in microbial community compositions of various temperature, the 66 hot spring samples were classified into the moderate temperature (32–73°C) and high temperature (73–86°C) groups (abbreviated as MT and HT hereinafter, respectively) depending on the upper temperature limit for photosynthesis (about 73°C) (Rothschild and Mancinelli, 2001). Similarity analysis (one-way ANOSIM) was performed based on the Bray-Curtis dissimilarity at the 97% cutoff to test for any significant dissimilarity in community compositions of the total, abundant, intermediate, and rare biosphere between the MT and HT groups of, respectively.

Nucleotide Sequence Accession Numbers

The sequences retrieved in this study were deposited at the Sequence Read Archive (SRA) in the National Center for Biotechnology Information (NCBI) under the BioProject accession no. SRP101393.

RESULTS

Environmental Parameters of the Sampled Hot Springs

The hot springs in this study possessed a range of temperature (32–86°C), pH (3.0–9.5), salinity (0.13–1.32 g/L), and DOC (0–958.60 mg/L) and TOC (0–12.60%) contents (**Supplementary Table S1**). Most of the QZM, QC, SM, and GD hot springs had nearly neutral pH (6.5–8.0), while most of the DGJ hot springs were neutral to slightly alkaline (pH 7.0–9.5), except the acidic DGJ_17 (pH = 3.0), DGJ_18 (pH = 4.0), and SM_3 (pH = 3.4) hot springs (**Supplementary Table S1**). Geochemistry clustering analysis showed that the sampled hot springs were clustered on the basis of their locations, suggesting that hot springs from different zones were distinct with respect to geochemistry (**Supplementary Figure S2**). Comparatively, the DGJ hot springs exhibited lower contents of DOC, TOC, SO_4^{2-}, and Cl^- than those in other four sampling zones (**Supplementary Table S1**). In addition, most of the samples from one sampling location were clustered together according to their temperature (i.e., MT vs. HT) in the QZM and DGJ zones.

Microbial Diversity and Composition of the Total, Abundant, Intermediate, and Rare Biosphere

A total of 4566560 quality sequence reads were obtained from the 66 hot springs samples with an average of 69190 sequence reads per sample. The Goods coverage was 96–100%, indicating that the number of sequence reads was sufficient to capture most taxa in each sample (**Table 1**). The observed OTUs, and

[1]http://www.drive5.com/usearch/

TABLE 1 | Alpha diversity indices at the 97% OTU level of 16S rRNA gene libraries of the studied hot spring samples (re-sampling 22938 reads in each sample was performed for 1000 replicates).

Sample ID	No. of obtained sequence reads	Observed species	Goods coverage	Simpson	Shannon	Equitability	Chao1
QZM-1	99313	188.63	0.98	0.84	3.75	0.50	324.95
QZM-2	101178	278.46	0.98	0.89	4.51	0.56	489.47
QZM-3	109007	200.39	0.98	0.83	3.47	0.45	352.13
QZM-4	49444	286.03	0.98	0.84	4.45	0.55	440.87
QZM-5	52532	340.44	0.97	0.91	5.25	0.62	527.17
QZM-6	57095	286.18	0.98	0.93	4.93	0.60	463.18
QZM-7	109986	294.10	0.97	0.91	5.05	0.62	489.71
QZM-9	63729	361.93	0.97	0.87	5.10	0.60	541.96
QZM-10	51200	326.03	0.98	0.94	5.53	0.66	472.67
QZM-11	50457	297.66	0.98	0.92	5.04	0.61	443.44
QZM-12	57524	302.96	0.98	0.88	4.96	0.60	446.97
QZM-13	67777	305.12	0.98	0.92	5.14	0.62	471.55
QZM-14	73807	296.95	0.98	0.93	5.07	0.62	447.69
QZM-15	117181	209.36	0.98	0.88	4.11	0.53	368.35
QZM-16	182398	190.90	0.98	0.55	2.32	0.31	359.79
QZM_17	29163	165.13	0.99	0.95	5.20	0.71	219.03
QZM_18	56895	516.85	0.96	0.96	6.53	0.72	758.66
QZM_19	26561	268.23	0.98	0.90	5.11	0.63	349.55
QZM_20	43788	231.58	0.98	0.91	4.70	0.60	331.58
QZM_21	62016	176.90	0.99	0.94	5.07	0.68	247.80
QZM_22	79462	298.12	0.98	0.94	5.61	0.68	405.51
QZM_23	70841	138.71	0.99	0.91	4.28	0.60	221.68
QZM_24	46399	99.06	0.99	0.89	4.04	0.61	147.17
DGJ-1	132844	251.24	0.98	0.91	4.65	0.58	423.53
DGJ-2	143530	219.09	0.98	0.77	3.38	0.43	397.54
DGJ-3	114267	271.51	0.98	0.68	3.59	0.44	475.56
DGJ-4	130429	225.44	0.98	0.78	3.70	0.47	383.50
DGJ-5	122686	283.36	0.98	0.86	4.46	0.55	463.98
DGJ-6	68683	315.41	0.98	0.87	4.68	0.56	484.45
DGJ-8	108040	200.73	0.98	0.85	3.68	0.48	354.82
DGJ-9	157980	193.38	0.98	0.73	2.92	0.38	354.23
DGJ-10	135547	189.06	0.98	0.78	3.35	0.44	344.29
DGJ-11	75643	294.15	0.98	0.90	4.75	0.58	480.93
DGJ-12	101400	234.22	0.98	0.86	4.02	0.51	386.64
DGJ-13	29279	162.03	0.99	0.85	3.56	0.49	241.14
DGJ-14	29294	352.43	0.98	0.94	5.75	0.68	508.37
DGJ-15	135450	237.17	0.98	0.70	3.39	0.43	428.67
DGJ-16	56534	385.42	0.97	0.94	5.65	0.66	587.64
DGJ_17	56762	102.70	0.99	0.87	3.90	0.58	140.52
DGJ_18	53381	113.17	0.99	0.88	3.73	0.55	164.94
DGJ_19	61567	173.37	0.99	0.81	3.82	0.51	285.08
DGJ_20	46615	114.25	0.99	0.91	4.03	0.59	184.79
DGJ_21	76521	208.24	0.99	0.90	4.75	0.62	308.89
DGJ_22	57436	88.71	1.00	0.88	3.91	0.60	109.95
DGJ_23	44419	245.29	0.98	0.94	5.42	0.68	352.14
DGJ_24	58987	112.92	0.99	0.85	3.57	0.52	181.97
DGJ_25	62974	65.78	1.00	0.84	3.47	0.57	100.14
DGJ_26	88622	78.31	1.00	0.84	3.55	0.57	115.61
DGJ_27	57592	108.92	0.99	0.86	3.75	0.55	146.63
DGJ_28	32667	102.34	0.99	0.79	3.22	0.48	154.84
DGJ_29	47858	363.72	0.97	0.96	5.94	0.70	527.37

(Continued)

TABLE 1 | Continued

Sample ID	No. of obtained sequence reads	Observed species	Goods coverage	Simpson	Shannon	Equitability	Chao1
DGJ_30	51493	100.60	0.99	0.90	3.91	0.59	171.92
QC01	46085	104.13	0.99	0.88	3.94	0.59	139.85
QC02	42925	247.94	0.98	0.90	4.65	0.58	350.54
QC03	34831	249.25	0.98	0.93	5.01	0.63	353.16
QC04	32549	193.66	0.99	0.92	4.84	0.64	252.14
QC05	36372	420.48	0.97	0.94	5.56	0.64	639.77
SM_1	60261	115.12	0.99	0.88	4.06	0.59	166.33
SM_2	55048	111.93	0.99	0.89	4.08	0.60	175.46
SM_3	42195	65.11	0.99	0.78	2.91	0.48	107.86
SM_4	52521	116.61	0.99	0.86	3.84	0.56	156.92
GD_1	32301	104.89	0.99	0.79	2.96	0.44	158.13
GD_2	28471	183.07	0.99	0.92	4.62	0.62	249.24
GD_3	22938	300.01	0.98	0.96	5.79	0.70	394.81
GD_4	50119	285.79	0.98	0.92	4.99	0.61	454.78
GD_5	33691	149.03	0.99	0.77	3.37	0.47	239.37

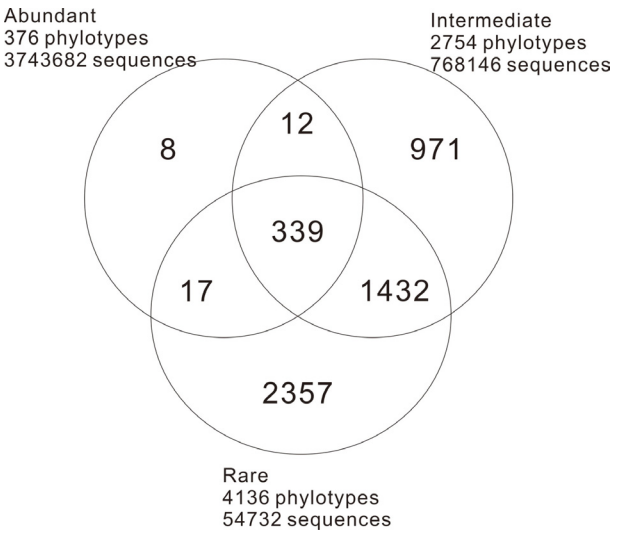

FIGURE 2 | Venn diagram illustrating the distribution structure of the abundant, intermediate, and rare phylotypes (OTUs at the 97% cutoff) in the sampled hot springs.

Shannon and Chao 1 indices ranged 65.11–516.85, 2.32–6.53, and 100.14–758.66 in the studied hot springs, respectively (**Table 1**). A total of 5136 OTUs were obtained in the total biosphere. A total of 376, 2754, and 4136 OTUs were identified as abundant, intermediate, and rare taxa, respectively. In total, 339 OTUs were common among the abundant, intermediate, and rare biosphere; 351 OTUs were common between the abundant and intermediate biospheres, 1762 OTUs were common between the intermediate and rare biospheres, and 356 OTUs were common between the abundant and rare biospheres (**Figure 2**). In addition, 8, 971 and 2357 OTUs were unique in the abundant, intermediate, and rare biospheres, respectively (**Figure 2**). These identified abundant, intermediate, and rare taxa covered 81.98, 16.82, and <2% of the total obtained quality sequence reads, respectively. Further phylogenic taxonomy analysis showed that about 91.26, 92.05, 87.70, and 90.43% of the obtained total, abundant, intermediate, and rare OTUs were affiliated with bacteria, and 8.74, 7.95, 12.30, and 9.57% of the total, abundant, intermediate, and rare OTUs were identified as archaea (**Figure 3**).

The abundant sub-community and total community were composed of similar dominant phyla and classes: the top 10 most dominant phyla of the abundant sub-community were *Chloroflexi*, *Proteobacteria*, *Deinococcus-Thermus*, *Aquificae*, *Bacteroidetes*, *Firmicutes*, *Cyanobacteria*, *Acetothermia*, *Thermodesulfobacteria,* and *Thermotogae* (**Figure 3** and **Supplementary Table S2**), and the top 10 most dominant classes were *Deinococci*, *Chloroflexia*, *Aquificae*, *Betaproteobacteria*, *Sphingobacteriia*, *Cyanobacteria*, *Gammaproteobacteria*, *Bacilli*, *Anaerolineae,* and *Thermodesulfobacteria* (**Figure 3** and **Supplementary Table S3**). In comparison, the phylogenetic composition of the intermediate sub-community showed little difference from the abundant sub-community. Specifically, the top 10 most dominant phyla in the intermediate sub-community were *Thermotogae*, *Armatimonadetes*, *Thermodesulfobacteria*, *Bacteroidetes*, *Ignavibacteriae*, *Acetothermia*, *Chlorobi, Planctomycetes*, *Verrucomicrobia,* and *Acidobacteria* (**Figure 3** and **Supplementary Table S2**), with *Thermotogae*, *Thermodesulfobacteria*, *Gammaproteobacteria*, *Ignavibacteria*, *Solibacteres*, *Alphaproteobacteria*, *Chlorobia*, *Sphingobacteriia*, *Planctomycetacia,* and *Nitrospira* being the top 10 most dominant Classes (**Supplementary Table S3**). In contrast, the rare sub-community showed apparently different phylogenetic composition from its abundant counterpart: the top 10 most dominant phyla in the rare biosphere were *Dictyoglomi*, *Hydrogenedentes*, *Atribacteria*, *Hadesarchaea*, *Aminicenantes*, *Microgenomates*, *Calescamantes*, *Omnitrophica*, *Altiarchaeales,* and *Chlamydiae*. Correspondingly, with *Acidimicrobiia*, *Opitutae*, *Coriobacteriia*, *Dictyoglomia*,

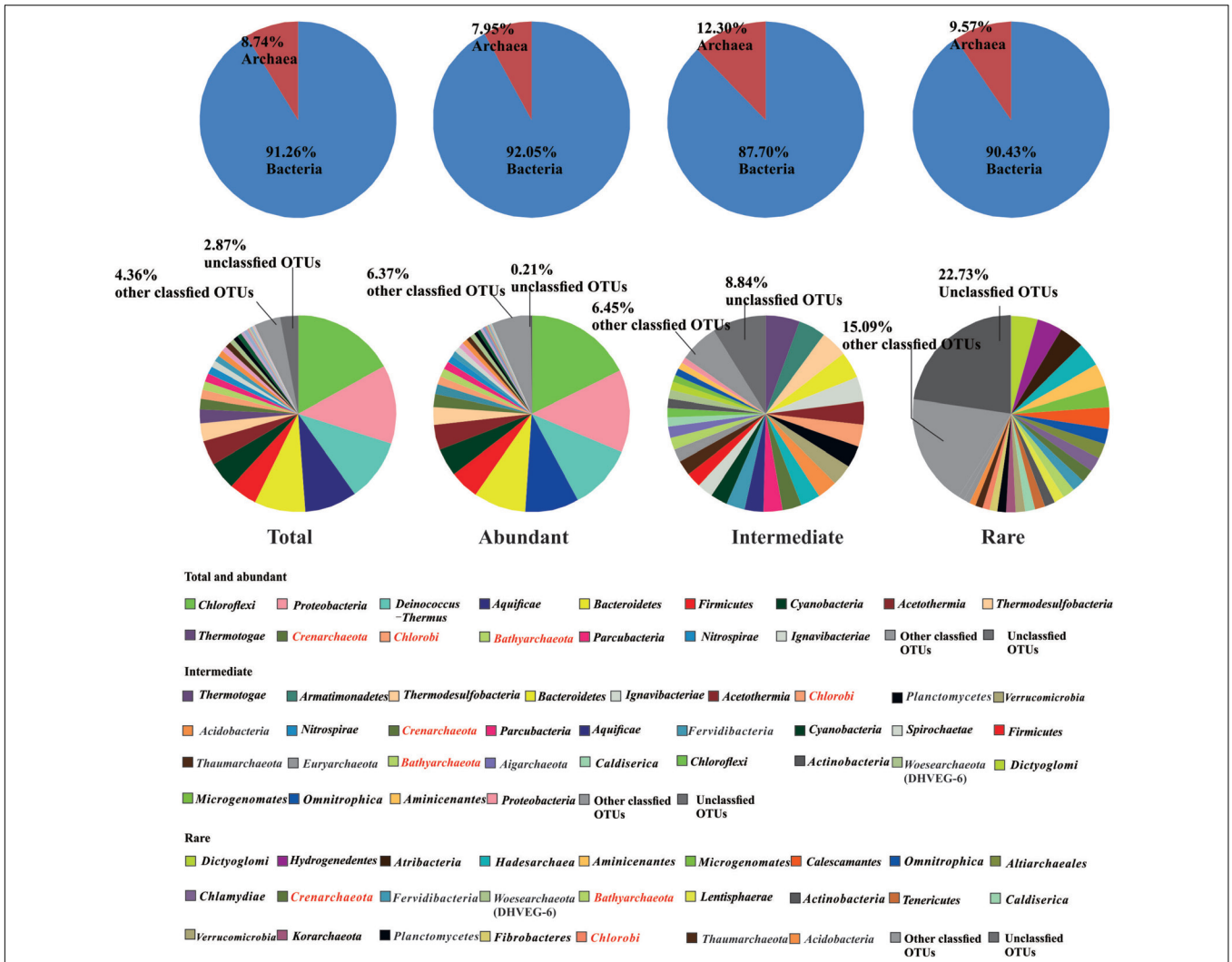

FIGURE 3 | Relative abundance of bacteria and archaea (the upper row), and microbial community composition (at the phylum level) of the total, abundant, intermediate, and rare biospheres (the lower row) (in the caption, characters in red indicated the phyla occurring among the abundant, intermediate, and rare biospheres).

Fimbriimonadia, *Chthonomonadetes*, *Thermomicrobia*, *Caldilineae*, *Verrucomicrobia*, and *Thermoleophilia* being dominant Classes (**Supplementary Table S2**).

Further analysis showed that all the detected dominant phyla in the abundant biosphere or most (44.09%) of the detected dominant phyla in the rare biosphere can be observed in the intermediate biosphere. Meanwhile, some phyla (e.g., *Crenarchaeota*, *Bathyarchaeota*, and *Chlorobi*) were common among the abundant, intermediate, and rare biospheres (**Figure 3** and **Supplementary Table S2**). The total and abundant biospheres showed similar community structures among the studied Tibetan hot springs, while they were different from the intermediate and rare biosphere (**Supplementary Figures S3A–D**). The HT samples tended to be clustered together for the total microbial communities, and abundant and rare sub-communities. In addition, the total and rare communities exhibited evident biogeographic patterns, in contrast with no biogeographic pattern in the intermediate and abundant biosphere (**Supplementary Figures S3A–D**). Furthermore, one-way ANOSIM test indicated that the community structures of the total, abundant and intermediate biospheres showed more significant ($p < 0.01$ vs. $p < 0.05$) difference between the MT and HT hot springs than that of the rare biosphere did (**Table 2** and **Supplementary Tables S4–S7**).

Influence of Environmental and Spatial Factors on the Microbial Distribution

The Mantel test showed that both environmental (temperature, pH, Fe^{2+}, salinity, DOC, and TOC) and spatial factors (GD, geographical distance) were significantly ($p < 0.05$) correlated with the total communities and the abundant, intermediate, and rare sub-communities (**Table 3**). Specifically, the total community was significantly ($p < 0.05$) correlated with temperature, salinity, DOC, GD, pH, Fe^{2+}, and TOC (**Table 3**);

TABLE 2 | One-way ANOSIM test on the difference in community structures of the total, abundant, intermediate, and rare biospheres between the MT and HT hot springs.

Biosphere	OTUs	R	P
Total	MT vs. HT	0.193	<0.001
Abundant	MT vs. HT	0.105	<0.01
Intermediate	MT vs. HT	0.211	<0.001
Rare	MT vs. HT	0.094	<0.05

the abundant sub-community was significantly correlated with temperature, GD, pH and salinity (**Table 3**). While the intermediate and rare sub-communities were significantly ($p < 0.05$) correlated with DOC, salinity and GD (**Table 3**). In addition, the common phyla (i.e., *Crenarchaeota*, *Chlorobi*, and *Bathyarchaeota*) of the abundant and rare biospheres showed different responses to the measured environmental factors (**Table 4**). For example, *Crenarchaeota* was only significantly correlated with DOC ($p < 0.01$), and *Chlorobi* was significantly correlated with salinity ($p < 0.001$), TOC ($p < 0.01$), pH ($p < 0.01$), and DOC ($p < 0.05$). While *Bathyarchaeota* showed no correlations with the measured environmental factors. In contrast, these three common phyla were significantly correlated with the graphical distance ($p < 0.01$) (**Table 4**).

The ABT analysis showed that the relative importance of the measured variables differed with respect to their contribution to shaping of the microbial compositions of the studied hot springs (**Table 3** and **Figure 4**). For shaping of the total community, spatial factors (GD) exhibited higher contribution (83.4 vs.

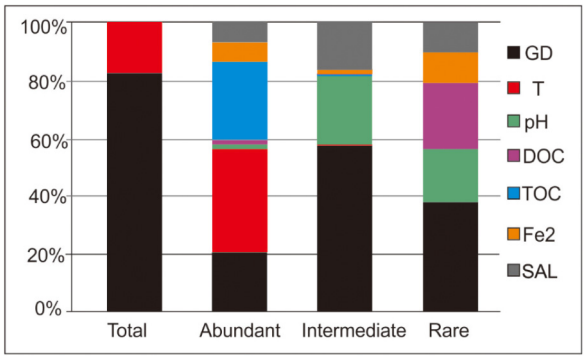

FIGURE 4 | ABT analysis showing the relative influence of individual environmental factors and geographic distance on shaping of microbial communities of the total, abundant, intermediate, and rare biospheres (SAL, salinity; DOC, dissolved organic carbon; TOC, total organic carbon; GD, geographic distance; Fe2, Fe^{2+}).

TABLE 3 | Mantel test showing correlation between the individual measured environmental parameters and the microbial communities (in the total, abundant, intermediate, and rare biospheres) of the sampled hot springs.

Physicochemical parameters	Total OTUs		Abundant OTUs		Intermediate OTUs		Rare OTUs	
	R	*P*	*R*	*P*	*R*	*P*	*R*	*P*
T	0.312	<0.001	0.320	<0.001	0.163	<0.05	0.019	0.600
pH	0.156	<0.05	0.149	<0.05	0.140	<0.05	0.066	0.223
SAL	0.225	<0.001	0.171	<0.01	0.236	<0.001	0.146	<0.05
Fe2	0.155	<0.05	0.034	0.206	−0.002	0.498	−0.045	0.805
DOC	0.306	<0.001	0.049	0.120	0.188	<0.001	0.282	<0.001
TOC	0.110	<0.05	0.739	0.059	0.117	<0.05	0.052	0.167
GD	0.159	<0.001	0.133	<0.001	0.137	<0.001	0.049	<0.05

P-value showing significant correlations (P < 0.05) were highlighted in gray. SAL, salinity; DOC, dissolved organic carbon; TOC, total organic carbon; GD, geographic distance; Fe2, Fe^{2+}.

TABLE 4 | Mantel test showing correlation between individual environmental parameters and phyla of *Crenarchaeota*, *Chlorobi,* and *Bathyarchaeota* common in the abundant, intermediate, and rare biospheres of the sampled hot springs.

Physicochemical parameters	*Crenarchaeota*		*Chlorobi*		*Bathyarchaeota*	
	R	*P*	*R*	*P*	*R*	*P*
T	0.083	0.053	0.100	0.029	-0.046	0.801
pH	0.013	0.394	0.191	<0.01	-0.030	0.644
SAL	0.079	0.081	0.297	<0.001	0.056	0.182
Fe2	−0.035	0.082	-0.033	0.797	-0.035	0.785
DOC	0.113	<0.01	0.088	<0.05	-0.001	0.472
TOC	0.043	0.148	0.135	<0.01	-0.032	0.740
GD	0.069	<0.01	0.101	<0.01	0.845	<0.01

P-value in gray background indicated a significant correlation (p < 0.05). SAL, salinity; DOC, dissolved organic carbon in hot spring water; TOC, total organic carbon in hot spring sediment; GD, geographic distance; Fe2, Fe^{2+}.

16.5%) than temperature, while other environmental factors (such as TOC, DOC, Fe^{2+}, and salinity) show no contribution; for shaping of the intermediate biosphere, spatial factors (GD) also exhibited higher contribution (56.8 vs. 43.2%) than the measured environmental factors. In contrast for shaping of the abundant and rare sub-communities, the environmental factors exhibited higher contributions (79.2 vs. 20.8% and 61.5 vs. 38.5%, respectively) than the spatial factors (**Figure 4**). For the abundant sub-community, the top three influencing factors were temperature, TOC and graphical distance, each contributing 36.2, 26.7, and 20.8% of the observed microbial variation, respectively. In contrast, for the intermediate sub-community, the top three influencing factor were spatial factors, pH and salinity, each contributing 56.8, 23.5, and 16.5% of the observed microbial variation, while temperature showed only 0.2% of contribution to shaping of the intermediate sub-community. Similarly, for the rare sub-community, the top three influencing factor were spatial factors, DOC content and pH, each contributing 38.5, 22.5, and 18.6% of microbial variation, respectively. However, temperature showed no observed contribution to shaping of the rare sub-community (**Figure 4**).

Correlations Between the Dominant Taxa of the Abundant, Intermediate, and Rare Biospheres and the Environmental Factors

Spearman correlation analysis revealed that the relative abundance of dominant taxa (at the phylum and class levels) were correlated with different environmental factors. The dominant taxa in the abundant biosphere were significantly correlated with temperature; the dominant taxa in the intermediate biosphere were significantly correlated with DOC and temperature; while the dominant taxa in the rare biosphere were significantly correlated with DOC (**Figure 5**). Specifically, different phyla and classes of one biosphere (abundant, intermediate or rare) exhibited diverse correlations with the measured environmental factors. Take the abundant biosphere for an example: the relative abundance of the phyla (and their corresponding Classes) such as *Aquificae* (*Aquificae*), *Deinococcus-Thermus*, *Firmicutes* (*Bacilli*), *Thermodesulfobacteria* (*Thermodesulfobacteria*), and *Crenarchaeota* (*Thermoprotei*) showed positive correlations ($p < 0.05$) with temperature. Conversely, relative abundance of *Chloroflexi* (*Chloroflexia*), *Bacteroidetes* (*Sphingobacteriia*), and *Cyanobacteria* (*Cyanobacteria*) showed negative correlations ($p < 0.05$) with temperature. In addition to these abovementioned major phyla or class in the abundant biosphere showing significant response to temperature, some phyla were significantly correlated with environmental variables rather than temperature. For example, *Thermotogae* (*Thermotogae*) and *Proteobacteria* (*Betaproteobacteria*) showed positive and negative correlations with TOC content ($p < 0.001$) and pH ($p < 0.05$), respectively.

Moreover, the common phyla (and their corresponding Classes) of the abundant and intermediate biospheres exhibited different responses to environmental factors. For example, *Aquificae* (*Aquificae*), *Bacteroidetes* (*Sphingobacteriia*), and *Thermotogae* (*Thermotogae*) in the intermediate biosphere exhibited positive correlations ($p < 0.05$) with DOC content, in contrast with their significant correlations ($p < 0.01$) with temperature in the abundant biosphere. Besides, the dominant phyla of the intermediate biosphere (and their corresponding classes) such as *Planctomycetes* (*Planctomycetacia*), *Verrucomicrobia, Nitrospirae* (*Nitrospira*), *Acidobacteria* (*Solibacteres*), and *Aquificae* (*Aquificae*) exhibited negative correlations ($p < 0.05$) with temperature (**Figure 5**). In contrast with the total, abundant and intermediate biospheres, only a few major phyla or classes in the rare biosphere exhibited correlations with the measured environmental factors. For example, *Aminicenantes* showed a significant positive correlation ($p < 0.01$) with pH; *Dictyoglomi* (*Dictyoglomia*) and *Calescamantes* showed a positive correlation with DOC content; and *Fervidibacteria* showed a positive correlation with temperature (**Figure 5**).

Potential Microbial Ecological Functions of the Total, Abundant, Intermediate, and Rare Communities and Their Correlation With Environmental Factors

About 1.87–62.65, 24.60–98.60, 3.83–86.48, and 67.97–93.34% of the obtained OTUs could be predicted with potential microbial ecological functions in the total, abundant, intermediate, and rare biospheres, respectively. In general, the predicted microbial ecological functions were related to carbon, sulfur and nitrogen cycles in these studied hot springs (**Figure 6** and **Supplementary Table S8**). In the total biosphere, twenty-two microbial ecological functions (relative abundance >0.01%) were identified, including chemoheterotrophy, dark sulfur oxidation, photoautotrophy, sulfur respiration, sulfate reduction, denitrification, ammonia oxidation, nitrification, nitrogen fixation, anoxygenic photoautotrophy, dark hydrogen oxidation, aromatic compound degradation, fermentation, knallgas bacteria, methanogenesis, xylan degradation, nitrite respiration, iron respiration, photoheterotrophy, methylotrophy, methanol oxidation, and hydrocarbon degradation. Fourteen of these predicted microbial functions were common among the abundant, intermediate, and rare biospheres, including chemoheterotrophy, dark sulfur oxidation, photoautotrophy, sulfur respiration, sulfate reduction, denitrification, nitrification, nitrogen fixation, anoxygenic photoautotrophy, dark hydrogen oxidation, fermentation, knallgas bacteria, methanogenesis, and iron respiration. In contrast, some of the predicted ecological functions were only present in the abundant, intermediate, or rare biosphere. For example, ammonia oxidation was only observed in the abundant biosphere, while photoheterotrophy, aromatic compound degradation, xylan degradation, methylotrophy, methanol oxidation, and hydrocarbon degradation were only found in the intermediate and rare biospheres (**Figure 6** and **Supplementary Table S8**).

In addition, some microbial ecological functions identified from the total, abundant and intermediate biospheres exhibited different relative abundance between the MT and HT hot springs (**Figure 7** and **Supplementary Table S9**). For example,

in the total and abundant biospheres, the relative abundance of photoautotrophy was higher (8.85 vs. 2.33% in the total biosphere and 7.09 vs. 3.88% in the abundant biosphere) in the MT hot springs than their counterparts in the HT hot springs, while the relative abundance of chemoheterotrophy (4.95 vs. 10.75% in the total biosphere and 19.46 vs. 33.82% in the abundant biosphere) and dark oxidation of sulfur compounds (6.21 vs. 8.11% in the total biosphere and 5.11 vs. 9.90% in the abundant biosphere) were lower in the MT hot springs than their counterparts in the HT hot springs. For the intermediate and rare biosphere, however, the identified microbial ecological functions varied little in their relative abundance between the studied MT and HT hot springs (**Figure 7** and **Supplementary Table S9**).

Spearman correlation analysis showed that temperature, DOC and TOC were the key factors influencing some of the predicted potential microbial ecological functions (relative abundance >1%) in the total, abundant and intermediate biospheres (**Figure 8**). For example, photoautotrophy showed negative and positive correlations with temperature ($p < 0.001$) and DOC ($p < 0.05$), respectively; ammonia oxidation and nitrification showed negative and positive correlations with temperature ($p < 0.001$) and TOC ($p < 0.05$), respectively; anoxygenic photoautotrophy showed negative and positive correlations with temperature ($p < 0.01$) and DOC ($p < 0.01$), respectively; and chemoheterotrophy showed a negative correlation with DOC ($p < 0.01$). In contrast, some dominant microbial ecological functions in the rare biosphere were significantly correlated with DOC content (**Figure 8**). For example, photoheterotrophy ($p < 0.001$) and sulfur respiration/dark sulfur oxidation ($p < 0.05$) showed positive and negative correlations with DOC content, respectively.

DISCUSSION

Discriminating Between the Abundant and Rare Sub-Communities Availed Better Understanding of the Microbial Structure in Tibetan Hot Springs

It is notable that differentiating the abundant and rare sub-communities from the total biosphere will improve our understanding of the microbial structure in the studied hot springs. The abundant sub-community in this study showed similar composition (at the phylum level as shown in **Figure 3** and **Supplementary Table S2**) to the total microbial community reported previously in neutral hot springs of China (Tibetan and Yunnan) and Malaysia (Song et al., 2013; Wang et al., 2013; Chan et al., 2017). However, the rare taxa were not differentiated from total biosphere in those previous studies. In contrast, rare taxa were separated from their abundant counterpart in this study, and most of them (at the phylum level as shown in **Figure 3** and **Supplementary Table S2**) belonged to either newly proposed phyla and/or candidate divisions, which were commonly detected at a lower relative abundance in the hot springs of the United States (Yellowstone National Park and California), Japan, and India (Hedlund et al., 2014; Badhai et al., 2015). So it is necessary to separate rare sub-communities from their abundant counterpart when assessing microbial diversity and community structures in hot springs. In addition, the bacterial diversity identified in this study was higher (49 vs. 42 phyla) than our previous study (Wang et al., 2013). Such difference could be ascribed to the intrinsic limitations of the sequencing techniques (Illumina sequencing vs. 454 Pyrosequencing between this and our previous study) (Jiang et al., 2018).

In addition, the abundant, intermediate, and rare status of some microbial taxa might transform to each other when environmental conditions or spatial factors differ. For example, in this study, the phyla of *Crenarchaeota* (belonging to Class of *Desulfurococcales*, *Thermoproteales*, *Sulfolobales,* and *Fervidicoccales*), *Bathyarchaeota*, and *Chlorobi* (belonging to class of *Chlorobiales*) were common among the abundant, intermediate, and rare sub-communities, but they showed different responses to environmental and spatial factors (**Table 4**). Besides, the rare phyla of *Dictyoglomi*, *Armatimonadetes,* and *Thaumarchaeota* identified in this study were ever detected as abundant phyla in previous researches on Tibetan hot springs (Song et al., 2013; Wang et al., 2013, 2014), such finding could be ascribed to the fact that the rare sub-community can serve as part of the seed bank and contribute to ecosystem dynamics and even become dominant under favorable conditions (Galand et al., 2009; Brazelton et al., 2010; Hugoni et al., 2013). Moreover, the common phyla of *Crenarchaeota*, *Bathyarchaeota*, and *Chlorobi* differed in their phylogenetic compositions between the abundant and rare sub-communities (e.g., the *Thermofilum* genus-like vs. unclassified OTUs in *Thermoproteales* between the rare and abundant sub-communities). These findings suggested that abundant and rare taxa may occupy different ecological niches and they together maintain ecological relevance in hot springs (Jousset et al., 2017). Note that the observed abundant, intermediate, and rare status transformation of some microbial taxa may be caused by sampling artifacts (e.g., random sampling) (Zhou et al., 2008) and intrinsic limitations of high-throughput sequencing techniques (Jiang et al., 2018), which could be improved by employing technical and biological replicates (Zhou et al., 2011). Due to lack of biological replicates, the rare biosphere diversity of the studied hot springs may be overestimated in this study. However, the current data in the present study could at least give a sketch of rare biosphere diversity in the studied Tibetan hot springs.

Different Influences of Environmental and Spatial Factors on the Total, Abundant and Rare Sub-Communities

It is noteworthy that total microbial community, abundant, intermediate, and rare sub-communities responded differently to environmental and geographical factors in the studied Tibetan hot springs. Previous microbial research in hot springs did not differentiate the abundant, intermediate, and rare taxa from the total microbial community, and temperature was shown

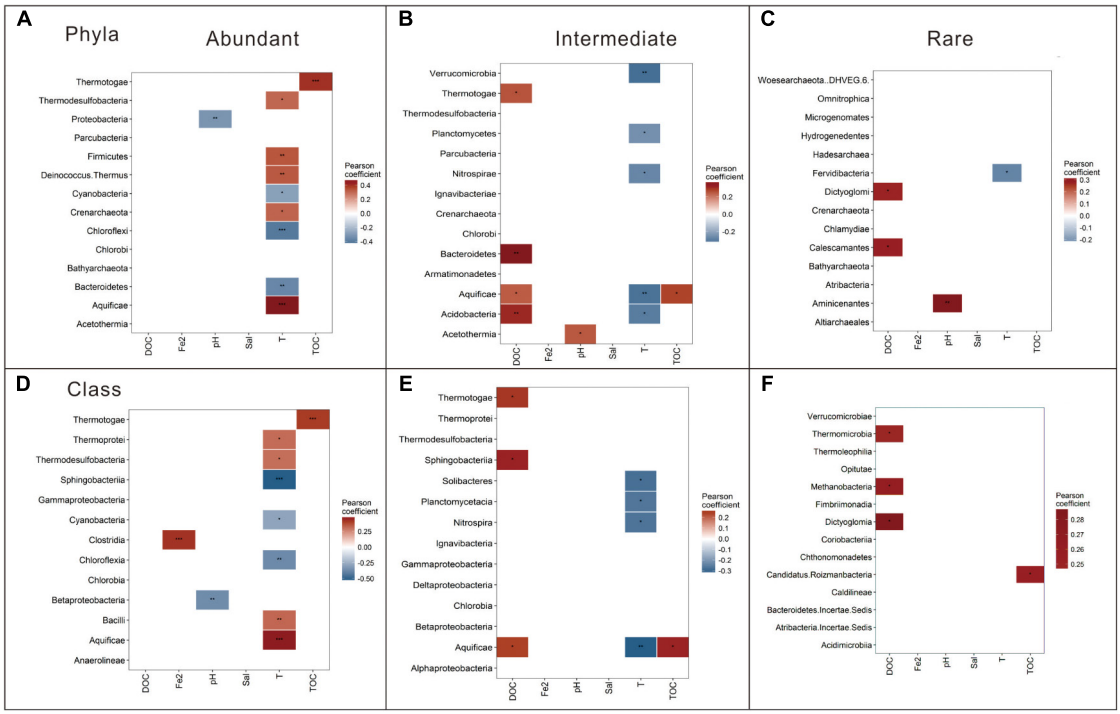

FIGURE 5 | Pearson correlation between the relative abundance of the dominant taxa (at the phylum and class levels) and the measured environmental variables for the abundant **(A,D)**, intermediate **(B,E)**, and rare **(C,F)** biospheres. ***$p < 0.001$; **$p < 0.01$; and *$p < 0.05$; Sal, salinity; DOC, dissolved organic carbon; TOC, total organic carbon; Fe2, Fe^{2+}.

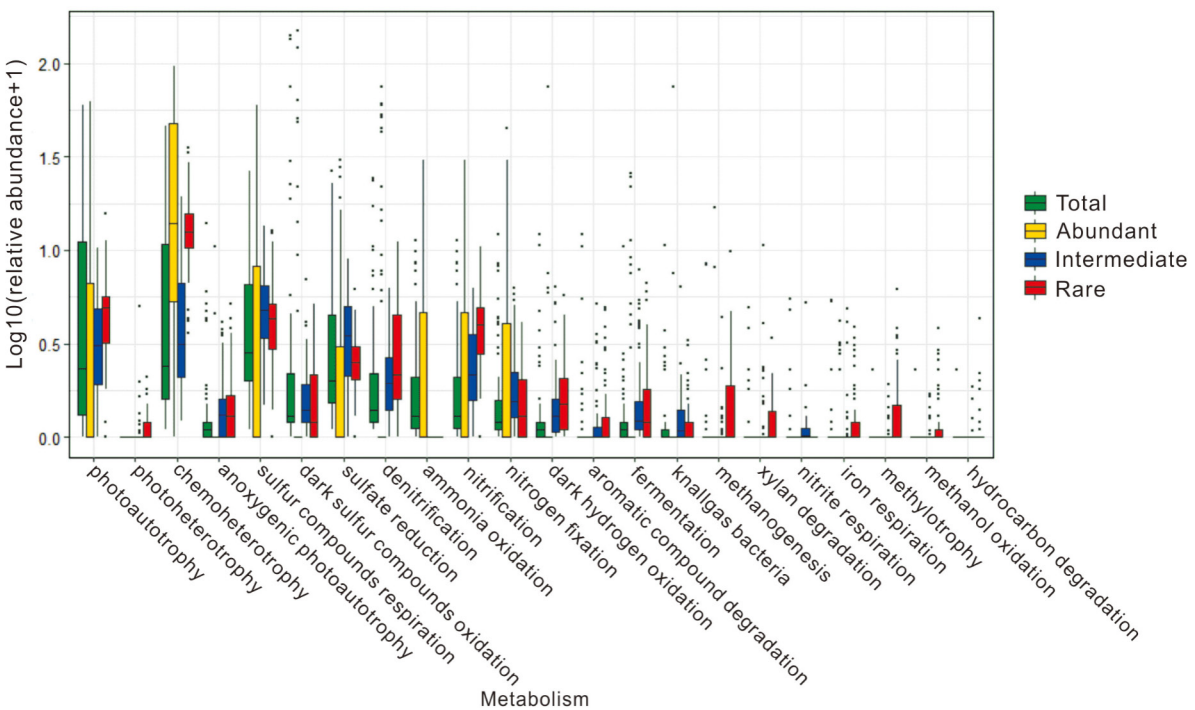

FIGURE 6 | The potential microbial ecological functions identified from prediction and their relative abundance in the total, abundant, intermediate, and rare biospheres of the studied hot springs.

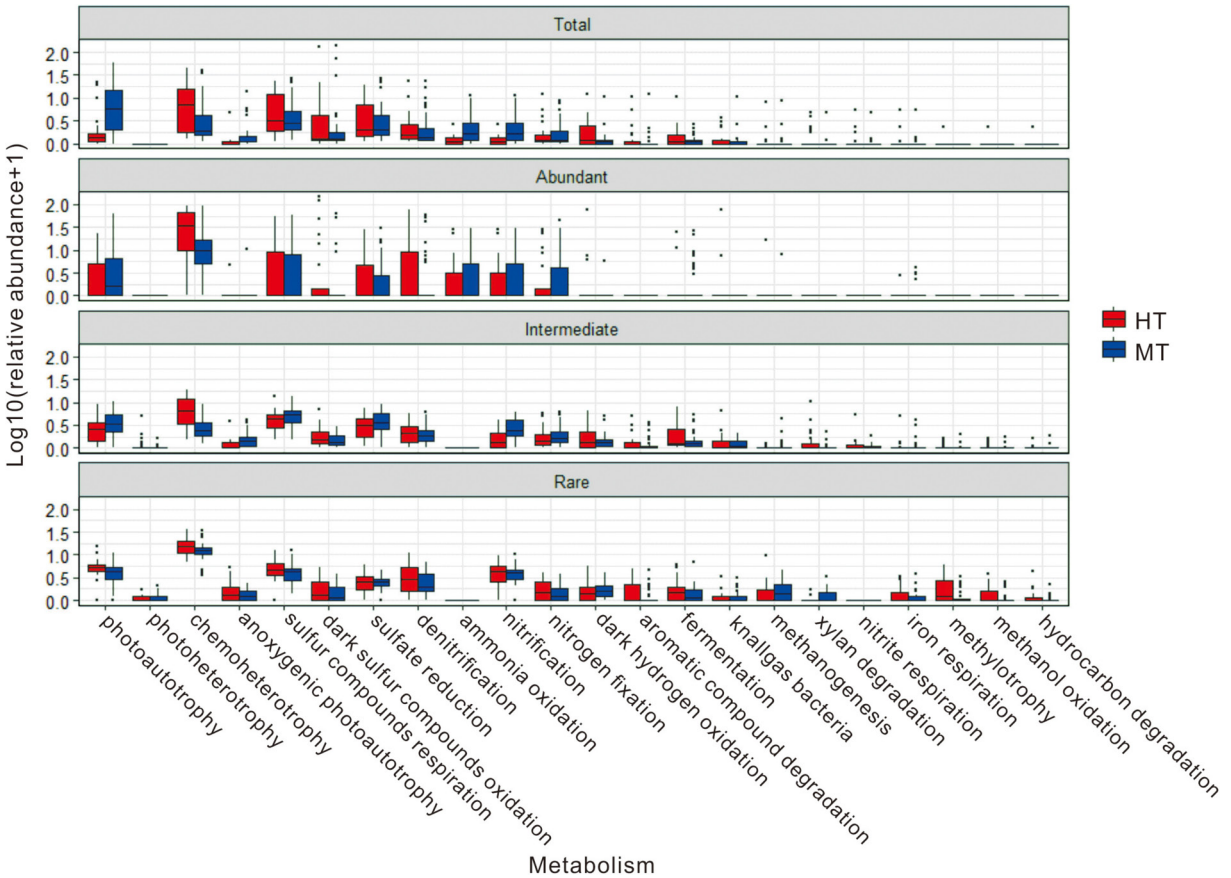

FIGURE 7 | Relative abundance of the predicted ecological functions in total, abundant, intermediate, and rare biospheres of the MT and HT hot springs.

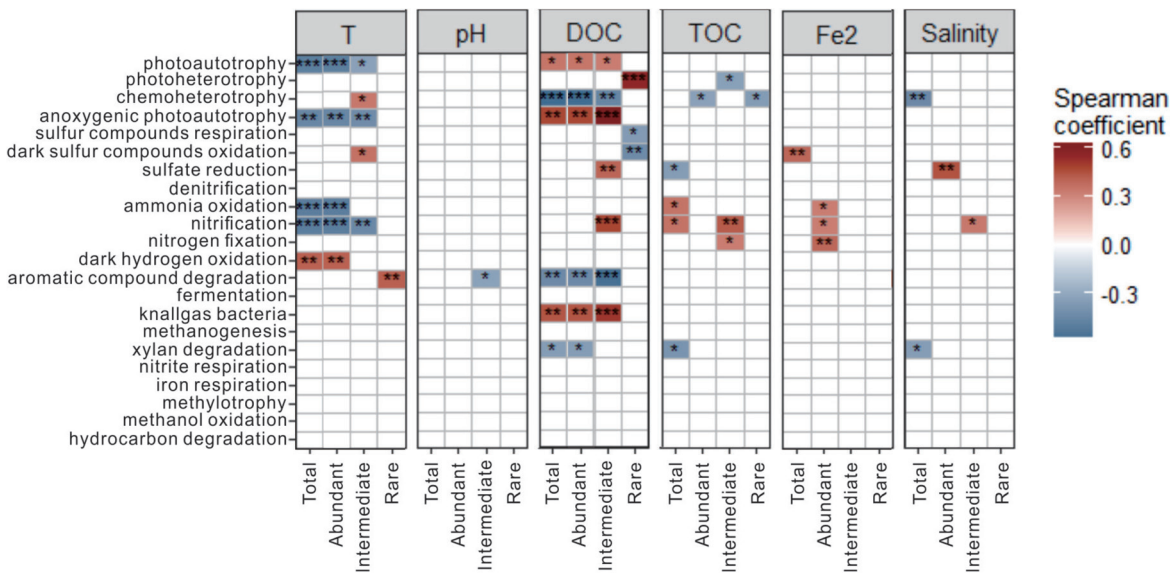

FIGURE 8 | Spearman correlations between the relative abundance of the identified microbial ecological functions and the measured environmental variables for the total, abundant, intermediate, and rare biospheres. ***$p < 0.001$; **$p < 0.01$; and *$p < 0.05$.

to be the key factor in shaping microbial structures in hot springs (Miller et al., 2009; Cole et al., 2013; Wang et al., 2013; Chan et al., 2017; Saxena et al., 2017). In contrast with this study, temperature was only found as the most important environmental factor affecting the abundant sub-community, whereas it was not among the most significant factors influencing the intermediate and rare sub-communities (**Figure 4**). In addition to temperature, organic substrates were shown to shape microbial diversity in other previous research, which did not discriminate abundant and rare sub-communities (Menzel et al., 2015; Chan et al., 2017). Such different responses of abundant and rare sub-communities to environmental variables suggested that different environmental factors could account for the distribution of various microbial taxa. In addition, the rare taxa contributed the majority of the microbial diversity (Galand et al., 2009; Pedrós-Alió, 2012). So it is reasonable to observe that different environmental factors shaped community structures of total, abundant and rare biospheres of the studied Tibetan hot springs, which was also in accordance with previous findings in oceans (Pedrós-Alió, 2012; Logares et al., 2014).

Moreover, the dominant taxa (at the phylum and class levels) in the abundant, intermediate, and rare sub-communities also responded differently to the measured environmental factors. For example, most phyla (class) of the abundant biosphere exhibited positive or negative correlations with temperature (as shown in **Figure 5**), which was consistent with previous findings for total microbial community in hot springs (Cole et al., 2013; Hou et al., 2013; Wang et al., 2013). In contrast, some phyla (class) in the abundant sub-community showed significant correlation with non-temperature environmental factors (For example, *Thermotoga* and *Proteobacteria* were significantly correlated with TOC content and pH, respectively). In addition, some common phyla between the abundant and intermediate sub-communities exhibited different responses to the measured environmental factors (For example, *Aquificae* in the intermediate sub-community exhibited a negative correlation with temperature and a positive correlation with DOC, while the *Aquificae* showed a positive correlation with temperature in the abundant sub-community). Such inconsistency could be ascribed to the fact that the common phyla between different sub-communities were composed of different taxa (**Supplementary Table S2**) and they might be characteristic of different growth and activity, as manifested in their relative abundance of the abundant (>1%), intermediate (0.01–1%) and rare (<0.01%) sub-communities.

It is also notable that spatial factors (e.g., GD) showed more contribution to shaping of the intermediate and rare sub-communities than to the abundant sub-community (**Figure 4**). This finding could be explained by the fact that the dispersal of rare taxa was more likely restricted among different ecosystems than that of their abundant counterparts (Logue, 2010; Liu et al., 2015). Furthermore, other unmeasured factors such as sediment mineralogy (Hou et al., 2013) and total nitrogen (Chan et al., 2017) might contribute to shaping of community structures of total, abundant and rare biospheres, which awaits further investigation.

Diverse Microbial Metabolic Phenotypes and Their Correlations With Environmental Factors in the Abundant, Intermediate, and Rare Biospheres

It is not surprising to observe more potential microbial ecological functions (20 and 21 vs. 15) (**Supplementary Table S6**) predicted in the intermediate and rare biospheres than that in the abundant biosphere because the former contained more diverse microbial taxa (OTUs) (Lynch and Neufeld, 2015). This finding may suggested that the intermediate and rare sub-communities in hot springs played important roles in the ecological function cache and thus ensured the ecosystem stability in response to environmental change (Ashley et al., 2012; Lynch and Neufeld, 2015). In addition, the intermediate and rare sub-communities contained some unique microbial functions related to organic matter degradation such as methylotrophy, methanol oxidation, aromatic compound degradation, xylan degradation, and hydrocarbon degradation (**Figure 6** and **Supplementary Table S8**), whereas such microbial functions were not identified in the abundant sub-community. Such contrasting results suggested that the intermediate and rare sub-communities in the studied hot springs may play more important roles than their abundant counterparts in organic matter degradation. In contrast, the abundant sub-community also contained unique microbial functions (e.g., ammonia oxidation) that were not identified in the intermediate and rare sub-communities. Such distinct distribution of microbial ecological functions between the abundant and rare sub-communities suggested that the abundant and rare taxa might occupy different ecological niches in hot spring ecosystems. However, further research is required to figure out the roles that the abundant and rare taxa each play in the ecological functions of the studied hot springs.

In addition to the abovementioned different ecological function compositions among the abundant, intermediate, and rare biospheres, it is also interesting to observe that some microbial functions shift in their abundance between the total/abundant biospheres of the MT and HT hot springs. For example, photoautotrophy was the main carbon fixation pathway in the MT hot springs (8.85 and 6.24% in relative abundance in total and abundant biosphere, respectively), while lower relative abundance was detected for photoautotrophy in the HT hot springs (2.33% the total biosphere and 4.02% in the abundant biosphere). Such abundance difference could be ascribed to the temperature limitation on photosynthesis (Boyd et al., 2009; De Leon et al., 2013); ammonia oxidation and nitrification were dominant in the MT hot springs but became minor in the HT hot springs, which was consistent with findings for microbial ammonia oxidation and nitrification in previous metagenomic studies (Reigstad et al., 2008; Zhang et al., 2008; Jiang et al., 2010). In contrast, chemoheterotrophy and chemolithotrophy pathways (e.g., dark oxidation of sulfur compounds, respiration of sulfur compounds, sulfate reduction, and denitrification) were minor in the MT hot springs but became dominant in the HT hot springs. So the observed abundance shift of microbial functions between MT and HT hot springs suggested that temperature could be an important factor influencing the distributions of

microbial ecological functions in the studied hot springs. In the meanwhile, other environmental factors (e.g., DOC and TOC) may also influence the distribution of the microbial ecological functions identified in this study. These findings were consistent previous metagenomic results (Badhai et al., 2015; Saxena et al., 2017).

Moreover, the predicted microbial functions in the abundant and rare sub-communities responded differently to the measured environmental variables. For examples, the relative abundance of photoautotrophy, anoxygenic photoautotrophy and nitrification was significantly correlated with temperature for the total, abundant and intermediate biospheres, but showed no correlation with temperature for the rare biosphere. In contrast, some of the identified microbial functions (e.g., photoheterotrophy, sulfur respiration, dark sulfur oxidation, and aromatic compound degradation) showed significant correlations with temperature and DOC for the rare biosphere, which however, was not observed for the total and abundant biospheres (**Figure 8**). Such different responses suggested that the potential ecological functions of abundant, intermediate, and rare taxa may differ among the hot springs of different environmental conditions (e.g., temperature, DOC, and TOC). Note that the obtained knowledge in this study may be limited about the environmental influence on microbial metabolic functions in the studied hot springs due to a large proportion of unclassified OTUs (**Figure 3**), a large proportion of OTUs without predicted ecological functions, and some unmeasured environmental variables, which awaits further investigation.

CONCLUSION

The abundant and rare sub-communities possessed different phylogenetic compositions and potential ecological functions, and they responded differently to environmental and spatial factors in the studied Tibetan hot springs. Temperature was the most important factor shaping the community compositions of the total and abundant biospheres, but it only showed little influence on the intermediate and rare sub-communities, suggesting that the abundant, intermediate, and rare biosphere may be sensitive to different environmental factors. Spatial factor (GD) contributed more influence to the variation of the rare sub-community than that of the abundant sub-community, indicating abundant taxa were more easily dispersed than rare taxa among different hot springs. The predicted microbial ecological functions of the abundant and rare sub-communities responded differently to the measured environmental factors, suggesting that they may occupy different ecological niches in hot spring ecosystems. In addition, the intermediate and rare taxa may play important roles in organic degradation than their abundant counterparts in the Tibetan hot springs.

AUTHOR CONTRIBUTIONS

YZ, GW, and HJ conceived and designed the experiments. YZ, GW, JY, and WS collected samples and performed the experiments. YZ, JY, WL, and HJ analyzed the data. All of the authors assisted in writing the manuscript, discussed the results, and commented on the manuscript.

FUNDING

This work was supported by the Special Foundation for Basic Research Program of China Ministry of Science and Technology (MOST) (No. 2015FY110100), the National Natural Science Foundation of China (Nos. 41502318 and 41521001), the 111 Program (State Administration of Foreign Experts Affairs and the Ministry of Education of China, grant B18049), the Key Project of International Cooperation of China Ministry of Science and Technology (No. 2013DFA31980), and the Fundamental Research Funds for the China Central Universities, China University of Geosciences (Wuhan).

SUPPLEMENTARY MATERIAL

The Supplementary Material for this article can be found online at: https://www.frontiersin.org/articles/10.3389/fmicb.2018.02096/full#supplementary-material

REFERENCES

Ashley, S., Hannes, P., Allison, S. D., Baho, D. L., Mercè, B., Helmut, B., et al. (2012). Fundamentals of microbial community resistance and resilience. *Front. Microbiol.* 3:416. doi: 10.3389/fmicb.2012.00417

Badhai, J., Ghosh, T. S., and Das, S. K. (2015). Taxonomic and functional characteristics of microbial communities and their correlation with physicochemical properties of four geothermal springs in Odisha. *India Front. Microbiol.* 6:1166. doi: 10.3389/fmicb.2015.01166

Boyd, E. S., Leavitt, W. D., and Geesey, G. G. (2009). CO2 uptake and fixation by a thermoacidophilic microbial community attached to precipitated sulfur in a geothermal spring. *Appl. Environ. Microbiol.* 75, 4289–4296. doi: 10.1128/aem.02751-08

Brazelton, W. J., Ludwig, K. A., Sogin, M. L., Andreishcheva, E. N., Kelley, D. S., Shen, C.-C., et al. (2010). Archaea and bacteria with surprising microdiversity show shifts in dominance over 1,000-year time scales in hydrothermal chimneys. *Proc. Natl. Acad. Sci.U.S.A.* 107, 1612–1617. doi: 10.1073/pnas.0905369107

Caporaso, J. G., Lauber, C. L., Walters, W. A., Berg-Lyons, D., Huntley, J., Fierer, N., et al. (2012). Ultra-high-throughput microbial community analysis on the Illumina HiSeq and MiSeq platforms. *ISME J.* 6, 1621–1624. doi: 10.1038/ismej.2012.8

Chan, C. S., Chan, K.-G., Ee, R., Hong, K.-W., Urbieta, M.-A. S., Donati, E. R., et al. (2017). Effects of physiochemical factors on prokaryotic biodiversity in malaysian circumneutral hot springs. *Front. Microbiol.* 6:177. doi: 10.3389/fmicb.2017.01252

Chan, C. S., Chan, K.-G., Tay, Y.-L., Chua, Y.-H., and Goh, K. M. (2015). Diversity of thermophiles in a Malaysian hot spring determined using 16S rRNA and shotgun metagenome sequencing. *Front. Microbiol.* 8:1252. doi: 10.3389/fmicb.2015.00177

Cole, J. K., Peacock, J. P., Dodsworth, J. A., Williams, A. J., Thompson, D. B., Dong, H., et al. (2013). Sediment microbial communities in Great Boiling

Spring are controlled by temperature and distinct from water communities. *ISME J.* 7, 718–729. doi: 10.1038/ismej.2012.157

Costa, K. C., Navarro, J. B., Shock, E. L., Zhang, C. L., Soukup, D., and Hedlund, B. P. (2009). Microbiology and geochemistry of great boiling and mud hot springs in the United States Great Basin. *Extremophiles* 13, 447–459. doi: 10.1007/s00792-009-0230-x

De Leon, K. B., Gerlach, R., Peyton, B. M., and Fields, M. W. (2013). Archaeal and bacterial communities in three alkaline hot springs in heart lake geyser basin, yellowstone national park. *Front. Microbiol.* 4:330. doi: 10.3389/fmicb.2013.00330

De'Ath, G. (2007). Boosted trees for ecological modeling and prediction. *Ecology* 88, 243–251. doi: 10.1890/0012-9658(2007)88[243:BTFEMA]2.0.CO;2

Edgar, R. C. (2013). UPARSE: highly accurate OTU sequences from microbial amplicon reads. *Nat. Methods* 10, 996–998. doi: 10.1038/NMETH.2604

Edgar, R. C., Haas, B. J., Clemente, J. C., Quince, C., and Knight, R. (2011). UCHIME improves sensitivity and speed of chimera detection. *Bioinformatics* 27, 2194–2200. doi: 10.1093/bioinformatics/btr381

Fuhrman, J. A. (2009). Microbial community structure and its functional implications. *Nature* 459, 193–199. doi: 10.1038/nature08058

Galand, P. E., Casamayor, E. O., Kirchman, D. L., and Lovejoy, C. (2009). Ecology of the rare microbial biosphere of the Arctic Ocean. *Proc. Natl. Acad. Sci. U.S.A.* 106, 22427–22432. doi: 10.1073/pnas.0908284106

Guo, Q., Nordstrom, D. K., and McCleskey, R. B. (2014). Towards understanding the puzzling lack of acid geothermal springs in Tibet (China): insight from a comparison with Yellowstone (USA) and some active volcanic hydrothermal systems. *J. Volcano. Geother. Res.* 288, 94–104. doi: 10.1016/j.jvolgeores.2014.10.005

Hedlund, B. P., Dodsworth, J. A., Murugapiran, S. K., Rinke, C., and Woyke, T. (2014). Impact of single-cell genomics and metagenomics on the emerging view of extremophile microbial dark matter. *Extremophiles* 18, 865–875. doi: 10.1007/s00792-014-0664-7

Hou, W., Wang, S., Dong, H., Jiang, H., Briggs, B. R., Peacock, J. P., et al. (2013). A comprehensive census of microbial diversity in hot springs of tengchong, yunnan province china using 16S rRNA gene pyrosequencing. *PLoS One* 8:e53350. doi: 10.1371/journal.pone.0053350

Huang, Q., Dong, C. Z., Dong, R. M., Jiang, H., Wang, S., Wang, G., et al. (2011). Archaeal and bacterial diversity in hot springs on the Tibetan Plateau, China. *Extremophiles* 15, 549–563. doi: 10.1007/s00792-011-0386-z

Hugoni, M., Taib, N., Debroas, D., Domaizon, I., Dufournel, I. J., Bronner, G., et al. (2013). Structure of the rare archaeal biosphere and seasonal dynamics of active ecotypes in surface coastal waters. *Proc. Natl.Acad.Sci.U.S.A.* 110, 6004–6009. doi: 10.1073/pnas.1216863110

Jiang, H., Huang, L., Yang, J., and Wu, G. (2018). "Chapter 23 - A Microbial Analysis Primer for Biogeochemists A2 - Vivo, Benedetto De," in *Environmental Geochemistry*, 2nd Edn, eds H. E. Belkin and A. Lima (New York, NY: Elsevier), 599–609. doi: 10.1016/B978-0-444-63763-5.00024-0

Jiang, H., Huang, Q., Dong, H., Wang, P., Wang, F., Li, W., et al. (2010). RNA-based investigation of ammonia-oxidizing archaea in hot springs of yunnan province, china. *Appl. Environ. Microbiol.* 76, 4538–4541. doi: 10.1128/AEM.00143-10

Jousset, A., Bienhold, C., Chatzinotas, A., Gallien, L., Gobet, A., Kurm, V., et al. (2017). Where less may be more: how the rare biosphere pulls ecosystems strings. *ISME J.* 11, 853–862. doi: 10.1038/ismej.2016.174

Kublanov, I. V., Perevalova, A. A., Slobodkina, G. B., Lebedinsky, A. V., Bidzhieva, S. K., Kolganova, T. V., et al. (2009). Biodiversity of thermophilic prokaryotes with hydrolytic activities in hot springs of Uzon Caldera, Kamchatka (Russia). *Appl. Environ. Microbiol.* 75, 286–291. doi: 10.1128/AEM.00607-08

Lau, M. C. Y., Aitchison, J. C., and Pointing, S. B. (2009). Bacterial community composition in thermophilic microbial mats from five hot springs in central Tibet. *Extremophiles* 13, 139–149. doi: 10.1007/s00792-008-0205-r3

Liu, L., Yang, J., Yu, Z., and Wilkinson, D. M. (2015). The biogeography of abundant and rare bacterioplankton in the lakes and reservoirs of China. *ISME J.* 9, 2068–2077. doi: 10.1038/ismej.2015.29

Logares, R., Audic, S., Bass, D., Bittner, L., Boutte, C., Christen, R., et al. (2014). Patterns of rare and abundant marine microbial eukaryotes. *Curr. Biol.* 24, 813–821. doi: 10.1016/j.cub.2014.02.050

Logares, R., Lindström, E. S., Langenheder, S., Logue, J. B., Paterson, H., Laybourn-Parry, J., et al. (2013). Biogeography of bacterial communities exposed to progressive long-term environmental change. *ISME J.* 7, 937–948. doi: 10.1038/ismej.2012.168

Logares, R., Mangot, J.-F., and Massana, R. (2015). Rarity in aquatic microbes: placing protists on the map. *Res. Microbiol.* 166, 831–841. doi: 10.1016/j.resmic.2015.09.009

Logue, J. B. (2010). *Factors Influencing the Biogeography of Bacteria in Fresh Waters - a Metacommunity Approach*. Ph.D. thesis, Acta Universitatis Upsaliensis, Uppsala.

Louca, S., Parfrey, L. W., and Doebeli, M. (2016). Decoupling function and taxonomy in the global ocean microbiome. *Science* 353:1272. doi: 10.1126/science.aaf4507

Lynch, M. D., and Neufeld, J. D. (2015). Ecology and exploration of the rare biosphere. *Nature Rev.Microbiol.* 13, 217–229. doi: 10.1038/nrmicro3400

Magoè, T., and Salzberg, S. L. (2011). FLASH: fast length adjustment of short reads to improve genome assemblies. *Bioinformatics* 27, 2957–2963. doi: 10.1093/bioinformatics/btr507

Menzel, P., Gudbergsdottir, S. R., Rike, A. G., Lin, L., Zhang, Q., Contursi, P., et al. (2015). Comparative metagenomics of eight geographically remote terrestrial hot springs. *Microb. Ecol* 70, 411–424. doi: 10.1007/s00248-015-0576-9

Meyer-Dombard, D. R., Shock, E. L., and Amend, J. P. (2005). Archaeal and bacterial communities in geochemically diverse hot springs of Yellowstone National Park. USA. *Geobiology* 3, 211–227. doi: 10.1111/j.1472-4669.2005.00052.x

Miller, S. R., Strong, A. L., Jones, K. L., and Ungerer, M. C. (2009). Bar-coded pyrosequencing reveals shared bacterial community properties along the temperature gradients of two alkaline hot springs in Yellowstone National Park. *Appl. Environ. Microbiol* 75, 4565–4572. doi: 10.1128/AEM.02792-08

Nemergut, D. R., Schmidt, S. K., Fukami, T., O'Neill, S. P., Bilinski, T. M., Stanish, L. F., et al. (2013). Patterns and processes of microbial community assembly. *Microbiol. Mol. Biol. Rev.* 77, 342–356. doi: 10.1128/MMBR.00051-12

Pearson, A., Pi, Y., Zhao, W., Li, W., Li, Y., Inskeep, W., et al. (2008). Factors controlling the distribution of archaeal tetraethers in terrestrial hot springs. *Appl. Environ. Microbiol.* 74, 3523–3532. doi: 10.1128/AEM.02450-07

Pedrós-Alió, C. (2012). The rare bacterial biosphere. *Annu. Rev. Mar. Sci* 4, 449–466. doi: 10.1146/annurev-marine-120710-100948

Purcell, D., Sompong, U., Yim, L. C., Barraclough, T. G., Peerapornpisal, Y., and Pointing, S. B. (2007). The effects of temperature, pH and sulphide on the community structure of hyperthermophilic streamers in hot springs of northern Thailand. *FEMS Microbiol. Ecol.* 60, 456–466. doi: 10.1111/j.1574-6941.2007.00302.x

Reigstad, L. J., Richter, A., Daims, H., Urich, T., Schwark, L., and Schleper, C. (2008). Nitrification in terrestrial hot springs of Iceland and Kamchatka. *FEMS Microbiol. Ecol.* 64, 167–174. doi: 10.1111/j.1574-6941.2008.00466.x

Rothschild, L. J., and Mancinelli, R. L. (2001). Life in extreme environments. *Nature* 409, 1092–1101. doi: 10.1038/35059215

Saxena, R., Dhakan, D. B., Mittal, P., Waiker, P., Chowdhury, A., Ghatak, A., et al. (2017). Metagenomic analysis of hot springs in central india reveals hydrocarbon degrading thermophiles and pathways essential for survivalin extreme environments. *Front. Microbiol.* 7:2123. doi: 10.3389/fmicb.2016.02123

Skirnisdottir, S., Hreggvidsson, G. O., Hjörleifsdottir, S., Marteinsson, V. T., Petursdottir, S. K., Holst, O., et al. (2000). Influence of sulfide and temperature on species composition and community structure of hot spring microbial mats. *Appl. Environ. Microbiol.* 66, 2835–2841. doi: 10.1128/AEM.66.7.2835-2841.2000

Sogin, M. L., Morrison, H. G., Huber, J. A., Welch, D. M., Huse, S. M., Neal, P. R., et al. (2006). Microbial diversity in the deep sea and the underexplored "rare biosphere". *Proc. Natl. Acad. Sci.U.S.A* 103, 12115–12120. doi: 10.1073/pnas.0605127103

Song, Z.-Q., Chen, J.-Q., Jiang, H.-C., Zhou, E.-M., Tang, S.-K., Zhi, X.-Y., et al. (2010). Diversity of crenarchaeota in terrestrial hot springs in Tengchong, China. *Extremophiles* 14, 287–296. doi: 10.1007/s00792-010-0307-6

Song, Z.-Q., Wang, F.-P., Zhi, X.-Y., Chen, J.-Q., Zhou, E.-M., Liang, F., et al. (2013). Bacterial and archaeal diversities in Yunnan and Tibetan hot springs. China. *Environ. Microbiol.* 15, 1160–1175. doi: 10.1111/1462-2920.12025

Tamaki, H., Wright, C. L., Li, X., Lin, Q., Hwang, C., Wang, S., et al. (2011). Analysis of 16S rRNA amplicon sequencing options on the Roche/454 next-generation titanium sequencing platform. *PLoS One* 6:e25263. doi: 10.1371/journal.pone.0025263

Wang, Q., Garrity, G. M., Tiedje, J. M., and Cole, J. R. (2007). Naive Bayesian classifier for rapid assignment of rRNA sequences into the new bacterial taxonomy. *Appl. Environ. Microbiol* 73, 5261–5267. doi: 10.1128/AEM.00062-07

Wang, S., Dong, H., Hou, W., Jiang, H., Huang, Q., Briggs, B. R., et al. (2014). Greater temporal changes of sediment microbial community than its waterborne counterpart in Tengchong hot springs, Yunnan Province, China. *Sci. Rep*. 4:7479. doi: 10.1038/srep07479

Wang, S., Hou, W., Dong, H., Jiang, H., Huang, L., Wu, G., et al. (2013). Control of temperature on microbial community structure in hot springs of the Tibetan Plateau. *PLoS One* 8:e62901. doi: 10.1371/journal.pone.0062901

Whitaker, R. J., Grogan, D. W., and Taylor, J. W. (2003). Geographic barriers isolate endemic populations of hyperthermophilic archaea. *Science* 301, 976–978. doi: 10.1126/science.1086909

Yang, J., Jiang, H., Dong, H., Wu, G., Hou, W., Zhao, W., et al. (2013). Diversity of Carbon Monoxide-Oxidizing Bacteria in Five Lakes on the Qinghai-Tibet Plateau. *China. Geomicrobiol. J.* 30, 758–767. doi: 10.1080/01490451.2013.769652

Yang, J., Jiang, H., Wu, G., Liu, W., and Zhang, G. (2016). Distinct factors shape aquatic and sedimentary microbial community structures in the lakes of western China. *Front. Microbiol.* 7:1782. doi: 10.3389/fmicb.2016.01782

Yim, L. C., Jing, H. M., Aitchison, J. C., and Pointing, S. B. (2006). Highly diverse community structure in a remote central Tibetan geothermal spring does not display monotonic variation to thermal stress. *FEMS Microbiol. Ecol.* 57, 80–91. doi: 10.1111/j.1574-6941.2006.00104.x

Zhang, C. L., Ye, Q., Huang, Z., Li, W., Chen, J., Song, Z., et al. (2008). Global occurrence of archaeal amoA genes in terrestrial hot springs. *Appl. Environ. Microbiol* 74, 6417–6426. doi: 10.1128/AEM.00843-08

Zhou, J., Wu, L., Deng, Y., Zhi, X., Jiang, Y.-H., Tu, Q., et al. (2011). Reproducibility and quantitation of amplicon sequencing-based detection. *ISME J.* 5, 1303–1313. doi: 10.1038/ismej.2011.11

Zhou, J. Z., Kang, S., Schadt, C. W., and Garten, C. T. (2008). Spatial scaling of functional gene diversity across various microbial taxa. *Proc. Natl. Acad. Sci. U.S.A.* 105, 7768–7773. doi: 10.1073/pnas.0709016105

Conflict of Interest Statement: The authors declare that the research was conducted in the absence of any commercial or financial relationships that could be construed as a potential conflict of interest.

frontiers in Microbiology

ORIGINAL RESEARCH
published: 06 July 2017
doi: 10.3389/fmicb.2017.01252

Effects of Physiochemical Factors on Prokaryotic Biodiversity in Malaysian Circumneutral Hot Springs

*Chia S. Chan[1], Kok-Gan Chan[2], Robson Ee[2], Kar-Wai Hong[2], María S. Urbieta[3], Edgardo R. Donati[3], Mohd S. Shamsir[1] and Kian M. Goh[1]**

[1] Faculty of Biosciences and Medical Engineering, Universiti Teknologi Malaysia, Skudai, Malaysia, [2] Division of Genetics and Molecular Biology, Faculty of Science, Institute of Biological Sciences, University of Malaya, Kuala Lumpur, Malaysia, [3] CINDEFI (CCT, La Plata-CONICET, UNLP), Facultad de Ciencias Exactas, Universidad Nacional de La Plata, La Plata, Argentina

Malaysia has a great number of hot springs, especially along the flank of the Banjaran Titiwangsa mountain range. Biological studies of the Malaysian hot springs are rare because of the lack of comprehensive information on their microbial communities. In this study, we report a cultivation-independent census to describe microbial communities in six hot springs. The Ulu Slim (US), Sungai Klah (SK), Dusun Tua (DT), Sungai Serai (SS), Semenyih (SE), and Ayer Hangat (AH) hot springs exhibit circumneutral pH with temperatures ranging from 43°C to 90°C. Genomic DNA was extracted from environmental samples and the V3–V4 hypervariable regions of 16S rRNA genes were amplified, sequenced, and analyzed. High-throughput sequencing analysis showed that microbial richness was high in all samples as indicated by the detection of 6,334–26,244 operational taxonomy units. In total, 59, 61, 72, 73, 65, and 52 bacterial phyla were identified in the US, SK, DT, SS, SE, and AH hot springs, respectively. Generally, Firmicutes and Proteobacteria dominated the bacterial communities in all hot springs. Archaeal communities mainly consisted of Crenarchaeota, Euryarchaeota, and Parvarchaeota. In beta diversity analysis, the hot spring microbial memberships were clustered primarily on the basis of temperature and salinity. Canonical correlation analysis to assess the relationship between the microbial communities and physicochemical variables revealed that diversity patterns were best explained by a combination of physicochemical variables, rather than by individual abiotic variables such as temperature and salinity.

Keywords: 16S rRNA amplicon sequencing, hot spring metagenome, saline pool, microbial community, thermophile diversity, microbial symbiosis, microbiome

OPEN ACCESS

Edited by:
Hongchen Jiang,
Miami University, United States

Reviewed by:
Song Zhaoqi,
Shangqiu Normal University, China
Weiguo Hou,
China University of Geosciences, China
Brandon Briggs,
University of Alaska Anchorage, United States

****Correspondence:***
Kian M. Goh
gohkianmau@utm.my

Specialty section:
This article was submitted to Extreme Microbiology, a section of the journal Frontiers in Microbiology

Received: *26 April 2017*
Accepted: *21 June 2017*
Published: *06 July 2017*

Citation:
Chan CS, Chan K-G, Ee R, Hong K-W, Urbieta MS, Donati ER, Shamsir MS and Goh KM (2017) Effects of Physiochemical Factors on Prokaryotic Biodiversity in Malaysian Circumneutral Hot Springs. Front. Microbiol. 8:1252. doi: 10.3389/fmicb.2017.01252

Abbreviations: AH, Ayer Hangat; BOD, biochemical oxygen demand; CCA, canonical correspondence analysis; C:N, carbon-to-nitrogen ratio; COD, chemical oxygen demand; DT, Dusun Tua; OTU, operational taxonomic unit; PCA, principal component analysis; PCoA, principal coordinate analysis; QIIME, Quantitative Insights Into Microbial Ecology; SE, Semenyih; SK, Sungai Klah; SS, Sungai Serai; TN, total nitrogen; TOC, total organic carbon; UPGMA, unweighted pair group method with arithmetic mean; US, Ulu Slim.

INTRODUCTION

The study of extremophiles provides insights into the origin and evolution of life. Biologists believe that extremophiles inhabiting extreme environments such as hot springs are the closest living descendents of the earliest life forms on earth (Woese et al., 1990; Olsen et al., 1994). Additionally, these extreme environments comprise relatively simple microbial ecosystems as compared with more complex environments such as soils (Xu et al., 2014), wastewater (Shanks et al., 2013), marine sediments (Zheng et al., 2014), and the human gastrointestinal tract (Trosvik and de Muinck, 2015). Therefore, studying the life in hot springs enables us to interrogate the interactions between organisms and the environment. Microbial communities in hot springs, especially those in Yellowstone National Park (USA) (Blank et al., 2002; Kan et al., 2011; Inskeep et al., 2013), Japan (Kubo et al., 2011; Nishiyama et al., 2013; Masaki et al., 2016), Iceland (Tobler and Benning, 2011; Menzel et al., 2015), China (Hou et al., 2013; Song et al., 2013), and India (Badhai et al., 2015; Sangwan et al., 2015), are extensively studied. Among these, the Octopus and Mushroom Springs at Yellowstone National Park have the longest history of research of nearly 50 years (Thiel et al., 2016). Recently, a research team in New Zealand initiated the 1,000 Springs Research Project to examine geothermal microbial biota in 1,000 hot-spring features in the Taupo Volcanic Zone[1]. Microbial populations in heated springs are influenced by physicochemical factors, such as temperature, pH, dissolved oxygen, and water chemistry (Mathur et al., 2007; Sharp et al., 2014; Chan et al., 2015). In hot springs with temperatures higher than 75°C, Aquificae, Deinococcus-Thermus, Thermodesulfobacteria, Thermotogae, and some thermophilic members of Proteobacteria and Firmicutes are the commonly found bacterial phyla (Blank et al., 2002; Hou et al., 2013; Song et al., 2013), in addition to archaeal phyla such as Crenarchaeota, Euryarchaeota, and Thaumarchaeota (Hou et al., 2013; Nishiyama et al., 2013; Chan et al., 2015). In hot springs with lower temperatures, thermophilic photosynthetic bacteria such as Cyanobacteria and Chloroflexi, together with phyla such as Proteobacteria may be the main population (Kubo et al., 2011; Nishiyama et al., 2013; Badhai et al., 2015). As the maximum temperature for photosynthesis is 75°C (Ferris and Ward, 1997), Cyanobacteria and Chloroflexi are therefore not predominantly present in hot springs with temperatures higher that this threshold.

The Banjaran Titiwangsa mountain range, with elevations of 900–2,100 m and a length of about 480 km, is the most prominent mountain cluster on Peninsular Malaysia. Most of the hot springs on the peninsula are located along the western flank of Banjaran Titiwangsa and are concentrated along major fault zones (Sum et al., 2010). The Malaysian hot springs differ from the geothermal systems in Yellowstone National Park, Japan, Kamchatka, and New Zealand in several aspects. Malaysia has a tropical climate and is located in a non-volcanic area. The water arising from these hot springs is heated geothermally; groundwater that percolates deeply into the Earth's crust comes in contact with the rocks that get heated as a result of the geothermal gradient originating from the Earth's interior. Pressure is generated and forces the water to discharge through pores and fissures within the Earth's crust toward the surface to form hot springs (Baioumy et al., 2015). In countries with volcanic activities in tectonically active zones, rain or melted snow comes in contact with near subsurface magma that may heat the water sufficiently to form superheated water bodies. Acidic hot springs (pH < 6.0) are often found in volcanic areas; however, hot springs in Malaysia are circumneutral or slightly alkaline. Hot-spring water usually has high concentrations of various elements owing to mineralization of dissolved solid elements from the adjacent areas. The composition of hot water is mainly determined by chemical interactions with reservoir rocks and rock-forming minerals along the ascent path, which may cause the spring water to be acidic or alkaline.

Earlier reports summarized the different physicochemical conditions in 46 known Malaysian hot springs (Samsudin et al., 1997; Sum et al., 2010). These hot springs have temperatures ranging from 36°C to 102°C, but predominantly lower than 80°C. Malaysian hot springs exhibit differences in physical appearance and chemical contents, which are expected to influence the microbial communities; nevertheless, limited studies have been conducted to understand the microbial diversity in Malaysian (Goh et al., 2011; Chan et al., 2015) and South-East Asian (Baker et al., 2001; Kanokratana et al., 2004; Huang et al., 2013) hot springs. In this report, a coordinated geochemical and molecular survey was conducted for six hot springs. Ulu Slim, Sungai Klah, and Dusun Tua were selected as these sites are the hottest geothermal springs in Malaysia. Ayer Hangat was chosen because it is the only saline hot spring in Malaysia. Semenyih and Sungai Serai hot springs were selected as they exhibit similar temperature (∼45°C) and pool size and are located close to each other. This work utilized 16S rRNA gene markers to understand microbial diversity and community structure. We expected our findings to elucidate possible relationships with hot-spring physicochemical variables.

MATERIALS AND METHODS

Study Sites and Water Physicochemical Characteristics

Hot springs at Ulu Slim (US) (3°53'55.79"N, 101°29'52.44"E), Sungai Serai (SS) (3°5'27.71"N, 101°47'39.06"E), Dusun Tua (DT) (3°8'21.23"N, 101°50'10.33'E), and Semenyih (SE) (3°2'32.81"N, 101°52'19.87"E) are located along the Banjaran Titiwangsa main mountain range (**Figure 1**). Additionally, the Ayer Hangat (AH) (6°25'22.31"N, 99°48'48.97"E) hot spring, located outside the main mountain range, was included in this study because of its high saline water content (**Table 1**). At each hot spring, water temperature was measured using a portable thermometer. Water and sediment samples were collected in sterile bottles that were closed immediately after sampling. Samples were collected in at least three sites at each hot spring. The samples were kept at ambient temperature

[1]http://www.1000springs.org.nz

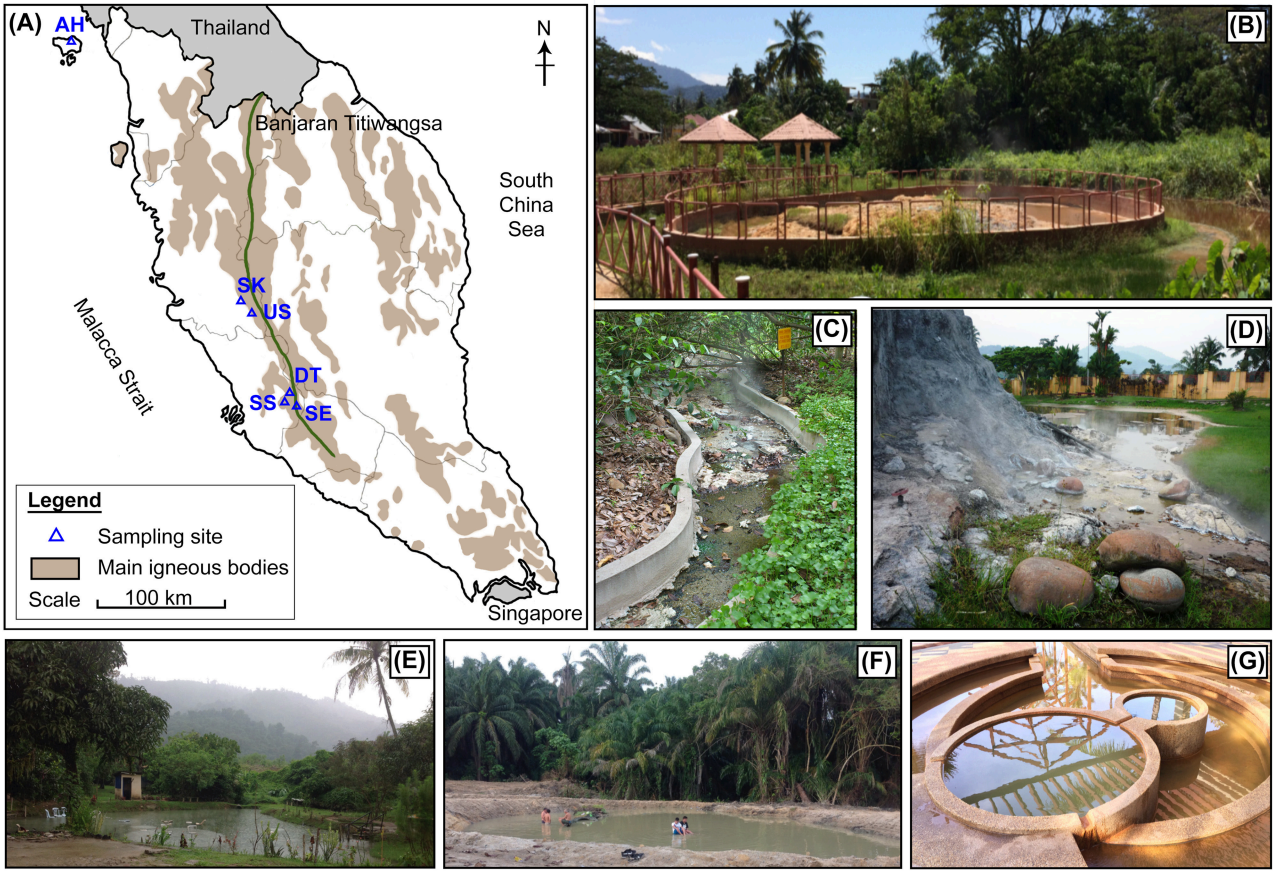

FIGURE 1 | (A) Map of the locations of six selected hot springs in Malaysia: Ayer Hangat (AH), Ulu Slim (US), Sungai Klah (SK), Dusun Tua (DT), Sungai Serai (SS), and Semenyih (SE). Photographs of Malaysian hot springs sampling sites; **(B)** US, **(C)** SK, **(D)** DT, **(E)** SS, **(F)** SE, and **(G)** AH.

and transferred immediately to the laboratory, where they were stored at 4°C prior to DNA extraction. Water samples of each site were sent to the Allied Chemists Laboratory Sdn. Bhd. (Malaysia) for physiochemical analyses in accordance with the American Public Health Association, Standard Methods for the Examination of Water and Wastewater (APHA) and United States Environmental Protection Agency (USEPA) guidelines (refer to **Table 2** for the list of analyses).

DNA Extraction and 16S rRNA Gene Sequencing

DNA extraction was conducted in the laboratory. Equal volumes of water and sediment samples for each hot spring were collected and pooled to represent the overall microbiome of each site. DNA extraction and amplicon generation from environmental samples were conducted as previously described (Chan et al., 2015), with modification of the amount of starting material used for DNA extraction. In brief, genomic DNA extracted from the samples was amplified and dual-index barcoded for multiplex sequencing using primer pair (S-D-Bact-0341-b-S17 and S-D-Bact-0785-a-A-21) targeted to the V3–V4 regions of the 16S rRNA gene (Klindworth et al., 2013). The forward (5′-TCGTCGGCAGCGTCAGATGTGTATAAGAGACAG-CCTACGGGNGGCWGCAG-3′) and reverse (5′-GTCTCGTGGGCTCGGAGATGTGTATAAGAGACAG-GACTACHVGGGTATCTAATCC-3′) primers contained Illumina overhang adapter sequences (underlined regions). Amplicons were paired-end (2 × 300 bp, MiSeq v3 reagent) sequenced on an Illumina MiSeq sequencer (San Diego, CA, USA) at the High Impact Research Institute at the University of Malaya, Malaysia. The sequence data have been submitted to NCBI SRA under Bioproject accession number PRJNA378468. To compare microbial profiles obtained in this study with those reported earlier for the Malaysian SK hot spring (Chan et al., 2015), the SRA for the latter (Bioproject no. PRJEB7059) was retrieved and processed similarly to the reads generated in this work.

Data Analysis

The raw sequence data were evaluated and filtered to ensure that >80% of the base calls in a sequence had a Phred quality score of 20 using the FASTQ Quality Filter ($q = 20$,

TABLE 1 | Descriptions of the hot springs studied.

Name	Sample type[a]	Descriptions
Ulu Slim (US)	Water and sediment (spring heads and pond)	• The hottest spring in Malaysia. • A roughly cylindrical shallow pool (∼4 m diameter, ∼10 cm depth) with two moderate spring heads (110°C). • Clear water and fine clays at the bottom. • Biofilms (<5 mm thickness) with colors of yellow, orange, light brown, and light green are formed on the spring.
Sungai Klah[b] (SK)	Water and sediment (middle of stream)	• Shallow water flow stream (∼150 m length, ∼1.5 m width, ∼5 cm depth) • Water temperatures between 50–110°C. • Multiple spring heads with clear running water. • Clays, rocks, and sands at the bottom.
Dusun Tua (DT)	Water and sediment (spring head and pond)	• A shallow pool with small spring source (75°C) outflow continually from a 1.5-m man-made cement-fountain landscape. • Multiple thick biomats (1–5 cm) of various colors (dark brown, red, white, dark green, and orange) are formed on the fountain, while a green filamentous mat is present on the bank of the collecting pool. • Clear water with silicate sands and clays at the bottom.
Sungai Serai (SS)	Water and sediment (center and edge of pool)	• Roughly round-shaped pool with diameter ∼10 m, and depth ∼0.5 m. • Many bubbling sources, but non-visible spring head. • Murky water with green biomats on the bank of the pool. • Loam soil at the bottom.
Semenyih (SE)	Water and sediment (center and edge of pool)	• Roughly round-shaped pool with diameter ∼10 m, and depth ∼0.7 m. • Many bubbling sources and no visible outflow. • Non-visible spring head. • Murky water with green biomats on the bank of the spring. • Fine silicate sands at the bottom.
Ayer Hangat (AH)	Water	• The only saline hot spring in Malaysia. • Water is trapped in a deep, cylindrical man-made pond with ∼1-m diameter. • Formation of small degassing bubbles with slow outflow. • Gray-yellowish water mixed with fine salt. • Thin light-brown and green biomats (<1 cm) are formed on the surrounding wall.

[a] *Sample type used for genomic DNA extraction.*

[b] *Data collected from Diversity of thermophiles in a Malaysian hot spring determined using 16S rRNA and shotgun metagenome sequencing (Chan et al., 2015).*

$p = 80$) of the FASTX-Toolkit[2]. Sequences that passed the quality filtering, were free from ambiguous characters, and of ≥200 bp were merged using PEAR (Zhang et al., 2014). Chimeric sequences were identified and discarded using the UCHIME algorithm (Edgar et al., 2011) implemented in the USEARCH package (Edgar, 2010). The sequences were then analyzed using the Quantitative Insights Into Microbial Ecology (QIIME) pipeline version 1.9.1 (Caporaso et al., 2010b) with default parameters unless otherwise noted. Briefly, sequences were clustered into operational taxonomic units (OTUs) at 97% similarity with USEARCH-based (Edgar, 2010) open-reference OTUs picking protocols using the Greengenes 13_8 reference sequences (McDonald et al., 2012). Taxonomy was assigned to sequences using UCLUST (Edgar, 2010), retrained on Greengenes 13_8 with a minimum of one OTU size, in QIIME. Representative sequences, which were selected as the centroid sequence of each OTU, were aligned using PyNAST aligner (Caporaso et al., 2010a) with a minimum sequence length of 26 bases, and those that failed to align were removed.

Statistical Analysis

Multivariate principal component analysis (PCA) of 23 physicochemical variables including sampling-site water temperature, pH, alkalinity, acidity, color, turbidity, aluminum, arsenic, chloride, fluoride, $CaCO_3$, iron, magnesium, phosphate, sodium, sulfate, sulfur, total nitrogen (TN), total organic carbon (TOC), biochemical oxygen demand under 5-day incubation (BOD; at 20, 60, and 80°C), and chemical oxygen demand (COD) was carried out to determine which physicochemical variables were related to the observed hot spring community patterns. All measured physicochemical variables were checked for normality and log-transformed before PCA. A PCA plot was generated using PAST software version 3.13 (Hammer et al., 2001).

To estimate species richness from the data sets, the original OTU table with singletons was used to conduct rarefaction analysis and estimate alpha diversity. Rarefaction curves based on observed OTUs were generated using QIIME. The

[2]http://hannonlab.cshl.edu/fastx_toolkit

TABLE 2 | Physicochemical properties of water samples from the six Malaysian hot springs studied.

Test variable	Methods	Unit	US	SK[a]	DT	SS	SE	AH
Temperature range	Thermometer	°C	80–110	60–110	55–75	40–45	40–50	40–50
Sampling temperature	Thermometer	°C	90	75	70	43	43	45
pH[b]	APHA 4500 H^+ B		7.2	8.2	7.0	6.9	6.9	7.1
Alkalinity	APHA 2320 B	mg L^{-1}	94	76	106	122	136	294
Acidity	APHA 2310 B	mg L^{-1}	<1	<1	<1	<1	20	<1
Color	APHA 2120 B	TCU	<5	75	<5	<5	<5	5
Turbidity	APHA 2130 B	NTU	1.0	130	<0.05	1.0	0.5	1.1
C:N ratio (TOC/TN)[c]			1.5	1.6	0.1	0.3	0.1	5.0
Aluminum (Al)	APHA 3030 F/USEPA 6010 B	mg L^{-1}	0.07	0.96	0.04	0.04	0.04	0.04
Arsenic (As)	APHA 3030 F/USEPA 6010 B	mg L^{-1}	0.03	0.07	ND (<0.01)	ND (<0.01)	ND (<0.01)	ND (<0.01)
Chloride (Cl^-)	APHA 4500-Cl^- B	mg L^{-1}	<1	2	1	3	4	13,832
Fluoride (F^-)	APHA 4500-F^- D	mg L^{-1}	0.4	1.1	6.9	11	9.4	21
Hardness ($CaCO_3$)	APHA 2340C	mg L^{-1}	13	<1	5	27	27	5,020
Iron (Fe)	APHA 3030 F/USEPA 6010 B	mg L^{-1}	ND (<0.02)	0.65	ND (<0.02)	0.03	ND (<0.02)	ND (<0.02)
Magnesium (Mg^+)	APHA 3030 F/USEPA 6010 B	mg L^{-1}	0.8	0.5	<0.1	0.2	0.2	394
Phosphate (PO_4^{3-})	APHA 3030 G/USEPA 6010 B	mg L^{-1}	0.1	0.2	0.1	0.3	0.7	0.4
Sodium (Na^+)	APHA 3030 F/USEPA 6010 B	mg L^{-1}	43	27	51	45	48	7,905
Sulfate (SO_4^{2-})	APHA 4500-SO_4 E	mg L^{-1}	3	8	6	1	1	947
Sulfur (S)	APHA 3030 F/USEPA 6010 B	mg L^{-1}	5.2	3.9	2.7	0.5	1.1	477
TN	APHA 3030 F/USEPA 6010 B	mg L^{-1}	<0.2	5.6	2.7	3.0	6.1	<0.2
TOC	APHA 5310 B	mg L^{-1}	0.3	9.04	0.4	0.8	0.9	1.0
BOD 5 days at 20°C	APHA 5210 B	mg L^{-1}	<5	5	<5	<5	<5	30
BOD 5 days at 60°C	APHA 5210 B	mg L^{-1}	<5	10	<5	<5	<5	20
BOD 5 days at 80°C	APHA 5210 B	mg L^{-1}	<5	5	<5	<5	<5	<5
COD	APHA 5220 B	mg L^{-1}	7.4	35	<5	<5	<5	90

[a] *Data collected from Diversity of thermophiles in a Malaysian hot spring determined using 16S rRNA and shotgun metagenome sequencing (Chan et al., 2015).*

[b] *The pH values were measured at room temperature.*

[c] *The C:N ratios were calculated on mass basis.*

Abbreviations: APHA, in accordance with American Public Health Association, Standard Methods for the Examination of Water and Wastewater; USEPA, United States Environmental Protection Agency; TN, total nitrogen; TOC, total organic carbon; BOD, Biochemical oxygen demand; COD, Chemical oxygen demand; ND, not detected.

alpha diversity estimates, including Good's coverage, Shannon–Wiener's diversity index, and Simpson's index of diversity, were calculated. Sampling completeness was evaluated using the Good's average estimator, which calculates the probability that a randomly selected amplicon sequence from a sample has already been sequenced (Good, 1953). The Shannon–Wiener diversity index (Spellerberg and Fedor, 2003) was used to explain the entropy, taking into account the species richness and evenness of the community, which varied from 0 for communities with a single taxon, to high values for highly diverse communities. Simpson's index of diversity (1-D) (Simpson, 1949) was used to describe the diversity in a community, ranging from 0 to 1, with 1 indicating maximum diversity in a sample.

Singletons were discarded and the OTU table was rarefied to a depth of 313,337 sequences per sample (75% sequences to the lowest number of sequences found among the sample dataset) to minimize the effect of sampling effort. Further, diversity analyses including beta diversity analysis were conducted using QIIME, with the script core_diversity_analyses.py. Jackknifed unweighted pair group method with arithmetic mean (UPGMA) clustering was performed to compare microbial community similarity among the hot spring samples based on UniFrac phylogenetic distances (weighted and unweighted) (Lozupone et al., 2007) and non-phylogenetic Bray–Curtis dissimilarity distances. A relative small UniFrac distance implies that two communities are compositionally similar, harboring lineages that share a common evolutionary history. Unweighted UniFrac only accounts for the community membership, while weighted UniFrac accounts for community structure (membership and relative abundance) (Lozupone et al., 2007). Biplots of principal coordinate analysis (PCoA) were generated in QIIME and visualized in 3D using Emperor (Vázquez-Baeza et al., 2013).

Canonical correspondence analysis (CCA) was performed using PAST software, to explore relationships of microbial community patterns at the phylum level with physicochemical variables. By considering that predominant species have greater influence within the communities, only 75 major OTUs with relative abundance of >0.001% across all sample data sets were used as a community matrix for CCA. The significance of the CCA models and the explanatory factors were tested using 999 permutations. The ordination on the x- and y-axis and the length of the corresponding arrows indicate the relative importance

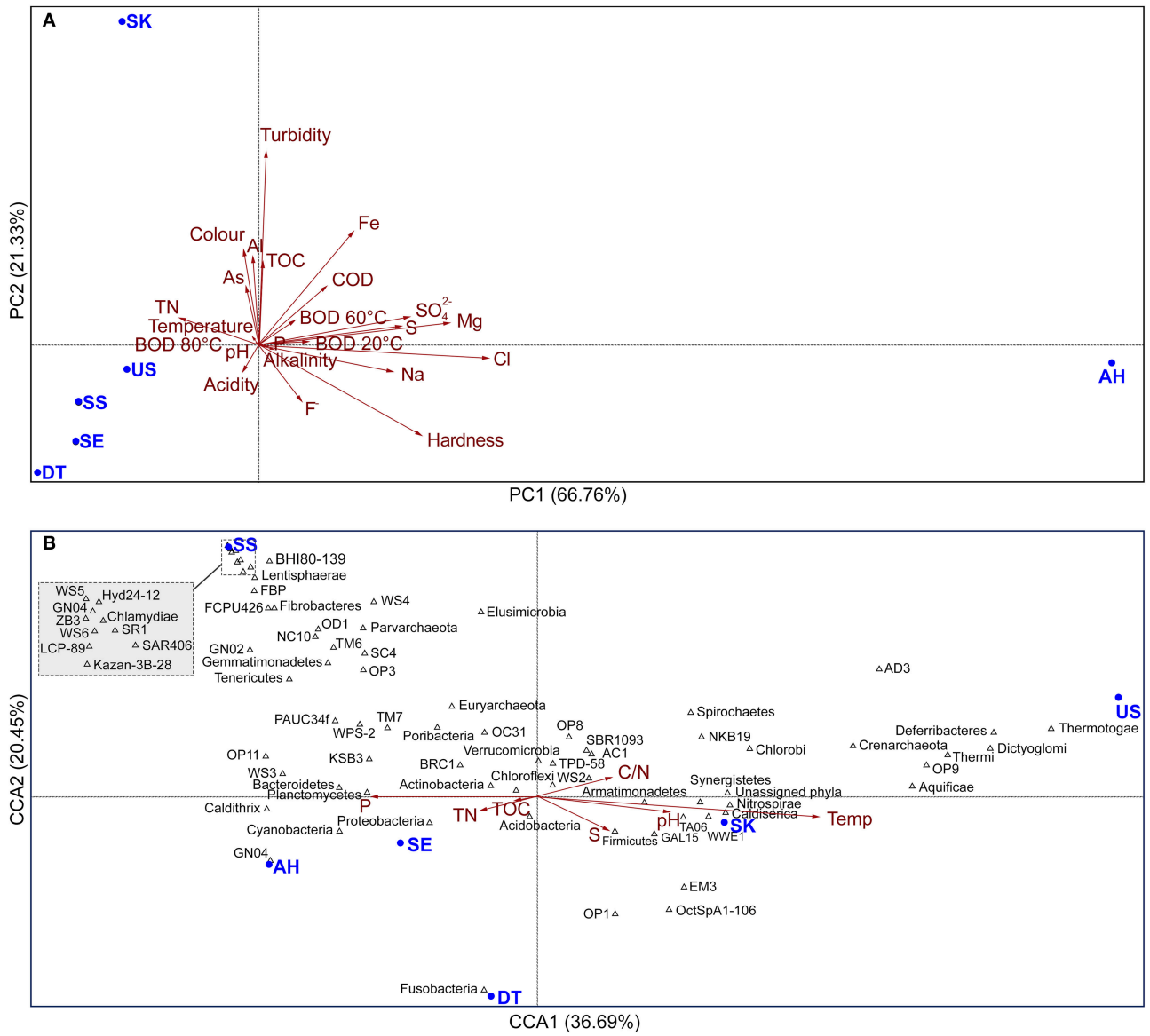

FIGURE 2 | (A) PCA of physicochemical variables and **(B)** CCA of microbial phyla (>0.001% of total phyla sequences) in relation to physicochemical variables. The percent variability explained by each principal component is shown in parentheses in the axis labels. Each hot spring sample is represented by 1 filled circle. Red arrows indicate the direction and magnitude of physicochemical variables associated with microbial community structures. C:N, C:N ratio; temp, sampling-site water temperature; S, sulfur content; TN, total nitrogen; TOC, total organic carbon; and p, phosphate content. Different phyla are represented by phyla names and triangles.

of physicochemical variables explaining the taxon distribution across communities. Unless specified otherwise, all statistical analyses were done in QIIME and/or PAST (Hammer et al., 2001).

RESULTS

Site Descriptions and Physicochemical Characteristics of Hot Springs

In this study, six hot springs with different physical and chemical conditions were studied (**Table 1**). Basically, the selected sites could be categorized as: (1) pond with high NaCl content (AH hot spring), (2) fast-flowing streamer (SK hot spring), and (3) non-saline pool with standing water (US, DT, SS, and SE hot springs). Data on microbial diversity in SK were previously reported by our group (Chan et al., 2015) and were compared with data for the other five hot springs studied in the current work (**Figure 1**, **Table 1**). The six hot springs exhibit different temperatures (40–110°C) and pH (6.9–8.2). The highest temperature was recorded at US (80–110°C) followed by SK (60–110°C) and DT (55–75°C). Hot springs SS, SE, and AH have lower temperatures (40–50°C). The water chemistry including alkalinity, acidity, color, turbidity, and major ions varied among the hot springs (**Table 2**). In comparison to other sites, SK water has the highest turbidity,

TABLE 3 | Sequencing data profiles and alpha diversity indexes.

	US	SK[a]	DT	SS	SE	AH
Number of raw sequences	1,053,625	480,983	1,028,376	1,761,134	1,167,238	1,100,225
Average size read (bp)	35–301	35–301	35–301	45–301	35–301	35–301
Mean GC content (%)	58	56	54	53	54	55
High quality sequences[b]	1,013,171	429,677	952,470	1,650,101	1,084,632	1,057,048
Cleaned sequences[c]	990,519	424,188	914,072	1,627,045	987,849	984,566
PyNAST aligned sequences	987,974	421,383	912,827	1,608,109	985,204	982,466
Sequences without singletons	974,062	417,783	898,358	1,569,331	970,574	968,368
Total OTUs[d]	7,326	6,334	9,083	26,244	11,504	6,430
Taxonomy assigned sequences	801,105	376,334	861,537	1,264,280	912,975	909,979
Bacteria	785,038	373,507	857,088	1,243,916	908,541	909,890
Archaea	16,067	2,827	4,449	20,364	4,434	89
Unassigned sequences	172,957	41,449	36,821	305,051	57,599	58,389
ALPHA DIVERSITY ANALYSIS						
Good's coverage	0.985	0.987	0.983	0.974	0.982	0.985
Shannon-Wiener	6.505	9.020	6.123	9.929	7.128	7.513
Simpson	0.962	0.992	0.933	0.984	0.955	0.977

[a] *Data collected from Bioproject accession number PRJEB7059.*
[b] *Sequences which passed the quality filtration and sequence read merging process.*
[c] *Sequences obtained after chimera removal.*
[d] *Amount of observed OTUs after singletons removal.*

TOC, aluminum, arsenic, and iron, while AH had distinctly high concentrations of chloride, fluoride, $CaCO_3$ (hardness), magnesium, sodium, sulfate, and sulfur. The chemical contents in water samples from high-temperature springs (US and DT) are relatively similar, except for the concentrations of fluoride, $CaCO_3$, magnesium, and TN. On the other hand, the water of two low-temperature hot springs (SE and SS) differs in the concentrations of iron, phosphate, TN, and acidity. Additionally, the sulfur content in AH, US, and SK is relatively high, probably associated with their location in the northern part of Peninsular Malaysia. The TN content in SK and SE is quite high, with 5.6 mg L^{-1} and 6.1 mg L^{-1}, respectively, while it is $<$0.2 mg L^{-1} for US and AH. Water in DT, SS, and SE has a carbon-to-nitrogen ratio (C:N) of 0.1–0.3, while the C:N for US and SK is quite similar (1.5–1.6). Besides its high COD and BOD levels, AH water has a high C:N ratio of 5.

PCA of the physicochemical variables separated the hot springs into three physicochemically distinct habitats (Group-1: AH; Group-2: SK, and Group-3: US, DT, SS, and SE). **Figure 2A** shows the distribution of the physicochemical variables formed by the first two components of the analysis, which explained 88.09% of the total variance. PC1 explained 66.76% of the observed variation, and clearly separated the saline hot spring AH from the non-saline hot springs (US, SK, DT, SS, and SE). PC1 was correlated with chloride, magnesium, sodium, sulfate ions, hardness, and sulfur, and high values for these variables might be related to the presence of seawater, as the AH hot spring is located on an island (**Figure 1A**). PC2, accounting for 21.33% of the total variation, was related primarily to pH, color, turbidity, aluminum, iron, and TOC. The relatively higher values of these variables in SK separated this hot spring from the other five springs; the presence of plant litter in SK increases the TOC (Chan et al., 2015). Group-3, a separate cluster of US, DT, SS, and SE, showed inverse correlations with most of the physicochemical variables, except temperature, TN, and acidity (**Figure 2A**).

16S rRNA Gene Microbial Profiles

As summarized in **Table 3**, the sizes of the six 16S rRNA gene sequence datasets ranged from 0.60 to 2.32 Gb, with between 480,983 and 1,761,134 paired-end reads. After quality filtering, sequence merging, and chimera removal, more than 98.8% of the cleaned sequences were aligned against Greengenes database using the PyNAST (Caporaso et al., 2010a) alignment algorithm. After removal of the singletons (sequences that are present exactly once in a sample), 80.6–95.9% of the aligned sequences were taxonomically classified. About 4.1–19.4% of these sequences could not be assigned to known taxa, perhaps due to a lack of suitable reference sequences in the database. The majority of the assigned OTUs were classified as bacteria, i.e., 97.99% for US, 99.25% for SK, 99.48% for DT, 98.39% for SS, 99.51% for SE, and 99.99% for AH. Archaeal OTUs comprised relatively small percentages: 2.01% for US and 1.61% for SS, and $<$1% of the total populations for other sites (SK: 0.75%, DT: 0.52%, SE: 0.49%, and AH: 0.01%).

Taxonomic Composition of the Prokaryotic Communities

Bacterial Diversity

Within the domain Bacteria, more than 99.4% of the assigned sequences were classified at the phylum level. In total, 59, 61, 72, 73, 65, and 52 bacterial phyla were detected in US, SK, DT, SS, SE, and AH, respectively, yet less than six phyla are dominant in each hot spring with $>$10% relative abundance of total sequences at the phylum level. The bacterial communities within

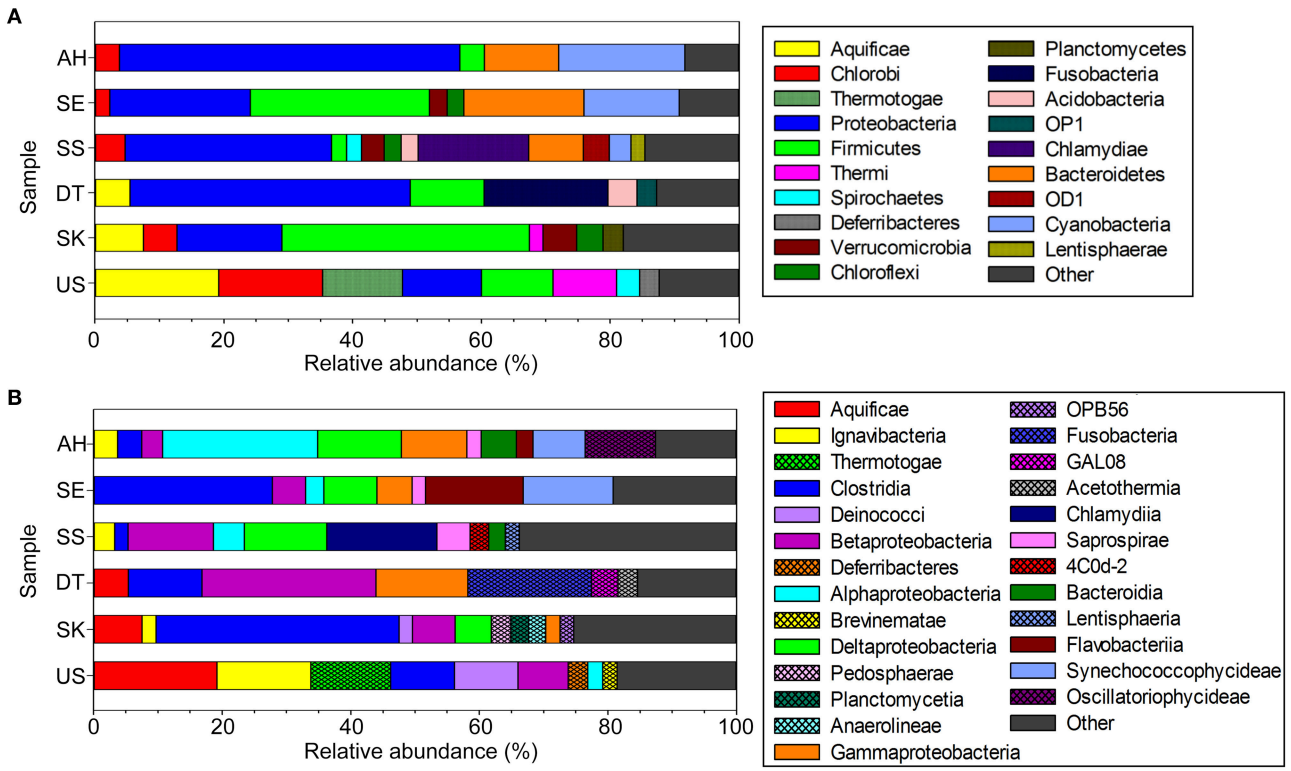

FIGURE 3 | Relative abundance of bacterial 16S rRNA gene sequences. **(A)** Phyla and **(B)** class taxonomic levels of bacterial community structures with relative abundances of <2% were grouped as "Other."

each site were unique. In general, the phyla Aquificae (relative abundance of 19.2%), Chlorobi (16.1%), Thermotogae (12.4%), Proteobacteria (12.2%), and Firmicutes (11.1%) dominated US. Phyla Firmicutes (38.5%) and Proteobacteria (16.3%) dominated SK, while Proteobacteria (43.5%), Fusobacteria (19.3%), and Firmicutes (11.5%) dominated DT. The SS hot spring was dominated by Proteobacteria (32.1%) and Chlamydiae (17.2%). SE water samples had great proportions of Firmicutes (27.8%), Proteobacteria (21.8%), Bacteroidetes (18.7%), and Cyanobacteria (14.8%). AH was dominated with Proteobacteria (52.8%), Cyanobacteria (19.6%), and Bacteroidetes (11.5%) (**Figure 3A**).

Firmicutes can be regarded as a signature phylum for circumneutral hot springs based on their abundance. Among the studied sites, SK and SE have the greatest dominance of Firmicutes (38.5 and 27.8% of total phyla, respectively), followed by US and DT (∼11%), while this phylum is relatively less abundant in SS and AH hot springs (<4%). In general, at least 89.6% of total Firmicutes OTUs were assigned to the class Clostridia (mainly in the order Clostridiales, comprising obligate anaerobe and endospore-forming bacteria) (**Figure 3B**), while the remaining classes were Bacilli and Erysipelotrichi. In SK and SE, Firmicutes were mainly represented by the genera *Pelosinus* (15.4% of total Firmicutes) and *Acidaminobacter* (74.7%). Furthermore, Firmicutes in SE were dominated by the genus *Acidaminobacter*, with 37.8% of the total genera.

Proteobacteria form another signature phylum as the phylum was dominant in DT, SS, and AH (43.5, 32.1, and 52.8% of total phyla, respectively). High abundance of Proteobacteria was also detected in the US (12.2%), SK (16.3%), and SE (27.8%) hot springs. Betaproteobacteria form the most abundant Proteobacteria class in US, SK, DT, and SS, while AH was dominated by Alphaproteobacteria (**Figure 3B**). Moreover, Alpha-, Beta-, Gamma-, and Deltaproteobacteria were detected in all six Malaysian hot springs, but at different percentages. DT was dominated by *Vogesella* (43.3% of total genera), a genus within Betaproteobacteria. *Vogesella* is frequently found in freshwater bodies and currently, seven species have been described in this genus. *Vogesella lacus* (Chou et al., 2009) and *Vogesella perlucida* (Chou et al., 2008) are the only species that can grow at temperatures <40°C. The genus *Hahella* represented the main Gammaproteobacteria in AH (13.9%). *Hahella* are marine bacteria that require NaCl to grow. To date, only three species within the genus *Hahella* have been described, i.e., *H. chejuensis* (Lee et al., 2001), *H. ganghwensis* (Baik et al., 2005), and *H. antarctica* (Lee et al., 2008). *H. chejuensis* is able to grow at temperatures of up to 45°C (Lee et al., 2001).

Owing to its high water temperature (80–110°C), hyperthermophilic phyla including Aquificae and Thermotogae prevailed in US. Both phyla were also detected in SK (7.5% Aquificae and 1.7% Thermotogae) which has a considerable high temperature, but were insignificant in SS, SE, and AH (<0.1% of

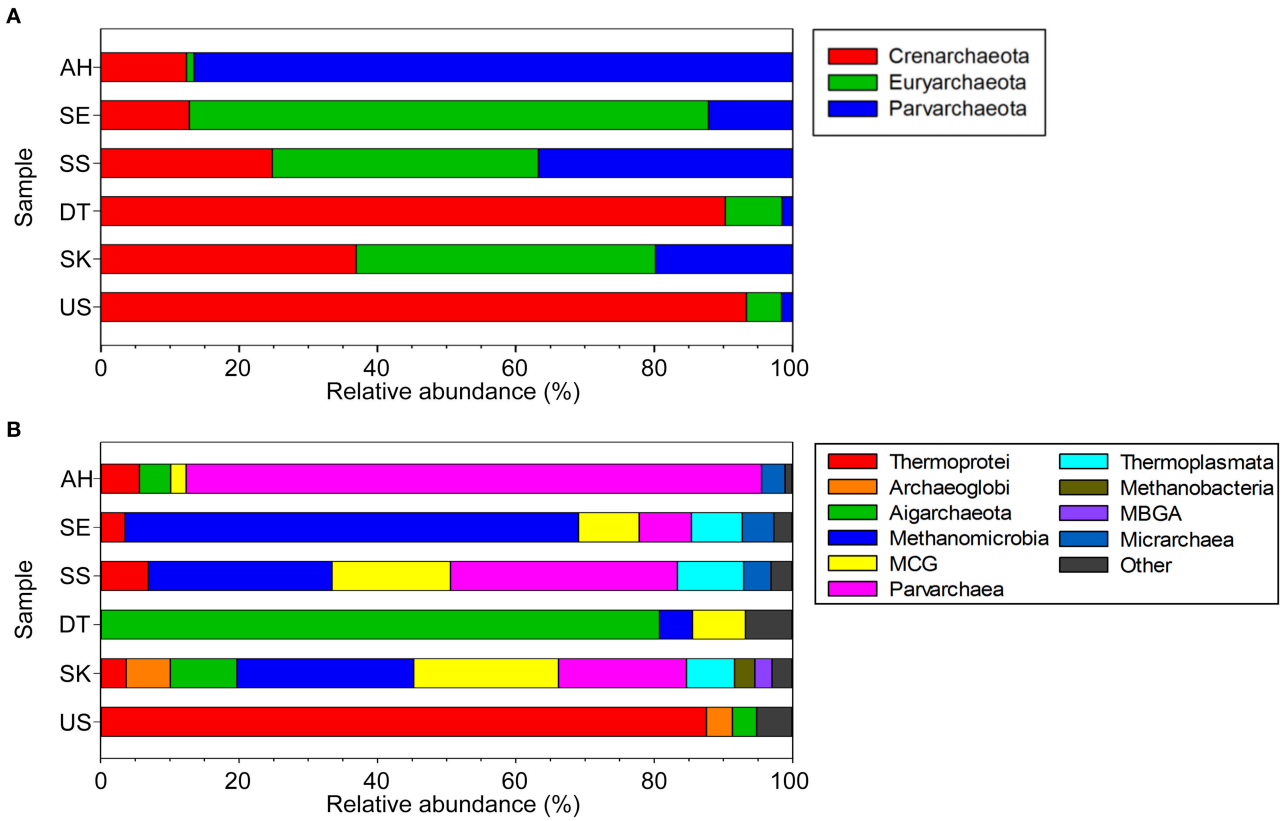

FIGURE 4 | Relative abundance of archaeal 16S rRNA gene sequences. **(A)** Phyla and **(B)** class taxonomic levels of archaeal community structures with relative abundances of <2% were grouped as "Other." Relative abundance is defined as the percentage of sequences in total successfully assignable sequences in the samples using Greengenes database.

total phyla). Aquificae in US and SK were mainly comprised of the genus *Hydrogenobacter*, with 98.9% in US and 88.6% in SK of total Aquificae, equivalent to 31.6 and 13.3% of total OTUs at the genus level, respectively. With an average temperature of 75°C, in DT, Aquificae (5.4% of total phyla) were more abundant than Thermotogae (0.2%).

Archaeal Diversity

Only 3 archaeal phyla, Euryarchaeota, Parvarchaeota, and Crenarchaeota, were detected in the studied sites (**Figure 4A**). Euryarchaeota were found to be the main archaea in SK (43.3% total archaea phylum), SS (38.5%), and SE (75.1%). Parvarchaeota prevailed in AH, with 86.5% of total archaeal phyla. An earlier metagenomics study elucidated that members of Parvarchaeota are very small in size (cells are <500 nm in diameter) and are from lineages without cultivated representatives that branch near the crenarchaeal/euryarchaeal divide (Baker et al., 2010). In SK, SS, and SE hot springs, the majority of the Euryarchaeota were methanogenic archaea of the class Methanomicrobia, genus, *Methanosaeta*. At present, *Methanosaeta* is the only genus affiliated to the Methanosaetaceae family. *Methanosaeta* spp. utilize acetate as a sole energy source to produce methane and carbon dioxide (Welte and Deppenmeier, 2011).

The phylum Crenarchaeota constituted the major archaeal member in the US (93.3%) and DT (90.3%) hot springs. In US, 93.7% of total Crenarchaeota were related to the class Thermoprotei. The hyperthermophilic genus *Aeropyrum* (90.4% of total genera) was identified in US; strains of this genus grow optimally at 85–95°C (Sako et al., 1996; Nakagawa et al., 2004). In DT (**Figure 4B**), 55% of the detected Aigarchaeota showed the closest similarity to the uncultivated archaeon "*Candidatus* Caldiarchaeum" (Nunoura et al., 2011). *Ca.* C. subterraneum was first discovered in a non-cultured metagenomic library from a microbial mat at a geothermal water stream of a sub-surface gold mine with a temperature of 70°C (Hirayama et al., 2005). It was proposed that *Ca.* C. subterraneum lives symbiotically with acetogenic "*Candidatus* Acetothermus autotrophicum" for organic carbon supply, since *Ca.* C. subterraneum has an extremely poor carbon fixation potential (Takami et al., 2015).

Alpha Diversity Analysis

Since rarefaction curves did not reach a plateau (Supplementary Figure 1), total species richness was not estimated. Therefore, Good's coverage estimator was used; all six hot spring samples had an estimated coverage of at least 97% of the entire sampled population (**Table 3**). Additionally, non-phylogeny-based metrics including Shannon–Wiener's and Simpson's

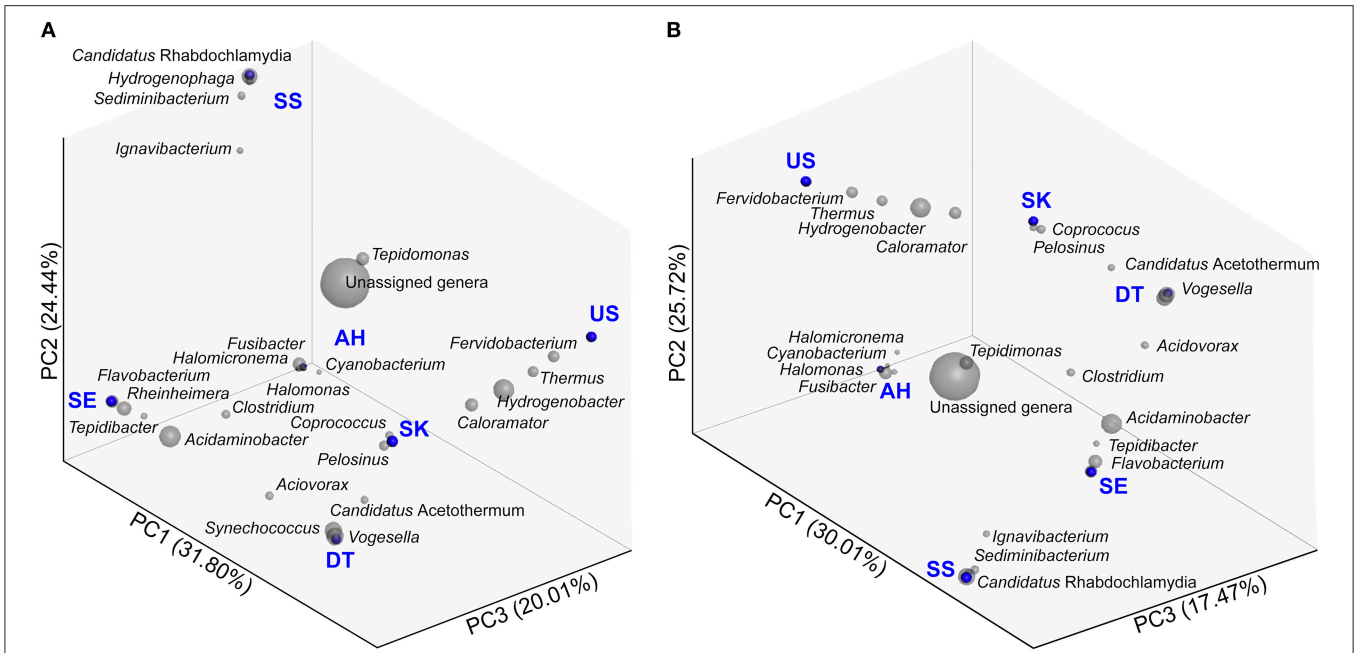

FIGURE 5 | Communities clustered using PCoA of the **(A)** weighted and **(B)** unweighted UniFrac distance matrixes. PC1, PC2, and PC3 are plotted on x-, y-, and z-axes with the percentage of variation explained by each axis noted in parentheses. Each point corresponds to a hot spring community.

diversity indexes were computed (**Table 3**). A greater (Shannon–Wiener) diversity of OTUs was found in SS (9.9) and SK (9.0), followed by AH (7.5) and SE (7.1). Both US (6.5) and DT (6.1) samples have relatively lower diversity, based on both the Shannon–Wiener and Simpson indexes. It has been reported that high temperature has a negative effect on diversity (Sharp et al., 2014; Li et al., 2015). The microbial communities in high-temperature hot springs (US and DT, >70°C) were dominated by fewer genera than those in low-temperature sites (SS, AH, and SE, <50°C). Nevertheless, although the SK hot spring has a high water temperature of 50–110°C, the diversity index for SK is high.

Beta Diversity Analysis

The above alpha diversity metrics provided an overview of the microbial diversity of each sampling site in this study. On the other hand, beta diversity is useful for documenting the structure of communities that may occur between samples categories or across environmental gradients (Lozupone and Knight, 2005). Here, we compared the six Malaysian hot spring samples using jackknifed UPGMA to cluster the community samples with weighted and unweighted UniFrac phylogenetic distances (Lozupone and Knight, 2005; Lozupone et al., 2007). Using PCoA with weighted UniFrac (**Figure 5A**), PC1 explains 32% of the variation, while PC2 and PC3 explain 24 and 20%, respectively. The AH hot spring presented as an outlier in PCoA owing to its high salinity. Weighted UniFrac PCoA and the corresponding dendrogram (Supplementary Figure 2A) were unable to show the effect of temperature on the microbial communities in the six hot springs. In comparison, PCoA with unweighted UniFrac (73% of total variation explained by PC1, PC2, and PC3) (**Figure 5B**) and the corresponding dendrogram (Supplementary Figure 2B) yielded a clearer clustering that sorted the hot springs into three groups in accordance to variation in temperature and salinity. The three groups are: Group-1: high salinity with moderate temperature (AH); Group-2: low salinity with moderate temperature (SE and SS); and Group-3: low salinity with high temperature (US, SK, and DT). A similar grouping pattern was identified based on Bray–Curtis dissimilarity using the jackknifed UPGMA dendrogram (Supplementary Figure 2C).

Relationships between Microbial Community and Physicochemical Variables

Multivariate analyses are widely used in ecology studies to elucidate the relationships between abundances of certain organisms and environmental parameters. In this study, the CCA approach (ter Braak and Verdonschot, 1995) was used to identify possible relationships between microbial communities in hot springs and local physicochemical variables. Only physicochemical variables with normally distributed values, including temperature, pH, C:N, TOC, TN, sulfur, and phosphate, were used in this study (**Figure 2B**). The placement of hot spring samples in the plot is influenced by their environmental characteristics. The eigenvalues for each axis generated by CCA indicate how much of the variation seen in the genera data can be explained by the canonical axis. In this analysis, 61% of the correlation between OTUs, hot spring samples, and physicochemical variables were explained by two axes.

Most variables, including temperature, pH, C:N, and sulfur content showed a positive correlation (**Figure 2B**), while inverse correlations were observed for TOC, TN, and phosphate content. Among the tested variables, temperature was the most influential variable affecting the distribution of OTUs. In **Figure 2B**, plots

for US and SK are situated in a right side, as these sites are characterized by high temperatures, while SS, AH, and SE hot springs fall in the opposite side of the plot. The right side was occupied by thermophilic phyla, including Thermotogae, Dictyoglomi, Thermi, Aquificae, Caldiserica, Crenarchaeota, Deferribacteres, candidate divisions OP9 ("Atribacter") (Nobu et al., 2016), OP1, EM3, and OctSpA1-106 (Youssef et al., 2015), with a strong, positive correlation with temperature. Additionally, candidate divisions EM3, OP1, and OctSpA1-106 are also positively correlated with sulfur content, and these OTUs were frequently found in US, SK, and DT, which are rich in sulfur (**Table 2**). Furthermore, phosphate is positively correlated with Caldithrix, Bacteroidetes, Cyanobacteria, Proteobacteria, WS3, and OP11, which were found in the AH and SE hot springs with slightly higher phosphate contents. Proteobacteria, Cyanobacteria, and Bacteroidetes were also positively correlated with TOC and TN, while Chlorobi, candidate division NKB19, and Spirochaetes were positively correlated with C:N. The microbial community from SS was negatively correlated with most of the measured physicochemical variables.

DISCUSSION

Microbial Community Composition and Diversity

All reported Malaysian hot springs have circumneutral pH. In the present study, the distributions of microbiota in six hot springs with different physical and physicochemical characteristics were studied. The five non-saline hot springs can be differentiated based on their water temperature, i.e., moderate-temperature (SS and SE) and high-temperature (US, SK, and DT) thermal springs. The moderate-temperature hot spring AH is especially interesting, as it is located 2 km away from an open sea, on an island. The concentrations of sodium, magnesium, chloride, fluoride, and sulfate ions in the AH hot spring were nevertheless lower than those in a seawater sample collected from Malaysia (data not shown). Therefore, it is possible that the water in the AH pond is a mixture of sea- and groundwater. The compounds in seawater (including chloride, magnesium, sodium, and sulfate ions) clearly influenced the microbial community that distinguishes AH from the non-saline US, SK, DT, SS, and SE hot springs. The microbial community structures in the US and SK hot springs are quite similar; both sites cluster together in the biplots in **Figures 5A,B** and share similar OTUs such as *Thermus*, *Hydrogenobacter*, and *Caloramator*.

Generally, the dominant phyla in the studied hot springs are similar, but the sites differ with respect to the overall composition (**Figures 3A**, **4A**). Firmicutes and Proteobacteria are the phyla consistently present in circumneutral hot springs. Site-specific taxa assigned at the genus level included *Fervidobacterium* in US; *Coprococcus* and *Pelosinus* in SK; *Vogesella* in DT; *Candidatus* Rhabdochlamydia, *Sediminibacterium*, and *Hydrogenophaga* in SS; *Rheinheimera* and *Flavobacterium* in SE; and *Halomicronema*, *Halomonas*, *Fusibacter*, and *Cyanobacterium* in AH (**Figure 5A**). Interestingly, *Candidatus* Rhabdochlamydia (Kostanjšek et al., 2004), an intracellular bacterium that was first found in the terrestrial isopod *Porcellio scaber* appeared to be one of the dominant genera in SE. This finding suggests that endosymbiosis of thermophilic microbiota can occur in the hot springs and is not restricted to SE, but also possibly occurs in DT, where we discovered tiny reddish crustaceans (order, Isopoda; data not shown).

In the current study, archaea appeared to be a minority in the prokaryotic community. This result is consistent with our previous shotgun metagenome analyses for SK (Chan et al., 2015) and US (data not shown). High-temperature environments were previously generally believed to be the realm of archaea (Urbieta et al., 2014; Li et al., 2015). However, recent studies applying molecular methods have revealed that bacteria rather are the predominant prokaryotic communities in such environments (Badhai et al., 2015; López-López et al., 2015). The factors that allow bacteria to dominate in high-temperature habitats are not well understood. Our findings revealed that archaea are not dominant in circumneutral hot springs, which in agreement with several recent reports with similar pH ranges (Wang et al., 2013; Merkel et al., 2017). Though insightful, the above findings are preliminary, as they are based on molecular methods, which inherently assume that both bacteria and archaea are detected at the same level. Moreover, other technical factors including DNA extraction method (Zielińska et al., 2017), primer selection (Cai et al., 2013), primer combinations, library preparation protocols, and sequencing platforms should be considered.

Higher Shannon–Wiener or Simpson diversity index values indicate greater species richness. The moderate-temperature springs SS, SE, and AH were more diverse than the higher-temperature springs at US and DT (**Table 3**). This shows that increments in habitat temperature result in decreased taxonomic richness and diversity, which is in agreement with earlier findings (Miller et al., 2009; Tobler and Benning, 2011; Inskeep et al., 2013; Sharp et al., 2014). Yet, markedly high microbial richness and diversity exist in SK, which may be owing to the stream-like physical appearance of this hot spring. Along the heated stream, the pH gradient varies by 1.5 unit, and the temperature fluctuates (60–110°C) because of the presence of multiple spring heads. Moreover, the stream is shallow and the water flows rapidly, thus generating sufficient aeration for aerophiles. Finally, the presence of plant litter in SK is associated with high TOC (additional carbon source) (Hou et al., 2013), which favors the growth of microorganisms. Thus, fluctuations in physicochemical features in a microenvironment likely enable a wider range of microbial species to survive.

Physicochemical Factors Regulating Microbial Community Structure

Quantitative weighted UniFrac analysis (**Figure 5A**) of our samples suggested that the five non-saline hot springs had similar microbial communities, while AH represented an outlier in the dendrogram (Supplementary Figure 2A). The high salinity of AH should be the main factor responsible for the unique microbial community based on the relative abundances of OTUs. Compared to quantitative weighted UniFrac, unweighted UniFrac is a qualitative distance metric that only considers the presence or absence of OTUs. Unweighted UniFrac further confirmed that microbial membership in the saline spring (AH) largely differs from that in the non-saline hot springs.

Besides salinity, unweighted UniFrac showed clustering of the microbial community structures by temperature for the non-saline hot springs (**Figures 5B** and Supplementary Figure 2B). This explained that temperature is a crucial factor in identifying the changes in community membership rather than community composition in this study. Taken together, our data indicate that salinity and temperature are the main factors in shaping the microbial community structures in these six Malaysian hot springs.

Besides temperature and salinity as the most influential factors, we were interested in identifying other factors potentially affecting the microbiota in circumneutral hot springs. Based on the CCA plot, it is possible that TOC and TN, or the C:N ratio affect growth efficiencies, and thus shape the microbial communities (Michaud et al., 2014; Wan et al., 2015). AH has the highest C:N among the six Malaysian hot springs, partly because seawater has a high C:N (Meyers, 1994). DT, SS, and SE hot springs are more species-rich, and these sites have low C:N (<0.5) (Touratier et al., 1999). Even though DT, US, and SK are high-temperature springs, the dominant genera in DT are different from those in the other two springs, probably owing to low C:N ratio. As SK is located in a forest, it has a relatively high TOC, possibly related to the presence of plant litter along the stream. The decomposition of plant litter is one of the processes involved in nutrient and carbon cycling in ecosystems, and results in the release of dissolved organic matter back to earth (Kindler et al., 2011). The high quantity of organic matter in SK might explain the high microbial diversity and richness of this hot spring in comparison to other springs.

CCA showed a positive correlation between phosphate content and phosphate-solubilizing bacteria from phyla Proteobacteria, Actinobacteria, and Bacteroidetes (Sharma et al., 2013). This suggests that Cyanobacteria, Planctomycetes, Caldithrix, candidate divisions OP11, and WS3 are likely involved in the process of releasing phosphorus from insoluble compounds to the environment. Additionally, the negative correlation between Cyanobacteria and water temperature was shown for high-temperature springs (US, SK, and DT hot springs). Such observation is explained by the restriction of photosynthesis when the temperature is higher than 75°C (Ferris and Ward, 1997). In another aspect, the positive correlation between sulfur content and candidate divisions OP1, EM3, and OctSpA1-106 suggests that sulfur may affect the growth of these uncultured prokaryotes. These candidate divisions may be important for sulfur cycling in hot springs. In comparison to aforementioned variables, other abiotic factors, including chloride, fluoride, sodium, sulfate, iron, magnesium, arsenic, and aluminum play less of a role in determining the predominant microbial members in the Malaysian hot springs.

CONCLUSION

The six Malaysian hot springs in this study have different physical and physicochemical characteristics. Investigating hot spring microbiomes with simple microbial composition is important for understanding microbe-mediated biogeochemical cycles and ecosystem functioning. This is the first study to identify the physicochemical factors that drive variations in microbial community structures in Malaysian hot springs. Firmicutes and Proteobacteria were the signature phyla in all six hot springs that along with the presence of site-specific taxa contributed to the uniqueness of each hot spring. Temperature was found to be the most influential factor shaping the microbiome of Malaysian hot springs, as was anticipated. Generally, overall microbial diversity and richness were negatively affected by temperature. As an exception, SK hosted high microbial richness and diversity despite its high temperature, probably due to its physical characters that enable a wider range of microbial species to survive. Variables such as salinity, C:N ratio, phosphate, and sulfur content are probably secondary factors that affect circumneutral hot spring microbial communities. Nevertheless, other variables should not be ignored in microbial ecology studies, as all abiotic factors collectively contribute to the dynamics of microbial populations. Understanding microbial community dynamics and genomic variability of community members in hot springs with different ecologies is important to elucidate community functions and their importance for the maintenance of hot spring ecosystems.

AUTHOR CONTRIBUTIONS

CC, KC, and KG contributed to the conception and design of the study. CC, RE, and KH produced data. CC, KH, MS, and KG conducted the bioinformatics and statistical analyses. CC, KC, and KG wrote and reviewed the manuscript. MU, ED, and MS helped in interpretation of data and contributed to the discussion of the results followed by reviewing the manuscript. All authors read and approved the final manuscript, and are agreement to be accountable for all aspects of the work in ensuring that questions related to the accuracy or integrity of any part of the work are appropriately investigated and resolved.

FUNDING

This work was supported by the University of Malaya via High Impact Research Grants (UM.C/625/1/HIR/MOHE/CHAN/01 [Grant No. A-000001-50001] and UM.C/625/1/HIR/MOHE/CHAN/14/1 [Grant No. H-50001-A000027]) awarded to KC. KG is grateful for funding received from Universiti Teknologi Malaysia GUP (Grant 15H50). Mohd Shahir Shamsir appreciates funding provided to this study by Universiti Teknologi Malaysia GUP (Grant 15H16).

ACKNOWLEDGMENTS

We are grateful to Teong Han Chew for assistance on part of the Python programming work.

SUPPLEMENTARY MATERIAL

The Supplementary Material for this article can be found online at: http://journal.frontiersin.org/article/10.3389/fmicb.2017.01252/full#supplementary-material

REFERENCES

Badhai, J., Ghosh, T. S., and Das, S. K. (2015). Taxonomic and functional characteristics of microbial communities and their correlation with physicochemical properties of four geothermal springs in Odisha, India. *Front. Microbiol.* 6:1166. doi: 10.3389/fmicb.2015.01166

Baik, K. S., Seong, C. N., Kim, E. M., Yi, H., Bae, K. S., and Chun, J. (2005). *Hahella ganghwensis* sp. nov., isolated from tidal flat sediment. *Int. J. Syst. Evol. Microbiol.* 55, 681–684. doi: 10.1099/ijs.0.63411-0

Baioumy, H., Nawawi, M., Wagner, K., and Arifin, M. H. (2015). Geochemistry and geothermometry of non-volcanic hot springs in West Malaysia. *J. Volcanol. Geotherm. Res.* 290, 12–22. doi: 10.1016/j.jvolgeores.2014.11.014

Baker, B. J., Comolli, L. R., Dick, G. J., Hauser, L. J., Hyatt, D., Dill, B. D., et al. (2010). Enigmatic, ultrasmall, uncultivated Archaea. *Proc. Natl. Acad. Sci. U.S.A.* 107, 8806–8811. doi: 10.1073/pnas.0914470107

Baker, G. C., Gaffar, S., Cowan, D. A., and Suharto, A. R. (2001). Bacterial community analysis of Indonesian hot springs. *FEMS Microbiol. Lett.* 200, 103–109. doi: 10.1111/j.1574-6968.2001.tb10700.x

Blank, C. E., Cady, S. L., and Pace, N. R. (2002). Microbial composition of near-boiling silica-depositing thermal springs throughout Yellowstone National Park. *Appl. Environ. Microbiol.* 68, 5123–5135. doi: 10.1128/AEM.68.10.5123-5135.2002

Cai, L., Ye, L., Tong, A. H. Y., Lok, S., and Zhang, T. (2013). Biased diversity metrics revealed by bacterial 16S pyrotags derived from different primer sets. *PLoS ONE* 8:e53649. doi: 10.1371/journal.pone.0053649

Caporaso, J. G., Bittinger, K., Bushman, F. D., DeSantis, T. Z., Andersen, G. L., and Knight, R. (2010a). PyNAST: a flexible tool for aligning sequences to a template alignment. *Bioinformatics* 26, 266–267. doi: 10.1093/bioinformatics/btp636

Caporaso, J. G., Kuczynski, J., Stombaugh, J., Bittinger, K., Bushman, F. D., Costello, E. K., et al. (2010b). QIIME allows analysis of high-throughput community sequencing data. *Nat. Methods* 7, 335–336. doi: 10.1038/nmeth.f.303

Chan, C. S., Chan, K.-G., Tay, Y.-L., Chua, Y.-H., and Goh, K. M. (2015). Diversity of thermophiles in a Malaysian hot spring determined using 16S rRNA and shotgun metagenome sequencing. *Front. Microbiol.* 6:177. doi: 10.3389/fmicb.2015.00177

Chou, J.-H., Chou, Y.-J., Arun, A. B., Young, C.-C., Chen, C. A., Wang, J.-T., et al. (2009). *Vogesella lacus* sp. nov., isolated from a soft-shell turtle culture pond. *Int. J. Syst. Evol. Microbiol.* 59, 2629–2632. doi: 10.1099/ijs.0.009266-0

Chou, Y.-J., Chou, J.-H., Lin, M.-C., Arun, A. B., Young, C.-C., and Chen, W.-M. (2008). *Vogesella perlucida* sp. nov., a non-pigmented bacterium isolated from spring water. *Int. J. Syst. Evol. Microbiol.* 58, 2677–2681. doi: 10.1099/ijs.0.65766-0

Edgar, R. C. (2010). Search and clustering orders of magnitude faster than BLAST. *Bioinformatics* 26, 2460–2461. doi: 10.1093/bioinformatics/btq461

Edgar, R. C., Haas, B. J., Clemente, J. C., Quince, C., and Knight, R. (2011). UCHIME improves sensitivity and speed of chimera detection. *Bioinformatics* 27, 2194–2200. doi: 10.1093/bioinformatics/btr381

Ferris, M. J., and Ward, D. M. (1997). Seasonal distributions of dominant 16S rRNA-defined populations in a hot spring microbial mat examined by denaturing gradient gel electrophoresis. *Appl. Environ. Microbiol.* 63, 1375–1381.

Goh, K. M., Chua, Y. S., Rahman, R. N. Z. R. A., Chan, R., and Illias, R. M. (2011). A comparison of conventional and miniprimer PCR to elucidate bacteria diversity in Malaysia Ulu Slim hot spring using 16S rDNA clone library. *Rom. Biotechnol. Lett.* 16, 6247–6255.

Good, I. J. (1953). The population frequencies of species and the estimation of population parameters. *Biometrika* 40, 237–264. doi: 10.1093/biomet/40.3-4.237

Hammer, Ø., Harper, D. A. T., and Ryan, P. D. (2001). PAST: Paleontological statistics software package for education and data analysis. *Palaeontol. Electron.* 4, 1–9.

Hirayama, H., Takai, K., Inagaki, F., Yamato, Y., Suzuki, M., Nealson, K. H., et al. (2005). Bacterial community shift along a subsurface geothermal water stream in a Japanese gold mine. *Extremophiles* 9, 169–184. doi: 10.1007/s00792-005-0433-8

Hou, W., Wang, S., Dong, H., Jiang, H., Briggs, B. R., Peacock, J. P., et al. (2013). A comprehensive census of microbial diversity in hot springs of Tengchong, Yunnan Province China using 16S rRNA gene pyrosequencing. *PLoS ONE* 8:e53350. doi: 10.1371/journal.pone.0053350

Huang, Q., Jiang, H., Briggs, B. R., Wang, S., Hou, W., Li, G., et al. (2013). Archaeal and bacterial diversity in acidic to circumneutral hot springs in the Philippines. *FEMS Microbiol. Ecol.* 85, 452–464. doi: 10.1111/1574-6941.12134

Inskeep, W. P., Jay, Z. J., Tringe, S. G., Herrgard, M. J., and Rusch, D. B. (2013). The YNP metagenome project: environmental parameters responsible for microbial distribution in the Yellowstone geothermal ecosystem. *Front. Microbiol.* 4:67. doi: 10.3389/fmicb.2013.00067

Kan, J., Clingenpeel, S., Macur, R. E., Inskeep, W. P., Lovalvo, D., Varley, J., et al. (2011). Archaea in yellowstone lake. *ISME J.* 5, 1784–1795. doi: 10.1038/ismej.2011.56

Kanokratana, P., Chanapan, S., Pootanakit, K., and Eurwilaichitr, L. (2004). Diversity and abundance of bacteria and archaea in the Bor Khlueng hot spring in Thailand. *J. Basic Microbiol.* 44, 430–444. doi: 10.1002/jobm.200410388

Kindler, R., Siemens, J. A. N., Kaiser, K., Walmsley, D. C., Bernhofer, C., Buchmann, N., et al. (2011). Dissolved carbon leaching from soil is a crucial component of the net ecosystem carbon balance. *Glob. Change Biol.* 17, 1167–1185. doi: 10.1111/j.1365-2486.2010.02282.x

Klindworth, A., Pruesse, E., Schweer, T., Peplies, J., Quast, C., Horn, M., et al. (2013). Evaluation of general 16S ribosomal RNA gene PCR primers for classical and next-generation sequencing-based diversity studies. *Nucleic Acids Res.* 41:e1. doi: 10.1093/nar/gks808

Kostanjšek, R., Štrus, J., Drobne, D., and Avguštin, G. (2004). Candidatus *Rhabdochlamydia porcellionis,* an intracellular bacterium from the hepatopancreas of the terrestrial isopod *Porcellio scaber* (Crustacea: Isopoda). *Int. J. Syst. Evol. Microbiol.* 54, 543–549. doi: 10.1099/ijs.0.02802-0

Kubo, K., Knittel, K., Amann, R., Fukui, M., and Matsuura, K. (2011). Sulfur-metabolizing bacterial populations in microbial mats of the Nakabusa hot spring, Japan. *Syst. Appl. Microbiol.* 34, 293–302. doi: 10.1016/j.syapm.2010.12.002

Lee, H. K., Chun, J., Moon, E. Y., Ko, S. H., Lee, D. S., Lee, H. S., et al. (2001). *Hahella chejuensis* gen. nov., sp. nov., an extracellular-polysaccharide-producing marine bacterium. *Int. J. Syst. Evol. Microbiol.* 51, 661–666. doi: 10.1099/00207713-51-2-661

Lee, K., Lee, H. K., and Cho, J.-C. (2008). *Hahella antarctica* sp. nov., isolated from Antarctic seawater. *Int. J. Syst. Evol. Microbiol.* 58, 353–356. doi: 10.1099/ijs.0.65389-0

Li, H., Yang, Q., Li, J., Gao, H., Li, P., and Zhou, H. (2015). The impact of temperature on microbial diversity and AOA activity in the Tengchong Geothermal Field, China. *Sci. Rep.* 5:17056. doi: 10.1038/srep17056

López-López, O., Knapik, K., Cerdán, M.-E., and González-Siso, M.-I. (2015). Metagenomics of an alkaline hot spring in Galicia (Spain): microbial diversity analysis and screening for novel lipolytic enzymes. *Front. Microbiol.* 6:1291. doi: 10.3389/fmicb.2015.01291

Lozupone, C. A., Hamady, M., Kelley, S. T., and Knight, R. (2007). Quantitative and qualitative β diversity measures lead to different insights into factors that structure microbial communities. *Appl. Environ. Microbiol.* 73, 1576–1585. doi: 10.1128/AEM.01996-06

Lozupone, C., and Knight, R. (2005). UniFrac: a new phylogenetic method for comparing microbial communities. *Appl. Environ. Microbiol.* 71, 8228–8235. doi: 10.1128/AEM.71.12.8228-8235.2005

Masaki, Y., Tsutsumi, K., Hirano, S. I., and Okibe, N. (2016). Microbial community profiling of the Chinoike Jigoku ("Blood Pond Hell") hot spring in Beppu, Japan: isolation and characterization of Fe(III)-reducing *Sulfolobus* sp. strain GA1. *Res. Microbiol.* 167, 595–603. doi: 10.1016/j.resmic.2016.04.011

Mathur, J., Bizzoco, R. W., Ellis, D. G., Lipson, D. A., Poole, A. W., Levine, R., et al. (2007). Effects of abiotic factors on the phylogenetic diversity of bacterial communities in acidic thermal springs. *Appl. Environ. Microbiol.* 73, 2612–2623. doi: 10.1128/AEM.02567-06

McDonald, D., Price, M. N., Goodrich, J., Nawrocki, E. P., DeSantis, T. Z., Probst, A., et al. (2012). An improved Greengenes taxonomy with explicit ranks for ecological and evolutionary analyses of bacteria and archaea. *ISME J.* 6, 610–618. doi: 10.1038/ismej.2011.139

Menzel, P., Gudbergsdóttir, S. R., Rike, A. G., Lin, L., Zhang, Q., Contursi, P., et al. (2015). Comparative metagenomics of eight geographically remote terrestrial hot springs. *Microb. Ecol.* 70, 411–424. doi: 10.1007/s00248-015-0576-9

Merkel, A. Y., Pimenov, N. V., Rusanov, I. I., Slobodkin, A. I., Slobodkina, G. B., Tarnovetckii, I. Y., et al. (2017). Microbial diversity and autotrophic activity in Kamchatka hot springs. *Extremophiles* 21, 307–317. doi: 10.1007/s00792-016-0903-1

Meyers, P. A. (1994). Preservation of elemental and isotopic source identification of sedimentary organic matter. *Chem. Geol.* 114, 289–302. doi: 10.1016/0009-2541(94)90059-0

Michaud, L., Lo Giudice, A., Interdonato, F., Triplet, S., Ying, L., and Blancheton, J. P. (2014). C/N ratio-induced structural shift of bacterial communities inside lab-scale aquaculture biofilters. *Aqua. Eng.* 58, 77–87. doi: 10.1016/j.aquaeng.2013.11.002

Miller, S. R., Strong, A. L., Jones, K. L., and Ungerer, M. C. (2009). Bar-coded pyrosequencing reveals shared bacterial community properties along the temperature gradients of two alkaline hot springs in Yellowstone National Park. *Appl. Environ. Microbiol.* 75, 4565–4572. doi: 10.1128/AEM.02792-08

Nakagawa, S., Takai, K., Horikoshi, K., and Sako, Y. (2004). Aeropyrum camini sp. nov., a strictly aerobic, hyperthermophilic archaeon from a deep-sea hydrothermal vent chimney. *Int. J. Syst. Evol. Microbiol.* 54, 329–335. doi: 10.1099/ijs.0.02826-0

Nishiyama, M., Yamamoto, S., and Kurosawa, N. (2013). Microbial community analysis of a coastal hot spring in Kagoshima, Japan, using molecular- and culture-based approaches. *J. Microbiol.* 51, 413–422. doi: 10.1007/s12275-013-2419-z

Nobu, M. K., Dodsworth, J. A., Murugapiran, S. K., Rinke, C., Gies, E. A., Webster, G., et al. (2016). Phylogeny and physiology of candidate phylum 'Atribacteria' (OP9/JS1) inferred from cultivation-independent genomics. *ISME J.* 10, 273–286. doi: 10.1038/ismej.2015.97

Nunoura, T., Takaki, Y., Kakuta, J., Nishi, S., Sugahara, J., Kazama, H., et al. (2011). Insights into the evolution of archaea and eukaryotic protein modifier systems revealed by the genome of a novel archaeal group. *Nucleic Acids Res.* 39, 3204–3223. doi: 10.1093/nar/gkq1228

Olsen, G. J., Woese, C. R., and Overbeek, R. (1994). The winds of (evolutionary) change: breathing new life into microbiology. *J. Bacteriol.* 176, 1–6. doi: 10.1128/jb.176.1.1-6.1994

Sako, Y., Nomura, N., Uchida, A., Ishida, Y., Morii, H., Koga, Y., et al. (1996). *Aeropyrum pernix* gen. nov., sp. nov., a novel aerobic hyperthermophilic archaeon growing at temperatures up to 100°C. *Int. J. Syst. Bacteriol.* 46, 1070–1077. doi: 10.1099/00207713-46-4-1070

Samsudin, A. R., Hamzah, U., Rahman, R. A., Siwar, C., Mohd, M. F., and Othman, R. (1997). Thermal springs of Malaysia and their potential development. *J. Asian Earth Sci.* 15, 275–284. doi: 10.1016/S1367-9120(97)00012-6

Sangwan, N., Lambert, C., Sharma, A., Gupta, V., Khurana, P., Khurana, J. P., et al. (2015). Arsenic rich Himalayan hot spring metagenomics reveal genetically novel predator–prey genotypes. *Environ. Microbiol. Rep.* 7, 812–823. doi: 10.1111/1758-2229.12297

Shanks, O. C., Newton, R. J., Kelty, C. A., Huse, S. M., Sogin, M. L., and McLellan, S. L. (2013). Comparison of the microbial community structures of untreated wastewaters from different geographic locales. *Appl. Environ. Microbiol.* 79, 2906–2913. doi: 10.1128/AEM.03448-12

Sharma, S. B., Sayyed, R. Z., Trivedi, M. H., and Gobi, T. A. (2013). Phosphate solubilizing microbes: sustainable approach for managing phosphorus deficiency in agricultural soils. *Springerplus* 2:587. doi: 10.1186/2193-1801-2-587

Sharp, C. E., Brady, A. L., Sharp, G. H., Grasby, S. E., Stott, M. B., and Dunfield, P. F. (2014). Humboldt's spa: microbial diversity is controlled by temperature in geothermal environments. *ISME J.* 8, 1166–1174. doi: 10.1038/ismej.2013.237

Simpson, E. H. (1949). Measurement of diversity. *Nature* 163:688. doi: 10.1038/163688a0

Song, Z.-Q., Wang, F.-P., Zhi, X.-Y., Chen, J.-Q., Zhou, E.-M., Liang, F., et al. (2013). Bacterial and archaeal diversities in Yunnan and Tibetan hot springs, China. *Environ. Microbiol.* 15, 1160–1175. doi: 10.1111/1462-2920.12025

Spellerberg, I. F., and Fedor, P. J. (2003). A tribute to Claude Shannon (1916–2001) and a plea for more rigorous use of species richness, species diversity and the 'Shannon–Wiener' index. *Glob. Ecol. Biogeogr.* 12, 177–179. doi: 10.1046/j.1466-822X.2003.00015.x

Sum, C. W., Irawan, S., and Fathaddin, M. T. (2010). "Hot springs in the Malay Peninsula," in *Proceedings World Geothermal Congress 2010* (Bali), 1–5.

Takami, H., Arai, W., Takemoto, K., Uchiyama, I., and Taniguchi, T. (2015). Functional classification of uncultured "*Candidatus* Caldiarchaeum subterraneum" using the MAPLE system. *PLoS ONE* 10:e0132994. doi: 10.1371/journal.pone.0132994

ter Braak, C. J. F., and Verdonschot, P. F. M. (1995). Canonical correspondence analysis and related multivariate methods in aquatic ecology. *Aquat. Sci.* 57, 255–289. doi: 10.1007/BF00877430

Thiel, V., Wood, J. M., Olsen, M. T., Tank, M., Klatt, C. G., Ward, D. M., et al. (2016). The dark side of the mushroom spring microbial mat: life in the shadow of chlorophototrophs. I. Microbial diversity based on 16S rRNA gene amplicons and metagenomic sequencing. *Front. Microbiol.* 7:919. doi: 10.3389/fmicb.2016.00919

Tobler, D. J., and Benning, L. G. (2011). Bacterial diversity in five Icelandic geothermal waters: temperature and sinter growth rate effects. *Extremophiles* 15, 473–485. doi: 10.1007/s00792-011-0378-z

Touratier, F., Legendre, L., and Vézina, A. (1999). Model of bacterial growth influenced by substrate C:N ratio and concentration. *Aquat. Microb. Ecol.* 19, 105–118. doi: 10.3354/ame019105

Trosvik, P., and de Muinck, E. J. (2015). Ecology of bacteria in the human gastrointestinal tract–identification of keystone and foundation taxa. *Microbiome* 3:44. doi: 10.1186/s40168-015-0107-4

Urbieta, M. S., Toril, E. G., Giaveno, M. A., Bazán, Á. A., and Donati, E. R. (2014). Archaeal and bacterial diversity in five different hydrothermal ponds in the Copahue region in Argentina. *Syst. Appl. Microbiol.* 37, 429–441. doi: 10.1016/j.syapm.2014.05.012

Vázquez-Baeza, Y., Pirrung, M., Gonzalez, A., and Knight, R. (2013). EMPeror: a tool for visualizing high-throughput microbial community data. *Gigascience* 2:16. doi: 10.1186/2047-217X-2-16

Wan, X., Huang, Z., He, Z., Yu, Z., Wang, M., Davis, M. R., et al. (2015). Soil C:N ratio is the major determinant of soil microbial community structure in subtropical coniferous and broadleaf forest plantations. *Plant Soil* 387, 103–116. doi: 10.1007/s11104-014-2277-4

Wang, S., Hou, W., Dong, H., Jiang, H., Huang, L., Wu, G., et al. (2013). Control of temperature on microbial community structure in hot springs of the Tibetan Plateau. *PLoS ONE* 8:e62901. doi: 10.1371/journal.pone.0062901

Welte, C., and Deppenmeier, U. (2011). Membrane-bound electron transport in *Methanosaeta thermophila*. *J. Bacteriol.* 193, 2868–2870. doi: 10.1128/JB.00162-11

Woese, C. R., Kandler, O., and Wheelis, M. L. (1990). Towards a natural system of organisms: proposal for the domains Archaea, Bacteria, and Eucarya. *Proc. Natl. Acad. Sci. U.S.A.* 87, 4576–4579. doi: 10.1073/pnas.87.12.4576

Xu, Z., Hansen, M. A., Hansen, L. H., Jacquiod, S., and Sørensen, S. J. (2014). Bioinformatic approaches reveal metagenomic characterization of soil microbial community. *PLoS ONE* 9:e93445. doi: 10.1371/journal.pone.0093445

Youssef, N. H., Couger, M. B., McCully, A. L., Criado, A. E. G., and Elshahed, M. S. (2015). Assessing the global phylum level diversity within the bacterial domain: a review. *J. Adv. Res.* 6, 269–282. doi: 10.1016/j.jare.2014.10.005

Zhang, J., Kobert, K., Flouri, T., and Stamatakis, A. (2014). PEAR: a fast and accurate Illumina Paired-End reAd mergeR. *Bioinformatics* 30, 614–620. doi: 10.1093/bioinformatics/btt593

Zheng, B., Wang, L., and Liu, L. (2014). Bacterial community structure and its regulating factors in the intertidal sediment along the Liaodong Bay of Bohai Sea, China. *Microbiol. Res.* 169, 585–592. doi: 10.1016/j.micres.2013.09.019

Zielińska, S., Radkowski, P., Blendowska, A., Ludwig-Gałęzowska, A., Loś, J. M., and Loś, M. (2017). The choice of the DNA extraction method may influence the outcome of the soil microbial community structure analysis. *Microbiologyopen*. doi: 10.1002/mbo3.453. [Epub ahead of print].

Conflict of Interest Statement: The authors declare that the research was conducted in the absence of any commercial or financial relationships that could be construed as a potential conflict of interest.

frontiers in Microbiology

ORIGINAL RESEARCH
published: 14 July 2017
doi: 10.3389/fmicb.2017.01336

Thioarsenate Formation Coupled with Anaerobic Arsenite Oxidation by a Sulfate-Reducing Bacterium Isolated from a Hot Spring

Geng Wu[1], Liuqin Huang[1], Hongchen Jiang[1], Yue'e Peng[1], Wei Guo[1], Ziyu Chen[1], Weiyu She[1], Qinghai Guo[1] and Hailiang Dong[2,3]*

[1] State Key Laboratory of Biogeology and Environmental Geology, China University of Geosciences, Wuhan, China, [2] State Key Laboratory of Biogeology and Environmental Geology, China University of Geosciences, Beijing, China, [3] Department of Geology and Environmental Earth Science, Miami University, Oxford, OH, United States

Thioarsenates are common arsenic species in sulfidic geothermal waters, yet little is known about their biogeochemical traits. In the present study, a novel sulfate-reducing bacterial strain *Desulfotomaculum* TC-1 was isolated from a sulfidic hot spring in Tengchong geothermal area, Yunnan Province, China. The *arxA* gene, encoding anaerobic arsenite oxidase, was successfully amplified from the genome of strain TC-1, indicating it has a potential ability to oxidize arsenite under anaerobic condition. In anaerobic arsenite oxidation experiments inoculated with strain TC-1, a small amount of arsenate was detected in the beginning but became undetectable over longer time. Thioarsenates ($AsO_{4-x}S_x^{2-}$ with x = 1–4) formed with mono-, di- and tri-thioarsenates being dominant forms. Tetrathioarsenate was only detectable at the end of the experiment. These results suggest that thermophilic microbes might be involved in the formation of thioarsenates and provide a possible explanation for the widespread distribution of thioarsenates in terrestrial geothermal environments.

Keywords: thioarsenate, hot springs, anaerobic arsenite oxidation, *arxA* gene, sulfate-reducing bacterium

OPEN ACCESS

Edited by:
Robert Duran, University of Pau and Pays de l'Adour, France

Reviewed by:
Ronald Oremland, United States Geological Survey, United States
Tim McDermott, Montana State University, United States

****Correspondence:***
Hongchen Jiang
jiangh@cug.edu.cn

Specialty section:
This article was submitted to Extreme Microbiology, a section of the journal Frontiers in Microbiology

Received: *17 April 2017*
Accepted: *30 June 2017*
Published: *14 July 2017*

Citation:
Wu G, Huang L, Jiang H, Peng Y, Guo W, Chen Z, She W, Guo Q and Dong H (2017) Thioarsenate Formation Coupled with Anaerobic Arsenite Oxidation by a Sulfate-Reducing Bacterium Isolated from a Hot Spring. Front. Microbiol. 8:1336. doi: 10.3389/fmicb.2017.01336

INTRODUCTION

High concentrations of arsenic have been reported in global terrestrial hot springs (McKenzie et al., 2001; Cleverley et al., 2003; Aiuppa et al., 2006; Pascua et al., 2007; Landrum et al., 2009; McCleskey et al., 2010). Traditionally, the predominant form of inorganic arsenic in aqueous environments is arsenate [As(V) as $H_2AsO_4^-$ and $HAsO_4^{2-}$] and arsenite [As(III) as $H_3AsO_3^0$ and $H_2AsO_3^-$] in oxic and anoxic environments, respectively (Oremland, 2003). However, recently pentavalent arsenic-sulfur species, so-called thioarsenates ($AsO_{4-x}S_x^{2-}$ with x = 1–4), have also been reported as important arsenic species in a number of sulfidic geothermal environments (Wilkin et al., 2003; Stauder et al., 2005; Planer-Friedrich et al., 2007, 2009; Härtig and Planer-Friedrich, 2012; Hug et al., 2014). For example, Hug et al. (2014) found that di- (x = 2) and tri-thioarsenates (x = 3) represented up to 25% of total arsenic in an acidic-sulfidic hot spring in New Zealand. Keller et al. (2014) investigated the arsenic speciation in natural alkaline-sulfidic geothermal waters (pH 8.56–9.60) and found that sulfide concentration and pH are the predominant factors determining the arsenic species distribution.

Extensive studies have shown that microbial activities can strongly influence the speciation and mobility of arsenic in natural environments through arsenic oxidation and reduction (Oremland et al., 2005; Paez-Espino et al., 2009). Most (if not all) of known arsenite-oxidizing microorganisms contain arsenite oxidases, which catalyze the transformation of arsenite [As(III)] to arsenate [As(V)] (Lett et al., 2012). The arsenite oxidases are encoded by *aioA* and *arxA* genes for aerobic and anaerobic arsenite-oxidizing bacteria, respectively. Thus the *aioA* and *arxA* genes have become molecular biomarkers to study the distribution and activity of arsenite-oxidizing bacteria in natural environments (Hamamura et al., 2009, 2010, 2014; Zargar et al., 2012; Engel et al., 2013; Jiang et al., 2014; Wu et al., 2015; Hernandez-Maldonado et al., 2016). Recently, it is speculated that filamentous microbial mats might play an important role in thioarsenate transformation in an alkaline, sulfidic hot spring in Yellowstone National Park, which is the first evidence showing microbially mediated thioarsenate species transformation by (hyper) thermophilic prokaryotes (Härtig and Planer-Friedrich, 2012). A subsequent investigation showed that the thermophilic microbial mats were mainly composed of *Aquificales* represented by *Thermocrinis* spp. and *Sulfurihydrogenibium* spp. (Planer-Friedrich et al., 2015). However, little is known about which microbial group was involved in the observed thioarsenate species transformation. In addition, one geochemical study on arsenic speciation in the Tengchong geothermal zone (TGZ) of Yunnan Province, China reported that thioarsenates are widely distributed in the high-sulfidic Tengchong hot springs (Guo et al., 2017). Thus, the TGZ hot springs are suitable sites for retrieving microorganisms potentially involved in thioarsenates transformation.

In the present study, we provided biological evidence on the potential involvement of a novel sulfate-reducing bacterium isolated from a TGZ hot spring, designated as *Desulfotomaculum* sp. TC-1, in the formation of thioarsenates. The strain TC-1 cells coupled sulfate reduction with arsenite oxidation, in which thioarsenates, instead of arsenate, were the main products. The results in this study suggested that microbial activities may be involved in the formation of thioarsenates in geothermal features and thus could explain the reported distribution of thioarsenates in sulfidic hot springs.

MATERIALS AND METHODS

Site Description and Sample Collection

The TGZ is located at the collision boundary between the Indian and Eurasian plates. The TGZ is known for its various geothermal features, which contains more than 800 hot springs (Du et al., 2005; Guo and Wang, 2012). Previous studies have shown that Tengchong hot springs host very diverse microbial communities (Hedlund et al., 2012; Hou et al., 2013; Song et al., 2013a; Briggs et al., 2014), which play important roles in the elemental cycling (e.g., carbon, nitrogen, sulfur) and arsenic transformation (Jiang et al., 2010, 2014; Song et al., 2013b; Li et al., 2015; Wu et al., 2015; Yang et al., 2015; Chen et al., 2016). A hot spring (N24.95318°; E98.43838°) was found downstream of the Dagunguo (DGG) spring in the Rehai Geothermal National Park in the TGZ and was therefore named Dagunguo-2 (DGG-2) (**Supplementary Figure S1**) (Guo et al., 2017). In June 2014, water temperature and pH were measured in the field with a portable meter (LaMotte, Chestertown, MD, United States). Water chemistry (S^{2-}, Fe^{2+}, NO_2^- and NH_4^+) measurements were performed by using Hach kits (Hach Company, Loveland, CO, United States). Sediment samples of the sampled hot spring were aseptically collected for cultivation.

Enrichment and Isolation of Thermophilic Sulfate Reducing Bacteria

Hungate techniques were used for enrichment and isolation. The hot spring sediment samples were transferred into 25 mL Balch tubes containing 5 mL DSMZ medium 63, which was pre-prepared anaerobically with the headspace filled with 100% N_2 gas. *In situ* enrichments (by putting the culture tubes in the hot spring) were incubated for 48 h and then the resulting enrichment cultures were transported to laboratory for further isolation and purification. To avoid light effects, the balch tubes were covered with foil *in situ* and *ex situ* during incubation. Inoculation, sampling, and isolation were performed in an anaerobic glove box (COY Laboratory Products, Grass Lake, MI, United States) with aseptic techniques (The gas chamber was filled with 100% N_2). The incubation temperature was 60°C. Cultures with positive growth (as indicated by the formation of black ferrous iron sulfide) were transferred three times for further purification. Isolation was performed by using the rolling-tube method with a high-melting-point agar, GELRITE gellan gum (Sigma) (Hungate and Macy, 1973).

SEM Observation

The morphology of strain TC-1 cells was examined with a Zeiss Supra 55 SAPPHIRE scanning electron microscope (SEM) using 7–10 keV accelerating voltage and 8.5 mm working distance. SEM sample preparation and observation were performed according to previously described methods (Zhao et al., 2013, 2015).

Phylogenetic Analysis of Strain TC-1

Total DNA of strain TC-1 was extracted with Bacterial DNA extraction kit (ABigen, Hangzhou, China) according to manufacturer's protocol. The 16S rRNA and *arxA* genes were amplified with the primer sets of Bac27F/Univ1492R and arxA_Deg_F_B (5′-CCA TCW SCT GGR ACG AGG CCY TSG-3′)/arxA_Deg_R_B (5′-GTW GTT GTA GGG GCG GAA S-3′) (Zargar et al., 2012), respectively. PCR amplification, sequencing, and phylogenetic analysis of the 16S rRNA and *arxA* genes were performed as previously described (Weisburg et al., 1991; Zargar et al., 2010, 2012). The *arxA* and 16S rRNA gene sequences of strain TC-1 were deposited in the GenBank under accession numbers of KX242336 and KX242337, respectively.

Test for Arsenite Oxidation of Strain TC-1

Strain TC-1 was grown at 60°C in anoxic DSMZ 63 medium (1 L) made of solution A [K_2HPO_4 0.5 g; NH_4Cl,1.0 g; Na_2SO_4,1.0 g; $CaCl_2 \times 2\ H_2O$, 0.1 g; $MgSO_4 \times 7\ H_2O$, 2.0 g; Na-DL-lactate,

2.0 g; yeast extract, 1.0 g; Na-resazurin solution (0.1% w/v), 0.5 ml; distilled water, 980.0 ml], solution B ($FeSO_4 \times 7\ H_2O$, 0.5 g; Distilled water, 10.0 ml) and solution C (ascorbic acid, 0.1 g; distilled water, 10.0 ml). The initial pH was 6.8, and pH varied less than 0.2 units during growth. To remove oxygen, the growth medium was boiled for >10 min, purged with N_2 upon cooling and immediately transferred into an anoxic chamber (100% N_2) for dispensing into glass serum bottles, which were subsequently sealed with thick butyl rubber stoppers. The sets of experiments were inoculated with TC-1 in DSMZ 63 medium with solution B replaced by 0.5 mM arsenite; Two types of abiotic controls were set up: one was in the DSMZ 63 medium with solution B replaced by 5 mM sulfide ($Na_2S{\cdot}9\ H_2O$, Sigma–Aldrich) and 0.5 mM arsenite (Sigma–Aldrich), and the other was in the DSMZ 63 medium with solution B replaced by 5 mM sulfide and 0.5 mM arsenate (Sigma–Aldrich). All experimental treatments were performed in triplicate. Liquid sampling for arsenic measurement was performed with aseptic syringes in an anaerobic chamber according to a previous method (Planer-Friedrich et al., 2015).

Arsenic Speciation Measurement for Total Arsenic, As (III) and As(V)

Total arsenic concentration and arsenic speciation (arsenite and arsenate) were measured according to previously described methods (Wu et al., 2015). Briefly, total arsenic concentration was measured with inductively coupled plasma atomic emission spectroscopy (ICP-AES) (iCAP ICP Spectrometer, Thermo Fisher Scientific, United States) with argon torch and iTeva software (Thermo Fisher Scientific, United States). Arsenic speciation (arsenite and arsenate) was determined with high performance liquid chromatography (HPLC)-atomic fluorescence spectroscopy (AFS). If the sum of measured As(III) and As (V) was not equal to total arsenic, those samples were oxidized by H_2O_2, in which As(III) and Thio-arsenate will be transferred to As(V) (Pettine et al., 1999), and then were measured for total As by ICP-AES.

Characterization of Thioarsenic Species with Liquid Chromatography-High Resolution Mass Spectrometry (LC-HRMS)

The relative abundances of four major thioarsenic species in the samples, including H_3AsSO_3, $H_3AsS_2O_2$, H_3AsS_3O and H_3AsS_4, were identified by injecting a liquid sample (5 μL) into a liquid chromatography-high resolution mass spectrometry (LC-HRMS, Q Exactive, Thermo Scientific, Germany) according to previously described methods (Chang et al., 2015; Yang et al., 2016). The mobile phase contained 50% acetonitrile (v/v) and 0.1% acetic acid (m/v) with a flow rate of 0.25 mL min^{-1}. The mass spectrometer system was operated with a heated electrospray ionization (HESI) source in a negative ion mode with a spray voltage of −3.2 kV, an S-lens RF level of 50%, a capillary temperature of 300°C, and a mass resolution of 70,000. The runtime was 2 min for each sample. The mass tolerance of the Precursor ion was below 5 ppm. Mass spectra were processed by using the Xcalibur 2.1 software (Thermo Scientific). The relative abundance of each thioarsenic species was calculated according to their corresponding chromatographic peak area.

RESULTS

Water Chemistry of the Dagunguo-2 Hot Spring

The pH and temperature of the Dagunguo-2 hot spring were 5.5 and 58.3°C, respectively. The spring water contained S^{2-} (1.53 μM), Fe^{2+} (5 μM), NO_2^- (0.065 μM), and NH_4^+ (37.8 μM).

Isolate Identification and Physiological Characterization

One strain was obtained and designated as strain TC-1 (**Supplementary Figure S2**). Phylogenetic analysis on the basis of 16S rRNA gene sequence identified strain TC-1as a close (sequence identity: 99.7%) relative of a sulfate-reducing bacterium *Desulfotomaculum carboxydivorans* CO-1-SRB, which was isolated from a sludge of an anaerobic bioreactor treating paper mill wastewater (Pettine et al., 1999) (see **Figure 1A** and **Table 1**). The *arxA* gene of strain TC-1 was successfully amplified and was closely related (sequence identity: 99%) to those recovered from Tukh Lake (represented by HJ1A27 in **Figure 1B**). The morphology of *Desulfotomaculum* TC-1 cells was rod-shaped with rounded ends, 0.8–1.5 μm in length and 0.2–0.4 μm in width (**Supplementary Figure S2**). The optimum growth temperature and pH for TC-1 were 60°C and 6.8, respectively. The optimum growth temperature was consistent with the environmental condition of the spring where the TC-1 strain was isolated (57°C). Under optimum conditions, the doubling time of strain TC-1 was approximately 30 h. Strain TC-1 cannot grow on As(III) in the DSMZ 63 medium (without lactate).

Variations of Total Arsenic, Arsenite and Arsenate during Arsenite Oxidation by Strain TC-1

Arsenic speciation was examined for 84 h after inoculation with strain TC-1 (**Figure 2**). Arsenite (0.5 mM) was nearly exhausted in 60 h. As arsenite was consumed, some amount of arsenate was initially detected after 24 h (**Figure 2**). After 60 h, both arsenite and arsenate were not detectable in the experimental tubes, but the total arsenic in the solution remained unchanged, indicating no formation of insoluble arsenic precipitates. In the abiotic control containing Na_2S and arsenite, white flocs formed in solution immediately. The resulting white flocs were separated by high speed centrifugation (12,000 rpm), and then were observed by SEM-EDS for element mapping. The results showed that arsenite could react with Na_2S to form the flocs which contained S and As (**Supplementary Figure S3**). The resulted supernatant was treated with H_2O_2 followed by ICP-AES measurement, but no arsenic was detected (data not shown).

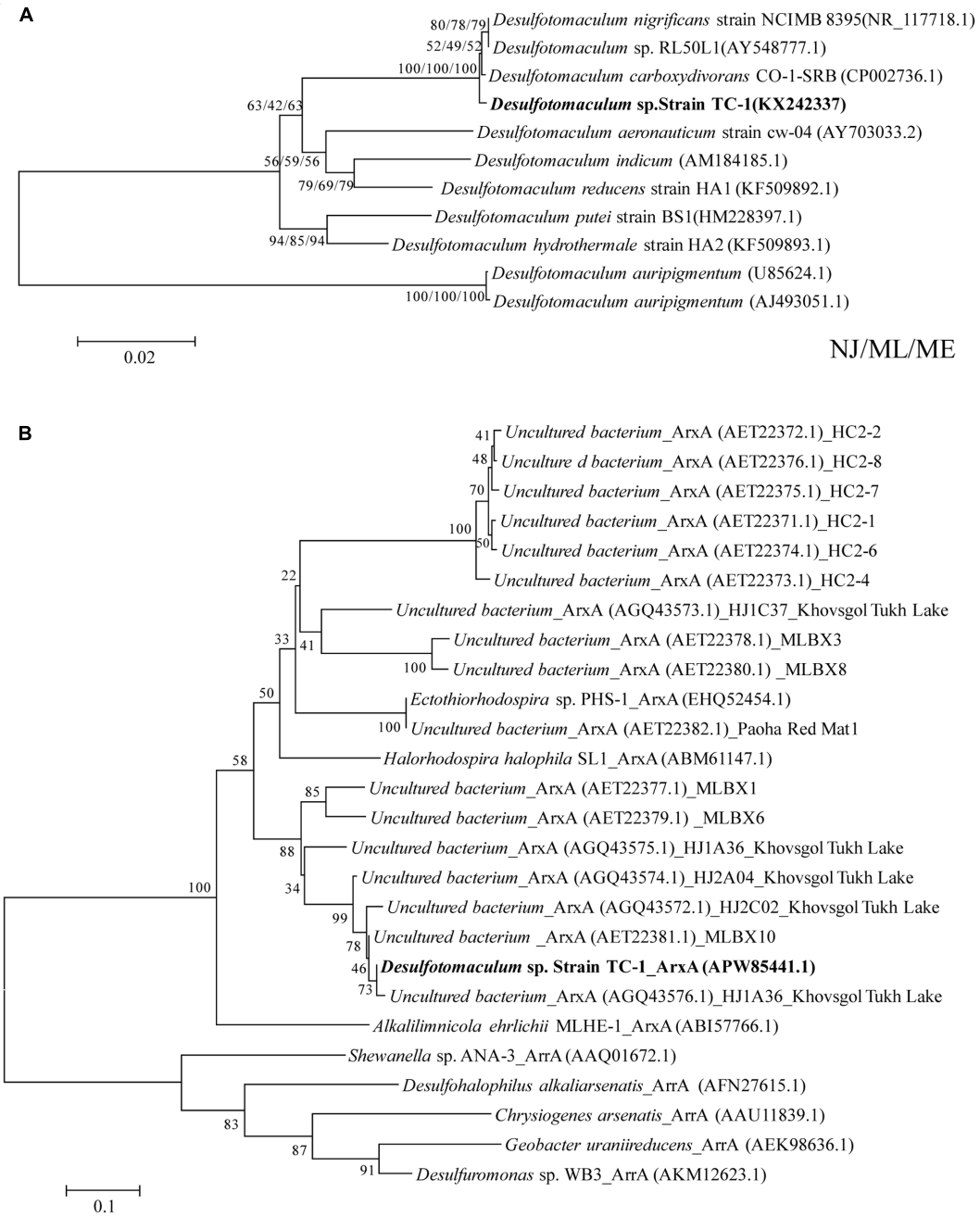

FIGURE 1 | Phylogenetic trees of 16S rRNA **(A)** and the deduced amino acid sequences of *ArxA* **(B)** encoded by *arxA* genes of strain TC-1 showing their relatedness to its close relatives in the GenBank. The GenBank accession numbers are listed in parentheses. Bootstrap values (per 1000 trials) > 50% are indicated. NJ/ML/ME indicates Neighbor-Joining/Maximum Likelihood/Minimum-Evolution algorithms.

Variation of Thioarsenic Species Formed during Arsenite Oxidation by Strain TC-1

The LC-HRMS analysis showed that the missing arsenite had been transformed to thioarsenic species (mono-thioarsenate $[HAsSO_3]^{2-}$, di-thioarsenate $[HAs^{V}S_2O_2]^{2-}$, tri-thioarsenate $[HAsS_3O]^{2-}$ and tetra-thioarsenate $[HAsS_4]^{2-}$) (**Figure 3**), and the relative concentrations of each identified thioarsenic species varied during the oxidation process: In the first 60 h, monothioarsenate, di-thioarsenate and tri-thioarsenate were dominant species in the solution, while no tetra-thioarsenate was detected. As arsenite oxidation experiment proceeded, a small amount of tetra-thioarsenate was detected at 84 h (at the end of the experiment) (**Figure 3**). In the abiotic control containing Na_2S and arsenate, only a tiny amount of di-thioarsenate was

TABLE 1 | Physiological, phylogenetic and phenotypic comparisons between strain TC-1 and known *arxA* gene-containing strains.

Strain name	Temperature (°C)	Species	Isolation source	Reference
Desulfotomaculum TC-1	60	*Firmicutes*	A hot spring of Tengchong, China	The present study
Alkalilimnicola ehrlichii str. MLHE-1	20	*Proteobacteria*	Water column of Mono Lake, CA, United States	Oremland et al., 2002; Zargar et al., 2010, 2012
Ectothiorhodospira strain PHS-1	43	*Proteobacteria*	A hot spring in Paoha Island of Mono Lake, CA, United States	Kulp et al., 2008
Halorhodospira halophila SL1	20	*Proteobacteria*	Summer Lake, OR, United States	Challacombe et al., 2013
Halomonas sp. ANAO-440	20	*Proteobacteria*	An alkaline saline lake in Mongolia	Hamamura et al., 2014

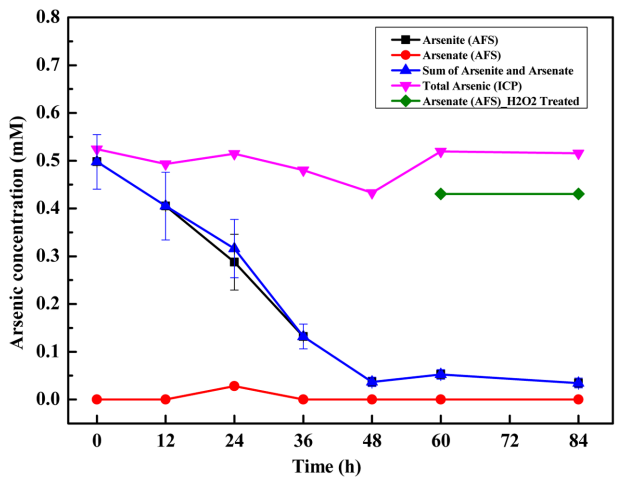

FIGURE 2 | Time-course variations of arsenite and arsenate concentrations and total arsenic concentration during anaerobic arsenite oxidation by strain TC-1. Triplicate samples were performed, and error bars were smaller than the sizes of the symbols.

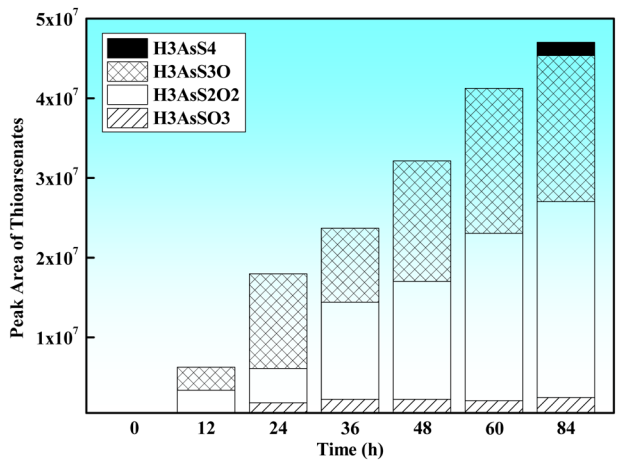

FIGURE 3 | Time-course variation of thioarsenate composition (expressed as the corresponding chromatographic peak area of each identified thioarsenic species) produced during anaerobic arsenite oxidation by strain TC-1.

observed, but other thioarsenic species (i.e., monothioarsenate, tri-thioarsenate, and tetra-thioarsenate) were not detected.

DISCUSSION

Anaerobic Arsenite Oxidation in Hot Springs

High levels of arsenic has been extensively reported in global terrestrial hot springs. Thus, terrestrial hot springs are an excellent setting for investigating arsenic biogeochemical cycling (Qin et al., 2009). In geothermal environments, microbially mediated aerobic arsenite oxidation has been frequently reported (Oremland, 2003), while few studies up to date discovered anaerobic arsenite oxidation by microbes. For example, Rhine et al. (2006) reported anaerobic arsenite oxidation phenomenon by novel denitrifying isolates from an arsenic contaminated industrial soil, while no function genes related to anaerobic arsenite oxidation were amplified; Zhao et al. (2015) reported anaerobic arsenite oxidation by an autotrophic arsenite-oxidizing bacterium from an arsenic-contaminated paddy soil and *aioA* gene was successfully amplified from those pure cultures, although the *aioA* gene is putatively involved in aerobic arsenic oxidation (Lett et al., 2012). Zargar et al. (2010) identified a novel arsenite oxidase gene, *arxA*, from *Alkalilimnicola ehrlichii* strain MLHE-1, an anaerobic arsenite-oxidizing bacterium from Mono Lake. However, little is reported on anaerobic arsenite oxidation by microbes in geothermal features. To our best knowledge, the only case of microbially mediated anaerobic arsenite oxidation in hot springs was reported in a hot spring (temperature 43°C) biofilm on the shore of the Paoha Island in Mono Lake (Kulp et al., 2008), which showed anaerobic photosynthetic arsenic(III) oxidation by strain *Ectothiorhodospira* strain PHS-1. However, in the present study, strain TC-1 can anaerobically oxidize arsenite at high temperature (60°C) independent of light or photosynthesis, indicating that photosynthesis-independent, microbially mediated anaerobic arsenic oxidation could take place in geothermal features.

To our best knowledge, strain TC-1 is the first known sulfate-reducing strain containing *arxA* gene. To date, only four other known *arxA* gene-containing strains have been obtained in pure cultures (**Table 1**) and they all fall within α-*Proteobacteria*, among which *A. ehrlichii* MLHE-1, *Halorhodospira halophila* SL1, and *Halomonas* sp. ANAO-440 were isolated from alkaline and/or saline environments, while *Ectothiorhodospira* strain PHS-1 was retrieved from a geothermal feature (temperature 43°C) (Oremland et al., 2002; Kulp et al., 2008; Zargar et al., 2010, 2012; Challacombe et al., 2013; Hamamura et al., 2014;

Hernandez-Maldonado et al., 2016). In contrast, strain TC-1 belongs to *Firmicutes* and is the only known strain within *Firmicutes* possessing the *arxA* gene. The affiliation of strain TC-1 with *Firmicutes* indicated that the microbes involved in anaerobic arsenic oxidation may be more phylogenetically diverse than currently known. It is possible that the *arxA* gene of strain TC-1 might have originated from other microbes via horizontal gene transfer as in strain PHS-1 (Zargar et al., 2012).

Formation of Thioarsenate under Anaerobic Conditions in Hot Springs

It is notable that thioarsenates could be formed by sulfate reducing bacteria under anaerobic conditions in hot springs. Previous work on arsenic speciation in geothermal environments reported the dominance of As(III) and As(V) in the bulk arsenic speciation (Ballantyne and Moore, 1988; Yokoyama et al., 1993; Macur et al., 2004). While studies with improved sample preservation techniques revealed that thioarsenate species were present or even abundant in geothermal features (Wilkin et al., 2003; Stauder et al., 2005; Planer-Friedrich et al., 2007; Wallschläger and Stadey, 2007; Guo et al., 2017), which can possibly make up to more than 50% of total dissolved arsenic in sulfidic waters (Wilkin et al., 2003; Hug et al., 2014). Most (if not all) of the geothermal features with reported high thioarsenates were sulfidic. The potential underlying reason for the formation of thioarsenates could be explained by the following equation:

$$[HAs^{V}O_4]^{2-} + [HS]^{-} \rightarrow [HAs^{V}S^{-II}{}_{x}O_{4-x}]^{2-} + [OH]^{-},$$

in which arsenate reacted with sulfide, leading to the formation of thioarsenate (Planer-Friedrich et al., 2015). The reactant arsenate could be extant or derived from arsenite oxidation. Commonly anoxic condition dominates sulfidic habitats, thus anaerobic arsenite oxidation could take place to produce arsenate. In the present study, strain TC-1 could oxidize As(III) to As(V), which reacted with S^{2-} or HS^{-} and thus formed thioarsenate species. This reaction could also explain the wide distribution of thioarsenates in sulfidic aquifers (Wood et al., 2002; Wilkin et al., 2003; Bostick et al., 2005; Hollibaugh et al., 2005; Stauder et al., 2005; Wallschläger and Stadey, 2007), although no exact reasons were provided for the predominance of thioarsenates in those previous studies. The present study provides evidence for possible microbial involvement in the formation of thioarsenates in hot springs.

Environmental Implication of Thioarsenate Formed by Sulfate Reducing Bacteria

Thioarsenate may be an important arsenic species in sulfidic and arsenic-rich environments (Hollibaugh et al., 2005; Hug et al., 2014; Guo et al., 2017). Based on the results presented above, high arsenic geological settings (e.g., groundwater and acid mine drainage that have the potential of sulfate reducing process) may contain significant amounts of thioarsenates, which to date have received little attention. Thioarsenates are more toxic than arsenate and tri-thioarsenate is almost as bioavailable and toxic as arsenite (Hinrichsen et al., 2015). Thus more attention should be paid to thioarsenates in high arsenic, sulfidic habitats. Previous studies have shown that arsenic in solution could be removed through combination with sulfide minerals derived from microbial SO_4^{2-} reduction (Moore et al., 1988; Rittle et al., 1995; Kirk et al., 2004), and that the enhanced SO_4^{2-} reduction may be useful for arsenic remediation (Rittle et al., 1995; Newman et al., 1997; Castro et al., 1999; Macy et al., 2000; Jong and Parry, 2003; Lee et al., 2005; Saunders et al., 2005; Keimowitz et al., 2007; Saunders et al., 2008; Kirk et al., 2010; Luo et al., 2013). However, recently an experiment with permeable reactive barriers (PRB) was performed to test the effect of arsenic remediation in the presence microbial sulfate reduction, and found that up to 47% of total As initially present in the sediment was leached out in the form of mobile thio-As species (Kumar et al., 2016). Thus, more cautions should be taken on the geochemical behaviors of arsenic and sulfate in the environment (where the arsenite and arsenate have the potential to transform to mobile thioarsenates) when sulfate reducing bacteria are employed for arsenic remediation (Burton et al., 2014; Stucker et al., 2014).

AUTHOR CONTRIBUTIONS

GW and HJ conceived and designed the experiments. LH and ZC isolated the strain. GW, YP, WG, HD, WS, and QG performed the experiments. GW analyzed the data. All of the authors assisted in writing the manuscript, discussed the results and commented on the manuscript.

ACKNOWLEDGMENTS

This work was supported by the National Natural Science Foundation of China grants (41502318, 41422208, 41521001, 41572335, 41630103), the Key Project of International Cooperation of China Ministry of Science and Technology (No. 2013DFA31980), and Special Foundation for Basic Research Program of China Ministry of Science and Technology (MOST) (No. 2015FY110100), and the Fundamental Research Funds for the Central Universities, China University of Geosciences (Wuhan) (No.CUGL170215).

SUPPLEMENTARY MATERIAL

The Supplementary Material for this article can be found online at: http://journal.frontiersin.org/article/10.3389/fmicb.2017.01336/full#supplementary-material

FIGURE S1 | The location **(A)** and geothermal features **(B)** of DGG-2 in the Rehai Geothermal Field, Tengchong, Yunnan, China.

FIGURE S2 | Scanning electron microscope images of strain *Desulfotomaculum* sp. TC-1 cells (Scale bar = 1 μm).

FIGURE S3 | Scanning electron microscope images of flocs and the S-As distribution in floc as indicated by the yellow line in **(A)**. **(A–C)** Indicate the SEM morphology of the flocs and the EDX multi element mapping/line scanning spectra for As (arsenic) and S (sulfur) elements, respectively.

REFERENCES

Aiuppa, A., Avino, R., Brusca, L., Caliro, S., Chiodini, G., D'alessandro, W., et al. (2006). Mineral control of arsenic content in thermal waters from volcano-hosted hydrothermal systems: insights from island of Ischia and Phlegrean Fields (Campanian Volcanic Province, Italy). *Chem. Geol.* 229, 313–330. doi: 10.1016/j.chemgeo.2005.11.004

Ballantyne, J. M., and Moore, J. N. (1988). Arsenic geochemistry in geothermal systems. *Geochim. Cosmochim. Acta* 52, 475–483. doi: 10.1016/0016-7037(88)90102-0

Bostick, B., Fendorf, S., and Brown, G. (2005). *In situ* analysis of thioarsenite complexes in neutral to alkaline arsenic sulphide solutions. *Mineral. Mag.* 69, 781–795. doi: 10.1180/0026461056950288

Briggs, B. R., Brodie, E. L., Tom, L. M., Dong, H., Jiang, H., Huang, Q., et al. (2014). Seasonal patterns in microbial communities inhabiting the hot springs of Tengchong, Yunnan Province, China. *Environ. Microbiol.* 16, 1579–1591. doi: 10.1111/1462-2920.12311

Burton, E. D., Johnston, S. G., and Kocar, B. D. (2014). Arsenic mobility during flooding of contaminated soil: the effect of microbial sulfate reduction. *Environ. Sci. Technol.* 48, 13660–13667. doi: 10.1021/es503963k

Castro, J. M., Wielinga, B. W., Gannon, J. E., and Moore, J. N. (1999). Stimulation of sulfate-reducing bacteria in lake water from a former open-pit mine through addition of organic wastes. *Water Environ. Res.* 71, 218–223. doi: 10.2175/106143098X121806

Challacombe, J. F., Majid, S., Deole, R., Brettin, T. S., Bruce, D., Delano, S. F., et al. (2013). Complete genome sequence of *Halorhodospira halophila* SL1. *Stand. Genomic Sci.* 8, 206–214. doi: 10.4056/sigs.3677284

Chang, Q., Peng, Y. E., Dan, C., Shuai, Q., and Hu, S. (2015). Rapid in situ identification of bioactive compounds in plants by in vivo nanospray high-resolution mass spectrometry. *J. Agric. Food Chem.* 63, 2911–2918. doi: 10.1021/jf505749n

Chen, S., Peng, X., Xu, H., and Ta, K. (2016). Nitrification of archaeal ammonia oxidizers in a high-temperature hot spring. *Biogeosciences* 13, 2051–2060. doi: 10.5194/bg-13-2051-2016

Cleverley, J. S., Benning, L. G., and Mountain, B. W. (2003). Reaction path modelling in the As–S system: a case study for geothermal As transport. *Appl. Geochem.* 18, 1325–1345. doi: 10.1016/S0883-2927(03)00054-4

Du, J., Liu, C., Fu, B., Ninomiya, Y., Zhang, Y., Wang, C., et al. (2005). Variations of geothermometry and chemical-isotopic compositions of hot spring fluids in the Rehai geothermal field, southwestern China. *J. Volcanol. Geotherm. Res.* 142, 243–261. doi: 10.1016/j.jvolgeores.2004.11.009

Engel, A. S., Johnson, L. R., and Porter, M. L. (2013). Arsenite oxidase gene diversity among *Chloroflexi* and *Proteobacteria* from El Tatio Geyser Field, Chile. *FEMS Microbiol. Ecol.* 83, 745–756. doi: 10.1111/1574-6941.12030

Guo, Q., Planer-Friedrich, B., Liu, M., Li, J., Zhou, C., and Wang, Y. (2017). Arsenic and thioarsenic species in the hot springs of the Rehai magmatic geothermal system, Tengchong volcanic region, China. *Chem. Geol.* 453, 12–20. doi: 10.1016/j.chemgeo.2017.02.010

Guo, Q., and Wang, Y. (2012). Geochemistry of hot springs in the Tengchong hydrothermal areas, Southwestern China. *J. Volcanol. Geotherm. Res.* 215, 61–73. doi: 10.1016/j.jvolgeores.2011.12.003

Hamamura, N., Itai, T., Liu, Y., Reysenbach, A. L., Damdinsuren, N., and Inskeep, W. P. (2014). Identification of anaerobic arsenite-oxidizing and arsenate-reducing bacteria associated with an alkaline saline lake in Khovsgol, Mongolia. *Environ. Microbiol. Rep.* 6, 476–482. doi: 10.1111/1758-2229.12144

Hamamura, N., Macur, R., Korf, S., Ackerman, G., Taylor, W., Kozubal, M., et al. (2009). Linking microbial oxidation of arsenic with detection and phylogenetic analysis of arsenite oxidase genes in diverse geothermal environments. *Environ. Microbiol.* 11, 421–431. doi: 10.1111/j.1462-2920.2008.01781.x

Hamamura, N., Macur, R. E., Liu, Y., Inskeep, W. P., and Reysenbach, A.-L. (eds). (2010). "Distribution of Aerobic Arsenite Oxidase Genes within the *Aquificales*," *Interdisciplinary Studies on Environmental Chemistry—Biological Responses to Contaminants*, (Tokyo: TERRAPUB), 47–55.

Härtig, C., and Planer-Friedrich, B. (2012). Thioarsenate transformation by filamentous microbial mats thriving in an alkaline, sulfidic hot spring. *Environ. Sci. Technol.* 46, 4348–4356. doi: 10.1021/es4015458

Hedlund, B. P., Cole, J. K., Williams, A. J., Hou, W., Zhou, E., Li, W., et al. (2012). A review of the microbiology of the Rehai geothermal field in Tengchong, Yunnan Province, China. *Geosci. Front.* 3, 273–288. doi: 10.1016/j.gsf.2011.12.006

Hernandez-Maldonado, J., Sanchez-Sedillo, B., Stoneburner, B., Boren, A., Miller, L. G., Mccann, S., et al. (2016). The genetic basis of anoxygenic photosynthetic arsenite oxidation. *Environ. Microbiol.* 19, 130–141. doi: 10.1111/1462-2920.13509

Hinrichsen, S., Geist, F., and Planer-Friedrich, B. (2015). Inorganic and methylated thioarsenates pass the gastrointestinal barrier. *Chem. Res. Toxicol.* 28, 1678–1680. doi: 10.1021/acs.chemrestox.5b00268

Hollibaugh, J. T., Carini, S., Gürleyük, H., Jellison, R., Joye, S. B., Lecleir, G., et al. (2005). Arsenic speciation in Mono Lake, California: response to seasonal stratification and anoxia. *Geochim. Cosmochim. Acta* 69, 1925–1937. doi: 10.1016/j.gca.2004.10.011

Hou, W., Wang, S., Dong, H., Jiang, H., Briggs, B. R., Peacock, J. P., et al. (2013). A comprehensive census of microbial diversity in hot springs of Tengchong, Yunnan Province China using 16S rRNA gene pyrosequencing. *PLoS ONE* 8:e53350. doi: 10.1371/journal.pone.0053350

Hug, K., Maher, W. A., Stott, M. B., Krikowa, F., Foster, S., and Moreau, J. W. (2014). Microbial contributions to coupled arsenic and sulfur cycling in the acid-sulfide hot spring Champagne Pool, New Zealand. *Front. Microbiol.* 5:569. doi: 10.3389/fmicb.2014.00569

Hungate, R., and Macy, J. (1973). The roll-tube method for cultivation of strict anaerobes. *Bull. Ecol. Res. Comm.* 17, 123–126.

Jiang, H., Huang, Q., Dong, H., Wang, P., Wang, F., Li, W., et al. (2010). RNA-based investigation of ammonia-oxidizing archaea in hot springs of Yunnan Province, China. *Appl. Environ. Microbiol.* 76, 4538–4541. doi: 10.1128/AEM.00143-10

Jiang, Z., Li, P., Jiang, D., Wu, G., Dong, H., Wang, Y., et al. (2014). Diversity and abundance of the arsenite oxidase gene *aioA* in geothermal areas of Tengchong, Yunnan, China. *Extremophiles* 18, 161–170. doi: 10.1007/s00792-013-0608-7

Jong, T., and Parry, D. L. (2003). Removal of sulfate and heavy metals by sulfate reducing bacteria in short-term bench scale upflow anaerobic packed bed reactor runs. *Water Res.* 37, 3379–3389. doi: 10.1016/S0043-1354(03)00165-9

Keimowitz, A., Mailloux, B., Cole, P., Stute, M., Simpson, H., and Chillrud, S. (2007). Laboratory investigations of enhanced sulfate reduction as a groundwater arsenic remediation strategy. *Environ. Sci. Technol.* 41, 6718–6724. doi: 10.1021/es061957q

Keller, N. S., Stefánsson, A., and Sigfússon, B. (2014). Arsenic speciation in natural sulfidic geothermal waters. *Geochim. Cosmochim. Acta* 142, 15–26. doi: 10.1016/j.gca.2014.08.007

Kirk, M. F., Holm, T. R., Park, J., Jin, Q., Sanford, R. A., Fouke, B. W., et al. (2004). Bacterial sulfate reduction limits natural arsenic contamination in groundwater. *Geology* 32, 953–956. doi: 10.1130/G20842.1

Kirk, M. F., Roden, E. E., Crossey, L. J., Brealey, A. J., and Spilde, M. N. (2010). Experimental analysis of arsenic precipitation during microbial sulfate and iron reduction in model aquifer sediment reactors. *Geochim. Cosmochim. Acta* 74, 2538–2555. doi: 10.1016/j.gca.2010.02.002

Kulp, T. R., Hoeft, S. E., Asao, M., Madigan, M. T., Hollibaugh, J. T., Fisher, J. C., et al. (2008). Arsenic(III) fuels anoxygenic photosynthesis in hot spring biofilms from Mono Lake, California. *Science* 321, 967–970. doi: 10.1126/science.1160799

Kumar, N., Couture, R.-M., Millot, R., Battaglia-Brunet, F., and Rose, J. (2016). Microbial sulfate reduction enhances arsenic mobility downstream of zerovalent-iron-based Permeable Reactive Barrier. *Environ. Sci. Technol.* 50, 7610–7617. doi: 10.1021/acs.est.6b00128

Landrum, J., Bennett, P., Engel, A., Alsina, M., Pastén, P., and Milliken, K. (2009). Partitioning geochemistry of arsenic and antimony, El Tatio Geyser Field, Chile. *Appl. Geochem.* 24, 664–676. doi: 10.1016/j.apgeochem.2008.12.024

Lee, M., Saunders, J. A., Wilkin, R. T., and Mohammad, S. (2005). "Geochemical modeling of arsenic speciation and mobilization: implications for bioremediation," in *Advances in Arsenic Research: Integration of Experimental and Observational Studies and Implications for Mitigation*, ed. P. A. O'Day (Washington, DC: American Chemical Society), 398–413.

Lett, M. C., Muller, D., Lievremont, D., Silver, S., and Santini, J. (2012). Unified nomenclature for genes involved in prokaryotic aerobic arsenite oxidation. *J. Bacteriol.* 194, 207–208. doi: 10.1128/JB.06391-11

Li, H., Yang, Q., Li, J., Gao, H., Li, P., and Zhou, H. (2015). The impact of temperature on microbial diversity and AOA activity in the Tengchong Geothermal Field, China. *Sci. Rep*. 5:17056. doi: 10.1038/srep17056

Luo, T., Tian, H., Guo, Z., Zhuang, G., and Jing, C. (2013). Fate of arsenate adsorbed on nano-TiO2 in the presence of sulfate reducing bacteria. *Environ. Sci. Technol.* 47, 10939–10946. doi: 10.1021/es400883c

Macur, R. E., Langner, H. W., Kocar, B. D., and Inskeep, W. P. (2004). Linking geochemical processes with microbial community analysis: successional dynamics in an arsenic-rich, acid-sulphate-chloride geothermal spring. *Geobiology* 2, 163–177. doi: 10.1111/j.1472-4677.2004.00032.x

Macy, J. M., Santini, J. M., Pauling, B. V., O'neill, A. H., and Sly, L. I. (2000). Two new arsenate/sulfate-reducing bacteria: mechanisms of arsenate reduction. *Arch. Microbiol.* 173, 49–57. doi: 10.1007/s002030050007

McCleskey, R. B., Nordstrom, D. K., Susong, D. D., Ball, J. W., and Taylor, H. E. (2010). Source and fate of inorganic solutes in the Gibbon River, Yellowstone National Park, Wyoming, USA. II. Trace element chemistry. *J. Volcanol. Geotherm. Res.* 196, 139–155. doi: 10.1016/j.jvolgeores.2010.05.004

McKenzie, E. J., Brown, K. L., Cady, S. L., and Campbell, K. A. (2001). Trace metal chemistry and silicification of microorganisms in geothermal sinter, Taupo Volcanic Zone, New Zealand. *Geothermics* 30, 483–502. doi: 10.1016/s0375-6505(01)00004-9

Moore, J. N., Ficklin, W. H., and Johns, C. (1988). Partitioning of arsenic and metals in reducing sulfidic sediments. *Environ. Sci. Technol.* 22, 432–437. doi: 10.1021/es00169a011

Newman, D. K., Beveridge, T. J., and Morel, F. M. M. (1997). Precipitation of arsenic trisulfide by *Desulfotomaculum auripigmentum*. *Appl. Environ. Microbiol.* 63, 2022–2028.

Oremland, R. S. (2003). The ecology of arsenic. *Science* 300, 939–944. doi: 10.1126/science.1081903

Oremland, R. S., Hoeft, S. E., Santini, J. M., Bano, N., Hollibaugh, R. A., and Hollibaugh, J. T. (2002). Anaerobic oxidation of arsenite in Mono Lake water and by a facultative, arsenite-oxidizing chemoautotroph, strain MLHE-1. *Appl. Environ. Microbiol.* 68, 4795–4802. doi: 10.1128/AEM.68.10.4795-4802.2002

Oremland, R. S., Kulp, T. R., Blum, J. S., Hoeft, S. E., Baesman, S., Miller, L. G., et al. (2005). A microbial arsenic cycle in a salt-saturated, extreme environment. *Science* 308, 1305–1308. doi: 10.1126/science.1110832

Paez-Espino, D., Tamames, J., De Lorenzo, V., and Canovas, D. (2009). Microbial responses to environmental arsenic. *Biometals* 22, 117–130. doi: 10.1007/s10534-008-9195-y

Pascua, C. S., Minato, M., Yokoyama, S., and Sato, T. (2007). Uptake of dissolved arsenic during the retrieval of silica from spent geothermal brine. *Geothermics* 36, 230–242. doi: 10.1016/j.geothermics.2007.03.001

Pettine, M., Campanella, L., and Millero, F. J. (1999). Arsenite oxidation by H_2O_2 in aqueous solutions. *Geochim. Cosmochim. Acta* 63, 2727–2735. doi: 10.1016/S0016-7037(99)00212-4

Planer-Friedrich, B., Fisher, J. C., Hollibaugh, J. T., Suss, E., and Wallschlager, D. (2009). Oxidative transformation of trithioarsenate along alkaline geothermal drainages - abiotic versus microbially mediated processes. *Geomicrobiol. J.* 26, 339–350. doi: 10.1080/01490450902755364

Planer-Friedrich, B., Härtig, C., Lohmayer, R., Suess, E., Mccann, S. H., and Oremland, R. (2015). Anaerobic chemolithotrophic growth of the *Haloalkaliphilic* bacterium strain MLMS-1 by disproportionation of monothioarsenate. *Environ. Sci. Technol.* 49, 6554–6563. doi: 10.1021/acs.est.5b01165

Planer-Friedrich, B., London, J., Mccleskey, R. B., Nordstrom, D. K., and Wallschlager, D. (2007). Thioarsenates in geothermal waters of yellowstone national park: determination, preservation, and geochemical importance. *Environ. Sci. Technol.* 41, 5245–5251. doi: 10.1021/es070273v

Qin, J., Lehr, C. R., Yuan, C., Le, X. C., Mcdermott, T. R., and Rosen, B. P. (2009). Biotransformation of arsenic by a Yellowstone thermoacidophilic eukaryotic alga. *Proc. Natl. Acad. Sci. U.S.A.* 106, 5213–5217. doi: 10.1073/pnas.0900238106

Rhine, E. D., Phelps, C. D., and Young, L. Y. (2006). Anaerobic arsenite oxidation by novel denitrifying isolates. *Environ. Microbiol.* 8, 899–908. doi: 10.1111/j.1462-2920.2005.00977.x

Rittle, K. A., Drever, J. I., and Colberg, P. J. S. (1995). Precipitation of arsenic during bacterial sulfate reduction. *Geomicrobiol. J.* 13, 1–11. doi: 10.1080/01490459509378000

Saunders, J. A., Lee, M.-K., Shamsudduha, M., Dhakal, P., Uddin, A., Chowdury, M., et al. (2008). Geochemistry and mineralogy of arsenic in (natural) anaerobic groundwaters. *Appl. Geochem.* 23, 3205–3214. doi: 10.1016/j.apgeochem.2008.07.002

Saunders, J. A., Lee, M.-K., Wolf, L. W., Morton, C. M., Feng, Y., Thomson, I., et al. (2005). Geochemical, microbiological, and geophysical assessments of anaerobic immobilization of heavy metals. *Bioremediat. J.* 9, 33–48. doi: 10.1080/01490459709378044

Song, Z., Wang, F., Zhi, X., Chen, J., Zhou, E., Liang, F., et al. (2013a). Bacterial and archaeal diversities in Yunnan and Tibetan hot springs. *China. Environ. Microbiol.* 15, 1160–1175. doi: 10.1111/1462-2920.12025

Song, Z., Wang, L., Wang, F., Jiang, H., Chen, J., Zhou, E., et al. (2013b). Abundance and diversity of archaeal *accA* gene in hot springs in Yunnan Province, China. *Extremophiles* 17, 871–879. doi: 10.1007/s00792-013-0570-4

Stauder, S., Raue, B., and Sacher, F. (2005). Thioarsenates in sulfidic waters. *Environ. Sci. Technol.* 39, 5933–5939. doi: 10.1021/es048034k

Stucker, V. K., Silverman, D. R., Williams, K. H., Sharp, J. O., and Ranville, J. F. (2014). Thioarsenic species associated with increased arsenic release during biostimulated subsurface sulfate reduction. *Environ. Sci. Technol.* 48, 13367–13375. doi: 10.1002/etc.2155

Wallschläger, D., and Stadey, C. J. (2007). Determination of (oxy) thioarsenates in sulfidic waters. *Anal. Chem.* 79, 3873–3880. doi: 10.1021/ac070061g

Weisburg, W. G., Barns, S. M., Pelletier, D. A., and Lane, D. J. (1991). 16S ribosomal DNA amplification for phylogenetic study. *J. Bacteriol.* 173, 697–703. doi: 10.1128/jb.173.2.697-703.1991

Wilkin, R. T., Wallschläger, D., and Ford, R. G. (2003). Speciation of arsenic in sulfidic waters. *Geochem. Trans.* 4:1. doi: 10.1186/1467-4866-4-1

Wood, S. A., Tait, C. D., and Janecky, D. R. (2002). A Raman spectroscopic study of arsenite and thioarsenite species in aqueous solution at 25 C. *Geochem. Trans.* 3, 31–39. doi: 10.1186/1467-4866-3-31

Wu, G., Jiang, H., Dong, H., Huang, Q., Yang, J., Webb, L., et al. (2015). Distribution of arsenite-oxidizing bacteria and its correlation with temperature in hot springs of the Tibetan-Yunnan geothermal zone in western China. *Geomicrobiol. J.* 32, 482–493. doi: 10.1080/01490451.2014.938206

Yang, J., Zhou, E., Jiang, H., Li, W., Wu, G., Huang, L., et al. (2015). Distribution and diversity of aerobic carbon monoxide-oxidizing bacteria in geothermal springs of China, the Philippines, and the United States. *Geomicrobiol. J.* 32, 903–913. doi: 10.1080/01490451.2015.1008605

Yang, Y., Peng, Y. E., Chang, Q., Dan, C., Guo, W., and Wang, Y. (2016). Selective identification of organic iodine compounds using liquid chromatography–high resolution mass spectrometry. *Anal. Chem.* 88, 1275–1280. doi: 10.1021/acs.analchem.5b03694

Yokoyama, T., Takahashi, Y., and Tarutani, T. (1993). Simultaneous determination of arsenic and arsenious acids in geothermal water. *Chem. Geol.* 103, 103–111. doi: 10.1016/0009-2541(93)90294-S

Zargar, K., Conrad, A., Bernick, D. L., Lowe, T. M., Stolc, V., Hoeft, S., et al. (2012). ArxA, a new clade of arsenite oxidase within the DMSO reductase family of molybdenum oxidoreductases. *Environ. Microbiol.* 14, 1635–1645. doi: 10.1111/j.1462-2920.2012.02722.x

Zargar, K., Hoeft, S., Oremland, R., and Saltikov, C. W. (2010). Identification of a novel arsenite oxidase gene, arxA, in the haloalkaliphilic, arsenite-oxidizing

bacterium *Alkalilimnicola ehrlichii* strain MLHE-1. *J. Bacteriol.* 192, 3755–3762. doi: 10.1128/jb.00244-10

Zhao, L., Dong, H., Kukkadapu, R., Agrawal, A., Liu, D., Zhang, J., et al. (2013). Biological oxidation of Fe (II) in reduced nontronite coupled with nitrate reduction by *Pseudogulbenkiania* sp. strain 2002. *Geochim. Cosmochim. Acta* 119, 231–247. doi: 10.1016/j.gca.2013.05.033

Zhao, L., Dong, H., Kukkadapu, R. K., Zeng, Q., Edelmann, R. E., Pentrák, M., et al. (2015). Biological redox cycling of iron in nontronite and its potential application in nitrate removal. *Environ. Sci. Technol.* 49, 5493–5501. doi: 10.1021/acs.est.5b00131

Conflict of Interest Statement: The authors declare that the research was conducted in the absence of any commercial or financial relationships that could be construed as a potential conflict of interest.

frontiers in Microbiology

ORIGINAL RESEARCH
published: 03 August 2018
doi: 10.3389/fmicb.2018.01759

Genomic Insights Into Energy Metabolism of *Carboxydocella thermautotrophica* Coupling Hydrogenogenic CO Oxidation With the Reduction of Fe(III) Minerals

Stepan V. Toshchakov[1,2], Alexander V. Lebedinsky[2], Tatyana G. Sokolova[2], Daria G. Zavarzina[2], Alexei A. Korzhenkov[1], Alina V. Teplyuk[1], Natalia I. Chistyakova[3], Vyacheslav S. Rusakov[3], Elizaveta A. Bonch-Osmolovskaya[2], Ilya V. Kublanov[2] and Sergey N. Gavrilov[2]**

[1] Laboratory of Microbial Genomics, Immanuel Kant Baltic Federal University, Kaliningrad, Russia, [2] Winogradsky Institute of Microbiology, FRC Biotechnology, Russian Academy of Sciences, Moscow, Russia, [3] Faculty of Physics, Lomonosov Moscow State University, Moscow, Russia

OPEN ACCESS

Edited by:
Nils-Kaare Birkeland,
University of Bergen, Norway

Reviewed by:
Hugh Morgan,
University of Waikato, New Zealand
Rudolf Kurt Thauer,
Max-Planck-Institut für Terrestrische Mikrobiologie, Germany

***Correspondence:**
Alexander V. Lebedinsky
a.lebedinsky@mail.ru
Sergey N. Gavrilov
sngavrilov@gmail.com

Specialty section:
This article was submitted to Extreme Microbiology, a section of the journal Frontiers in Microbiology

Received: 28 April 2018
Accepted: 13 July 2018
Published: 03 August 2018

Citation:
Toshchakov SV, Lebedinsky AV, Sokolova TG, Zavarzina DG, Korzhenkov AA, Teplyuk AV, Chistyakova NI, Rusakov VS, Bonch-Osmolovskaya EA, Kublanov IV and Gavrilov SN (2018) Genomic Insights Into Energy Metabolism of Carboxydocella thermautotrophica Coupling Hydrogenogenic CO Oxidation With the Reduction of Fe(III) Minerals. Front. Microbiol. 9:1759. doi: 10.3389/fmicb.2018.01759

The genus *Carboxydocella* forms a deeply branching family in the class *Clostridia* and is currently represented by three physiologically diverse species of thermophilic prokaryotes. The type strain of the type species, *Carboxydocella thermautotrophica* 41^T, is an obligate chemolithoautotroph growing exclusively by hydrogenogenic CO oxidation. Another strain, isolated from a hot spring at Uzon caldera, Kamchatka in the course of this work, is capable of coupling carboxydotrophy and dissimilatory reduction of Fe(III) from oxic and phyllosilicate minerals. The processes of carboxydotrophy and Fe(III) reduction appeared to be interdependent in this strain. The genomes of both isolates were sequenced, assembled into single chromosome sequences (for strain 41^T a plasmid sequence was also assembled) and analyzed. Genome analysis revealed that each of the two strains possessed six genes encoding diverse Ni,Fe-containing CO dehydrogenases (maximum reported in complete prokaryotic genomes), indicating crucial role of carbon monoxide in *C. thermautotrophica* metabolism. Both strains possessed a set of 30 multiheme *c*-type cytochromes, but only the newly isolated Fe-reducing strain 019 had one extra gene of a 17-heme cytochrome, which is proposed to represent a novel determinant of dissimilatory iron reduction in prokaryotes. Mössbauer studies revealed that strain 019 induced reductive transformation of the abundant ferric/ferrous-mica mineral glauconite to siderite during carboxydotrophic growth. Reconstruction of the *C. thermautotrophica* strains energy metabolism is the first comprehensive genome analysis of a representative of the deep phylogenetic branch Clostridia Incertae Sedis, family V. Our data provide insights into energy metabolism of *C. thermautotrophica* with an emphasis on its ecological implications.

Keywords: *Carboxydocella*, thermophile, Kamchatka hot springs, genomics, hydrogenogenic carboxydotrophy, Fe(III) reduction, Fe(III) silicate minerals, Firmicutes

INTRODUCTION

Carbon monoxide (CO) is a common although minor component of gasses in terrestrial hot springs. In the hot springs of Yellowstone National Park (United States) and Uzon Caldera (Kamchatka, Russia), its concentration was reported to be about 1–6 10^{-7} mole fraction in the gas bubbling through the water (Shock et al., 2005, 2010) or 20–30 nM of dissolved gas (Kochetkova et al., 2011). The main sources of CO in hydrothermal vents are volcanic gasses (Menyailov and Nikitina, 1980; Symonds et al., 1994; Allard et al., 2004) and thermochemical or photochemical decomposition of organic matter (Hellebrand and Schade, 2008). Carbon monoxide is a strong reductant [$E^{0'}{}_{(CO/CO2)}$ is ca. −520 mV at pH 7.0], and can be involved in a number of microbial metabolic redox reactions (Shock et al., 2005, 2010; Diender et al., 2015) coupled with the reduction of various inorganic electron acceptors.

Key enzymes of CO oxidation pathways are carbon monoxide dehydrogenases (CODHs), which catalyze the oxidation of CO with water to CO_2. CODHs from aerobes, encoded by *cox* genes, contain Cu and Mo as cofactors, while anaerobic CODHs, encoded by the distantly homologous *cooS* or *cdh* genes, contain Ni and Fe in active centers, where Ni activates CO and Fe provides the nucleophilic water. As distinct from the water-gas shift reaction, where the electrons and protons generated by CO oxidation are directly released as H_2, CODHs keep the protons and electrons separated, and the electrons are transferred to the terminal acceptors via electron-carrier proteins. In case of hydrogenogenic carboxydotrophs and their [Ni,Fe]-CODHs, protons may serve as these terminal acceptors, and H_2 is eventually released. [Ni,Fe]-CODHs are frequently associated with acetyl-CoA synthases (ACSs), where the [Ni,Fe]-CODH component reduces CO_2 to CO, condensed with a methyl group and CoA by ACS to produce acetyl-CoA, or oxidizes CO formed upon acetyl-CoA cleavage (Jeoung et al., 2014).

A number of prokaryotes are capable of using CO as an electron donor, and some of them can also use CO as a carbon source (King and Weber, 2007; Oelgeschläger and Rother, 2008; Sokolova and Lebedinsky, 2013; Tiquia-Arashiro, 2014; Diender et al., 2015). In various terrestrial hydrotherms, potential activity or the presence of CO-oxidizing anaerobes has been revealed (Kochetkova et al., 2011; Brady et al., 2015; Yoneda et al., 2015), and the number of newly isolated CO-oxidizers is increasing permanently (Balk et al., 2009; Yoneda et al., 2012, 2013; Sokolova and Lebedinsky, 2013; Tiquia-Arashiro, 2014). Among cultivated thermophilic anaerobic CO-oxidizing species, hydrogenogenic carboxydotrophs are in majority, moreover, in certain hot springs, they comprise a significant portion of the microbial population (Yoneda et al., 2015). These bacteria oxidize carbon monoxide via the following reaction: $CO + H_2O \rightarrow CO_2 + H_2$ ($\Delta G^{0'} = -20$ kJ). A representative of thermophilic hydrogenogenic CO-trophic microorganisms, *Carboxydocella thermautotrophica*, is the type species of the genus *Carboxydocella,* which forms a deep phylogenetic branch of the order Clostridiales, Incertae Sedis, family V (Sokolova et al., 2009; Sokolova, 2015). *Carboxydocella* species were found to be widely distributed in neutral hot springs with moderately thermophilic conditions (Slepova et al., 2006, 2007; Kochetkova et al., 2011; Slobodkina et al., 2012; Brady et al., 2015; Sokolova, 2015). So far, three *Carboxydocella* species have been validly described: *C. thermautotrophica* (Sokolova et al., 2002), *C. sporoproducens* (Slepova et al., 2006), and *C. manganica* (Slobodkina et al., 2012). While *C. thermautotrophica* and *C. sporoproducens* are carboxydotrophs, *C. manganica* is unable to oxidize CO.

Some thermophilic anaerobes isolated from various sedimentary environments of volcanic origin are capable of both hydrogenogenic CO-oxidation and dissimilatory ferric iron reduction from Fe(III) oxides (Sokolova et al., 2004; Slobodkin et al., 2006; Zavarzina et al., 2007; Slepova et al., 2009; Yoneda et al., 2012, 2013). At the moment, the interconnections between the oxidative and reductive branches of energy metabolism in these organisms remain unclear. Fe-bearing silicates (clay and mica minerals) comprising the most abundant Fe(III) source in volcanic areas (Eroschev-Shak et al., 1998, 2005) have not been tested as electron acceptors for growth of carboxydotrophs. Microbial redox transformation of these minerals is poorly understood so far, especially at elevated temperatures. Dissimilatory reduction of structural Fe from clays has been documented for a few thermophilic species (Pentráková et al., 2013). Less is known about bioreduction of Fe-rich micas, which are widely distributed in igneous and sedimentary rocks. The ability to reduce structural Fe in the mica mineral biotite was only demonstrated for resting cell suspensions of two mesophilic Fe(III)-reducing bacteria *Geobacter sulfurreducens* and *Shewanella oneidensis* (Brookshaw et al., 2014a,b). Bacteria of these species are the main models used for the investigation of microbial redox interactions with Fe(III) minerals, and the current concept of extracellular electron transfer in prokaryotes is mostly based on the data obtained for these microorganisms. Recent reviews of this concept (Shi et al., 2016; White et al., 2016) highlight the key role of multiheme *c*-type cytochromes in this process and the existence of two major pathways for direct electron transfer from respiratory chain to electron acceptor outside the cell. The first pathway is mediated by porin-cytochrome complexes linking intracellular electron shuttles and Fe(III)-reducing cytochromes on the cell surface. The second pathway is based on electrically conductive cell appendages (pili or "nanowires"). Genomic studies revealed that the determinants of both pathways are widespread among prokaryotes, although *in vivo* activity of porin-cytochrome complexes or nanowires has been documented for a restricted number of Fe(III)-reducers (Shi et al., 2012, 2014, 2016).

Here we report physiological and genomic characterization of two strains of *Carboxydocella thermautotrophica*. The type strain *C. thermautotrophica* 41^T is an obligate chemolithoautotroph growing exclusively by hydrogenogenic CO oxidation (Sokolova et al., 2002), while a new isolate of the same species, obtained during the current work (strain 019), differs significantly in its physiology, namely, by its capacity for Fe(III) reduction from oxic and mica minerals, which depends on CO availability. This physiological versatility of *C. thermautotrophica* strains has lead us to the proposal of an important ecological role for this taxon, such as coupling the transformation of carbon oxides and Fe

minerals in terrestrial sedimentary environments of Kamchatka hot springs.

MATERIALS AND METHODS

Strains

The type strain *C. thermautotrophica* 41^T (Sokolova et al., 2002) was obtained from DSMZ collection (DSMZ 1236). The strain 019 has been isolated from a core sample of the ground taken at East Thermal Field at Uzon Caldera (Kamchatka Peninsula, Russia).

Sampling

A core was taken at East Thermal Field at Uzon Caldera (Kamchatka Peninsula) at an edge of Zavarzin Pool. Zavarzin Pool, 2.5 m in diameter, is formed by several hot springs discharging inside it. In the pool, thin brown layers of microbial mats were developed covered with a thick layer of sulfur. Temperature and pH of the water varied in different spots at the pool from 46 to 57°C and from 6.10 to 6.75, respectively. The core was taken at a 0.5-m distance from the pool and to 40-cm depth. The upper 10 cm of the core were black, next 15 cm in the middle had vertical black and white stripes, and the bottom 15 cm were almost white. The pH of the water filling the core was 5.8, its temperature was 55°C, and E_h was −225 mV (hereafter all the E_h values are presented vs. the potential of standard hydrogen electrode [SHE] at pH 6.5). Subsamples of top, middle and bottom layers of the core were taken anaerobically in tightly sealed bottles and designated as DC03-018, DC03-019, and DC03-020, respectively.

Enrichment and Isolation

For enrichment and isolation of hydrogenogenic carboxydotrophic prokaryotes and their subsequent cultivation Media 1 and 2 were used. Medium 1 contained (g l^{-1}): NH_4Cl, 1; $MgCl_2{\cdot}6H_2O$, 0.33; $CaCl_2{\cdot}6H_2O$, 0.1; KCl, 0.33; KH_2PO_4, 0.5; resazurin, 0.001; 1 ml l^{-1} of trace mineral solution (Kevbrin and Zavarzin, 1992); 1 ml l^{-1} of vitamin solution (Wolin et al., 1963), $NaHCO_3$ (0.5 g l^{-1}). Medium 1 was reduced with $Na_2S{\cdot}\ 9H_2O$ (1.0 g l^{-1}), and pH was adjusted to 6.8 with 6N HCl. Medium 2 had the composition similar to Medium 1 except the presence of hydromorphic ferric oxide (ferrihydrite), while sodium sulfide was omitted. Medium 1 had a redox potential characteristic of strictly anaerobic conditions (E_h value of −430 mV), and Medium 2 had a redox potential of −90 mV. Hereafter, strictly anaerobic conditions of Medium 1 are referred to as "low E_h" and anaerobic conditions of Medium 2 are referred to as "high E_h". Microaerobic or aerobic growth conditions are specified where necessary. Yeast extract (0.5 g l^{-}1) or sodium acetate (0.2 g l^{-1}) or lactate (0.3 g l^{-1}) were added as additional carbon sources when indicated. Glass vessels (60 ml total volume) sealed with butyl rubber stoppers (Bellco Glass Inc.) and containing 10 ml of liquid Medium 2 and 50 ml gas phase (100% CO) were inoculated with suspended core samples and incubated at 60°C. In chemical controls with non-inoculated media 1 or 2, equilibrium concentration of gaseous CO_2, released due to thermal decomposition of bicarbonate at 60°C, was under the detection level at the beginning of incubation and did not exceed 0.03% (v/v) of the gas phase within further 6 days of incubation. Growth was determined using light microscopy and by monitoring CO utilization and gaseous products formation as described previously (Sokolova et al., 2002). After a number of serial end point dilution transfers in Medium 2 pure cultures were isolated from colonies obtained in roll-tubes prepared in 15-ml Hungate tubes with Medium 1 solidified by 5% agar, under 100% CO in the gas phase. Well-separated colonies were transferred to the liquid Medium 1.

Physiological Studies

Utilization of molecular hydrogen, CO_2, acetate, lactate (2 g/l) or glycerol (0.2%, v/v) by the new isolate was tested in liquid Medium 1 with 100% N_2 or 80:20% H_2/CO_2 as the gas phase in presence or absence of potential electron acceptors. The acceptors tested were sodium nitrate, nitrite, sulfate, thiosulfate, AQDS, as well as mineral acceptors ferrihydrite (prepared as described by Gavrilov et al., 2012), glauconite (from Severo-Stavropol'skoye underground gas storage reservoir, Russia), nontronite (from the collection of clay minerals of the Faculty of Soil Science, Lomonosov Moscow State University) and diatomite (from Inzenskoye deposit, Russia). Soluble acceptors were added from pre-sterilized stock solutions to a concentration of 10 mM (5 mM in case of nitrite); Fe(III) minerals were added to Medium 2 before sterilization to achieve initial Fe(III) content of 90 mM in case of ferrihydrite and 20 mM in case of glauconite, nontronite, or diatomite.

CO, CO_2, and H_2 were analyzed using a '3700' custom-modified gas chromatograph (ZIOC RAS Special Design Tech. Dept., Russia) supplied with Phoenix v.3.6.0 analytical software (BSoft, Russia) and equipped with zeolite NaX 80–100 mesh and Chromosorb-102 60-80 mesh 3 m columns and TCD detector, which were all conditioned at 30°C. Extra pure grade Ar was used as the carrier gas. Volatile fatty acids were determined by high performance liquid chromatography (HPLC) on a Stayer chromatograph (Aquilon, Russia) equipped with an Aminex HPX_87H column (Bio-Rad) and a Smartline 2300 refractometric detector (Knauer, Germany), with 5 mM H_2SO_4 as the eluent. Growth on iron-containing minerals was traced by the increase of the content of HCl-extractable Fe(II) in the mineral phase of Medium 2. The cell density was determined by direct cell counting under a CX41 phase-contrast microscope (Olympus). Temperature and pH growth optima were deduced from growth rates determined on Medium 1.

Mössbauer Studies

Mössbauer spectra of ^{57}Fe nuclei were recorded at room temperature on a custom-modified MS-1104Em spectrometer (Research Institute of Physics, Southern Federal University, Russia), which was equipped with a ^{57}Co-source in a Rh matrix and operated in a constant acceleration mode. The spectrometer was calibrated using standard α-Fe absorbent. The SpectrRelax software (Matsnev and Rusakov, 2014) was used to analyze the Mössbauer spectra. Iron species were determined colorimetrically in HCl extracts of culture subsamples with

ferrozine (Fe^{2+}) or potassium thiocyanate (Fe^{3+}), as previously described (Gavrilov et al., 2012). Insoluble parts of silicate minerals were separated from HCl extracts by centrifugation at 12 kG for 10 min on an Eppendorf table top centrifuge. Non-extractable iron content of glauconite was estimated from Mössbauer spectral data under the assumption that the recoil-free fraction (probability of Mössbauer effect) is equal for iron atoms located in different positions in various mineral phases, and accordingly, relative intensities of subspectra (area of subspectra) are equal to the relative content of iron atoms in these positions.

DNA Isolation

For DNA isolation cells were cultivated on Medium 1 in the absence of minerals under optimal conditions, collected by centrifugation at 9 kG for 15 min and disrupted with glass beads using Minilys homogenizer (Bertin Technologies). DNA was extracted using QIAamp DNA mini kit (Qiagen).

Phylogenetic Reconstructions

Phylogenetic trees were constructed using the Maximum Likelihood method based on the Jones–Taylor–Thornton model (Jones et al., 1992) in MEGA6 (Tamura et al., 2013).

For the putative iron reducing cytochrome, separate reconstructions were performed for C-terminus (first 500 aa residues) and the remaining part of the sequence (501–1486 aa residues), containing all the conservative multiheme cytochrome domains (i.e., putative "catalytic" domain of the protein). Blastp analysis was performed against UniProtKB prokaryotic database on April, 2018. For the catalytic domain of the protein, only the hits with $E_v < 0.001$, query coverage $\geq$50% and identity >20% (which is relevant for multiheme cytochromes, Sharma et al., 2010) from cultivated strains were considered. The analysis retrieved 57 sequences, which were then filtered through 0.9 filter using CD-hit utility[1] and the resulting set of 50 sequences was aligned with built-in Muscle at default parameters in MEGA6.

Genome Sequencing and Assembly

Sequencing projects were started in May 2013 and finished in August 2014. For sequencing of the genomes of *C. thermautotrophica* strains both paired-end and mate-paired DNA libraries were used. Paired end libraries were prepared from 1 μg of genomic DNA with NEBNext™ Ultra DNA library preparation kit (New England Biolabs, United States) according to manufacturer's instructions to obtain mean library size of 500 bp. Mate-paired libraries were prepared with Nextera™ Mate Pair Library Prep Kit (Illumina Inc., United States) using bead-based size selection protocol. Both paired-end mate-paired libraries were sequenced using 2 × 250 bp reads with MiSeq™ Personal Sequencing System (Illumina Inc., United States). After sequencing all reads were subjected to stringent quality filtering with CLC Genomics Workbench 8.5 (Qiagen, Germany). After filtering, overlapping paired-end library reads were merged with SeqPrep tool[2], resulting in 215,048 and 227,940 single merged reads; and 895,488 and 892,408 read pairs for strains 41^T and 019, respectively. Fragment size of both paired-end libraries was 500–700 bp. Mate-paired reads were treated with NextClip tool (Leggett et al., 2014), resulting in 2,382,016 and 2,123,106 read pairs with mean insert sizes of 2,439 and 2,382 bp for strains 41^T and 019, respectively. Reads were assembled with both ALLPATHS-LG (Butler et al., 2008) and SPADES 3.8.0 (Nurk et al., 2013) assemblers and refined manually using CLC Genomics Workbench 8.5 software (Qiagen, Germany). Orientation of contigs and final filling of sequence gaps was made by PCR with outward-oriented primers to contigs termini and subsequent Sanger sequencing of resulting amplicons. Final average genome coverage was 247× and 218× for strains 41^T and 019, respectively. During assembly of strain 41^T genome an additional circular contig, corresponding to plasmid, was also assembled.

The complete genome sequences of the *C. thermautotrophica* type strain 41^T and strain 019 have been deposited in DDBJ/EMBL/GenBank under accession numbers CP028491 (strain 019), CP028514 (strain 41^T) and CP028515 (plasmid of strain 41^T). Related projects information and sample details have been deposited in NCBI database under accession numbers PRJEB11520, PRJEB11521, and SAMN07757920, SAMN07757921, respectively.

Genome Annotation

Gene prediction and primary annotation was performed with IMG/M ER System (Chen et al., 2017). Refining of the automated annotations and other predictions were done manually according to genome annotation protocol (Toshchakov et al., 2015).

Subcellular localization of multiheme cytochromes was predicted based on the results of six different on-line prediction services – SignalP 4.1, TatP 1.0, SecretomeP 2.0a and TMHMM 2.0 (all at CBS Prediction Servers[3]), as well as PSORTb 3.0.2[4] and Phobius[5].

Conserved domains were predicted with HMMSCAN[6] considering Pfam, TIGRFAM, Gene3D, Superfamily, PIRSF and TreeFam protein families databases.

RESULTS

Enrichment and Isolation of Strain 019, Cell Morphology of the New Isolate

The *C. thermautotrophica* Fe(III)-reducing strain 019 was obtained from a core sample taken near Zavarzin thermal pool at Uzon Caldera (Kamchatka). The bottles with anaerobic Medium 2 (high E_h) containing sodium acetate and ferrihydrite under a 100% CO atmosphere and inoculated with the middle (black-to-white) part of the core sample (subsample DC03-019) showed an increase in pressure from 140 to 170 kPa after 2 days of incubation at 60°C. Growth of small rod-shaped cells was observed. The CO content in the gas phase decreased to 40% and about 30%

[1] http://weizhongli-lab.org/cdhit_suite/cgi-bin/index.cgi

[2] https://github.com/jstjohn/SeqPrep

[3] http://www.cbs.dtu.dk/services

[4] http://www.psort.org/psortb/

[5] http://phobius.sbc.su.se/

[6] https://www.ebi.ac.uk/Tools/hmmer/search/hmmscan

H_2 and 30% CO_2 were formed. After several transfers in the same medium the enrichments were serially tenfold diluted and transferred to the Medium 1 (low E_h) with sodium acetate and without Fe(III) under 100% CO, and then to roll-tubes with the same solidified Medium 1. After 2 days of incubation at 60°C, round white colonies about 0.5 mm in diameter were observed, which were transferred to a similar liquid medium. As a result, an isolate designated strain 019 was obtained.

Cells of the isolate 019 were straight rods with a length of 1–1.5 μm and a width of about 0.4–0.5 μm, arranged singly or in pairs. Cells were motile due to lateral flagella but singular cell aggregates on magnetite were also observed (**Supplementary Figure S1**).

Growth Characteristics of the New Isolate

Physico-Chemical Parameters

Growth of strain 019 was observed in the temperature range of 45–68°C, with an optimum at 58°C, and in the pH range 6.5–7.6, with an optimum at pH 7.0. Strain 019 grew anaerobically in a wide range of culture conditions: autotrophically or heterotrophically, by respiration or by fermentation. Aerobic or microaerobic growth was not observed with any of the tested concentrations of oxygen in the gas phase, i.e., under 100% air, a mixture of CO and air (4:1 v/v), or CO with 0.5, 1, or 2% O_2.

Carbon Substrates

Autotrophic growth of strain 019 under CO was observed in the absence of any organic carbon sources. H_2 as the electron donor with Fe(III), thiosulfate or nitrate as electron acceptors did not support autotrophic growth under a H_2/CO_2 gas phase. Organic substrates either stimulated carboxydotrophic growth or supported the growth in the absence of CO. Acetate and lactate but not pyruvate were utilized concomitantly with complete CO oxidation and hydrogen formation, the presence of the organic acid salt raising the cell yield up to 10 times compared to autotrophic growth conditions. Fermentative growth of strain 019 was observed on yeast extract, sucrose, glucose, maltose, or pyruvate under pure N_2 or CO atmosphere. Galactose, cellobiose, cellulose, lactose, glycerol, peptone were not utilized. Glucose was fermented to lactate, acetate and H_2.

Electron Donors and Acceptors

During autotrophic growth on CO coupled to hydrogenogenic carboxydotrophy, strain 019 utilizes protons as electron acceptors in its energy metabolism. Among electron acceptors other than protons, only Fe(III) stimulated growth of the strain, but it was exclusively utilized in the presence of CO (**Figure 1**). Thiosulfate and nitrate did not affect growth of the organism with organic acids under CO and inhibited autotrophic growth under CO (data not presented). Sulfate, nitrite or AQDS inhibited growth of strain 019 under any of the conditions tested.

Utilization of protons and Fe(III) as electron acceptors by strain 019 during autotrophic or heterotrophic (with lactate) growth appeared to depend on redox potential of the culture medium (**Figure 1**). In high E_h anaerobic medium, the growth was only possible in the presence of both CO and an Fe(III) mineral. In contrast, in low E_h culture medium, strain 019 grew either by carboxydotrophy in the absence of electron acceptors other than protons or by fermentation, i.e., with organic electron donors in the absence of both CO and Fe(III). Checking the Fe(III) reducing ability of strain 019 in low E_h medium appeared to be impossible due to rapid chemical redox interactions at 60°C between insoluble Fe(III) and sulfides, added to decrease the redox potential.

In parallel experiments, the type strain 41^T grew only at low E_h by autotrophic hydrogenogenic CO oxidation without additional electron acceptors (**Figure 1**), as described previously by Sokolova et al., 2002.

Fe(III) Reduction From Minerals by Strain 019

The growth of strain 019 in the presence of both Fe(III) and CO was accompanied by Fe(III) reduction, complete CO oxidation and the formation of apparently equimolar quantities of CO_2 and H_2. In our experiments we used insoluble Fe(III) forms, which are typical for physico-chemical conditions in natural habitats of *C. thermautotrophica*. No soluble Fe(II) or Fe(III) was detected in cultures during their growth with various Fe(III) minerals.

Fe(III) Reduction From Ferrihydrite

Fe(III) supplied as an oxic mineral ferrihydrite provided maximal cell yield of strain 019 (**Figure 1**). During the growth, about 23% of insoluble Fe(III) from ferrihydrite was reduced to Fe(II) in the form of a black magnetic mineral (presumably, magnetite) with concomitant decrease of the culture E_h down to −360 mV. The cell yield of autotrophic cultures grown on CO increased three times in the presence of ferrihydrite, in spite of the high initial E_h of the medium. Lactate stimulated the growth on CO with ferrihydrite (**Figure 1**). Consumption of 2.3 mM lactate was accompanied by the formation of 1.1 mM acetate (**Figure 2B**), indicating that about half of the oxidized lactate was utilized as an electron donor in catabolic reactions, while the rest of lactate was likely consumed as a carbon source. In contrast, only 0.6 mM lactate was consumed by cultures grown on CO and lactate in the absence of Fe(III) at low E_h, and no acetate production was detected in these growth conditions. Kinetic experiments revealed that maximal growth rate in high E_h medium containing ferrihydrite, CO and lactate was observed within the first 24 h of incubation simultaneously with the highest rates of Fe(III) reduction and lactate conversion to acetate. About 77% of the lactate consumed by the end of this growth phase was converted to acetate (**Figure 2B**), while only 10% of CO was oxidized with equimolar H_2 formation. Maximal rate of hydrogenogenic carboxydotrophy was achieved later, when cell growth and Fe(III) reduction slowed down (**Figure 2**).

Fe(III) Reduction From Phyllosilicates

As strain 019 was isolated from a mineral core sample, it was tested for the ability to utilize structural Fe(III) from crystal lattice of phyllosilicates – the group of minerals previously detected in Zavarzin hot pool (Rozanov et al., 2014) right nearby the site where samples for our enrichments were obtained. We tested mixed valence Fe(III/II) minerals: the Fe-mica glauconite, clay

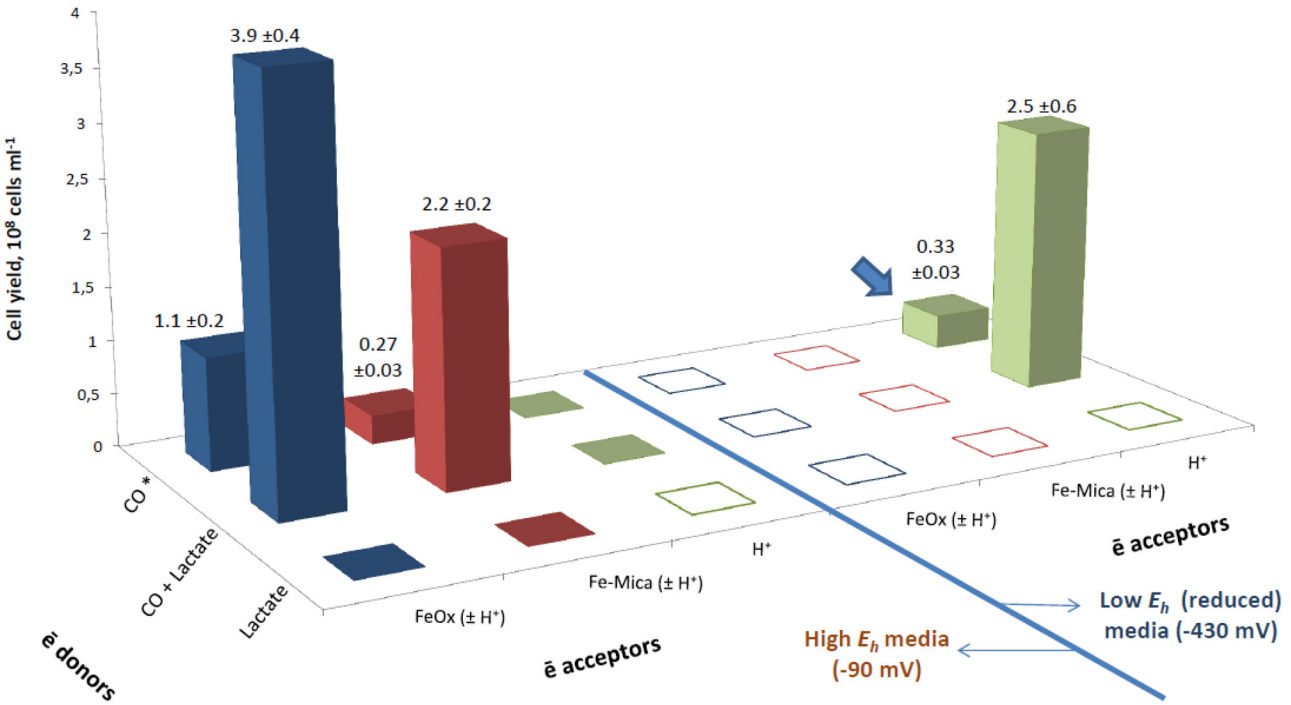

FIGURE 1 | Cell yield of strain 019 cultures as dependent on availability of Fe(III), organic carbon and a reductant in the medium. Indicated above the bars are cell yields and corresponding error limits ($\times 10^8$ cells ml^{-1}). Note that two types of anaerobic culture media (high E_h and low E_h) were used to test each couple of electron donor and acceptor with both *C. thermautotrophica* strains. The initial E_h values were identical in the culture media of a particular type and are indicated on the diagram. Low E_h medium was pre-reduced with sodium sulfide (refer to "Materials and Methods" section for details). Electron donor/acceptor couples which have been tested but did not support the growth of a *C. thermautotrophica* strain are shown as flat filled squares. Empty squares indicate donor/acceptor couples which are biochemically senseless (lactate and H^+) or physico-chemically restricted [rapid chemical reduction of Fe(III) minerals by sulfides]. Asterisk indicates autotrophic growth conditions when CO was the only carbon source and electron donor available in the culture medium. Thick arrow indicates the conditions supporting the growth of the type strain 41^T; data on its cell yields are not presented.

mineral nontronite and siliceous sedimentary rock diatomite containing admixtures of natural Fe oxides (Distanov, 1987). Growth of strain 019 was observed in three consecutive transfers with diatomite and glauconite (**Figure 3**). Growth with diatomite was observed only in the presence of lactate as a potential carbon source, while growth with glauconite was observed both in the presence and in the absence of organic substrates. Growth with glauconite correlated with an increase in HCl-extractable Fe(II) (**Figure 4**) and non-extractable structural Fe(II) content (**Supplementary Figure S2**) of the Fe-mica mineral. During autotrophic growth, only a minor increase of glauconite Fe(II) content (by ca. 0.2 mM) was observed and the cell yield correlated with that detected in the absence of Fe(III) minerals at low E_h. Lactate stimulated the growth with glauconite 10-fold (**Figure 1**) and Fe(II) production from glauconite sevenfold (up to 1.42 mM). About 1 mM of lactate was consumed concomitantly with glauconite reduction but no acetate production was detected, indicating utilization of lactate as the carbon source only (**Figure 4B**). The growth was accompanied by a pronounced decrease of E_h down to −520 mV. In a control experiment, simulating the initial Fe(III)/Fe(II) ratio of glauconite by using a mixture of ferrihydrite and magnetite, the E_h value of the cultures rapidly decreased from −90 to −320 mV within the first 8 h of incubation. Changes in E_h of uninoculated controls with glauconite or ferrihydrite/magnetite mixture were much lower. The growth of strain 019 in the presence of lactate, CO and glauconite started with active CO oxidation and H_2 formation. The rates of lactate consumption and Fe(III) reduction were minimal in this growth phase, but after 49 h of incubation, maximal rates of growth and of all of the mentioned metabolic processes were achieved simultaneously (**Figure 4**). Fe(III) reduction from the mica mineral by strain 019 rapidly ceased upon exhaustion of CO, followed by a start of cell lysis (**Figure 4**). However, to trace possible minor structural changes in glauconite, induced by microbial Fe(III) reduction but not leading to an increase in the HCl-extractable Fe(II) content of the mineral, we continued incubation of the cultures further on. Mössbauer investigations revealed that the relative amounts of Fe^{2+} and Fe^{3+} atoms in glauconite remained virtually constant within the first 78 h of incubation, until cell lysis started. During subsequent incubation, the relative content of ferrous atoms in glauconite increased almost twice from 2.2 ± 0.5% to 5.7 ± 0.4% by the 166th hour, and this trend was strengthening within further 794 h of incubation, until all the cells have been completely lysed (**Supplementary Figure S2**). Mössbauer spectra of the studied samples within all the incubation period were of

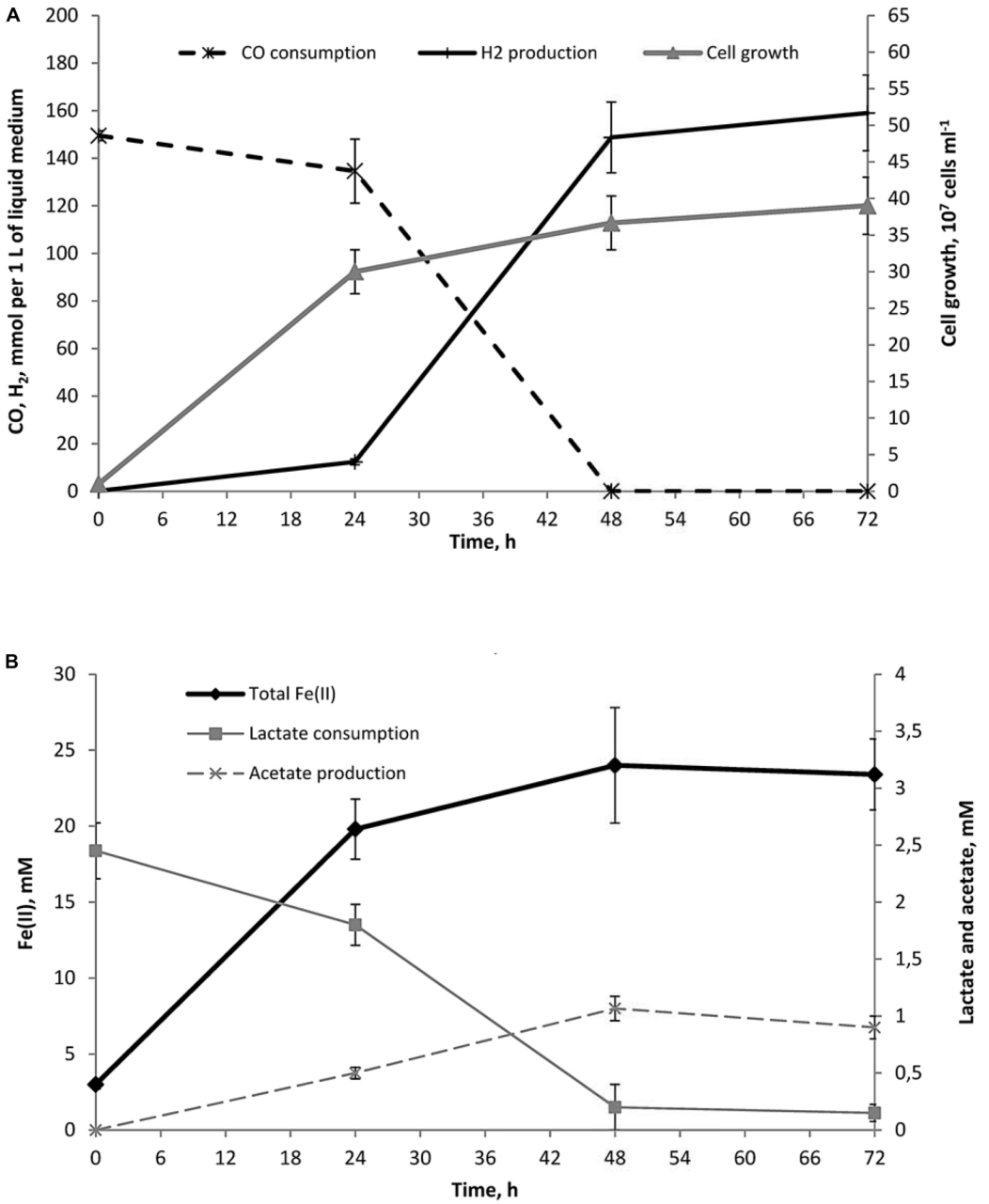

FIGURE 2 | Dynamics of growth, Fe(II) production, lactate consumption, acetate formation and concomitant hydrogenogenic carboxydotrophy of *C. thermautotrophica* strain 019 growing on CO and lactate with ferrihydrite. **(A)** Cell growth, CO consumption and H_2 production; **(B)** Fe(II) production, lactate consumption and acetate formation.

paramagnetic type with a superposition of quadrupole doublets. Final spectra, captured at the 960th hour (**Figure 5**), were clearly fitted by four quadrupole doublets with equal line widths, depicting the formation of a small relative amount of a new mineral phase containing Fe^{2+} atoms in the octahedral oxygen environment. This phase was identified as siderite ($FeCO_3$), which indicated the reduction of Fe^{3+} atoms in glauconite lattice structure. The relative concentration of siderite in the sample, obtained at the end of the entire 960-h incubation period, was $I = 3.9 \pm 1.3\%$. No changes in the mineral structure were detected in abiotic controls (**Figure 5**), as well as no production of H_2 or Fe(II), no decrease in lactate concentration, and no interactions of CO or H_2 with Fe(III) were observed within the same incubation period.

No growth or Fe(III) reduction from any of the tested Fe(III) minerals was observed with the type strain 41^T under the same cultivation conditions. Neither could the type strain grow by fermentation.

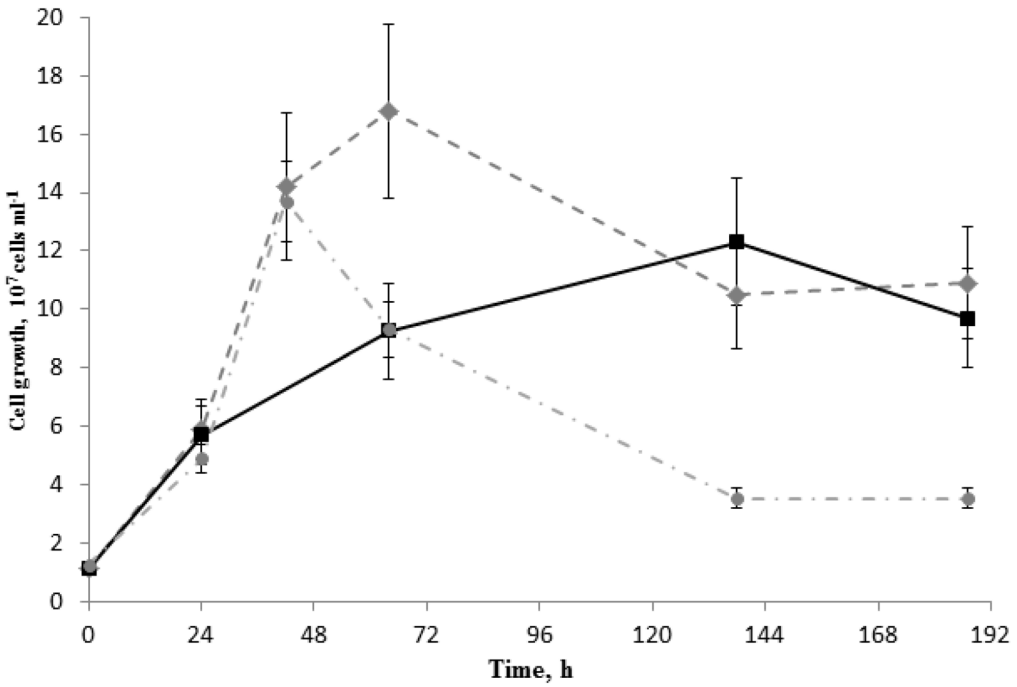

FIGURE 3 | Growth of *C. thermautotrophica* strain 019 with Fe(III)-containing silica mineral and rock on lactate under 100% CO. Diamonds – growth with glauconite at high E_h (–90 mV); squares – growth with diatomite at high E_h; circles – control growth without external electron acceptors at low E_h (–430 mV).

Phylogenetic Position of Strain 019

The average nucleotide identity (ANI) value between the genomes of strains 019 and 41^T, calculated using ANI calculator[7] with default parameters, was 99.7%; while the species-delimiting value, corresponding to the 70% level of *in vitro* DNA–DNA hybridization, is 95% (Goris et al., 2007). Thus, *in silico* hybridization of the genomes shows the affiliation of strains 019 and 41^T with the same species, *Carboxydocella thermautotrophica*.

Genomic Properties of *C. thermautotrophica* Strains 019 and 41^T

The genome of *C. thermautotrophica* type strain consists of one circular chromosome of a total length of 2690058 base pairs (49,14% GC content) and one circular plasmid of 53067 nucleotides (41% GC content). Read coverage of plasmid was 3.5 times higher than average chromosome coverage, suggesting 3–5 copies of plasmid per cell. The length of *C. thermautotrophica* strain 019 circular chromosome is 2676584 base pairs (49,14% GC content), and no plasmids have been identified in this strain.

For the *C. thermautotrophica* 041^T chromosome, 2810 genes were predicted, 2697 of which are protein-coding genes and 113 are RNA genes (**Table 1**). 65.5% of genes were assigned to at least one COG cluster with IMG annotation pipeline (Huntemann et al., 2015). The distribution of hits to COG functional categories is presented in **Supplementary Table S1**. Genome has five complete ribosomal operons with 16S rRNA genes showing at least 99.6% identity with each other. General genomic features of *C. thermautotrophica* strain 019 were similar to those of the type strain chromosome and are presented in **Table 1** and **Figure 6**.

The plasmid of strain 41^T encoded 51 proteins, 21 of their ORFs showed dispersed weak to moderate (23–58%) hits to the chromosome-encoded *in silico* proteomes of both strains, and two of the ORFs revealed weak hits to the proteome of strain 019 only. Little if any of these proteins are of clear metabolic relevance. Presence in the plasmid of the IS1182 mobile element, along with genes of restriction-modification system, suggests that it may be a selfish mobile element (Kobayashi, 2001; Koonin, 2011).

Comparative Genome Analysis of CO and Fe(III) Metabolism in *C. thermautotrophica* Strains 019 and 41^T

Oxidative Phosphorylation

A set of genes of the proton-translocating type I NADH-dehydrogenase (complex I) *nuoABCDHIJKLMN* is encoded in the same order by CFE_1311–1321 in strain 019 and CTH_1331–1341 in strain 41^T. Subunits NuoEFG, essential to provide the catalytic site for NADH oxidation, are encoded separately in both genomes: CFE_2217–2219 in strain 019 and CTH_2319–2321 in strain 41^T. NuoEFG proteins in both strains share

[7]http://enve-omics.ce.gatech.edu/ani/

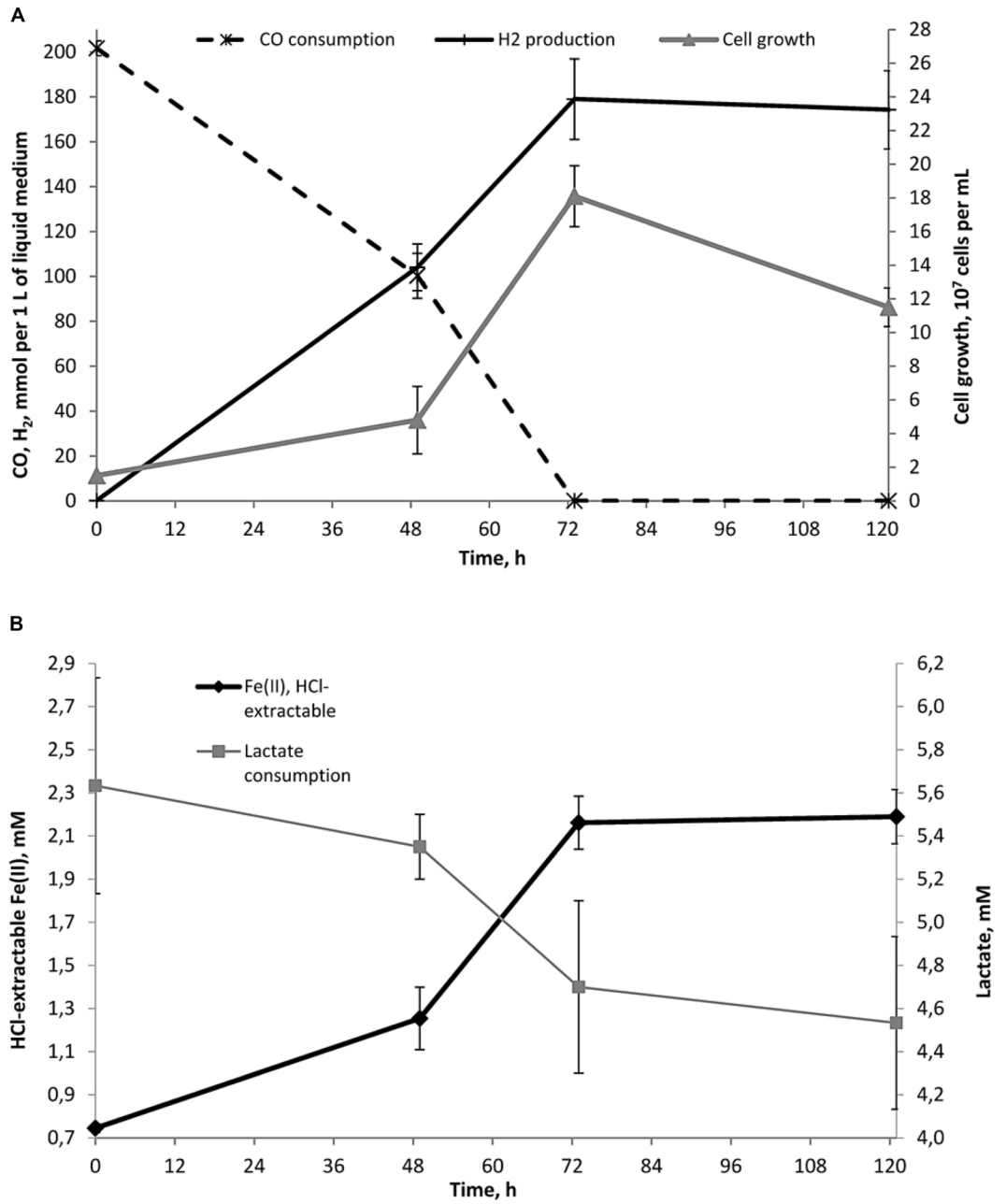

FIGURE 4 | Dynamics of growth, Fe(II) production, lactate consumption and concomitant hydrogenogenic carboxydotrophy of *C. thermautotrophica* strain 019 growing on CO and lactate with glauconite. **(A)** Cell growth, CO consumption and H_2 production; **(B)** lactate consumption and Fe(II) formation. No acetate production has been recorded during the growth with glauconite.

weak sequence similarity with their homologs from UniProt database. Gene clusters of the respiratory complex II (succinate dehydrogenase) are duplicated in both genomes (CFE_1726–1728 and CFE_2117–2119 in strain 019, and CTH_1740–1742 and CTH_2150–2152 in strain 41^T). Oxidative phosphorylation in both strains is performed via F_0F_1-type bacterial ATP-synthases, encoded by CFE_0343–0352 in strain 019 and CTH_0352–0361 in strain 41^T.

Inorganic Carbon Assimilation

Both *C. thermautotrophica* strains possess full sets of genes for the Wood–Ljungdahl pathway of inorganic carbon assimilation. The genes of the so-called Western (carbonyl) branch of the pathway and genes of the final steps of the Eastern (methyl) branch are encoded in each of the strains in a large gene cluster (**Supplementary Table S2**) similar to the *acs* gene cluster of *Moorella thermoacetica* ATCC 39073 (Pierce et al., 2008),

TABLE 1 | General features of replicons of *C. thermautotrophica* strains.

	C. thermautotrophica 019 chromosome	*C. thermautotrophica* 041^T chromosome	*C. thermautotrophica* 041^T plasmid
Replicon length, bp	2676584	2690058	53067
GC mol %	49.14	49.14	41.3
Number of genes	2809	2810	51
RNA genes	120	113	0
tRNA	71	73	0
rRNA	15	15	0
Protein-coding genes	2689	2697	51
Assigned to COG	1775	1787	14
Number of GIs	9	8	NA
Total length of GIs, bp	214072	211619	NA

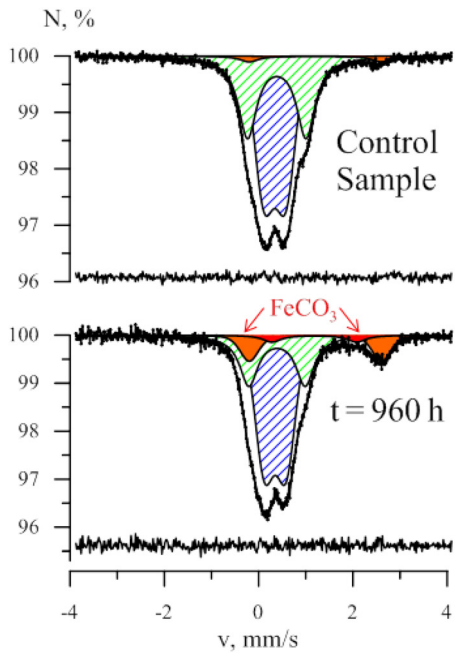

FIGURE 5 | Mössbauer spectra of the mineral phase formed in glauconite-reducing culture of *C. thermautotrophica* strain 019 grown with CO and lactate. Characteristic peaks of siderite are marked red. Samples of the mineral phase were collected for analysis at the 960th hour of incubation after complete cell lysis.

a model organism to study the Wood–Ljungdahl pathway. Interestingly, in *C. thermautotrophica* strains additional genes of methylenetetrahydrofolate reductase subunits MetVF are also present in a smaller gene cluster (**Supplementary Table S2**), and here they occur together with *hdrCBA* and *mvhD* genes, which in *M. thermoacetica* adjoin the *metVF* genes in the large *acs* cluster. Other Wood–Ljungdahl pathway genes of *C. thermautotrophica* strains are dispersed over the chromosomes (**Supplementary Table S2**), as it is in *M. thermoacetica*. Genes encoding key enzymes of other known autotrophic pathways (Fuchs, 2011; Nunoura et al., 2018; Mall et al., 2018) could not be found.

Both *C. thermautotrophica* strains also possess genes that might extend the anabolic function of the Wood–Ljungdahl pathway to the catabolic capacity for acetogenesis, including acetogenesis on $H_2 + CO_2$. The genomes harbor genes of phosphotransacetylase (two non-homologous genes in each genome) and acetate kinase (**Supplementary Table S2**), which provide for acetate and ATP production from acetyl-CoA and ADP + P_i, and genes encoding close homologs (49–73% amino acid sequence identity, **Supplementary Table S2**) of the subunits of enzymatic complexes that promote reductant balance and energy conservation during acetogenesis by *M. thermoacetica* (Schuchmann and Müller, 2014; Basen and Müller, 2017), including an energy converting hydrogenase additional to the CO-induced one, considered in the next subsection.

However, despite the apparent presence of all required acetogenesis determinants, we failed to obtain growth of strains 41^T and 019 on $H_2 + CO_2$ mixture or to detect acetate production during autotrophic growth under CO.

Genomic Determinants of Carboxydotrophy

A common metabolic feature of *C. thermautotrophica* strains is their ability to grow at the expense of hydrogenogenic oxidation of carbon monoxide. In the type strain 41^T, this ability appeared to be restricted by the redox potential of the culture medium, manifesting itself only at its low values. In contrast, strain 019 grew by CO oxidation also at relatively high E_h of −90 mV, but only in the presence of Fe(III) minerals, which were utilized as electron acceptors in parallel with protons.

Each of the genomes of *C. thermautotrophica* strains 41^T and 019 harbors six *cooS* genes, encoding anaerobic (Ni,Fe-containing) CODHs, and no genes encoding aerobic (Mo,Cu-containing) CODHs. Quite recently (see the "Discussion" section for the latest data), the highest number of [Ni,Fe]-CODHs encoded in available completely sequenced genomes was five, one of such few genomes belonging to the well-studied hydrogenogenic carboxydotroph *Carboxydothermus hydrogenoformans* (see Svetlitchnyi et al., 2004; Wu et al., 2005 for substantiation of the integrity of the *cooS3* gene in the original isolate of *C. hydrogenoformans*). The functional roles of the five [Ni,Fe]-CODHs of *C. hydrogenoformans* have been studied by various approaches, and for four of them functions have been established (Svetlitchnyi et al., 2001, 2004; Soboh et al., 2002; Hedderich, 2004; Wu et al., 2005). The phylogenetic relations

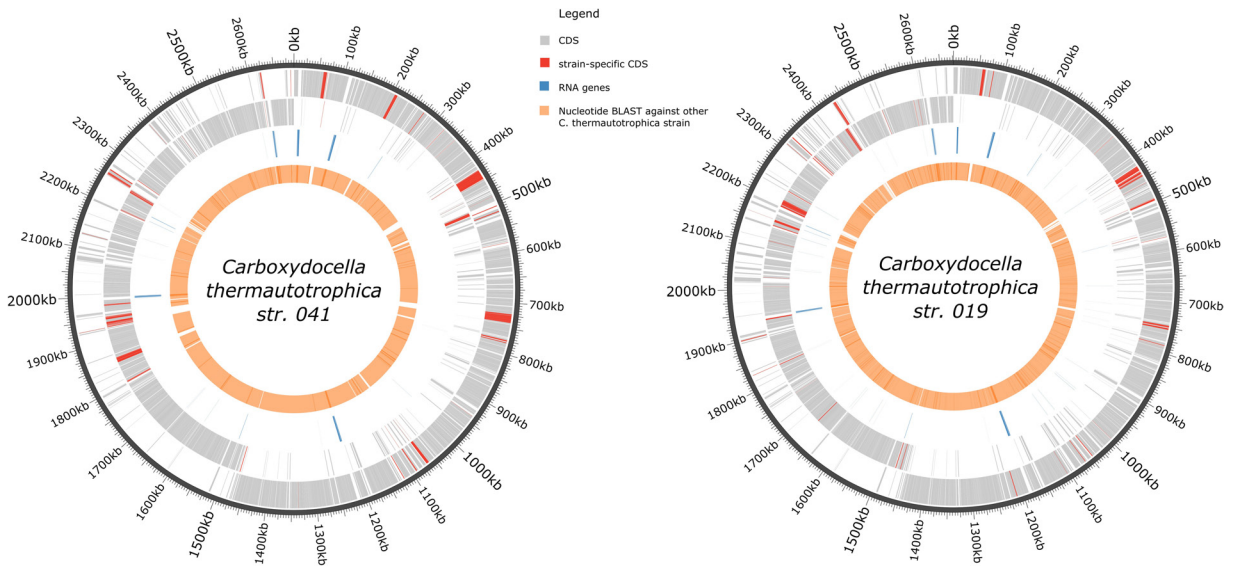

FIGURE 6 | Graphic representation of the genomes of *C. thermautotrophica* strains. Rings from outside to inside: genomic coordinates (dark gray); plus-strand common (gray) and strain-specific (red) CDSs; minus-strand common (gray) and strain-specific (red) CDSs; RNA genes (blue); blastn hits with e-value cutoff 10^{-5} vs. the other *C. thermautotrophica* strain.

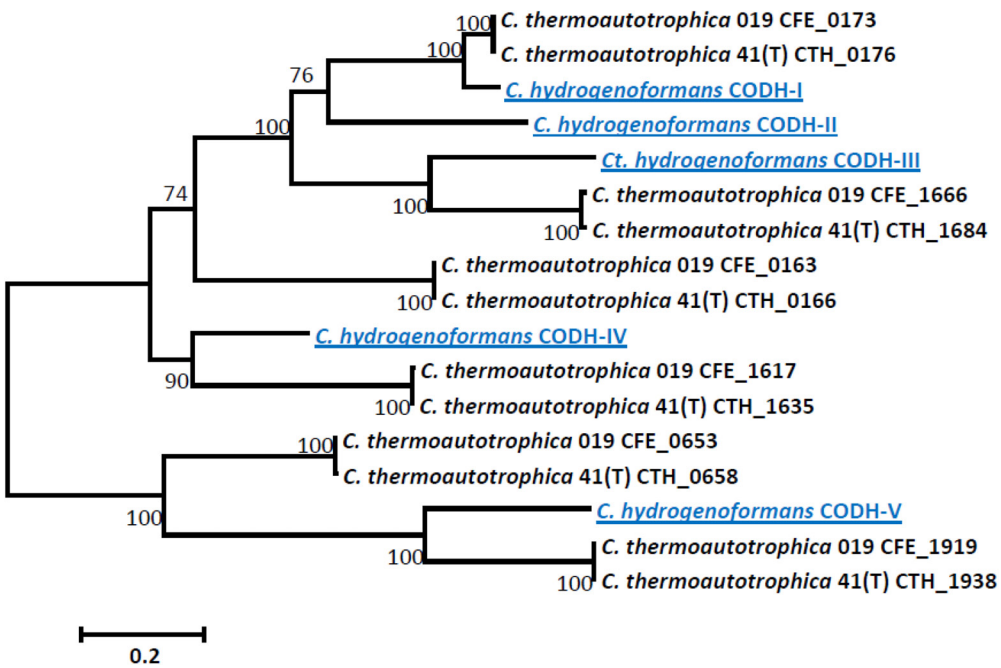

FIGURE 7 | Phylogenetic tree of *Carboxydocella thermautotrophica* [Ni,Fe]-CODHs. The tree was constructed by Maximum Likelihood method using MEGA6 (Tamura et al., 2013) at default parameters after aligning sequences with built-in Muscle at default parameters. Underlined blue are the [Ni,Fe]-CODHs of *Carboxydothermus hydrogenoformans*, which were used as references for function prediction.

C. thermautotrophica [Ni,Fe]-CODHs with the [Ni,Fe]-CODHs of *C. hydrogenoformans* are shown in **Figure 7**.

The roles of two [Ni,Fe]-CODHs in each *C. thermautotrophica* strain can be deduced from high similarity of their amino acid sequences and genomic contexts with [Ni,Fe]-CODH-I and [Ni,Fe]-CODH-III of *C. hydrogenoformans*. The *cooSI*-like genes CFE_0173 and CTH_0176 are parts of gene clusters (**Figure 8**) highly similar to the *C. hydrogenoformans* gene cluster that includes, along with *cooSI*, genes of an energy-converting hydrogenase (ECH) and is responsible for hydrogen formation

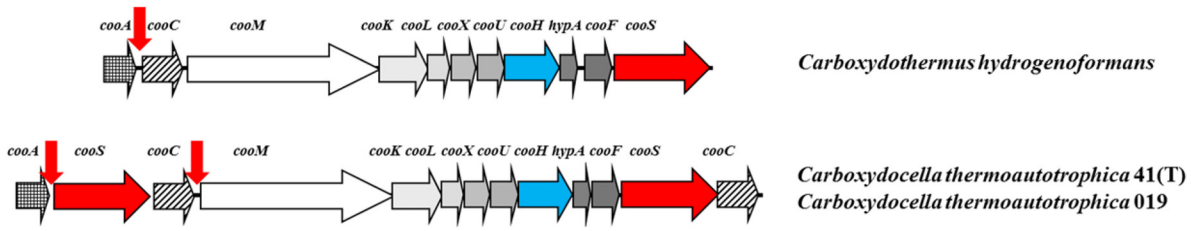

FIGURE 8 | Gene clusters determining hydrogenogenic carboxydotrophy in *Carboxydothermus hydrogenoformans* and *Carboxydocella thermautotrophica* strains 41^T and 019. *cooA*: gene of redox- and CO-sensitive transcriptional regulator; *cooS* (red horizontal arrow): [Ni,Fe]-CODH gene; *cooC*: gene of [Ni,Fe]-CODH accessory nickel-insertion protein; *cooMKLXUH*: genes of energy-converting hydrogenase (ECH); *hypA*: gene of hydrogenase maturation protein; *cooF*: gene of ferredoxin-like protein; *cooH* (blue horizontal arrow): gene of ECH catalytic subunit. Red vertical arrows show locations of CooA-binding sites. The locus tags for the gene clusters are CHY_1835-1824, CTH_0165-0177, and CFE_0162-0174. Note that the exact role of the upstream 'enigmatic' *cooSC* operon (CTH_0166-167 and CFE_0163-0164) in carboxydocellas remains unclear (refer to the text for details).

from CO + H_2O with transmembrane potential generation (Svetlitchnyi et al., 2001, 2004; Soboh et al., 2002; Hedderich, 2004). However, in the *C. thermautotrophica* strains this gene cluster has a more complicated pattern, including a second *cooC* gene in the downstream region and a second *cooS* gene (CFE_0163 and CTH_0166) in the upstream region, between the *cooC* gene and the *cooA* gene of the CO- and redox-sensing transcription regulator protein CooA (Roberts et al., 2001). This additional *cooS* gene does not have close homologs in *C. hydrogenoformans*.

The operon formula of the cluster in *C. thermautotrophica* strains is apparently *cooA-cooSC-cooMKLXUHhypAcooFSC-*, i.e., the two [Ni,Fe]-CODHs are encoded in distinct operons. However, these operons are evidently co-regulated by the above-mentioned CO- and redox-sensing regulator protein CooA. In both *C. thermautotrophica* strains, CooA-specific binding sites, conforming to the long-known consensus formula TGTCRNNNNNNYGACR (Fox et al., 1996), are located upstream of the *cooSC* and *cooMKLXUHhypAcooFSC* operons (**Figure 8**). The role of the *cooSC* operon is obscure, but the fact that it is regulated by CooA, sensing CO at low redox potential conditions (Roberts et al., 2001), provides grounds to speculate that the [Ni,Fe]-CODHs CFE_0163 and CTH_0166 have a role to play in CO oxidation with hydrogen production.

The [Ni,Fe]-CODHs of *C. thermautotrophica* strains that are similar to *C. hydrogenoformans* [Ni,Fe]-CODH-III, involved in the Wood–Ljungdahl pathway of acetyl-CoA synthesis from C1 units and low-potential reductants (Svetlitchnyi et al., 2004; Wu et al., 2005), are encoded by CTH_1684 in strain 41^T and CFE_1666 in strain 019. The genes of these [Ni,Fe]-CODHs occur in gene clusters (**Supplementary Table S2**) similar to the *acs* gene clusters of *C. hydrogenoformans* (Wu et al., 2005) and *M. thermoacetica* ATCC 39073 (Pierce et al., 2008). The genes of the Wood–Ljungdahl pathway, which evidently provides for the autotrophic capacity of *C. thermautotrophica* strains, are considered in more detail above, in the subsection Inorganic carbon assimilation.

The [Ni,Fe]-CODHs of *C. thermautotrophica* strains CFE_1617 and CTH_1635 are similar to the *C. hydrogenoformans* [Ni,Fe]-CODH-IV (**Figure 7**), thought to be involved in defense against oxidative stress (Wu et al., 2005). However, these *C. thermautotrophica* [Ni,Fe]-CODH genes differ in their genomic context from the *C. hydrogenoformans* [Ni,Fe]-CODH-IV gene: they are in gene clusters that do not include rubrerythrin gene, which in *C. hydrogenoformans* is thought to be responsible for the final step in a chain of reactions performing hydrogen peroxide reduction to water at the expense of electrons derived from CO. Thus, currently, we do not have any hypothesis about the role of the [Ni,Fe]-CODHs CFE_1617 and CTH_1635.

The remaining fifth and sixth [Ni,Fe]-CODHs of *C. thermautotrophica* strains (CFE_0653, CFE_1919, CTH_0658, CTH_1938) are similar to *C. hydrogenoformans*' [Ni,Fe]-CODH-V, whose function has not been even hypothetically supposed (Wu et al., 2005). CFE_0653 and CTH_0658 seem to be alone in their operons (judging from the 70-100 bp intergenic spaces upstream and downstream), and CFE_1919 and CTH_1938 are alone judging from the directions of transcription of the neighboring genes. Thus, we are unable to make any predictions about the functions of these [Ni,Fe]-CODHs from purely genomic analysis. Moreover, the genomically lone [Ni,Fe]-CODHs CFE_1919 and CTH_1938 have an altered pattern of the ligands of the active site [Ni-4Fe-5S] C-cluster (Dobbek et al., 2001): they lack the Cys295 residue (*C. hydrogenoformans* CooSII numbering), thought to be important for Ni-coordination in the C-cluster (Inoue et al., 2013).

Fe(III) Respiration

Screening of both *C. thermautotrophica* genomes revealed 30 genes in each strain possessing various *c*-type multiheme cytochrome domains. Almost all the encoded proteins are 99–100% identical in the two organisms (**Supplementary Table S3**). Four of the cytochrome genes comprise typical *nrfAH* loci of dissimilatory nitrite reductase complexes and were excluded from further screening of putative Fe(III) reductases. Some of the rest multiheme cytochrome genes could be involved in extracellular electron transfer chain. We found no homologs of putative quinol oxidizing multiheme CymA, regarded to initiate extracellular electron transfer in *S. oneidensis* (Coursolle and Gralnick, 2010). However, both *C. thermautotrophica* strains possess homologs of inner membrane cytochromes ImcH and CbcL from *G. sulfurreducens*, which have been shown to determine high- and low-potential pathways for metal reduction, respectively

(Levar et al., 2017). The homologs of ImcH are encoded by CFE_1714 in strain 019 and CTH_1728 in strain 041^T, located in identical clusters with two other multiheme cytochrome genes. The homologs of CbcL (Zacharoff et al., 2016) are encoded in two Cbc-like gene clusters in each *C. thermautotrophica* genome. Those are CFE_2192-2193 and CFE_2225-2226 in strain 019 and CTH_2221-2222 and CTH_2327-2328 in strain 041^T. In each of these clusters, one gene encodes a transmembrane *b*-type diheme domain protein, which could serve for quinol oxidation, and the other encodes a protein with a predicted transmembrane helix and a *c*-type multiheme domain facing the cell surface, which could accept electrons from the *b*-type cytochrome and initiate their further transfer to terminal Fe(III) reductases.

As described above, strain 041^T does not reduce any forms of Fe(III). Interestingly, among predicted *c*-type multihemes of *C. thermautotrophica* strains, only one 17-heme cytochrome was identified exclusively in the Fe(III)-reducing strain 019 (**Supplementary Table S3**). The protein is encoded by CFE_2239 downstream of a 15-heme and a hexaheme *c*-type cytochromes CFE_2242-2243 with unknown function and upstream of two cytochrome *c* maturation proteins and an *S*-layer homology domain-containing protein CFE_2230. The cytochrome CFE_2239 is predicted to contain signal peptide in its C-terminal part and no transmembrane helixes, and thus is likely to be a secreted protein. Topology prediction with CW-PRED service (Fimereli et al., 2012) indicates probable anchoring of CFE_2239 in the cell wall. However, the protein shares no homology with any of the outer surface cytochromes or proteins related to porin-cytochrome complexes that are suggested to perform the final step of extracellular electron transfer in *Shewanella* and *Geobacter* species (Coursolle and Gralnick, 2010; Aklujkar et al., 2013; Shi et al., 2016). The cytochrome CFE_2239 consists of two parts which are likely to have different origin and functions. In the cytochrome CFE_2239, putative catalytic N-terminal part (from 501st to 1486th amino acid residue) harbors all the 17 heme-binding motives organized in several conservative multiheme domains. It has distant homologs among many different multihemes, mainly of proteobacterial origin. Phylogeny reconstruction indicates (**Supplementary Figure S3**) that this putative catalytic domain could have been acquired by horizontal gene transfer from *Geobacter* species. The C-terminal part of the protein CFE_2239 was not reliably predicted to contain homologs of any conservative protein domains, however, the search against SwissProt database revealed a few weak homologs among bacterial adhesin proteins and eukaryotic secreted proteins involved in receptor-ligand interactions and adhesion.

DISCUSSION

Bacteria of the genus *Carboxydocella* represent a distinct metabolic group of thermophilic hydrogenogenic carboxydotrophs (Sokolova et al., 2009). The members of this group are either obligately dependent on CO or capable of gaining energy using other catabolic processes (fermentation or different types of anaerobic respiration). Three species of the genus *Carboxydocella* have been isolated from various thermal habitats of Kamchatka peninsula (Sokolova et al., 2002; Slepova et al., 2006; Slobodkina et al., 2012). The metabolism of these organisms differs significantly (**Supplementary Table S4**). Our new isolate 019, obtained from a core sample near Zavarzin thermal pool at Uzon Caldera, shares some features with all validly described *Carboxydocella* species. However, it belongs phylogenetically to the species with the type strain of which it has the lowest number of common metabolic features: in contrast to strain 019, *C. thermautotrophica* 41^T can only grow autotrophically and cannot reduce Fe(III). Two metabolic processes are manifestly common to both *C. thermautotrophica* strains – those are inorganic carbon assimilation and hydrogenogenic carboxydotrophy.

Diversity of CO-Dehydrogenases

The genomes of *C. thermautotrophica* strains 41^T and 019 encode six [Ni,Fe]-CODHs each. Until the recent isolation and genomic study of *Calderihabitans maritimus* (six [Ni,Fe]-CODH genes, including one frameshifted gene (Omae et al., 2017), and the publication of the genome of *Clostridium formicaceticum* (six [Ni,Fe]-CODH genes, CP020559.1, Karl et al., 2017), the highest number of [Ni,Fe]-CODHs encoded in available completely sequenced genomes was five. Our analysis performed in April 2018 by tblastn in the NCBI Complete Prokaryote Genome Database (20,008 genomes) revealed 379 genomes encoding at least one [Ni,Fe]-CODH; of them, 208 genomes encoded more than one [Ni,Fe]-CODH. Six genomes encoded five [Ni,Fe]-CODHs each, and the genome of *Clostridium formicaceticum* encoded six [Ni,Fe]-CODHs. Thus, the genomes of *C. thermautotrophica* strains are top-ranking with respect to the number of [Ni,Fe]-CODHs encoded.

The functional roles of multiple [Ni,Fe]-CODHs have been best studied in *Carboxydothermus hydrogenoformans*, and to four of them functions have been ascribed (Svetlitchnyi et al., 2001, 2004; Soboh et al., 2002; Hedderich, 2004; Wu et al., 2005). Based on comparison of amino acid sequences and genomic contexts, we managed to ascribe functions to only two of the six [Ni,Fe]-CODHs in each of the *C. thermautotrophica* strains and to tentatively suppose a possible role for one more [Ni,Fe]-CODH in each strain.

The [Ni,Fe]-CODH encoded immediately adjacent to ECH genes (apparently in a single operon) is evidently responsible in *C. thermautotrophica* strains for hydrogen formation from $CO + H_2O$ with transmembrane potential generation. [Ni,Fe]-CODH–ECH gene clusters occur in all of the sequenced genomes of hydrogenogenic carboxydotrophs, the only exception known so far being *Carboxydothermus pertinax* Ug1 (Fukuyama et al., 2017). Three types of such gene clusters have been described, composed of homologous genes that, however, differ in their order and phylogeny (genes specific to a particular cluster type are quite few). The gene cluster found in the genomes of *C. thermautotrophica* strains belongs to the long-known *coo*-type gene cluster. The first [Ni,Fe]-CODH–ECH gene cluster to be described was the *coo* gene cluster of *Rhodospirillum rubrum* S1^T (Fox et al., 1996; Kerby et al., 1997). Similar (*coo*-type) gene clusters were then described in *C. hydrogenoformans*

Z-2901^T (Soboh et al., 2002; Wu et al., 2005) (**Figure 8**), *Thermosinus carboxydivorans* Nor1^T (Techtmann et al., 2012), *Desulfotomaculum caboxydivorans* CO-1-SRB^T (Visser et al., 2014), *Calderihabitans maritimus* KKC1 (Omae et al., 2017), and mentioned to occur in *Carboxydothermus islandicus* SET (Fukuyama et al., 2017). Gene clusters of *coo*-type also occur in the genomes of some other hydrogenogenic carboxydotrophs ('*Thermincola potens*' JR (CP002028.1), *Thermincola ferriacetica* Z-0001^T (LGTE00000000)), as well as in some bacteria for which the capacity has not been tested. A peculiar variant of the *coo* gene cluster was described in *Rubrivivax gelatinosus* CBS (Wawrousek et al., 2014). Also known are two other types of [Ni,Fe]-CODH–ECH gene clusters that differ from the *coo* cluster in the order of homologous genes and their phylogeny. One was found in *Caldanaerobacter subterraneus* subspecies (Sant'Anna et al., 2015), and the other was revealed in several representatives of the archaeal genus *Thermococcus* (Lim et al., 2010; Kozhevnikova et al., 2016; Oger et al., 2016). Some of the organisms harboring the gene clusters of the latter two types are known to be capable of hydrogenogenic carboxydotrophy, for others the capacity has not been tested.

Thus, the [Ni,Fe]-CODH–ECH gene cluster peculiar to *C. thermautotrophica* strains belongs to the long-known, best studied, and most widely occurring *coo*-type gene clusters. However, in the *C. thermautotrophica* strains this gene cluster has a more complicated pattern; in particular, it includes a second *cooS* gene in an adjacent and apparently co-regulated *cooSC* operon. This co-regulation, performed by the CO- and redox-sensing transcription regulator protein CooA, provides grounds to speculate that this enigmatic [Ni,Fe]-CODH (CFE_0163 in strain 019 or CTH_0166 in strain 41^T), which does not have close homologs in *C. hydrogenoformans* or in finished genomes represented in the NCBI nr database, has a role to play in CO oxidation with hydrogen production. It was shown by Soboh et al. (2002) that the CO-oxidizing:H_2-evolving enzyme complex that these authors isolated from *C. hydrogenoformans* contained both CooS1 and CooS2 at a ratio of about 10:1, although the main function of CooS2 has been proposed to be generation of NADPH for anabolic purposes (Svetlitchnyi et al., 2001). The physiological relevance of the dual composition of the [Ni,Fe]-CODH–ECH enzymatic complex has not been discussed; and we can only mention that CooS1 and CooS2 do not differ significantly in their apparent K_m values (Svetlitchnyi et al., 2001). No close homologs of CooS2 are encoded in the genomes of *C. thermautotrophica* strains, and it is possible that the discussed 'enigmatic' [Ni,Fe]-CODH encoded upstream of the [Ni,Fe]-CODH–ECH gene cluster is a minor substitute in the CO-oxidizing:H_2-evolving enzyme complex of *C. thermautotrophica.*

None of the other *C. thermautotrophica* [Ni,Fe]-CODHs seem to be co-regulated with the CO-oxidizing:H_2-evolving enzyme complex, since no CooA-binding sites could be found in proximity of other [Ni,Fe]-CODH genes. Moreover, since the CooA transcription regulator is sensitive both to CO and redox conditions, it may be speculated that the remaining four [Ni,Fe]-CODHs are expressed and active both in the absence and in the presence of electron acceptors other than proton [nitrate for both strains, nitrate or Fe(III) for strain 019]. However, only for one of these [Ni,Fe]-CODHs can we predict function from sequence comparisons with well-studied [Ni,Fe]-CODHs and from genomic context. This [Ni,Fe]-CODH (CTH_1684 and CFE_1666) must be involved in the Wood–Ljungdahl pathway. Interestingly, in some hydrogenogenic autotrophic carboxydotrophs the gene encoding this [Ni,Fe]-CODH becomes frameshifted as a result of cultivation at high CO concentrations. The laboratory-acquired origin of the frameshift and its cause are evident for *C. hydrogenoformans* (Svetlitchnyi et al., 2004; Wu et al., 2005) and can be supposed for *Calderihabitans maritimus*. Svetlitchnyi et al. (2004) showed that in a *C. hydrogenoformans* strain variant with non-frameshifted [Ni,Fe]-CODH, acetyl-CoA synthase existed predominantly as monomer at high CO concentrations and used exogenous CO instead of the CO produced from CO_2 by the [Ni,Fe]-CODH. Such one-step assimilation of CO should be more beneficial. In the *C. thermautotrophica* strains the [Ni,Fe]-CODHs involved in the Wood–Ljungdahl pathway are not impaired despite repeated culture transfers under 100% CO.

In *M. thermoacetica* the Wood–Ljungdahl pathway plays the roles of both carbon assimilation and energy generation, depending on whether acetyl-CoA is further carboxylated or converted to acetate with ATP formation (Pierce et al., 2008). *C. hydrogenoformans* has been reported (Henstra and Stams, 2011) to switch to acetogenesis from CO under conditions where hydrogen production from CO becomes thermodynamically unfavorable (low substrate and high product concentrations). Both *C. thermautotrophica* strains possess genes closely homologous to those thought to be responsible for the acetogenic growth of *M. thermoacetica* (Schuchmann and Müller, 2014; Basen and Müller, 2017). Especially remarkable is that each of their genomes encodes two methylenetetrahydrofolate reductase homologs and that one of these *metVF* gene variants is clustered with *hdrCBA* and *mvhD* genes, indicative of the formation of the HdrCBA+MetVF+ MvhD methylenetetrahydrofolate-reducing electron-bifurcating complex, which is highly efficient in terms of bioenergetics since it produces low-potential reductant (Mock et al., 2014).

The genomes of each of the *C. thermautotrophica* strains encoded three [Ni,Fe]-CODHs for which we could not predict or suppose a definite function. We can only make some very general comments about the remaining [Ni,Fe]-CODHs. In both strains, particular [Ni,Fe]-CODH(s) may be involved in autotrophic carboxylation reactions that follow acetyl-CoA synthesis, supplying reducing equivalents to carboxylating enzymes, as it was supposed for one of the [Ni,Fe]-CODHs of *Calderihabitans maritimus* based on the genomic proximity of its gene with genes of ferredoxin:oxoacid oxidoreductase (Omae et al., 2017). However, in case of the *C. thermautotrophica* strains, there are no such hints from the genomic contexts.

Anyway, it is evident that CO is an important nutrient in the natural habitat of the *C. thermautotrophica* strains, and they largely base on it their survival strategy.

Physiology of Fe(III) Reduction

The most intriguing physiological feature of *C. thermautotrophica* strain 019 appeared to be dissimilatory reduction of Fe(III) from minerals, which is obviously coupled to hydrogenogenic CO oxidation. Minerals of Fe(III) are the only form of electron acceptors sustaining *C. thermautotrophica* growth at elevated E_h of −90 mV (**Figure 1**). Hydrogenogenic carboxydotrophy with protons as electron acceptors was exclusively performed by the organism under strongly reduced conditions (−430 mV). Notably, strain 019 appeared to reduce structural Fe(III) from silica mineral glauconite. This process has not been previously reported in Fe(III) reducers. In our recent report, we have demonstrated oxidation of structural Fe(II) but not the reduction of Fe(III) from glauconite by the alkaliphilic dissimilatory iron-reducer *Geoalkalibacter ferrihydriticus* during acetogenic growth (Zavarzina et al., 2016). In contrast to that finding, *C. thermautotrophica* performed the reduction of structural Fe(III) from the same mineral, as clearly indicated by the formation of siderite (**Figure 5**) and the increase of extractable Fe(II) concentration (**Figure 4**) during strain 019 cultivation with glauconite. Achievement of the highest possible Fe(II) content of glauconite during its reduction is clearly marked by decreased line width of Mössbauer spectra (**Supplementary Figure S2**, Inlay), which is an indicator of the decrease in the ordering of glauconite crystal lattice. Such disordering results from the attack of Fe^{3+} atoms at the mineral surface, e.g., by bacterial redox systems. Further increase in Mössbauer spectral line width and Fe(II) content of the mineral after the start of cell lysis could be explained by the formation of new solid phase siderite (**Supplementary Figure S2**). No such changes were observed in abiotic controls, indicating biologically induced process of siderite formation, which, however, is not directly controlled by the redox systems of live cells and proceeds after their lysis.

The reduction of mixed valence Fe(III/II) silica minerals and the oxic Fe(III) mineral ferrihydrite have different impacts on the metabolism of strain 019. When Fe(III) was provided as an electron acceptor in the form of ferrihydrite, cultures of strain 019 revealed two clearly distinguishable growth phases. During the first 24-h phase with high initial E_h and low initial Fe(II) content, maximal growth rate correlated with maximal rates of Fe(III) reduction, lactate conversion to acetate and low rates of carboxydotrophy and hydrogen formation. The second phase started upon accumulation of Fe(II) and concomitant E_h decrease. This 'high Fe(II)' phase was characterized by pronounced slowdown of growth and Fe(II) formation, but at the same time, the rate of hydrogenogenic carboxydotrophy increased to its maximum.

We may assume that during the first stage of growth both CO and lactate could be simultaneously utilized as electron donors for Fe(III) reduction in parallel with hydrogenogenic carboxydotrophy. Accordingly, three reactions are likely to sustain the growth of strain 019 at this stage:

$$C_3H_5O_3^- + H_2O + 4Fe^{3+} \rightarrow C_2H_3O_2^- + CO_2 + 4Fe^{2+} + 4H^+, \quad (1)$$

$$CO + H_2O + 2Fe^{3+} \rightarrow CO_2 + 2Fe^{2+} + 2H^+, \quad (2)$$

$$CO + H_2O \rightarrow CO_2 + H_2 \quad (3)$$

Data on metabolite concentrations (**Figure 2**) allow us to propose the following brutto-equation for energy metabolism of strain 019 at the first stage of its growth on CO and lactate with ferrihydrite:

$$C_3H_5O_3^- + 30CO + 31H_2O + 30Fe^{3+} \rightarrow C_2H_3O_2^- + 31CO_2 + 30Fe^{2+} + 30H^+ + 17H_2 \quad (4)$$

Given that each lactate molecule donates 4 electrons to Fe^{3+} and each CO molecule donates 2 electrons to either Fe^{3+} or H^+, reaction (4) implies that the ratio of carbon monoxide spent for iron(III) reduction and for hydrogenogenesis was 13:17, i.e., about 43% of the consumed carbon monoxide was utilized for Fe(III) reduction during the first phase of growth of strain 019 with ferrihydrite and CO. Protons produced in this reaction could be translocated by type I NADH-dehydrogenase or ECH complexes. During further growth of the culture, when Fe(II) accumulates and E_h decreases, hydrogenogenic carboxydotrophy becomes much more active and seems to play the major role in the energy metabolism of strain 019 (**Figure 2**). Indeed, redox-control of the [Ni,Fe]-CODH–ECH cluster transcription in *C. thermautotrophica* via CooA regulator could restrict employment of this energy generating complex under high E_h growth conditions. On the other hand, both *C. thermautotrophica* strains possess four more [Ni,Fe]-CODH clusters which do not depend on CooA and thus on low redox potential. At least three of those could be active at elevated E_h being coupled to Fe(III) reduction in yet unknown way. Formation of magnetite during cell growth coupled to ferrihydrite reduction decreases E_h down to −360 mV and switches on the [Ni,Fe]-CODH–ECH energy generating complex at the second, 'high Fe(II),' growth phase of strain 019. As the [Ni,Fe]-CODH–ECH complex deals with soluble electron donor and acceptor inside the cell and includes a single step proton translocation via ECH, it outcompetes the more complicated Fe(III)-reducing extracellular electron transfer pathway for electrons derived from CO oxidation. Metabolite concentrations monitoring (**Figure 2**) allows us to propose the following brutto-equation for the 'high Fe(II)' phase of strain 019 growth with ferrihydrite, lactate and CO:

$$C_3H_5O_3^- + 270CO + 271H_2O + 10Fe^{3+} \rightarrow C_2H_3O_2^- + 271CO_2 + 10Fe^{2+} + 10H^+ + 267H_2 \quad (5)$$

This reaction, in contrast to reaction (4), implies that the main portion of carbon monoxide consumed during the second growth phase of strain 019 was spent for hydrogenogenesis, and only 1% of it (3 moles of 270) was utilized for ferrihydrite reduction. This switch of the electron acceptor for CO oxidation from Fe(III) to more accessible but less energetically favorable intracellular protons, together with magnetite accumulation, which restricts the access of the cells to Fe(III) atoms on the mineral surface, decreases the growth rate of the organism at high Fe(II) content, in spite of intensified consumption of CO and lactate.

Key Role of CO in Fe(III) Reduction

The inability of strain 019 to reduce any forms of Fe(III) with lactate in the absence of CO indicates the key metabolic role of carbon monoxide utilization pathways in the organism. In particular, even lactate utilization is likely linked to [Ni,Fe]-CODH activity. Lactate enters the metabolic network of *C. thermautotrophica* via pyruvate-forming lactate dehydrogenase. Pyruvate can be converted to formate and acetyl-CoA by pyruvate-formate lyase (formate *C*-acetyltransferase, CFE_0574-575). Formate in its turn could further enter Wood–Ljungdahl pathway via formate-tetrahydrofolate ligase (CFE_0088) and finally be condensed with a CO molecule by the ACS complex (**Supplementary Table S2**) to form acetyl-CoA, which is then converted to acetate with substrate-level phosphorylation (**Supplementary Table S2**). Previously, acetogenesis from formate and CO via the Wood–Ljungdahl pathway has been proposed for the acetogen *Acetobacterium woodii* (Bertsch and Müller, 2015). *C. thermautotrophica* strains possess all the necessary genes for acetogenesis (**Supplementary Table S2**), including those of the HdrCBA+MetVF+MvhD electron-bifurcating complex, which does not seem to be crucial when the energy requirements are covered by hydrogenogenesis from CO, but is highly efficient in case of acetogenesis. In our experiments, conditions favoring acetogenesis by *C. thermautotrophica* strain 019 seem to have existed in the high E_h culture medium, when the activity of [Ni,Fe]-CODH–ECH was restricted by redox potential. However, from purely genomic analysis, it is difficult to predict whether or not the acetyl-CoA synthase of *C. thermautotrophica* strains can directly use exogenous CO under certain conditions. One should also remember that Fe(III) is indispensable electron acceptor for *C. thermautotrophica* at elevated E_h, and that metabolic link between acetogenesis and Fe(III) reduction in this organism remains to be understood.

Of note is the fact that during organotrophic growth with the Fe(III)-mica mineral glauconite there was no acetate production, and maximal rates of growth, carboxydotrophy, lactate consumption and Fe(III) reduction were observed simultaneously. The most probable cause is the ferrous iron content of the mixed valence mineral glauconite. This Fe(II) could act as an immobilized reductant rapidly decreasing redox potential of the culture medium in the close vicinity of mineral particles and thus stimulating redox-controlled carboxydotrophic growth of the organism. Such a decrease of the E_h value in the medium containing both ferric and ferrous iron mineral forms is enhanced by growing cultures, as revealed in our control experiment with a ferrihydrite/magnetite mixture. In contrast to ferrihydrite, glauconite did not stimulate autotrophic growth of strain 019 on CO (**Figure 1**). This fact indicates that glauconite reduction is not as energetically favorable as ferrihydrite reduction, and Fe(II) production from glauconite is rather caused by secondary activity of the extracellular electron transfer chain of strain 019. The absence of acetate production during growth on lactate with glauconite and CO, as well as the cessation of Fe(III) reduction from glauconite upon exhaustion of CO, indicate that carbon monoxide serves as the only electron donor for the reduction of this mica mineral.

Genomic Determinants of Extracellular Electron Transfer to Fe(III) Minerals

Utilization of Fe(III) minerals as electron acceptors is challenging and requires extracellular electron transfer chain to be established between enzymatic respiratory system of an organism and Fe atoms on the mineral surface or in the silicate lattice. Crystalline Fe-silicate minerals are less energetically favorable electron acceptors than amorphous or poorly crystalline Fe(III) oxyhydroxides. Nonetheless, the reduction of structural Fe(III) within phyllosilicate clay minerals has been documented for mesophilic, thermophilic and hyperthermophilic microorganisms (Kashefi et al., 2008; Pentráková et al., 2013). However, molecular mechanisms of this process remain poorly understood, as well as no information is still available on microbial reduction of Fe(III) within mica minerals, which are widespread in the Earth's crust, being precursors of clay minerals in weathering processes. Comprehensively studied are the mechanisms of Fe(III) reduction from oxyhydroxides, such as ferrihydrite. Key genes determining the extracellular electron transfer to these minerals have been revealed and their products have been extensively characterized in model mesophilic proteobacteria (Shi et al., 2016). Extensive data on biochemical mechanisms for Fe(III) oxide reduction have also been obtained for two thermophilic Firmicutes (Carlson et al., 2012; Gavrilov et al., 2012) and three hyperthermophilic archaea of the family *Archaeoglobaceae* (Manzella et al., 2015; Mardanov et al., 2015; Smith et al., 2015), although their pathways for extracellular electron transfer remain less studied than in mesophilic models. In all the mentioned organisms three major groups of multiheme *c*-type cytochromes are considered to drive dissimilatory Fe(III) reduction (Shi et al., 2016), those are: cytochromes associated with the cytoplasmic membrane that accept electrons from the quinone pool of the electron transfer chain; intermediate electron-shuttling cytochromes; and a group of cytochromes associated with the outer membrane (or the *S*-layer), which accept electrons from the shuttles and transfer them to an Fe(III) oxide contacting the cell surface (Xiong et al., 2006; Zhang et al., 2008). Terminal step of electron transfer to Fe(III) oxides is regarded to be provided by porin-cytochrome complexes of pcc-type, first described in *Geobacter* species, or Mtr-type, first described in Fe-reducing *Shewanella* spp. Such complexes, albeit not related phylogenetically to each other, have been recently shown to be widespread among various Fe(III)-reducing and Fe(II)-oxidizing prokaryotes (see White et al., 2016 for review), although it is still unclear whether these complexes are universal for all the prokaryotes reducing Fe(III) from insoluble forms. In our work, comparative genome analysis of two strains of a single species, which differ from each other by the ability to reduce Fe(III), revealed the only gene of a cytochrome which exclusively exists in the genome of the iron-reducing strain 019. Thus, this cytochrome is supposed to determine the ability to reduce Fe(III) from both high-potential iron oxides and low-potential Fe-mica minerals. This gene appeared to encode a secreted multiheme *c*-type cytochrome which

shares no homology with any of the components of porin-cytochrome complexes, although its heme-containing part does share homology with some cytochromes of *Geobacter* species. The C-terminus of the putative terminal Fe(III) reductase gene of strain 019 is homologous to secreted adhesins but not to porins or any other beta-barrel structures inherent in porin-cytochrome complexes involved in redox cycling of iron. We assume the putative Fe(III) reductase of strain 019 (CFE_2239) to appear by a fusion of genes encoding an adhesion protein and a cytochrome acquired from deltaproteobacteria by horizontal gene transfer. Most probable source organisms of this cytochrome gene belong to *Geobacteraceae* family (**Supplementary Figure S3**), well known for their Fe(III) reducing activity. This correlates with ecological data indicating proteobacteria to comprise 3–6% of prokaryotic diversity in Zavarzin hot spring (Gumerov et al., 2011; Rozanov et al., 2014), adjoining the natural habitat of strain 019. However, the reduction of structural Fe(III) from mica minerals has not been previously reported either in geobacters or in any other Fe(III) reducers.

Acquiring an Fe(III) reductase that is able to interact with Fe(III)-mica minerals by *C. thermautotrophica* strain 019 significantly impacts the fitness of this species in an unstable hydrothermal environment. Fe(III) is the only electron acceptor that allows the organism to proliferate at elevated redox values and utilize various organic and inorganic carbon sources and electron donors, depending on their availability. The presence of genes which are supposed to determine high- and low-potential pathways for extracellular electron transfer (ImcH-like and CbcL-like cytochromes) in strain 019 makes the organism less dependent on the form of Fe(III) available. So, upon oxygenation of the environment, enhancing the formation of Fe(III) oxides, the organism can utilize these high-potential electron acceptors both for energy conservation and redox control of its ecological microniche via Fe(II) production. A decrease of redox potential would not inhibit iron reduction in the organism, as its catabolism can be switched to another pathway for extracellular electron transfer – to a low-potential form of the acceptor, namely, to the structural Fe(III) of mica minerals, which are abundant in sedimentary environments. Both pathways for the reduction of Fe(III) minerals could be linked to the electron transfer chain in the cell membrane by CbcL-like quinol-oxidizing multiheme cytochrome complexes. Details of these pathways for Fe(III) reduction are to be studied further.

CONCLUSION

Our results improve current knowledge on metabolic features of deeply branching Clostridia, and indicate possible ecological importance of *C. thermautotrophica* in its sedimentary thermal habitats. For the first time dissimilatory reduction of structural Fe(III) from ubiquitous silicate mineral glauconite is described.

Genome analysis provided insights in such ecologically relevant properties of *C. thermautotrophica* as hydrogenogenic CO-trophy and Fe(III) reduction. An outstanding number of CO dehydrogenases and a novel type of putative terminal reductase of insoluble Fe(III) compounds have been identified in the organism.

The variety of [Ni,Fe]-CODHs in both *C. thermautotrophica* genomes is supposed to reflect high affinity of the species to this substrate, which is common gaseous component of sedimentary environments of volcanic origin. Fe(III) reducing ability of strain 019 allows it to couple carboxydotrophy with utilization of this high-potential electron acceptor in anoxic sediments. In a more global scale, coupling of Fe(III) reduction with CO oxidation by *C. thermautotrophica* hardwires the electron flow from carbon monoxide to the mineral constituent of the environment that could be further used as an electrical conductor, facilitating direct interspecies electron transfer ("DIET"), or as an electron-storage material, which supports microbial metabolism of other community members (Shi et al., 2016) and could be called a "biogeobattery."

The difference in the ability of two *C. thermautotrophica* strains to reduce Fe(III) correlates with peculiar ecological factors encouraging strain 019 to evolve or acquire the determinants of extracellular electron transfer to Fe(III) minerals. While strain 41^T was isolated from the surface layer of hot spring sediments (Sokolova et al., 2002), strain 019 was obtained from a transition (anaerobic to aerobic) zone of a core rich in Fe-bearing silicates (Rozanov et al., 2014). Further on, a biofilm-like lifestyle in a sedimentary environment with restricted free volume of the mineral phase and tight cell-to-cell contacts favor horizontal gene transfer (Madsen et al., 2012).

Further ecological studies are needed to assess the distribution of *C. thermautotrophica* and prokaryotes with similar phenotypes in various terrestrial hydrothermal vents, widely represented on the Eurasian continent. This would help to estimate the global role of microbial processes coupling the transformation of carbon monoxide and one of the key components of the Earth's crust, mica minerals.

AUTHOR CONTRIBUTIONS

SG, TS, and EB-O convened the research. ST, TS, DZ, AL, and SG designed the research. TS, DZ, and SG performed the cultivation studies. NC and VR performed the Mössbauer studies. ST, AK, and AT performed the genome sequencing and assembling. AL, ST, SG, and IK performed the genome analysis. ST, TS, DZ, NC, EB-O, IK, AL, and SG wrote the manuscript.

FUNDING

The work of ST, TS, DZ, EB-O, IK, AL, and SG was supported by the RSF project # 17-74-30025.

SUPPLEMENTARY MATERIAL

The Supplementary Material for this article can be found online at: https://www.frontiersin.org/articles/10.3389/fmicb.2018.01759/full#supplementary-material

REFERENCES

Aklujkar, M., Coppi, M. V., Leang, C., Kim, B. C., Chavan, M. A., Perpetua, L. A., et al. (2013). Proteins involved in electron transfer to Fe(III) and Mn(IV) oxides by *Geobacter sulfurreducens* and *Geobacter uraniireducens*. *Microbiology* 159, 515–535. doi: 10.1099/mic.0.064089-0

Allard, P., Burton, M., and Muré, F. (2004). High resolution FTIR sensing of magmatic gas composition during explosive eruption of primitive Etna basalt. *Geophys. Res. Abstr.* 6:6493.

Balk, M., Heilig, H. G. H. J., van Eekert, M. H. A., van Stams, A. J. M., van Rijpstra, I. C., van Sinninghe-Damsté, J. S., et al. (2009). Isolation and characterization of a new CO-utilizing strain, *Thermoanaerobacter thermohydrosulfuricus* subsp. carboxydovorans, isolated from a geothermal spring in Turkey. *Extremophiles* 13, 885–894. doi: 10.1007/s00792-009-0276-9

Basen, M., and Müller, V. (2017). "Hot" acetogenesis. *Extremophiles* 21, 15–26. doi: 10.1007/s00792-016-0873-3

Bertsch, J., and Müller, V. (2015). CO metabolism in the acetogen *Acetobacterium woodii*. *Appl. Environ. Microbiol.* 81, 5949–5956. doi: 10.1128/AEM.01772-15

Brady, A. L., Sharp, C. E., Grasby, S. E., and Dunfield, P. F. (2015). Anaerobic carboxydotrophic bacteria in geothermal springs identified using stable isotope probing. *Front. Microbiol.* 6:897. doi: 10.3389/fmicb.2015.00897

Brookshaw, D. R., Coker, V. S., Lloyd, J. R., Vaughan, D. J., and Pattrick, R. A. D. (2014a). Redox interactions between Cr(VI) and Fe(II) in bioreduced biotite and chlorite. *Environ. Sci. Technol.* 48, 11337–11342. doi: 10.1021/es5031849

Brookshaw, D. R., Lloyd, J. R., Vaughan, D. J., and Pattrick, R. A. D. (2014b). Bioreduction of biotite and chlorite by a *Shewanella* species. *Am. Mineral.* 99, 1746–1754. doi: 10.2138/am.2014.4774ccby

Butler, J., MacCallum, I., Kleber, M., Shlyakhter, I. A., Belmonte, M. K., Lander, E. S., et al. (2008). ALLPATHS: *de novo* assembly of whole-genome shotgun microreads. *Genome Res.* 18, 810–820. doi: 10.1101/gr.7337908

Carlson, H. K., Iavarone, A. T., Gorur, A., Yeo, B. S., Tran, R., Melnyk, R. A., et al. (2012). Surface multiheme c-type cytochromes from *Thermincola potens* and implications for respiratory metal reduction by Gram-positive bacteria. *Proc. Natl. Acad. Sci. U.S.A.* 109, 1702–1707. doi: 10.1073/pnas.1112905109

Chen, I. M. A., Markowitz, V. M., Chu, K., Palaniappan, K., Szeto, E., Pillay, M., et al. (2017). IMG/M: Integrated genome and metagenome comparative data analysis system. *Nucleic Acids Res.* 45, D507–D516. doi: 10.1093/nar/gkw929

Coursolle, D., and Gralnick, J. A. (2010). Modularity of the Mtr respiratory pathway of Shewanella oneidensis strain MR-1. *Mol. Microbiol.* 77, 995–1008. doi: 10.1111/j.1365-2958.2010.07266.x

Diender, M., Stams, A. J. M., and Sousa, D. Z. (2015). Pathways and bioenergetics of anaerobic carbon monoxide fermentation. *Front. Microbiol.* 6:1275. doi: 10.3389/fmicb.2015.01275

Distanov, U. G. (1987). "Geological-industrial types of deposits of sedimentary siliceous rocks of the USSR. The criteria of prognosis and searches," in *The Origin and Practical Use of Siliceous Rocks. [In Russian]*, eds V. N. Kholodov and V. I. Sadnicki (Moscow: Nauka), 157–167.

Dobbek, H., Svetlitchnyi, V., Gremer, L., Huber, R., and Meyer, O. (2001). Crystal structure of a carbon monoxide dehydrogenase reveals a [Ni-4Fe-5S] cluster. *Science* 293, 1281–1285. doi: 10.1126/science.1061500

Eroschev-Shak, V. A., Zolotarev, B. P., and Karpov, G. A. (2005). Clay minerals in present-day volcano- hydrothermal systems. *Volcanol. Seismol.* 4, 11–24.

Eroschev-Shak, V. A., Zolotarev, B. P., Karpov, G. A., Grigoriev, V. S., Pokrovsky, B. G., and Artamonov, A. V. (1998). Secondary alterations of basalts and dacites in the Uzon Caldera, Kamchatka. *Lithol. Miner. Resour.* 2, 195–206.

Fimereli, D. K., Tsirigos, K. D., Litou, Z. I., Liakopoulos, T. D., Bagos, P. G., and Hamodrakas, S. J. (2012). "CW-PRED: a HMM-based method for the classification of cell wall-anchored proteins of Gram-positive bacteria," in *Proceedings of the 7th Hellenic Conference on AI, SETN 2012 Artificial Intelligence: Theories and Applications*, Lamia, 285–290. doi: 10.1007/978-3-642-30448-4_36

Fox, J. D., Yiping, H. E., Shelver, D., Roberts, G. P., and Ludden, P. W. (1996). Characterization of the region encoding the CO-induced hydrogenase of Rhodospirillum rubrum. *J. Bacteriol.* 178, 6200–6208. doi: 10.1128/jb.178.21.6200-6208.1996

Fuchs, G. (2011). Alternative pathways of carbon dioxide fixation: insights into the early evolution of life? *Annu. Rev. Microbiol.* 65, 631–658. doi: 10.1146/annurev-micro-090110-102801

Fukuyama, Y., Omae, K., Yoneda, Y., Yoshida, T., and Sako, Y. (2017). Draft Genome Sequences of *Carboxydothermus pertinax* and *C. islandicus*, hydrogenogenic carboxydotrophic bacteria. *Genome Announc.* 5:e01648-16. doi: 10.1128/genomeA.01648-16

Gavrilov, S. N., Lloyd, J. R., Kostrikina, N. A., and Slobodkin, A. I. (2012). Fe(III) oxide reduction by a gram-positive thermophile: physiological mechanisms for dissimilatory reduction of poorly crystalline Fe(III) oxide by a thermophilic gram-positive bacterium *Carboxydothermus ferrireducens*. *Geomicrobiol. J.* 29, 804–819. doi: 10.1080/01490451.2011.635755

Goris, J., Konstantinidis, K. T., Klappenbach, J. A., Coenye, T., Vandamme, P., and Tiedje, J. M. (2007). DNA-DNA hybridization values and their relationship to whole-genome sequence similarities. *Int. J. Syst. Evol. Microbiol.* 57, 81–91. doi: 10.1099/ijs.0.64483-0

Gumerov, V. M., Mardanov, A. V., Beletsky, A. V., Bonch-Osmolovskaya, E. A., and Ravin, N. V. (2011). Molecular analysis of microbial diversity in the Zavarzin Spring, Uzon Caldera, Kamchatka. *Microbiology* 80, 244–251. doi: 10.1134/S002626171102007X

Hedderich, R. (2004). Energy-converting [NiFe] hydrogenases from archaea and extremophiles: ancestors of complex I. *J. Bioenerg. Biomembr.* 36, 65–75. doi: 10.1023/B:JOBB.0000019599.43969.33

Hellebrand, H. J., and Schade, G. W. (2008). Carbon monoxide from composting due to thermal oxidation of biomass. *J. Environ. Qual.* 37, 592–598. doi: 10.2134/jeq2006.0429

Henstra, A. M., and Stams, A. J. M. (2011). Deep conversion of carbon monoxide to hydrogen and formation of acetate by the anaerobic thermophile *Carboxydothermus hydrogenoformans*. *Int. J. Microbiol.* 2011:641582. doi: 10.1155/2011/641582

Huntemann, M., Ivanova, N. N., Mavromatis, K., James Tripp, H., Paez-Espino, D., Palaniappan, K., et al. (2015). The standard operating procedure of the DOE-JGI microbial genome annotation pipeline (MGAP v.4). *Stand. Genomic Sci.* 10, 4–9. doi: 10.1186/s40793-015-0077-y

Inoue, T., Takao, K., Yoshida, T., Wada, K., Daifuku, T., Yoneda, Y., et al. (2013). Cysteine 295 indirectly affects Ni coordination of carbon monoxide dehydrogenase-II C-cluster. *Biochem. Biophys. Res. Commun.* 441, 13–17. doi: 10.1016/j.bbrc.2013.09.143

Jeoung, J., Fesseler, J., Goetzl, S., and Dobbek, H. (2014). Carbon monoxide. Toxic gas and fuel for anaerobes and aerobes: carbon monoxide dehydrogenases. *Met. Ions Life Sci.* 14, 37–69. doi: 10.1007/978-94-017-9269-1_3

Jones, D. T., Taylor, W. R., and Thornton, J. M. (1992). The rapid generation of mutation data matrices from protein sequences. *Comput. Appl. Biosci.* 8, 275–282. doi: 10.1093/bioinformatics/8.3.275

Karl, M. M., Poehlein, A., Bengelsdorf, F. R., Daniel, R., and Dürre, P. (2017). Complete genome sequence of the autotrophic acetogen *Clostridium formicaceticum* DSM 92T using nanopore and illumina sequencing data. *Genome Announc.* 5:e00423-17. doi: 10.1128/genomeA.00423-17

Kashefi, K., Shelobolina, E. S., Elliott, W. C., and Lovley, D. R. (2008). Growth of thermophilic and hyperthermophilic Fe(III)-reducing microorganisms on a ferruginous smectite as the sole electron acceptor. *Appl. Environ. Microbiol.* 74, 251–258. doi: 10.1128/AEM.01580-07

Kerby, R. L., Ludden, P. W., and Roberts, G. P. (1997). In vivo nickel insertion into the carbon monoxide dehydrogenase of *Rhodospirillum rubrum*: molecular and physiological characterization of cooCTJ. *J. Bacteriol.* 179, 2259–2266. doi: 10.1128/jb.179.7.2259-2266.1997

Kevbrin, V. V., and Zavarzin, G. A. (1992). The effect of sulfur compounds on growth of halophilic homoacetic bacterium *Acetohalobium arabaticum*. *Microbiology* 61, 812–817.

King, G. M., and Weber, C. F. (2007). Distribution, diversity and ecology of aerobic CO-oxidizing bacteria. *Nat. Rev. Microbiol.* 5, 107–118. doi: 10.1038/nrmicro1595

Kobayashi, I. (2001). Behavior of restriction-modification systems as selfish mobile elements and their impact on genome evolution. *Nucleic Acids Res.* 29, 3742–3756. doi: 10.1093/nar/29.18.3742

Kochetkova, T. V., Rusanov, I. I., Pimenov, N. V., Kolganova, T. V., Lebedinsky, A. V., Bonch-Osmolovskaya, E. A., et al. (2011). Anaerobic transformation of carbon monoxide by microbial communities of Kamchatka hot springs. *Extremophiles* 15, 319–325. doi: 10.1007/s00792-011-0362-7

Koonin, E. V. (2011). *The Logic of Chance: The Nature and Origin of Biological Evolution*. Upper Saddle River, NJ: FT Press Science, 295.

Kozhevnikova, D. A., Taranov, E. A., Lebedinsky, A. V., Bonch-Osmolovskaya, E. A., and Sokolova, T. G. (2016). Hydrogenogenic and sulfidogenic growth of thermococcus archaea on carbon monoxide and formate. *Microbiology* 85, 400–410. doi: 10.1134/S0026261716040135

Leggett, R. M., Clavijo, B. J., Clissold, L., Clark, M. D., and Caccamo, M. (2014). Next clip: an analysis and read preparation tool for nextera long mate pair libraries. *Bioinformatics* 30, 566–568. doi: 10.1093/bioinformatics/btt702

Levar, C. E., Hoffman, C. L., Dunshee, A. J., Toner, B. M., and Bond, D. R. (2017). Redox potential as a master variable controlling pathways of metal reduction by *Geobacter sulfurreducens*. *ISME J.* 11, 741–752. doi: 10.1038/ismej.2016.146

Lim, J. K., Kang, S. G., Lebedinsky, A. V., Lee, J. H., and Lee, H. S. (2010). Identification of a novel class of membrane-bound [NiFe]-Hydrogenases in *Thermococcus onnurineus* NA1 by in silico analysis. *Appl. Environ. Microbiol.* 76, 6286–6289. doi: 10.1128/AEM.00123-10

Madsen, J. S., Burmølle, M., Hansen, L. H., and Sørensen, S. J. (2012). The interconnection between biofilm formation and horizontal gene transfer. *FEMS Immunol. Med. Microbiol.* 65, 183–195. doi: 10.1111/j.1574-695X.2012.00960.x

Mall, A., Sobotta, J., Huber, C., Tschirner, C., Kowarschik, S., Bačnik, K., et al. (2018). Reversibility of citrate synthase allows autotrophic growth of a thermophilic bacterium. *Science* 359, 563–567. doi: 10.1126/science.aao2410

Manzella, M. P., Holmes, D. E., Rocheleau, J. M., Chung, A., Reguera, G., and Kashefi, K. (2015). The complete genome sequence and emendation of the hyperthermophilic, obligate iron-reducing archaeon "*Geoglobus ahangari*" strain 234T. *Stand. Genomic Sci.* 10:77. doi: 10.1186/s40793-015-0035-8

Mardanov, A. V., Slododkina, G. B., Slobodkin, A. I., Beletsky, A. V., Gavrilov, S. N., Kublanov, I. V., et al. (2015). The *Geoglobus acetivorans* genome: Fe(III) reduction, acetate utilization, autotrophic growth, and degradation of aromatic compounds in a hyperthermophilic archaeon. *Appl. Environ. Microbiol.* 81, 1003–1012. doi: 10.1128/AEM.02705-14

Matsnev, M. E., and Rusakov, V. S. (2014). Study of spatial spin-modulated structures by Mössbauer spectroscopy using SpectrRelax. *AIP Conf. Proc.* 1622, 40–49. doi: 10.1063/1.4898609

Menyailov, I. A., and Nikitina, L. P. (1980). Chemistry and metal contents of magmatic gases: the new Tolbachik volcanoes case (Kamchatka). *Bull. Volcanol.* 43, 195–205. doi: 10.1007/BF02597621

Mock, J., Wang, S., Huang, H., Kahnt, J., and Thauer, R. K. (2014). Evidence for a hexaheteromeric methylenetetrahydrofolate reductase in *Moorella thermoacetica*. *J. Bacteriol.* 196, 3303–3314. doi: 10.1128/JB.01839-14

Nunoura, T., Chikaraishi, Y., Izaki, R., Suwa, T., Sato, T., Harada, T., et al. (2018). A primordial and reversible TCA cycle in a facultatively chemolithoautotrophic thermophile. *Science* 359, 559–563. doi: 10.1126/science.aao3407

Nurk, S., Bankevich, A., Antipov, D., Gurevich, A. A., Korobeynikov, A., Lapidus, A., et al. (2013). Assembling single-cell genomes and mini-metagenomes from chimeric MDA products. *J. Comput. Biol.* 20, 714–737. doi: 10.1089/cmb.2013.0084

Oelgeschläger, E., and Rother, M. (2008). Carbon monoxide-dependent energy metabolism in anaerobic bacteria and archaea. *Arch. Microbiol.* 190, 257–269. doi: 10.1007/s00203-008-0382-6

Oger, P., Sokolova, T. G., Kozhevnikova, D. A., Taranov, E. A., Vannier, P., Lee, H. S., et al. (2016). Complete genome sequence of the hyperthermophilic and piezophilic archaeon *Thermococcus barophilus* Ch5, capable of growth at the expense of hydrogenogenesis from carbon monoxide and formate. *Genome Announc.* 4:e01534-15. doi: 10.1128/genomeA.01534-15

Omae, K., Yoneda, Y., Fukuyama, Y., Yoshida, T., and Sako, Y. (2017). Genomic analysis of *Calderihabitans maritimus* KKC1, a thermophilic, hydrogenogenic, carboxydotrophic bacterium isolated from marine sediment. *Appl. Environ. Microbiol.* 83:e00832-17. doi: 10.1128/AEM.00832-17

Pentráková, L., Su, K., Pentrák, M., and Stucki, J. W. (2013). A review of microbial redox interactions with structural Fe in clay minerals. *Clay Miner.* 48, 543–560. doi: 10.1180/claymin.2013.048.3.10

Pierce, E., Xie, G., Barabote, R. D., Saunders, E., Han, C. S., Detter, J. C., et al. (2008). The complete genome sequence of *Moorella thermoacetica* (f. *Clostridium thermoaceticum*). *Environ. Microbiol.* 10, 2550–2573. doi: 10.1111/j.1462-2920.2008.01679.x

Roberts, G. P., Thorsteinsson, M. V., Kerby, R. L., Lanzilotta, W. N., and Poulos, T. (2001). CooA: a heme-containing regulatory protein that serves as a specific sensor of both carbon monoxide and redox state. *Prog. Nucleic Acid Res. Mol. Biol.* 67, 35–63. doi: 10.1016/S0079-6603(01)67024-7

Rozanov, A. S., Bryanskaya, A. V., Malup, T. K., Meshcheryakova, I. A., Lazareva, E. V., Taran, O. P., et al. (2014). Molecular analysis of the benthos microbial community in Zavarzin thermal spring (Uzon Caldera, Kamchatka, Russia). *BMC Genomics* 15:S12. doi: 10.1186/1471-2164-15-S12-S12

Sant'Anna, F. H., Lebedinsky, A. V., Sokolova, T. G., Robb, F. T., and Gonzalez, J. M. (2015). Analysis of three genomes within the thermophilic bacterial species *Caldanaerobacter subterraneus* with a focus on carbon monoxide dehydrogenase evolution and hydrolase diversity. *BMC Genomics* 16:757. doi: 10.1186/s12864-015-1955-9

Schuchmann, K., and Müller, V. (2014). Autotrophy at the thermodynamic limit of life: a model for energy conservation in acetogenic bacteria. *Nat. Rev. Microbiol.* 12, 809–821. doi: 10.1038/nrmicro3365

Sharma, S., Cavallaro, G., and Rosato, A. (2010). A systematic investigation of multiheme c-type cytochromes in prokaryotes. *J. Biol. Inorg. Chem.* 15, 559–571. doi: 10.1007/s00775-010-0623-4

Shi, L., Dong, H., Reguera, G., Beyenal, H., Lu, A., Liu, J., et al. (2016). Extracellular electron transfer mechanisms between microorganisms and minerals. *Nat. Rev. Microbiol.* 14, 651–662. doi: 10.1038/nrmicro.2016.93

Shi, L., Fredrickson, J. K., and Zachara, J. M. (2014). Genomic analyses of bacterial porin-cytochrome gene clusters. *Front. Microbiol.* 5:657. doi: 10.3389/fmicb.2014.00657

Shi, L., Rosso, K. M., Zachara, J. M., and Fredrickson, J. K. (2012). Mtr extracellular electron-transfer pathways in Fe(III)-reducing or Fe(II)-oxidizing bacteria: a genomic perspective. *Biochem. Soc. Trans.* 40, 1261–1267. doi: 10.1042/BST20120098

Shock, E. L., Holland, M., Meyer-Dombard, D., Amend, J. P., Osburn, G. R., and Fischer, T. P. (2010). Quantifying inorganic sources of geochemical energy in hydrothermal ecosystems, Yellowstone National Park, USA. *Geochim. Cosmochim. Acta* 74, 4005–4043. doi: 10.1016/j.gca.2009.08.036

Shock, E. L., Holland, M., Meyer-Dombard, D. R., and Amend, J. P. (2005). "Geochemical sources of energy for microbial metabolism in hydrothermal ecosystems: Obsidian Pool, Yellowstone National Park," in *Geothermal Biology and Geochemistry in Yellowstone National Park Thermal Biology Institute*, eds W. P. Inskeep and T. R. McDermott (Bozeman, MT: Montana State University), 95–112

Slepova, T. V., Rusanov, I. I., Sokolova, T. G., Bonch-Osmolovskaia, E. A., and Pimenov, N. V. (2007). Radioisotopic assays of rates of carbon monoxide conversion by anaerobic thermophilic prokaryotes. *Microbiology* 76, 523–529. doi: 10.1134/S0026261707050025

Slepova, T. V., Sokolova, T. G., Kolganova, T. V., Tourova, T. P., and Bonch-Osmolovskaya, E. A. (2009). *Carboxydothermus siderophilus* sp. nov., a thermophilic, hydrogenogenic, carboxydotrophic, dissimilatory Fe(III)-reducing bacterium from a Kamchatka hot spring. *Int. J. Syst. Evol. Microbiol.* 59, 213–217. doi: 10.1099/ijs.0.000620-0

Slepova, T. V., Sokolova, T. G., Lysenko, A. M., Tourova, T. P., Kolganova, T. V., Kamzolkina, O. V., et al. (2006). *Carboxydocella sporoproducens* sp. nov., a novel anaerobic CO-utilizing/H2-producing thermophilic bacterium from a Kamchatka hot spring. *Int. J. Syst. Evol. Microbiol.* 56, 797–800. doi: 10.1099/ijs.0.63961-0

Slobodkin, A. I., Sokolova, T. G., Lysenko, A. M., and Wiegel, J. (2006). Reclassification of *Thermoterrabacterium ferrireducens* as *Carboxydothermus ferrireducens* comb. nov., and emended description of the genus Carboxydothermus. *Int. J. Syst. Evol. Microbiol.* 56, 2349–2351. doi: 10.1099/ijs.0.64503-0

Slobodkina, G. B., Panteleeva, A. N., Sokolova, T. G., Bonch-Osmolovskaya, E. A., and Slobodkin, A. I. (2012). *Carboxydocella manganica* sp. nov., a thermophilic, dissimilatory Mn(IV)- and Fe(III)-reducing bacterium from a Kamchatka hot spring. *Int. J. Syst. Evol. Microbiol.* 62, 890–894. doi: 10.1099/ijs.0.027623-0

Smith, J. A., Aklujkar, M., Risso, C., Leang, C., Giloteaux, L., and Holmes, D. E. (2015). Mechanisms involved in Fe(III) respiration by the hyperthermophilic archaeon *Ferroglobus placidus*. *Appl. Environ. Microbiol.* 81, 2735–2744. doi: 10.1128/AEM.04038-14

Soboh, B., Linder, D., and Hedderich, R. (2002). Purification and catalytic properties of a CO-oxidizing:H2-evolving enzyme complex from *Carboxydothermus hydrogenoformans*. *Eur. J. Biochem.* 269, 5712–5721. doi: 10.1046/j.1432-1033.2002.03282.x

Sokolova, T., and Lebedinsky, A. (2013). "CO-Oxidizing anaerobic thermophilic prokaryotes," in *Thermophilic Microbes in Environmental and Industrial*

Biotechnology. Biotechnology of Thermophiles, eds T. Satyanarayana, J. Littlechild, and Y. Kawarabayasi (Dordrecht: Springer), 203–231. doi: 10.1007/978-94-007-5899-5_7

Sokolova, T. G. (2015). *"Carboxydocella," in Bergey's Manual of Systematics of Archaea and Bacteria*. Hoboken, NJ: John Wiley & Sons, Inc, 1–4.

Sokolova, T. G., González, J. M., Kostrikina, N. A., Chernyh, N. A., Slepova, T. V., Bonch-Osmolovskaya, E. A., et al. (2004). *Thermosinus carboxydivorans* gen. nov., sp. nov., a new anaerobic, thermophilic, carbon-monoxide-oxidizing, hydrogenogenic bacterium from a hot pool of Yellowstone National Park. *Int. J. Syst. Evol. Microbiol.* 54, 2353–2359. doi: 10.1099/ijs.0.63186-0

Sokolova, T. G., Henstra, A. M., Sipma, J., Parshina, S. N., Stams, A. J. M., and Lebedinsky, A. V. (2009). Diversity and ecophysiological features of thermophilic carboxydotrophic anaerobes. *FEMS Microbiol. Ecol.* 68, 131–141. doi: 10.1111/j.1574-6941.2009.00663.x

Sokolova, T. G., Kostrikina, N. A., Chernyh, N. A., Tourova, T. P., Kolganova, T. V., and Bonch-Osmolovskaya, E. A. (2002). Carboxydocella thermoautotrophica gen. nov., sp. nov., a novel anaerobic, CO-utilizing thermophile from a Kamchatkan hot spring. *Int. J. Syst. Evol. Microbiol.* 52, 1961–1967. doi: 10.1099/ijs.0.02173-0

Svetlitchnyi, V., Dobbek, H., Meyer-Klaucke, W., Meins, T., Thiele, B., Römer, P., et al. (2004). A functional Ni-Ni-[4Fe-4S] cluster in the monomeric acetyl-CoA synthase from *Carboxydothermus hydrogenoformans*. *Proc. Natl. Acad. Sci. U.S.A.* 101, 446–451. doi: 10.1073/pnas.0304262101

Svetlitchnyi, V., Peschel, C., Acker, G., and Meyer, O. (2001). Two membrane-associated NiFeS-carbon monoxide dehydrogenases from the anaerobic carbon-monoxide-utilizing eubacterium *Carboxydothermus hydrogenoformans*. *J. Bacteriol.* 183, 5134–5144. doi: 10.1128/JB.183.17.5134-5144.2001

Symonds, R. B., Rose, W. I., Bluth, G. J. S., and Gerlach, T. M. (1994). Volcanic gas studies- methods, results, and applications. *Rev. Mineral.* 30, 1–66.

Tamura, K., Stecher, G., Peterson, D., Filipski, A., and Kumar, S. (2013). MEGA6: molecular evolutionary genetics analysis version 6.0. *Mol. Biol. Evol.* 30, 2725–2729. doi: 10.1093/molbev/mst197

Techtmann, S. M., Lebedinsky, A. V., Colman, A. S., Sokolova, T. G., Woyke, T., Goodwin, L., et al. (2012). Evidence for horizontal gene transfer of anaerobic carbon monoxide dehydrogenases. *Front. Microbiol.* 3:132. doi: 10.3389/fmicb.2012.00132

Tiquia-Arashiro, S. M. (2014). *Thermophilic Carboxydotrophs and their Applications in Biotechnology (Extremophilic Bacteria)*. Berlin: Springer, 131.

Toshchakov, S. V., Kublanov, I. V., Messina, E., Yakimov, M. M., and Golyshin, P. N. (2015). "Genomic analysis of pure cultures and communities," in *Hydrocarbon and Lipid Microbiology Protocols. Springer Protocols Handbooks*, eds T. McGenity, K. Timmis, and B. Nogales (Berlin: Springer), 5–27. doi: 10.1007/8623_2015_126

Visser, M., Parshina, S. N., Alves, J. I., Sousa, D. Z., Pereira, A. C., Muyzer, G., et al. (2014). Genome analyses of the carboxydotrophic sulfate-reducers *Desulfotomaculum nigrificans* and *Desulfotomaculum carboxydivorans* and reclassification of *Desulfotomaculum caboxydivorans* as a later synonym of *Desulfotomaculum nigrificans*. *Stand. Genomic Sci.* 9, 655–675. doi: 10.4056/sig

Wawrousek, K., Noble, S., Korlach, J., Chen, J., Eckert, C., Yu, J., et al. (2014). Genome annotation provides insight into carbon monoxide and hydrogen metabolism in *Rubrivivax gelatinosus*. *PLoS One* 9:e114551. doi: 10.1371/journal.pone.0114551

White, G. F., Edwards, M. J., Gomez-Perez, L., Richardson, D. J., Butt, J. N., and Clarke, T. A. (2016). Mechanisms of bacterial extracellular electron exchange. *Adv. Microb. Physiol.* 68, 87–138. doi: 10.1016/bs.ampbs.2016.02.002

Wolin, E. A., Wolin, M. J., and Wolfe, R. S. (1963). Formation of methane by bacterial extracts. *J. Biol. Chem.* 238, 2882–2886. doi: 10.1016/S0016-0032(13)90081-8

Wu, M., Ren, Q., Durkin, A. S., Daugherty, S. C., Brinkac, L. M., Dodson, R. J., et al. (2005). Life in hot carbon monoxide: the complete genome sequence of *Carboxydothermus hydrogenoformans* Z-2901. *PLoS Genet.* 1:e65. doi: 10.1371/journal.pgen.0010065

Xiong, Y., Shi, L., Chen, B., Mayer, M. U., Lower, B. H., Londer, Y., et al. (2006). High-affinity binding and direct electron transfer to solid metals by purified metal reducing protein OmcA Decaheme cytochrome. *J. Am. Chem. Soc.* 128, 13978–13979. doi: 10.1021/ja063526d

Yoneda, Y., Kano, S. I., Yoshida, T., Ikeda, E., Fukuyama, Y., Omae, K., et al. (2015). Detection of anaerobic carbon monoxide-oxidizing thermophiles in hydrothermal environments. *FEMS Microbiol. Ecol.* 91, 1–9. doi: 10.1093/femsec/fiv093

Yoneda, Y., Yoshida, T., Kawaichi, S., Daifuku, T., Takabe, K., and Sako, Y. (2012). *Carboxydothermus pertinax* sp. nov., a thermophilic, hydrogenogenic, Fe(III)-reducing, sulfur-reducing carboxydotrophic bacterium from an acidic hot spring. *Int. J. Syst. Evol. Microbiol.* 62, 1692–1697. doi: 10.1099/ijs.0.031583-0

Yoneda, Y., Yoshida, T., Yasuda, H., Imada, C., and Sako, Y. (2013). A thermophilic, hydrogenogenic and carboxydotrophic bacterium, *Calderihabitans maritimus* gen. nov., sp. nov., from a marine sediment core of an undersea caldera. *Int. J. Syst. Evol. Microbiol.* 63, 3602–3608. doi: 10.1099/ijs.0.050468-0

Zacharoff, L., Chan, C. H., and Bond, D. R. (2016). Reduction of low potential electron acceptors requires the CbcL inner membrane cytochrome of *Geobacter sulfurreducens*. *Bioelectrochemistry* 107, 7–13. doi: 10.1016/j.bioelechem.2015.08.003

Zavarzina, D. G., Chistyakova, N. I., Shapkin, A. V., Savenko, A. V., Zhilina, T. N., Kevbrin, V. V., et al. (2016). Oxidative biotransformation of biotite and glauconite by alkaliphilic anaerobes: the effect of Fe oxidation on the weathering of phyllosilicates. *Chem. Geol.* 439, 98–109. doi: 10.1016/j.chemgeo.2016.06.015

Zavarzina, D. G., Sokolova, T. G., Tourova, T. P., Chernyh, N. A., Kostrikina, N. A., and Bonch-Osmolovskaya, E. A. (2007). *Thermincola ferriacetica* sp. nov., a new anaerobic, thermophilic, facultatively chemolithoautotrophic bacterium capable of dissimilatory Fe(III) reduction. *Extremophiles* 11, 1–7. doi: 10.1007/s00792-006-0004-7

Zhang, H., Tang, X., Munske, G. R., Zakharova, N., Zheng, C., Wolff, M. A., et al. (2008). In vivo identification of outer membrane protein OmcA-MtrC interaction network in *Shewanella oneidensis* MR-1 cells using novel chemical cross-linkers. *J. Proteome Res.* 7, 1712–1720. doi: 10.1021/pr700767658

Conflict of Interest Statement: The authors declare that the research was conducted in the absence of any commercial or financial relationships that could be construed as a potential conflict of interest.

frontiers in Microbiology

ORIGINAL RESEARCH
published: 30 June 2017
doi: 10.3389/fmicb.2017.01228

Respiratory Pathways Reconstructed by Multi-Omics Analysis in *Melioribacter roseus*, Residing in a Deep Thermal Aquifer of the West-Siberian Megabasin

Sergey Gavrilov[1], Olga Podosokorskaya[1], Dmitry Alexeev[2], Alexander Merkel[1], Maria Khomyakova[1], Maria Muntyan[3], Ilya Altukhov[4,5], Ivan Butenko[4], Elizaveta Bonch-Osmolovskaya[1], Vadim Govorun[4,5] and Ilya Kublanov[1,6]*

[1] Winogradsky Institute of Microbiology, Research Center of Biotechnology, Russian Academy of Sciences, Moscow, Russia, [2] Saint Petersburg State University of Information Technologies, Mechanics and Optics, St. Petersburg, Russia, [3] Belozersky Institute of Physico-Chemical Biology, Lomonosov Moscow State University, Moscow, Russia, [4] Federal Research and Clinical Centre of Physico-Chemical Medicine, Moscow, Russia, [5] Moscow Institute of Physics and Technology, Dolgoprudny, Russia, [6] Laboratory of Microbial Genomics, Immanuel Kant Baltic Federal University, Kaliningrad, Russia

OPEN ACCESS

Edited by:
Nils-Kaare Birkeland, University of Bergen, Norway

Reviewed by:
Christiane Dahl, University of Bonn, Germany
Ronald Oremland, United States Geological Survey, United States

***Correspondence:**
Sergey Gavrilov
sngavrilov@gmail.com

Specialty section:
This article was submitted to Extreme Microbiology, a section of the journal Frontiers in Microbiology

Received: *17 March 2017*
Accepted: *16 June 2017*
Published: *30 June 2017*

Citation:
Gavrilov S, Podosokorskaya O, Alexeev D, Merkel A, Khomyakova M, Muntyan M, Altukhov I, Butenko I, Bonch-Osmolovskaya E, Govorun V and Kublanov I (2017) Respiratory Pathways Reconstructed by Multi-Omics Analysis in Melioribacter roseus, Residing in a Deep Thermal Aquifer of the West-Siberian Megabasin. Front. Microbiol. 8:1228. doi: 10.3389/fmicb.2017.01228

Melioribacter roseus, a representative of recently proposed Ignavibacteriae phylum, is a metabolically versatile thermophilic bacterium, inhabiting subsurface biosphere of the West-Siberian megabasin and capable of growing on various substrates and electron acceptors. Genomic analysis followed by inhibitor studies and membrane potential measurements of aerobically grown *M. roseus* cells revealed the activity of aerobic respiratory electron transfer chain comprised of respiratory complexes I and IV, and an alternative complex III. Phylogeny reconstruction revealed that oxygen reductases belonged to atypical *cc(o/b)o*$_3$-type and canonical *cbb*$_3$–type cytochrome oxidases. Also, two molybdoenzymes of *M. roseus* were affiliated either with Ttr or Psr/Phs clades, but not with typical respiratory arsenate reductases of the Arr clade. Expression profiling, both at transcripts and protein level, allowed us to assign the role of the terminal respiratory oxidase under atmospheric oxygen concentration for the *cc(o/b)o*$_3$ cytochrome oxidase, previously proposed to serve for oxygen detoxification only. Transcriptomic analysis revealed the involvement of both molybdoenzymes of *M. roseus* in As(V) respiration, yet differences in the genomic context of their gene clusters allow to hypothesize about their distinct roles in arsenate metabolism with the 'Psr/Phs'-type molybdoenzyme being the most probable candidate respiratory arsenate reductase. Basing on multi-omics data, the pathways for aerobic and arsenate respiration were proposed. Our results start to bridge the vigorously increasing gap between homology-based predictions and experimentally verified metabolic processes, what is especially important for understudied microorganisms of novel lineages from deep subsurface environments of Eurasia, which remained separated from the rest of the biosphere for several geological periods.

Keywords: deep subsurface environment, West-Siberian megabasin, thermophilic bacteria, respiratory metabolism, cytochrome oxidases, arsenate reductase

INTRODUCTION

Recently the discovery and study of *Ignavibacterium album* and *Melioribacter roseus* (Iino et al., 2010; Podosokorskaya et al., 2013), the first two cultivated representatives of previously uncultured candidate division ZB1 (Elshahed et al., 2003) led to the proposal of Ignavibacteriae phylum, a member of the Chlorobi-Bacteroidetes-Ignavibacteriae group (Podosokorskaya et al., 2013). Besides two cultured species Ignavibacteriae includes numerous clones found in various environments all around the world, including hot springs, oil reservoirs, mines, and seafloor sediments (Tiodjio et al., 2014; Kato et al., 2015). *Melioribacter roseus* was isolated from a microbial mat proliferating in a geothermal water discharge (Podosokorskaya et al., 2013). The organism is a moderate thermophile and originates from subsurface biosphere, as 16S rRNA genes of closely related organisms were identified in arsenic-containing water samples from 2725 m depth at the same site (Frank Y. A. et al., 2016).

Physiological studies revealed that both cultured representatives of the phylum Ignavibacteriae are facultatively anaerobic organotrophs capable of fermentative growth on various carbohydrates and of oxygen or arsenate respiration with acetate as the electron donor. Primary genome analysis of *M. roseus* highlighted key determinants of electron transport chains, providing important insights into the organism's ability to oxidize various electron donors during aerobic or anaerobic respiration. Genes for the electron transfer chain membrane complexes I and II, alternative complex III (ACIII) and several terminal oxidoreductases transferring electrons to oxygen and arsenate were found. Among those, the three different oxygen reductases and two different molybdopterin oxidoreductases have been proposed to determine most active respiratory processes performed by *M. roseus*—aerobic respiration and dissimilatory arsenate reduction, respectively (Kadnikov et al., 2013; Podosokorskaya et al., 2013), although their specific roles in respiratory metabolism were not assigned.

All the currently known energy-transducing oxygen reductases of respiratory chains in prokaryotes are subdivided into two large superfamilies. One of them, that encloses the enzymes with heme-copper binuclear center, is subdivided into three large clades known as A(I)-, B(II)-, and C(III)-type oxygen reductases (Mattar and Engelhard, 1997; Sousa et al., 2012). The other one, lacking copper, is represented by cytochrome *bd* oxygen reductases. With respect to the mode of energy transduction, the *bd*-type oxidases were shown to be the redox loops without ion-pumping activity (Borisov et al., 2011), while the heme-copper oxidases were demonstrated to pump protons (Wikström, 1977; Rauhamäki et al., 2012; Rauhamäki and Wikström, 2014) or sodium ions (Muntyan et al., 2015) across the cell membrane. In the respiratory chains of prokaryotic aerobes, the heme-copper oxygen reductases are highly diverse. Each of their clades, A, B and C, encloses enzymes accepting electrons from different donors, whether quinols or cytochromes *c*. As regarding the heme content, these enzymes can include hemes of *a*, *b*, *c*, and *o* types. However, molecular phylogeny of heme-copper oxidases superfamily reflects only one structural parameter affecting their catalytic activity. Namely, the position of conserved amino acid motifs that determine the structure of proton pumping channels is considered upon phylogenetic reconstructions (Sousa et al., 2012; Gennis, 2013). Recent multivariate analysis of genomic, structural, functional and thermodynamic information pertinent to the evolution of heme-copper oxidases has also highlighted correlation of their phylogeny-based grouping into three clades (A, B, and C) with the affinity to oxygen, and led to the proposal of the low O_2-affinity A-type enzymes as the most recent evolutionary innovation and the high-affinity O_2 reductases (B and C) arising from NO-reducing precursor enzymes (Ducluzeau et al., 2014).

Currently known respiratory arsenate reductases belong to the Arr family within a complex iron–sulfur molybdopterin oxidoreductase superfamily (CISM) — a group of molybdenum-containing enzymes, highly diverse by the catalyzed reaction. Among arsenate reductases only Arr-type enzymes are known to serve for energy generation during As(V) reduction to As(III), although functional flexibility of CISM superfamily enzymes could not rule out the presence of arsenate-reducing activity in the groups of molybdopterin oxidoreductases other than Arr (Duval et al., 2008; Rothery et al., 2008).

Here we describe the results of the phylogenetic analysis of putative oxygen and arsenate reductases genes in *M. roseus*, transcriptomic and proteomic experimental evaluation of their involvement in energy metabolism of the organism, and propose the mechanisms for aerobic respiration and arsenate reduction in this representative of the novel bacterial phylum. This information may cast light on yet poorly understood metabolic processes, occurred in thermophilic microbial communities residing in deep subsurface.

MATERIALS AND METHODS

Cultivation of *M. roseus*

Melioribacter roseus P3M-2^T was incubated at 52–54°C in the modified anaerobic S medium (Podosokorskaya et al., 2013). Sodium sulfide and resazurin were only added to a strictly anaerobic variant of the medium for fermentative growth testing (see below). In all the cases of anaerobic growth, the strain was incubated in the dark without shaking. For aerobic or microaerobic cultivation, the same medium was used, but in this case, boiling and flushing of the medium with nitrogen were omitted, and inoculated tubes or bottles were incubated with shaking. Oxygen level in aerobic and microaerobic cultures was determined at the initial point and at the end of incubation by gas chromatography as previously described (Frank Y. A. et al., 2016).

All tests were performed in the presence of 10 mM Tricine buffer and yeast extract added as a source of growth factors (0.1 g l^{-1} under anaerobic conditions and 0.05 g l^{-1} under aerobic conditions).

Inhibitory Analysis

Two inhibitors of electron transfer—rotenone and 2-*n*-heptyl-4-hydroxyquinoline-*N*-oxide (HQNO)—were used for the analysis. The inhibitors (each by 15 μM) were added to the medium

from anaerobic (N_2) stock solutions in 100% DMSO before cultivation. Negative control without inhibitors and additional positive controls, containing cells, acetate or maltose, air in the gas phase, and 0.1% (v/v) DMSO but no inhibitors, were used to provide data normalized to 100% activity to help estimate the impact of the inhibitors. Hydrogen was added to the gas phase (1 gauge atmosphere) to eliminate the possibility of fermentative growth of the strain on yeast extract (added to the medium as a growth factor at a concentration of 0.1 g l^{-1}).

Transmembrane Electrical Potential and Respiratory Activity

The transmembrane electrical potential ($\Delta\psi$) of the bacterial cells grown under atmospheric oxygen was detected using tetraphenylphosphonium (TPP^+) penetrating cation at the final concentration of 1.6 μM and a TPP^+-selective electrode, as described earlier (Kamo et al., 1979) with our modifications (Muntyan et al., 2012). The experiments were conducted with washed resting cell suspensions (3 mg ml^{-1} of total cell protein), prepared in fresh sterile aerobic culture medium (pH 7.0) lacking organic growth factors, in a conical thermostated glass cell at 52°C under vigorous aeration with a magnetic stirring bar. To evaluate the respiratory activity of bacterial cells grown under atmospheric oxygen, the rate of oxygen consumption was measured in the cell suspensions using a standard oxygen Clark-type electrode and a polarograph LP7e (LP, Czech Republic) at 52°C. All the measurements were performed in three biological replicas, i.e., with three different cell suspensions. Each cell suspension was divided into halves for simultaneous determination of $\Delta\psi$ and respiratory activity.

Sequence Analysis

Phylogenetic analysis of CISM proteins was performed in the same manner as described by Sorokin et al., 2016. Phylogenetic analysis of cytochrome oxidases was performed as follows: all 725 seed sequences of Pfam PF00115 (COX1) family were downloaded from http://pfam.xfam.org/family/PF00115#tabview=tab3. The sequences were clustered based on 50% identity threshold using CD-hit (Huang et al., 2010), and 1 representative of each cluster was left (112 sequences). Upon addition of two *M. roseus* homologs (MROS_0038 and MROS_1513) to this 96-sequence dataset, the sequences were aligned in MAFFT v. 7 (Katoh et al., 2002). The Le Gascuel (+I + G) model was revealed by ProtTest 2.4 (Abascal et al., 2005) to give the highest likelihood. Phylogenetic analysis was performed in MEGA v. 6 (Tamura et al., 2013).

Localization of molybdoenzymes was predicted basing on the results of six different on-line prediction services – SignalP 4.1, TatP 1.0, SecretomeP 2.0a and TMHMM 2.0 (all at CBS Prediction Servers[1]), as well as PSORTb 3.0.2[2] and Phobius[3].

[1]http://www.cbs.dtu.dk/services

[2]http://www.psort.org/psortb/

[3]http://phobius.sbc.su.se/

Membrane Fraction Preparation

For preparation of membrane fractions for proteomic analysis, *M. roseus* was grown fermentatively with maltose on a strictly anaerobic (E_h −130 mV vs. standard hydrogen electrode [SHE]) medium and by aerobic respiration (atmospheric oxygen) with acetate in three biological replicas, 2 liters each. Growth was controlled microscopically, and the cells were collected on the boundary of exponential and stationary growth phases by centrifugation at 14 000 *g*, 4°C for 15 min. Cell pellets were washed in 50 mM Tris-HCl, pH 7.5 and centrifuged at 14 000 *g*, 4°C for 20 min. After that, cell pellets were resuspended in 50 mM Tris-HCl, pH 7.5 with 0.1 mg ml^{-1} DNAse I (Fermentas) and protease inhibitor cocktail (prepared from Protease Inhibitor Tablet, Sigma, according to manufacturer's recommendations), and then they were sonicated on ice using Soniprep 150 Plus disintegrator (MSE, UK) for 5 min at a frequency of 12 kHz. Cell debris was separated by centrifugation at 14 000 *g*, 4°C for 8 min and discarded, while the supernatants were further ultracentrifuged at 100 000 *g*, 4°C for 1 h. Precipitated membrane fractions were stored at −80°C before analysis. Each fraction contained ca. 200 μg total cell protein as determined by the Bradford Protein Assay Kit (BioRad) and according to the manufacturer's recommendations.

Protein Extraction and Trypsin Digestion

The membrane fractions were treated with 5 μl of 10% RapiGest SF (Waters) and 1 μl nuclease mix (GE Healthcare) for 30 min at 4°C, resuspended in 45 μl of 100 mM NH_4HCO_3, vortexed and heated at 100°C for 5 min. After cooling to room temperature, insoluble material was removed by centrifugation at 15 000 *g* for 5 min. The supernatant was separated, checked for protein concentration, subjected for disulfide bonds reduction with 10 mM 1,4-dithiothreitol (DTT, BioRad) in 100 mM ammonium bicarbonate at 60°C for 30 min, and subsequently alkylated with 30 mM iodoacetamide (BioRad) at room temperature in dark for 30 min. DTT and 100 mM ammonium bicarbonate were added iteratively. After that, alkylated trypsin (Trypsin Gold, Mass Spectrometry Grade, Promega) was added to the supernatant in the ratio of 1/50 (mg per mg total protein) and incubated at 37°C overnight. For trypsin inactivation and degradation of the acid-labile surfactant, an aliquot of trifluoroacetic acid (Sigma) was added to the final concentration of 0.5% (m/v), and the mixture was incubated at 37°C for 45 min. Residual surfactant was removed by centrifugation at 15 000 *g* for 10 min. The obtained hydrolysate was desalted using a Discovery DSC-18 Tube (Supelco) according to the manufacturer's protocol. Peptides were eluted with 700 μL 75% acetonitrile (ACN), 0.1% trifluoroacetic acid (TFA), dried in a SpeedVac (Labconco) and resuspended in 3% ACN, 0.1% TFA to the final concentration of 5 μg μl^{-1}.

LC-MS/MS Analysis

The LC-MS/MS was performed on a TripleTOF 5600+ mass-spectrometer operating in a data-dependent mode with a NanoSpray III ion source (ABSciex, Canada) coupled to a

NanoLC Ultra 2D+ nano-HPLC system (Eksigent) configured as described by Ziganshin et al. (2016).

Protein Identification

The raw LC/MS-MS datasets (.wiff file format) were converted to Mascot Generic Format (.mgf file format) using AB SCIEX MS Data Converter (version 1.3). Proteins were identified with the Mascot search engine (version 2.5.1) against the *Melioribacter roseus* str. P3M sequence database (RefSeq: NC_018178, which contains 2840 amino acid sequences). The Mascot searches were performed with the following parameters: tryptic-specific peptides, maximum of one missed cleavages, a peptide charge state limited to 1+, 2+, and 3+, a peptide mass tolerance of 10 ppm, a fragment mass tolerance of 0.5 Da, and variable modifications caused by Oxidation(M) and Carbamidomethylation(C). The False Discovery Rate (FDR) was calculated using the decoy database analysis with Mascot. Individual ions score higher than 11 indicate identity or extensive homology with $p < 0.05$ and FDR <1%. The mass spectrometry proteomics data have been deposited to the ProteomeXchange Consortium (Vizcaíno et al., 2014) via the PRIDE partner repository with the dataset identifier PXD003662 (refer to additional information below for details).

Quantitative Proteomics

For comparative analysis of protein amount, emPAIs (Ishihama et al., 2005) were calculated. Data were normalized using the scaling method. Proteins were considered to be statistically different according to the unpaired two-tailed Student's *t*-test (*p*-value <0.05) with the Benjamini and Hochberg (1995) adjustment for *p*-values.

Transcriptomic Analysis

For transcriptomic analysis, seven sets of primers for *M. roseus* genes encoding the catalytic subunits of three oxygen reductases (*coxI*, *ccoNO*, *cydA*) and two molybdopterin-containing oxidoreductases (*ttrA* and *psr/phsA*), as well as for the reference housekeeping genes *rpoB* (encoding the DNA-directed RNA polymerase subunit beta, MROS_0223) and *atpA* (encoding the alpha subunit of F0F1–type ATP-synthase, MROS_0272), were designed using the Primer-BLAST service (http://www.ncbi.nlm.nih.gov/tools/primer-blast/). The specificity of the primers was verified by the Sanger sequencing of amplicons. The primers are summarized in Supplementary Table S1. RT-PCR analysis was performed with the cells grown at five different cultivation conditions: aerobic respiratory growth at atmospheric O_2 concentration in the gas phase, microaerobic respiratory growth at 2% O_2 in the gas phase, anaerobic respiratory growth with arsenate, fermentative growth in the absence of external electron acceptors at positive E_h value of the medium (+200 mV vs SHE) or negative E_h (–130 mV vs SHE, corresponding to strict anaerobiosis achieved by addition of 1 mM sodium sulfide to the culture medium). At all three respiratory cultivation conditions, a non-fermentable substrate acetate was used, while at both fermentative cultivation conditions, the anaerobic media were amended with a fermentable substrate maltose. In all the cases, the total RNA was extracted using ExtractRNA and CleanRNA Standard kits followed by DNAse I treatment. To prepare cDNA, 2 μg of the total RNA was reverse-transcribed using the MMLV RT kit. All the chemicals at this stage were from Evrogen, Russia. Quantitative PCR (qPCR) was performed using the qPCRmix-HS SYBR kit (Evrogen, Russia) on a StepOnePlus™ Real-Time PCR System (Applied Biosystems, United States). Calibration curves were constructed based on fivefold dilutions of genomic DNA of *M. roseus*. All growth experiments, as well as all qPCR measurements, were performed in triplicate. Transcription of the target oxidoreductase genes was normalized using the transcription level of both *rpoB* and *atpA*, which were transcribed at all the tested growth conditions in a similar ratio to each other (Supplementary Figure S1). Our final analysis was based on *rpoB*-normalized data.

RESULTS AND DISCUSSION

Disclosure of the Aerobic Electron Transfer Chain Activity

Previous genome analysis revealed the presence of the major components of respiratory electron transfer chain (ETC) in *M. roseus* (Podosokorskaya et al., 2013): proton-translocating NADH-dehydrogenase complex I, membrane-bound succinate dehydrogenase/fumarate reductase, isoprenoid quinones, and quinol oxidizing alternative complex III (ACIII). To confirm the activity of this ETC in *M. roseus,* the influence of rotenone and HQNO on aerobic growth with maltose or acetate (a non-fermentable substrate) was evaluated. Each of the inhibitors completely arrested *M. roseus* growth at these conditions. Neither HQNO nor rotenone had affected fermentative growth of the organism on maltose without electron acceptors.

Rotenone is known as an inhibitor of type I NADH-dehydrogenases. This compound binds to the membranous quinone-binding subunit NuoH/Nqo8 or the interface of the subunits NuoB/D/H (Sazanov, 2012; Nichols, 2013).

2-*n*-heptyl-4-hydroxyquinoline-*N*-oxide can serve as an inhibitor of several quinone interacting enzymes. In particular, HQNO demonstrates strong inhibitory effect on complex II (Smirnova et al., 1995), as well as partial inhibition of ACIII (Refojo et al., 2010, 2012). Complete inhibition of *M. roseus* aerobic growth with HQNO suggests the blockage of the main electron flow leading to energy production. According to genomic analysis (Podosokorskaya et al., 2013) we can assume that the points of HQNO action could be the *M. roseus* complex II and the alternative complex III. Anyway, the observed inhibition of *M. roseus* aerobic growth with either rotenone or HQNO supports the presence and activity of at least two energy-transducing complexes – the complex I and, most probably, the alternative complex III.

The washed resting cells grown aerobically with acetate maintained a transmembrane electrical potential ($\Delta\psi$) in the absence of added exogenous substrates, as was detected using the TPP^+-selective electrode. The transmembrane potential dissipated upon the addition of 1 μM carbonyl cyanide

m-chlorophenyl hydrazone (CCCP), which passively balances proton gradient across the cytoplasmic membrane (**Figure 1**, gray dotted line). Aliquots of these same cell preparations exhibited no respiration, as determined by a standard oxygen Clark-type electrode, unless they were supplied with exogenous energy substrates. In the presence of acetate, the cells began to respire with the oxygen consumption rate of 1.9 nmol O_2 min^{-1} mg^{-1} of the cell protein (kinetic data are not presented). The $\Delta\psi$ value on the membranes of the respiring cells was maintained at the level observed in the absence of acetate (**Figure 1**, black solid line). Apparently, acetate serves as an external respiratory substrate in *M. roseus* cells, being presumably metabolized via the acetyl-CoA synthetase-catalyzed pathway and further through the TCA cycle predicted by genome analysis (Kadnikov et al., 2013). This pathway could directly fuel the respiratory ETC via the activity of succinate dehydrogenase, resulting in initiation of oxygen consumption by the cells. The presence of the respiratory complex II in *M. roseus* was previously revealed by genome analysis (Kadnikov et al., 2013) and its expression under aerobic condition is supported by our proteomic data (see below, Supplementary Table S2). In the presence of the respiratory substrate (acetate) and $\Delta\psi$ across the bacterial cell membranes (i.e., when the respiratory chain was in partially reduced state), cyanide inhibited respiratory activity of whole resting cells. The cyanide effect on oxygen respiration was comparatively high, as 50% inhibition was observed within 10 minutes in the presence of 35 μM KCN (without preincubation) with reductive substrate, and 65% inhibition was reached at 100 μM KCN within 20 min (Supplementary Figure S2). Noteworthily, our measurements were performed under optimal growth conditions of *M. roseus* (pH 7.0, 52°C), at which 99% cyanide (pK = 9.2) exists in the form of easily sublimating cyanic acid (boiling point 26°C). Consequently, the active concentration of cyanide in the incubation mixture for the respiratory activity measurements was to be well below the mentioned estimated value. Additionally, the inhibitory effect of cyanide on cytochrome oxidases depends on pH of the medium, membrane environment and RedOx state of the pentacoordinated oxygen-binding heme (that is heme a_3/o_3) in the enzyme reaction center (Wilson and Erecińska, 1978; Cooper and Brown, 2008). Considering these facts and reasons, and that our measurements were performed with the whole cells and incompletely oxidized heme proteins (when the cytochrome oxidases of clade A form unstable complexes with cyanide, i.e., reversibly bind it), we assume that the actual cyanide inhibitory effect on *M. roseus* cytochrome oxidases is much higher, than the apparent one registered in our study. Anyway, such an effect manifests the efficiency of cyanide as an inhibitor, thus suggesting that mainly the heme-copper oxidases comprise the terminus of the respiratory chain (Nichols, 2013) in the cells grown at atmospheric oxygen concentration.

Taken together, the results of inhibitory analysis of aerobic respiration and $\Delta\psi$ measurements performed with *M. roseus* whole cells clearly highlight the activity of aerobic respiratory electron transfer chain in the microorganism. The variety and functionality of three different oxygen reductases in *M. roseus* are analyzed in the next section on the basis of the genomic, proteomic and transcriptomic data.

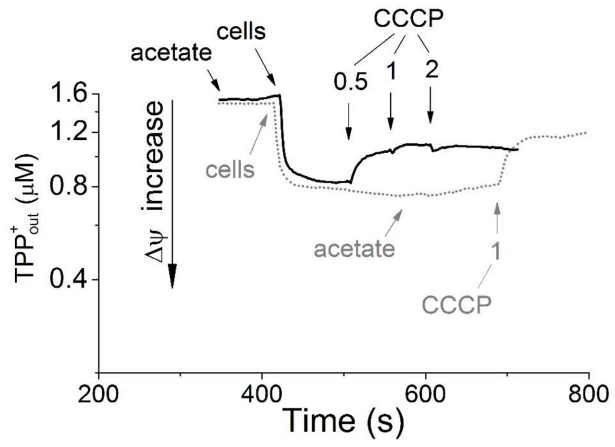

FIGURE 1 | Generation of transmembrane electrical potential in aerobically grown resting cells of *Melioribacter roseus*. The incubation medium (pH 7.0) was the same as the growth medium with the exception that the growth factors were omitted, but TPP-Cl was added to the final concentration of 1.6 μM. Small arrows indicate time points of the following additions to the incubation mixture: the cells to achieve 3 mg ml^{-1} of total cell protein; sodium acetate to achieve 10 mM final concentration; and CCCP in micromolar concentrations as indicated in the panel. Membrane potential is shown in the intact cells preincubated without acetate before its addition (gray dotted line) and in the cells incubated for 5 min with acetate (black solid line). All measurements were carried out at 52°C.

Identification of the Key Terminal Oxygen Reductases

During previous preliminary genome analysis of *M. roseus*, three putative terminal oxidoreductases were revealed: two heme-copper cytochrome *c* oxidases and a quinol oxidase of the *bd*-type (Podosokorskaya et al., 2013). Sequence analysis of the catalytic subunits MROS_0038 and MROS_1513 (CoxI and CcoNO, respectively) and the analysis of the genomic context of their genes (Podosokorskaya et al., 2013; Karnachuk et al., 2015) revealed that CoxI is highly similar (66% amino acid sequence identity at 97% query coverage) to the atypical heme-copper $cc(o/b)o_3$ cytochrome oxidase with an unusual heme content, which was recently described in a strict anaerobe *Desulfovibrio vulgaris* Hildenborough as a proton-translocating enzyme involved in oxygen detoxification (Ramel et al., 2013). The CcoNO of *M. roseus* was proposed to be a typical cbb_3-type oxidoreductase with homologs in various Bacteroidetes, mainly aerobic ones (Podosokorskaya et al., 2013; Karnachuk et al., 2015). The phylogenetic analysis of *coxI* and *ccoNO* genes, performed within this work, generally reproduced the currently accepted phylogeny of heme-copper oxidoreductases (HCO; Sousa et al., 2012; Ducluzeau et al., 2014; Muntyan et al., 2015). The CoxI protein from *M. roseus* displayed close relation to the catalytic subunit of the $cc(o/b)o_3$ cytochrome oxidase described in *D. vulgaris*, while both enzymes appeared in the same distinct subclade of A-type oxidoreductases (**Figure 2**), which possess low affinity to O_2 and are proposed to be best adapted to

modern atmospheric oxygen concentration (Ducluzeau et al., 2014). Analysis of protein sequences from the '*M. roseus* subclade' (**Figure 2**) with a web-based HCO classifying tool (Sousa et al., 2011, www.evocell.org/hco) recognized all of them as A2-subtype oxidoreductases possessing several peculiar residues in their proton channels (Sousa et al., 2012). The CcoNO protein of *M. roseus* fell within the clade of the authentic cbb_3 oxidoreductases of C-type (**Figure 2**) notable for the mandatory Glu in the active center (Muntyan et al., 2015).

Sequence analysis of the catalytic subunit, CydA, of the *bd*-type quinol oxidase (MROS_0843) put this enzyme into the most widespread subfamily A of cytochromes *bd* with a "short Q-loop" between transmembrane helixes 6 and 7 (Borisov et al., 2011). Sequences from Bacteroidetes prevail in the first 100 best BLAST hits of MROS_0843 (UniProt database search on March 2017, Supplementary Table S3). In recent reviews, sporadic distribution of different cytochrome *bd*-type oxidases within the phylum Bacteroidetes was demonstrated and supposed to be a result of horizontal gene transfer. These cytochrome *bd* oxidases were proposed to perform various physiological functions apart from proton motive force generation, such as facilitating the colonization of O_2-poor environments or detoxifying oxygen under oxidative stress and other stressful conditions (Borisov et al., 2011; Giuffrè et al., 2014).

To investigate which of the predicted oxidases and accessory proteins are involved in oxygen respiration at atmospheric O_2 concentration, the results of a shotgun proteomic analysis of transmembrane and membrane-bound proteins were compared across two cultivation conditions: growth by aerobic respiration (at atmospheric O_2 with acetate) and maltose fermentation under strictly anaerobic conditions (at negative E_h of –130 mV vs SHE). Totally, at both growth conditions, each in three biological replicas, 1239 proteins were identified with a minimum of two unique peptides. The number of proteins identified per

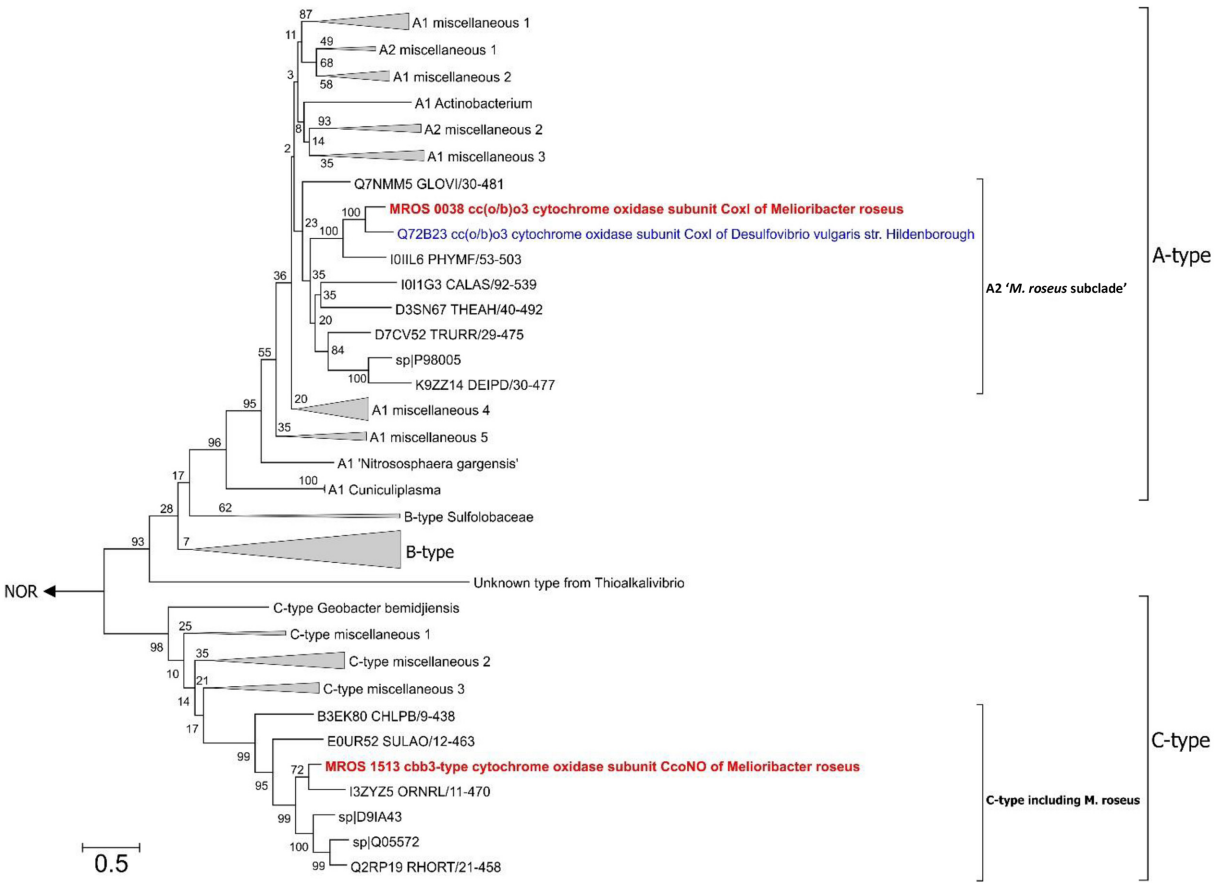

FIGURE 2 | Maximum Likelihood phylogenetic tree of PF00115 domain (COX1 family, heme-copper oxygen reductases) sequences. Refer to the text for the description of A2 '*M. roseus* subclade'. After 50% sequence identity filtering of PF00115 sequences from the "seed" data-set (http://pfam.xfam.org/family/pf00115#tabview=tab3) a total of 112 sequences were used for the analysis. The tree with the highest log likelihood is shown. The bootstrap values (1000 replicates) are shown next to the branches. All positions with less than 95% site coverage were eliminated. There were a total of 367 positions in the final dataset. The tree was constructed in MEGA6 (Tamura et al., 2013). The "unknown group" was first introduced by Muntyan et al. (2015). Nitric oxide reductases (NOR) were used as an outgroup. CoxI protein of the $cc(o/b)o_3$ cytochrome oxidase (A2-subtype) and CcoNO protein of the cbb_3 oxygen reductase (C-type) of *M. roseus* are in bold red, and CoxI protein of oxygen detoxificating $cc(o/b)o_3$ cytochrome oxidase of *D. vulgaris* str. Hildenborough is in bold blue. Bar is 0.5 substitutions per site.

each sample is provided in Supplementary Tables S4–S6. For quantitative proteome analysis, exponentially modified protein abundance indexes (emPAIs) were calculated: 304 proteins were significantly different (adjusted p-value <0.05) between the cells grown by aerobic respiration and the cells grown by fermentation under strictly anaerobic conditions (Supplementary Table S2). Some proteins were identified reliably in aerobically grown cells only. Included among those proteins were (i) the catalytic subunit CoxI and the subunit CoxII of the *cc(o/b)o*$_3$ cytochrome oxidase, (ii) its redox partner class I soluble cytochrome c_{551}/c_{552} (MROS_0033), (iii) two subunits of the alternative complex III, ActC and fused ActDE, encoded in the same cluster with the *cc(o/b)o*$_3$ oxidase by MROS_0043 and MROS_0042, respectively, and (iv) the metal ion-binding subunit of copper-transporting ATPase, MROS_1511, proposed to participate in the biogenesis of heme-copper oxidases in *M. roseus* (Karnachuk et al., 2015). Upregulation at aerobic versus fermentative growth was statistically significant for the following proteins (**Figure 3**): (i) the catalytic subunit of the ACIII complex, ActB (encoded by MROS_0044), (ii) the NADH-dehydrogenase subunit, NuoG (encoded by MROS_2032), essential to provide the catalytic site for NADH oxidation in respiratory complex I, (iii) the SCO1/SenC domain protein encoded by MROS_0039, which is located in the same cluster (MROS_0034-0039) as the *cc(o/b)o*$_3$ oxidase genes and could determine the post-translational step in the accumulation of heme-copper oxidase subunits, CoxI and CoxII (Buchwald et al., 1991), (iv) the cytochrome *c* biogenesis protein F, encoded by MROS_0623 (CcmF). It should be mentioned that 3-fold upregulation at aerobic conditions was also significant in the case of subunit III of the *cbb*$_3$-type oxygen reductase, while the catalytic subunit, CcoNO, of this complex was detected in only one biological replica, which does not allow for the prediction of the influence of aerobiosis on its abundance in the cells. Among proteins detected at fermentative conditions only (Supplementary Table S2) are hydrogenases of the [FeFe]-family (MROS_0634, 0635, 2480-2482, 2487, 2488), which were proposed to oxidize NADH to produce H_2 during the fermentation of sugars (Kadnikov et al., 2013), and the subunit alpha of pyruvate:ferredoxin oxidoreductase (MROS_2663), which catalyzes the final step in the Embden-Meyerhof-Parnas pathway (Kletzin and Adams, 1996). This result seems logical considering that all of the

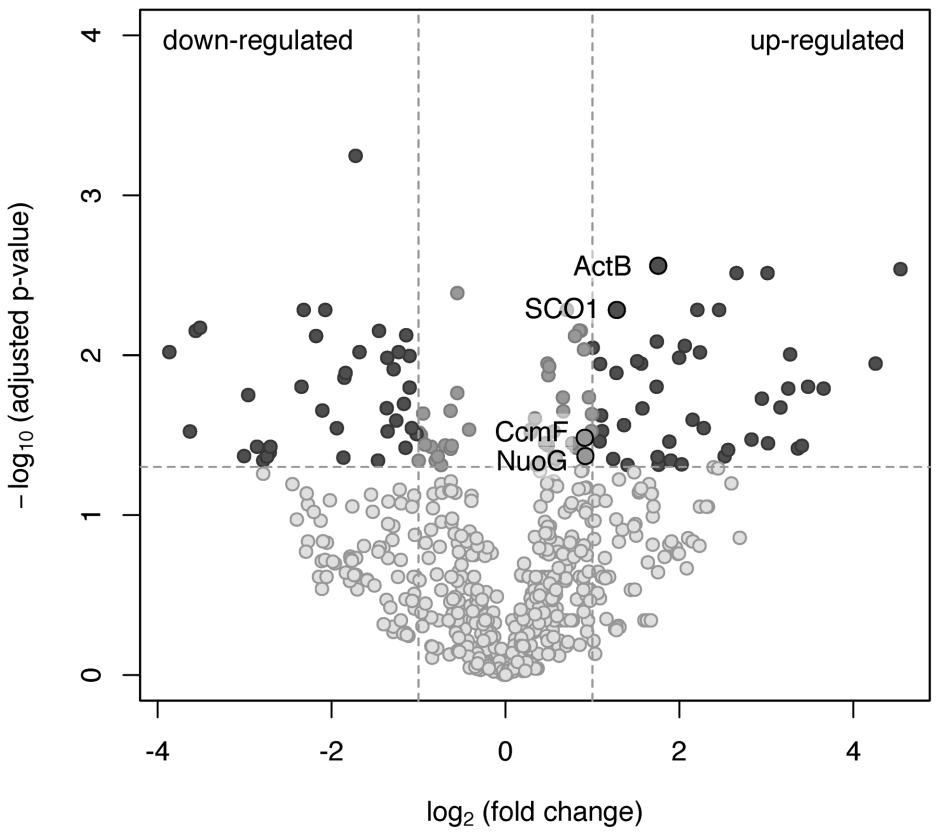

FIGURE 3 | A volcano plot representation of the differentially expressed genes in a pairwise comparison of *M. roseus* cultures grown at aerobic and fermentative (strictly anaerobic) conditions. The significance cut-off was set to a p-value of 0.05 ($-\log_{10}$(adjusted p-value) >1.3), and the biological cut-off was set to a fold change of 2 ($-1 \geq \log_2$(fold change) ≥ 1). The three colors differentiate genes with minor or insignificant changes in expression (grayish), statistically and biologically up-regulated or down-regulated genes (dark gray) and statistically but not biologically up-regulated or down-regulated genes (light gray). Proteins detected solely at aerobic or fermentative conditions are not the subjects of this analysis. Upregulated proteins captured in black circles are related to oxygen respiration (refer to the text for details).

proteins suppressed under aerobic conditions are involved in the fermentative catabolism of prokaryotes. Notably, insensitivity of the cytochrome *bd* oxidase to the change of growth conditions supports the prediction that this enzyme does not play a role of a terminal oxygen reductase during the aerobic growth of *M. roseus*.

Overall, the results of the proteomic analysis, in concordance with the abovementioned biochemical data, clearly indicate the involvement of complexes I, ACIII and the atypical heme-copper *cc(o/b)o*$_3$ cytochrome oxidase in aerobic respiration in *M. roseus*, what is supported by the expression pattern of the proteins involved in heme-copper enzymes' biogenesis. To our knowledge, this is the first reported evidence at protein level of the involvement of ACIII in conjunction with the *cc(o/b)o*$_3$ cytochrome oxidase in aerobic respiration. The homolog of the *cc(o/b)o*$_3$ cytochrome oxidase of *M. roseus* has been comprehensively characterized only in *D. vulgaris*, in which the involvement of this enzyme in oxygen reduction coupled to proton motive force generation was demonstrated. However, no growth stimulation by oxygen was observed for this organism, and transcriptomic data only suggested a detoxifying role of this enzyme in the metabolism of the strict anaerobe, *D. vulgaris* (Lamrabet et al., 2011; Ramel et al., 2013). In general, our proteomic analysis revealed induction of the *cc(o/b)o*$_3$ cytochrome oxidase (MROS_0035-0038) during aerobic growth of *M. roseus* in comparison to fermentative growth, while the differences in expression of the *cbb*$_3$ cytochrome oxidase proteins (MROS_1513-1515) and the *bd*-type oxidase (MROS_0842-0843) were not reliably detected.

Differentially Expressed Genes of Oxidoreductases at Various Growth Conditions

Comparative transcriptomics approach was used to confirm the findings of proteomic analysis and distinguish the metabolic roles of the two different HCOs and the cytochrome *bd* oxidase in *M. roseus.* Thus, the results of the RT-PCR analysis, targeted at *M. roseus* genes encoding the catalytic subunits of the three oxidoreductases (*coxI*, *ccoNO*, *cydA*), were compared across four different cultivation conditions: respiratory aerobic growth with acetate at atmospheric O_2 concentration, microaerobic growth with acetate at 2% O_2 in the gas phase, maltose fermentation at positive E_h value of the medium (see Methods section) or at negative E_h value (i.e., at strict anaerobiosis). An anaerobic medium with positive E_h was used to assess possible involvement of the cytochrome oxidases in the oxidative stress response under the absence of oxygen in the gas phase but the presence of dissolved oxidized compounds. Strikingly, the genes of all three oxidases were transcribed at aerobic, microaerobic and both anaerobic growth conditions, although the normalized transcription level differed significantly (**Figure 4**). The highest normalized transcription level was observed for the *coxI* gene of the *cc(o/b)o*$_3$ cytochrome oxidase at aerobic conditions; the level decreased ca. 1.5-fold under microaerobic conditions (adjusted *p*-value 0.073, *p*-value 0.029) and significantly lowered 4 to 6-fold at anaerobic fermentative

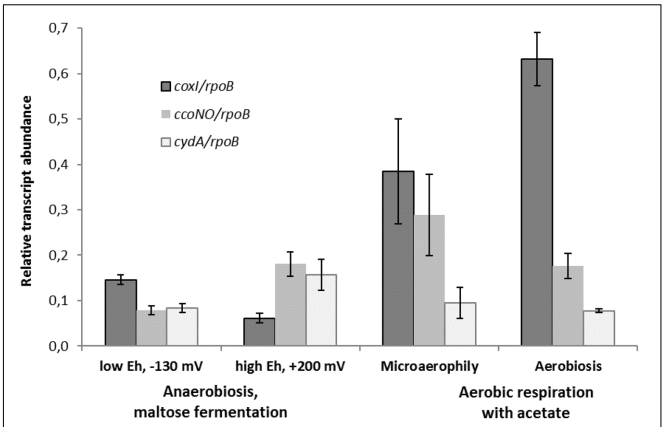

FIGURE 4 | Relative transcript abundance of catalytic subunits of three different terminal oxygen reductases in aerobically or anaerobically (fermentatively) grown cells of *M. roseus*. Represented are the genes of catalytic subunits of the following terminal oxidases: *coxI* – heme-copper *cc(o/b)o*$_3$ cytochrome oxidase, *ccoNO* – heme-copper *cbb*$_3$-type oxidase and *cydA* – cytochrome *bd* oxidase. All the transcript abundances are normalized for the transcription level of the *rpoB* gene.

growth, both at negative and positive E_h (adjusted *p*-value $\ll 0.05$ for both pairwise comparisons). Different pattern was observed for *ccoNO* gene of the *cbb*$_3$-type cytochrome oxidase, the transcription level of which was maximal at microaerobic cultivation conditions, did not statistically change at both aerobic or positive-E_h anaerobic fermentative conditions and approached its minimum at strict anaerobiosis, at negative E_h (adjusted *p*-value 0.028 for the comparison of maximal and minimal *ccoNO* transcription levels). Cytochrome *bd* oxidase demonstrated the lowest transcription levels among all three oxygen reductases at respiratory growth conditions (**Figure 4**). Although, transcript abundance of *cydA* gene was statistically indistinguishable at all tested growth conditions (adjusted *p*-values > 0.05 for all pairwise comparisons).

The results of transcriptomic studies demonstrate the key role of the A2-subtype *cc(o/b)o*$_3$ cytochrome oxidase as the terminal oxidoreductase in *M. roseus* aerobic respiration, while another heme-copper *cbb*$_3$-type oxidase is supposed to play an auxiliary role in aerobic respiration, which, however, becomes important at microaerobic conditions when a higher affinity to O_2 is needed to support the cell growth by oxygen respiration. Indeed, the oxidases of the *cbb*$_3$-type possess a high affinity to oxygen (Pitcher et al., 2002) compared to the affinity measured for a *cc(o/b)o*$_3$ cytochrome oxidase in *D. vulgaris* (Ramel et al., 2013). Thus, the *cbb*$_3$ oxidase of *M. roseus* is likely to play a major role in aerobic respiration at microaerobic conditions or, alternatively, serve for oxygen scavenging upon anaerobic fermentative growth at positive E_h (i.e., when dissolved O_2 could be present in the environment at a concentration insufficient for the activity of the *cc(o/b)o*$_3$ cytochrome oxidase). Comparatively low transcription levels of the cytochrome *bd* oxidase at all tested conditions allows us to suggest that this enzyme mainly serves for the scavenging or detoxification of oxygen and is not directly involved in the aerobic energy

metabolism of *M. roseus*. Of further note, the transcription of the *coxI* gene was significantly higher at strict anaerobiosis than at positive-E_h fermentative conditions (adjusted *p*-value 0.028, **Figure 4**), what could reflect the similarity between the functional properties of the *cc(o/b)o*$_3$ cytochrome oxidase from *M. roseus* and its close homolog from the strict anaerobe, *D. vulgaris*, in which the detoxificating role of this oxidoreductase has been evidenced.

Interestingly, transcription of *atpA* (Supplementary Figure S1) and the genes of cytochrome oxidases (**Figure 4**) was still observed at strictly anaerobic conditions during maltose fermentation, although several enzymes involved in fermentative catabolism clearly were upregulated at these conditions, according to our proteomic analysis. The transcription of *atpA* during fermentation correlates with the expression data on four major F_0F_1-ATPase subunits (Supplementary Table S2) and could be explained in the view of probable functioning of the ATPase in the reverse direction of ATP hydrolysis for the dissipation of proton excess to prevent cytoplasm acidification. This function was proposed first for F_0F_1 ATPases in *Clostridium pasteurianum* and *Thermotoga maritima* pathways of acetogenic glucose fermentation, in which the key role was assigned to electron bifurcating [FeFe]-hydrogenases driving the thermodynamically unfavorable oxidation of NADH through the exergonic oxidation of ferredoxin to produce H_2 (Buckel and Thauer, 2013). In the case of *M. roseus*, H_2, acetate and CO_2 are the main products of maltose fermentation (Podosokorskaya et al., 2013), and one of two putative [FeFe]-hydrogenases (MROS_0634) was upregulated during maltose fermentation. Accordingly, *M. roseus* is likely to possess a mode of fermentative catabolism similar to that proposed for *C. pasteurianum* and *T. maritima*, involving hydrolytic activity of F_0F_1 ATPase (Buckel and Thauer, 2013). Low-level transcription of cytochrome oxidases genes during fermentative growth could be explained by the "semper paratus" state of catabolic machinery in *M. roseus*, considering the instability of its natural environmental conditions (Podosokorskaya et al., 2013; Frank Y. et al., 2016), that is, the low biosynthesis level of key respiratory enzymes is probably sustained by a regulome of *M. roseus* in order to outcompete for electron acceptors upon sharp changes to the geochemical setting.

Screening for Respiratory Arsenate Reductases

We have previously reported on arsenate respiration in growth experiments with *M. roseus* (Podosokorskaya et al., 2013). Preliminary genome analysis (Podosokorskaya et al., 2013) pointed out the genes of two oxidoreductase complexes belonging to the CISM superfamily (Duval et al., 2008). Phylogenetic analysis of their molybdopterin catalytic subunits MROS_1076 and MROS_1774 (Supplementary Figure S3), performed in the frames of the current work, revealed their affiliation to tetrathionate- (Ttr) and polysulfide/thiosulfate- (Psr/Phs) reductase branches, respectively, but not to dissimilatory arsenate reductases (Arr). According to our (Supplementary Figure S3) and previous (Duval et al., 2008; Sorokin et al., 2016) reconstructions, the Ttr clade originates from the same root as the Arr clade, which, in its turn, has a common ancestor with the Psr/Phs cluster. To the moment, the only organism reported to use a non-Arr-type oxidoreductase to respire arsenate is *Pyrobaculum aerophilum*. This hyperthermophilic archaeon, similarly to *M. roseus*, possesses Ttr- and Psr/Phs-type, but not Arr-type, oxidoreductases of the CISM superfamily (Cozen et al., 2009).

Considering that no other candidates for arsenate respiration were found in *M. roseus*, the transcription pattern of molybdopterin catalytic subunits MROS_1076 and MROS_1774 was studied for the cells grown by respiration with acetate as the electron donor and arsenate as the sole electron acceptor under anaerobic cultivation conditions. The cells, grown with acetate under aerobic or microaerobic conditions and those grown by maltose fermentation under strict anaerobiosis (E_h –130 mV), were used as negative controls. Two sets of primers for *M. roseus* genes, encoding the molybdopterin catalytic subunits, were designed, and normalized transcription levels were compared across all four cultivation conditions (arsenate, aerobic, microaerobic respiration, and maltose fermentation).

The transcription of *ttrA* and *psr/phsA* genes was almost negligible in the absence of arsenate but dramatically increased in cells grown with arsenate (**Figure 5**). These results suggest that both 'Psr/Phs' and 'Ttr' molybdopterin oxidoreductases are involved in arsenate respiration. Yet we should note, that only the induction of *psrA/phsA* was clearly statistically distinguishable (adjusted *p*-value 0.03) in arsenate-grown cells of *M. roseus*. Interestingly, despite the presence of Ttr- and Psr/Phs-type enzymes as candidate arsenate reductases in both *P. aerofilum* and *M. roseus* (Supplementary Figure S3), As(V) did induce only one molybdopterin oxidoreductase in *P. aerofilum* – the TtrA (PAE1265, Cozen et al., 2009), while in *M. roseus* both

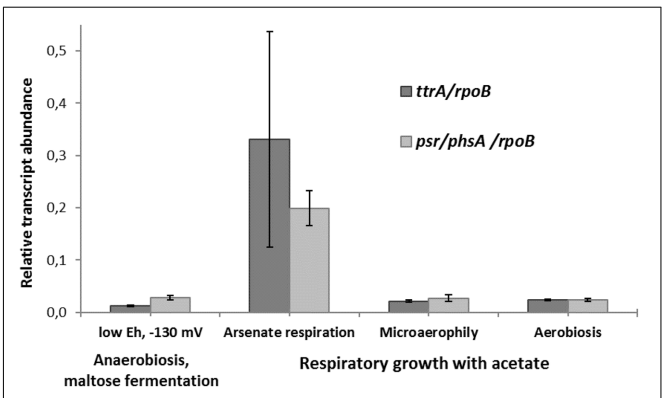

FIGURE 5 | Relative transcript abundance of *ttrA* and *psr/phsA* genes involved in arsenate respiration of *M. roseus* grown at different growth conditions. Represented are the genes of catalytic subunits of the following CISM family oxidoreductases: *ttrA* – tetrathionate-like reductase, presumably involved in arsenate detoxification cascade, and *psr/phsA* – polysulfide/thiosulfate-like reductase, presumed to serve as the terminal dissimilatory arsenate reductase. All the transcript abundances are normalized for the transcription level of the *rpoB* gene.

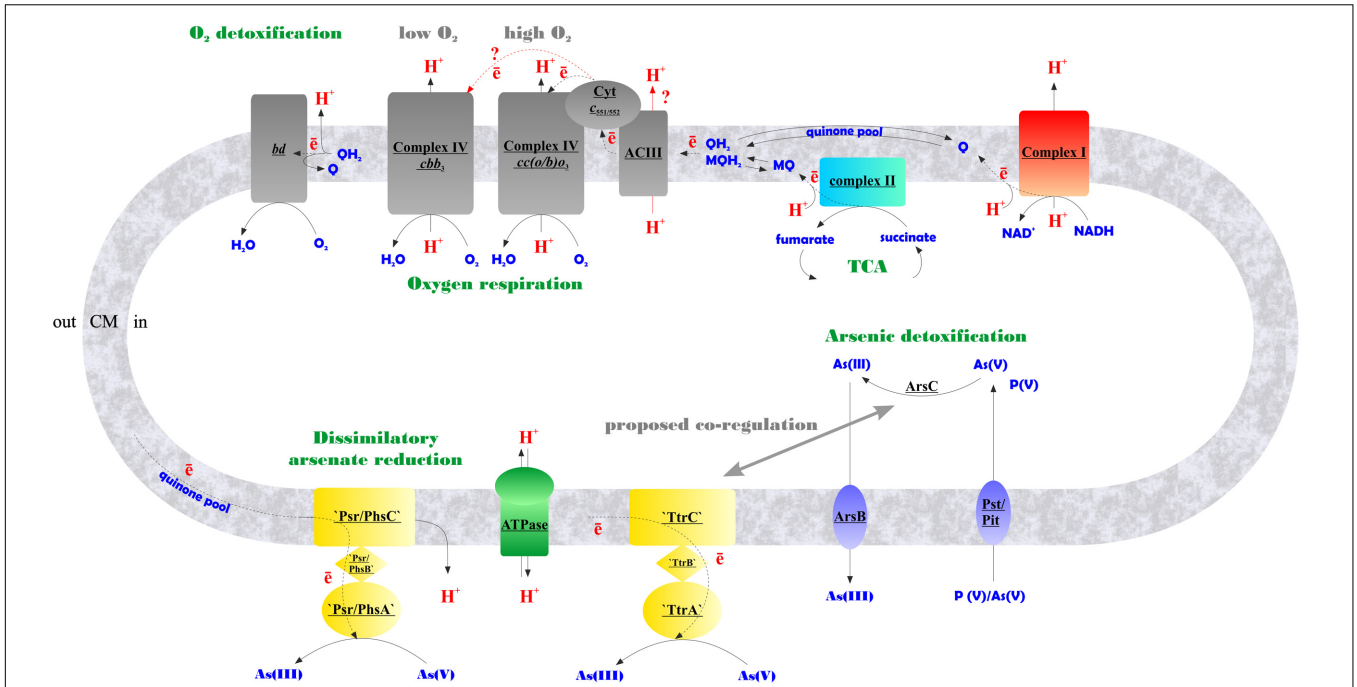

FIGURE 6 | Schematic representation of aerobic and arsenate respiratory pathways of *M. roseus* summarized from our data. Contracted notations: bd – quinol oxidase of the *bd*-type; ACIII – alternative respiratory complex III; Cyt $c_{551/552}$ – soluble monoheme *c*-type cytochrome transferring electrons from ACIII to heme-copper terminal oxidoreductases of A-type – *cc(o/b)o*$_3$, or C-type – *cbb*$_3$, upregulated at atmospheric O_2 concentration or at microaerobic conditions, respectively; 'Psr/PhsABC,' polysulfide/thiosulfate-like reductase complex of CISM family; 'TtrABC', tetrathionate-like reductase complex of CISM family (A, B and C stand for molybdopterin-containing catalytic subunits, Fe–S subunits, and membrane-bound subunits of CISM complexes, respectively); ArsC, detoxifying arsenate reductase; ArsB, arsenite efflux pump; Pst/Pit, phosphate transporter systems, non-specifically transporting arsenate into the cell (Paez-Espino et al., 2009), encoded by MROS_2637-2640, and MROS_1319 in *M. roseus*; TCA, tricarboxylic acid cycle; Q/MQ, oxidized quinones (in particular, menaquinones); QH_2/MQH_2, reduced quinones/menaquinones; CM, cytoplasmic membrane. Firm lines with arrows indicate proton flows, dotted lines indicate electron flows, red lines with red query marks indicate putative electron and proton transfer pathways.

the 'Ttr' and the 'Psr/Phs' oxidoreductases were induced with arsenate and the 'Psr/Phs' induction was more pronounced (**Figure 5**). Although, we cannot exclude participation of the 'Ttr' oxidoreductase in arsenate metabolism of *M. roseus*, considering occurrence of transcriptional response of the *ttrA* gene to arsenate and its peculiar genomic neighborhood. Encoded right upstream of the *ttr* locus in *M. roseus* genome is an 'ArrTSR' two-component regulatory system (Saltikov, 2011), including a phosphorylated response regulator ('ArrR', MROS_1070), a sensory histidine kinase ('ArrS', MROS_1069) and a hypothetical protein (MROS_RS05510 according to the recent NCBI RefSeq reannotation), homologous to a periplasmic phosphonate binding protein 'ArrT' (Saltikov, 2011), a part of phosphonate ABC transporters (Alicea et al., 2011). The 'ArrTSR' system is supposed to induce transcription of dissimilatory arsenate reductases in response to periplasmic arsenate via the 'ArrR' regulator (Saltikov, 2011). Finally, in *M. roseus* in close vicinity to *arrT* gene is an ars-type arsenic resistance locus *arsRPCB* (MROS_1063-1067, Kadnikov et al., 2013), encoding detoxificating glutathione:arsenate oxidoreductase ArsC, an arsenite exporter ArsB and a specific regulator ArsR, which induces transcription of *arsPCB* in the presence of arsenite (Saltikov, 2011). In contrast to *ttr*, the *psr*/*phs* locus is preceded by the gene of MerR-like transcription activator (MROS_1773), which can respond to heavy metal ions and chemical stresses (Brown et al., 2003). Peculiarities of genomic environment of *ttrA* and *psrA*/*phsA* genes allow us to hypothesize that 'PsrA/PhsA' and 'TtrA' enzymes play different roles in arsenate respiration of *M. roseus*. We propose the 'PsrA/PhsA' to be the major arsenate reductase, as its transcription could be directly induced by As(V) and such an induction is supported by our experimental data. On the other hand, 'TtrA' could act as an auxiliary arsenate reductase which activity could be co-regulated with arsenic detoxification complex ArsPCB. Thus, our results indicate utilization of two non-Arr arsenate reductases by *M. roseus* in arsenic respiratory metabolism (**Figure 6**), yet further studies are definitely needed to cast light on their exact physiological functions.

CONCLUSION

In this study, we present multiple evidences on the involvement of atypical respiratory enzymes in the energy metabolism of an extremophilic bacterium representing deep phylogenetic lineage and originating from one of Eurasian deep subsurface environments, which remained separated from the rest of the biosphere for several geological periods.

By using a combination of biochemical, bioinformatic, transcriptomic and proteomic approaches, we have evidenced the functioning of the electron transfer chain during aerobic respiration of *M. roseus*, which is comprised of NADH-dehydrogenase I, respiratory complex II, alternative complex III and an atypical A2-subtype *cc(b/o)*o_3 cytochrome oxidase. The *cc(b/o)*o_3 cytochrome oxidase has been previously characterized exclusively in *D. vulgaris,* where it was shown to serve only for oxygen detoxification. Here is the first evidence of the involvement of this enzyme in aerobic respiration. Furthermore, a wide distribution of homologs of this type of enzyme among aerobes (Lamrabet et al., 2011) might suggest its involvement in oxygen respiration in many of these microorganisms. Based on our results, we propose the metabolic scheme of aerobic respiration in *M. roseus* (**Figure 6**), in which the *cc(b/o)*o_3 cytochrome oxidase is the major terminal oxidoreductase upon atmospheric O_2 concentration, while at microaerobic growth conditions another heme-copper oxidase, belonging to the *cbb*$_3$-type, solos in energy transduction in this organism. The third oxidoreductase detected in *M. roseus*—the cytochrome *bd* oxidase—most likely serves for oxygen scavenging at both aerobic and anaerobic growth conditions. Our transcriptomic studies have supported comparative genomics predictions on participation of two molybdopterin oxidoreductases, not belonging to the Arr clade, in arsenate respiration. We further hypothesize that these two molybdoenzymes are involved differently in arsenic metabolism of *M. roseus*: while one of them acts as the major dissimilatory arsenate reductase, the other is likely to be linked with arsenic detoxification pathway (**Figure 6**).

AUTHOR CONTRIBUTIONS

SG, IK, EB-O convened the research. SG, IK, AM, DA, VG designed the research. SG, IK, OP, AM, MK, MM, IA, IB performed experimental work. SG, IK, MM, OP, IA, EB-O wrote the manuscript.

FUNDING

The work of SG, OP, AM, MK, EA, and IK on respiratory metabolism (major growth experiments, phylogenetic, genomic, and transcriptomic studies) was supported by the RSF project # 14-24-00165. The work of IB and VG on proteomic studies was supported by the RSF project # 14-24-00159. The work of MM was supported by the RSF project # 14-50-00029 (respiratory activity and membrane potential measurements) and the RFBR project # 17-04-02173 (part of genomic analysis).

ACKNOWLEDGMENT

We would like to thank Dr. Dmitry Yu. Sorokin for his thoughtful comments on bacterial oxygen metabolism.

SUPPLEMENTARY MATERIAL

The Supplementary Material for this article can be found online at: http://journal.frontiersin.org/article/10.3389/fmicb.2017.01228/full#supplementary-material

REFERENCES

Abascal, F., Zardoya, R., and Posada, D. (2005). ProtTest: selection of best-fit models of protein evolution. *Bioinformatics* 21, 2104–2105. doi: 10.1093/bioinformatics/bti263

Alicea, I., Marvin, J. S., Miklos, A. E., Ellington, A. D., Looger, L. L., and Schreiter, E. R. (2011). Structure of the *Escherichia coli* phosphonate binding protein PhnD and rationally optimized phosphonate biosensors. *J. Mol. Biol.* 414, 356–369. doi: 10.1016/j.jmb.2011.09.047

Benjamini, Y., and Hochberg, Y. (1995). Controlling the false discovery rate: a practical and powerful approach to multiple testing. *J. R. Stat. Soc. Series B Stat. Methodol.* 57, 289–300.

Borisov, V. B., Gennis, R. B., Hemp, J., and Verkhovsky, M. I. (2011). The cytochrome *bd* respiratory oxygen reductases. *Biochim. Biophys. Acta* 1807, 1398–1413. doi: 10.1016/j.bbabio.2011.06.016

Brown, N. L., Stoyanov, J. V., Kidd, S. P., and Hobman, J. L. (2003). The MerR family of transcriptional regulators. *FEMS Microbiol. Rev.* 27, 145–163. doi: 10.1016/S0168-6445(03)00051-2

Buchwald, P., Krummeck, G., and Rodel, G. (1991). Immunological identification of yeast SCO1 protein as a component of the inner mitochondrial membrane. *Mol. Gen. Genet.* 229, 413–420. doi: 10.1007/BF00267464

Buckel, W., and Thauer, R. K. (2013). Energy conservation via electron bifurcating ferredoxin reduction and proton/Na+ translocating ferredoxin oxidation. *Biochim. Biophys. Acta* 1827, 94–113. doi: 10.1016/j.bbabio.2012.07.002

Cooper, C. E., and Brown, G. C. (2008). The inhibition of mitochondrial cytochrome oxidase by the gases carbon monoxide, nitric oxide, hydrogen cyanide and hydrogen sulfide: chemical mechanism and physiological significance. *J. Bioenerg. Biomembr.* 40, 533–539. doi: 10.1007/s10863-008-9166-6

Cozen, A. E., Weirauch, M. T., Pollard, K. S., Bernick, D. L., Stuart, J. M., and Lowe, T. M. (2009). Transcriptional map of respiratory versatility in the hyperthermophilic Crenarchaeon *Pyrobaculum aerophilum*. *J. Bacteriol.* 191, 782–794. doi: 10.1128/JB.00965-08

Ducluzeau, A.-L., Schoepp-Cothenet, B., van Lis, R., Baymann, F., Russell, M. J., and Nitschke, W. (2014). The evolution of respiratory O2/NO reductases: an out-of-the-phylogenetic-box perspective. *J. R. Soc. Interface* 11:20140196. doi: 10.1098/rsif.2014.0196

Duval, S., Ducluzeau, A.-L., Nitschke, W., and Schoepp-Cothenet, B. (2008). Enzyme phylogenies as markers for the oxidation state of the environment: the case of respiratory arsenate reductase and related enzymes. *BMC Evol. Biol.* 8:206. doi: 10.1186/1471-2148-8206

Elshahed, M. S., Senko, J. M., Najar, F. Z., Kenton, S. M., Roe, B. A., Dewers, T. A., et al. (2003). Bacterial diversity and sulfur cycling in a mesophilic sulfide-rich spring. *Appl. Environ. Microbiol.* 69, 5609–5621. doi: 10.1128/AEM.69.9.5609-5621.2003

Frank, Y., Banks, D., Avakian, M., Antsiferov, D., Kadychagov, P., and Karnachuk, O. (2016). Firmicutes is an important component in water-injected and pristine oil reservoirs; Western Siberia Russia. *Geomicrobiol. J.* 33, 387–400. doi: 10.1080/01490451.2015.1045635

Frank, Y. A., Kadnikov, V. V., Gavrilov, S. N., Banks, D., Gerasimchuk, A. L., Podosokorskaya, O. A., et al. (2016). Stable and variable parts of microbial community in siberian deep subsurface thermal aquifer system revealed in a long-term monitoring study. *Front. Microbiol.* 7:2101. doi: 10.3389/fmicb.2016.02101

Gennis, R. B. (2013). "Bacterial respiratory oxygen reductases," in *Encyclopedia of Biophysics*, ed. G. C. K. Roberts (Berlin: Springer-Verlag), 178–181. doi: 10.1007/978-3-642-16712-6_33

Giuffrè, A., Borisov, V. B., Arese, M., Sarti, P., and Forte, E. (2014). Cytochrome *bd* oxidase and bacterial tolerance to oxidative and nitrosative stress. *Biochim. Biophys. Acta* 1837, 1178–1187. doi: 10.1016/j.bbabio.2014.01.016

Huang, Y., Niu, B., Gao, Y., Fu, L., and Li, W. (2010). CD-HIT Suite: a web server for clustering and comparing biological sequences. *Bioinformatics* 26, 680–682. doi: 10.1093/bioinformatics/btq003

Iino, T., Mori, K., Uchino, Y., Nakagawa, T., Harayama, S., and Suzuki, K. (2010). *Ignavibacterium album* gen. nov., sp. nov., a moderately thermophilic anaerobic bacterium isolated from microbial mats at a terrestrial hot spring and proposal of *Ignavibacteria classis* nov., for a novel lineage at the periphery of green sulfur bacteria. *Int. J. Syst. Evol. Microbiol.* 60, 1376–1382. doi: 10.1099/ijs.0.012484-0

Ishihama, Y., Oda, Y., Tabata, T., Sato, T., Nagasu, T., Rappsilber, J., et al. (2005). Exponentially modified protein abundance index (emPAI) for estimation of absolute protein amount in proteomics by the number of sequenced peptides per protein. *Mol. Cell. Proteomics* 4, 1265–1272. doi: 10.1074/mcp.M500061-MCP200

Kadnikov, V. V., Mardanov, A. V., Podosokorskaya, O. A., Gavrilov, S. N., Kublanov, I. V., Beletsky, A. V., et al. (2013). Genomic analysis of *Melioribacter roseus*, facultatively anaerobic organotrophic bacterium representing a novel deep lineage within Bacteriodetes/Chlorobi group. *PLoS ONE* 8:e53047. doi: 10.1371/journal.pone.0053047

Kamo, N., Muratsugu, M., Hongoh, R., and Kobatake, Y. (1979). Membrane potential of mitochondria measured with an electrode sensitive to tetraphenyl phosphonium and relationship between proton electrochemical potential and phosphorylation potential in steady state. *J. Membr. Biol.* 49, 105–121. doi: 10.1007/BF01868720

Karnachuk, O. V., Gavrilov, S. N., Avakyan, M. R., Podosokorskaya, O. A., Frank, Y. A., Bonch-Osmolovskaya, E. A., et al. (2015). Diversity of copper proteins and copper homeostasis systems in *Melioribacter roseus*, a facultatively anaerobic thermophilic member of the new phylum Ignavibacteriae. *Microbiology* 84, 135–143. doi: 10.1134/S0026261715020058

Kato, S., Ikehata, K., Shibuya, T., Urabe, T., Ohkuma, M., and Yamagishi, A. (2015). Potential for biogeochemical cycling of sulfur, iron and carbon within massive sulfide deposits below the seafloor. *Environ. Microbiol.* 17, 1817–1835. doi: 10.1111/1462-2920.12648

Katoh, K., Misawa, K., Kuma, K., and Miyata, T. (2002). MAFFT: a novel method for rapid multiple sequence alignment based on fast Fourier transform. *Nucleic Acids Res.* 30, 3059–3066. doi: 10.1093/nar/gkf436

Kletzin, A., and Adams, M. W. (1996). Molecular and phylogenetic characterization of pyruvate and 2-ketoisovalerate ferredoxin oxidoreductases from *Pyrococcus furiosus* and pyruvate ferredoxin oxidoreductase from *Thermotoga maritima*. *J. Bacteriol.* 178, 248–257. doi: 10.1128/jb.178.1.248-257.1996

Lamrabet, O., Pieulle, L., Aubert, C., Mouhamar, F., Stocker, P., Dolla, A., et al. (2011). Oxygen reduction in the strict anaerobe *Desulfovibrio vulgaris* Hildenborough: characterization of two membrane-bound oxygen reductases. *Microbiology* 157, 2720–2732. doi: 10.1099/mic.0.049171-0

Mattar, S., and Engelhard, M. (1997). Cytochrome ba3 from *Natronobacterium pharaonis*. *Eur. J. Biochem.* 250, 332–341. doi: 10.1111/j.1432-1033.1997.0332a.x

Muntyan, M. S., Cherepanov, D. A., Malinen, A. M., Bloch, D. A., Sorokin, D. Y., Severina, I. I., et al. (2015). Cytochrome cbb3 of *Thioalkalivibrio* is a Na+-pumping cytochrome oxidase. *Proc. Natl. Acad. Sci. U.S.A.* 112, 7695–7700. doi: 10.1073/pnas.1417071112

Muntyan, M. S., Morozov, D. A., Klishin, S. S., Khitrin, N. V., and Kolomijtseva, G. Y. (2012). Evaluation of the electrical potential on the membrane of the extremely alkaliphilic bacterium *Thioalkalivibrio*. *Biochemistry (Moscow)* 77, 917–924. doi: 10.1134/S0006297912080135

Nichols, D. G. (2013). *Bioenergetics*, 4th Edn. Amsterdam: Academic Press.

Paez-Espino, J. T., Tamames, J., de Lorenzo, V., and Canovas, D. (2009). Microbial responses to environmental arsenic. *Biometals* 22, 117–130. doi: 10.1007/s10534-008-9195-y

Pitcher, R. S., Brittain, T., and Watmough, N. J. (2002). Cytochrome cbb(3) oxidase and bacterial microaerobic metabolism. *Biochem. Soc. Trans.* 30, 653–658. doi: 10.1042/bst0300653

Podosokorskaya, O. A., Kadnikov, V. V., Gavrilov, S. N., Mardanov, A. V., Merkel, A. Y., Karnachuk, O. V., et al. (2013). Characterization of *Melioribacter roseus* gen. nov., sp. nov., a novel facultatively anaerobic thermophilic cellulolytic bacterium from the class Ignavibacteria, and a proposal of a novel bacterial phylum Ignavibacteriae. *Environ. Microbiol.* 15, 1759–1771. doi: 10.1111/1462-2920.12067

Ramel, F., Amrani, A., Pieulle, L., Lamrabet, O., Voordouw, G., Seddiki, N., et al. (2013). Membrane-bound oxygen reductases of the anaerobic sulfate-reducing *Desulfovibrio vulgaris* Hildenborough: roles in oxygen defense and electron link with periplasmic hydrogen oxidation. *Microbiology* 159, 2663–2673. doi: 10.1099/mic.0.071282-0

Rauhamäki, V., Bloch, D. A., and Wikström, M. (2012). Mechanistic stoichiometry of proton translocation by cytochrome cbb_3. *Proc. Natl. Acad. Sci. U.S.A.* 109, 7286–7291. doi: 10.1073/pnas.1202151109

Rauhamäki, V., and Wikström, M. (2014). The causes of reduced proton-pumping efficiency in type B and C respiratory heme-copper oxidases, and in some mutated variants of type A. *Biochim. Biophys. Acta* 1837, 999–1003. doi: 10.1016/j.bbabio.2014.02.020

Refojo, P. N., Teixeira, M., and Pereira, M. M. (2010). The alternative complex III of *Rhodothermus marinus* and its structural and functional association with caa3 oxygen reductase. *Biochim. Biophys. Acta* 1797, 1477–1482. doi: 10.1016/j.bbabio.2010.02.029

Refojo, P. N., Teixeira, M., and Pereira, M. M. (2012). The alternative complex III: properties and possible mechanisms for electron transfer and energy conservation. *Biochim. Biophys. Acta* 1817, 1852–1859. doi: 10.1016/j.bbabio.2012.05.003

Rothery, R. A., Workun, G. J., and Weiner, J. H. (2008). The prokaryotic complex iron–sulfur molybdoenzyme family. *Biochim. Biophys. Acta* 1778, 1897–1929. doi: 10.1016/j.bbamem.2007.09.002

Saltikov, C. W. (2011). "Regulation of arsenic metabolic pathways in prokaryotes," in *Microbial Metal and Metalloid Metabolism: Advances and Applications*, eds J. F. Stolz and R. S. Oremland (Washington, DC: ASM Press), 195–210. doi: 10.1128/9781555817190.ch11

Sazanov, L. A. (2012). "Structural perspective on respiratory complex I," in *Structure and Function of NADH: Ubiquinone Oxidoreductase*, ed. L. Sazanov (Dordrecht: Springer), doi: 10.1007/978-94-007-4138-6

Smirnova, I. A., Hägerhäll, C., Konstantinov, A. A., and Hederstedt, L. (1995). HOQNO interaction with cytochrome b in succinate: menaquinone oxidoreductase from *Bacillus subtilis*. *FEBS Lett.* 359, 23–26. doi: 10.1016/0014-5793(94)01442-4

Sorokin, D. Y., Kublanov, I. V., Gavrilov, S. N., Rojo, D., Roman, R., Golyshin, P. N., et al. (2016). Elemental sulfur and acetate can support life of a novel strictly anaerobic haloarchaeon. *ISME J.* 10, 240–252. doi: 10.1038/ismej.2015.79

Sousa, F. L., Alves, R. J., Pereira-Leal, J. B., Teixeira, M., and Pereira, M. M. (2011). A bioinformatics classifier and database for heme–copper oxygen reductases. *PLoS ONE* 6:e19117. doi: 10.1371/journal.pone.0019117

Sousa, F. L., Alves, R. J., Ribeiro, M. A., Pereira-Leal, J. B., Teixeira, M., and Pereira, M. M. (2012). The superfamily of heme-copper oxygen reductases: types and evolutionary considerations. *Biochim. Biophys. Acta* 1817, 629–637. doi: 10.1016/j.bbabio.2011.09.020

Tamura, K., Stecher, G., Peterson, D., Filipski, A., and Kumar, S. (2013). MEGA6: molecular evolutionary genetics analysis version 6.0. *Mol. Biol. Evol.* 30, 2725–2729. doi: 10.1093/molbev/mst197

Tiodjio, R. E., Sakatoku, A., Nakamura, A., Tanaka, D., Fantong, W. Y., Tchakam, K. B., et al. (2014). Bacterial and archaeal communities in Lake Nyos (Cameroon, Central Africa). *Sci. Rep.* 4:6151. doi: 10.1038/srep06151

Vizcaíno, J. A., Deutsch, E. W., Wang, R., Csordas, A., Reisinger, F., Ríos, D., et al. (2014). ProteomeXchange provides globally coordinated proteomics data submission and dissemination. *Nat. Biotechnol.* 32, 223–226. doi: 10.1038/nbt.2839

Wikström, M. K. (1977). Proton pump coupled to cytochrome c oxidase in mitochondria. *Nature* 266, 271–273. doi: 10.1038/266271a0

Wilson, D. F., and Erecińska, M. (1978). Ligands of cytochrome c oxidase. *Methods Enzymol.* 53, 191–201. doi: 10.1016/S0076-6879(78)53024

Ziganshin, R. H., Ivanova, O. M., Lomakin, Y. A., Belogurov, A. A. Jr., Kovalchuk, S. I., Azarkin, I. V., et al. (2016). The pathogenesis of the demyelinating form of Guillain-Barre syndrome: proteopeptidomic and immunological profiling of physiological fluids. *Mol. Cell. Proteomics* 15, 2366–2378. doi: 10.1074/mcp.M115.056036

Conflict of Interest Statement: The authors declare that the research was conducted in the absence of any commercial or financial relationships that could be construed as a potential conflict of interest.

frontiers in Microbiology

ORIGINAL RESEARCH
published: 02 November 2017
doi: 10.3389/fmicb.2017.02140

Sugar Metabolism of the First Thermophilic Planctomycete *Thermogutta terrifontis*: Comparative Genomic and Transcriptomic Approaches

Alexander G. Elcheninov[1†], Peter Menzel[2,3†], Soley R. Gudbergsdottir[2], Alexei I. Slesarev[4], Vitaly V. Kadnikov[5], Anders Krogh[2], Elizaveta A. Bonch-Osmolovskaya[1], Xu Peng[2] and Ilya V. Kublanov[1,6*]*

[1] Winogradsky Institute of Microbiology, Research Center of Biotechnology, Russian Academy of Sciences, Moscow, Russia, [2] Department of Biology, University of Copenhagen, Copenhagen, Denmark, [3] Max Delbrück Center for Molecular Medicine, Berlin, Germany, [4] Fidelity Systems, Inc., Gaithersburg, MD, United States, [5] Institute of Bioengineering, Research Center of Biotechnology, Russian Academy of Sciences, Moscow, Russia, [6] School of Life Sciences, Immanuel Kant Baltic Federal University, Kaliningrad, Russia

OPEN ACCESS

Edited by:
Nils-Kaare Birkeland, University of Bergen, Norway

Reviewed by:
Magnus Øverlie Arntzen, Norwegian University of Life Sciences, Norway
Harold J. Schreier, University of Maryland, Baltimore County, United States

***Correspondence:**
Ilya V. Kublanov
kublanov.ilya@gmail.com
Alexander G. Elcheninov
elcheninov.ag@gmail.com

† These authors have contributed equally to this work.

Specialty section:
This article was submitted to Extreme Microbiology, a section of the journal Frontiers in Microbiology

Received: *08 September 2017*
Accepted: *19 October 2017*
Published: *02 November 2017*

Citation:
Elcheninov AG, Menzel P, Gudbergsdottir SR, Slesarev AI, Kadnikov VV, Krogh A, Bonch-Osmolovskaya EA, Peng X and Kublanov IV (2017) Sugar Metabolism of the First Thermophilic Planctomycete Thermogutta terrifontis: Comparative Genomic and Transcriptomic Approaches. Front. Microbiol. 8:2140. doi: 10.3389/fmicb.2017.02140

Xanthan gum, a complex polysaccharide comprising glucose, mannose and glucuronic acid residues, is involved in numerous biotechnological applications in cosmetics, agriculture, pharmaceuticals, food and petroleum industries. Additionally, its oligosaccharides were shown to possess antimicrobial, antioxidant, and few other properties. Yet, despite its extensive usage, little is known about xanthan gum degradation pathways and mechanisms. *Thermogutta terrifontis*, isolated from a sample of microbial mat developed in a terrestrial hot spring of Kunashir island (Far-East of Russia), was described as the first thermophilic representative of the *Planctomycetes* phylum. It grows well on xanthan gum either at aerobic or anaerobic conditions. Genomic analysis unraveled the pathways of oligo- and polysaccharides utilization, as well as the mechanisms of aerobic and anaerobic respiration. The combination of genomic and transcriptomic approaches suggested a novel xanthan gum degradation pathway which involves novel glycosidase(s) of DUF1080 family, hydrolyzing xanthan gum backbone beta-glucosidic linkages and beta-mannosidases instead of xanthan lyases, catalyzing cleavage of terminal beta-mannosidic linkages. Surprisingly, the genes coding DUF1080 proteins were abundant in *T. terrifontis* and in many other *Planctomycetes* genomes, which, together with our observation that xanthan gum being a selective substrate for many planctomycetes, suggest crucial role of DUF1080 in xanthan gum degradation. Our findings shed light on the metabolism of the first thermophilic planctomycete, capable to degrade a number of polysaccharides, either aerobically or anaerobically, including the biotechnologically important bacterial polysaccharide xanthan gum.

Keywords: planctomycetes, thermophiles, CAZymes, xanthan gum, comparative genomics, transcriptomics, metabolism reconstruction

INTRODUCTION

Planctomycetes is a bacterial phylum, comprising only a few cultivated species, while a large number of ribosomal RNA sequences from various uncultured planctomycetes have been observed in the SILVA Ref database (release 128, Quast et al., 2013). Altogether, around a hundred sequenced planctomycetes genomes are available today, including 38 genome sequences of cultivated and ca. twice that amount of uncultivated ones (IMG database, March 2017, Markowitz et al., 2012). Cultivated planctomycetes with validly published names comprise 2 classes, 3 orders, 5 families, 25 genera, and 29 species. Until recently, all of these were characterized as strictly aerobic, heterotrophic and peptidoglycan-less microorganisms, which reproduce by budding and grow at mesophilic and slightly psychrophilic conditions (Liesack et al., 1986; Fuerst and Sagulenko, 2011). However, all of these features were reconsidered during the past few years. Their cell walls have been shown to contain a uniquely thin peptidoglycan layer (Jeske et al., 2015), representatives of the novel class *Phycisphaerae* divide by binary fission (Fukunaga et al., 2009; Kovaleva et al., 2015) instead of budding, and, finally, a few thermophilic and facultative anaerobic representatives were recently isolated (Kovaleva et al., 2015; Slobodkina et al., 2015). Even though no autotrophic planctomycetes were isolated and cultivated so far, members of the third class-level lineage, represented by uncultivated anammox planctomycetes (van de Graaf et al., 1995), are thought to fix CO_2 via the acetyl-CoA pathway (Strous et al., 2006).

Thermogutta terrifontis was characterized as the first thermophilic representative of the phylum *Planctomycetes* (Slobodkina et al., 2015). Among two species of the genus one, *T. hypogea*, was isolated from a subsurface environment of a Beatrix gold mine, SAR, while the second, *T. terrifontis*, was isolated from a microbial mat, developed in a terrestrial hot spring of Kunashir island (Far-East of Russia). As other cultivated planctomycetes, *T. terrifontis* grew well on various carbohydrates including oligo- and polysaccharides. At the same time its capability of anaerobic growth by either fermentation or anaerobic respiration was a novel finding among the representatives of this phylum. Yet, nothing is known on the mechanisms underlying these novel capabilities. *T. terrifontis* strain R1 has been shown to grow on xanthan gum (Slobodkina et al., 2015) – a complex polysaccharide synthesized by *Xanthomonas campestris*, comprising a beta-1,4-glucan backbone and mannosyl–glucuronyl–mannose side chains. Xanthan gum itself has numerous biotechnological applications in cosmetics, agriculture pharmaceuticals, food and petroleum industries (García-Ochoa et al., 2000). Moreover, its oligosaccharides were described as elicitors, stimulating plants in their defense response against pathogens (Liu et al., 2005); as antimicrobial compounds (Qian et al., 2006) and as antioxidants (Xiong et al., 2013). At the moment, not much is known about its decomposition pathways, especially on mechanisms and involved proteins. A few key enzymes needed to break xanthan gum side chains (xanthan lyases, beta-glucuronyl hydrolases, and alpha-mannosidases) are known, yet still no glycosidases acting on the glucan backbone of xanthan gum have been characterized. Here, we reconstructed the central carbohydrate metabolism of *T. terrifontis* strain R1 using genomic and transcriptomic sequencing with a special emphasis on xanthan gum degradation.

MATERIALS AND METHODS

Cultures and DNA/RNA Extraction

Thermogutta terrifontis R1 cells were grown under microaerophilic conditions for 2–4 days in glass bottles, sealed with butyl rubber plug with aluminum cap, on modified Pfenning medium supplemented with xanthan gum or trehalose as a growth substrate. Mineral growth medium (Podosokorskaya et al., 2011) was prepared aerobically; 50 mg l^{-1} of yeast extract (Sigma) was added as a source of indefinite growth factors. Atmospheric air was in the gas phase and no reducing agents or resazurin were added. pH was adjusted to 6.1 with 5 M NaOH. Xanthan gum (1 g/l) [KELTROL®T (food grade Xanthan Gum, Lot#2F5898K) CP Kelco] or trehalose (2 g/l) (Sigma, T9531) were added from sterile stock solutions before inoculation.

For genome sequencing 2000 ml of *T. terrifontis* grown culture was centrifuged at 17664 G, and cells pellet was harvested. Total DNA was extracted from the cell pellet by freezing and thawing in TNE buffer (Tris 20 mM, NaCl 15 mM, EDTA 20 mM). After treating with lysozyme, RNase A, SDS, and proteinase K the DNA was extracted with phenol/chloroform and precipitated with EtOH and dissolved in 2 mM TE buffer (Gavrilov et al., 2016).

For the transcriptomic experiment, cultures on both xanthan gum and trehalose were grown for 4 days. Then, three samples of each culture (cultivated on xanthan gum and trehalose) were used for RNA extraction. RNA was extracted using TRI-reagent (Sigma), following standard protocol with the addition of two freeze and thaw cycles of the cells in TRI-reagent, as well as addition of chloroform and washing twice with 75% EtOH. RNA pellet was dissolved in RNAase-free water.

Sequencing, Assembly, and Mapping

The genome was sequenced using a combination of Illumina GA II, and Roche/454 sequencing platforms. All general aspects of 500 bp paired-end (PE) library construction and sequencing, as well as 454 single-end sequencing can be found at the corresponding company website. A hybrid assembly of Illumina and 454 datasets was done using the Newbler assembler (Margulies et al., 2005). The initial Newbler assembly consisting of seven unique contigs was used to identify repeat regions that were subsequently screened out. At this point a 2 kb mate-pair Illumina library was constructed and sequenced and obtained paired end information was used to arrange multiple screened contigs into a single scaffold using the Phred/Phrap/Consed software package (Gordon et al., 1998). This package was also used for further sequence assembly and quality assessment in the subsequent finishing process. Sequence gaps between contigs that represented repeats were filled with Dupfinisher (Han and Chain, 2006), and a single scaffold was manually created and verified using available paired-end information. Illumina reads were used to correct potential base errors and increase consensus quality.

Together, the combination of the Illumina and 454 sequencing platforms provided 320× coverage of the genome.

Genome Annotation

The assembled chromosome was uploaded to the RAST server (Aziz et al., 2008) for *de novo* gene prediction using Glimmer-3 (Delcher et al., 2007) and initial detection of homologs. Furthermore, the predicted genes were searched against the protein databases Pfam 27.0 (Finn et al., 2014), COG 2003–2014 (Galperin et al., 2015), MEROPS 9.12 (Rawlings et al., 2016), CAZy/dbCAN (Yin et al., 2012; Lombard et al., 2014), and TCDB (Saier et al., 2014) in order to expand the initial RAST annotation. The positive hits from these searches were manually curated using Uniprot/NCBI BLASTp. Signal peptides were predicted with the SignalP 4.1 web server (Petersen et al., 2011), and transmembrane helices were predicted with the TMHMM 2.0 web server (Krogh et al., 2001). Infernal 1.1.1 (Nawrocki and Eddy, 2013) was used in conjunction with the covariance models from Rfam 12.0 (Nawrocki et al., 2015) to search for non-coding RNA genes.

Transcriptome Sequencing and Assignment

Extracted total RNA was converted to cDNA by reverse transcriptase. Total cDNA was sequenced from the three samples of each culture by strand-specific paired-end Illumina sequencing using an insert size of 270 bp and read length of 90 bp. RNA-seq reads were mapped to the genome using BWA ver 0.7.8 (Li and Durbin, 2009) requiring properly mapped pairs. Read assignment to genes was done using the featureCounts program from the Subread package (Liao et al., 2013). Only uniquely assigned read pairs were counted. Differential gene expression between the two groups was measured using edgeRun (Dimont et al., 2015) and genes were called differentially expressed using a BH-corrected *p*-value of 0.05.

Phylogenetic Analysis

Phylogenetic analyses were performed according to Sorokin et al. (2016) using the maximum likelihood method in MEGA6 (Tamura et al., 2013). Initial multiple amino acid sequence alignments were done in Mafft 7 (Katoh and Standley, 2013).

RESULTS AND DISCUSSION

Genome Assembly and General Genome Characteristics

The genome of *T. terrifontis* strain R1 was sequenced and assembled into a single circular chromosome with a length of 4,810,751 bp and GC content of 57.34%. Genome annotation was performed using the RAST server and Infernal. In total, 4,504 protein coding genes were found in the genome, of which 2,412 could not be annotated by our database search and are therefore designated as "hypothetical protein."

Both RAST and Infernal identified the same set of the 3 rRNAs and 46 tRNAs. Additionally, the ribonuclease P (RNase P), SRP, and tmRNA genes were identified by Infernal. No homolog was found for the non-coding 6S RNA gene. A recent computational screen for 6S RNA across all bacterial phyla (Wehner et al., 2014) reported the absence of 6S RNA in *Pirellula staleyi* and *Rhodopirellula baltica*, which are the closest related species to *T. terrifontis* in the 16S rRNA phylogeny (Slobodkina et al., 2015). This suggests that this gene is also likely to be absent in *T. terrifontis*. The Infernal search also revealed three riboswitches: cyclic di-GMP-I (RF01051), cobalamin (RF00174), and fluoride (RF01734).

The genome was submitted to GenBank with the accession number CP018477.

Transcriptome Sequencing and General Transcriptome Characteristics

Thermogutta terrifontis R1 cells were cultured in growth media containing trehalose or xanthan gum, each in triplicates (see section "Materials and Methods"). Transcriptome sequencing using Illumina paired-end sequencing resulted in between 11.5 and 12.1 m read pairs for the 2 × 3 replicates. Across these, between 91.3 and 98.5% of the read pairs could be mapped uniquely to the genome. Differential expression analysis reported that 665 genes are up- and 617 genes are down-regulated on xanthan gum compared to trehalose-grown culture (**Figure 1** and Supplementary Table S1).

Genome-Scale Reconstruction of Oligo- and Polysaccharide Degradation

Thermogutta terrifontis R1 was shown to be able to grow using the following oligo- and polysaccharides as substrates: sucrose, trehalose, cellobiose, starch, xylan, pectin, or xanthan gum (Slobodkina et al., 2015). No growth was detected when maltose, lactose, agarose, alginate, cellulose, chitin, or inulin were added to the medium as sole carbon sources (Slobodkina et al., 2015).

Our analysis of the *T. terrifontis* R1 genome revealed 101 genes encoding glycosidases (GHs), 14 genes encoding polysaccharide lyases (PLs) and 3 genes encoding carbohydrate esterases (CEs) (Supplementary Table S2). Among these, 54 genes encode proteins that were predicted to be secreted outside the cells (whether anchored on the cells surface or being released into the culture broth). No dominant CAZy (GH, PL, or CE) families (Lombard et al., 2014) were observed among *T. terrifontis* R1 CAZymes, yet the most numerous were GH5 (10 proteins) and putative glycosidases (9 proteins), including DUF1080 domain. Detailed analysis of the CAZymes specificities revealed following activities: trehalose can be degraded by trehalose synthase (Qu et al., 2004) acting in opposite direction (THTE_2039). Sucrose hydrolysis may occur by the action of intracellular fructosidase (THTE_0696). Alpha-1,4-bonds and alpha-1,6-bonds in starch can be hydrolyzed by a number of GH13 and GH77 glycosidases (THTE_1477, THTE_2143, THTE_3153, and THTE_3783), producing maltooligosaccharides and finally D-glucose. Cellobiose can be hydrolyzed by the putative beta-glucosidase (THTE_0963), or one of the GH2 and GH5 glycosidases with currently uncertain function. Xylan can be decomposed to xylooligosaccharides

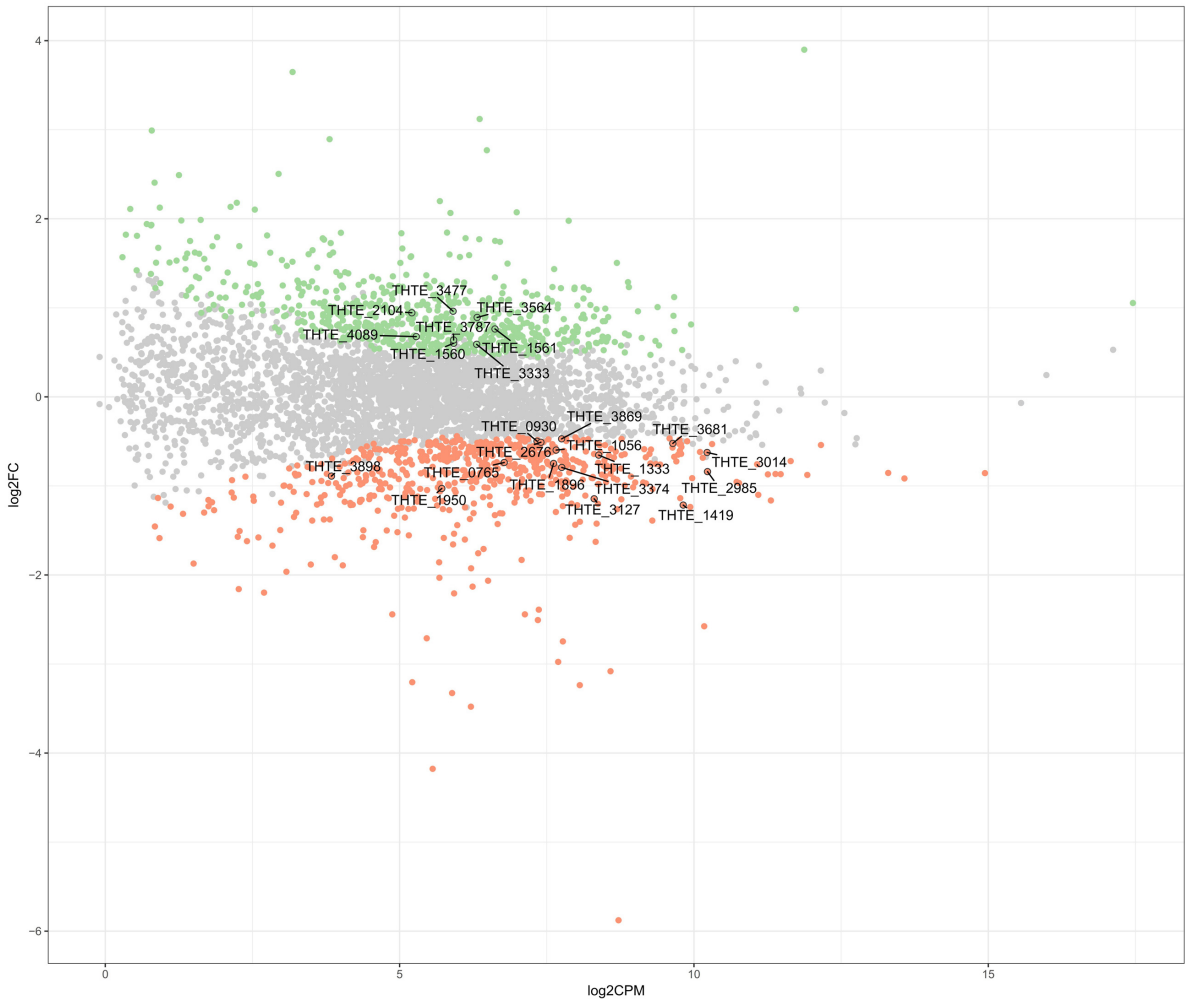

FIGURE 1 | Differently expressed genes between xanthan gum-grown and trehalose-grown *Thermogutta terrifontis* R1 cells. Green and red dots indicate significantly up-regulated and down-regulated genes in xanthan gum culture compared with trehalose culture (*P*-value < 0.05). Annotated data points show locus tag identifiers of differentially expressed genes encoding proteins that are involved either in xantham gum / trehalose degradation pathways or in the central carbon metabolism. Y axis: log2 Fold Change between trehalose and xanthan gum-grown cultures. X axis: Read count of each gene per million mapped reads, averaged across all samples.

by means of endoxylanases (THTE_2600 and THTE_3961) and to xylose by beta-xylosidases (THTE_0688, THTE_1819, THTE_1884, and THTE_2108). Pectin degradation occurs, most probably, by the action of a pectate lyase (THTE_1993) and several polygalacturonases (THTE_0436, THTE_1516, and THTE_2121), releasing D-galacturonic residues, that are further metabolized to D-glyceraldehyde 3-phosphate and pyruvate (see below). A large number of glycosidases was predicted to be involved in xanthan gum hydrolysis (see section "Xanthan Gum and Trehalose Utilization Pathways, Revealed by Comparative Genomic and Transcriptomic Analyses").

Genome-Scale Reconstruction of Central Carbohydrate Metabolism

According to the results of genome analysis, the final products of oligo- and polysaccharides decomposition were predicted to comprise glucose, fructose, mannose, xylose, galacturonate, and glucuronate. Some of these (glucose, mannose, xylose) as well as galactose were also shown to be used as growth substrates by *T. terrifontis* R1 according to Slobodkina et al., 2015. D-Glucose and D-fructose oxidation seems to occur via the Embden-Meyerhof (EM) pathway (**Figures 2**, **3** and Supplementary Table S3). Interestingly, the genome contains four genes encoding phosphofructokinases: one ATP-dependent (THTE_2190) and three pyrophosphate-dependent (THTE_0093, THTE_1056, THTE_2629). Since no genes for fructose-1,6-bisphosphatase were found, and PPi-dependent phosphofructokinases are thought to be reversible, at least one of them should be a part of gluconeogenesis. Additionally, analysis of the nearest characterized homologs supports two of them to be involved in xylose utilization (see below). The Entner-Doudoroff pathway seems to be inoperative due to the absence of the gene

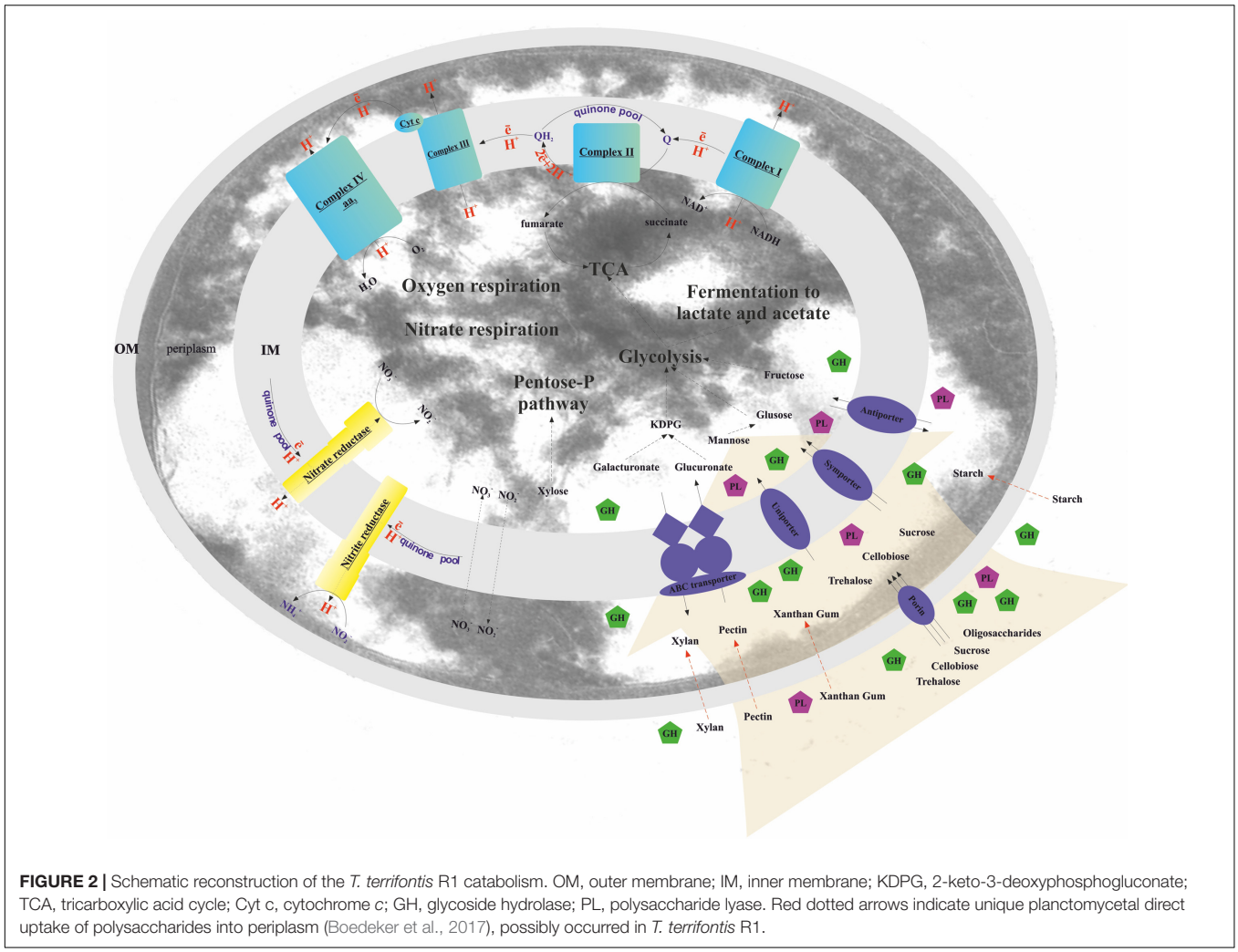

FIGURE 2 | Schematic reconstruction of the *T. terrifontis* R1 catabolism. OM, outer membrane; IM, inner membrane; KDPG, 2-keto-3-deoxyphosphogluconate; TCA, tricarboxylic acid cycle; Cyt c, cytochrome *c*; GH, glycoside hydrolase; PL, polysaccharide lyase. Red dotted arrows indicate unique planctomycetal direct uptake of polysaccharides into periplasm (Boedeker et al., 2017), possibly occurred in *T. terrifontis* R1.

encoding 6-phosphogluconate dehydratase, a key enzyme of the pathway. Glucose-1-dehydrogenase, gluconokinase, and gluconate dehydratase genes are also absent in the genome.

The first step of galactose utilization – phosphorylation to galactose-1-phosphate – is catalyzed by galactokinase (THTE_0177). Next, the putative galactose-1-P-uridyltransferase (THTE_3784) transfers the UDP-group from UDP-glucose to galactose-1-P, producing UDP-galactose and glucose-1-P. This protein belongs to the type 1 galactose-1-P-uridyltransferases family, however, its closest characterized homolog was ADP-glucose:phosphate adenylyltransferase (UniProt ID Q9FK51). While phylogenetic analysis (Supplementary Figure S1) supports this finding, the sequence identity of these two proteins is rather low (Identity 35%, Coverage 97%), leaving the function of this enzyme unclear. However, since no other putative galactose-1-P-uridyltransferase genes were found, the assignment of the function to THTE_3784 remains plausible. Finally UDP-galactose is converted to UDP-glucose by the UDP-glucose 4-epimerase (THTE_2863), whereas the glucose-1-phosphate is converted to glucose-6-phosphate by the phosphoglucomutase (THTE_3829).

Xylose utilization was predicted to occur as follows: xylose is isomerized to xylulose by xylose isomerase (THTE_2111); xylulokinase (THTE_0598) phosphorylates xylulose to xylulose-5-phosphate, which finally enters the pentose-phosphate pathway. All genes encoding proteins of both oxidative and synthetic parts of this pathway were found in the genome with transaldolase gene as an exception (**Figure 3** and Supplementary Table S4). Yet, sedoheptulose-7-phosphate (S-7-P), formed under action of transketolase, could be phosphorylated by PPi-dependent phosphofructokinases THTE_0093 and THTE_2629, of which the nearest characterized homolog from *Methylococcus capsulatus* (UniProt Q609I3, Reshetnikov et al., 2008) was shown to reversibly phosphorylate S-7-P with higher activity and affinity than fructose-6-phosphate (F-6-P). The resulting sedoheptulose-1,7-bisphosphate could be eliminated to erythrose-4-phosphate and dihydroxyacetone-phosphate by fructose-1,6-bisphosphate aldolase (THTE_1419) as it was proposed by Susskind et al. (1982) and Schellenberg et al. (2014).

D-Galacturonate, released in the course of pectin degradation, is presumably oxidized to glyceraldehyde-3-phosphate and

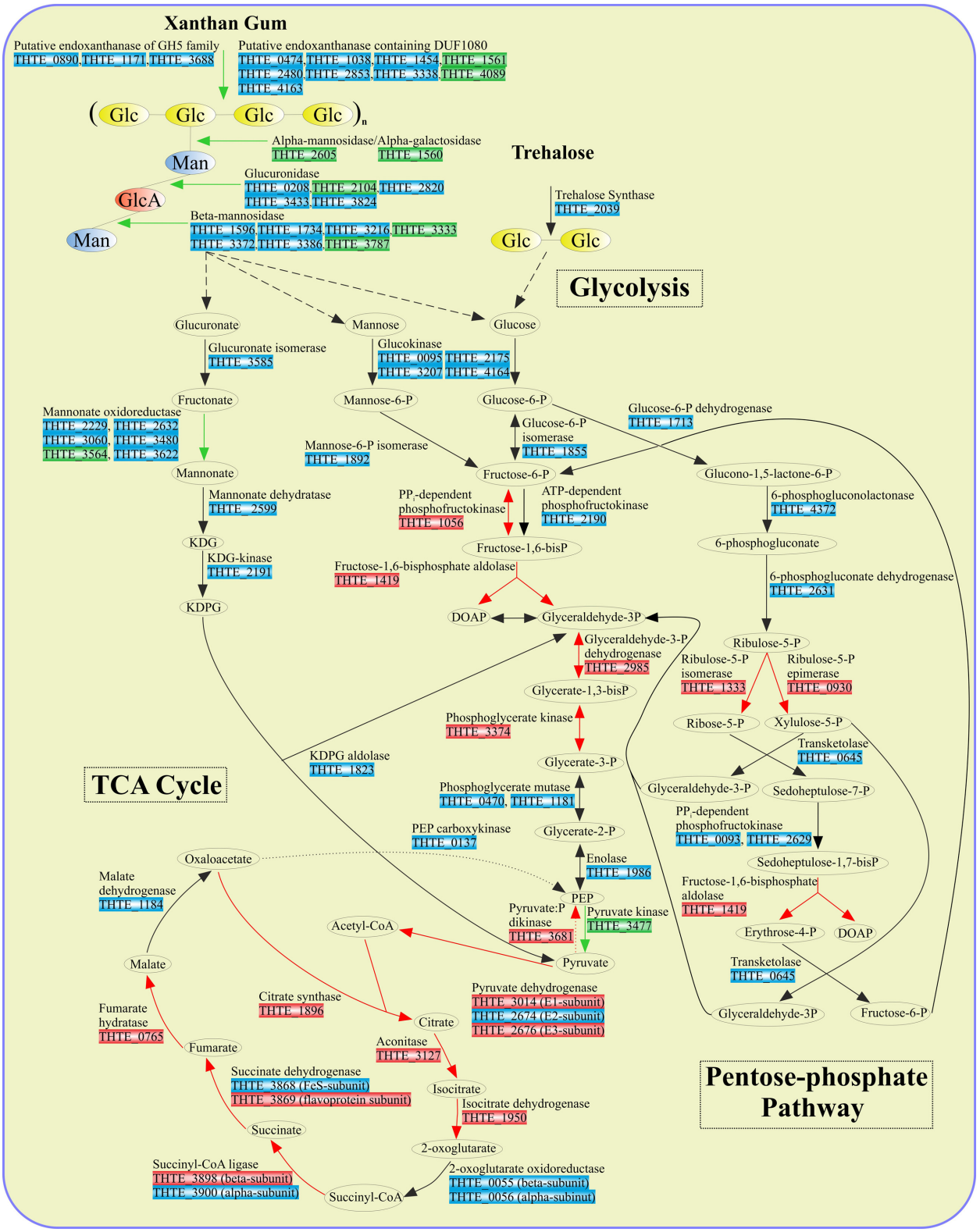

FIGURE 3 | Enzymes involved in sugar turnover. Color boxes indicate the differential expression of the genes, indicated by the transcriptomic analysis. Green: up-regulation with xanthan gum; Red: down-regulation with xanthan gum; Blue: genes are not significantly differentially expressed between xanthan gum and trehalose.

pyruvate through a number of reactions (Supplementary Figure S2) catalyzed by uronate isomerase (THTE_3585), putative altronate oxidoreductase (see below), altronate dehydratases (THTE_0455 and THTE_0456), KDG kinase (THTE_2191), and KDPG aldolase (THTE_1823). No genes encoding altronate oxidoreductase belonging to the polyol-specific long-chain dehydrogenase/reductase family (Klimacek et al., 2003) were found. However, the genome contains several genes (*THTE_0865*, *THTE_1784*, *THTE_2229*, *THTE_2632*, *THTE_3060*, *THTE_3480,* and *THTE_3564*), probably encoding proteins of the short-chain dehydrogenase/reductase family (Jörnvall et al., 1995). One of its biochemically characterized representatives, an oxidoreductase UxaD from the hyperthermophilic anaerobic bacterium *Thermotoga maritima*, was shown to possess mannonate oxidoreductase activity (Rodionova et al., 2012).

The metabolism of xanthan gum degradation products – glucose, glucuronate, and mannose – is described in Section "Xanthan Gum and Trehalose Utilization Pathways, Revealed by Comparative Genomic and Transcriptomic Analyses."

Pyruvate, generated in the course of degradation of sugars and sugar acids, is further oxidized to acetyl-CoA in the reactions catalyzed by the pyruvate dehydrogenase complex (**Figure 3**): pyruvate dehydrogenase (E1) (THTE_3014), dihydrolipoamide acetyltransferase (E2) (THTE_2674), and lipoamide dehydrogenase (E3) (THTE_2676).

It has been shown by Slobodkina et al. (2015), that the products of *T. terrifontis* R1 glucose fermentation were hydrogen, lactate and acetate. Lactate could be produced from pyruvate by lactate dehydrogenase (THTE_3348), while the mechanism of acetate formation remains unclear. Although two acetate kinases were found (THTE_1319 and THTE_2274), no genes coding for phosphate-acetyl transferase were detected in the genome. It is therefore possible that acetate could be formed due to the action of CoA-acylating aldehyde dehydrogenase (THTE_1321), catalyzing the NADH-dependent reduction of acetyl-CoA to acetaldehyde (Toth et al., 1999), and aldehyde dehydrogenase (THTE_2212) catalyzing the oxidation of acetaldehyde to acetate along with formation of NADH (Ho and Weiner, 2005). Finally, acetate could be formed under the action of putative ADP-forming acetyl-CoA synthetase (THTE_2996), as it was shown for few hyperthermophilic archaea (Musfeldt et al., 1999; Musfeldt and Schönheit, 2002). Surprisingly, the genome encoded an ATP-dependent acetyl-CoA synthase (THTE_1589), which catalyzes the irreversible activation of acetate, whereas acetate was not listed among the substrates, supporting the growth of *T. terrifontis* R1 in Slobodkina et al. (2015).

Hydrogen formed by *T. terrifontis* R1 in the course of fermentation apparently results from the operation of group 3c [NiFe]-hydrogenase (Vignais and Billoud, 2007) THTE_4311-4313 and/or [FeFe]-hydrogenases (Vignais and Billoud, 2007) THTE_2884, THTE_2882, THTE_2881, THTE_3842-THTE_3844. On the other hand, according to our analysis, all the genomes of planctomycetes, available in the IMG database (34 genomes of planctomycetes with assigned genus and species names. The analysis was performed 03.07.17), lack genes of [FeFe]-hydrogenase. Since, *T. terrifontis* is the first planctomycete known to synthesize hydrogen in the course of fermentation, and it is currently the only one in which genes for [FeFe]-hydrogenases have been found, at least some of its [FeFe]-hydrogenases could be involved in hydrogen production.

All genes, coding the citrate cycle (TCA cycle) enzymes were found in the *T. terrifontis* R1 genome (**Figures 2**, **3** and Supplementary Table S5).

Genome-Scale Reconstruction of Nitrate Reduction

Genes for all three subunits of the respiratory cytoplasmic nitrate reductase Nar (Simon and Klotz, 2013) were found in the genome. The alpha subunit (NarG) THTE_1509 belongs to the deep lineage within the Nar-DMSO cluster (Supplementary Figure S3) of the molybdopterine superfamily (Duval et al., 2008). *THTE_1508* and *THTE_1507* encode the other two subunits NarH and NarI, respectively, while *THTE_1506* encodes a chaperon subunit (TorD). The NarGHI complex might form a supercomplex with an electrogenic membrane-bound NADH dehydrogenase (Simon and Klotz, 2013, **Figure 2** and Supplementary Table S6). No diheme subunit NarC was found, yet the genes of cytochrome b/c_1 complex (complex III, *THTE_1510-THTE_1512*) are located in close vicinity to the NarGHI genes (*THTE_1509-THTE_1507*), what might reflect the involvement of the complex III in the electron and proton transfer during *T. terrifontis* anaerobic growth with nitrate. Nitrite is reduced to ammonium by means of non-electrogenic periplasmic membrane-bound nitrite reductase Nrf, the catalytic subunit NrfA and the membrane-bound subunit NrfH (Simon and Klotz, 2013) of which are encoded by *THTE_1450* and *THTE_1449*, respectively.

Genome-Scale Reconstruction of Aerobic Respiration

The complete aerobic respiratory electron transfer chain (ETC), including H^+-translocating NADH-dehydrogenase (complex I), succinate dehydrogenase (complex II), cytochrome b/c_1-complex (complex III), and terminal cytochrome c oxidase aa_3-type (complex IV) was found (**Figure 2** and Supplementary Table S6). We did not find the typical cytochrome *c* gene or the plastocyanin gene, involved in transferring electrons from complex III to complex IV, yet *THTE_3354* encodes a putative large (258 amino acids) cytochrome *c* containing two monoheme domains. No genes encoding terminal quinol oxidases (bd-type, bo_3-type, or ba_3-type) were found in the genome.

Xanthan Gum and Trehalose Utilization Pathways, Revealed by Comparative Genomic and Transcriptomic Analyses

In order to decipher the mechanisms of xanthan gum degradation, *T. terrifontis* R1 was grown on xanthan gum and trehalose (as the control), and the transcriptomes were sequenced

and analyzed for genes that are up-regulated in the cultures with xantham gum as the substrate. Trehalose is a disaccharide consisting of 1-1-alpha-linked glucose molecules, and it was chosen as one of the simple sugars, supporting growth of the strain. Interestingly, *T. terrifontis* R1 genomic analysis revealed no genes coding for known trehalose-hydrolyzing enzymes of GH15, GH37, and GH65 families. Furthermore, two GH13 proteins (THTE_1477 and THTE_3153) have no trehalose-converting enzymes among their nearest characterized relatives. Therefore, the only remaining reasonable candidate involved in decomposition of trehalose is a trehalose synthase of GT4 family (THTE_2039), acting in reverse direction, leading to a release of D-glucose and NDP-D-glucose molecules. The level of its expression in cells, grown on trehalose and xanthan-gum was similar (**Figure 3**), what could be explained by reversibility of its action (Qu et al., 2004; Ryu et al., 2005) at various growth conditions: trehalose degradation when trehalose is being sole substrate and trehalose synthesis when other substrates are used.

Despite its ubiquitous usage in pharmaceutical and food industries, not much is known about xanthan gum (beta-1,4-glucan with mannosyl–glucuronyl–mannose side chains) degradation mechanisms. For the complete hydrolysis of the molecule the following linkages should be broken: β-mannose-1–4-α-glucuronate, β-glucuronate-1–2-α-mannose, α-mannose-1–3-β-glucose linkages in side chains, and β-1,4-glucosidic linkages in polyglucose backbone (**Figure 4**).

Among the enzymes currently known to be involved in xanthan gum decomposition, there are few removing terminal mannose residues xanthan lyases (Hashimoto et al., 1998; Ruijssenaars et al., 1999), belonging to the PL8 family, and an endoxanthanase (xanthan-specific endoglucanase, Li et al., 2009), hydrolyzing the glucan backbone (**Figure 4A**). The latter has been biochemically characterized, yet its sequence is still unknown, preventing structure analysis and evolutionary reconstructions using sequence comparison.

No homologs of PL8 family lyases, to which all known xanthan lyases belong, were found in the *in silico* translated *T. terrifontis* R1 proteome. They were probably replaced by several putative endomannanases/beta-mannosidases of GH5 family (THTE_1596, THTE_1734, THTE_3216, THTE_3333, THTE_3372, THTE_3386 and THTE_3787, Supplementary Figure S4), cleaving Man(1β–4α)GlcA linkages. Four of them (THTE_1596, THTE_3216, THTE_3333, and THTE_3386) were predicted to be extracellular. Transcriptomic analysis showed two genes *THTE_3333* and *THTE_3787* to be up-regulated in the xanthan gum cultures, assuming their involvement in its decomposition.

For cleavage of the GlcA(β1–2α)Man linkage the action of beta-glucuronidase is needed. All known beta-glucuronidases belong to the GH1, GH2, GH30, and GH79 families. While no genes encoding GH1, GH30, and GH79 proteins were found, five genes encoding GH2 family glycosidases (*THTE_0208*, *THTE_2104*, *THTE_2820*, *THTE_3433*, and *THTE_3824*) were revealed in the *T. terrifontis* R1 genome. The family GH2 contains a number of enzymes with various specificities. We compared *T. terrifontis* GH2s with the previously characterized members of the GH2 family, to predict whether the putative five *T. terrifontis* GH2 proteins act as beta-glucuronidases. All five genes formed a monophyletic group, adjoined to the cluster with characterized beta-galactosidases and beta-glucuronidases (Supplementary Figure S5). Given that one of these (*THTE_2104*) was significantly up-regulated in the cells growing on xanthan gum, the beta-glucuronidase activity seems to be characteristic of at least this one, yet possibly all five GH2 from this monophyletic group possess this activity. It should be noted that THTE_2104 and also THTE_0208 were predicted to be secreted.

The Man(1α–β3)Glc linkage could be hydrolyzed by an alpha-mannosidase of GH38 family (THTE_2605). Another option is an extracellular putative alpha-galactosidase of GH36 family

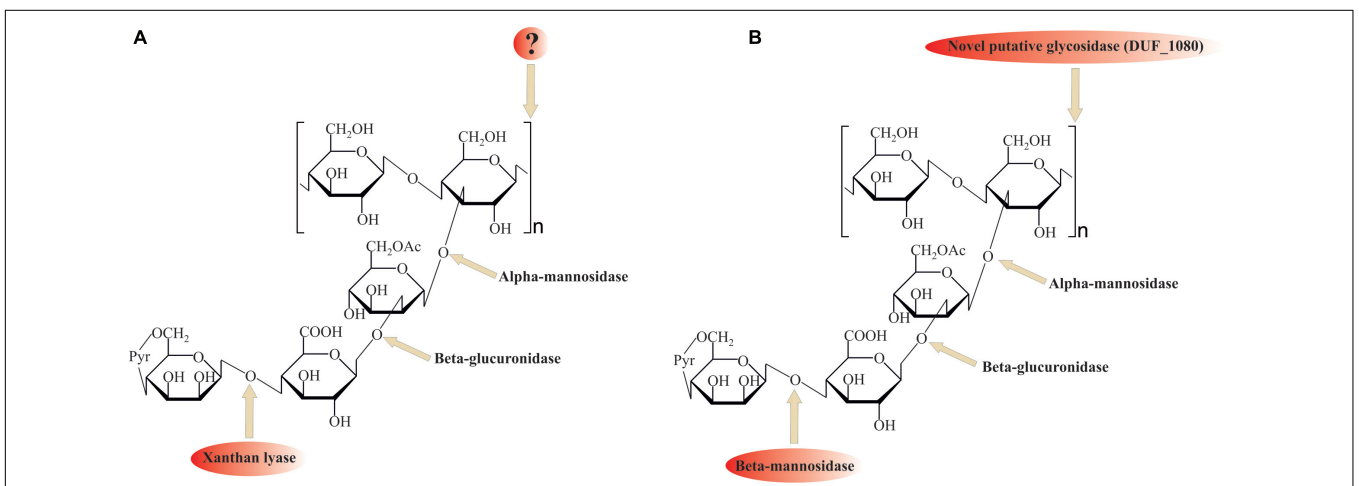

FIGURE 4 | Comparison of **(A)** known (with xanthan lyase) and **(B)** proposed novel (without xanthan lyase) xanthan gum degradation pathways. ? question mark indicates no sequence data available for these enzymes. Please, see the text for details.

(THTE_1560), whose characterized homologs are known to hydrolyze a number of oligosaccharides of various structures (Merceron et al., 2012). Both *THTE_2605* and *THTE_1560* genes were up-regulated during the growth on xanthan gum.

Finally, the hydrolysis of a Glc(β1–4)Glc linkage in xanthan gum backbone could be catalyzed by the GH5 enzymes THTE_0890, THTE_1171 and THTE_3688, however, only one of them was predicted to be extracellular (THTE_1171) and none of them were up-regulated on xanthan gum.

Search of the other putative glycosidases of *T. terrifontis* R1 revealed nine proteins (THTE_0474, THTE_1038, THTE_1454, THTE_1561, THTE_2480, THTE_2853, THTE_3338, THTE_4089, and THTE_4163) containing a domain of unknown function (DUF1080). All of these proteins, except THTE_1454 and THTE_3338, were predicted to be extracellular, and two of them (*THTE_1561* and *THTE_4089*) were up-regulated on xanthan gum. These proteins may be representatives of a novel family of glycosidases according to TOPSAN annotation[1]. Such a high number of genes encoding putative glycosidases with unknown function in a xanthan gum degrading microorganism might be an indication on their involvement in the process, most probably for hydrolysis of the backbone linkage (**Figure 4B**). Interestingly, proteins containing DUF1080 are highly overrepresented among all *Planctomycetes* (Supplementary Table S7) in comparison with other organisms. This, together with our observation that xanthan gum being a selective substrate for many planctomycetes, suggest an important role of DUF1080 proteins in xanthan gum degradation. Finally, five of nine *T. terrifontis* R1 DUF1080 proteins, including THTE_1561, have a CBM66 domain, which was found mainly among *Firmicutes* representatives and helps binding the terminal fructoside residue in fructans (Cuskin et al., 2012). Yet, the DUF1080 and CBM66 domains overlap each other, indicating two different designations of the same domain occurred.

The predicted products of xanthan gum degradation are mannose, glucuronic acid, and glucose. Although no mannokinase genes were found in the *T. terrifontis* R1 genome, mannose could be phosphorylated to mannose-6-P by the variety of its putative glucokinases from the ROK family (THTE_0095, THTE_2175, THTE_3207, THTE_4164), representatives of which are known to be capable of acting on various hexoses (Conejo et al., 2010; Nakamura et al., 2012). Mannose-6-phosphate upon conversion to fructose-6-phosphate by mannose-6-phopshate isomerase (THTE_1892) enters the EM pathway (**Figures 2**, **3**). However, none of the genes coding these proteins were up-regulated on xanthan gum in our experiment, possibly due to their wide specificity and hence constitutive expression.

An oxidation of glucuronate, released during xanthan gum hydrolysis, might occur through formation of fructonate, followed by reduction to mannonate, dehydration to 2-keto-3-desoxy-6-phosphogluconate (KDPG) and its elimination to pyruvate and glyceraldehyde-3-phosphate (**Figure 3**). All genes encoding the respective proteins, except mannonate oxidoreductase, were found in the genome. As it was hypothesized for altronate oxidoreductases (see above), we suggest that some of short-chain reductases/dehydrogenases (THTE_2229, THTE_2632, THTE_3060, THTE_3480, THTE_3564 and THTE_3622) with unknown specificity, especially the up-regulated THTE_3564, may act as a mannonate oxidoreductase.

In most cases, the majority of enzymes involved in both the trehalose and xanthan gum-dependent pathways of the central carbohydrate metabolism were expressed on the same level or were down-regulated in the cells grown on xanthan gum. This could be due to the lower structural complexity of trehalose in comparison with xanthan gum, which requires fewer degradation steps and determines easier import into the cell: one transporter and one enzymatic step are enough to transport and decompose trehalose to the basic metabolites (D-glucose and NTP-α-D-glucose) compared with most certainly multiple transporters and four steps of xanthan gum decomposition, coupled with two- and five-step mannose and glucuronate, respectively, conversions to EM pathway metabolites (**Figure 3**). Finally, the majority of flagellar, as well as pili IV and secretion system proteins, were up-regulated (Supplementary Table S1) in the cells grown on xanthan gum. This might be a reflection of viscosity of the substrate, which force cells to be more agile and capable of binding to the substrate.

CONCLUSION

The central carbohydrate metabolism of *T. terrifontis* R1 was deciphered using genomic and transcriptomic approaches, and the novel xanthan gum degradation pathway was proposed. The pathway involves endomannanases/beta-mannosidases instead of xanthan lyases as well DUF1080 proteins for the hydrolysis of xanthan gum backbone. Surprisingly, the genes coding DUF1080 proteins were highly abundant in *T. terrifontis* R1, as well as in many other *Planctomycetes* genomes. These results are relevant due to lack of the information on microorganisms degrading xanthan gum and its degradation pathways, which has so far been limited to few representatives of *Actinobacteria* and *Firmicutes* and their enzymes. Yet, further studies including proteomics of xanthan gum-growing cultures, as well as, purification and characterization of the respective enzymes are needed to verify the predicted pathway.

DATA AVAILABILITY

The *T. terrifontis* R1 genome is available via GenBank accession number CP018477.

AUTHOR CONTRIBUTIONS

IK, XP, and EB-O conceived the study. SG and PM contributed to cultivation and transcriptome sequencing. AS, VK, PM, and AK

[1]http://www.topsan.org/Proteins/JCSG/4jqt

contributed to genome sequencing and assembly. AE, PM, and IK contributed to genome and transcriptome analysis. AE, PM, XP, and IK wrote the manuscript.

FUNDING

The work was supported by the European Union 7th Framework Programme FP7/2007-2013 under grant agreement no. 265933 (*Hotzyme*). The work of AE, EB-O and IK was supported by RSF grant 17-74-30025. The work of VK was supported by the Federal Agency for Scientific Organisations of Russia.

ACKNOWLEDGMENT

We would like to thank Drs. S. N. Gavrilov, O. L. Kovaleva and A. V. Lebedinsky for their valuable comments and advices. This work was performed using the scientific equipment of Core Research Facility "Bioengineering".

SUPPLEMENTARY MATERIAL

The Supplementary Material for this article can be found online at: https://www.frontiersin.org/articles/10.3389/fmicb.2017.02140/full#supplementary-material

REFERENCES

Aziz, R. K., Bartels, D., Best, A. A., DeJongh, M., Disz, T., Edwards, R. A., et al. (2008). The RAST server: rapid annotations using subsystems technology. *BMC Genomics* 9:75. doi: 10.1186/1471-2164-9-75

Boedeker, C., Schüler, M., Reintjes, G., Jeske, O., van Teeseling, M. C. F., Jogler, M., et al. (2017). Determining the bacterial cell biology of Planctomycetes. *Nat. Commun.* 8:14853. doi: 10.1038/ncomms14853

Conejo, M. S., Thompson, S. M., and Miller, B. G. (2010). Evolutionary bases of carbohydrate recognition and substrate discrimination in the ROK protein family. *J. Mol. Evol.* 70, 545–556. doi: 10.1007/s00239-010-9351-1

Cuskin, F., Flint, J. E., Gloster, T. M., Morland, C., Baslé, A., Henrissat, B., et al. (2012). How nature can exploit nonspecific catalytic and carbohydrate binding modules to create enzymatic specificity. *Proc. Natl. Acad. Sci. U.S.A.* 109, 20889–20894. doi: 10.1073/pnas.1212034109

Delcher, A. L., Bratke, K. A., Powers, E. C., and Salzberg, S. L. (2007). Identifying bacterial genes and endosymbiont DNA with Glimmer. *Bioinformatics* 23, 673–679. doi: 10.1093/bioinformatics/btm009

Dimont, E., Shi, J., Kirchner, R., and Hide, W. (2015). edgeRun: an R package for sensitive, functionally relevant differential expression discovery using an unconditional exact test. *Bioinformatics* 31, 2589–2590. doi: 10.1093/bioinformatics/btv209

Duval, S., Ducluzeau, A.-L., Nitschke, W., and Schoepp-Cothenet, B. (2008). Enzyme phylogenies as markers for the oxidation state of the environment: the case of respiratory arsenate reductase and related enzymes. *BMC Evol. Biol.* 8:206. doi: 10.1186/1471-2148-8-206

Finn, R. D., Bateman, A., Clements, J., Coggill, P., Eberhardt, R. Y., Eddy, S. R., et al. (2014). Pfam: the protein families database. *Nucleic Acids Res.* 42, 222–230. doi: 10.1093/nar/gkt1223

Fuerst, J. A., and Sagulenko, E. (2011). Beyond the bacterium: planctomycetes challenge our concepts of microbial structure and function. *Nat. Rev. Microbiol.* 9, 403–413. doi: 10.1038/nrmicro2578

Fukunaga, Y., Kurahashi, M., Sakiyama, Y., Ohuchi, M., Yokota, A., and Harayama, S. (2009). *Phycisphaera mikurensis* gen. nov., sp nov., isolated from a marine alga, and proposal of *Phycisphaeraceae* fam. nov., *Phycisphaerales* ord. nov and *Phycisphaerae* classis nov in the phylum *Planctomycetes*. *J. Gen. Appl. Microbiol.* 55, 267–275. doi: 10.2323/jgam.55.267

Galperin, M. Y., Makarova, K. S., Wolf, Y. I., and Koonin, E. V. (2015). Expanded Microbial genome coverage and improved protein family annotation in the COG database. *Nucleic Acids Res.* 43, D261–D269. doi: 10.1093/nar/gku1223

García-Ochoa, F., Santos, V. E., Casas, J. A., and Gómez, E. (2000). Xanthan gum: production, recovery, and properties. *Biotechnol. Adv.* 18, 549–579. doi: 10.1016/S0734-9750(00)00050-1

Gavrilov, S. N., Stracke, C., Jensen, K., Menzel, P., Kallnik, V., Slesarev, A., et al. (2016). Isolation and characterization of the first xylanolytic hyperthermophilic euryarchaeon *Thermococcus* sp. strain 2319x1 and its unusual multidomain glycosidase. *Front. Microbiol.* 7:552. doi: 10.3389/fmicb.2016.00552

Gordon, D., Abajian, C., and Green, P. (1998). Consed: a graphical tool for sequence finishing. *Genome Res.* 8, 195–202. doi: 10.1101/gr.8.3.195

Han, C., and Chain, P. (2006). "Finishing repetitive regions automatically with dupfinisher," in *Proceeding of the 2006 International Conference on Bioinformatics & Computational Biology*, eds H. R. Arabnia and H. Valafar (Las Vegas, NV: REA Press), 141–146.

Hashimoto, W., Miki, H., Tsuchiya, N., Nankai, H., and Murata, K. (1998). Xanthan lyase of *Bacillus* sp. strain GL1 liberates pyruvylated mannose from xanthan side chains. *Appl. Environ. Microbiol.* 64, 3765–3768.

Ho, K. K., and Weiner, H. (2005). Isolation and characterization of an aldehyde dehydrogenase encoded by the aldB gene of *Escherichia coli* isolation and characterization of an aldehyde dehydrogenase encoded by the *aldB* gene of *Escherichia coli*. *J. Bacteriol.* 187, 1067–1073. doi: 10.1128/JB.187.3.1067

Jeske, O., Schüler, M., Schumann, P., Schneider, A., Boedeker, C., Jogler, M., et al. (2015). Planctomycetes do possess a peptidoglycan cell wall. *Nat. Commun.* 6:7116. doi: 10.1038/ncomms8116

Jörnvall, H., Persson, B., Krook, M., Atrian, S., Gonzàlez-Duarte, R., Jeffery, J., et al. (1995). Short-chain dehydrogenases/reductases(SDR). *Biochemistry* 34, 6003–6013. doi: 10.1021/bi00018a001

Katoh, K., and Standley, D. M. (2013). MAFFT multiple sequence alignment software version 7: improvements in performance and usability. *Mol. Biol. Evol.* 30, 772–780. doi: 10.1093/molbev/mst010

Klimacek, M., Kavanagh, K. L., Wilson, D. K., and Nidetzky, B. (2003). *Pseudomonas fluorescens* mannitol 2-dehydrogenase and the family of polyol-specific long-chain dehydrogenases/reductases: sequence-based classification and analysis of structure-function relationships. *Chem. Biol. Interact.* 14, 559–582. doi: 10.1016/S0009-2797(02)00219-3

Kovaleva, O. L., Merkel, A. Y., Novikov, A. A., Baslerov, R. V., Toshchakov, S. V., and Bonch-Osmolovskaya, E. A. (2015). *Tepidisphaera mucosa* gen. nov., sp. nov., a moderately thermophilic member of the class *Phycisphaerae* in the phylum *Planctomycetes*, and proposal of a new family, *Tepidisphaeraceae* fam. nov., and a new order, *Tepidisphaerales* ord. nov. *Int. J. Syst. Evol. Microbiol.* 65, 549–555. doi: 10.1099/ijs.0.070151-0

Krogh, A., Larsson, B., von Heijne, G., and Sonnhammer, E. L. L. (2001). Predicting transmembrane protein topology with a hidden Markov model: application to complete genomes. *J. Mol. Biol.* 305, 567–580. doi: 10.1006/jmbi.2000.4315

Li, B., Guo, J., Chen, W., Chen, X., Chen, L., Liu, Z., et al. (2009). Endoxanthanase, a novel β-D-Glucanase hydrolyzing backbone linkage of intact xanthan from newly isolated *Microbacterium* sp. XT11. *Appl. Biochem. Biotechnol.* 159, 24–32. doi: 10.1007/s12010-008-8439-1

Li, H., and Durbin, R. (2009). Fast and accurate short read alignment with Burrows-Wheeler transform. *Bioinformatics* 25, 1754–1760. doi: 10.1093/bioinformatics/btp324

Liao, Y., Smyth, G. K., and Shi, W. (2013). The subread aligner: fast, accurate and scalable read mapping by seed-and-vote. *Nucleic Acids Res.* 41:e108. doi: 10.1093/nar/gkt214

Liesack, W., König, H., Schlesner, H., and Hirsch, P. (1986). Chemical composition of the peptidoglycan-free cell envelopes of budding bacteria of the *Pirella/Planctomyces* group. *Arch. Microbiol.* 145, 361–366. doi: 10.1007/BF00470872

Liu, H., Huang, C., Dong, W., Du, Y., Bai, X., and Li, X. (2005). Biodegradation of xanthan by newly isolated *Cellulomonas* sp. LX, releasing elicitor-active xantho-oligosaccharides-induced phytoalexin synthesis in soybean

cotyledons. *Process Biochem.* 40, 3701–3706. doi: 10.1016/j.procbio.2005.05.006

Lombard, V., Golaconda Ramulu, H., Drula, E., Coutinho, P. M., and Henrissat, B. (2014). The carbohydrate-active enzymes database (CAZy) in 2013. *Nucleic Acids Res.* 42, D490–D495. doi: 10.1093/nar/gkt1178

Margulies, M., Egholm, M., Altman, W. E., Attiya, S., Bader, J. S., Bemben, L. A., et al. (2005). Genome sequencing in open microfabricated high density picoliter reactors. *Nat. Biotechnol.* 437, 376–380. doi: 10.1038/nature03959

Markowitz, V. M., Chen, I. M. A., Palaniappan, K., Chu, K., Szeto, E., Grechkin, Y., et al. (2012). IMG: the integrated microbial genomes database and comparative analysis system. *Nucleic Acids Res.* 40, 115–122. doi: 10.1093/nar/gkr1044

Merceron, R., Foucault, M., Haser, R., Mattes, R., Watzlawick, H., and Gouet, P. (2012). The molecular mechanism of thermostable α-galactosidases AgaA and AgaB explained by X-ray crystallography and mutational studies. *J. Biol. Chem.* 287, 39642–39652. doi: 10.1074/jbc.M112.394114

Musfeldt, M., and Schönheit, P. (2002). Novel type of ADP-forming acetyl coenzyme A synthetase in hyperthermophilic *Archaea*: heterologous expression and characterization of isoenzymes from the sulfate reducer *Archaeoglobus fulgidus* and the methanogen *Methanococcus jannaschii*. *J. Bacteriol.* 184, 636–644. doi: 10.1128/JB.184.3.636

Musfeldt, M., Selig, M., and Schönheit, P. (1999). Acetyl coenzyme A synthetase (ADP forming) from the hyperthermophilic archaeon *Pyrococcus furiosus*: identification, cloning, separate expression of the encoding genes, *acdAI* and *acdBI*, in *Escherichia coli*, and in vitro reconstitution of the active heterotetrameric enzyme from its recombinant subunits. *J. Bacteriol.* 181, 5885–5888.

Nakamura, T., Kashima, Y., Mine, S., Oku, T., and Uegaki, K. (2012). Characterization and crystal structure of the thermophilic ROK hexokinase from *Thermus thermophilus*. *J. Biosci. Bioeng.* 114, 150–154. doi: 10.1016/j.jbiosc.2012.03.018

Nawrocki, E. P., Burge, S. W., Bateman, A., Daub, J., Eberhardt, R. Y., Eddy, S. R., et al. (2015). Rfam 12.0: updates to the RNA families database. *Nucleic Acids Res.* 43, D130–D137. doi: 10.1093/nar/gku1063

Nawrocki, E. P., and Eddy, S. R. (2013). Infernal 1.1: 100-fold faster RNA homology searches. *Bioinformatics* 29, 2933–2935. doi: 10.1093/bioinformatics/btt509

Petersen, T. N., Brunak, S., von Heijne, G., and Nielsen, H. (2011). SignalP 4.0: discriminating signal peptides from transmembrane regions. *Nat. Methods* 8, 785–786. doi: 10.1038/nmeth.1701

Podosokorskaya, O. A., Merkel, Y. A., Kolganova, T. V., Chernyh, N. A., Miroshnichenko, M. L., Bonch-Osmolovskaya, E. A., et al. (2011). *Fervidobacterium riparium* sp. nov., a thermophilic anaerobic cellulolytic bacterium isolated from a hot spring. *Int. J. Syst. Evol. Microbiol.* 61, 2697–2701. doi: 10.1099/ijs.0.026070-0

Qian, F., An, L., He, X., Han, Q., and Li, X. (2006). Antibacterial activity of xanthooligosaccharide cleaved from xanthan against phytopathogenic *Xanthomonas campestris* pv. *campestris*. *Process Biochem.* 41, 1582–1588. doi: 10.1016/j.procbio.2006.03.003

Qu, Q., Lee, S., and Boos, W. (2004). TreT, a novel trehalose glycosyltransferring synthase of the hyperthermophilic archaeon *Thermococcus litoralis*. *J. Biol. Chem.* 279, 47890–47897. doi: 10.1074/jbc.M404955200

Quast, C., Pruesse, E., Yilmaz, P., Gerken, J., Schweer, T., Yarza, P., et al. (2013). The SILVA ribosomal RNA gene database project: improved data processing and web-based tools. *Nucleic Acids Res.* 41, 590–596. doi: 10.1093/nar/gks1219

Rawlings, N. D., Barrett, A. J., and Finn, R. (2016). Twenty years of the MEROPS database of proteolytic enzymes, their substrates and inhibitors. *Nucleic Acids Res.* 44, D343–D350. doi: 10.1093/nar/gkv1118

Reshetnikov, A. S., Rozova, O. N., Khmelenina, V. N., Mustakhimov, I. I., Beschastny, A. P., Murrell, J. C., et al. (2008). Characterization of the pyrophosphate-dependent 6-phosphofructokinase from *Methylococcus capsulatus* bath. *FEMS Microbiol. Lett.* 288, 202–210. doi: 10.1111/j.1574-6968.2008.01366.x

Rodionova, I. A., Scott, D. A., Grishin, N. V., Osterman, A. L., and Rodionov, D. A. (2012). Tagaturonate-fructuronate epimerase UxaE, a novel enzyme in the hexuronate catabolic network in *Thermotoga maritima*. *Environ. Microbiol.* 14, 2920–2934. doi: 10.1111/j.1462-2920.2012.02856.x

Ruijssenaars, H. J., De Bont, J. A. M., and Hartmans, S. (1999). A pyruvated mannose-specific xanthan lyase involved in xanthan degradation by *Paenibacillus alginolyticus* XL-1. *Appl. Environ. Microbiol.* 65, 2446–2452.

Ryu, S., Park, C., Cha, J., Woo, E., and Lee, S. (2005). A novel trehalose-synthesizing glycosyltransferase from *Pyrococcus horikoshii*: molecular cloning and characterization. *Biochem. Biophys. Res. Commun.* 329, 429–436. doi: 10.1016/j.bbrc.2005.01.149

Saier, M. H., Reddy, V. S., Tamang, D. G., and Västermark, Å. (2014). The transporter classification database. *Nucleic Acids Res.* 42, 251–258. doi: 10.1093/nar/gkt1097

Schellenberg, J. J., Verbeke, T. J., McQueen, P., Krokhin, O. V., Zhang, X., Alvare, G., et al. (2014). Enhanced whole genome sequence and annotation of *Clostridium stercorarium* DSM8532T using RNA-seq transcriptomics and high-throughput proteomics. *BMC Genomics* 15:567. doi: 10.1186/1471-2164-15-567

Simon, J., and Klotz, M. G. (2013). Diversity and evolution of bioenergetic systems involved in microbial nitrogen compound transformations. *Biochim. Biophys. Acta* 1827, 114–135. doi: 10.1016/j.bbabio.2012.07.005

Slobodkina, G. B., Kovaleva, O. L., Miroshnichenko, M. L., Slobodkin, A. I., Kolganova, T. V., Novikov, A. A., et al. (2015). *Thermogutta terrifontis* gen. nov., sp. nov. and *Thermogutta hypogea* sp. nov., thermophilic anaerobic representatives of the phylum *Planctomycetes*. *Int. J. Syst. Evol. Microbiol.* 65, 760–765. doi: 10.1099/ijs.0.000009

Sorokin, D. Y., Kublanov, I. V., Gavrilov, S. N., Rojo, D., Roman, P., Golyshin, P. N., et al. (2016). Elemental sulfur and acetate can support life of a novel strictly anaerobic haloarchaeon. *ISME J.* 10, 240–252. doi: 10.1038/ismej.2015.79

Strous, M., Pelletier, E., Mangenot, S., Rattei, T., Lehner, A., Taylor, M. W., et al. (2006). Deciphering the evolution and metabolism of an anammox bacterium from a community genome. *Nature* 440, 790–794. doi: 10.1038/nature04647

Susskind, B. M., Warren, L. G., and Reeves, R. E. (1982). A pathway for the interconversion of hexose and pentose in the parasitic amoeba *Entamoeba histolytica*. *Biochem. J.* 204, 191–196.

Tamura, K., Stecher, G., Peterson, D., Filipski, A., and Kumar, S. (2013). MEGA6: molecular evolutionary genetics analysis version 6.0. *Mol. Biol. Evol.* 30, 2725–2729. doi: 10.1093/molbev/mst197

Toth, J., Ismaiel, A. A., and Chen, J. S. (1999). The *ald* gene, encoding a coenzyme A-acylating aldehyde dehydrogenase, distinguishes *Clostridium beijerinckii* and two other solvent-producing clostridia from *Clostridium acetobutylicum*. *Appl. Environ. Microbiol.* 65, 4973–4980.

van de Graaf, A., Mulder, A., Bruijn, P. D. E., Jetten, M. S. M., Robertson, L. A., and Kuenen, J. G. (1995). Anaerobic oxidation of ammonium is a biologically mediated process. *Appl. Environ. Microbiol.* 61, 1246–1251.

Vignais, P. M., and Billoud, B. (2007). Occurrence, classification, and biological function of hydrogenases: an overview. *Chem. Rev.* 107, 4206–4272.

Wehner, S., Damm, K., Hartmann, R. K., and Marz, M. (2014). Dissemination of 6S RNA among bacteria. *RNA Biol.* 11, 1467–1478. doi: 10.4161/rna.29894

Xiong, X., Li, M., Xie, J., Jin, Q., Xue, B., and Sun, T. (2013). Antioxidant activity of xanthan oligosaccharides prepared by different degradation methods. *Carbohydr. Polym.* 92, 1166–1171. doi: 10.1016/j.carbpol.2012.10.069

Yin, Y., Mao, X., Yang, J., Chen, X., Mao, F., and Xu, Y. (2012). DbCAN: a web resource for automated carbohydrate-active enzyme annotation. *Nucleic Acids Res.* 40, 445–451. doi: 10.1093/nar/gks479

Conflict of Interest Statement: The authors declare that the research was conducted in the absence of any commercial or financial relationships that could be construed as a potential conflict of interest.

frontiers in Microbiology

ORIGINAL RESEARCH
published: 20 August 2018
doi: 10.3389/fmicb.2018.01931

Fermentation of Mannitol Extracts From Brown Macro Algae by Thermophilic *Clostridia*

*Theo Chades, Sean M. Scully, Eva M. Ingvadottir and Johann Orlygsson**

Faculty of Natural Resource Sciences, University of Akureyri, Akureyri, Iceland

Mannitol-containing macro algae biomass, such as *Ascophyllum nodosum* and *Laminaria digitata*, are a potential feedstock for the production of biofuels such as bioethanol. The purpose of this work was to evaluate the ability of thermophilic anaerobes within Class *Clostridia* to ferment mannitol and mannitol-containing algal extracts. Screening of the type strains of six genera, *Caldanaerobius*, *Caldanaerobacter*, *Caldicellulosiruptor*, *Thermoanaerobacter*, *Thermobrachium*, and *Thermoanaerobacterium*) was conducted on 20 mM mannitol and revealed that 11 of 41 strains could utilize mannitol with ethanol being the dominant end-product. Mannitol utilization seems to be most common within the genus of *Thermoanaerobacter* (7 of 16 strains) with yields up to 88% of the theoretical yield in the case of *Thermoanaerobacter pseudoethanolicus*. Six selected mannitol-degrading strains (all *Thermoanaerobacter* species) were grown on mannitol extracts prepared from *A. nodosum* and *L. digitata*. Five of the strains produced similar amounts of ethanol as compared with ethanol yields from mannitol only. Finally, *T. pseudoethanolicus* was kinetically monitored using mannitol and mannitol extracts made from two macro algae species, *A. nodosum* and *L. digitata* for end-product formation.

Keywords: third generation biomass, bioethanol, *Thermoanaerobacter*, seaweed, bioprocessing, extremophiles, *Ascophyllum nodosum*, *Laminaria digitata*

OPEN ACCESS

Edited by:
Nils-Kaare Birkeland,
University of Bergen, Norway

Reviewed by:
Hugh Morgan,
University of Waikato, New Zealand
Sachin Kumar,
Sardar Swaran Singh National Institute of Renewable Energy, India

***Correspondence:**
Johann Orlygsson
jorlygs@unak.is

Specialty section:
This article was submitted to Extreme Microbiology, a section of the journal Frontiers in Microbiology

Received: *28 April 2018*
Accepted: *30 July 2018*
Published: *20 August 2018*

Citation:
Chades T, Scully SM, Ingvadottir EM and Orlygsson J (2018) Fermentation of Mannitol Extracts From Brown Macro Algae by Thermophilic Clostridia. Front. Microbiol. 9:1931. doi: 10.3389/fmicb.2018.01931

INTRODUCTION

Due to the worldwide energy crisis and environmental problems associated with the utilization of petroleum products, the need for biofuel production from renewable feedstocks that do not compete with agriculture has been of increased interest over the past several decades (Sánchez and Cardona, 2008; Scully and Orlygsson, 2015). While the production of bioethanol from lignocellulosic biomass has made advances in terms of pretreatment of the biomass and the development of microorganisms well-suited to this task, substantially less work has been done on the utilization of marine biomass, such as macro algae, as a raw material. The utilization of macro algae (third generation biomass) as a feedstock is of special interest as marine biomass often has high productivity and does not compete with arable land (Daroch et al., 2013; Wei et al., 2013). The utilization of third generation biomass remains challenging due to the diversity of chemical compositions of macro algae and as well as lack of well-established methodologies for the saccharification of this type of biomass (Daroch et al., 2013). While macro algae do not contain lignin like terrestrial plants, many macro algae contain phlorotannins which are similarly structured to lignin in that it is composed of phloroglucinol, an aromatic

molecule (Kawai and Murata, 2016). Brown macro algae have complex carbohydrate composition containing alginate, fucoidan, mannitol, and laminarin (Wei et al., 2013; Xia et al., 2015; Kawai and Murata, 2016). Mannitol and laminarin function as reserve carbohydrates and are accumulated during summer months of the northern hemisphere (Adams et al., 2011) reaching concentrations as high as 25–30% on a dry weight basis (Daroch et al., 2013; Wei et al., 2013). Brown macroalgae are harvested commercially in large quantities in Asia and Europe (Muty and Banerjee, 2012). In 2012, 24 million tons of macro algae were harvested globally with only a handful of nations responsible indicating that there is great potential to exploit these materials (Radulovich et al., 2015). In the west of Iceland, *Laminaria digitata* and *Ascophyllum nodosum* have been dried using geothermal heat since the 1970s which was commercialized by Thorverk, ehf in the mid-1980s although harvested quantities are less than 20 tons per year. As a raw material for bioprocessing, brown macro algae have been used for biogas production while for bioethanol production the complexity of the biomass still presents a serious challenge for economic success due to the diversity of carbohydrates present as well as pretreatment methodologies still being in their infancy (Wei et al., 2013; Enquist-Newman et al., 2014; Milledge et al., 2014; Jiang et al., 2016).

Thermophilic species within Class *Clostridia*, including genera such as *Caldicellulosiruptor, Thermoanaerobacter,* and *Thermoanaerobacterium,* have been isolated from a wide range of thermal environments including many in terrestrial geothermal areas in Eurasia including Iceland, and the Kamchatka Peninsula, Russia (Burgess et al., 2007). As with thermoanaerobes in general, work at higher operating temperatures improves substrate solubility and reduces viscosity, improves the thermodynamics of many fermentative processes, and could potentially allow for *in situ* distillation of volatile end products such as ethanol. Many thermophilic *Clostridia* are of interest for their inherent tolerance to extreme environmental conditions and their ability to produce potential biofuels from a broad range of substrates including monosaccharides present in lignocellulosic biomass although highly reduced sugar alcohols have received little attention. Many of these thermophilic *Clostridia* also have the ability to degrade polymeric carbohydrates which often includes starch, xylan, and even crystalline cellulose (Ren et al., 2009; Taylor et al., 2009; Chang and Yao, 2011; Scully and Orlygsson, 2015). Several *Caldicellulosiruptor* species in particular are highly versatile bioprocessing platforms with diverse capabilities involving the deconstruction of complex carbohydrates including cellulose and hemicelluloses (Blumer-Schuette et al., 2012; Carere et al., 2012). Due to the broad substrate spectra and diverse metabolic capabilities demonstrated by the aforementioned thermophilic anaerobes, they make natural prospecting candidates for the utilization of algal biomass, particularly mannitol. While the utilization of sugar alcohols, such as D-mannitol, are often reported in the work describing novel species, end product spectra are seldom reported.

Sugar alcohols, such as mannitol, are naturally occuring or can be produced by the catalytic dehydrogenation of their correpsonding hexose or pentose or can be produced by yeast during fermentation (Tanghe et al., 2005). Mannitol, in addition to being an inexpensive substrate, can be easily isolated from brown algae such as *A. nodosum*, *Laminaria* species, and *Macrocystis pyrifera*, such as sorbitol (glucitol), and mannitol. Beyond their applications as artificial sweeteners and laxatives, other potential applications of mannitol include clinical applications and as a fermentation feedstock (Daroch et al., 2013; Wei et al., 2013). Mannitol is interesting for biofuel production since its heating value is higher than that of glucose (3025 kJ/mol versus 2805 kJ/mol) and is a more reduced fermentation substrate as compared to hexoses and thus is an unexploited resource for bioethanol production (Daroch et al., 2013; Wei et al., 2013).

Mannitol utalization is a fairly ubiquitous trait with organisms including yeast such as *Candida albicans* and *Pichia angophorae* (Horn et al., 2000) although some strains of *Saccharomyces cerevisiae* have been adapted to utilize mannitol (Quain and Boulton, 1987). Mesophilic bacteria capable of mannitol utilization include *Staphylococcus aureus*, *Escherichia coli* (Kim et al., 2011), *Zymobacter palmae* (Horn et al., 2000), *Vibrio tritonius* (Matsumura et al., 2014), *Clostridium butyricum* (Heyndrickx et al., 1989), *Clostridium difficile* (Kazamias and Sperry, 1995), *Clostridium acetobutylicum* (Kaid et al., 2016), and *Anaerobium acetethylicum* (Patil et al., 2015). Thermophilic bacteria known to degrade mannitol anaerobically include the recently described *Defluviitalea phaphyphila* which is capable of degrading multiple macro algae components (Ji et al., 2016a,b), *Caldicoprobacter algeriensis* (Bouanane-Darenfed et al., 2011), *Thermoanaerobacter wiegelii* which yields ethanol (Cook et al., 1996), and *Thermoanaerobacter pentosaceus* (Sittijunda et al., 2013; Tomás et al., 2013).

As brown algae commonly contain high concentrations of mannitol, commercially harvested brown algae species such as *L. digitata* and *A. nodosum* make logical choices of raw material. *Macrocystis pyrifera* contains up to 12.4% mannitol by weight (Mateus et al., 1977) while the mannitol content in *L. digitata* has been found to vary between 3 and 21% (Black et al., 1952) although more recent reports have reported results above 30% on a weight basis (Adams et al., 2011). The extraction of mannitol from brown algae can be accomplished using solid-liquid extraction using weakly acidic solutions as has been reported for brown algae such as *Macrocystis pyrifera* (Mateus et al., 1977).

The present work examines the extraction of mannitol from macro algae and its subsequent fermentation to ethanol by thermophilic *Clostridia*. Comparisons between dilute acid solid-liquid extraction conditions under mild (50°C or less) conditions were performed. The ability of thermophilic *Clostridia* in the genera of *Caldanaerobius*, *Caldicellulosiruptor*, *Caldanaerobacter*, *Thermoanaerobacterium*, *Thermoanaerobacter*, and *Thermobrachium* to utilize mannitol as the sole substrate as well as mannitol extracted by dilute acid extraction from two ubiquitous mannitol-containing brown algae species, *A. nodosum* and *L. digitata* were tested. A kinetic experiment with a promising strain, *Thermoanaerobacter pseudoethanolicus*, was also performed. This study demonstrates the ease with which mannitol can be

extracted and fermented to bioethanol from readily available brown algae.

MATERIALS AND METHODS

Strains and Cultivation Conditions

Organisms were cultivated in Basal Mineral (BM) medium prepared as previously described (Sveinsdottir et al., 2009) with modifications; the medium consisted of (per liter): $NaH_2PO_4 \cdot 2H_2O$ 3.04 g, $Na_2HPO_4 \cdot 2H_2O$ 5.43 g, NH_4Cl 0.3 g, NaCl 0.3 g, $CaCl_2 \cdot 2H_2O$ 0.11 g, $MgCl_2 \times 6H_2O$ 0.1 g, yeast extract 2.0 g, resazurin 1 mg, trace element solution 1 mL, vitamin solution (DSM141) 1 mL, and $NaHCO_3$ 0.8 g. The trace element solution consisted of the following on a per liter basis: $FeCl_2 \times 4H_2O$ 2.0 g, EDTA 0.5 g, $CuCl_2$ 0.03 g, H_3BO_3, $ZnCl_2$, $MnCl_2 \times 4H_2O$, $(NH_4)Mo_7O_{24}$, $AlCl_3$, $CoCl_2 \times 6H_2O$, $NiCl_2$, and 0.05 g, $Na_2S \times 9H_2O$ 0.3 g, and 1 mL of concentrated HCl. The final mannitol concentration was 20 mM in all cases. The medium was prepared by adding the buffer to distilled water containing resazurin and boiled for 10 min and cooled under nitrogen flushing (<5 ppm O_2). The mixture was then transferred to serum bottles using the Hungate technique (Hungate, 1969; Miller and Wolin, 1974) and autoclaved for 60 min. Media preparations containing algal extracts were sterilized by Tindallization to avoid browning of the media; these serum bottles were heated twice at 90°C for 60 min. All other components of the medium were added separately through filter (0.45 μm) sterilized solutions. All experiments were conducted at 65°C and at pH of 7.0 with a liquid-gas phase (L-G) ratio of 1:1 in which the gas phase consists of nitrogen. In all cases, experiments were performed in triplicate.

Forty one strains of thermophilic anaerobes from the genera of *Caldicellulosiruptor, Caldanaerobacter, Thermoanaerobacter,* and *Thermoanaerobacterium* were purchased from Deutsche Sammlung von Mikroorganismen und Zellkulturen (DSMZ); *Thermoanaerobacterium thermostercoris* (DSM 22141), *Thermoanaerobacterium thermosulfurigenes* (DSM 2229), *Thermoanaerobacterium aotearoense* (DSM 10170), *Thermoanaerobacterium thermosaccharolyticum* (DSM 571), *Thermoanaerobacterium saccharolyticum* (DSM 7060), *Thermoanaerobacterium xylanolyticum* (DSM 7097), *Thermoanaerobacterium aciditolerans* (DSM 16487), *Caldanaerobius polysaccharolyticus* (DSM 13641), *Caldanaerobius zeae* (DSM 13642), *Caldanaerobius fijiensis* (DSM 17918), *Thermobrachium celere* (DSM 13655), *Caldicellulosiruptor changbaiensis* (DSM 26941), *Caldicellulosiruptor saccharolyticus* (DSM 8903), *Caldicellulosiruptor owensis* (DSM 13100), *Caldicellulosiruptor bescii* (DSM 6725), *Caldicellulosiruptor acetigenus* (DSM 7040), *Caldicellulosiruptor lactoaceticus* (DSM 9545), *Caldicellulosiruptor kristjanssonii* (DSM 12137), *Caldicellulosiruptor hydrothermalis* (DSM 18901), *Caldicellulosiruptor kronotskiensis* (DSM 18902), *Thermoanaerobacter acetoethylicus* (DSM 2359), *Thermoanaerobacter brockii* subsp. *brockii* (DSM 1457), *T. brockii* subsp. *finnii* (DSM 3389), *T. brockii* subsp. *lactiethylicus* (DSM 9801), *Thermoanaerobacter italicus* (DSM 9252), *Thermoanaerobacter ethanolicus* (DSM 2246), *Thermoanaerobacter kivui* (DSM 2030), *Thermoanaerobacter mathrani* subsp. *mathrani* (DSM 11426), *T. pentosaceus* (DSM 25963), *T. pseudoethanolicus* (DSM 2355), *Thermoanaerobacter siderophilus* (DSM 12299), *Thermoanaerobacter sulfurigignens* (DSM 17917), *Thermoanaerobacter sulfurophilus* (DSM 11584), *Thermoanaerobacter thermohydrosulfuricus* (DSM 567), *Thermoanaerobacter uzonensis* (DSM 18761), *T. wiegelii* (DSM 10319), *Caldanaerobacter subterraneus* subsp. *yonseiensis* (DSM 13777), *C. subterraneus* subsp. *subterraneus* (DSM 13054), *C. subterraneus* subsp. *pacificus* (DSM 12653), *C. subterraneus* subsp. *tengcongensis* (DSM 15242), and *Caldanaerobacter uzonensis* (DSM 18923). All cultivations were conducted at pH 7.0 at the organism's T_{opt} which is listed in **Supplementary Table S1**.

All inoculation stocks of the strains were taken from frozen (−20°C) cultures with rigorously degassed 30% (v/v) glycerol and reactivated on BM medium containing glucose (20 mM). Reactivated cultures were inoculated (2% v/v) from exponential growth phase to 25 mL serum bottles (liquid-gas ratio 1:1). Cultures were grown for 7 days and screened for end-product formation.

Macro Algae Collection and Preparation

Multi-kilogram quantities of brown algae were collected in the summer of 2015. *A. nodosum* was obtained from the shores just north of Akureyri, Iceland (65°41′53.31″N, 18°6′32.80″W) in July of 2015. *L. digitata* was obtained from a coastal area north of Husavik, Iceland (66°3′38.64″N, 17°21′18.92″W) in August of 2015. Collected samples were transported to the laboratory and briefly washed with cold tap water; material was then dried in an oven at 45°C for 48 h. Dried algae was milled in a Waring blender and then milled to less than 2 μm in a Herzog HSM 50 pulverizing mill. The resultant algal meal was stored in air tight containers prior to use.

Extraction of Mannitol From Macro Algae

The solid-liquid extraction of mannitol from *A. nodosum* and *L. digitata* was investigated by varying both temperature (0, 25, 50°C) and HCl concentration (0, 50, 100 mM). One gram of algal meal was placed in a 50 mL polypropylene tube with 10 mL of extraction solution (0, 0.05 M, or 0.1 M HCl) and mixed at 250 rpm for 15 min at a 45° angle to ensure thorough mixing. The supernatant was collected by centrifugation (4700 rpm, 15 min, 4°C). This was repeated for a total of four extraction. Extraction solutions were stored at −40°C prior to analysis for mannitol, total phenolics, and protein.

Extraction Kinetics of Algal Meal

10 g of algal meal was extracted in triplicate on a 10 g scale with 100 mL of extraction solution (50 mM HCl for *A. nodosum* or dH_2O for *L. digitata*) based on results of the previous experiment. Samples were mixed at 250 rpm and supernatant was withdrawn over 15 min in 3 min intervals, centrifuged at 13,000 rpm, and stored at −40°C prior to analysis for mannitol, total phenolics, and protein.

Large-Scale Extraction of Mannitol From Algal Meal

100 g of algal meal was extracted with 1 L of either 50 mM HCl (*A. nodosum*) or dH_2O (*L. digitata*) at 200 rpm for 10 min at 25°C. The extract was centrifuged at 4700 rpm for 15 min at 4°C. 10 g of $CaCl_2$ was then added to precipitate alginate present and the resultant solution was centrifuged at 4700 rpm at 4°C for 15 min. The supernatant solution was adjusted to pH 7.0 with 12 M NaOH and filtered sequentially through 53 and 5 μm nylon mesh. Extracts were analyzed for mannitol and total phenolic content.

Screening of Thermophilic *Clostridia* for Mannitol Utilization

All strains were screened for mannitol utilization by adding mannitol (20 mM) in Hungate tubes (16 mm × 150 mm, ChemGlass, United Kingdom) with an L-G ratio of 1:1. Pressure and optical density were determined after 7 days of incubation where after they were analyzed for end products.

Fermentation of Mannitol-Extracts From Macro Algae

BM medium was prepared with algal extract diluted to 20 mM mannitol equivalence. Media was prepared in 25 mL serum bottles. Pressure and optical density were determined after 7 days of incubation where after they were analyzed for end products.

Kinetic Fermentation of Mannitol and Mannitol-Extracts From Macro Algae by *T. pseudoethanolicus*

Thermoanaerobacter pseudoethanolicus was cultivated on mannitol (20 mM) and mannitol extracts from macroalgae (equivalent to 20 mM mannitol) in 125 mL serum bottles. Samples were collected over time for 290 h with the most intensive sampling at early stage of the fermentations. Samples were analyzed as previously described.

Analytical Methods

Hydrogen was analyzed using a Perkin Elmer gas chromatograph equipped with thermo conductivity detector as previously described Orlygsson and Baldursson (2007). Volatile fatty acids and alcohols were analyzed by gas chromatograph (Perkin Elmer Clarus 580) using a FID detector with 30 m DB-FFAP capillary column (Agilent Industries Inc., Palo Alto, CA, United States) as previously described Orlygsson and Baldursson (2007). Pressure was determined using a PendoTech PMAT-DPG Handheld PressureMAT. Mannitol was analyzed using the colorimetric method described by Sanchez (1998). Briefly, 25 μL of diluted sample (less than 5 mM of mannitol) was added to a microplate to which 125 μL of 500 mM formate buffer (pH 3.0) and 75 μL of 5 mM periodic acid. 75 μL of freshly prepared reaction solution (100 mM acetylacetone, 2 M ammonium acetate, 20 mM thiosulfate) was added, the plate briefly mixed at 150 rpm and then incubated at 100°C on a microplate heating block for 2 min. Samples were then read on a Bioscreen C (Growth Curves Ltd., Finland) at 412 nm against a blank prepared as described except substituting reaction solution for distilled water to correct for colored solutions. Standards were prepared from authentic mannitol at a concentration range of 0.5–5 mM.

Total phenolic compounds were analyzed colorimetrically by transferring 250 μL of sample and 1.25 mL of dH_2O to a microtube to which 125 μL of Folin-Ciocalteu Reagent was added. After 5 min, 375 μL of 20% (w/v) sodium carbonate was added followed by 500 μL of dH_2O and incubated at ambient temperature for 2 h. Samples were read at 760 nm on a Shimadzu UV-1800 UV-Visible spectrophotometer in a quartz cuvette (l = 1 cm) against a water blank. Results are calculated as gallic acid equivalent (GAE) using a standard curve prepared from gallic acid standards (0–100 μg/mL).

Lactate was analyzed spectrophotometrically according to Ingvadottir et al. (2017). Bradford protein was analyzed according to (Bradford, 1976) with modifications. 300 μL of Bradford reagent was added to a microplate well containing 10 μL of sample and shaken for 30 s at 150 rpm on a microplate shaker. Plates were then read at 600 nm on a Bioscreen C (Growth Curves Ltd., Finland) against a water blank. Bovine Serum Albumin was (0.1–1.25 mg/mL) was used as a standard.

Conductivity was determined using a EC 300 portable conductivity meter (YSI Environmental, United States). Viscosity was measured using a Brookfield DV-II+ Pro EXTRA Programmable Rheometer. Proximate analysis of biomass (protein, fat, ash, and carbohydrate content) was conducted according to standard methods.

RESULTS

Two types of macroalgal biomass were used in present study to investigate its mannitol content and its extraction. The mannitol present in the macroalgal extracts were then tested as a substrate for six genera of thermophilic bacteria.

Proximate Analysis of Macro Algae

The two macro algae species used in the present investigation *A. nodosum* and *L. digitata* were analyzed for protein, fat, ash, and total carbohydrates. The bulk of the material was greater than 70% (dw) for both algae although the protein and fat content of *A. nodosum* were higher as compared to *L. digitata* but ash and carbohydrate content of the latter were higher (**Table 1**).

TABLE 1 | Proximate analysis of *A. nodosum* and *L. digitata* collected from Akureyri and Husavik, Iceland, respectively.

	Brown algae species	
	A. nodosum	***L. digitata***
Protein	6.94 ± 0.32	4.03 ± 0.97
Ash	15.60 ± 1.32	18.07 ± 1.07
Fat	5.21 ± 0.69	0.46 ± 0.24
Carbohydrates	72.24 ± 0.92	77.43 ± 0.98

Values represent the average of triplicate measurements ± SD.

Extraction of Mannitol From Macroalgae

Ascophyllum nodosum

Mannitol was extracted from *A. nodosum* with three different concentrations of acid (0, 50, and 100 mM), at three temperatures (0, 25, and 50°C) for four consecutive times. This was also done for protein and total phenolic content (as GAE). The total amounts of mannitol extracted from this macroalgae varied from 7.95 to 39.6 mM (**Figure 1A**). When end concentrations of mannitol extracted are compared with mannitol concentrations obtained after the first extraction, most often more than 50% of mannitol was extracted in this first round (range from 47.2% (0°C, 0.1 M) to 68.5% (25°C, 0.1 M) (**Figure 1A** and **Supplementary Table S2**). Temperature has a clear effect on the amount of mannitol released, with the lowest amounts always found at 0°C and highest at 25°C. Similarly, the effect of acid was profound with little mannitol released without acid but little difference was observed between 50 and 100 mM HCl. Protein extraction from *A. nodosum* is shown in **Figure 1B**. The amount of protein extracted ranged from 0.19 to 0.23 mg/mL with the highest protein amounts observed when the samples were extracted with distilled water at ambient temperature (0.23 mg/mL). Temperature did not greatly impact the amount of protein solubilized during mannitol extraction (**Supplementary Table S3**). The content of phenolic compounds were also analyzed for *A. nodosum* under these same conditions (**Figure 1C**). The only difference with regard to temperature and the concentration of HCl is that lower amounts of phenolic compounds were extracted at 0°C as compared with higher temperatures with and without acid addition (**Supplementary Table S4**).

Laminaria digitata

Mannitol extraction from *L. digitata* resulted in much higher concentrations (ranging from 71.3 to 86.9 mM) as compared with *A. nodosum* (**Figure 2A**). First extraction always resulted in more than 50% mannitol extraction when compared with the total amounts extracted (**Supplementary Table S5**). Interestingly, much less variation was found between the use of HCl and temperature as compared with *A. nodosum*. Protein extraction from *A. nodosum* were highest at 50°C with 50 and 100 mM HCl

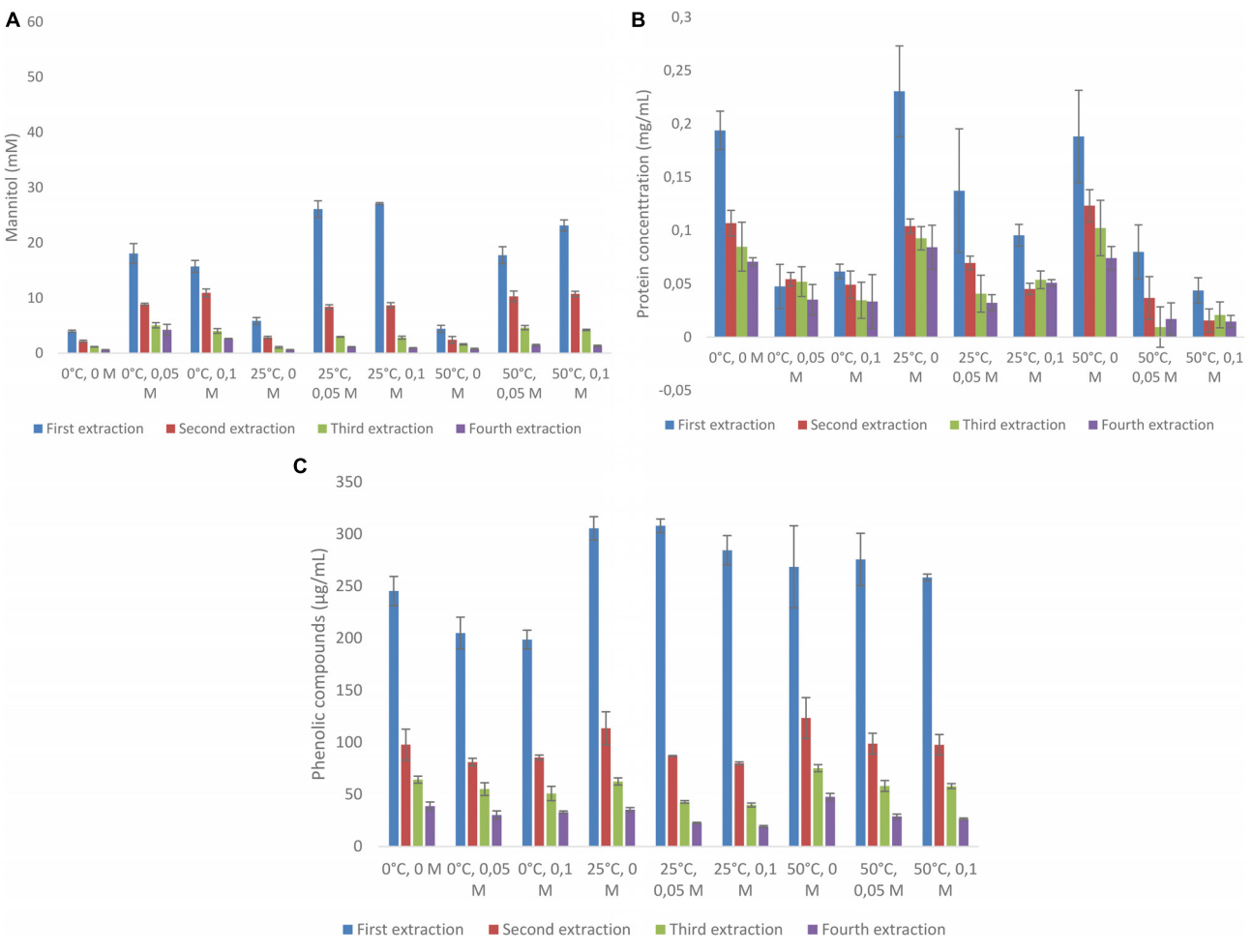

FIGURE 1 | Sequential solid-liquid extraction of mannitol from *Ascophyllum nodosum* at various temperature and HCl concentrations. **(A)** mannitol concentration, **(B)** protein concentration, **(C)** total phenolic compounds as gallic acid equivalent.

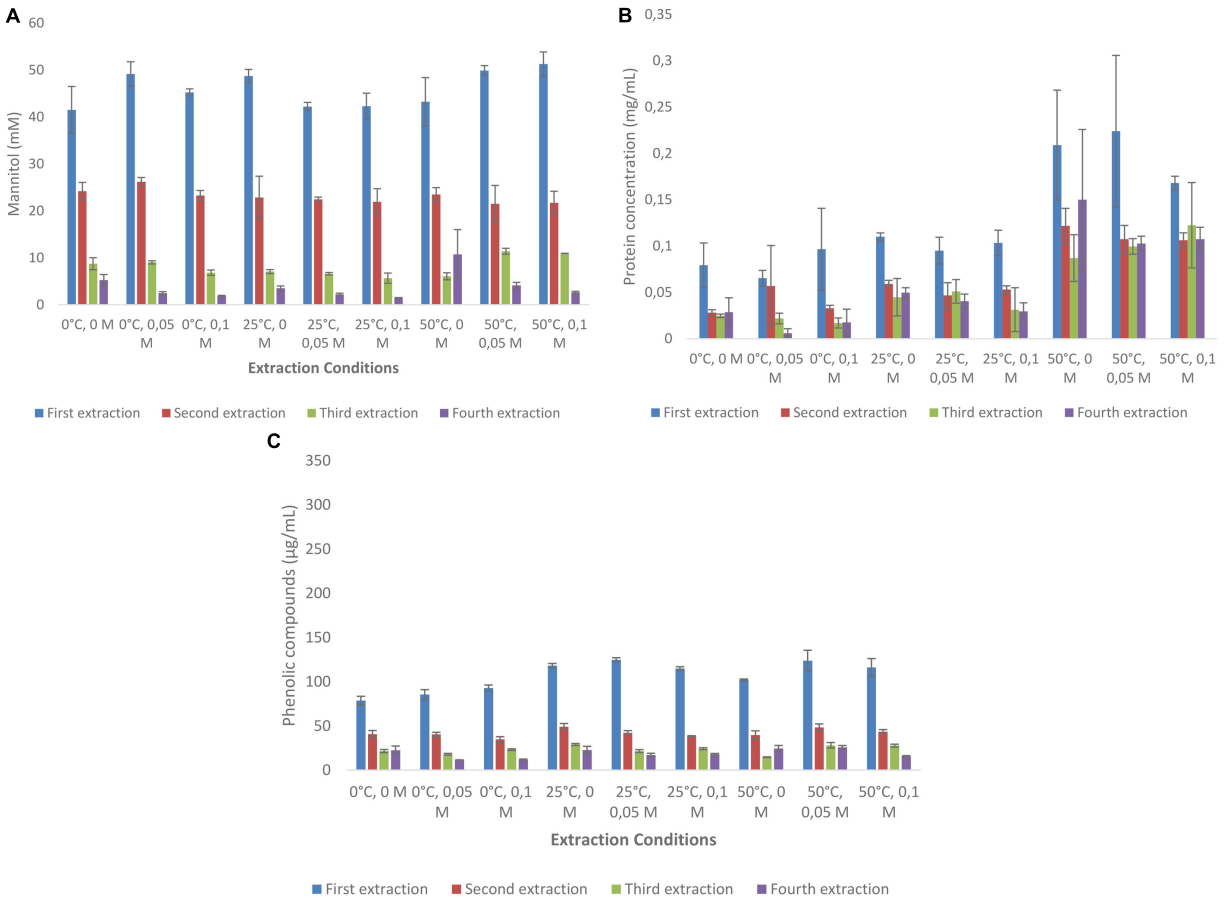

FIGURE 2 | Sequential solid-liquid extraction of mannitol from *Laminaria digitata* at various temperature and HCl concentrations. **(A)** Mannitol concentration, **(B)** protein concentration, **(C)** total phenolic compounds as gallic acid equivalent.

concentrations (0.21–0.22 mg/mL). Much lower concentrations of protein was extracted at other conditions (**Figure 2B**). The concentrations of phenolic compounds from *A. nodosum* (**Figure 2C**) were much lower as compared with *L. digitata* and little difference was between different experimental set up.

Extraction Kinetics of Mannitol and Phenolics From Macroalgal Meal

In one set of experiments the extraction of both mannitol and phenolic compounds was done kinetically with samples taken every 3 min for 15 min. Conditions chosen were 25°C and 50 mM HCl. **Figures 3A,B** shows that most of the mannitol and phenolic compounds are extracted during the first 3 min of the experiments (more than 75% of the total quantity extracted). As before, mannitol extraction for *L. digitata* were more than twice of that of *A. nodosum* and the concentrations of phenolic compounds were 50% lower (**Supplementary Tables S6**, **S7**).

Large Scale Extraction (100 g Scale)

The preparative scale extraction of mannitol from macro algal meal was conducted on a 100 g scale using the optimum conditions (25°C, 50 mM HCl) for each brown algae based on previous experiments as summarized in **Table 2**. As before, the first extraction from both algal meal yielded the highest concentrations of mannitol (19.91 and 65.15 mM, from *A. nodosum* and *L. digitata*, respectively). To reduce the viscosity, $CaCl_2$ was added to precipitate any co-extracted alginate.

Screening of Thermophilic *Clostridia* for Mannitol Utilization

Forty one strains of thermophilic *clostridia* were screened for the degradation and end product formation from 20 mM of mannitol. Most of the strains that were positive on mannitol utilization belong to the genus *Thermoanaerobacter*. Positives within each genera were *Caldanaerobacter* (1 of 5 species), *Caldicellulosiruptor* (2 of 9, both weakly positive), *Thermoanaerobacter* (7 of 16), and *Thermoanaerobacterium* (1 of 7). *T. celere*, and *Caldanaerobius* strains did not utilize mannitol (**Table 3**). End products of mannitol fermentation are presented in **Table 3**.

Four of *Thermoanaerobacter* strains are highly ethanologenic producing more than 30 mmol of ethanol from 20 mM of mannitol but the other three produce between 19.7 and 26.8 mM. Other products were lactate, acetate and hydrogen. Only one

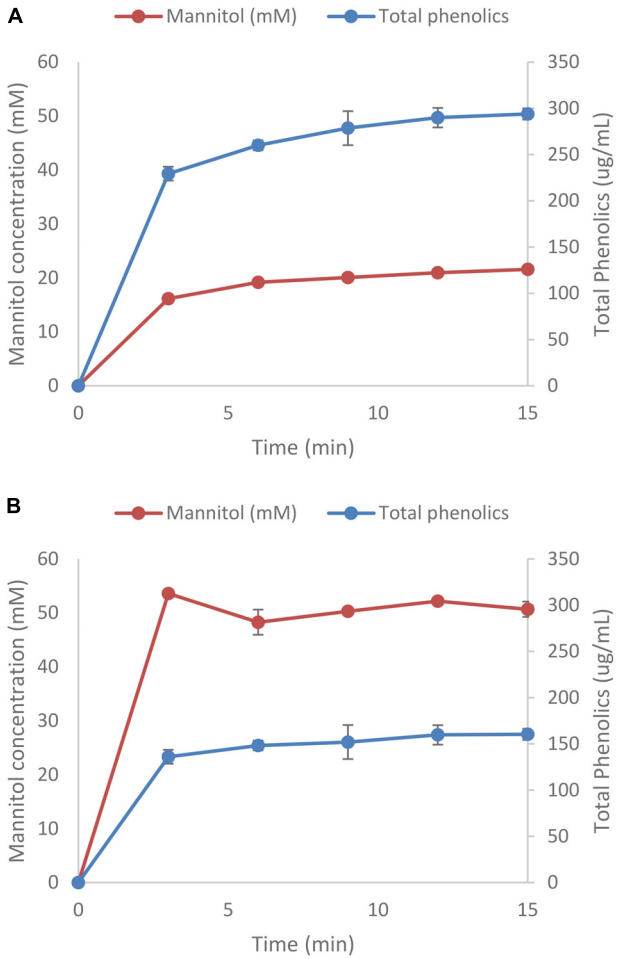

FIGURE 3 | Extraction of mannitol from *Ascophyllum nodosum* **(A)** and *Laminaria digitata* **(B)**. Protein was less then 0.2 mg/mL (data not shown).

strain, *C. subterraneus* subsp. *pacificus*, was found positive of the five *Caldanaerobacter* species but produced less ethanol as compared to *Thermoanaerobacter* species. Also, only one of the *Thermoanaerobacterium* strain was found positive, *Th. xylanolyticum* producing 18.2 mM of ethanol, 2.7 mM of acetate, and 3.8 mM of lactate. Two of the *Caldicellulosiruptor* species were weakly positive on mannitol degradation produced low amounts of all end products but above controls.

Fermentation of Macroalgal Extracts by Selected Strains

Strains demonstrating end product formation on mannitol were then grown on extracts of *A. nodosum* and *L. digitata* diluted to a concentration equivalent to 20 mM of mannitol as shown in **Figures 4A,B**, respectively. The only strains showing end-product formation from the extracts belong to the genus of *Thermoanaerobacter*.

Five species (*T. siderophilus*, *T. pseudoethanolicus*, *T. brockii* subsp. *finnii*, *T. brockii* subsp. *brockii, and T. sulfurigignens*) produced considerable amounts of ethanol from both macroalgae species (**Figures 4A,B**). *T. uzonensis* however, only produced ethanol on *A. nodosum* hydrolysate. Ethanol yields (assuming that the only carbon source is mannitol) on the *A. nodosum* extract ranged from 52.5% (*T. sulfurigignens*) to 92.3% (*T. pseudoethanolicus*) and fermentation of the *L. digitata* extract yielded between 52.1% (*T. sulfurigignens*) and 67.6% (*T. pseudoethanolicus*) of the theoretical yield.

Kinetic Experiment

One of the strains yielding high ethanol yields on mannitol and macroalgal extracts was *T. pseudoethanolicus* (**Table 4**). To further investigate mannitol fermentation by this bacterium, kinetic experiments were conducted on glucose and mannitol, as well as the algal extracts from *A. nodosum* and *L. digitata*. **Supplementary Figure S1** shows that glucose is rapidly fermented to ethanol by *T. pseudoethanolicus* reaching 35 mM (87.5% of theoretical) around 48 h. For comparison, fermentation without added carbon source is presented in **Supplementary Figure S2**. The fermentation of mannitol (**Figure 5A**), however, shows the production profile of end-products revealing a rather rapid growth rate and most of the ethanol was already produced within 110 h (final concentration was 28.1 mM which is slightly lower as compared with the screening data on mannitol). Interestingly most of the ethanol is produced after the bacterium reaches stationary growth phase. As previously, the other minor products were acetate, lactate, and hydrogen. During growth on *Laminaria* and *Ascophyllum* extracts similar results were obtained (**Figures 5B,C**) with ethanol being the main end product and acetate and hydrogen were observed below 10 mmol/L.

DISCUSSION

Chemical Composition and Extraction of Mannitol From Macroalgae Biomass

The middle of summer was selected for the sampling period as previous work has shown that the mannitol content peaks around this time in other locations (Adams et al., 2011). While seasonal variation studies on the composition of brown macro algae have not been reported in Iceland, the observed values for protein, fat, and ash were within the ranges previously reported (Indergaard and Minsaas, 1991 and references therein). The bulk of both *A. nodosum* and *L. digitata* collected were carbohydrates (>70% on a dry weight basis) with a large ash fraction (**Table 1**). The collected *L. digitata* contained less than 1% fat which is lower than the range commonly reported but could potentially be attributed to a relatively low quantity of material extracted (approximately 10 g).

Mannitol is an inexpensive carbon source readily extracted from brown macro algae under mild conditions (**Figures 1A**, **2A**). Increasing the length of the extraction may result in the co-extraction of phenolics (**Figures 1C**, **2C**) which could potentially be inhibitory to fermentative organisms (Daglia, 2012). Relative to the amount of protein present in the algal meal (4–7% w/w), relatively low quantities (<0.2 mg/mL) were extracted under most conditions examined in the present

TABLE 2 | Preparative scale extraction of mannitol from brown macro algae.

Macro algae	Extraction no.	Mannitol (mM)	Total phenolics (μg/mL)	Salt (ppt)	Viscosity (cP)
A. nodosum	1	19.91 ± 0.25	267.87 ± 0.76	7.4	1950.0
	2	8.02 ± 0.09	114.64 ± 0.5	4.9	24.0
	Total	27.93	382.51		
L. digitata	1	65.16 ± 0.52	125.42 ± 2.20	11.2	4580.0
	2	26.12 ± 0.03	65.01 ± 9.18	7.3	1620.0
	Total	91.28	190.43		

All values represent triplicate analyses of single extraction solutions with SD presented as error bars.

TABLE 3 | End product formation from strains degrading mannitol (20 mM).

		End products (mmol/L)				
Strain	**Substrate**	**Ethanol**	**Lactate**	**Acetate**	**Hydrogen**	**Carbon balance (%)**
C. subterraneus subsp. *pacificus* (DSM 12653)	Mannitol	17.3 ± 5.5	2.76 ± 0.81	5.6 ± 1.3	1.7 ± 0.7	64.2
	Control (YE)	0.8 ± 0.2	0.0 ± 0.0	4.8 ± 0.2	5.7 ± 0.7	ND
T. uzonensis (DSM 18761)	Mannitol	30.0 ± 1.8	4.33 ± 0.46	3.0 ± 0.1	8.4 ± 1.4	93.5
	Control (YE)	0.8 ± 0.2	0.0 ± 0.0	3.3 ± 0.5	4.0 ± 1.2	ND
T. sulfurigignens (DSM 17917)	Mannitol	24.8 ± 1.6	3.89 ± 1.01	4.1 ± 0.8	11.9 ± 1.6	81.8
	Control (YE)	1.7 ± 0.4	0.0 ± 0.0	1.8 ± 0.7	2.2 ± 0.5	ND
T. siderophilus (DSM 12299)	Mannitol	33.2 ± 3.2	2.52 ± 1.4	3.0 ± 0.3	9.0 ± 1.7	96.8
	Control (YE)	0.9 ± 0.1	0.0 ± 0.0	2.7 ± 0.7	2.7 ± 0.8	ND
T. pseudoethanolicus (DSM 2355)	Mannitol	36.6 ± 6.3	3.40 ± 0.9	3.1 ± 0.2	8.1 ± 1.2	107.7
	Control (YE)	1.4 ± 0.3	0.0 ± 0.0	1.9 ± 0.6	3.2 ± 1.2	ND
T. italicus (DSM 9252)	Mannitol	19.7 ± 7.9	6.89 ± 1.48	3.1 ± 0.7	8.5 ± 0.7	74.3
	Control (YE)	0.9 ± 0.3	0.0 ± 0.0	1.4 ± 0.5	2.2 ± 0.6	ND
T. brockii subsp *finni* (DSM 3389)	Mannitol	33.4 ± 0.5	3.12 ± 0.24	3.1 ± 0.2	8.9 ± 0.9	99.3
	Control (YE)	1.7 ± 0.5	0.0 ± 0.0	2.7 ± 0.4	3.0 ± 0.8	ND
T. brockii subsp *brockii* (DSM 1457)	Mannitol	26.8 ± 6.3	5.27 ± 0.98	3.6 ± 0.3	10.1 ± 1.6	89.2
	Control (YE)	2.2 ± 0.8	0.0 ± 0.0	3.2 ± 0.1	3.6 ± 1.1	ND
Th. xylanolyticum (DSM 7097)	Mannitol	18.2 ± 2.2	3.78 ± 0.38	2.6 ± 0.4	3.3 ± 2.8	ND
	Control (YE)	0.6 ± 0.0	0.0 ± 0.0	1.5 ± 0.2	1.4 ± 0.2	ND
Ca. lactoaceticus (DSM 9545)	Mannitol	10.0 ± 5.2	5.83 ± 1.23	4.4 ± 0.1	2.2 ± 0.6	38.5
	Control (YE)	0.0 ± 0.0	0.0 ± 0.0	1.0 ± 0.2	1.7 ± 0.2	ND
Ca. kristjanssonii (DSM 12137)	Mannitol	8.3 ± 2.3	0.67 ± 0.29	2.4 ± 0.1	3.0 ± 0.2	24.9
	Control (YE)	0.0 ± 0.0	0.0 ± 0.0	2.3 ± 0.2	0.8 ± 0.2	ND

Values represent the average of triplicate measurements ± SD. C, Caldanaerobacter; T, Thermoanaerobacter; Th, Thermoanaerobacterium; Ca, Caldicellulosiruptor.

investigation (**Figures 1B**, **2B**). The main reason for this difference could be the fact that the proteins present have limited solubility under these conditions or are bound to other components in the matrix. Furthermore, other algal polymers, such as laminarin, fucoidan, alginate, and agar could be co-extracted although this can likely be minimized by using mild conditions and short extraction times as the traditional methodologies for the extraction of these carbohydrates necessitates hot acid extraction (Black et al., 1952; Mateus et al., 1977). For the selective extraction of mannitol, the use of other mineral acids, such as sulfuric acid, maybe more relevant due to HCl's volatility, especially at elevated temperatures. Kinetic experiments of mannitol extraction under selected conditions reveal that mannitol is rapidly extracted with peak concentrations for the first and second rounds of extraction being achieved in less than 5 min (**Figures 3A,B**). This is more rapid than mannitol extraction reported for other species such as *Macrocystis pyrifera* (Mateus et al., 1977).

In order to reduce the viscosity after large-scale extraction, an extra step involving the addition of calcium chloride to precipitate the alginate was added. This did not adversely affect the concentration of mannitol although increasing the salinity of the solution may adversely affect a number of the organisms being studied.

Screening of Thermophilic *Clostridia* for Mannitol Utilization

The utilization of mannitol is not routinely reported in characterization papers for most thermophilic *Clostridia* although the type strains of *Caloramator* were not included in this study, *Caloramator boliviensis* and *Caloramator*

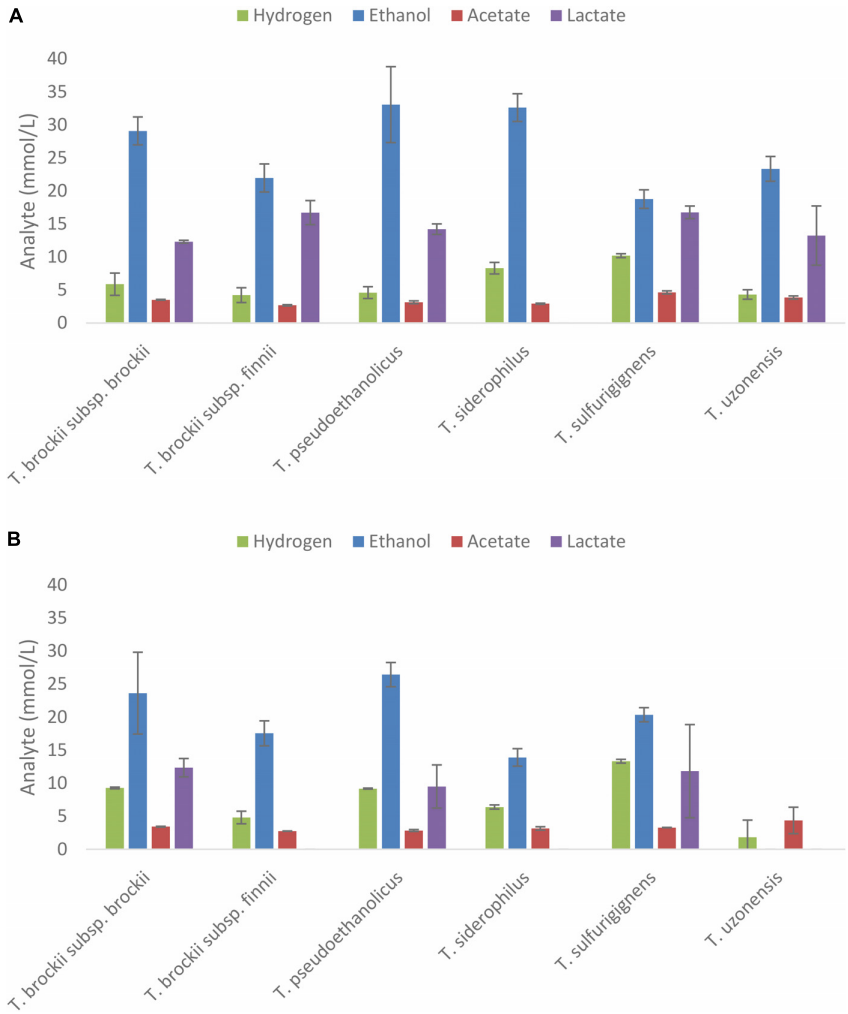

FIGURE 4 | Fermentation products after 5 days from selected thermophilic *Clostridia* on extracts of *Ascophyllum nodosum* **(A)** and *Laminaria digitata* **(B)** adjusted to 20 mM mannitol equivalent. End products were analyzed after 10 days of fermentation; values represent the average of triplicate fermentations with SD presented as error bars.

quimbayensis have been noted to utilize mannitol (Crespo et al., 2012; Rubiano-Labrador et al., 2013).

From the data presented the general trend seems to be that mannitol utilization is largely restricted to the genera of *Thermoanaerobacter* although some strains within *Caldicellulosiruptor* demonstrated weakly positive results evidenced by low ethanol yields (**Table 3**). Generally, the mannitol utilization results reported here are in good agreement with the results which have been previously reported with a few exceptions. The subspecies of *C. subterraneus* have been reported to degrade mannitol qualitatively (Fardeau et al., 2004 and references therein) while in this study only *C. subterraneus* subsp. *pacificus* degrades mannitol with ethanol as the major end product. Furthermore, *T. pentosaceus* was originally reported to utilize mannitol although our results are negative.

Four of the *Thermoanaerobacter* species produce more than 0.4 g ethanol/g mannitol in the present investigation of which the maximum theoretical yields are 0.51 g ethanol/g mannitol (1.5 mol ethanol/mol mannitol). This is comparable with several mesophilic bacteria like *Escherichia coli* and *Zymobacter palmae* which have been reported to produce 0.41 and 0.38 g/g, respectively (Horn et al., 2000; Kim et al., 2011). Other mesophilic microorganism have been reported to produce lower amounts of ethanol, such as *Enterobacter* sp., *Pichia angophorae*, and *Vibrio tritonius* AM2, with 0.29, 0.29, and 0.36 g ethanol/g substrate, respectively. The thermophilic bacterium belonging to Class *Clostridia*, *Defluviitalea phaphyphila,* has recently been shown to produce high ethanol titers from mannitol with yields of up to 0.44 g/g being reported (Ji et al., 2016a,b).

Fermentation of Mannitol in Macroalgal Extracts by Selected Strains

Despite positive growth and end product formation on mannitol, strains from the genera of *Caldicellulosiruptor, Caldanaerobacter,* and *Thermoanaerobacterium* did not utilize

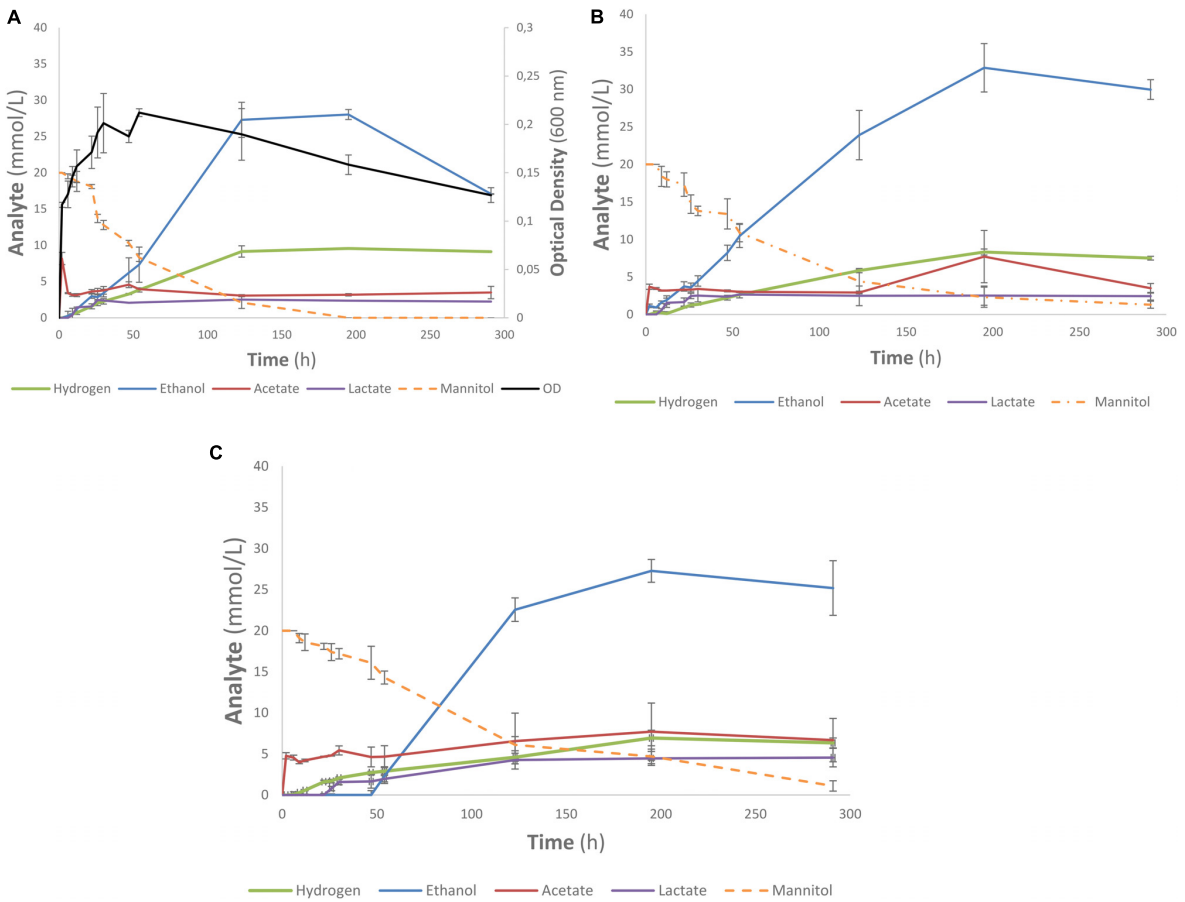

FIGURE 5 | Profile of mannitol-containing media using *Thermoanaerobacter pseudoethanolicus* (DSM 2355). **(A)** 20 mM mannitol, **(B)** *Ascophyllum nodosum* extracted diluted to 20 mM mannitol, **(C)** *Laminaria digitata* extract diluted to 20 mM mannitol. Data points represent the average values of triplicates with SD presented as error bars.

the mannitol-containing extracts from *A. nodosum* or *L. digitata*. The five mannitol-degrading strains of *Thermoanaerobacter* yielded good ethanol yields from the macro algal extracts, the highest ethanol concentration, 33.1 mM were obtained from *T. pseudoethanolicus* on *A. nodosum* extracts. In general higher ethanol yields were obtained on *Ascophyllum* extracts (between 18.8 and 33.1 mM) compared to *Laminaria* extracts (0.0–26.4 mM). Assuming that mannitol is the only sugar left in the extracts after extraction the ethanol yields are in good correlation with ethanol yields from mannitol only (**Figures 4A,B**). Several studies have been performed using various types of macro algae for ethanol production. When the recently isolated thermophile *Defluviitalea phaphyphila* was cultivated on the alginates from the brown macroalgae *Saccharina japonica* the bacterium produced 2.7 g of ethanol and 3.0 g of acetate from 7.6 g of alginate (Ji et al., 2016a,b). The study by Matsumura et al. (2014) on the brown macroalgae *Saccharina sculpera* using the facultative anaerobe *Vibrio tritonius* resulted in production of 11.5 g of ethanol from 30 g of seaweed hydrolysate. In a study with *E. coli* cultivated on enzyme pretreated hydrolysate of *L. japonica* the maximum ethanol production observed was 0.29 g/g biomass (Kim et al., 2011). Finally, *Saccharomyces cerevisiae* has been reported to produce between 4 and 5 g/L of ethanol in a SSF fermentation of

TABLE 4 | Features of kinetic experiments with *Thermoanaerobacter pseudoethanolicus* (DSM 2355) on mannitol and macro algal extracts.

		Ethanol yield		
Substrate	**Fermenation time (h)**	**Yield (%)**	**Ethanol (g/g substrate)**	**Volumetric productivity (mM per hour)**
Mannitol	123	70.1	0.36	0.29
A. nodosum extract	195	82.2	0.42	0.22
L. digitata extract	195	68.2	0.35	0.33

S. japonica (Li et al., 2013). It is difficult to compare these results since the concentration of the extracts used, species type and pretreatment methods used vary to a great extent. Clearly however, the best *Thermoanaerobacter* species producing more than 30 mM of ethanol from macroalgal extracts containing 20 mM of mannitol are among the higher yields observed in literature with other microorganism.

As the end products were analyzed after 5 days, it is possible that some strains could exhibit delayed ethanol formation as observed in the kinetic experiments with *T. pseudoethanolicus* on both 20 mM mannitol and the brown algal extracts adjusted to 20 mM of mannitol. Furthermore, the lack of observed end product formation on mannitol-containing algal extracts could be due to inhibition phenomena from co-extracted salts or other inhibitory compounds. The salt concentrations in the macroalgal extracts in our study was 0.5 and 1.1% (**Table 2**). While salt tolerance has not been widely investigated for the type strains of these genera although some data on *Caldicellulosiruptor* species have been reported; *Ca. kristjansson* is inhibited below 0.2% NaCl, *Ca. acetigenus* is inhibited at 0.2% while many other members of the genus only tolerate up to 1% (Onyenwoke et al., 2006; Bing et al., 2015).

Kinetic Studies of Anntiol and Algal Extract Fermentation

Fermentation of mannitol by *T. pseudoethanolicus* is comparatively slow compared to other substrates (such as glucose, **Supplementary Figure S1**) only reaching a maximum ethanol after 120 h (**Figure 5A**). Ethanol formation continued into the stationary phase which could indicate a bottleneck in feeding mannitol catabolism intermediates into glycolysis pathway. Further work is needed to understand the nature of mannitol utilization by *T. pseudoethanolicus* and to explain why the formation of reduced end products is slower as compared with glucose. It is worth noting that optical density of the culture was approximately 30% higher on glucose as compared with mannitol and three times as high compared with control (yeast extract only) (**Supplementary Figures S1**, **S2** and **Figure 5A**). The fermentation of the mannitol-containing algal extracts were more slowly fermented to ethanol than with mannitol only (**Figures 5B,C**). The mannitol may have been less accessible to the microorganism due to other compounds in the sample matrix. The optical density was not measured during these fermentations due to the highly turbid nature of the algal extracts. Additionally, fermentation of other compounds present in the extract such as laminarin are possible since some *Clostridia* have been reported to have glucosidases capable of cleaving a β-1,3-*O* glycosidic bond although this capability has not been systematically investigated (Leschine, 2005). As the end product were analyzed after 5 days, it is possible that some strains exhibited delayed ethanol formation as observed in the kinetic experiments with *T. pseudoethanolicus* on both 20 mM mannitol and the brown algae extracts adjusted to 20 mM of mannitol. Furthermore, the lack of observed end product formation on mannitol-containing algae extracts could be due inhibition phenomena from co-extracted salts or other inhibitory compounds.

The slow degradation of mannitol by *T. pseudoethanolicus* could be problematic for commercialization of bioethanol production from macro algae. This could potentially be overcome by increasing the cell density by immobilization, by using continuous culture, as well as the optimization of culture conditions, and genetic engineering of the strain. Furthermore, the utilization of other components of brown macro algae, such as laminarin and alginate, could be approached by hydrolyzing the macro algae using commercially available enzymes. Also, hydrolysates prepared from species known to degrade these polysaccharides could lead to a greater utilization of the biomass perhaps using a cascading biorefinery scheme that couples the removal of higher-value products to the fermentation of lower value fractions such as mannitol.

CONCLUSION

Mannitol is a potentially viable source of carbon for the fermentative production of bioethanol by thermophilic anaerobes isolated from diverse environments. Mannitol can be rapidly extracted from *A. nodosum* and *L. digitata* under mild conditions with good yields. The amount of mannitol released from the two species of brown macroalgae varied to a great extent; always lower than 40 mM from *A. nodosum* but higher than 72 mM from *L. digitata*. The amount of protein and phenolic compounds released were also different between macroalgae species (about 300 μg/mL for *A. nodosum* and 100 μg/mL for *L. digitata*). Of 41 thermophilic *Clostridia* species tested for mannitol utilization, 11 were positive mainly species within the genus *Thermoanaerobacter*. Four species showed more than 75% ethanol yields on the sugar alcohol. Six *Thermoanaerobacter* species degraded macroalgal extracts resulting in ethanol as the main end-product. *T. pseudoethanolicus* was the best ethanol producer both from pure mannitol as well as from macroalgae biomass.

AUTHOR CONTRIBUTIONS

EI, SS, and TC designed and performed the experiments and analysis. SS and JO drafted the manuscript.

FUNDING

This work was supported by AVS research fund, grant R15 065-15. The project was funded by AVS (Aukið verðmæti sjávarafurða), an Icelandic Research Funding which is not listed in the Funding body above.

SUPPLEMENTARY MATERIAL

The Supplementary Material for this article can be found online at: https://www.frontiersin.org/articles/10.3389/fmicb.2018.01931/full#supplementary-material

REFERENCES

Adams, J. M. M., Ross, A. B., Anastasakis, K., Hodgson, E. M., Gallagher, J. A., Jones, J. M., et al. (2011). Seasonal variation in the chemical composition of the bioenergy feedstock *Laminaria digitata* for thermochemical conversion. *Bioresour. Technol.* 102, 226–234. doi: 10.1016/j.biortech.2010.06.152

Bing, W., Wang, H., Zheng, B., Zhang, F., Zhu, G., Feng, Y., et al. (2015). *Caldicellulosiruptor changbaiensis* sp. nov., a cellulolytic and hydrogen-producing bacterium from a hot spring. *Int. J. Syst. Evol. Microbiol.* 65, 293–297. doi: 10.1099/ijs.0.065441-0

Black, W. A. P., Dewar, E. T., and Woodward, F. N. (1952). Manufacture of algal chemicals. IV.-laboratory-scale isolation of fucoidin from brown marine algae. *J. Sci. Food Agric.* 3, 122–129. doi: 10.1002/jsfa.2740030305

Blumer-Schuette, S. E., Giannone, R. J., Zurawski, J. V., Ozdemir, I., Ma, Q., Yin, Y., et al. (2012). *Caldicellulosiruptor* core and pangenomes reveal determinants for noncellulosomal thermophilic deconstruction of plant biomass. *J. Bacteriol.* 194, 4015–4028. doi: 10.1128/JB.00266-12

Bouanane-Darenfed, A., Fardeau, M.-L., Greégoire, P., Manon, J., Kebbouche-Gana, S., Benayad, T., et al. (2011). *Caldicoprobacter algeriensis* sp. nov. a new thermophilic anaerobic, xylanolytic bacterium isolated from an algerian hot spring. *Curr. Opin. Microbiol.* 62, 826–832. doi: 10.1007/s00284-010-9789-9

Bradford, M. M. (1976). A rapid and sensitive method for the quantitation of microgram quantities of protein utilizing the principle of protein-dye binding. *Anal. Biochem.* 72, 248–254. doi: 10.1016/0003-2697(76)90527-3

Burgess, E. A., Wagner, I. C., and Wiegel, J. (2007). "Thermophile environments and biodiversity," in *Physiology and Biochemistry of Extremophiles*, eds C. Gerday and N. Glansdorff (Washington, DC: ASM Press), 13–29. doi: 10.1128/9781555815813.ch2

Carere, C. R., Rydzak, T., Verbeke, T. J., Cicek, N., Levin, D. B., and Sparling, R. (2012). Linking genome content to biofuel production yields: a meta-analysis of major catabolic pathways among select H2 and ethanol-producing bacteria. *BMC Microbiol.* 12:295. doi: 10.1186/1471-2180-12-295

Chang, T., and Yao, S. (2011). Thermophilic, lignocellulolytic bacteria for ethanol production: current state and perspectives. *Appl. Microbiol. Biotechnol.* 92, 13–27. doi: 10.1007/s00253-011-3456-3

Cook, G. M., Rainey, F. A., Patel, B. K. C., and Morgan, H. W. (1996). Characterization of a new obligately anaerobic thermophile, *Thermoanaerobacter wiegelii* sp. nov. *Int. J. Syst. Bacteriol.* 46, 123–127. doi: 10.1099/00207713-46-1-123

Crespo, C., Pozzo, T., Karlsson, E. N., Alvarez, M. T., and Mattiasson, B. (2012). *Caloramator boliviensis* sp. nov., a thermophilic, ethanol-producing bacterium isolated from a hot spring. *Int. J. Syst. Evol. Microbiol.* 62, 1679–1686. doi: 10.1099/ijs.0.032664-0

Daglia, M. (2012). Polyphenols as antimicrobial agents. *Curr. Opin. Biotechnol.* 23, 174–181. doi: 10.1016/j.copbio.2011.08.007

Daroch, M., Geng, S., and Wang, G. (2013). Recent advances in liquid biofuel production from algal feedstocks. *Appl. Energy* 102, 1371–1381. doi: 10.1016/j.apenergy.2012.07.031

Enquist-Newman, M., Faust, A. M. E., Bravo, D. D., Santos, C. N. S., Raisner, R. M., Hanel, A., et al. (2014). Efficient ethanol production from brown macroalgae sugars by a synthetic yeast platform. *Nature* 505, 239–243. doi: 10.1038/nature12771

Fardeau, M., Salinas, M. B., L'Haridon, S., Jeanthon, C., Verhé, F., Cayol, J., et al. (2004). Isolation from oil reservoirs of novel thermophilic anaerobes phylogenetically related to *Thermoanaerobacter subterraneus*: reassignment of *T. subterraneus*, *Thermoanaerobacter yonseiensis*, *Thermoanaerobacter tengcongensis* and *Carboxydibrachium pacificum*. *Int. J. Syst. Evol. Microbiol.* 54, 467–474. doi: 10.1099/ijs.0.02711-0

Heyndrickx, M., De Vos, P., Speybrouck, A., and De Ley, J. (1989). Fermentation of mannitol by *Clostridium butyricum*: role of acetate as an external hydrogen acceptor. *Appl. Microbiol. Biotechnol.* 31, 323–328. doi: 10.1007/BF00257597

Horn, S. J., Aasen, I. M., and Ostgaard, K. (2000). Ethanol production from seaweed extract. *J. Ind. Microbiol. Biotechnol.* 25, 249–254. doi: 10.1038/sj.jim.7000065

Hungate, R. E. (1969). A roll tube method for cultivation of strict anaerobes, in *Methods in Microbiology,* eds J. R. Norris and D. W. Ribbons (New York, NY: Academic Press), 117–132.

Indergaard, M., and Minsaas, J. (1991). "Animal and human nutrition," in *Seaweed Resources in Europe: Uses and Potential*, eds M. D. Guiry and G. Blunden (Chichester: John Wiley & Sons, Ltd.), 21–64.

Ingvadottir, E. M., Scully, S. M., and Orlygsson, J. (2017). Evaluation of the genus of *Caldicellulosiruptor* for producation of 1,2-propanediol from methylpentoses. *Anaerobe* 47, 86–88. doi: 10.1016/j.anaerobe.2017.04.015

Ji, S. Q., Wang, B., Lu, M., and Li, F. L. (2016a). Biotechnology for biofuels direct bioconversion of brown algae into ethanol by thermophilic bacterium *Defluviitalea phaphyphila*. *Biotechnol. Biofuels* 9, 1–10. doi: 10.1186/s13068-016-0494-1

Ji, S. Q., Wang, B., Lu, M., and Li, F. L. (2016b). *Defluviitalea phaphyphila* sp. nov., a novel thermophilic bacterium that degrades brown algae. *Appl. Environ. Microbiol.* 82, 868–877. doi: 10.1128/AEM.03297-15

Jiang, R., Ingle, K. N., and Golberg, A. (2016). Macroalgae (seaweed) for liquid transportation biofuel production: what is next? *Algal Res.* 14, 48–57. doi: 10.1016/j.algal.2016.01.001

Kaid, N., Al-shorgani, N., Hafez, M., Isa, M., Mohtar, W., Yusoff, W., et al. (2016). Isolation of a *Clostridium acetobutylicum* strain and characterization of its fermentation performance on agricultural wastes. *Renew. Energy* 86, 459–465. doi: 10.1016/j.renene.2015.08.051

Kawai, S., and Murata, K. (2016). Biofuel production based on carbohydrates from both brown and red macroalgae: recent developments in key biotechnologies. *Int. J. Mol. Sci.* 145, 1–17. doi: 10.3390/ijms17020145

Kazamias, M. T., and Sperry, J. F. (1995). Enhanced fermentation of mannitol and release of cytotoxin by *Clostridium difficile* in alkaline culture media. *Appl. Environ. Microbiol.* 61, 2425–2427.

Kim, N., Li, H., Jung, K., Nam, H., and Cheon, P. (2011). Ethanol production from marine algal hydrolysates using *Escherichia coli* KO11. *Bioresour. Technol.* 102, 7466–7469. doi: 10.1016/j.biortech.2011.04.071

Leschine, S. (2005). "Degradation of polymer: cellulose, xylan, pectin, starch," in *Handbook on Clostridia*, ed. P. Durre (Boca Raton, FL: CRC Press), 101–131.

Li, P., Lee, J., Jin, H., and Keun, K. (2013). Ethanol production from *Saccharina japonica* using an optimized extremely low acid pretreatment followed by simultaneous saccharification and fermentation. *Bioresour. Technol.* 127, 119–125. doi: 10.1016/j.biortech.2012.09.122

Mateus, H., Regenstein, J. M., and Baker, R. C. (1977). Studies to improve the extraction of mannitol and alginic acid from *Macrocystis pyrifera*, a marine brown algae. *Econ. Bot.* 31, 24–27. doi: 10.1007/BF02860648

Matsumura, Y., Sato, K., Al-saari, N., Nakagawa, S., and Sawabe, T. (2014). Enhanced hydrogen production by a newly described heterotrophic marine bacterium, *Vibrio tritonius* strain AM2, using seaweed as the feedstock. *Int. J. Hydrogen Energy* 39, 7270–7277. doi: 10.1016/j.ijhydene.2014.02.164

Milledge, J. J., Smith, B., Dyer, P. W., and Harvey, P. (2014). Macroalgae-derived biofuel: a review of methods of energy extraction from seaweed biomass. *Energies* 7, 7194–7222. doi: 10.3390/en7117194

Miller, T. L., and Wolin, M. J. (1974). A serum bottle modification of the Hungate technique for cultivating obligate anaerobes. *Appl. Microbiol.* 27, 985–987.

Muty, U. S., and Banerjee, A. K. (2012). "Seaweeds: the wealth of oceans," in *Handbook of Marine Macroalgae: Biotechnology and Applied Phycology*, ed. S.-K. Kim (Hoboken, NJ: Wiley-Blackwell), 36–44.

Onyenwoke, R. U., Lee, Y., Dabrowski, S., Ahring, B. K., and Wiegel, J. (2006). Reclassification of *Thermoanaerobium acetigenum* as *Caldicellulosiruptor acetigenus* comb. nov. and emendation of the genus description. *Int. J. Syst. Evol. Microbiol.* 56, 1391–1395. doi: 10.1099/ijs.0.63723-0

Orlygsson, J., and Baldursson, S. R. B. (2007). Phylogenetic and physiological studies of four hydrogen-producing thermoanareobes. *Icel. Agric. Sci.* 20, 93–105.

Patil, Y., Junghare, M., Pester, M., and Mu, N. (2015). *Anaerobium acetethylicum* gen. nov., sp. nov., a strictly anaerobic, gluconate-fermenting bacterium isolated from a methanogenic bioreactor. *Int. J. Syst. Evol. Microbiol.* 65, 3289–3296. doi: 10.1099/ijsem.0.000410

Quain, D. E., and Boulton, C. A. (1987). Growth and metabolism of mannitol by strains of *Saccharomyces cerevisiae*. *J. Gen. Microbiol.* 133, 1675–1684. doi: 10.1099/00221287-133-7-1675

Radulovich, R., Neori, A., Valderrama, D., Reddy, C. R. K., Cronin, H., and Forster, J. (2015). "Farming of seaweeds," in *Seaweed Sustainability: Food and Non-Food Applications*, eds B. K. Tiwori and D. J. Troy

(New York, NY: Academic Press), 27–59. doi: 10.1016/B978-0-12-418697-2.00003-9

Ren, N., Wang, A., Cao, G., Xu, J., and Gao, L. (2009). Bioconversion of lignocellulosic biomass to hydrogen: potential and challenges. *Biotechnol. Adv.* 27, 1051–1060. doi: 10.1016/j.biotechadv.2009.05.007

Rubiano-Labrador, C., Baena, S., Díaz-Cárdenas, C., and Patel, B. K. C. (2013). *Caloramator quimbayensis* sp. nov., an anaerobic, moderately thermophilic bacterium isolated from a terrestrial hot spring. *Int. J. Syst. Evol. Microbiol.* 63, 1396–1402. doi: 10.1099/ijs.0.037937-0

Sanchez, J. (1998). Colorimetric assay of alditols in complex biological samples. *J. Agric. Food Chem.* 46, 157–160. doi: 10.1021/jf970619t

Sánchez, O. J., and Cardona, C. A. (2008). Trends in biotechnological production of fuel ethanol from different feedstocks. *Bioresour. Technol.* 99, 5270–5295. doi: 10.1016/j.biortech.2007.11.013

Scully, S., and Orlygsson, J. (2015). Recent advances in second generation ethanol production by thermophilic bacteria. *Energies* 8, 1–30. doi: 10.3390/en8010001

Sittijunda, S., Tomás, A. F., Reungsang, A., O-thong, S., and Angelidaki, I. (2013). Ethanol production from glucose and xylose by immobilized *Thermoanaerobacter pentosaceus* at 70 °C in an up-flow anaerobic sludge blanket (UASB) reactor. *Bioresour. Technol.* 143, 598–607. doi: 10.1016/j.biortech.2013.06.056

Sveinsdottir, M., Beck, S. R., and Orlygsson, J. (2009). Ethanol production from monosugars and lignocellulosic biomass by thermophilic bacteria isolated from Icelandic hot springs. *Icel. Agric. Sci.* 22, 45–58.

Tanghe, A., Prior, B., and Thevelein, J. M. (2005). "Yeast responses to stresses," in *The Yeast Handbook: Biodiversity and Ecophysiology of Yeasts*, eds C. A. Rosa and G. Péter (New York, NY: Springer), 175–195.

Taylor, M. P., Eley, K. L., Martin, S., Tuffin, M. I., Burton, S. G., and Cowan, D. A. (2009). Thermophilic ethanologenesis: future prospects for second-generation bioethanol production. *Trends Biotechnol.* 27, 398–405. doi: 10.1016/j.tibtech.2009.03.006

Tomás, A. F., Karakashev, D., and Angelidaki, I. (2013). *Thermoanaerobacter pentosaceus* sp. nov., an anaerobic, extreme thermophilic, high ethanol-yielding bacterium isolated from household waste. *Int. J. Syst. Evol. Microbiol.* 63, 2396–2404. doi: 10.1099/ijs.0.045211-0

Wei, N., Quarterman, J., and Jin, Y.-S. (2013). Marine macroalgae: an untapped resource for producing fuels and chemicals. *Trends Biotechnol.* 31, 70–77. doi: 10.1016/j.tibtech.2012.10.009

Xia, A., Jacob, A., Herrmann, C., Tabassum, M. R., and Murphy, J. D. (2015). Production of hydrogen, ethanol and volatile fatty acids from the seaweed carbohydrate mannitol. *Bioresour. Technol.* 193, 488–497. doi: 10.1016/j.biortech.2015.06.130

Conflict of Interest Statement: The authors declare that the research was conducted in the absence of any commercial or financial relationships that could be construed as a potential conflict of interest.

Advantages of publishing in Frontiers

OPEN ACCESS
Articles are free to read for greatest visibility and readership

FAST PUBLICATION
Around 90 days from submission to decision

HIGH QUALITY PEER-REVIEW
Rigorous, collaborative, and constructive peer-review

TRANSPARENT PEER-REVIEW
Editors and reviewers acknowledged by name on published articles

Frontiers
Avenue du Tribunal-Fédéral 34
1005 Lausanne | Switzerland

Visit us: www.frontiersin.org
Contact us: info@frontiersin.org | +41 21 510 17 00

REPRODUCIBILITY OF RESEARCH
Support open data and methods to enhance research reproducibility

DIGITAL PUBLISHING
Articles designed for optimal readership across devices

FOLLOW US
@frontiersin

IMPACT METRICS
Advanced article metrics track visibility across digital media

EXTENSIVE PROMOTION
Marketing and promotion of impactful research

LOOP RESEARCH NETWORK
Our network increases your article's readership